

AD-A090 117

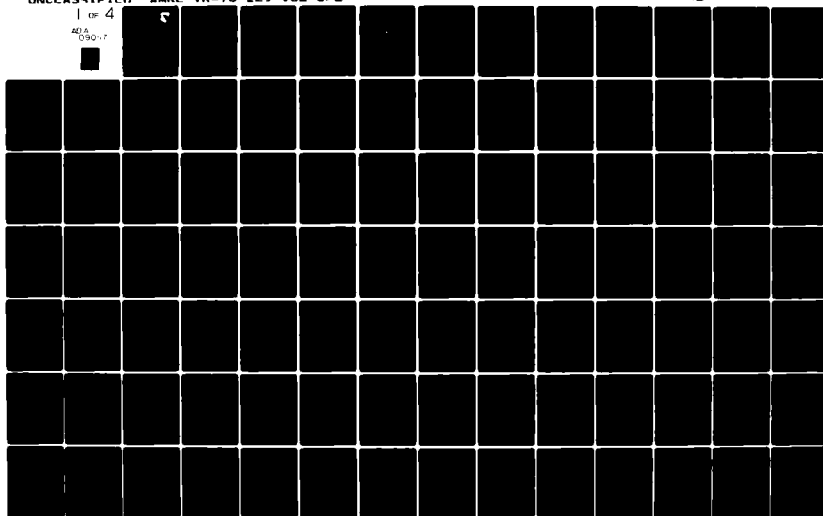
AIR FORCE AEROSPACE MEDICAL RESEARCH LAB WRIGHT-PATT--ETC F/G 6/16  
VISUAL INFORMATION PROCESSING BASED ON SPATIAL FILTERS CONSTRAI--ETC(U)  
DEC 78 A P GINSBURG  
AMRL-TR-78-129-VOL-1/2

UNCLASSIFIED

NL

1 of 4

AD-A  
090-117



h  
14 AMRL-TR-78-129, Volumes I & II - 1/2 12

LEVEL II



AD A090117

6 **VISUAL INFORMATION PROCESSING BASED ON  
SPATIAL FILTERS CONSTRAINED BY BIOLOGICAL DATA**

9 Doctoral thesis,

10 Arthur P. Ginsburg, PhD

16 2313

17 Y-1

11 December 1978

12 36

RECEIVED  
A

DDC FILE COPY

Approved for public release; distribution unlimited

AEROSPACE MEDICAL RESEARCH LABORATORY  
AEROSPACE MEDICAL DIVISION  
AIR FORCE SYSTEMS COMMAND  
WRIGHT-PATTERSON AIR FORCE BASE, OHIO

00967

80 10 9 011

## NOTICES

When US Government drawings, specifications, or other data are used for any purpose other than a definitely related Government procurement operation, the Government thereby incurs no responsibility nor any obligation whatsoever, and the fact that the Government may have formulated, furnished, or in any way supplied the said drawings, specifications, or other data, is not to be regarded by implication or otherwise, as in any manner licensing the holder or any other person or corporation, or conveying any rights or permission to manufacture, use, or sell any patented invention that may in any way be related thereto.

Please do not request copies of this report from Air Force Aerospace Medical Research Laboratory. Additional copies may be purchased from:

National Technical Information Service  
5285 Port Royal Road  
Springfield, Virginia 22161

Federal Government agencies and their contractors registered with Defense Documentation Center should direct requests for copies of this report to:

Defense Documentation Center  
Cameron Station  
Alexandria, Virginia 22314

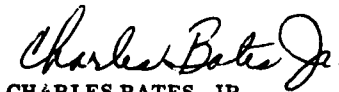
## TECHNICAL REVIEW AND APPROVAL

AMRL-TR-78-129  
(Vols I & II)

This report has been reviewed by the Office of Public Affairs (PA) and is releasable to the National Technical Information Service (NTIS). At NTIS, it will be available to the general public, including foreign nations.

This technical report has been reviewed and is approved for publication.

FOR THE COMMANDER



CHARLES BATES, JR.  
Chief  
Human Engineering Division  
Air Force Aerospace Medical Research Laboratory

REPORT DOCUMENTATION PAGE		READ INSTRUCTIONS BEFORE COMPLETING FORM
1. REPORT NUMBER AMRL-TR-78-129, Volumes I and II	2. GOVT ACCESSION NO. AD-H090	3. REPORT'S CATALOG NUMBER 127
4. TITLE (and Subtitle) VISUAL INFORMATION PROCESSING BASED ON SPATIAL FILTERS CONSTRAINED BY BIOLOGICAL DATA		5. TYPE OF REPORT & PERIOD COVERED Doctoral Dissertation
7. AUTHOR(s) Arthur P. Ginsburg		6. PERFORMING ORG. REPORT NUMBER
9. PERFORMING ORGANIZATION NAME AND ADDRESS Aerospace Medical Research Laboratory, Aerospace Medical Division, Air Force Systems Command, Wright-Patterson Air Force Base, Ohio 45433		8. CONTRACT OR GRANT NUMBER(s)
11. CONTROLLING OFFICE NAME AND ADDRESS		10. PROGRAM ELEMENT, PROJECT, TASK AREA & WORK UNIT NUMBERS 61102F, 2313-V1-22
14. MONITORING AGENCY NAME & ADDRESS (if different from Controlling Office)		12. REPORT DATE December 1978
		13. NUMBER OF PAGES 334
		15. SECURITY CLASS. (of this report) UNCLASSIFIED
		15a. DECLASSIFICATION/DOWNGRADING SCHEDULE N/A
16. DISTRIBUTION STATEMENT (of this Report) Approved for public release; distribution unlimited		
17. DISTRIBUTION STATEMENT (of the abstract entered in Block 20, if different from Report)		
18. SUPPLEMENTARY NOTES Library of Congress Catalog Card Number 79-600156		
19. KEY WORDS (Continue on reverse side if necessary and identify by block number) contrast matching, visual channels, spatial vision, contrast sensitivity, spatial frequency, filters, biological data, visual psychophysics, neurophysiology, visual perception, digital image processing, form perception, visual textures, illusions, abnormal vision, Snellen acuity, visual acuity, object detection, object identification, amblyopia, and multiple sclerosis, and multistability.		
20. ABSTRACT (Continue on reverse side if necessary and identify by block number) Visual perception is investigated using spatial filters that are constrained by biological data. This report has four major parts: (1) a theoretical background to Fourier analysis, (2) a review of the literature relating to the spatial filtering characteristics of mammalian visual systems, (3) visual information processing in terms of spatial filtering, (4) the relating of contrast sensitivity to the identification of complex objects. The common denominator to all the investigations is spatial filtering. The major goal of the dissertation was the attempt to explain certain aspects of visual perception using a single concept: filtering.		



20. ABSTRACT CONTINUED The results of this attempt are summarized as follows:

(1) Biological data from cat, monkey, and man, using neurophysiological and psychophysical methods, provide much evidence for the existence of mechanisms tuned to different regions of spatial frequency and orientation. In general, the spatial frequency bandwidth is one to two octaves and the orientation bandwidth is  $\pm 15$  degrees. The overall filtering characteristics of the visual system is the envelope of the activity of those mechanisms and can be determined by contrast sensitivity and contrast matching functions.

(2) Two-dimensional spatial filters were made based upon the general and specific filtering properties of the overall (MTF) and individual mechanisms (channels). These spatial filters were used to filter a wide variety of objects.

(3) The perceptual problems of the classification of simple and complex objects, Gestalt principles, visual textures, visual illusions, and multi-stability, with few exceptions, yielded gracefully to the concept of spatial filtering. Parsimony reigned as explanations for these seemingly disparate visual phenomena were given in terms of the known two-dimensional filtering properties of the visual system.

(4) A detailed study using generalized and biologically derived band-pass spatial filters further demonstrated the power of a general filter concept for visual perception. The full spectrum of perceptual information about a complex object from basic form to the finest detail was available with only seven two-octave-wide band-pass filters (channels). These results led to the concept of a hierarchy of filtered images.

(5) In general, the MTF filter provided the details of objects that corresponded to what is seen. One-to two-octave band-pass filters appeared to provide the generalized information that is perceived about objects. The specific bandwidth and shape of the spatial filters were not important for the class of objects and perceptual problems discussed.

(6) Combining the filtering results of the minimum information required for the identification of objects with data from an experiment that determined the minimum amount of contrast required for the identification of Snellen letters demonstrated the predictive power of the filter concept. The Snellen acuity of 17 of 22 eyes of amblyopes and patients suffering from multiple sclerosis could be predicted within one Snellen line. The increase of spatial sensitivity over a narrow range of spatial frequency of one amblyope resulted in a concomitant increase in Snellen letter acuity. Especially interesting was that the increased Snellen acuity could be explained from the minimum number of spatial frequencies required for letter identification. These results appear to provide the first direct evidence for the existence of narrow-band mechanisms in the visual system which are used in the identification of complex objects. Thus, the ability to establish a relationship between Snellen letter acuity and contrast sensitivity suggests that the filter concept is neither blind nor empty.

In general, these results support the view that the MTF is the window which reduces the range of size of objects that can be seen. The much narrower and orientation-selective filters that make up the MTF appear to filter relevant form information. The outputs of all the individual filters appear to be presented simultaneously to create the global picture that is seen.

The picture that emerges from these studies is that visual perception may be structured from a hierarchy of filtered images, each image representing one level of visual information. This hierarchy of filtered images may be the keyboard from which the harmony of visual perception is obtained.

# VOLUME I

Accession For		
PTIS	GRA&I	<input checked="checked" type="checkbox"/>
DTIC TAB		<input type="checkbox"/>
Unannounced		<input type="checkbox"/>
Justification		
By		
Distribution/		
Availability Codes		
Avail and/or		
Dist	Special	
A		

## PREFACE

This report is a dissertation submitted to the University of Cambridge for a Ph.D. in Biophysics which is being made available to the larger research community. Alluding to early advances in Greek arts and sciences, John Platt categorized the two general classes of scientific minds as Dionysian and Apollonian. Although dissertations can be typically categorized as Apollonian (since novel major thrusts in science can be risky and quite unsettling to the scientific status quo), this dissertation is primarily Dionysian. It offers a new synthesis of visual perception within a single conceptual framework—filtering—to explain how we see objects. It is a different way of thinking and quantifying perception not found in contemporary texts. It attempts to provide a logical bridge between current knowledge about visual science and perception using engineering systems analysis.

General theories about perception do not usually consider the physics of the visual system—how the great masses of spatial information are physically transmitted up the visual pathway. Since the visual system is a physical processing system, it is reasonable to suggest that the physical filtering properties of the mechanisms that encode and transmit spatial information determine to a large extent the kind of processing that can occur. It seems, therefore, crucially important to understand the filtering characteristics of those mechanisms. This means that the bandwidth, center frequencies, and weighting functions of the filters, their degree of linearity, and how they interact must be determined to fully understand how they create the global picture that we see. Thus the general approach here is to use such data to filter objects to determine what kinds of information can be provided by such a system of filters. Our ordinary perception of objects becomes the boundary conditions to which the filtered images are compared. In this way, perhaps a physical foundation for perception can be created.

It became clear at the beginning of this research that one could easily devote full time to one small aspect of perception—illusions, for example. However, the successful modelling of one small aspect of perception does not guarantee that the insights and results of the model can collapse across all other perceptual problems within that single framework. Since there exists no general quantitative theory of perception, it seemed crucial in the early stages to extend the concept of filtering to many perceptual areas as quickly as possible to test the parsimony of the notion. The first-order approximation of results was sought—90% of the solution. Thus the major criteria set for the results of each stage of this work were: are these results internally and externally consistent with one another and with current knowledge in visual science, and are they testable? Once those criteria were achieved for each area of perception, parsimony could be tested rapidly while simultaneously maintaining scientific credibility. Relating the ability of the filtering characteristics of the visual system to predict the detection and identification of complex objects of persons having normal and abnormal vision represents an attempt to tie earlier filtering results into direct measurements of the filtering properties of the mechanisms of the visual system. Time will tell whether this approach continues to prove helpful.

There is no attempt in this dissertation to argue every point and offer alternatives to each possible explanation for each demonstration. There are many questions that still remain unanswered. The reason for this approach is simple. It is almost impossible (and not desirable at our state of ignorance) to travel down each stream while trying to reach a source of a river. Only intuition can be used to guide such travel. Thus the intuition derived from the preceding research directed the next step. Since one person's path is another's maze, this approach will not please all readers. Indeed, it would be disappointing if it did, for it would represent agreement in areas full of differences, hardly representative of a fresh approach to long-standing problems.

This strategy means that the explanation for certain phenomena written here is not suggested to be the only possible explanation. However, the explanations are internally consistent. Since there was no other general model to test these ideas against, no other approach seemed tenable at that time. Science is the best story that is constructed from all the currently known facts. It will be quite surprising if most interpretations here stand for long periods of time in terms of completely explaining how each perceptual phenomenon occurs. This research represents the beginning of a quantitative approach to understanding the important spatial information in objects for various aspects of perception.

Since this work attempts to replace words by numbers, it offers an approach to many applied problems. The transfer of this technology from basic to applied research areas, applicable to certain military and civilian problems in vision, is currently under way. It is hoped that this work will help to create a firm foundation for such applied areas as display design and object detection and identification by man and machine. Since this research uses the same mathematical language to describe the filtering properties of the observer and the spatial information of objects that are being used to describe certain sensor and display parameters, it may provide the basis for unified metrics in those areas. The results of the next series of experiments attempting to transfer this technology will determine the effectiveness of this approach.

No research can be done effectively in a complete vacuum. It wasn't until I received feedback about my early work on filtering and visual perception in 1971 and 1972, after initial lectures at the Neurosciences Research Program in Boston and The Physiological Laboratory in Cambridge, England, and other scientific institutions that I became aware of the work done by others in psychophysics and neurophysiology that supported some of the original filtering results. This dissertation represents the major integration and extension of those early filtering results into contemporary visual science.

Thus, there are many individuals to whom I would like to express my gratitude: Dr. D. Pollen, who first took an interest in my work, and Dr. R. Held, whose comment on the filtering after my first lecture: "It is an idea whose time has come," helped spur me on to the next stages. Similarly, Dr. F. Campbell, also provided early encouragement and acted as my research supervisor at Cambridge. I am also grateful to Dr. J. Robson, Dr. D. Tolhurst, Dr. C. Furchner, Dr. R. Sekuler, Dr. J. Mollon, Dr. J. Foley, and Dr. H. Howland for their interesting discussions at various stages of this work. For the technical assistance *par excellence* of Clive Hood at Cambridge goes a special thank you. I have been fortunate enough to have been invited to lecture on the early results of this work in the United States, Great Britain, Europe, and the U.S.S.R. I have benefited greatly from that exposure and thank the numerous individuals for their interest and criticism.

The assistance provided by Dr. R. Zimmern, Ms. R. Banks, and Ms. J. Lowry of Addenbrooks Hospital, Cambridge, for securing and examining patients used in the clinical studies reported in this dissertation is gratefully acknowledged.

I am also grateful to Dr. O. Saxton, Dr. D. M. Horner, and Mr. T. Pitt of the Electron Microscopy Branch of Applied Physics at the University of Cambridge for sharing their SEMPER system with me.

Dr. M. Cannon, Dr. M. Nelson, Mrs. A. Elshoff, and Mrs. M. Whitaker are thanked for their help with the final editing and proofing. I would also like to thank Ms. F. Hake for the illustrations and Mr. P. Starling and Mr. R. Brooks for photographing the figures. I am also grateful to Ms. J. Jackson who typed the final copy of this dissertation. Thanks also to Mr. S. Fullenkamp and Lt. D. Evans for help with the logistics of putting this report physically together.

# CONTENTS

<b>VOLUME I</b>		<i>Page</i>
<b>INTRODUCTION</b>		10
<b>PART I</b>	<b>A THEORETICAL BACKGROUND TO FOURIER ANALYSIS AND SPATIAL FILTERING</b>	12
<b>CHAPTER 1</b>	<b>LINEAR SYSTEMS ANALYSIS</b>	13
	1.1 Introduction	13
	1.2 Linearity, Nonlinearity, and the Power of Superposition	13
	1.3 Periodic and Nonperiodic Stimuli	13
	1.4 Basis Functions	14
	1.4.1 Orthogonality	14
	1.4.2 Integral Squared Error	15
<b>CHAPTER 2</b>	<b>FOURIER ANALYSIS</b>	16
	2.1 The Trigonometric Fourier Series	16
	2.2 Complex Fourier Series	17
	2.3 The Fourier Transform Pair	17
	2.4 The One-Dimensional Discrete Finite Fourier Transform	17
	2.5 The Two-Dimensional Discrete Finite Fourier Transform	18
	2.5.1 Two-Dimensional Sinusoids	19
<b>CHAPTER 3</b>	<b>DIGITAL IMAGE PROCESSING</b>	21
	3.1 The Image Analysis Facility	21
	3.2 The SEMPER Image Processing System	22
	3.3 A Demonstration: Two-Dimensional Fourier Magnitude Spectra of Squares	23
	3.3.1 The Relationship Between Space and Spatial Frequency	23
<b>CHAPTER 4</b>	<b>SPATIAL FILTERING</b>	24
	4.1 Convolution Versus Fourier Transformation	24
	4.2 Spatial Filtering in the Fourier Transform Domain	24
	4.2.1 One-Dimensional Ideal Band-Pass Filters	24
	4.2.2 Two-Dimensional Band-Pass Spatial Filters	25
	4.2.3 Spatial Filtering of a Complex Scene	25
	4.3 Summary of Fourier Analysis and Spatial Filtering	26
<b>PART II</b>	<b>THE SPATIAL FILTERING CHARACTERISTICS OF MAMMALIAN VISUAL SYSTEMS</b>	27
<b>CHAPTER 5</b>	<b>THE OVERALL SPATIAL FILTERING CHARACTERISTICS OF THE HUMAN VISUAL SYSTEM</b>	28
	5.1 Some Basics: Spatial Frequency, Contrast, and Contrast Sensitivity	28
	5.2 The Contrast Sensitivity Function	28
	5.2.1 Factors Which Affect the Shape of the Contrast Sensitivity Function	29

	<i>Page</i>
5.3 Single- Versus Multi-channel Visual Models .....	30
5.4 The Filtering Characteristics of Suprathreshold Vision .....	30
5.5 Summary .....	31
<b>CHAPTER 6 THE SPATIAL FILTERING PROPERTIES OF CHANNELS DETERMINED FROM PSYCHOPHYSICAL DATA .....</b>	<b>32</b>
6.1 The Measurement of the Spatial Bandwidth of Channels .....	32
6.1.1 Selective Adaptation .....	32
6.1.2 Masking .....	32
6.1.3 Threshold Summation .....	32
6.1.4 Visual Evoked Response .....	33
6.2 The Measurement of the Orientation Selectivity of Channels .....	33
6.2.1 Selective Adaptation .....	33
6.2.2 Masking .....	33
6.2.3 Threshold Summation .....	34
6.2.4 Monocular Rivalry .....	34
6.2.5 Visual Evoked Response .....	34
<b>CHAPTER 7 THE SPATIAL FILTERING PROPERTIES OF CHANNELS DETERMINED FROM NEUROPHYSIOLOGICAL DATA .....</b>	<b>35</b>
7.1 The Receptive Field .....	35
7.2 Feature Detectors .....	35
7.3 Evidence for Spatial Filters in the Mammalian Visual System .....	35
7.4 Differences Between Bandwidths of Channels .....	36
<b>CHAPTER 8 CREATING TWO-DIMENSIONAL SPATIAL FILTERS FROM BIOLOGICAL DATA .....</b>	<b>38</b>
8.1 Two-Dimensional Spatial Filters Based on Contrast Sensitivity Data .....	38
8.2 Two-Dimensional Spatial Filters Based on Biological Channels .....	39
8.2.1 Comparison Between an Ideal Low-Pass Filter and Filters Obtained from Biological Data .....	40
<b>PART III VISUAL INFORMATION PROCESSING IN TERMS OF SPATIAL FILTERING .....</b>	<b>42</b>
<b>CHAPTER 9 SPATIAL FILTERING AND THE GENERALIZATION OF FORM: SIMPLE CONTINUOUS AND DISCRETE OBJECTS .....</b>	<b>43</b>
9.1 Introduction .....	43
9.2 Letter T .....	44
9.3 Letter E .....	45
9.4 Discrete Letter G .....	45
9.4.1 Similar Forms from Four Discriminably Different Letter Gs .....	46
9.5 Dot Letter R in Noise .....	46
9.6 Gestalt Principles of Perceptual Organization .....	46
9.7 Summary .....	46

	<i>Page</i>
<b>CHAPTER 10</b>	
<b>SPATIAL FILTERING AND THE GENERALIZATION OF FORM: COMPLEX OBJECTS (VARIATIONS OF A PORTRAIT)</b> .....	48
10.1 Introduction .....	48
10.2 Filtering the Original Portrait .....	48
10.3 Filtering Coarsely Quantized Portraits .....	49
10.3.1 Why Does Coarse Quantization Reduce Form Perception? .....	50
10.4 Filtering a Portrait with Random Noise Added .....	51
10.4.1 Artifacts from a Portrait with Random Noise Added .....	51
10.5 Filtering a Portrait with Inclusive OR Random Noise .....	52
10.6 Filtering a Binary Line Portrait .....	52
10.7 Perception of Reversed Contrast Portraits .....	53
10.8 Summary .....	53
<b>CHAPTER 11</b>	
<b>VISUAL TEXTURES</b> .....	55
11.1 Introduction .....	55
11.2 Two General Figure-Ground Problems .....	55
11.2.1 Isolating a Rectangular Form from Oblique Lines by Spatial Filtering .....	55
11.2.2 Isolating Oblique Structure in a Real Scene by Spatial Filtering .....	55
11.3 Similarity Grouping of Letter Arrays .....	55
11.3.1 Similarity Grouping Due to Orientation Differences .....	56
11.3.2 Similarity Grouping Due to Configuration Differences .....	56
11.3.3 Second Order Effects of Grouping: Symmetry .....	57
11.4 Isolating Objects from Random Dots .....	58
11.4.1 Isolating Form and Symmetry from a Random Dot Pattern .....	58
11.4.2 Isolating Objects of Different Size in a Random Dot Pattern .....	58
11.5 Analysis of a Complex Scene .....	58
11.6 Monocular Texture Gradients .....	59
11.7 Summary .....	59
<b>CHAPTER 12</b>	
<b>VISUAL ILLUSIONS</b> .....	60
12.1 Introduction .....	60
12.2 Illusions of Noncollinearity .....	60
12.2.1 Variations and a "Correction" of the Poggendorff Illusion .....	60
12.2.2 An Illusion Due to Error in Aligning Edges .....	61
12.3 Illusions of Line Length .....	62
12.3.1 Variations of the Müller-Lyer Illusion .....	62
12.3.2 The Ponzo Illusion .....	62
12.3.3 Variations of the Horizontal-Vertical (H-V) Line Illusion With and Without a Frame .....	62
12.3.4 Simple Line Illusions .....	63
12.4 Illusions of Misjudged Size and Distance .....	63
12.4.1 The Titchener Illusion .....	63
12.4.2 An Illusion of Misjudged Distance .....	63
12.5 Illusion of Nonparallel Lines: the Zöllner Illusion .....	64
12.6 Illusions of Contrast .....	64
12.6.1 The Hermann Grid Illusion .....	64
12.6.2 The Ehrenstein Illusion .....	64
12.6.3 The Benussi Ring Illusion .....	64

12.7 Subjective Contours: the Kanizsa Triangle .....	65
12.7.1 Comparison Between Solid and Outline Kanizsa Triangle .....	65
12.8 Discussion .....	66
12.8.1 Predicting the Perceived Length of the Müller-Lyer Illusion from Filtered Images .....	67
12.8.2 Filtered Images, Eye Scans, and Illusions .....	68
12.8.3 Why are the Details of Illusions Seen as Distorted? .....	69
12.9 Summary .....	69
 <b>CHAPTER 13      MULTISTABLE OBJECTS .....</b>	 70
13.1 Introduction .....	70
13.2 Multistability Due to the Different Sizes of Objects in One Scene .....	70
13.3 The Bisected Circle .....	71
13.3.1 An Experiment: Segregation of Two Areas by a Line .....	71
13.4 The Rubin Face-Vase Object .....	72
13.5 Multistable Dot Patterns .....	72
13.6 Multistable Triangles .....	73
13.7 Summary .....	74
 <b>CHAPTER 14      SPATIAL INFORMATION FROM A BANK OF CHANNELS .....</b>	 76
14.1 Introduction .....	76
14.2 Methods .....	76
14.3 Comparing Band-Pass and Channel Filtering of a Portrait .....	76
14.3.1 General Discussion .....	77
14.3.1.1 Information Contained in a Hierarchy of Filtered Images .....	78
 <b>CHAPTER 15      GENERAL DISCUSSION AND SUMMARY OF THE RESULTS                     OF SPATIAL FILTERING .....</b>	 79
15.1 The Classification of Simple and Complex Objects .....	79
15.2 Visual Textures .....	79
15.3 Visual Illusions .....	79
15.4 Multistable Objects .....	79
15.5 A Hierarchy of Filtered Images .....	79
15.6 Why Don't We See the Basic Forms of Objects? .....	80
15.7 Predicting the Identification of Complex Objects by the Filtering Characteristics of the Human Visual System .....	80
 <b>PART IV          RELATING CONTRAST SENSITIVITY TO THE IDENTIFICATION                     OF COMPLEX OBJECTS .....</b>	 83
 <b>CHAPTER 16      SNELLEN LETTER ACUITY AND SPATIAL FREQUENCY .....</b>	 84
16.1 Introduction .....	84
16.2 The Theoretical Minimum Number of Spatial Frequencies Necessary for Identification of Snellen Letters .....	84
16.3 Spatial Filtering of Snellen Letters .....	84



	<i>Page</i>
<b>CHAPTER 17</b>	
<b>THE MINIMUM CONTRAST REQUIRED FOR THE DETECTION AND IDENTIFICATION OF SNELLEN LETTERS</b> .....	86
17.1 Introduction .....	86
17.2 Methods .....	86
17.3 Results and Discussion .....	86
<b>CHAPTER 18</b>	
<b>THE RELATIONSHIP BETWEEN CONTRAST SENSITIVITY AND SNELLEN LETTER ACUITY IN NORMAL AND ABNORMAL VISION</b> .....	89
18.1 Introduction .....	89
18.2 Predicting Snellen Acuity of Subjects Having Amblyopia, Abnormal Retinal Correspondence, and Multiple Sclerosis .....	89
18.3 Relating Snellen Letter Acuity to the Contrast Sensitivity of an Amblyope with a Notch in Her Contrast Sensitivity Function .....	90
18.4 Predicting Snellen Acuity from Data of Other Amblyopes .....	90
18.5 Summary .....	91
<b>CHAPTER 19</b>	
<b>GENERAL DISCUSSION AND CONCLUSIONS ABOUT HOW THE FILTER CONCEPT RELATES TO THE OVERALL PROBLEMS OF PERCEPTION</b> .....	92
19.1 Introduction .....	92
19.2 The Relationship between Spatial Filtering and Higher Visual Processing .....	92
19.3 Implications for Machine Pattern Recognition .....	92
19.4 Some Problems in Object Recognition That the Spatial Filter Concept Can Help to Solve .....	93
19.4.1 Size Invariance .....	93
19.4.2 Invariance to Retinal Position .....	93
19.4.3 Recognition of Objects When Their Contrast Is Reversed .....	94
19.4.4 Equivalence of Objects That Are Solid or Outline .....	94
19.4.5 Nonequivalence of Recognizing Rotated Shapes .....	94
19.4.6 Similarity and Confusion Between Shapes .....	94
19.4.7 Recognition with Local Variations of Shape .....	95
19.4.8 Segmentation .....	95
19.4.9 Recognition of Complex Scenes .....	95
19.4.10 Perceptual Learning .....	96
19.4.11 Redundancy .....	96
19.4.12 Physiological Evidence .....	97
19.4.13 Summary .....	97
19.5 Why Are the Low Spatial Frequencies More Important than the High Spatial Frequencies? .....	97
19.6 What Is the Bandwidth and Shape of the Channels? .....	98
19.7 What Could Be the Basis for the One- to Two-Octave-Wide Channels? .....	98
19.8 What Is the Minimum Number of Spatial Frequencies Necessary for the Identification of Objects? .....	99
19.9 The Roles That Fourier Analysis Can Play in Spatial Vision .....	99
19.9.1 Fourier Analysis as a Metric .....	99
19.9.2 Fourier Analysis as a Tool for Spatial Filtering .....	99
19.9.3 The Fourier Transform as a Model of Visual Information Processing .....	100
19.9.3.1 From a Local to a Global Harmonic Analysis .....	100
19.10 Future Investigations .....	102

<b>SUMMARY</b> .....	103
<b>REFERENCES</b> .....	104

## **VOLUME II**

### **LIST OF FIGURES**

### **FIGURES**

<b>APPENDIX A</b>	<b>INVESTIGATIONS INTO THE FILTERING CHARACTERISTICS OF ABNORMAL VISION</b> .....	<b>A-1</b>
<b>Chapter A-1</b>	<b>THE FILTERING CHARACTERISTICS OF ABNORMAL VISION</b> .....	<b>A-2</b>
	A-1.1 Why Investigate Abnormal Vision? .....	A-2
	A-1.2 Amblyopia .....	A-2
	A-1.2.1 Early Psychophysical Studies of Amblyopia .....	A-5
	A-1.2.2 Recent Studies of Amblyopia .....	A-6
<b>Chapter A-2</b>	<b>THE GENERATION OF STIMULI AND EXPERIMENTAL PROCEDURES</b> .....	<b>A-9</b>
	A-2.1 The Generation of Spatial Stimuli .....	A-9
	A-2.1 Contrast .....	A-9
	A-2.1.2 The Stimuli .....	A-10
	A-2.1.2.1 Stationary Gratings .....	A-10
	A-2.1.2.2 Moving Gratings .....	A-10
	A-2.1.2.3 Split-Screen Gratings .....	A-11
	A-2.1.3 Determining Contrast .....	A-12
	A-2.2 Measuring Contrast Sensitivity .....	A-13
	A-2.3 Measuring a Contrast Match .....	A-15
	A-2.4 Changing Contrast by Polarizers .....	A-17
<b>Chapter A-3</b>	<b>CONTRAST SENSITIVITY FUNCTIONS OF AMBLYOPES</b> .....	<b>A-20</b>
	A-3.1 Methods .....	A-20
	A-3.2 Sensitivity Loss at All Spatial Frequencies .....	A-20
	A-3.3 Sensitivity Loss at High Spatial Frequencies .....	A-21
	A-3.4 Selective Loss at Mid-spatial Frequencies .....	A-23
	A-3.4.1 Stationary Sine-Wave Gratings .....	A-23
	A-3.4.2 Moving Sine-Wave Gratings .....	A-26
	A-3.4.3 Sine-Wave Versus Square-Wave Gratings .....	A-29
	A-3.5 Changes in Contrast Sensitivity in the Amblyopic Eye .....	A-30
	A-3.6 Summary .....	A-34
<b>Chapter A-4</b>	<b>SUPRATHRESHOLD VISION OF AN AMBLYOPE</b> .....	<b>A-35</b>
	A-4.1 Contrast Matching of a Normal Observer .....	A-36
	A-4.2 Contrast Matching by an Amblyope .....	A-37
	A-4.3 Discussion .....	A-40

Chapter A-5	THE FILTERING CHARACTERISTICS OF PATIENTS HAVING MULTIPLE SCLEROSIS .....	A-44
	A-5.1 Introduction .....	A-44
	A-5.2 Methods and Results .....	A-44
	A-5.3 Discussion .....	A-45
APPENDIX B	TABLE OF CONTRAST SENSITIVITY FROM CAMPBELL, KULIKOWSKI, AND LEVINSON (1966) .....	B-2
APPENDIX C	OBJECTS THAT ARE BLURRED BY OPTICAL DEFOCUS TO ABOUT THE FOURTH HARMONIC .....	C-2

## INTRODUCTION

The everyday objects that we see contain a tremendous amount of information. Our remarkably sensitive eye uses more than 110,000,000 rods and about 6,000,000 cones to sample objects into at least 100 different levels of brightness and about 50 distinguishable colours. It is highly unlikely that the visual system can process all that information. Indeed, any real system must have limits as to the amount of information it can process. As will be shown, it is the nature of the visual system to throw away much of the detailed information about objects. One way to describe the data reduction is in terms of filtering, that is, the selection of a certain range of a particular physical property.

Kenneth Craik (1966) suggested as a general principle that a filter is needed to separate one object from another: "The essential part of physical 'recognizing' instruments is usually a filter — whether it be mechanical sieve, an optical filter, or a tuned electrical circuit — which passes any quantities it is required to identify and rejects all others."

One filter alone cannot provide the information to perform all the tasks required for perception. Several filters are required and they cannot be too broad or too narrow. As Craik noted: "Our ordinary perception hovers uncertainly between overgeneralization, which would lead us to ignore initial differences between objects, and overspecificity, which would lead us never to recognize the identity of objects unless they were in every detail indistinguishable; the first would end us in confusion, the second in inability to draw general conclusions about the world we see." Applying these concepts to object recognition implies at least one filter to capture the general form of an object and another filter to capture the details.

The application of filtering to perception suggests that certain information about objects must be redundant for certain tasks. Here, redundant means information that is extra, not needed for the task. For example, serifs found on letters are redundant for the classification of the letter. However, information about the serif is required if the type of font of the letter is to be determined. The importance of redundancy in visual processing has been stressed by Attneave (1954) and Barlow (1961).

The first parts of this dissertation deal with certain fundamental questions: Can the concept of filtering unify the understanding of visual information processing? How much of visual perception can be accounted for by the information contained in mechanisms that inevitably lose information in the filtering process? To answer these questions, many of the important general phenomena of perception must be considered: object recognition, illusions, textures, and multistable objects. A general theory of visual perception should encompass all of these phenomena within a unified, quantitative structure. Such a theory will be attempted in this dissertation. However, in order to provide realistic interpretations of how the visual system could be processing spatial information, certain constraints must be imposed.

The main constraint on the filtering presented here is that it be based upon the filtering properties of known mechanisms in the visual system. This constraint, however, begs the question: What is known about the filtering properties of the visual system? A review of the neurophysiological and psychophysical literature reveals much information about the spatial filtering characteristics of mechanisms in the visual system. Although a wealth of data is available, it has not been integrated into a general understanding of visual information processing. Thus, the first parts of the dissertation will attempt to answer the question: What could the large amounts of data collected over the last fifteen years about the spatial processing of the visual system explain about the perception of everyday objects?

As the filtering properties of the visual system are examined, it will be shown that the spatial information that is selectively lost by certain mechanisms determines the appearance of objects under certain viewing conditions. The use of filters based on biological data will make it possible to see objects as the various stages of visual processing would "see" them. The information that remains after certain stages of data reduction can be shown to account for a variety of phenomena including the classification of patterns that range from letters to faces, Gestalt laws of perceptual organization, many geometric and contrast illusions, the isolation of form from texture, and multistable objects. Furthermore, a limited range of information will be shown to be sufficient for form generalization. Indeed, it will be shown that only a few ripples from the tidal wave of information that washes over the retina are needed to account for much of how we see objects.

The later chapters in this dissertation relate a conventional measure of visual acuity to a psychophysical measure that provides more detailed and quantitative information about the filtering characteristics of the visual system. Experimental data are used to offer an explanation of why certain filtering characteristics of the visual system will not be detected by conventional measurements of visual acuity. Further, these data provide additional quantitative support for the notion that relatively little spatial information is required to correctly identify complex objects—a major finding of the earlier chapters of this dissertation.

Appendix A contains the details of experiments on abnormal vision that were used to test the ability of certain data to predict a conventional measure of visual acuity. These data were collected in an attempt to provide more insight into visual processing by investigating the filtering characteristics of abnormal vision. In particular, studies of one amblyope showed highly tuned mechanisms in each eye that have not been revealed before and that appear to compensate for the different filtering characteristics of each eye under certain circumstances. Further studies with patients suffering from multiple sclerosis provided filtering characteristics that substantiate complaints of poor vision which appears normal when conventional acuity measurements are used.

In summary, this dissertation presents the argument that the concept of spatial filtering can provide a quantitative and parsimonious means of explaining many phenomena of spatial vision. It will be argued that it is impossible for the visual system to process all the information available about the objects that are seen. The reduction of spatial information that occurs at various stages of processing in the visual system can be examined by filtering objects using spatial filters based on biological data about the shape and size of certain visual mechanisms. The consequences of such filtering provide images that relate to how objects are seen and suggest that a major role of the organization of the visual system is to extract information from a relatively small numbered hierarchy of filtered images.

First, however, some mathematical theory that will be needed to understand the relationship between filtering and visual perception will be presented.

**PART I**

**A THEORETICAL BACKGROUND TO  
FOURIER ANALYSIS AND SPATIAL FILTERING**

*"Man tries to make for himself in the fashion that suits him best a simplified and intelligible picture of the world . . . . The supreme task . . . is to arrive at those universal elementary laws from which the cosmos can be built up by pure deduction. There is no logical path to these laws; only intuition, resting on sympathetic understanding of experience, can reach them . . . ."*

**Albert Einstein**

## CHAPTER 1

### LINEAR SYSTEMS ANALYSIS

#### 1.1 Introduction

The use of Fourier analysis by visual scientists is becoming increasingly widespread. However, it is important to point out how Fourier analysis fits into the general and powerful framework of linear systems analysis. This understanding is necessary in order to appreciate why Fourier analysis is unique in the spatial analysis of complex objects. A brief discussion of systems analysis that leads to the Fourier transform and spatial filtering may aid this understanding. Some aspects of this discussion are amplified in Cooper and McGillem (1967).

The Fourier transform will play three roles: first, as a quantitative description of the spatial information of objects; second, as a means to filter the spatial information of objects; third, as a general model of how the visual system appears to be processing local and global spatial information. It is extremely important for the reader to be aware of how the Fourier transform is being used throughout this dissertation.

A *system* consists of mechanisms that are assembled and interact with one another to perform some function. For example, the eye-brain system is composed of mechanisms assembled to perform the function of detecting and classifying objects. The tools that have been developed to analyze systems constitute systems analysis. The major problem of system analysis is to define the response of a system when the system and the input are known. The solutions to this problem provide predictive power about the behaviour of the system under certain conditions. One part of this problem is the determination of a mathematical description, or model, for the system which allows the predictions to be quantitative.

#### 1.2 Linearity, Nonlinearity, and the Power of Superposition

Two of the terms used to classify systems are *linear* and *non-linear*. A linear system obeys the law of *superposition*. If

$$R_1(x) = \text{system response to stimulus } S_1(x)$$

$$R_2(x) = \text{system response to stimulus } S_2(x)$$

and

$$AR_1(x) + BR_2(x) = \text{system response to } AS_1(x) + BS_2(x)$$

for all  $A$ ,  $B$ ,  $S_1(x)$  and  $S_2(x)$ , then the system is linear. If this is not true, then the system is nonlinear. The power of the law of superposition comes from allowing calculations of the response of a system to complex stimuli simply by taking the sum of the responses of a system to individual simple stimuli.

All real systems have some degree of nonlinearity. However, the nonlinearities can be ignored if they are small in comparison to the overall operating characteristics of the system. If the nonlinearity cannot be ignored, then a piecewise analysis is used in which each section of the response is approximated by a linear function.

In probing an unknown system, linear analysis is very powerful. The deviation from linearity can be used to determine the amount of nonlinearity in the system.

#### 1.3 Periodic and Nonperiodic Stimuli

The input to a system is the stimulus. For the visual system, the stimulus is a pattern of light intensity that varies over space (excluding temporal aspects for the moment). Pattern and object will be used somewhat interchangeably as loose descriptions of the stimuli in this dissertation. In general, pattern will refer to a simple stimulus, whereas object will refer to a more complex stimulus. In order to carry out a systems analysis, a mathematical representation of the pattern is used.

Patterns may be classified as *periodic* or *nonperiodic*. A periodic pattern is one that repeats the sequence of values over a fixed distance, called the period. More precisely, a pattern,  $p(x)$ , is periodic if there is a number  $\bar{x}$  such that

$p(x) = p(x + \bar{X})$  for all  $x$ ; all other patterns are nonperiodic. The smallest positive number that satisfies the previous relationship is the period,  $\bar{X}$ , which also defines the duration of one complete cycle of the pattern. Integral submultiples of  $\bar{X}$  are called *harmonics*. The fundamental frequency,  $f_1$ , of a periodic pattern is inversely related to the distance  $\bar{X}$  where  $f_1 = 1/\bar{X}$ .

Sinusoids are an example of periodic patterns. As shall be shown, however, even nonperiodic patterns can be represented in terms of periodic functions. From the standpoint of the mathematical representation of patterns, the periodic class is of considerable theoretical importance.

#### 1.4 Basis Functions

Most patterns observed are not periodic. Therefore, a set of periodic functions is needed with which to represent both periodic and nonperiodic patterns. To create a quantitative description of a pattern, it is necessary to represent it in terms of explicit space functions whose numerical values are exactly defined. These considerations raise an important question: What criteria should govern the selection of the space function? There are many different ways in which this representation might be realized with the same objective. The choice of any particular method is usually dictated by mathematical convenience.

Mathematical convenience usually suggests that a pattern  $p(x)$  be represented as a linear combination of a set of elementary space functions  $\lambda_n(x)$ . These elementary functions, called *basis functions*, are selected to have certain convenient properties.

A set of basis functions is given by  $\lambda_0(x)$ ,  $\lambda_1(x)$ ,  $\lambda_2(x)$ , . . . ,  $\lambda_n(x)$ , where  $n$  can range to infinity ( $\infty$ ). A linear combination of basis functions can be written as

$$B(x) = \sum_{n=0}^N a_n \lambda_n(x) \quad (1)$$

where  $a_n$  is the corresponding coefficient of the basis function  $\lambda_n(x)$ . There is no general solution to the selection of the best set of basis functions  $\lambda_n(x)$  for any given application. However, there are many known results available for functions that have certain properties which can guide the particular selection in any given application.

##### 1.4.1 Orthogonality

One important property for a set of basis functions is called *finality of coefficients*. This property allows the determination of any given coefficient without the need to know any other coefficient; that is, the value of each coefficient  $a_n$  is independent of the value of any other coefficient. For example, more terms can be added to the representation to allow greater accuracy without making any changes in the earlier coefficients. Finality of coefficients is achieved when the basis functions are said to be *orthogonal* over the space for which the pattern is defined.

The condition of orthogonality for real basis functions requires that

$$\int_{x_1}^{x_2} \lambda_n(x) \lambda_k dx = 0 \text{ for } k \neq n \\ = \eta_k \text{ for } k = n \quad (2)$$

for all  $k$  and  $n$  over the space  $x_1$  to  $x_2$ . If  $\eta_k = 1$  for all  $k$ , then the basis functions are orthogonal. In words, Equation 2 simply requires that the basis functions have no components in common.

When the basis functions are orthogonal and real, then the coefficient  $a_n$  can be found by

$$a_n = \frac{1}{\lambda_n} \int_{x_1}^{x_2} \lambda_n(x) B(x) dx \quad (3)$$



#### 1.4.2 Integral Squared Error

There is another property of orthogonal functions which is quite important. In many situations, the accuracy of the representation of a pattern when only some and not all the terms are used must be determined. Any real pattern stored, for example, in a digital computer (or the visual system), can be represented only by a finite number of terms. A practical problem which arises is how to select a set of basis functions that minimizes the error of representation of the pattern for a limited number of terms. One measure used is called the *integral squared error* (I), the integral of the square of the differences between the pattern,  $p(x)$ , and its approximation,  $\hat{p}(x)$ , given by

$$I = \int_{x_1}^{x_2} [p(x) - \hat{p}(x)]^2 dx \quad (4)$$

The integral squared error is zero only when  $p(x) = \hat{p}(x)$ . If not, then I is always positive, and the smaller it is, the better the approximation. It can be shown that orthogonal basis functions not only have the property of finality of coefficients but also minimize the integral squared error of the representation, e.g., Cooper and McGillem (1967).

Other criteria could be used to select basis functions; however, they take us beyond the scope of this discussion.

So far, only a general discussion of basis functions has been provided and no suggestions about the most desirable types of functions to use have been offered. The requirement of orthogonality does little to restrict this selection since many different functions can be made orthogonal by suitable definitions. Therefore, the selection of basis functions depends primarily upon how the functional representation is to be used. In systems analysis, sinusoids are very useful functions because they remain sinusoids after the performance of various mathematical operations needed in such an analysis. Addition and subtraction of two sinusoids of the same frequency results in a sinusoid. The derivative and the integral of sinusoids are sinusoids. These properties, combined with superposition, suggest that representing a pattern as a sum of sinusoids can be quite convenient as well as powerful.

## CHAPTER 2

### FOURIER ANALYSIS

#### 2.1 The Trigonometric Fourier Series

The power of using sinusoids to represent complex functions was first shown by the French physicist Fourier (1768-1830) who used them to solve problems in heat transmission. Out of his work has come Fourier's theorem:

$$f(x) = C_0 + C_1 \cos\left(\frac{2\pi}{\bar{X}} x + \phi_1\right) + C_2 \cos\left(\frac{2\pi}{\bar{X}/2} x + \phi_2\right) + \dots + C_n \cos\left(\frac{2\pi}{\bar{X}/n} x + \phi_n\right) \quad (5)$$

where  $C_0, \dots, C_n$ , are constants. Fourier's theorem states that a periodic function  $f(x)$ , with a spatial period  $\bar{X}$ , can be synthesized by a sum of harmonic functions that are integral submultiples of  $\bar{X}$  and have a phase angle given by  $\phi$ . The accuracy of this representation of a function is increased by increasing the number of terms. In order to maintain the proper phase relationship between the harmonics and yet remove the cumbersome phase term in each harmonic, a trigonometric identity is used:

$$C_n \cos(nkx + \phi_n) = A_n \cos nkx + B_n \sin nkx \quad (6)$$

where  $k = 2\pi/\bar{X}$ ,  $A_n = C_n \cos \phi_n$ , and  $B_n = -C_n \sin \phi_n$ . Equation 5 in more compact form is given by

$$f(x) = A_0 + \sum_{n=1}^{\infty} A_n \cos nkx + \sum_{n=1}^{\infty} B_n \sin nkx \quad (7)$$

Equation 7 is called the *trigonometric Fourier series*.

The process of determining the values of the coefficients  $A_0$ ,  $A_n$ , and  $B_n$  is called *Fourier analysis*. They are determined from

$$A_0 = \frac{1}{\bar{X}} \int_0^{\bar{X}} f(x) dx$$

$$A_n = \frac{1}{\bar{X}} \int_0^{\bar{X}} f(x) \cos nkx dx \quad (8)$$

and

$$B_n = \frac{1}{\bar{X}} \int_0^{\bar{X}} f(x) \sin nkx dx$$

where  $A_0$  is the average value of  $f(x)$ , the zero frequency component. The *magnitude*,  $M_n$ , of the coefficients  $A_n$  and  $B_n$ , is given by

$$M_n = \sqrt{A_n^2 + B_n^2} \quad (9)$$

and their *phase angle*,  $\phi_n$ , the relative position or phase shift between the coefficients  $A_n$  and  $B_n$ , is given by

$$\phi_n = \tan^{-1} \frac{B_n}{A_n} \quad (10)$$

$M_n$  and  $\phi_n$  provide a description of  $f(x)$  in the frequency domain of the function  $f(x)$ , called a magnitude and phase *spectrum*, in contrast to  $f(x)$  which is a description in the space domain. Magnitude and phase will be discussed further in the following sections.

## 2.2 Complex Fourier Series

Integration can be computed with ease if the real sinusoids are expressed in terms of complex exponentials,  $\exp-Jknx$ , where  $J = \sqrt{-1}$ . The coefficients of the exponential Fourier series are found from

$$\alpha_n = \frac{1}{\bar{X}} \int_0^{\bar{X}} f(x) \exp-Jknx \, dx \quad (11)$$

and since  $\alpha_{-n} = \alpha_n^*$  (where  $*$  denotes the complex conjugate)

$$f(x) = \sum_{n=-\infty}^{\infty} \alpha_n \exp Jknx \quad (12)$$

## 2.3 The Fourier Transform Pair

As the period  $\bar{X}$  is increased, more and more of the function  $f(x)$  will be included in the expression. As  $\bar{X} \rightarrow \infty$ , the spacing between the harmonics becomes differential,  $x \rightarrow dx$ , and the number of components becomes infinite,  $n \rightarrow \infty$ . The summation formally passes into an integral and leads to the *Fourier transform* of  $f(x)$  given by

$$F(Jk) = \int_{-\infty}^{\infty} f(x) \exp-Jkx \, dx \quad (13)$$

$f(x)$  can be recovered from

$$f(x) = \frac{1}{2\pi} \int_{-\infty}^{\infty} F(Jk) \exp Jkx \, dk \quad (14)$$

which is called the *inverse Fourier transform* of  $F(x)$ . The functions  $f(x)$  and  $F(jk)$  are called a *Fourier transform pair*. The general practice is followed using lower case letters for space functions and capital letters for the transform.

## 2.4 The One-Dimensional Discrete Finite Fourier Transform

The previous Fourier transform pair describes a continuous function  $f(x)$  that lends itself to optical Fourier transforms (e.g., O'Neill, 1963; Lipson and Lipson, 1969; Hecht and Zajac, 1974). However, because digital filtering techniques will be used in the Fourier transform domain, the finite, discrete Fourier transform is used here. Brigham (1974) provides a lucid theoretical development (as well as amplification of what follows) of the continuous to the discrete Fourier transform. The modifications of going from a continuous to a discrete representation are concerned with space domain sampling, truncation effects from the limited number of components, and frequency domain sampling.

Briefly, the continuous function  $f(x)$  is sampled at discrete points by delta functions,  $\delta(x - k\bar{X})$ , over the sampling interval  $\bar{X}$ . The sampled function  $f_s(x)$  is given by

$$f_s(x) = \sum_{k=-\infty}^{\infty} f(k\bar{X}) \delta(x - k\bar{X}) \quad (15)$$

If equal interval sampling occurs at equal to or greater than two samples for the highest frequency component present in  $f_s(x)$  (called the Nyquist frequency), then the sampled function  $f_s(x)$  will be a good representation of  $f(x)$ . However, if a more coarse sampling rate occurs, the result is *aliasing*: distortion introduced into the sampled function due to spectrum overlap.

Neither the visual system nor a digital computer can deal with an infinite number of samples. Therefore, the sampled function  $f_s(x)$  is truncated by some function. A rectangular function is given by

$$\begin{aligned} t(x) &= 1 & 0 \leq x \leq \bar{X} \\ &= 0 & \text{elsewhere} \end{aligned} \quad (16)$$

where  $\bar{X}$  is the length of the truncation function. The sampled truncated function now becomes

$$f_{st}(x) = \sum_{k=0}^{N-1} f(k\bar{X}) \delta(x - k\bar{X}) \quad (17)$$

Improper truncation, e.g., truncating  $f(x)$  at each end of the sample points, results in additional frequency components in the frequency domain, called *leakage*, because each  $N$ th point of one period adds to the first point of the next period.

Such considerations lead to the *finite discrete Fourier transform pair*.

$$F\left(\frac{n}{N\bar{X}}\right) = \sum_{k=0}^{N-1} f(k\bar{X}) \exp^{-j2\pi nk/N} \quad (18a)$$

where  $n = 0, 1, 2, \dots, N-1$

$$f(k\bar{X}) = \frac{1}{N} \sum_{n=0}^{N-1} F\left(\frac{n}{N\bar{X}}\right) \exp j2\pi nk/N \quad (18b)$$

where  $k = 0, 1, 2, \dots, N-1$ . The discrete Fourier transform is a special case of the continuous Fourier transform. If the samples of the original function  $f(x)$  are one period of a periodic function, then the Fourier transform of this periodic function is given by Equation 18a.

It must be stressed that the discrete Fourier transform is a complete transform in its own right. Only under special conditions will there be equivalence between the discrete and continuous Fourier transforms. Differences between the two transforms are due to the sampling and truncation requirements of the discrete Fourier transform.

The discrete and continuous Fourier transforms will be exact (within a scaling constant) if:

- (1)  $f(x)$  is periodic
- (2)  $f(x)$  is band-limited
- (3) the sampling rate is at least two times the highest frequency component of  $f(x)$  and
- (4) the truncation function is non-zero over exactly one period (or an integer multiple period) of  $f(x)$ .

Recall that improper sampling results in aliasing. Improper truncation results in *leakage*. There are techniques for reducing the effects of aliasing and leakage when nonperiodic functions are Fourier transformed. However, these techniques are beyond the scope of the present discussion and can be found in Brigham (1974).

## 2.5 The Two-Dimensional Discrete Finite Fourier Transform

So far, only one-dimensional transforms have been discussed. The everyday patterns that are seen are two-dimensional intensity distributions on the retina (excluding depth and time) and require a *two-dimensional finite, discrete Fourier transform* for analysis:

$$P\left(\frac{u}{U\bar{X}}, \frac{v}{V\bar{Y}}\right) = \sum_{x=1}^{\bar{X}} \sum_{y=1}^{\bar{Y}} p(x, y) \exp \left[ -j2\pi \left( \frac{xu}{\bar{X}} + \frac{yv}{\bar{Y}} \right) \right] \quad (19a)$$

$$p(x, y) = \frac{1}{\bar{X}\bar{Y}} \sum_{u=-U}^U \sum_{v=-V}^V P\left(\frac{u}{U\bar{X}}, \frac{v}{V\bar{Y}}\right) \exp \left[ -j2\pi \left( \frac{xu}{\bar{X}} + \frac{yv}{\bar{Y}} \right) \right] \quad (19b)$$

where  $x = 2u + 1$ ,  $y = 2v + 1$  and  $2\pi \frac{xu}{\bar{X}}$ ,  $2\pi \frac{yv}{\bar{Y}}$  are the spatial frequencies (cycles per unit length  $x, y$ ) in the Fourier transform plane ( $u, v$ ). Bracewell (1956) and Brigham (1974) provide good discussions of the properties of the one- and two-dimensional transforms.

Insight into the two-dimensional Fourier transform can be gained by using Euler's identity to separate the complex exponential term into complex trigonometric functions. Equation 19a then becomes

$$P\left(\frac{u}{U\bar{X}}, \frac{v}{V\bar{Y}}\right) = \sum_{x=1}^{\bar{X}} \sum_{y=1}^{\bar{Y}} p(x, y) \cos 2\pi \left[ \left( \frac{xu}{\bar{X}} + \frac{yv}{\bar{Y}} \right) \right] - j \sin 2\pi \left[ \left( \frac{xu}{\bar{X}} + \frac{yv}{\bar{Y}} \right) \right] \quad (20)$$

The arguments of the cosine and sine terms determine the spatial frequency and the orientation of the two-dimensional sinusoids. The spatial frequency,  $f$ , and orientation of the sinusoids,  $\theta$ , is given by

$$f = \left( \sqrt{u^2 + v^2} \right)^{-1} \quad (21)$$

$$\theta = \tan^{-1} \frac{u}{v}$$

The cosine term is the even symmetric, real (Re) part of the Fourier transform; the sine term is the odd symmetric, imaginary (Im) part of the Fourier transform. As with the trigonometric series, the magnitude  $M$  and phase  $\phi$  of the Fourier transform are given by

$$M_n = \sqrt{\text{Re}_n^2 + \text{Im}_n^2}$$

and

$$\phi_n = \tan^{-1} \frac{\text{Im}_n}{\text{Re}_n} \quad (22)$$

### 2.5.1 Two-Dimensional Sinusoids

The two-dimensional Fourier transform can be interpreted as a filter process by which patterns are filtered by a bank of two-dimensional sinusoids of different spatial frequency and orientation. The degree to which the spatial frequency component is present in the spatial structure of a pattern that is "captured" by a particular sinusoid is given by the magnitude. The phase is needed to determine where the magnitude belongs with respect to the spatial position of the pattern.

These two-dimensional sinusoidal (cosine and sine function) filters are shown in Figure 1. Three vertical, integrally related spatial frequencies—harmonics—are shown. Horizontal and oblique harmonics are also needed to define the three-harmonic set of filters for the two-dimensional Fourier transform. They would be identical to those shown but at a different orientation. A three-dimensional view of these sinusoids is shown in Figure 2.

The previous analysis has shown that any pattern can be decomposed into sinusoids. Any system that processes patterns can be described completely by specifying the properties of sinusoids, spatial frequency and orientation or magnitude and phase, as they are processed by the system. The reduction in magnitude of the sinusoids by an *isotropic* (no change in magnitude with orientation) system can be measured in terms of *contrast* (the difference in luminance

between the light and dark bars referenced to the mean luminance). The relationship which specifies the ratio of input to output contrast is the *modulation transfer function* [MTF]. The MTF, then, specifies the ability of any system to process spatial contrast information about patterns.

Now that the theory of the discrete Fourier transform has been outlined, the next section will provide a discussion of the digital techniques that are used to compute the discrete Fourier transform of objects.

## CHAPTER 3

### DIGITAL IMAGE PROCESSING

The previous chapter provided some theory about the two-dimensional discrete Fourier transform. This chapter presents a discussion of the digital computer techniques that are used to implement the theory. Digital techniques are used to compute the two-dimensional Fourier transform of simple objects—squares. Finally, the relationship between size and bandwidth will be demonstrated using digitally computed Fourier transforms.

Two special purpose digital image processing systems and two general purpose digital computer systems were used to perform digital filtering to create the filtered images that are shown in this dissertation. General information on digital image processing may be found in Andrews (1970).

#### 3.1 The Image Analysis Facility

Most of the digital filtering was done using the Image Analysis Facility (Ginsburg, Cook, Mott-Smith, 1972) at the Air Force Cambridge Research Laboratories in the United States. The Image Analysis Facility (IAF) used a vidicon camera to scan complex grey-level pictures, transforming intensity levels into video signals. The video was then filtered, sampled, and channeled to an analogue-to-digital (A/D) converter by a 32-channel multiplexer. The A/D converter digitized the sampled video, creating data acceptable to the digital computer, a PDP-1. A digital computer programme stored one sampled vertical line of the picture video into computer memory line by line. Each line was stored successively on a digital magnetic drum. After drum storage, the unprocessed picture was transferred and stored on magnetic tape for future processing or returned to the computer for immediate processing. The picture was displayed on a cathode ray tube (CRT) for observation or photographing before and/or after processing.

Although the IAF was very efficient for most picture processing, it was too slow to be considered for use as an interactive processor for the two-dimensional Fourier transform. Therefore, a much faster digital computer, a CDC 6600, was used to transform and filter the pictures. Computer programmes were written to link the data, which were transferred by magnetic tape from one computer system to the other. The pictures, filtered using the CDC 6600 general purpose computer, were returned to the IAF for photographing. This method proved most efficient for routine filtering. Furthermore, high speed printers and plotters, coupled to the CDC 6600 system, quickly produced numerical printouts and plots of the pictures, Fourier spectra, and filtered images, as desired. The numerical printouts contain 10 or 64 amplitude levels of the filtered images. The contour plots contain 10 or 16 amplitude levels that have been equally spaced between the maximum and minimum values of the filtered images.

Another advantage of the CDC system was that simple patterns, such as two-tone alphanumerics, could be coded onto punch cards and read directly into the CDC computer for processing, thereby saving scanning time.

The two-tone patterns were cardpunched for 32 by 32 *pel* (picture element) grids. The Fourier spectra were obtained from a Fast Fourier Transform programme, e.g., see Brigham (1974), available on the CDC 6600 computer. Spatial filtering was accomplished in the transform domain as previously discussed. The filtered spectra were inverse Fourier transformed to create the filtered images. Interpolation programmes on the IAF were used to enlarge the patterns to 256 by 256 pels. Except for the original patterns, the transforms and filtered images were extrapolated using sinc

$x = \frac{\sin \pi x}{\pi x}$  as a general smoothing function to avoid coarse quantization artifacts when they were viewed. Compare, for example, the smoothed and original filtered images in Figure 62,c,d. The differences between the original and extrapolated data are negligible when viewed at the appropriate viewing distances discussed later.

The grey-level (multi-tone) patterns were digitized by the video scanner of the IAF for 128 by 128 pel grids. Filtering was done as before on the CDC 6600 computer. The 128 by 128 pel patterns were enlarged to 420 by 448 pels using extrapolation programmes on the IAF. However, no smoothing function was necessary for these larger patterns.

In general, it is necessary to band-limit objects that are digitally processed to avoid the effect of aliasing (Section 2.4).

An object is typically sampled 5 to 10 times more than the Nyquist sample and then filtered to the Nyquist frequency. This technique insures that spatial frequencies up to and including the Nyquist frequency have been sampled adequately and that the object is adequately band-limited. This technique was not needed in the studies made in this dissertation. The simple binary objects processed in this dissertation were not created by a digital sampling system, but were defined analytically on digital grids. Thus, those objects are band-limited to begin with. Further, since the Fourier transform produces spatial frequencies only up to and including the Nyquist frequency, there will be no aliasing. However, the grey-level pictures in this dissertation were sampled by a digital scanning device. Therefore, it is possible that the finest details of the pictures were not adequately sampled. However, any artifacts from this sampling should be evident from viewing the sampled picture. Since there were not any artifacts seen between the original and sampled pictures, it was assumed that there were no serious aliasing problems. Further, since those objects were also spatial filtered in the Fourier transform domain, only spatial frequencies through the Nyquist frequency were used and no further aliasing effects occurred. Finally, aliasing maximally affects the higher spatial frequencies. Since almost all the objects are low pass filtered to some degree, any possible results of aliasing are greatly attenuated.

The original objects, Fourier spectra, and filtered images were photographed from the CRT of the IAF using Polaroid 55 P/N film to create the 64 grey-level pictures shown in this dissertation.

### 3.2 The SEMPER Image Processing System

Some of the digital filtering was done with an image processing system called SEMPER, developed for the analysis of electron microscopy imagery in the Electron Microscopy Branch of Applied Physics at the University of Cambridge.

The input scanning device for SEMPER (a commercial system called SCANDIG built by Technical Operations, Inc.; Joyce Loebel Ltd. in the U.K.) is a high-speed rotating microdensitometer which converts pictorial information into digital form. It measures and records optical densities in two dimensions through any flexible photographic transparency at the rate of 20,000 readings per second.

Light from a 50-watt halogen lamp passed through an iris, was deflected by a mirror, and focused onto the sample mounted on the drum. The transmitted light was collected by an objective lens and passed through a variable aperture onto the face of a photomultiplier tube. The photomultiplier tube converted the collected light into an electrical signal proportional to the amount of light transmitted. A log amplifier converted the electrical signal into units of density which were input into an A/D converter. The A/D converted changed the signal into 8-bit binary data which were then stored on magnetic tape.

The data on magnetic tape were then processed using the SEMPER system. The heart of the SEMPER system is a PDP-8/E digital computer with moving-head disk storage. The picture data were processed using the SEMPER executive language commands under teletype control. Operations performed on the pictures were monitored on a display oscilloscope.

The digital data of the processed pictures were used to create photographs containing 256 grey levels. The Photowrite system (P-1500, Optronics International, Inc.; Joyce Loebel, Ltd., in the U.K.) is a high-speed digital film-writing system which consists of an unexposed film clamped to the outside of a circular rotating drum. The light from a light-emitting diode modulated by the digital data was passed through an aperture and focused onto the film. The drum, film, and optical path were enclosed in a light tight enclosure which is removed to develop the film.

Kodak high-speed Infrared film (4143 Thick; 10.2 by 12.7 cm) was used to create negatives. The exposed film was developed in Ilford PW Universal developer (1:4, 78°F) for 2.5 minutes, given a normal bath in water, then "fixed" for 2.5 minutes using Super Amfix (1:3). Prints were made from the developed film using Ilfospeed Grade O 0.1 M paper exposed at F5.6 for 1 to 1.5 seconds. The linearity of the developing and printing processes was determined from step wedges placed along the sides of the pictures.

Although simple band-pass spatial filtering could be done using the SEMPER system, practical considerations, such as available storage space and time required for computation, made it necessary to use the central computer system, an



IBM 370, for much of the picture processing. Therefore, as with previous picture processing, the spatial filter design and much of the spatial filtering were accomplished on a large computer system and the SEMPER system was used as an input/output device to digitize and create pictures of the filtered objects.

### 3.3 A Demonstration: Two-Dimensional Fourier Magnitude Spectra of Squares

The two-dimensional Fourier transforms of two different size squares were computed, using the previously described techniques, to create the magnitude spectra shown in Figure 3.

Both the magnitude and phase components of the transform are required to describe a pattern uniquely. The magnitude components are the amplitudes associated with each spatial frequency and orientation in the frequency domain. The phase components represent the position and orientation of the associated spatial frequencies in the original pattern space. Since the phase of the transform has not been modified for the results presented in this dissertation, the phase is not shown.

The two spatial coordinates,  $x$  and  $y$ , of the original squares correspond to two spatial frequency coordinates in the transform domain,  $u$  and  $v$ . These spectra have been arranged like the diffraction patterns that would be observed in a device performing an optical Fourier transform, e.g., Lipson and Lipson (1969). The spectra are bilaterally symmetrical across any axis that goes through the centre of the transform. The central spectral component at the origin ( $f_u = 0$ ,  $f_v = 0$ ) is the zero frequency or average intensity value of the pattern. The spatial frequencies go from low to high, radially outward from the centre of the spectrum. The central high-intensity region is the central maximum which contains about 90 percent of the pattern energy.

#### 3.3.1 The Relationship Between Space and Spatial Frequency

An important point about a linear transform, such as the Fourier transform, is that no information is gained or lost in transformation. However, the spatial information about an object is rearranged, as shown by the magnitude spectra of Figure 3. In more complex patterns, the large parts of the pattern will be found in the low spatial frequencies and the small parts will be found in the high spatial frequencies. This rearrangement of spatial information in the frequency domain makes the filtering of spatial information such as size and orientation of complex patterns quite simple, as will be shown in the next chapter.

## CHAPTER 4

### SPATIAL FILTERING

In this chapter the Fourier transform is put to work to spatially filter patterns. First, the difference between using the Fourier transform rather than convolution techniques to filter patterns is discussed. Demonstration of spatial filtering of a complex scene will follow.

#### 4.1 Convolution Versus Fourier Transformation

There are two general techniques by which spatial filtering can be accomplished. A pattern can be spatially filtered by *convolution*, that is, multiplying the pattern point by point with a filter function that is translated over the entire pattern and adding the results, e.g., Bracewell (1965). An alternative method is to, first, *transform (change)* the pattern from the space domain into a spatial frequency domain, e.g., Fourier transformation, then directly attenuate (that is, reduce in amplitude) or extract certain unattenuated spatial frequency information and, finally, perform an inverse transform to reconstruct the pattern from that attenuated or extracted information. These techniques can produce identical results. Indeed, there is a theorem that states that the Fourier transform of the convolution of two functions is equal to the product of the Fourier transforms of the functions taken separately, e.g., Bracewell (1965).

Although convolution can be used to spatially filter a pattern, it does not provide explicit spatial frequency and phase information about the pattern. Unlike transform methods of spatial filtering, convolution is an implicit filtering operation. In other words, only limited insight into the filtering of patterns is gained using convolution.

Considerable insight can be gained, however, by noting how the Fourier transform filters spatial information. Putting Equation 20 into words: The two-dimensional Fourier transform yields spatial frequency/orientation information by multiplying the pattern point by point with two-dimensional arrays of sinusoids (e.g., Figure 2) of different spatial frequency and orientation, and then summing over all the points for each sinusoidal array. Thus, although the computations are different, results of a Fourier transformation can be viewed as similar to convolution; and, because sinusoids are symmetric patterns, it can also be looked upon as a cross-correlation of the input pattern with two-dimensional sinusoidal arrays over a range of spatial frequencies and orientations. Fourier transformation differs from convolution in two ways: It does not require that one of the patterns be reversed, and it does not translate or move one pattern across the other. The Fourier transform does its filtering with functions that remain fixed in position. This important difference between transform and convolution techniques should be kept in mind when either technique is suggested as a model of visual processing, as will be discussed in Section 19.9.3.

#### 4.2 Spatial Filtering in the Fourier Transform Domain

##### 4.2.1 One-Dimensional Ideal Band-Pass Filters

Spatial filtering in the Fourier transform domain is done by multiplying the spectral components of the pattern by some filter function. Mathematically, a simple one-dimensional band-pass filter is given by

$$H_{bp}(u) = 1 \text{ for some } -u \leq U \leq u \quad (23)$$

$$= 0 \text{ elsewhere}$$

An ideal low-pass filter simply multiplies some central portion of the magnitude spectrum by one and the rest of the transform by zero. The inverse process results in high-pass filtering. An ideal band-pass filter is made by multiplying some finite region away from the centre of the magnitude by one and the rest of the transform by zero.

Examples of one-dimensional ideal low-, high-, and band-pass filters are shown in Figure 4.a,1,2,3. The equivalent *line-spread functions* (the Fourier transform of the filters above) that would produce similar filtering by convolution are shown in Figure 4.b,1,2,3. The *general* effect of each filter on a square wave (the *square-wave response*) is shown in Figure 4.c,1,2,3. The specific shapes of the filtered squares will depend on the specific bandwidths and shapes of the filters.

The filtered spectrum can be synthesized back into the space domain by an inverse Fourier transform,  $P^{-1}$ , which results in a filtered object called an *image*. This method enables the observer to determine what spatial information about the original object was contained in certain parts of the spectrum. The filtered image,  $P_f(x)$ , is given by

$$P_f(x) = P^{-1}(u) \{ [P(u)H_{bp}(u)] \} \quad (24)$$

#### 4.2.2 Two-Dimensional Band-Pass Spatial Filters

The properties of the one-dimensional filters discussed in the previous section can be extended to two-dimensions, as shown in Figure 5,a,b,c. Other general shapes and configurations of two-dimensional filters are shown in Figure 5,d,e,f. The shaded areas shown in these figures are the regions of spatial frequencies that are passed by the filter. These spatial filters will be used to select various bands of spatial frequency and orientation of many different patterns in subsequent sections.

A three-dimensional view of two-dimensional ideal low-pass circular and square filters and their respective *point-spread functions* is shown in Figure 6,a,1,b,1,a,2,b,2. The relationship between these filters and single channels in the visual system is discussed in Section 8.2.1.

#### 4.2.3 Spatial Filtering of a Complex Scene

This section demonstrates spatial filtering in the two-dimensional discrete Fourier domain using a complex visual scene—part of the Bridge of Sighs at St. John's College, Cambridge. This scene was chosen because of its rich periodic structure in both the horizontal and vertical orientations.

The digitized scene and its magnitude spectrum are shown in Figure 7,a,1,2. Figure 7,a,3 shows the magnitude spectrum that was sectioned, normalized, and recombined to show the high frequencies. The repetitive structure along the vertical and horizontal orientations in the magnitude spectra generally reflects the periodicity in the scene.

First, the high spatial frequencies were removed (Figure 7,b). (The diagonal lines shown in the pictures of the spectra in Figure 7,d-h represent the region of spatial frequencies that are passed by the spatial filter.) Only the general form of the bridge remains when the scene contains only 12 and 18 low spatial frequencies, Figure 7,b,c.

Figure 7,d,e shows the result of passing only the high spatial frequencies—those greater than 12 and 18. Removing the low spatial frequencies greatly reduces the contrast over broad spatial regions. The details of the scene now predominate.

The previous filtering was isotropic; the same bandwidth was used at all orientations. Next, a predominant range of horizontal components was passed (Figure 7,f). Since the horizontal spatial frequencies result from vertical objects in the scene, it is not surprising to see generally vertical objects that reflect the overall vertical periodicity in the original scene. Note the vertical bars in the portals of the bridge. Filtering most of the vertical components produced broad horizontal objects, as shown in Figure 7,g. Filtering the left oblique parts of the spectrum produces generally right oblique parts of the scene (Figure 7,h).

The periodicity of the windows can be detected on the horizontal axis of the spectrum shown by the circle in Figure 7,i. This small amount of information was filtered out to create Figure 7,i, where the repeated light and dark bars are plainly seen. This repeated structure appears sinusoidal because only relatively few components of the spectrum have been passed. Since each point in the spectrum represents the filtering of the original pattern with one sinusoid, it is reasonable to expect that filtering out that component results in the sinusoidal appearance.

Such demonstrations show the power of spatial filtering in two dimensions. Form and detail of different size and orientation can be extracted in a global manner quite easily from even the most complex scene.

### **4.3 Summary of Fourier Analysis and Spatial Filtering**

The previous chapters have shown sinusoids to be powerful tools in both the theoretical and practical aspects of describing patterns. Their use in Fourier analysis resulted in two-dimensional spectra that were used as a means of spatially filtering a complex scene. The next chapter provides the experimental data that are needed to make spatial filters to probe the filtering characteristics of the visual system using the preceding methods.

**PART II**  
**THE SPATIAL FILTERING CHARACTERISTICS**  
**OF MAMMALIAN VISUAL SYSTEMS**

**"How do we see faces and animals and maps in clouds, or in the blots of a Rorschach test?"**

**Norbert Wiener**

## CHAPTER 5

### THE OVERALL SPATIAL FILTERING CHARACTERISTICS OF THE HUMAN VISUAL SYSTEM

#### 5.1 Some Basics: Spatial Frequency, Contrast, and Contrast Sensitivity

Recall that a sine-wave grating is a repeated sequence of light and dark bars whose luminance profile varies sinusoidally about a mean luminance with distance (Figures 1,2). Here two variables of a sine-wave grating are considered: spatial frequency and contrast. The width of one light and one dark bar of a grating is one cycle, or the period of the grating. The reciprocal of the period is the spatial frequency. Spatial frequency is expressed by the number of cycles of the grating that occur over a particular distance. The spatial frequency of an object can be expressed by cycles per object (c/o) dimension or, more commonly, by cycles per unit of visual angle. The number of cycles per object dimension is determined by the size of the particular dimension of some part of or the entire object and is independent of viewing distance. Cycles per unit of visual angle, more commonly called cycles per degree (c/d), is determined by the viewing distance.

The luminance difference of the light and dark bars determines the contrast of the grating. The definition of contrast most often used is that first given by Michelson (1927):

$$C = \frac{L_{\max} - L_{\min}}{L_{\max} + L_{\min}}$$

where  $L_{\max}$  and  $L_{\min}$  are the maximum and minimum luminance of the bars of the grating.

Figure 8 shows a sine-wave grating whose contrast is constant but whose spatial frequency is changing logarithmically. (Figures 8, 9, and 10 are unpublished photographs supplied by F. W. Campbell and J. G. Robson.) The wider bars at the left are low spatial frequencies when compared to the narrow bars on the right which are high spatial frequencies.

The effect of contrast on a grating of a fixed spatial frequency is shown in Figure 9. There is a square-wave grating on the left side and a sine-wave grating on the right. The medium contrast of the grating at the bottom is reduced logarithmically towards the top of the grating. Note near the top that the contrast of the grating is so low that only a uniform grey area is seen. The length of the visible grating will change with viewing distance.

If the contrast of a grating is increased from below visibility to where the grating is just seen, then the grating is said to have reached threshold contrast. Gratings of different spatial frequencies require different amounts of contrast to reach threshold for the observer. The reciprocal of the threshold contrast is called *contrast sensitivity*. If the log spatial frequency grating is shown with log contrast, as in Figure 10, the limit of visible grating results in the inverted U-shaped function found by contrast sensitivity measurements.

The importance of contrast in enabling one to see various spatial information in objects cannot be stressed too much. The loss of spatial information as contrast is reduced is demonstrated by a portrait shown in Figure 11. Various details about the portrait, such as the hair over the forehead, are selectively lost as the contrast is reduced from 100 percent to 6 percent. At the lowest contrast, 6 percent, only a ghost-like face remains.

#### 5.2 The Contrast Sensitivity Function

There must be a limit in any real system to the range of information it can process. Just as the retina is sensitive to the limited range of electromagnetic energy that is called light, the eye is also sensitive to a limited range of size of objects. Microscopes and telescopes were invented to extend the range of object sizes that can be seen. The contrast sensitivity function describes the range of object sizes that can be passed by a visual system.

The range of object sizes that can be seen became a major concern with the advent of telecommunications. It is not too

surprising that Schade (1956), an electrical engineer faced with the problem of how much spatial information to transmit for television, made the first measurements of the spatial bandwidth of the visual system. He found that the human visual system responded best to a limited range of spatial frequencies.

The importance of such measurements was realized and techniques improved by Campbell and Robson (1964, 1968). Figure 12 shows a typical *contrast sensitivity function* that they obtained with sine-wave gratings. Note that the visual system is more sensitive at about 1 to 5 c/d and less sensitive at higher and lower spatial frequencies.

Carlson, Cohen, and Gorog (1977) used one- and two-dimensional sine-wave gratings to measure contrast sensitivity. The contrast sensitivity obtained with two-dimensional gratings agrees well with the sensitivity obtained with one-dimensional gratings from 0.2 to 20 c/d (mean luminances of 0.034 to 34 millilamberts). Thus, the contrast sensitivity function can be viewed as the "window" through which spatial objects are viewed under threshold conditions.

### 5.2.1 Factors Which Affect the Shape of the Contrast Sensitivity Function

The general shape of the contrast sensitivity function is affected by the grating waveform, luminance, focus, pupil size, orientation, the number of bars of the grating, which part of the retina is tested, and whether the gratings are stationary or change in phase by either flicker or movement. For example, Campbell and Robson (1968) showed that the low-spatial-frequency loss that increases with decreasing spatial frequency below about 1 c/d, when measured with sine-wave gratings, becomes relatively less when square-wave gratings are used to measure contrast sensitivity.

Decreasing the mean retinal luminance causes the peak sensitivity and the high-frequency cutoff of the contrast sensitivity to shift to lower spatial frequencies, e.g., Patel (1966); Van Nes, Koenderink, Nas, and Bouman (1967). The low-frequency falloff disappears at scotopic luminances, and the visual system acts as a low-pass filter rather than a band-pass filter.

The effect of focus and pupil size on contrast sensitivity was studied by Campbell and Green (1965). In general, they found that the sensitivity to high spatial frequencies decreased as defocus increased. Optimum contrast sensitivity, which agreed with a diffraction limited system, was obtained with a 2 mm diameter pupil. Increased pupil size caused a shift in performance from that of a diffraction limited optical system.

The contrast sensitivity to gratings changes as a function of orientation (e.g., Campbell and Kulikowski, 1966; Mitchell, Freeman, and Westheimer, 1967). In general, contrast sensitivity is greatest for vertical gratings, slightly less for horizontal, and least for oblique gratings, especially at the high spatial frequencies.

It is important to consider how many bars make a grating. Estevez and Cavanus (1976) showed that fewer than about eight bars caused a decrease in the low-frequency falloff of the contrast sensitivity function. Furthermore, by using fewer bars, they showed that edge effects and surround luminance can affect contrast sensitivity. For example, sine-wave gratings that ended in sine phase and had a dark surround resulted in reduced contrast sensitivity when compared to similar gratings having a uniform light surround.

It is important to note that moving gratings (Robson, 1966) and flickering gratings (Kulikowski and Tolhurst, 1973) result in a substantial decrease in the low-frequency falloff. These effects are important because the retinal image of an object is never perfectly stationary under normal viewing conditions.

There is less sensitivity to high spatial frequency gratings seen in the periphery than in the fovea (Daitch and Green, 1969; Sharpe and Tolhurst, 1973). The reduction in peripheral sensitivity is not due to the optics (Daitch and Green, 1969). Hilz and Cavanus (1974) showed that sensitivity to gratings decreased by a factor of 10 from the central retina to 16 degrees in the periphery.

As Schade (1956) pointed out, a linear optical system cannot selectively reduce low spatial frequencies to a greater degree than high spatial frequencies. The observed low-frequency falloff must therefore represent the filtering properties of neurological mechanisms in the visual system.

The filter characteristics for the optics and the retinal-brain system have been separated in the elegant experiments of Campbell and Green (1965) and Campbell and Gubisch (1966). The contrast sensitivity to gratings is not limited by the optics of the eye under normal viewing conditions. Thus, the high frequency cutoff also represents the filtering by neurological mechanisms in the visual system.

### 5.3 Single- Versus Multi-channel Visual Models

A *channel* is defined as one or more neural mechanisms that respond best to some region along a stimulus dimension and less or not at all to other regions of that same dimension, e.g., spatial frequency (size) and orientation.

Does the overall contrast sensitivity reflect the cascaded result of optics and neurons that can be treated as a single spatial filter? This single-channel view has been used by some researchers, e.g., Ratliff (1965), Patel (1966), Cornsweet (1970), to account for certain observations—for example, Mach bands. However, it predicts the largest Mach bands with square waves, not ramps, e.g., Cornsweet (1970), which does not agree with observation (McCullough, 1955). Furthermore, such a model cannot account for other observations, such as the independent detection of spatial frequency components of patterns at threshold, as is discussed in later sections.

An alternative to the single-channel model is the multi-channel model. The multi-channel model, first proposed by Campbell and Robson (1968), suggests that the visual system contains a number of channels (filtering mechanisms), each selective to a limited range of spatial frequencies. They showed that the ratio of the contrast thresholds for a sine-wave versus a square-wave grating of the same spatial frequency was  $4/\pi$ , a value predicted from the amplitude of the fundamental Fourier components of the two gratings. The important aspect of this result was that the value  $4/\pi$  was more or less invariant for gratings of spatial frequencies greater than about 1 c/d. A single filter model would have predicted a greater sine-to-square threshold ratio for low and medium frequencies because the higher harmonics of the square waves could contribute to the output of the filter. The ratio of  $4/\pi$  would be predicted only when the third harmonic ( $3f$ ) of the square wave was outside the range of the filter, e.g., when  $3f$  was greater than about 30 to 60 c/d. These findings strongly demonstrated linearity of detection at threshold and led Campbell and Robson to suggest that there are a number of channels in the human visual system, each tuned to a different range of spatial frequencies. The overall contrast sensitivity function, then, represents the envelope of the combined activity of all of the individual channels.

As was shown in Section 3.3.1, size and spatial frequency are inversely related to one another. Thus, any research done in terms of size can be reinterpreted in terms of spatial frequency. Certain researchers who have preferred to work in the space domain have found results similar to those researchers working in the spatial frequency domain. Evidence for independent size mechanisms was provided by Pantle and Sekuler (1968). They found that the detection of gratings was affected most by adapting (see Section 6.1.1) to square-wave gratings of similar spatial frequencies. Thomas (1970) discussed the need for size-tuned mechanisms to account for the detection of certain objects.

### 5.4 The Filtering Characteristics of Suprathreshold Vision

The shape of the contrast sensitivity function is based upon the threshold detection of gratings. Other techniques, such as contrast matching, provide a family of curves that relate the overall filter characteristics of the visual system to suprathreshold levels of contrast. Although initially investigated by Davidson (1968) and Watanabe, Mori, Nagata, and Hiwatashi (1968), the most thorough investigation of contrast matching has been done by Georgeson and Sullivan (1975). They investigated contrast matching using sine-wave gratings in the peripheral retina, as well as central vision, and in different orientations.

Figure 13 shows results of contrast matching by the author (see Section A-2.3 for methods). This family of curves shows that the familiar contrast sensitivity curve, found at low contrasts (uppermost curve), smooths into almost linear horizontal curves (lower curves) at high contrast.

These kinds of results prompted Georgeson and Sullivan (1975) to postulate that the constant valued sensitivity seen at high contrast was due to independent spatial frequency channels. Each channel reached peak sensitivity due to individual gain mechanisms sensitive to contrast.



## 5.5 Summary

This chapter has presented the techniques and examples that provide information about the overall filtering characteristics of the visual system from threshold to suprathreshold. Further discussion introduced the concept of channels in the visual system. The bandwidth and shape of these channels are discussed in the next sections.

Many pages could easily be devoted to all the psychophysical experiments that provide evidence for the existence of mechanisms in the human visual system tuned to different ranges of spatial frequency (size) and orientation, i.e., channels. Readers interested in the details of that evidence are referred to several recent reviews (Campbell, 1974; Sekuler, 1974; Robson, 1975; Breitmeyer and Ganz, 1976; Braddick, Campbell, and Atkinson, 1977; and Graham, 1977). Also, readers interested in the phase specificity of channels, difference between low and high spatial frequency channels, suprathreshold effects such as the spatial frequency shift, and interactions among channels and edge and bar channels are referred to the same reviews. Since the main concern here is with the filtering characteristics of channels, only those papers that provide bandwidth and orientation measurements about channels are discussed in certain following sections.

## CHAPTER 6

### THE SPATIAL FILTERING PROPERTIES OF CHANNELS DETERMINED FROM PSYCHOPHYSICAL DATA

#### 6.1 The Measurement of the Spatial Bandwidth of Channels

Several psychophysical techniques have been used to determine the spatial frequency and orientation selectivity of channels in the human visual system. They include selective adaptation, masking, threshold summation, and visual evoked responses. Selected results of each will be discussed.

##### 6.1.1 Selective Adaptation

*Selective adaptation* is determined from the reduction in sensitivity to one stimulus due to prolonged exposure to another.

The first information about the bandwidth of channels came from Blakemore and Campbell (1969). They found selective threshold elevation (reduced contrast sensitivity) after adaptation to sine-wave gratings of different spatial frequencies from 3 to 20 c/d. Their data suggested that the bandwidth of the channels, measured by the half-height of the threshold elevation of the test grating, was about 1.2 octaves. Blakemore, Muncey, and Ridley (1973) replicated the adaptation method with similar techniques; they found a bandwidth of 1.5 octaves.

Lange, Sigel, and Stecher (1973) extended the findings of narrow bandwidth channels by Sachs, Nachmias, and Robson (1971) (see Section 6.1.3). They had subjects adapt to single components of stimuli that consisted of two sine-wave gratings. They found that the narrow bandwidth within which the two gratings were not detected independently remained the same even after threshold elevation of the component gratings. Their results were used to estimate the channel bandwidth to less than 1 octave.

##### 6.1.2 Masking

Another technique for measuring channel bandwidth is to simultaneously present a *masking* and test signal. The bandwidth of the channel is measured by the reduced effect of the masking signal as its frequency is shifted from the test frequency.

Carter and Henning (1971) used one-dimensional, broad-band filtered noise as a masking stimulus for gratings. They found that the most effective masking was achieved by noise whose bandwidth was 1 to 2 octaves around the mean of the test frequency.

Stromeyer and Julesz (1972) also used band-limited noise to mask gratings. They found that threshold elevation decreased by one-half when the frequency of the test grating was about 0.6 octave away from the band-limited noise. However, after increasing the width of the band-limited noise, they found that the most effective masking centered over the test frequency occurred within a noise bandwidth of 2 octaves.

##### 6.1.3 Threshold Summation

The *threshold summation* technique determines the contrast threshold of a stimulus measured alone and when it is superimposed on another subthreshold stimulus. The sensitivity of the mechanism that detects the original stimulus is measured by the reduction in threshold produced by the presence of the second stimulus.

Graham and Nachmias (1971) used threshold summation to measure contrast thresholds for the detection of different phase combinations of two sine-wave gratings having a spatial frequency ratio of 1 to 3. Since the peak-to-trough amplitude was quite different for each phase condition, if single waveforms were detected by different channels, then different thresholds should have occurred. However, independent thresholds were found whether the gratings were in peaks-add or peaks-subtract phase. In addition to providing good evidence for a multi-channel model, their results also

suggest that the channels are not affected by gratings whose frequencies are separated by a factor of 3.

Very narrow bandwidth measurements were made by Sachs, et al. (1971) using threshold summation. They used a complex analysis designed to distinguish between the detection of complex gratings by a single- and a multi-channel model. In support of the multi-channel model, they found independent detection of the two components of a complex grating with frequency relationships  $f_1/f_2 = 4/5$  or  $5/4$ . The resulting channel bandwidth was only about 0.4 octave at a centre frequency of 14 c/d. Narrow bandwidths were also found with similar techniques by Quick and Reichert (1975).

An elegant attempt to provide the two-dimensional structure of a single channel was made by Mostafavi and Sakrison (1976). Their model represents a channel as an *incoherent detector* (one which sums similar frequency components from different parts of the visual field independent of phase) consisting of a band-pass filter, followed by a transformation and spatial summation. From the detection of pseudo-random images (band-pass filtered Gaussian white noise), they found a bandwidth of about 1 octave around the centre frequency and an angular bandwidth of 20 degrees.

#### 6.1.4 Visual Evoked Response

Campbell and Maffei (1970) used measurements of the *visual evoked response* (VER) to determine the spatial tuning of channels. The VER is an electrical potential, recorded from electrodes placed on the scalp, which is produced by responses to visual stimuli. A signal is obtained by averaging the voltage sensed by the electrodes over a large number of trials. The averaging process is needed to cancel out the random noise in the signal. The stimuli were sine-wave gratings that were alternated in phase at a rate of 8 cycles/second. A linear relationship was found between the logarithm of the stimulus contrast and the amplitude of the evoked response. The slope of the graph of log contrast versus amplitude was used to measure the channel bandwidth. Two gratings of different spatial frequencies were presented, one in the upper half of the field and the other in the lower. The slope of the curve increased as the difference between the spatial frequency of the two gratings increased. The maximum slope was found when the difference between the spatial frequency of the two gratings was 1 octave or more. They concluded that channels separated by 1 octave are independent.

### 6.2 The Measurement of the Orientation Selectivity of Channels

#### 6.2.1 Selective Adaptation

Blakemore and Nachmias (1971) presented a high contrast grating at different orientations to adapt orientation-selective mechanisms in central vision. The orientation tuning characteristics were measured from the threshold elevation of a sine-wave grating of the same frequency as the adapting grating. Threshold elevation decreased as the difference between the orientation of the adapting grating and test grating increased. Threshold elevation decreased to half of maximum when the orientation difference was  $\pm 7$  degrees.

Movshon and Blakemore (1973), using the same adaptation technique, found similar orientation selectivity,  $\pm 7.5$  degrees averaged from two subjects. Furthermore, they showed that the orientation tuning did not vary with the spatial frequency of the gratings.

The orientation selectivity in peripheral vision was measured by Sharpe and Tolhurst (1973). Using the same adaptation technique as Blakemore and Nachmias (1971), they found that the orientation tuning was somewhat broader, 12 to 20 degrees.

#### 6.2.2 Masking

Campbell and Kulikowski (1966) measured the orientation selectivity of the visual system with the technique of masking. A masking grating varying in orientation was superimposed on a test grating of the same spatial frequency. Maximum masking effect, reduced contrast sensitivity, occurred when the two gratings were of the same orientation and was reduced to half when the difference in orientation between the two gratings was 12 degrees for vertical test

gratings and 15 degrees for oblique test gratings.

#### 6.2.3 Threshold Summation

Kulikowski, Abadi, and King-Smith (1973) used threshold summation to measure the orientation selectivity of gratings. They found quite narrow tuning characteristics. Threshold elevation was decreased to half at about  $\pm 3$  degrees and virtually disappeared at about  $\pm 18$  degrees.

#### 6.2.4 Monocular Rivalry

Campbell and Howell (1972) reported what they termed *monocular rivalry* with sine-wave gratings. When two sine-wave gratings are superimposed perpendicularly to one another, they appear to alternate —only one being visible at a time. One grating fades in while the other fades out. Atkinson, Campbell, Fiorentini, and Maffei (1973) found that the rate of alternation can appear to be quite rapid under certain conditions. Campbell, Gilinsky, Howell, Riggs, and Atkinson (1973) measured the rate of alternation as the orientation of the two gratings was changed. They found that the gratings alternated only when the orientation difference between them was greater than 15 degrees.

It is quite difficult to explain such tuning without the concept of independent channels. The  $\pm 15$  degrees found to produce monocular rivalry is similar to the bandwidth of orientation mechanisms found using other psychophysical techniques. Since orientation-selective neurons have been found only in the cortex, some aspects of monocular rivalry are presumably a function of the tuning properties of cortical mechanisms. It may be that monocular rivalry due to crossed gratings occurs when two different groups of orientation-selective mechanisms are stimulated.

#### 6.2.5 Visual Evoked Response

Campbell and Maffei (1970) used the visual evoked response to measure the orientation selectivity to gratings. After adaptation to a high contrast grating, the subject observed low contrast gratings and the evoked potential was recorded. This adaptation resulted in a reduction of the amplitude of the evoked response. However, the reduction found when the two gratings were at the same orientation virtually disappeared when the orientation difference between the gratings was 20 degrees.

This chapter has presented some of the literature that provides psychophysical and electrophysiological evidence for mechanisms in the visual system that are selective for spatial frequency (size) and orientation. These results reflect the overall response of the visual system to grating stimuli. Do they reflect the measurements of individual mechanisms in the visual system? These measurements are discussed in certain following sections.

## CHAPTER 7

### THE SPATIAL FILTERING PROPERTIES OF CHANNELS DETERMINED FROM NEUROPHYSIOLOGICAL DATA

The notion that the overall envelope of the filter characteristics of the visual system results from the activity of quasi-independent spatial frequency channels would seem to follow naturally from the single cell recordings from animals by many early researchers, e.g., Kuffler (1953). That notion has not always been accepted, as was discussed in Section 5.3.

#### 7.1 The Receptive Field

Kuffler (1953) showed that the *receptive fields* (the visual space to which neurons respond) in the retina of the cat were of two types: "on-centre" and "off-centre." The firing rate of an "on-centre" neuron increased if a small spot of light, placed in the centre of the receptive field, was turned on. Some cells that have a maintained discharge in the absence of stimulation increase their discharge rate temporarily when a small spot of light, placed in the centre of the receptive field, is turned off. These are "off-centre" neurons. Small spots of light turned on in the surround of "on-centre" neurons or turned off for the "off-centre" neurons reduced their characteristic response. This effect is called *lateral inhibition*.

#### 7.2 Feature Detectors

Many researchers have interpreted receptive fields from the pioneering research of Kuffler (1953) and Hubel and Wiesel (1959) as feature detectors. Barlow, Narashimhan, and Rosenfeld (1972) provide an extensive review of literature related to feature detectors.

Feature detectors are composed of receptive fields that are uniquely selective to disks, edges, etc.: they respond maximally when a perfect match between the receptive field and a stimulus with a particular geometric shape occurs. In other words, a disk of light is signaled because a receptive field of the correct size and position with respect to the visual field has been excited.

An alternative view of receptive fields has developed over the last 10 years. It removes the criterion of feature detection from the receptive field and replaces it with a far more useful concept, that of a channel. The substitution of the word channel for feature detector is no mere play on words. Within the concept of channel lies the recognition that complex visual objects can be analyzed with a far more general range of spatial parameters than that considered by advocates of feature detectors. This is not to say that there is no use for some of the properties of feature detectors such as edge detectors. Such concepts can be quite useful, but not to the exclusion of other conceptual mechanisms. The existence of channels, with their concomitant selection of spatial frequency (size), orientation, and phase, and the importance of contrast, allows the concept of spatial filter theory for perception to be investigated more fully.

#### 7.3 Evidence for Spatial Filters in the Mammalian Visual System

This section briefly samples the research that underlies the concept of neurophysiological channels and provides the basic parameters for describing spatial filters. Robson (1975) provides a more extensive review.

Enroth-Cugell and Robson (1966) provided the first investigations of the filter characteristics of single cells using sine-wave gratings. They found that the retinal ganglion cells of the cat are optimally tuned to particular ranges of spatial frequency. Each cell has its own contrast sensitivity function. The spatial frequency that produces the maximum response varies from cell to cell.

The most important finding of that research was not the individual tuning characteristics of the retinal ganglion cells but that, in general, there are two types of cells: X and Y. The more narrowly tuned X-cells, which predominate in the central retina, provide linear spatial summation. The relatively broader tuned Y-cells are nonlinear. This evidence for linear processing by one class of cells in the mammalian retina suggests that the linear transmission of spatial information of objects is important for subsequent visual processing.

Maffei and Fiorentini (1973) also investigated the tuning characteristics of retinal ganglion cells. Robson (1975) interpreted their results as showing that the response amplitude of the cells was proportional to the contrast of gratings at low contrast levels; but at higher levels of contrast, a logarithmic relationship was found. Although some behaviour of the retinal ganglia is not completely linear, Robson (1975) still argued that contrast rather than absolute luminance variation is the more appropriate stimulus variable to measure.

The tuning characteristics of the retinal ganglion cells are relatively broad when compared to those of the cells found at the lateral geniculate nucleus (LGN) and the striate cortex (Maffei and Fiorentini, 1973). Furthermore, the predominantly isotropic (circularly symmetric) receptive fields found in the retina and LGN give way to anisotropic receptive fields in the striate cortex (Hubel and Wiesel 1959, 1962, 1968). The rectangularly shaped receptive fields in the striate cortex occur in a variety of sizes and orientations and have different numbers of excitatory and inhibitory zones. It is not surprising that such cells respond maximally to gratings whose orientation and spatial frequency best match the orientation and width of the areas that form the receptive field. The close relationship between the spatial weighting of cortical cells and sinusoidal gratings is seen in Figure 2. The maxima and minima of the sinusoidal gratings can be related to the excitation (+) and the inhibition (-) shown by the rectangular plots to the upper right corner of each grating.

The first tuning characteristics of cortical cells in the cat were obtained by Campbell, Cooper, and Enroth-Cugell (1969). They found that the optimum contrast sensitivity was orientation-specific and varied from cell to cell with response falling off above and below the optimum spatial frequency. Further grating studies on cortical cells in the cat were done by Glezer, Ivanoff, and Tscherbach (1973), and by Maffei and Fiorentini (1973). They found that the bandwidth of simple cells was about 2 octaves; that of complex cells was somewhat larger. Glezer et al. (1973) and Pollen and Ronner (1975) found that complex and hyper-complex cells were optimally stimulated by periodic rather than single stripes.

Simple cells appear to be excited by X-cells and complex cells by Y-cells (Stone and Dreher, 1973). Simple cells are also more position-sensitive to the receptive field than are complex cells. These findings, coupled with the narrow tuning of the simple cells, suggest that it is perhaps more appropriate to consider the behaviour of simple cells than complex cells as linear spatial filters. In general, these studies show optimum tuning in simple cells of about  $\pm 15$  degrees in orientation and about 2 octaves in spatial frequency.

Recent investigations by DeValois (1976) of the tuning properties of simple cells in monkey found very narrow tuning in both orientation and spatial frequency. Bandwidths at half-amplitude varied from 0.7 to greater than 2 octaves. Orientation tuning varied from  $\pm 4$  degrees to greater than  $\pm 50$  degrees. About 25 percent of the cells were tuned to only 0.7 to 1.2 octaves in spatial frequency and  $\pm 4$  to  $\pm 10$  degrees in orientation.

In addition to the very narrow filtering characteristics of cortical cells, an interesting picture of the organization of spatial frequency and orientation columns in the cortex has been provided by neurophysiologists. Hubel and Wiesel (1974) found a systematic change of orientation selectivity in neurons from measurements made perpendicularly through a column in the visual cortex. This systematic orientation tuning was confirmed by Maffei and Fiorentini (1977), who found that tangential penetrations through a column resulted in systematic changes in the spatial frequency selectivity of the cells.

These data provide the exciting view of the striate cortex composed of columns of "two-dimensional machines" (Hubel and Wiesel, 1974) that act as a two-dimensional array of sieves systematically tuned for orientation and spatial frequency and are repeated throughout the striate cortex like a lattice structure of the finest crystal.

#### 7.4 Differences Between Bandwidths of Channels

The bandwidth estimates determined from psychophysical measurements of Sachs et al. (1971), Lange et al. (1973), and Quick and Reichert (1975) are quite narrow, about 0.5 octave. Graham (1975, 1977) and Stromeyer and Klein (1975) argued that considerations of *probability summation*—detection occurring from a pooled, weighted response of independent channels—suggested that the bandwidth of these narrow channels may be underestimated.

If the bandwidth of channels determined by threshold summation is underestimated, then what about the veracity of bandwidth estimates as determined by masking and adaptation? Pantle (1974) derived relative bandwidths from different types of psychophysical data. He showed that the narrowest bandwidth resulted from threshold summation, a broader bandwidth resulted from selective adaptation, and masking produced the greatest bandwidth.

Dealy and Tolhurst (1974) showed that contrast sensitivity is reduced with gratings of any contrast above threshold. Their results suggested that adaptation may be due to inhibition from which Braddick, et al. (1977), argued that the range of spatial frequencies that can adapt a channel is wider than that which can stimulate it for detection. This suggests that adaptation and masking experiments provide an overestimate of the channel bandwidth.

Although different bandwidths appear to arise from different psychophysical methods, there is at least one other factor to consider. It is also possible that these different bandwidths are the result of the channels being at different levels of stimulation or because the channels being stimulated have a wide range of different bandwidths. Since DeValois (1976) showed that there are quite narrowly tuned receptive fields in monkey visual cortex, it seems likely that the human visual system also contains receptive fields of similar narrow bandwidth.

What is surprising is not that different psychophysical methods yield different bandwidths, but that they generally agree within 1 octave. Such good agreement suggests an important general bandwidth for filtered images. However, it should be kept in mind that a complex object that extends over the central retina is most likely being filtered with narrow-band as well as medium- and broad-band mechanisms due to the different sizes of receptive fields that exist across the retina.

In summary, many psychophysical and neurophysiological studies have found mechanisms whose spatial bandwidths averaged 1 to 2 octaves. Orientation bandwidths average  $\pm 15$  degrees. The next sections will present spatial filters based on the overall filtering characteristics of the visual system and the bandwidth and shape of channels that have been discussed.

## CHAPTER 8

### CREATING TWO-DIMENSIONAL SPATIAL FILTERS FROM BIOLOGICAL DATA

The previous chapters presented some of the psychophysical and neurophysiological data about the spatial filtering properties of the mammalian visual system. Here those data are used to create spatial filters with which to filter objects.

#### 8.1 Two-Dimensional Spatial Filters Based on Contrast Sensitivity Data

In Section 5.2 it was argued that the visual system can process spatial information about objects only through a window that can be described by the contrast sensitivity and contrast matching functions. Furthermore, it was shown that the visual system is anisotropic; that is, sensitivity to detection of objects varies as a function of orientation. Both spatial frequency and orientation sensitivities depend upon the contrast of the object, e.g., Georgeson and Sullivan (1975).

A two-dimensional spatial filter can simulate the effects of such filtering properties on complex objects. A two-dimensional filter allows the determination of how much spatial information about an object is passed through the early stages of the visual system and of the consequences for spatial information contained in objects at different orientations.

There is a continuum of filter functions that changes from threshold to suprathreshold (see Section 5.2). The limiting case for spatial information is the contrast sensitivity function. Therefore, a two-dimensional filter was created based on contrast sensitivity data (Ginsburg, 1973). Since objects will be filtered using a static filter as a modulation transfer function, the two-dimensional contrast sensitivity filter will be called an MTF.

Two general assumptions are made in using the contrast sensitivity function as an MTF. First, as mentioned in Section 5.2, the visual system does not have one MTF but, rather, a family of MTFs that range from threshold to suprathreshold and change as a function of the variables discussed in Section 5.2.1. Thus, the particular conditions under which the contrast sensitivity function was obtained must be specified in order for it to be used as an MTF. Second, MTFs based on contrast sensitivity measurements obtained at threshold imply that the response (output) of the system is constant and that it changes as a function of the amplitude and frequency of the input sinusoids; in other words, the system is linear (see Section 1.2). This is perhaps the most stringent assumption that has to be made. Hay and Chesters (1972) argued that signal-transfer functions cannot be deduced solely from threshold measurements because those measurements depend greatly on system noise. Since they found that noise varied as a function of retinal distance, the visual system is nonlinear at threshold. Henning, Hertz, and Broadbent (1975) found that gratings with three sinusoidal components of high spatial frequency interacted with a sinusoidal grating two octaves lower in frequency. That finding suggests nonlinear distortion of high, but not low, spatial frequencies. Although it must be accepted that any real system has some degree of nonlinearity, the important point is the degree of nonlinearity that can be assumed for the overall operation of the system. If the visual system were not linear to a first approximation, Campbell and Robson (1968) and Campbell, Carpenter, and Levinson (1969) could not have predicted the visibility of complex waveforms from the response of the visual system to sine waves. Thus, it is highly unlikely that the nonlinearity findings by researchers such as Hay and Chesters should refute the use of the contrast sensitivity function as an MTF. It is in this spirit of first order approximation of linearity that a two-dimensional MTF was constructed from contrast sensitivity data. Unless this linear systems approach is taken, the relative importance of the nonlinearities of the visual system will be difficult to determine.

Since the single most complete set of contrast sensitivity data then available for spatial frequency and orientation was that of Campbell, Kulikowski, and Levinson (1966), their data were used to calculate the parameters for the MTF filter. The contrast sensitivity values for spatial frequencies from 1 to 32 c/d for sine-wave gratings presented at 0, 45, and 90 degrees of rotation were obtained from Figures 2 and 5 of their report. Lines were drawn by eye through the data points of the three subjects and averaged for the spatial frequencies shown in Appendix B. The contrast sensitivities were normalized to the maximum value (213.3 at 6 c/d at 0 degrees orientation). The normalized functions are plotted with solid lines in Figure 14. Values of percent contrast sensitivity at integer spatial frequencies were



placed on a rectangular grid. The off-axis values between 0, 45, and 90 degrees were interpolated by eye, especially noting the spatial frequency values of Figures 1 and 4 of Campbell, et al. (1966). These values were arranged in digitized circles that approximated a polar representation for the rectangular grid that was used for the digital filtering (Figure 15,a).

Note that only one quadrant of the two-dimensional MTF was created. The grating data collected at 135 degrees were not used because they differed little from the data at 45 degrees, and two-fold symmetry was desired as a first approximation for the filter. The single quadrant values were replicated in the other three quadrants to provide the desired symmetry. This filter will be called MTF(L).

To investigate the effects of increased contrast sensitivity at the lower spatial frequencies, 1 to 5 c/d, found in other studies, e.g., Blakemore and Campbell (1969), a different set of values based upon their data for the low spatial frequencies was used. These are shown in Figure 15,b. This filter will be called MTF(H). The magnitude spectra of the Fourier transformed objects were multiplied by the values of the MTF filters and then inverse Fourier transformed. The effects of the MTF spatial filters were determined from numerical printouts, contour plots, and photographs of the filtered images (see Section 3.1).

The fundamental frequencies of the patterns were attenuated by the contrast sensitivity corresponding to 2 c/d for the 32 by 32 pel objects and 0.5 c/d for the 128 by 128 pel objects. Therefore, the MTF filtered images should be viewed at about 0.5 degree (about 120 times the width of the object) for the 32 by 32 pel objects and about 2 degrees (about 30 times the width of the object) for the 128 by 128 pel objects in order to compare them with the original objects and to determine the fidelity of the digital filtering to the filtering characteristics of the reader's own visual system.

The contrast sensitivity for both spatial frequency and orientation can be seen most easily from the pictures of the MTF filters shown in Figure 16. Figure 16,a shows the MTF(L). Figure 16,b shows the MTF(H). Figure 16,c and d are due to shorter exposures of the MTF(H) to show the details of the filter characteristics at higher spatial frequencies. The lighter and darker regions correspond to higher and lower contrast sensitivities. Note also the differences between different spatial frequencies and orientations. Figure 16,e shows a three-dimensional view of MTF(H). Note the familiar shape of the contrast sensitivity function on each side of the x-axis.

It should be clear from this MTF filter that objects of the same size and intensity but at different orientations will be attenuated differently. Vertical objects will be attenuated less than objects oriented horizontally or at 45 or 135 degrees. Since the greatest contrast sensitivity occurs at 3 to 6 c/d, medium size objects will be attenuated less than smaller or larger objects. Very fine details about an object (high spatial frequencies) will be attenuated more by the filter than will intermediate spatial frequencies.

An alternative to these digital methods is the use of pictures of the MTF filters to create spatial filters for an optical Fourier transform device. The negative of these filters, suitably reduced by microphotographic techniques, could be placed in the Fourier transform plane to produce filtered objects similar to those produced using digital techniques. One caution in using this optical technique is the possibility of nonuniform phase due to variations in the thickness of the material used for the negative.

## 8.2 Two-Dimensional Spatial Filters Based on Biological Channels

Several attempts using psychophysical techniques have been made to determine the shape of channels in the human visual system, e.g., Blakemore and Campbell (1969); Stromeyer and Klein (1975); Mostafavi and Sakrison (1976); Legge (1977). However, each used different methods and each found a line- or point-spread function that was somewhat different. The present approach is to use spatial filters that have the general filtering characteristics of channels: ideal low-pass and band-pass filters. By changing the shape and bandwidth of these filters, a range of different point-spread functions may be obtained, some closely approximating those based on data. The effect of these changes in the filter shapes can be seen in the filtered images. Previous spatial filtering by Ginsburg (1971,a,b; 1973) and Ginsburg, et al. (1976), suggested that such changes had little effect on the ability to classify similar complex objects as being similar. It was found that a general bandwidth of low spatial frequencies was the most important variable for the classification of objects. Therefore, the majority of the spatial filtering presented here was done using ideal low-pass and band-pass filters. In Section 14.3, a direct comparison will be made on a large set of data between

ideal band-pass and psychophysically derived channel band-pass filters to justify this basic approach.

Do low-pass digital filters correspond to mechanisms in the visual system? Recall that the channels in the visual system may be thought of as discrete spatial filters with finite bandwidths. They are not ideal low-pass or high-pass optical filters. They are band-pass filters whose bandwidth is a function of the size of receptive fields.

One point that should be understood is that the discrete finite Fourier transform that is implemented by using a Fast Fourier Transform (FFT) is also band-limited. Only a finite number of spatial harmonics can be obtained from any object. If the size of the object is the same as the sampling grid, then an integer multiple number of harmonics that range from 1 cycle per object to the Nyquist frequency is determined. For example, an object sampled on a 32 by 32 pel grid yields 1 to 16 spatial harmonics in each dimension. Therefore, high- and low-pass filters in the discrete Fourier transform domain are band-pass filters with respect to an optical Fourier transform which would contain higher and lower spatial frequencies.

A closer look is taken at the line weighting function of the one-dimensional ideal low-pass filter shown in Figure 4.b.1. This space filter, convolved with an object, will produce the same filtered image as if the spectrum of the object were multiplied by the ideal band-pass filter and inverse Fourier transformed.

But is the rippling nature of this space filter like that of mechanisms in the visual system? Mathematically, the space filter is a sinc function, given by

$$\text{sinc } x = \frac{\sin \pi x}{\pi x}$$

with properties such that  $\text{sinc}(0) = 1$ ,  $\text{sinc}(n) = 0$  for  $n = 1, 2, 3, \dots, n$  (Bracewell, 1965).

It is interesting to note the different names attached to the same parts of the sinc function, depending upon the discipline that described them. In optics, the central peak is called the central maximum and the subsidiary peaks and valleys, the maxima and minima or side lobes. The neurophysiologist and psychophysicist describe spatially tuned mechanisms having weighting characteristics similar to those given by the sinc function as excitatory (the central maximum) and inhibitory and disinhibitory flanks (minimum and maximum side lobes). The ideal low-pass filter is sometimes called a gate function in electrical engineering because of its selective filtering properties; i.e., it "gates" certain signals through some communication channel.

#### 8.2.1 Comparison Between an Ideal Low-Pass Filter and Filters Obtained from Biological Data

The sinc function and normalized line-spread functions based on neurophysiological and psychophysical data are shown in Figure 17. The solid line is from table values of the sinc function found in Bracewell (1965). The filled circles are data obtained from the on-off response of a flashing light moved through the receptive field of a simple cell in the visual cortex of a cat, from Tolhurst and Movshon (1976). The line-spread function is similar to that obtained by Bishop, Henry, and Smith (1971) using different techniques. The dashed lines are from the curve  $[e^{-x} - e^{-4x^2}]^3$  that fits the shape of a psychophysical channel determined from the adaptation studies of Blakemore and Campbell (1969).

Several of the data points from the on-off response of the cortical cell (filled circles) were shifted slightly along the horizontal axis to allow the curves to coincide with the zero crossings of the sinc function. These shifts are justified because there is a range of different size channels; in general, they represent a change in size, and the main concern is with the relative amplitudes of the central maximum and side lobes.

There is good agreement between the general shape of these curves. The sinc function usually has lower side lobes (less "inhibition"), but it extends farther in space than the channel and cell data. The greatest amount of inhibition is seen in the psychophysical channel. It should be pointed out that prefiltering the spectrum with an MTF filter and then using the ideal low-pass filter will increase the inhibition of the corresponding line-spread function. An ideal band-pass filter will further increase the inhibition, as can be seen by comparing the line-spread function in Figure 4.b.1 with 4.b.3.

Are the two-dimensional ideal band-pass filters neurophysiologically realizable? The corresponding point-spread functions of ideal circle- and square-shaped spatial filters were shown in Figure 6. The point-spread function of the circle-shaped filter is called a Bessel function of the first kind, order zero (e.g., see Hecht and Zajac, 1974). It is similar to the isotropic receptive fields found in the retina and LGN.

The square-shaped spatial filter has vertical and horizontal line-spread functions that are given by the sinc function. It can be viewed as a generalized channel or as the superposition of several channels having the same or different bandwidths with different orientation.

By intuition, one might expect that the different two-dimensional shapes of filters having similar bandwidths would greatly affect the shape of objects. However, Ginsburg (1971,a,b) has shown that although there are discriminable differences between objects that are optically low-pass filtered with square, circular, and rectangular (1:0.6) filters having similar bandwidths, the objects can still be easily classified as the same. Similar results will be shown later using digital filters having different shapes and weighting functions.

A diagram of an ideal low-pass digital transform filter that passes the first four harmonics is shown in Figure 18 (Ginsburg, 1971,a). This filter has a  $\pm 1$  octave band-pass centred at  $2c/\text{width}$  of the sampling grid. The orientation selectivity of this kind of digital filter is given by  $45/n$  degrees where  $n$  is the number of the  $n^{\text{th}}$  harmonic. From Figure 18, it can be seen that the orientation selectivity required to pass the first, second, third, and fourth harmonics is 45, 22.5, 15, and 11.25 degrees, respectively.

The reader is reminded that the bandwidth and orientation selectivity required by such digital filters are easily found in both neurophysiological and psychophysical data from cat, monkey, and man, as was discussed in Chapters 6 and 7.

In summary, very simple band-pass filters in the Fourier transform domain were shown to provide filtering properties whose counterparts in the space domain exhibit the general filtering properties of single channels in the visual system. The next chapters show how these filters demonstrate possible visual processing of spatial information of simple and complex objects.

**PART III**

**VISUAL INFORMATION PROCESSING  
IN TERMS OF SPATIAL FILTERING**

**"Percepts without concepts are blind; concepts without percepts are empty."**

***Immanuel Kant***

## CHAPTER 9

### SPATIAL FILTERING AND THE GENERALIZATION OF FORM: SIMPLE CONTINUOUS AND DISCRETE OBJECTS

#### 9.1 Introduction

The preceding sections presented the theoretical background and experimental data needed to create certain spatial filters. These spatial filters are constrained by biological data and are used to determine the spatial information about objects which can be extracted by those filters.

This dissertation deals with only a few of the ranges of objects studied. The examples discussed have been selected to bring out distinct problems for space domain pattern recognition techniques or because they represent a particular class of perceptual problem. In general, these objects are similar to those used in previous investigations of spatial filtering using optical spatial filtering techniques (Ginsburg, 1971,a,b). The results presented here, in addition to replicating the previous results, also extend them.

*Space domain pattern recognition means the recognition of patterns by the explicit extraction and manipulation of pattern features such as lines, angles, or edges without considering how the visual system filters the various spatial frequencies that are present in those patterns. In contrast, the transform filtering approach extracts information from patterns as a whole, that is, extracts pattern information in a way that interrelates all of the pattern features. That information is then filtered into different ranges of spatial frequency and orientation that are based on the filtering processes of the visual system. The reader is encouraged to test the parsimony of the filter results against other possible space domain techniques.*

The usage of classification, recognition, and identification is sometimes blurred. For example, the classification of objects by machines is commonly termed pattern recognition. The following general definitions of detection, classification, recognition, and identification are used. Detection is the perception of the minimum amount of spatial information about an object with which a performance measure can be obtained; e.g., an object is seen 75 percent of the presentation time. Classification is the perception of that spatial information required to place an object in a group, e.g., "The object is a face." Recognition is the perception of the spatial information required to determine whether an object has been seen before, e.g., "That is the same face seen yesterday." Identification is the perception of that information required to name a particular object, e.g., "That is Mary's face."

Some questions asked in this section are: What are the effects of the MTF filters on the details of objects? What does the low frequency attenuation of the MTF do to low-pass filtered images? What is the effect of removing very low spatial frequencies from a filtered image, i.e., using a band-pass filter? Finally, what is the minimum number of spatial frequencies needed to classify an object?

In these next sections it is important to keep in mind how the spatial frequencies relate to the dimensions of the objects. A measure is needed to relate the spatial frequencies of an object independent of its viewing distance. The fundamental frequency, or first harmonic, will refer to one cycle across some given size dimension of the object. For example, the fundamental frequency of a letter width means one cycle across the width of the letter. Referring back to Figures 1 and 2, if the width of the letter is the same as the width of the pictures that contain one cycle, then the sine and cosine functions provide spatial information about one harmonic of the letter in the vertical orientation. The magnitude of this vertical harmonic could be placed in the first horizontal square in the two-dimensional spectrum. Rotating this fundamental harmonic 45 and 90 degrees provides the magnitude of the fundamental harmonic for the other two orientations (see Figure 18).

For the following filtered objects, only the filter size will be given, not the number of harmonics that the filter passes. Since the particular bandwidth required to show various effects is not critical (Ginsburg, 1971,a,b and Ginsburg, et al., 1976), the filter size will be a simpler measure to use. However, the fundamental frequency will be given for the width of selected objects and the actual spatial frequencies that are passed by the filter can be easily computed. The

fundamental frequency of the object,  $f_{01}$ , is given by the number of pels of the sampling grid divided by the number of pels of some dimension of the object. For example, the letter T in Figure 19,a is 15 pels long. The sampling grid is 32 pels. Thus,  $f_{01} = 32/15 = 2.13$  cycles/sampling grid (c/g),  $f_{02} = 4.26$  c/g, and  $f_{03} = 6.39$  c/g.

The particular harmonic of the object,  $f_{hn}$ , given by the fundamental spatial frequency in the magnitude spectrum, is the size of object divided by the grid size, or the inverse of  $f_{01}$ , multiplied by the number of the harmonic. For example, the first harmonic of the magnitude spectra of the letter T in Figure 19,a is  $f_{h1} = 15/32 = 0.47$  cycles across the object (c/o). Thus,  $f_{h2} = 0.94$  c/o,  $f_{h3} = 1.4$  c/o, etc. It can be seen from these calculations that a 5 by 5 low-pass spatial filter will capture more than the second but not more than the third harmonic of the object. Thus, a 5 by 5 means a low-pass filter that captures  $5 \times 0.47$  or 2.35 spatial frequencies of the object in the u, v dimensions of the transform plane.

The important point is that low spatial frequencies will always refer to the low spatial frequencies of the object relative to the fundamental spatial frequency of some dimension of the object. Generally, they will refer to the bandwidth of the lowest four harmonics.

## 9.2 Letter T

The effects of the MTF filter on a very simple two-dimensional pattern, a letter T, are shown in Figure 19. (This pattern also represents a version of the horizontal-vertical line illusion, as is discussed in Section 12.3.3.) The filtered magnitude spectra are shown on the left side and the filtered images on the right. There are only slight differences between the brightness distribution of the T from the MTF(L), Figure 19,b, and MTF(H), Figure 19,c, spatial filters. Both filters result in a substantial reduction in contrast of the vertical and horizontal lines and create maximum intensities at their intersections. The vertical lines are slightly brighter than the horizontal lines, most noticeably as the vertical line extends away from the intersection. Note that these results (and other results to follow) suggest that the differences between the low frequency attenuation characteristics of the two filters have only a small effect on the overall shape of the object. However, the MTF(H) filter provides slightly more homogeneity in the brightness distribution of the lines than the MTF(L) filter.

It is important for the reader to note that the brightness distributions shown in the pictures in this dissertation accurately represent the results of the digital filtering and are not artifacts of the filtering characteristics of his own visual system (assuming, of course, that the reader is an emmetrope). The fidelity of these pictures to the numbers used to create them is shown in the two- and three-dimensional contour plots of Figure 20. Careful study of these contour plots and the pictures will show excellent agreement between the peaks of the contours and the grey levels in the pictures. The similarity between the shape and detail of these filtered pictures, whether amplitude or intensity values are used, is shown by comparing Figure 19 with Figure 20. Thus, such nonlinearities as occur between an amplitude and an intensity representation of a filtered image will have little effect on the overall two-dimensional shape and the amplitude relationship between different parts of the filtered image.

The MTF filters act as differentiators at the low spatial frequencies. This results in a reduction in contrast between the original letter T and the MTF filtered Ts. In order to enable the details of the filtered images to be seen better, the intensity values of the MTF filtered images were multiplied by a logarithmic (log) function. This operation does not alter the general structure of the object; it just increases the contrast to make it easier to visualize details of the object. The log transform increases the contrast of the low contrast details of the images by multiplying the intensity values of the images by a logarithmic function scaled between the extremes of the intensity values 0 (white) and 63 (black). Multiplication of the values of the intensity by the log function results in increasing the lowest intensities to a greater extent than the highest intensities. The overall effect is to compress the larger range of intensities of the images into a more narrow range that becomes more visible with the limited range of intensity than was captured on the Polaroid film that was used. The log transform increases the lower intensities while preserving the overall smoothing effects of the filter on the object. This can be verified by comparing the log transformed, MTF filtered letter T in Figure 19,d with the 10-level contour plot of Figure 20,b.

The values of the MTF filtered spectra have also been log transformed in order to increase the visibility of the low contrast details of the spectra. Compare the spectra in Figure 19,c and d.

What is the minimum number of spatial frequencies required to identify this letter T? Also, what are the effects of the MTF(L) and MTF(H) filters on the low spatial frequencies? Both of these questions are answered by the next demonstrations in which the letter T is synthesized from 1 to 6 c/o using both filters. The results are shown in Figures 21 and 22 in which a T-shaped object can be recognized from about 1.5 to almost 3 c/o (Figures 21 and 22,c,d,e).

There is little difference between the shapes of these filtered images in these bands of spatial frequency. This result implies that the particular bandwidth required to provide the basic form of an object is not critical over a range of at least  $\pm 1$  c/o.

A final demonstration shows that an anisotropic spatial filter and the removal of very low spatial frequencies of the letter T still provide sufficient information for the identification of the object. The results of filtering the original T with a rectangular filter,  $f(u, v) = 6, 4$ , with and without the low spatial frequencies removed ( $f_H = 0.47$  c/o) are shown in Figure 19,f,g. The spectra and filtered images have not been log transformed because the MTF filters were not used. Note that rectangular filtered letter T in Figure 19,f is comparable to the MTF filtered letter T in Figure 19,e even though quite different spatial filters have been used.

This invariance of form with changes in the filter characteristics using filters that can be related to mechanisms in the visual system will be shown several times with many different objects.

The major differences between the objects filtered by the two MTF filters are the magnitudes of the ripples distant from the object that can be seen in several of the contour plots. The MTF(L) filter produces ripples of greater magnitude than does the MTF(H) filter. This is due to increased inhibition, i.e., the greater low frequency attenuation of the MTF(L) filter. In general, these ripples are of relatively small value. For example, the ripples seen in the photograph of the low-pass filtered T (Figure 19,e) are not seen in the contour plot of the same object in Figure 22,f. This means that those ripples are less than 10 percent of the maximum value.

Now that one object has been filtered in detail, only the general results of similar filtering of other objects will be shown. In general, only the MTF(H) spatial filter will be used to represent the filtering effects of the two-dimensional contrast sensitivity function on objects. The small differences between the MTF(L) and MTF(H) filters are more important for contrast illusions than general form information, as is discussed in Chapter 12. Numerical printouts and contour plots will be used only to make specific points about certain objects that are not immediately apparent from the pictures.

The results of filtering more complex objects are shown in Figure 23. The original objects are shown in Column 1. The MTF(H) filtered spectra are shown in Column 2. Column 3 shows the MTF(H) filtered images. Columns 4, 5, and 6 show the low-pass filtered images. Column 4 shows filtered images containing only four cycles prefiltered with the MTF(H) followed by an ideal low-pass filter. An ideal low-pass filter was used to capture four cycles of the filtered images shown in Column 5. The filtered images in Column 6 contain only three harmonics after removal of the lowest harmonic (about the 0.5 cycle of the object) and those harmonics greater than four.

### 9.3 Letter E

The MTF(H) filter does little to the letter E (Figure 23,a,1), except to smooth the corners and lines (Figure 23,a,3). Except for contrast, there is little difference between the form of the letter E created from four harmonics with (Figure 23,a,4) and without (Figure 23,a,5) the MTF(H) filter. Intuition suggests that the lowest harmonic of the letter should provide just contrast, not form, information. That intuition is confirmed in Figure 23,a,6 where the removal of the lowest harmonic has reduced contrast but has had little effect on the form as compared to the low-pass filtered Es of Figure 23,a,4,5. Thus, only three harmonics are required for the identification of this letter E.

### 9.4 Discrete Letter G

This next experiment investigates how objects that are made of discrete elements can be perceived as a whole unit of form if man or machine can isolate the low spatial frequencies. The discrete squares of the letter G in Figure 23,b,1 perceptually close to provide the G form information. Can the filter concept offer any clues as to how a global form could emerge from such discrete pattern elements? First, the effects of the MTF spatial filter on the discrete pattern

are noted. Figure 23.b.3 shows that the MTF filter has only smoothed the squares. They can still be resolved even after the log transform. Thus, a global G has not emerged by filtering the original pattern according to the contrast sensitivity data. In other words, the G form has not been generalized from its discrete elements by the single overall spatial filtering characteristics of the visual system as processed by the MTF filter that has been used. However, when the higher spatial frequencies of the discrete G pattern are sequentially removed, the square dots are not resolved and the generalized G form is found in three ranges of low frequency from 1 to 3, 1 to 4, 1 to 5 c/o (Figure 24.c,d,e). The best subjective G form is present in a frequency band of 1 to 4 c/o (Figures 23.b.4,5, and 24.d). Similar results are obtained with the ideal low-pass filter. Removing the fundamental frequency demonstrates once again a reduction in contrast in the filtered pattern. The basic form, however, remains with only 2 to 4 c/o shown in Figure 23.b.6.

Can the generalized G form be found in a range of high spatial frequencies? The answer to this question is "no," noting the results of sequentially filtering out the lower spatial frequencies as shown in Figure 25. Thus, excluding the lower spatial frequencies results in either the dots or nondescript forms. Only a band-pass region of low spatial frequencies contains the generalized form.

#### 9.4.1 Similar Forms from Four Discriminably Different Letter Gs

The previous results suggest that the discriminable differences between objects are removed by low-pass filtering and that the particular elements that make up the object are, in general, irrelevant for the classification of the object. This suggestion is shown to have considerable merit in the following demonstration. Four discriminably different letter Gs, Full G, Dot G, Serif G, and Slash G, are shown to have similar forms when created from their low spatial frequencies in Figure 26.

#### 9.5 Dot Letter R in Noise

Similar results were obtained with a figure-ground problem of a dot R buried in random dot noise (Figure 23.c.11). Clearly, any system that analyzes this object in terms of local features will have difficulty in discriminating the dots of the R from the noise. However, separating the R form from the noise by spatial filtering is simple because their main spectral energy occurs in different spatial frequency bands (Figure 23.c.4,5,6).

Of course, using the spatial filter to extract embedded figures would be difficult if the size of the noise were to approach the size of the elements making up the object. But it should be noted that the human observer would also have increased difficulty.

#### 9.6 Gestalt Principles of Perceptual Organization

The preceding experiments have demonstrated that a low spatial frequency band that contains only three harmonics is sufficient to provide generalized form information of objects that have names, i.e., that can be classified. The next experiment investigates the effects of spatial filtering on more general dot/line patterns. These patterns illustrate fundamental laws of perceptual organization enunciated by early Gestalt psychologists: whole (Figure 23.d.11), proximity (Figure 23.e.1), similarity (Figure 23.f.1) and proximity/similarity (Figure 23.g.1). Pattern elements perceptually close and group to form units of information different from the sum of their parts, e.g., Koffka (1935).

As before, the MTF spatial filter just smooths the pattern elements and the low-pass spatial filter isolates the basic forms. Thus, the perceived groupings—uniform field for the whole, three uniform groups for the proximity, two similar groups separated by a central dissimilar group for the similarity, and three uniform groups for the proximity/similarity—can be found in a low spatial frequency band,  $f = 1, 4$  c/o (Figure 23.d-g.4-6). Note that the removal of the lowest harmonic of the dot pattern has the additional benefit of providing generalized grouping information. It has also reduced the contrast difference between dissimilar pattern features in Figure 23.d-g.6. There are many other examples of closure. For example, Figure 27, a shows a letter H made up of line segments. The low-spatial frequencies of this object provide the completed form as shown in Figure 27.c.

#### 9.7 Summary

The previous sections have shown that, in general, the basic form of many different objects can be seen from only three



harmonics of the original object. Can such simple but powerful filtering also work on more complex objects such as portraits? This is investigated in the next chapter.

## CHAPTER 10

### SPATIAL FILTERING AND THE GENERALIZATION OF FORM: COMPLEX OBJECTS (VARIATIONS OF A PORTRAIT)

#### 10.1 Introduction

The previous experiments have shown that spatial filters based on biological data can provide details and general forms of simple objects that agree well with the way the visual system seems to filter and extract information about objects. In this section a more complex object is investigated—a portrait.

An original portrait (Figure 28.a.1) is used as a control in the following demonstrations. Four variations of this original portrait have been made: coarse quantization (Figure 28.b.1), added random noise (Figures 28.c.1; 31.a.1), inclusive "OR" random noise (Figure 31.b.1), and line configuration (Figure 31.c.1). Each portrait is discriminably different from the others and yet is able to convey similar general face information. As in the previous demonstrations, the fidelity of the MTF will be noted in determining the resolution of the portrait features that are seen. The low spatial frequencies, as predicted from the previous filtering results, will be examined for similar portrait form information. Answers to several questions will be sought as the effects of the MTF and low-pass filters are observed: Why do the portrait features look different at different viewing distances? How do these portrait configurations convey similar face information? What is the minimum amount of information needed to recognize and identify a face?

Harmon (1973) provided an interesting investigation concerned with the recognition of faces using both blurring and coarse quantization. His basic findings were that 60 percent correct face recognition can be obtained even under severe blur and that a 16 by 16 matrix of quantized squares was close to the minimum resolution required for identification. Unfortunately, it is difficult to translate the space averaging blur that he used into spatial frequency terms. Clearly, it is not band-pass filtering. Furthermore, the 16 by 16 matrix that provided the minimum resolution for identification appears to be related to the sampling grid and not relevant portrait dimensions. A 16 by 16 sampling matrix can provide a maximum of eight harmonics. However, previous filtering results predict that only about four harmonics should be necessary for face identification. An examination of the coarsely quantized portraits that were shown in Harmon's article reveals an average of 10 blocks across the face. Thus, the sampling that was used provided about five harmonics per face width, a value more in agreement with predictions.

In another study, Harmon and Julesz (1973) investigated the masking effect of visual noise on the perception of a portrait by coarsely quantizing a portrait of Abraham Lincoln into large blocks. Their general conclusion was that noise due to the high frequencies of the blocks masked the low frequencies that carry the portrait information. They termed this effect "critical-band masking." In one demonstration, they removed a two-octave band of frequencies just above the block frequency. The result was a low frequency portrait that also contained the edges of the blocks. The face was more easily recognized in comparison to a face in which the removal of some high frequencies eliminated the sharp edges. However, the recognition of that filtered face was not so good as would be expected taking into consideration that the edge frequencies are two octaves higher than the face frequency and that psychophysical studies (see Chapter 6) have shown spatial frequency interaction within about a two-octave bandwidth. In a further demonstration, they added random noise that was spectrally adjacent to but two octaves higher than that of the blurred portraits of Lincoln. Again the perceived differences between the two portrait configurations were not so great as one would expect from critical-band masking. These demonstrations, especially from the latter results, imply that perceptual mechanisms, in addition to frequency specific channels, may cause or contribute to our difficulty in recognizing coarsely quantized portraits.

#### 10.2 Filtering the Original Portrait

An original continuous tone portrait was digitized to 105 by 112 pels containing 64 grey levels per element and processed on a 128 by 128 pel grid. The width of the face was about 64 pels. Appropriate aperture tapering functions to reduce leakage (see Section 2.4) were not used in this study because portraits normally do have borders around them and it is interesting as an aside to examine leakage effects from such abrupt pattern edges.

The amplitude values of the original, variations of the original, and the filtered portraits were normalized to the same maximum and minimum values except where noted. The portraits were Fourier transformed by a digital Fast Fourier Transform technique (see Section 3.1). The resulting spectra were filtered by attenuating according to a two-dimensional contrast sensitivity function,  $MTF(H)$ , and/or ideal low-pass filtered. The filtered portraits were then reconstructed by performing an inverse Fourier transform.

The fundamental frequency is attenuated by the contrast sensitivity data obtained at 0.5 c/d. Thus the MTF filtered portraits should be viewed at about 2 degrees of visual angle (about 1.2 meters) to determine the fidelity of the MTF filtered picture to one's own visual filtering characteristics.

The reconstructed portraits were enlarged to 420 by 448 pels by creating a 4 by 4 block of uniform intensity for each of the 105 by 112 pels. Pictures of both one- and two-dimensional spectra were obtained. A log transform of these spectra was performed in order to increase the contrast of the low energy spectral components on the film (see Section 9.2). The spectra represent  $\pm 64$  spatial frequencies in two dimensions. The fundamental frequency of the face is  $f_1 = 2 \text{ c/picture width (c/pw)}$ .

The one- and two-dimensional magnitude spectra of the portraits in Figure 28 are shown in Figure 29. The one-dimensional magnitude spectra represent the spectra along the vertical axis of the adjacent two-dimensional spectra. The periodic structure in the transforms is due to truncation from a 23 by 16 pel border around the portrait that occurred when the original portrait was digitized to 105 by 112 pels for a 128 by 128 grid. The effect of this artifact is to multiply the spectrum of the portrait by the spectrum of a square pulse (e.g., see Figure 3). This resulting periodic structure hinders the visual analysis of the spectrum but has little effect on the filtered image, as shall be shown. Note the elliptical spectral form in all the two-dimensional spectra around the low spatial frequencies that is due to the basic shape of the face. Also note the relatively lower amplitude of the high frequency ray-like spectral forms (Figure 29,a) due to the details of the original portrait.

The filtered portrait in Figure 28,a,2 shows general smoothing of the portrait detail due to the high frequency attenuation. Note that there is no sharpening of the edges from the MTF filter. When these portraits are viewed at the appropriate distance of 2 degrees of visual angle, the resolution of the details of the original and MTF filtered portraits is in good agreement. Note, for example, the hair patch and the eyebrows. This result suggests that the shape of the MTF, even though primarily derived from threshold contrast sensitivity data, does provide a reasonable first-order approximation of our visual filtering characteristics over about 2 degrees of visual angle for suprathreshold vision.

The portrait information that is in the low frequencies is examined next. The previous filtering results suggest that about four harmonics should be required for the general face information. The face covers about half the width of the portrait. Therefore,  $8 \text{ c/pw}$ ,  $4 \text{ c/face(f)}$ , should provide the general form of the face. The results of such low-pass filtering are shown in Figure 28,a,3 where a very smoothed portrait is seen, as would be expected from low-pass filtering.

The same question that was asked in the previous chapter on the simple forms is asked: Do the low frequency attenuation characteristics of the MTF affect this important range of frequencies? This question is answered by low-pass filtering the portrait without prefiltering with the MTF. The result is shown in Figure 28,a,4 where, except for an increase in contrast, the forms are almost identical. Therefore, it is concluded that the low frequency attenuation characteristics from the MTF—moderate differentiation up to 6 c/d in this case—do not impair the basic form of even complex portraits.

### 10.3 Filtering Coarsely Quantized Portraits

Coarsely quantized spatial information greatly reduces the amount of information that can be extracted from an object. It is a crude form of low-pass filtering. There are certain visual displays that present coarsely quantized objects. It is important to determine how much usable information can be extracted from such displays (Ginsburg, 1973).

Harmon (1973) and Harmon and Julesz (1973) have previously demonstrated that a coarsely quantized portrait of Abraham Lincoln contained sufficient feature resolution for recognition. The coarse quantization of a portrait is, by

itself, a low-pass spatial filter operation that replaces the original spectral information with spectral energy at the fundamental sampling frequency of the coarsely quantized block and its harmonics. Harmon noted that recognition of the coarsely quantized portrait is improved by squinting, defocusing, or by viewing at a distance. These results suggest that the noise energy introduced at the higher spatial frequencies by the coarsely quantized blocks masks the perception of the low spatial frequency form information (Harmon and Julesz, 1973). Reducing that noise by means of high frequency attenuation allows the low spatial frequency form information to be more readily perceived.

This study will further investigate the similarity of form information contained in the original and coarsely quantized portraits by means of low-pass spatial filtering. Also, as in the original portrait, the effects of the MTF attenuation characteristics on the coarsely quantized portrait will be shown.

The original 420 by 448 pel portrait was coarsely quantized into 15 by 16 square blocks of uniform amplitude values; each block averaged over 28 by 28 pels. The result is shown in Figure 28.b.1 where the inhibited perception of the portrait is observed.

A certain amount of care has to be used to coarsely quantize a portrait to ensure that the original features, e.g., eyes, nose, and mouth, are sufficiently sampled. As Harmon (1973) noted, overall recognition increased from about 10 percent to 95 percent with optimally placed sampling blocks. This result can be understood in terms of sampling theory. There are 15 and 16 blocks in the horizontal and vertical directions, respectively. The sampling theorem states that a wave function must be sampled by at least twice the highest frequency that is to be unambiguously recovered (reconstructed) from that function. Undersampling the original portrait by the coarse blocks produces aliasing, i.e., false frequency energy introduced by the sampling function around the sampling frequency. Thus, at most, 7.5 and 8 c/pw spatial frequency information in the horizontal and vertical directions from the original portrait can be recovered, and spurious energy that does not contain portrait information will be introduced above the sampling frequency. This implies that the placement of the sampling blocks is critical in order to preserve accurately the low spatial frequency information below 8 c/pw, and one has to consider the particular features that are sampled by each block. Thus, the sampling blocks should be placed to sample the relevant low spatial frequency information of the original pattern — in the present case, the eyes, nose, and mouth, etc. — in order to maintain the original low frequency spatial information previously demonstrated to carry the basic form information.

The one- and two-dimensional log transforms are shown in Figure 29.a,b.1,2. The coarse quantization process removes all but the low spatial frequency elliptical structure to about 8 c/pw and replaces the original high frequency oblique ray structure with periodic rectangular components due to the block harmonics. Similarity exists between the line spectra of the original and coarsely quantized portraits only up to about 10 c/pw.

The effect of the MTF filter on this portrait is shown in Figure 28.b.2. The MTF spatial filter reduces the contrast, as expected from the low-spatial frequency attenuation characteristics of the filter, and only local smoothing occurs. Observation of the original and MTF spatial filtered portraits at about 2 degrees of visual angle reveals similar feature resolution even though substantial contrast reduction is evident. Again the high frequency attenuation of the MTF spatial filter appears to provide a good first approximation for resolution of features under suprathreshold viewing conditions.

MTF spatial filtering followed by low-pass spatial filtering,  $f \approx 4$  c/f, results in the coarsely quantized portrait shown in Figure 28.b.3. Figure 28.b.4 shows the results of low-pass filtering on its own, appearing very similar to Figure 28.b.3 except for contrast. Thus, the low spatial frequency attenuation characteristics of the MTF—differentiation up to 6 c/pw—have little affect upon the low spatial frequency form information of this portrait. However, a comparison between MTF low-pass spatial filtered original and coarsely quantized portraits demonstrates a marked decrease in contrast of the eyes, nose, and mouth, as well as left cheek and shoulder, in the coarsely quantized portrait. But, again, these results should be tempered with the realization of the importance of the block placement in sampling the original pattern features.

#### 10.3.1 Why Does Coarse Quantization Reduce Form Perception?

Although Harmon and Julesz (1973) suggested that portraits were masked by the noise introduced by coarse

quantization, there would seem to be other factors that reduce the perception of coarsely quantized portraits.

First, the degree of quantization in both this study and that of Harmon and Julesz (1973) occurs at the sampling limit for the basic features such as the eyes, nose, mouth, and overall shape. In addition to being almost impossible to sample such general features to the same degree because of the uniform sampling size that was used, such coarse sampling reduces the amount of spatial information about the portrait to almost zero and introduces aliasing. The lack of details (the higher spatial frequencies of the eyes, etc.) and the result of aliasing (spurious patterns resulting from spurious spectral energy) can be seen quite clearly by comparing the original and coarsely quantized filtered portraits in Figure 30. These original and coarsely quantized portraits have been low-pass filtered from  $f = 24, 16$ , and  $12$  c/pw.

A second factor arises if it is accepted that mechanisms in the visual system perform piece-wise Fourier-like filtering over finite areas of an object. An object is bounded by its edges. The higher the contrast of the edges, the more likely it is that the object has distinguishable boundaries. In such a scheme each block and/or multiples of blocks with similar amplitudes that make up the coarsely quantized picture would be considered to share the same boundary and could be analyzed separately. That would create difficulty in determining the lower harmonics for the overall form of the portrait. This point is discussed further in Sections 13.3.1 and 19.9.3.1.

A third factor is the creation of Mach bands by coarse quantization (Ginsburg, 1973). Note that many of the blocks of low contrast that are adjacent to blocks of similar contrast in Figure 28b,1 do not appear to have uniform brightness distributions. The narrow region of lighter and darker brightness distribution along the edges of those blocks appears similar to the brightness distributions of Mach bands. Thus, the amplitude of the original blocks will not be completely uniform and the average values will change, depending upon the magnitude of the Mach bands. This will further reduce the already minimal fidelity of spatial information from sampling considerations about the object that could be extracted by other visual processes.

All of these effects need to be investigated further. It seems clear, however, that critical band masking is not the only factor to be considered in such problems.

#### 10.4 Filtering a Portrait with Random Noise Added

This next demonstration investigates the appearance of the woman's portrait to which a two-dimensional random noise pattern with a uniform amplitude distribution was added. The amplitudes of the pels were normalized so the maximum amplitude of the picture did not exceed the limits of the computer range.

The result of adding random noise to the original portrait is shown in Figure 28,c,1 where the main effect of the noise is to greatly reduce the detail, particularly in the eyes, nose, and mouth.

The one- and two-dimensional spectra (Figure 29,c,1,2) contain very little structure except at the low spatial frequencies, below  $8$  c/pw, where the two-dimensional elliptical structure from the basic face form persists. The line spectrum reveals a profile more similar to the original line spectrum than that of the coarsely quantized portrait. The spectra again suggest that the basic portrait form is relatively intact below  $f = 4$  c/f.

The effect of the  $MTF(H)$  spatial filter reveals a smoother, more cosmetically appealing portrait (Figure 28,c,2) with quite similar feature resolution of the eyes, nose, and mouth, although with increased contrast.

Low-pass spatial filtering the filtered noise portrait with and without MTF prefiltering to  $f = 4$  c/f (Figure 28,c,3,4) once again reveals similar form information virtually unaffected by the MTF attenuation characteristics.

##### 10.4.1 Artifacts from a Portrait with Random Noise Added

It is important to realize that random noise can be correlated with pictures in specific ways. In other words, the same size random noise with a constant amplitude distribution that results in a uniform amplitude spectrum, created with different random values, will affect the original picture differently. This is demonstrated in Figure 31,a,1 where another random noise pattern with the same parameters as before is added to the original portrait. Note especially the

eyes, nose, mouth, and left cheek differences between this portrait and that of Figure 28.c.1. The different spectrum resulting from this second added random noise portrait is apparent upon observation. The low-pass spatial filtered portrait for  $f = 4 \text{ c/f}$ , shown in Figure 31.a.3, demonstrates similar form information; however, note the difference between the resolution of the hair and the displaced mouth in comparison to Figure 28.c.3. These results suggest caution in experiments based upon picture correlated random noise, because even those features that contain only low spatial frequencies can be affected differently by different random noise obtained from a similar noise generating process.

### 10.5 Filtering a Portrait with Inclusive OR Random Noise

The portrait with added random noise has a uniform amplitude distribution that will increase the average intensity of the portrait if the average noise exceeds that of the original portrait. That result may account for some of the decreased contrast of the pattern information after spatial filtering. In addition, it has been demonstrated that adding different patterns of random noise with a uniform amplitude distribution constructed from elements of the same size affects the basic portrait form. This next study was undertaken to reduce the average pattern intensity as well as to combine the same random noise pattern in a nonadditive fashion. The desired result was achieved by inclusive OR-ing the original portrait with the random noise, as shown in Figure 31.b.1. (The inclusive OR is a logical binary bit operation that places a 1 if either or both the random noise value and the portrait value have a 1 in the same picture value bit position). Note the decreased perception of the nose and mouth in comparison to the added noise portraits.

The two-dimensional log magnitude spectrum (Figure 31.b.2) reveals an elliptical low spatial frequency structure similar to that of the other portrait configurations. In addition, spectral energy is less random, as well as reduced, along the vertical and horizontal axes, due primarily to the reduced intensity differences along the portrait edges.

The low-pass spatial filter results are shown in Figure 31.b.3 for  $f = 4 \text{ c/pw}$  in which the filtered portrait is seen to contain the general form information. However, the general homogeneous contrast of the features of the face found in the original or random noise portraits is lacking. In particular, note the decreased resolution of the mouth in comparison to the other portrait configurations. However, even with this portrait, a system that can extract similar form information appears to provide sufficient information for classification.

### 10.6 Filtering a Binary Line Portrait

One of the most interesting aspects of perception is that line patterns can represent complex forms such as portraits. That line patterns can abstract and provide basic pattern information was demonstrated by Attneave (1954). He showed that information about forms could be obtained from edges or contour lines of a form at points of change in gradients and points of greatest change of contour direction. But how do edges and lines contain form information? In general, edges and, particularly, lines contain high spatial frequency information. This might seem to be at odds with the notion of basic form information being provided by low spatial frequencies; however, it has been demonstrated (see Section 9.6) that the low spatial frequencies of the lines of the similarity groupings contain homogeneous group information. Perhaps the lines of complex patterns can also provide form information in the low spatial frequencies. If line configurations contain low frequency information which is similar to that in normal grey-scale portraits, then perhaps one can consider lines not as explicit features to be detected and manipulated (therefore explicitly carrying the form information) but as pattern elements that can provide low spatial frequencies that have been shown to convey the basic form information of objects. The subsequent demonstrations will amplify this point.

To test this hypothesis, a binary line portrait was created from an edge portrait (Figure 32.a.1) by replacing all the picture values less than a certain value by 1 (white) and those greater than that value by 0 (black), as shown in Figure 31.c.1. Note that the most distinct lines come from regions of greatest contrast in the original portrait.

The two-dimensional log magnitude spectrum, shown in Figure 31.c.2, reveals a loss of elliptical spatial frequency structure found at the low spatial frequencies of the other portraits. The medium spatial frequencies reveal slight off-axis ray structure in comparison to the original portrait. Although the low frequency energy of lines is quite low compared to that found in a normal portrait, the lines still provide more energy at the low spatial frequencies than is found at the high frequencies.

Low-pass spatial filtering to  $f = 4 \text{ c/f}$  demonstrates basic portrait form information comparable to the previous portrait

configurations (Figure 31,c,3). Note the hair, cheek, chin, and shoulder outlines. The eyes, nose, and mouth are the most prominent features in the reconstruction. Note that the right eye is the most emphasized feature and that the nose and mouth cannot be resolved.

It appears that the low spatial frequency forms of line objects are similar to the other portrait configurations. It is worth noting that the prominent features in the original line portrait — the eyes, nose, and mouth — that are most dissimilar from the original portrait configuration also remain most dissimilar in the low spatial frequency reconstructed line portrait. This result suggests that even complex linear binary patterns can convey certain form information, from only low spatial frequency bands, that can be used for classification, recognition, and identification. Of course, in these and other comparisons, the similarities of the filtered images are based on subjective evaluation. This is adequate for these studies. More quantitative comparison can be made by correlating the filtered spectra or images (e.g., see Ginsburg, et al., 1976).

### 10.7 Perception of Reversed Contrast Portraits

The preceding filtered line portrait revealed similar form information in low spatial frequencies when compared to other portrait configurations. This suggests that the low spatial frequency structure of lines may be important information for perceived similarity of objects. However, an alternative hypothesis is that the edge information of the original and line portraits is similar and thus explicitly provides similar portrait information (implying that the similar low spatial frequency information is coincidental). Is there a method for obtaining the same edge and line information while varying the spatial frequency information? The answer is yes, based upon a consideration of the spatial frequencies of the negative of an object. A reversed contrast object, that is, one with black and white interchanged, contains identical edge information but dissimilar spatial frequency information (e.g., see Lipson and Lipson, 1969, Section 7.4.7). If the edges provide the basic information explicitly (that is, identification results from the detection and manipulation of the edges), then it would be expected that changing a black edge into a white edge, and vice versa, would have no major effect on the perceived portrait information. It is well known that photograph negatives are harder to recognize and identify than positives, a result that immediately suggests that edges may not carry the primary information for form. This fact is demonstrated by two positive and negative portraits shown in Figure 32,a,1,2.

These portraits obviously contain similar information. Figure 32,a,2 has reversed picture values that, although they contain identical edge information, notably affect the perception of the eyes, nose, and mouth in such a way that portrait similarity and, hence, identification are decreased.

A more interesting example of the inadequacy of isolating edge and line information for perception is shown in Figure 32,b,1,2 where the original grey-scale portrait was converted by a binary programme that made all the picture values between two levels white and all other values black. Again, similarity between this and the original portrait is easily seen. However, when these values are reversed, as shown in Figure 32,b,2, portrait similarity is greatly decreased. Except from critical examination of the head, neck, and shoulder outline, portrait information is very dissimilar. Note, in particular, that even with much effort, the mouths of the two portrait configurations do not convey the same information. The two black spots are highlights in the lower lip of the positive portrait but appear as two teeth in the negative portrait. No matter how conscious an attempt is made to isolate these features from the influence of the surrounding mouth, segregation resulting in another interpretation does not seem possible. These effects are even more apparent when the portraits are viewed at about 2 degrees of visual angle.

These results further demonstrate the classic Gestalt view that the sum of the parts is different than the whole. In a filter concept of perception, highlights cannot be extracted explicitly but must be analyzed as a whole with surrounding mouth features. These results also suggest that it is the low spatial frequency information that carries the basic portrait frequency information. By viewing the portraits from a distance, the high spatial frequencies are more attenuated than the low spatial frequencies, and the relative dissimilarities between the portrait configurations are seen to remain.

### 10.8 Summary

This chapter extended the application of the concept of filtering from simple to complex objects: portraits. Subjectively

similar form information was shown to exist within a two-octave band of low spatial frequencies for a wide variety of different portrait configurations, including noise and line versions. Visual texture in terms of spatial filtering is investigated next.



## CHAPTER 11

### VISUAL TEXTURES

#### 11.1 Introduction

Our visual world is rich in textures—multiple patterns that share some common spatial properties. Understanding how the visual system extracts information from texture is important because of the role that texture plays in separating objects from their background (figure-ground), e.g., Julesz (1971). Furthermore, this understanding is necessary if machines are to be made to perform similar functions (Ginsburg, 1973).

Textures can be defined in terms of either spatial features or transformations. The explicit extraction of spatial features, such as edges, lines, orientation, contrast, etc., has been suggested by many researchers, e.g., Hawkins (1970). This section shows how much simpler and parsimonious filtering can be in extracting certain textures when used in conjunction with operations consistent with known visual processes.

Spatial frequency content has been shown to distinctly characterize certain textures, e.g., Cutrona (1965); Lendaris and Stanley (1970). For example, certain geographical characteristics can be distinguished by their spatial frequency content, e.g., Goldstein and Rosenfeld (1964). Although substantial overlap can occur in spectra from certain complex scenes (Johnston, El-Sum, Rudin, Sikorsky, and Feigenbaum, 1964), there still can be good separation in certain regions of spatial frequencies, (see Figure 4 of Hawkins, 1970). The search for different spectral bands to separate various textures may prove more fruitful than an analysis of the complete spectrum, just as generalized forms were shown to exist from only the low spatial frequencies of objects when the rest of the spectrum was filtered out.

#### 11.2 Two General Figure-Ground Problems

It was shown in Section 9.6 that low-pass filtering can offer an explanation for the perception of figure-ground from textures made of dots and lines. Here, an initial investigation of figure-ground is made in terms of the anisotropic filter characteristics and the spatial frequency/orientation-selective nature of channels in the visual system.

##### 11.2.1 Isolating a Rectangular Form from Oblique Lines by Spatial Filtering

Consider the figure-ground object in Figure 33.a. The problem here is to extract the rectangular form from the background. This is a simple task for an anisotropic spatial filter, such as the  $MTF(H)$ , that attenuates the oblique structure in Figure 33.b. Similar extraction of the rectangle could be achieved if the spectral components in the obliques were removed. Note that low-pass filtering (Figure 33.c,d.) only signals that there is an object in the original pattern.

##### 11.2.2 Isolating Oblique Structure in a Real Scene by Spatial Filtering

Another example of the power of spatial filtering that can enhance specific regions of spatial frequency in a global manner is shown in Figure 34. Note that all the collinear lines in this real scene can be attended to in one orientation at a time. Filtering out the two different oblique regions of the spectrum separates the linear objects into two groups, as shown in Figure 34.b and c.

It should be clear, once any object is analyzed into quasi-independent channels of different spatial frequencies (size) and orientation, that such isolation of objects is quite simple. However, does the filter concept have predictive power with other figure-ground problems such as letter arrays, random dot patterns, and more complex scenes? Furthermore, how can those objects that are filtered be separated from the field? These questions are examined next.

#### 11.3 Similarity Grouping of Letter Arrays

The variables of similarity grouping found important by Julesz (1962), Beck (1966,a,b; 1967; 1972), and Olson and Attneave (1970) are shape, slope, and brightness. The results of Pickett (1970) agree with those findings and also with

the results of Julesz (1971) which suggest that the visual system contains a "slicer" mechanism that operates on texture clusters of similar brightness. Ginsburg (1971,a,b; 1973), and Ginsburg, et al. (1976), have shown that anisotropic low-pass filtering can segregate certain textures into objects of homogeneous brightness. Here, similar groupings using the MTF filter are shown.

### 11.3.1 Similarity Grouping Due to Orientation Differences

Texture fields that contain repeated objects differing only in orientation will not be considered because, as previous examples of orientation-selective filtering have shown, they can be easily separated from one another by quasi-independent orientation channels.

One of the major problems with present theories of feature analysis is typified by a basic dichotomy that emerges from the results of Beck (1966,a,b) and Eichelman (1970). Similarity judgements of paired letters had little predictive power in determining how the letters would group when they were made into arrays. An example is shown in Figure 35,a, in which the tilted T (TT) may be seen as more similar to the upright T (UT) than is the L. However, when these same letters are arranged in arrays (Figure 35,b) the opposite grouping occurs.

Ginsburg, et al. (1976), have suggested that the paired letters are judged for similarity with the same metric used for machine pattern classification tasks—Euclidean distance (cross-correlation) of the low spatial frequencies of the letters. However, the arrays of letters appear to be processed in a global manner. Comparing the features of the individual letters would provide the same grouping as paired letters. However, the letter arrays can be segregated by a more global property, e.g., brightness distribution due to the anisotropic spatial filtering of the visual system (Ginsburg, et al., 1976). Note that the cross-correlation is a measure of the similarity of the letters, whereas the effects of brightness provide measurable differences between the letters.

The segregation of the letters in letter arrays by the MTF filter is shown in Figure 36. The TTs are clearly less visible than the UTs and Ls (Figure 36,c). (These results are general demonstrations of the effects of the MTF filtering because the coarse quantization of the TTs in these pictures provides additional information by which the letters can be segregated.)

The effects of the MTF filter are particularly relevant to the objects used by Beck (1966,a,b; 1967; 1972). The size of the objects ranged from only 10 to 31 minutes and luminance values were scotopic, 0.025 to 0.29 foot-lamberts. These values suggest that similarity judgements were being made with high spatial frequency patterns of low contrast. From the discussion in Section 5.2.1, these are the conditions that produce the greatest degree of anisotropy in the human visual system. Experimental predictions based on this analysis are discussed in the next section.

### 11.3.2 Similarity Grouping Due to Configuration Differences

Beck (1966,b) used simple geometric objects and letters to determine the effect of orientation and shape similarity on perceptual grouping by having subjects partition arrays of different patterns into two regions. Studies by the author with anisotropic filtering readily segregated the patterns in terms of orientation. Independent orientation channels easily handle such tasks. However, some of his arrays contained objects with only shape, not orientation differences. Can these results also be explained by brightness differences due to the MTF filtering? The answer appears to be yes, based on the results of the MTF filter on a typical array in Figure 37. Here the Ls segregate from UTs and sideways Ts (ST) by brightness also because of the low-pass filtering characteristics of the MTF.

The magnitude spectra for both the T and L in Figure 37, normalized from 0 to 10, are shown in Figure 38. (The spectrum of the sideways T is not shown because it is the same as the UT rotated by 90 degrees.) Note that L has less spectral energy at the low spatial frequencies than does the T (see the squares in Figure 38). Thus, it is not too surprising that the L will be affected more by the low-pass filtering characteristics of the MTF than the T.

The numerical printouts of the filtered array (Figure 39,a,b) confirm the observations with the pictures. Also note that the intensity distribution of the same letters is not equal. This result suggests that grouping of such objects depends on

some local average brightness, not on precise values. Furthermore, this example suggests that changes in the brightness distribution occur with different pattern configurations. Thus, the proximity of similar patterns affects judgements based on local brightness. The magnitude of such effects on similarity judgements must be determined experimentally.

Many of the other results of Beck and Olson and Attneave were analyzed in a similar manner, but these results would require a lengthy discussion. The effects of low-pass filtering on grouping of these kinds of arrays can be demonstrated easily by squinting or viewing the arrays (Figure 40) at a distance. Different brightness distributions occur as Figure 40 is rotated to different orientations. In general, it appears that not only the primary results of the experiments of Beck and Olson and Attneave can be explained in terms of filtering but also the second and third order effects.

### 11.3.3 Second Order Effects of Grouping: Symmetry

One example of a second order effect will be discussed. Beck (1966,a) reported in two experiments that the TT grouped further away from the UT than the X. These results cannot be explained by differences in orientation because the TT and X have the same orientation. However, the X has two-fold symmetry; the TT does not. Thus, the X will have more energy in the lowest spatial frequencies than will the TT. This may be seen by comparing the numerical printouts of the normalized intensity values of the filtered X and TT shown in Figure 41,a,b. The total intensity for values of the images equal to or greater than 30 for the X is 418 and only 314 for the TT. Thus the TT contains about 25 percent of the intensity of the X for values of intensity equal to or greater than 30.

Noting the intensity distributions of the MTF filtered UT and X and UT and TT (Figure 41,a,b), it is quite evident that the X would provide a brighter object than the TT. This result helps to explain why subjects reduced the brightness of the UTs in an array of UTs and Xs less than in an array of UTs and TTs. There is a greater difference between the brightness of the UT and TT than the UT and X.

The filter analysis is consistent with the information about the intensity of the letters that were presented to the subjects in the experiments. The array sizes used by Beck (1966,a) ranged from 5 degrees, 10 minutes to about 10 degrees, 30 minutes. As Beck (1972) pointed out, peripheral acuity blurred peripheral objects. Beck used that fact to suggest that the poor grouping of the Xs occurred because they would readily lose discriminability with blur. However, the major difference between the filtered letters (Figure 41,b) is the increased intensity at the centre of the X compared to the TT. Although the overall extent of the X is slightly reduced in comparison to the TT after filtering (as these filtered letters show), the central intensity values of these letters suggest that the X will retain more form information than the TT.

Beck further supports his argument with his finding that when the Xs were larger, they grouped as well as the tilted Ts (Beck, 1972, p. 16). However, the size of the letters was changed by only a factor of 1.2 (5 mm to 6 mm) in the two experiments that he discusses. The mean luminance of the standard pattern in the two experiments differed only by a factor of 2.5 (0.114 to 0.29 foot-lamberts). Finally, his statistical analysis showed no significant difference between the grouping strength of the X and TT in the second experiment; the difference between the mean luminance values required for grouping in the two different experiments were quite similar, 0.015 and 0.013 foot-lamberts. This analysis of his results suggests that there was little if any difference between the grouping of the X and TT in the two experiments—a result that is consistent with filtering. Other filtering by the author suggests that small changes in size (a factor of 1.2) would produce too little difference in the intensity distribution of these objects to change the general results. This analysis further suggests that it is the relative brightness, i.e., contrast, between the objects due to filtering and not the relative discriminability that is the major grouping variable in these experiments. Of course, further investigation is required to assess the relative importance of each of these variables.

These filtered letters suggest a counter-intuitive prediction—The similarity judgements are based primarily on the brightness differences of the different letters due to the filtering effects on shape and orientation. This suggestion predicts that *increasing* the brightness of tilted objects in an array will reduce their discriminability under certain conditions. Experiments support this prediction (Eichelman and Ginsburg, 1977).

To summarize, arrays of patterns such as those used by Beck (1966,a,b; 1967; 1972) and Olson and Attneave (1970) appear to group in a manner consistent with those predicted by brightness effects based on anisotropic spatial filtering of the slope and shape of the patterns. These arrays are made up of relatively simple patterns. Is the filter concept

relevant to more complex figure-ground patterns such as random dot patterns? These are investigated in the next section.

#### 11.4 Isolating Objects from Random Dots

##### 11.4.1 Isolating Form and Symmetry from a Random Dot Pattern

Perhaps some of the most complicated figure-ground problems involve the extraction of objects from random patterns. An example is given in Figure 42,a—a random dot pattern created by Julesz (1971). The problem here is to understand how the visual system so rapidly and seemingly effortlessly extracts symmetry information and the face-like objects from such a noisy pattern. Julesz (1971, 1975) suggested that textures differing in first order statistics (e.g., intensity values) are easily seen. However, he does not provide any insight into how the visual system performs such tasks. Marr (1976) also suggested that first order discrimination and grouping processes were used to extract forms from filtered textures. Unfortunately, Marr's complex techniques were based upon *ad* and *post hoc* assumptions of what makes up and extracts information from objects. Ginsburg (1973) showed that the filter characteristics of the visual system—the two-dimensional MTF—can create somewhat homogeneous forms whose first order statistics (intensity) were used to begin isolation and extraction of form from a random dot pattern.

The result of that spatial filtering is shown in Figure 42. The original pattern is filtered by the MTF (Figure 42,b) or a low-pass (24 by 24) filter (Figure 42,c) to cluster proximate dots of similar intensity. This result demonstrates that *general* filtering processes in the visual system can form homogeneous clusters in a simple manner. Furthermore, when retinal inhomogeneity is considered, such filtered information *has* to exist in at least the peripheral retina when the original pattern is viewed. The general symmetry of this complex pattern can be found easily from the low spatial frequencies of the pattern, as shown in Figure 41,d,e. It is suggested that higher-order visual processes can attend to symmetry in objects filtered from channels whose bandwidth captures relatively low spatial frequencies. More detail about this point is provided in Section 19.4.9.

##### 11.4.2 Isolation Objects of Different Size in a Random Dot Pattern

Another example of how a filtered image separates figure from ground by creating different areas of intensity from similar random distributions of different size objects is shown in Figure 43. Here, the small square can be seen immediately in the lower right corner. The region of small squares is seen to have different average contrast than the rest of the picture after MTF filtering. The high frequency attenuation characteristics of the MTF filter reduce the average contrast of the region of small squares. The binary picture in Figure 43,c is created from the upper 30 percent of the intensity values of Figure 43,b to show the differences between the peak intensities inside and outside the square region.

#### 11.5 Analysis of a Complex Scene

Results of previous research into texture analysis (Ginsburg, 1973)—some of which were presented here—were used to analyze the complex scene shown in Figure 44,a. The problem is the identification of letters in the words by using filtering methods that may be similar to those used by the visual system. Figure 44,b represents the selected area of interest and the general amount of information that may be contained within the parafoveal region. A log transform of the picture in Figure 44,b, shown in Figure 44,c, improves the contrast of the features of the letters. Figure 44,d shows the result of low-pass filtering. The lack of general form information demonstrates that a global analysis based on filtered images of this kind would be unsuccessful in providing sufficient information for the identification of these letters.

How can letters be isolated and recognized on such a noisy background? Previous results on texture analysis suggested that objects could be extracted from differences in brightness. First, the picture is digitized into 128 by 128 pels for computer processing. This is a crude method of low-pass filtering. Digitally slicing approximately 30 percent of the lowest intensities contained in the picture (shown as the brightest objects in Figure 44,e) and using them to create the picture in Figure 44,f captures the elements that make up each letter, plus a small amount of noise. (A  $\pm 5$  percent change in the intensity values that were selected works equally well.) The solution to the remaining problem of

classifying the letters from these discrete features has already been offered for man and machine (Ginsburg, 1971,a,b). The "Gestalt" of these objects is found from the low spatial frequencies, as seen from Figure 44,g using the MTF filter or Figure 44,h using ideal low-pass filtering. In practice, each letter would be isolated and processed separately as done by the fovea when these pictures are held at normal reading distance.

There are, of course, many other possible ways to extract similar information from the original picture. The point here is that it has been accomplished using simple methods believed to correspond to the filtering properties of the human visual system. Furthermore, these results have gone beyond simply the extraction of the relevant features. The information that was extracted is sufficient for classification by man and machine (Ginsburg, 1973).

### 11.6 Monocular Texture Gradients

Certain lighting conditions can create shadows (contrast gradients) that cause certain patterns to be perceived in depth. Gibson (1950) has shown that certain textures whose elements have the same contrast and size and converge at some point can also convey a perception of depth with monocular viewing (Figure 45,a). Can any relationship be shown to exist between contrast gradients of the filtered image and of similar textures and the perception of depth? The author noted that pattern elements that were close to one another or were of different size generally had different contrast after filtering. These results prompted filtering of a digitized textured field taken from Gibson and shown in Figure 45,b. Note that the pattern elements originally having the same contrast but different sizes and proximity give the impression of perceived depth. The MTF filtered image (Figure 45,c) shows that the pattern elements of different sizes and proximity have different contrast. It is possible that one aspect of perceived monocular depth is the different relative intensity levels (contrast) of the features in the filtered image of a channel (See Section 13.6 for other examples.)

### 11.7 Summary

This chapter provided demonstrations of techniques based on suggested processing capabilities of the visual system which attempt to solve problems of the perception of visual textures. The important grouping variables that other researchers have found—object shape, orientation, and brightness—were shown to be provided by filtering mechanisms in the visual system. The success of a counter-intuitive experiment based on these results suggested the predictive power of these techniques and analyses. A complex scene was analyzed for the extraction of objects sufficient for machine classification using filtering methods based on the previous analysis. Finally, an example of a texture gradient that provides monocular depth cues was examined by spatial filtering. Next, the same spatial filtering is applied to offer an explanation for the perception of visual illusions.

## CHAPTER 12

### VISUAL ILLUSIONS

#### 12.1 Introduction

An understanding of visual illusions is important because they demonstrate instances in which the visual system fails seemingly simple tasks. Lines and angles in very simple geometric patterns are seen distorted into different shapes, lengths, and orientations. A full understanding of perception would have to include an explanation of visual illusions.

A number of theories of visual illusions have been proposed. Contemporary theories to account for the appearance of illusions have invoked such factors as distortions due to diffraction and optical aberrations in the eye, (e.g., Chiang, 1968), physiological mechanisms, e.g., lateral inhibition (e.g., Ganz and Day, 1965; von Békésy, 1968; Blakemore, Carpenter, and Georgeson, 1970), and cognitive explanations (e.g., Gregory, 1963; Day, 1972). The reader is referred to an excellent review by Robinson (1972) on illusions and the various theories used to attempt to explain them.

The analysis of visual illusions presented here represents a continuation of research by the author that regards illusions as a consequence of the manner in which the visual system processes all spatial objects: by spatial filtering (Ginsburg, 1971,a,b; 1973; 1975; Ginsburg, et al., 1976).

In the introduction of this dissertation, it was stressed that the visual system must be throwing away large amounts of detailed information. In Chapters 5, 6, and 7, the neurophysiological and psychophysical evidence for the limits of spatial resolution in the fovea as well as the parafovea was discussed. Furthermore, the spatial bandwidth of mechanisms farther up the visual pathway becomes increasingly narrow.

There must be some consequence to the throwing away of certain details about objects at the various stages of visual processing. Two consequences of losing detail are that intensity and spatial information are distorted, as has been shown previously in many of the filtered images. From this point of view, visual illusions result primarily from the spatial filtering properties of the visual system. Thus, filtering geometric and contrast illusions with spatial filters based on the filtering characteristics of the visual system generally resulted in the distortions that are perceived when they are viewed, as shall now be shown.

#### 12.2 Illusions of Noncollinearity

##### 12.2.1 Variations and a "Correction" of the Poggendorff Illusion

In the Poggendorff illusion (Zöllner, 1862), the collinear oblique lines that transverse the parallel lines are not perceived as collinear (Figure 46,a,1). Since this illusion depends upon judgement made on the collinearity of lines that form an angle with other lines, the spatial filtering results on the Müller-Lyer illusion (Ginsburg, 1971,a,b; Ginsburg, et al., 1976) would predict a shift in the intensity distribution at the intersection of the collinear oblique lines and the parallel lines into the acute angle.

The result of MTF filtering and low-pass filtering with and without MTF prefiltering is shown in Figure 46,a,3,4,5. Placing a straight edge over the peaks of the intensity distribution of the collinear lines demonstrates the lack of collinearity, especially in the low-pass filtered images. However, even though the filtered objects have been shown to well represent the intensity distribution of the computer plots and printouts, the numerical printouts shown in Figure 47,a,b provide objective quantitative measures of the distortions due to spatial filtering. The filtered images and the numerical printouts confirm the prediction and suggest that the illusion is due to bending of collinear lines at their junction with the parallel lines.

In this filtered image and those that follow, the magnitude of the distortions is assumed to be determined by the following rules. The orientation of a line is judged on the basis of the axis connecting the two highest intensity peaks after filtering. The length of a line is judged on the basis of distance from the peak-to-peak intensity values of the line

and/or the distance from intensity edge to intensity edge, depending upon which measure is easier to determine in these demonstrations. An experiment discussed in Section 12.8.1 attempted to determine the relevant intensity features of the filtered images of an illusion.

If similar spatial filtering in the visual system accounts for the distortion in the Poggendorff illusion, then an inverse MTF filter should provide the intensity distribution that cancels the distortion. An inverse filter,  $MTF^{-1}$ , filtered the original illusion with the general result that the collinear lines were shifted in the opposite direction at the junctions with the parallel lines (Figure 47,c).

It is emphasized, however, that this inverse filter technique is only an approximation because the minimum MTF values become infinitely large, and vice versa, when the original values of the MTF are inverted. This is why the parallel lines are almost absent in the  $MTF^{-1}$  numerical printout; they are greatly reduced in the  $MTF^{-1}$  filtered image in comparison to the obliques. Furthermore, the inverse filter technique appears useful only for geometric illusions that involve angles and not absolute line length such as the horizontal-vertical line illusion of Figure 53,a. Other studies by the author suggest that the inverse filter cannot distribute intensities to places where none existed in the original object; it appears to be only able to shift existing intensity distributions.

The original results of the filtering suggest that the "correction" to this configuration of the Poggendorff illusion is to bend the collinear lines at the junction opposite the filtered illusion. This correction is shown in Figure 48,b where, in comparison to the standard Poggendorff illusion (Figure 48,a), the corrected illusion shows a substantial reduction in, if not a complete loss of, the perceived distortion. The reader is encouraged to place a straight edge across the collinear lines to see the small degree of curvature at the junction that is present.

It is interesting to note that Helmholtz (1909) suggested that the original Poggendorff illusion was due to the bending of collinear lines at the junction where the obliques meet the parallel lines, similar to that found in the numerical printouts of the MTF filtered illusion.

Koboyashi (1956) first demonstrated that the Poggendorff illusion disappeared when the obliques were bent at the intersection with the parallel lines. The filtered data presented here show why such a demonstration works.

The corrected illusion does not seem to be greatly dependent upon viewing distance. An interesting fact is observed at about 0.5 degrees: The corrected illusion exhibits negligible distortion even though the correction is not seen at that distance. Also note that the illusion persists (although somewhat decreased in comparison to the original illusion) when the intersections of the oblique lines with the parallel lines are removed (Figure 48,c). It should be clear from the earlier examples of filtered images that low-pass filtering this particular illusion will still cause a shift in the intensity distribution in the same direction as perceived distortion. These two observations (as well as other arguments presented later) suggest that perceived distortions are based upon spatial information present in low spatial frequency channels.

Two variations of the Poggendorff illusion (Pressey and den Heyer, 1968) are shown in Figure 46,b,1,c,1. The original Poggendorff illusion persists with the oblique angles only (Figure 46,b,1). However, the illusion is diminished (Pressey and den Heyer, 1968) or reversed (Restle, 1969) when only the acute angles of the Poggendorff illusion are present (Figure 46,c,1). In this case, if judgements are made of the vertical position of the obliques based on the peak intensities or extremities of the filtered objects, a continuum of judgements can be made which result in a decreased or reversed illusion.

There are other attributes of the filtered illusion such as small changes in angle and curvature of the collinear lines whose relative importance to the illusion appears to be second order and will not be discussed further here.

### 12.2.2 An Illusion Due to Error in Aligning Edges

A very simple geometric illusion, shown in Figure 49,a, was reported by Loeb (1895). The short line at the right is seen slightly above the longer bottom line at the left with which it is collinear. This illusion is stronger when it is rotated 45 degrees (Hotopf, 1975). The MTF filtered image shows the perceived distortions in the numerical printout of Figure 49,b. Note the relative shift of the average intensity on each side of the original line. The parallel lines on the left shift

away from each other. The line on the right remains in essentially the same position. The overall effect is that the line on the right appears to be displaced upwards. These effects are increased when the illusion is rotated 45 degrees (not shown), due to the anisotropy of the two-dimensional MTF.

### 12.3 Illusions of Line Length

#### 12.3.1 Variations of the Müller-Lyer Illusion

A digitized representation of the Müller-Lyer illusion (1889) is shown in Figure 50,a,1. Lines of equal length are perceived to be longer and shorter if out-pointing and in-pointing fins are added to the ends of the lines.

A variation of the Müller-Lyer illusion has the fins only (Brentano, 1892), as shown in Figure 50,b,1. Here the illusion is that the distance between the tips of the out-going fins is less than the distance between the tips of the in-going fins.

The MTF (Figure 50,a,b,3) and low-pass filtered images of both illusions (Figure 50,a,b,4,5) show the perceived distortions, confirming the optical filtering results of Ginsburg (1971,a,b).

Müller-Lyer (1896) created a variant of his original illusion, a digitized version of which is shown in Figure 50,c,1. Here the extension of the fins causes a perceived decrease in line length compared to the same line with shorter fins.

This illusion provides one counter-example against a general optical blur, smoothing, or assimilation theory for geometric illusions. Any averaging process would keep the lines the same length or increase the length of the line with the longer fins because there would be more spatial information over which to average from the longer fins than the shorter ones.

The magnitude of the digitized version of this illusion is small. It is also very slight in the MTF filtered object (Figure 50,c,3) but stronger in the low-pass filter results (Figure 50,c,4,5). These distortions can be seen more clearly in the contour plot, Figure 51. The shorter line length with the longer fins is not seen in the blurred image shown in Appendix C. Note also that the blurred image still appears to provide the illusion.

#### 12.3.2 The Ponzo Illusion

The original Ponzo illusion (Ponzo, 1912) contains two parallel lines equal in length which are seen as unequal in length when they are placed between two converging lines (Figure 52,a).

The results of filtering this illusion using the MTF and low-pass filter are shown in Figure 52,c,d,e. The upper horizontal line (apical) is extended into the vertical oblique lines, an effect not seen with the lower horizontal line (distal). Note the decreased intensity at the ends of both lines. Thus, the apical line seems longer from such spatial extension; the distal line appears shorter. This particular result is consistent with the experimental findings of Quina and Pollack (1972), who found, in addition to overestimations of the length of the apical line, that the length of the distal line was consistently underestimated.

Attneave (1972) pointed out that the distance between the horizontal and oblique lines was an important variable relating to the magnitude of the illusion. Variations of the Ponzo illusion similarly filtered show such changes. However, the general distortions persist with low-pass filtering. Shultz (1976) noted that, in addition to the standard distortions, the distance increased between the two horizontal lines. The intensity distributions of the two horizontal lines of the filtered Ponzo illusion of Figure 52,c,d,e show that effect. The increased distance between the average intensity values of the two parallel horizontal lines of Figure 49 is also evident.

#### 12.3.3 Variations of the Horizontal-Vertical (H-V) Line Illusion With and Without a Frame

Perhaps the simplest geometric illusion is a vertical line which appears longer when it intersects a horizontal line of equal length to form a +, T, or L (Fick, 1851).



The results of filtering the T configuration of the H-V illusion were shown in Section 9.2. The vertical line is about 4 percent longer than the horizontal line after MTF filtering, measured from the farthest distance of the peaks of the contours of Figure 20,b. However, the filtered image reveals about an 11 percent increase in the length of the vertical line for the farthest distance of the contours of the 4 by 4 low-pass filtered plot (Figure 21,d). Suto (1959), reported by Oyama (1960), had subjects compare the length of each line of the inverted T with a standard horizontal line. The horizontal line length was underestimated by about 4 percent and the vertical line length was overestimated by 14 percent. This close agreement between the filtered image and experimental findings suggests again that the distortions may be due to low-spatial frequency channels which provide the spatial information used in the estimation of perceived line length.

The T configuration of the illusion changes with orientation. The vertical line of a T rotated 90 degrees is seen as shorter (Kunnapas, 1955,b). This effect is shown in Figures 53 and 54 where the intensities and the length of the vertical lines are greater than those of the horizontal lines.

Several researchers, e.g. Kunnapas (1955,a) and Wenderoth and Beh (1977), have investigated the effect of putting frames around variations of the L or T line figures. The general effect of rotating such figures in frames is to change the apparent relative length of certain components. These changes in length depend upon the size and shape, etc., of the frame. Slight variations in the intensity distributions of the lines in the L figure with and without surrounding lines are shown in Figure 55. Note also the difference in intensity distributions of the same filtered images of the texture patterns shown in Section 11.3.2 due to their proximity to other objects (e.g., Figure 39,b). These results suggest that some interactions between figures and frames may be accounted for by the spatial interactions that occur due to the spatial filtering properties of the visual system.

#### 12.3.4 Simple Line Illusions

Even the simplest line patterns can produce distortions. The two examples shown in Figure 56,a,b are from Müller-Lyer (1889) and Wundt (1898). In Figure 56,a the centre segment of the line on the right appears smaller than the centre segment on the left. The opposite distortion occurs in Figure 56,b. The line on the right appears smaller than the centre section of the line on the left.

The perceived distortions are seen in the numerical printouts (Figure 56,c,d) and the contour plots (Figure 56,e,f) of the MTF filtered illusions. (To compare the size of similar contours, measure from the outside of the image, the lowest level, to the inside of the image. Measurements made on the smallest diamond-shaped objects in the left of Figure 56,e,f are at the highest contour level and are not found in the object at the right. Therefore, the next lowest contour is used for the appropriate comparison.)

### 12.4 Illusions of Misjudged Size and Distance

#### 12.4.1 The Titchener Illusion

When two circles of equal size are each surrounded by circles of different sizes, the circle surrounded by the smaller circles appears larger than the circle surrounded by the larger circles. This illusion is called the Titchener circles (Wundt, 1898). Variations of this illusion use squares (Obonai, 1954), as shown in Figure 57,a,1,b,1. Here the squares on the left have different perceived size than the squares on the right of the same size. The square surrounded by the larger squares appears smaller and the square surrounded by the smaller squares appears larger. These effects are shown in the difference between the intensity values in the numerical printouts and the size of the contour plots after MTF filtering (Figure 57,a,2,b,2,a,3,b,3).

#### 12.4.2 An Illusion of Misjudged Distance

An illusion reported by Ebbinghaus (1902) is shown in Figure 58,a. Here the bottom pair of shorter parallel lines appears farther apart than the larger upper pair of parallel lines. The perceived distortion is evident in the numerical computer printout shown in Figure 58,b. The smoothed lines show average intensity shifts that reduce the distance between the upper lines, while the reverse is true for the lower pair of lines.

## 12.5 Illusion of Nonparallel Lines: the Zöllner Illusion

One illusion that does not appear to be explained by the kind of spatial filtering that has been presented here is the Zöllner illusion (Zöllner 1862). As shown in the digitized version of the Zöllner illusion (Figure 59,a), the three sections formed by the parallel lines appear to be bent in opposite directions. This illusion is much stronger in nondigitized form. The MTF and low-pass filtered pictures shown in Figure 59,b,c do not show any such distortion. If anything, the intensity distributions go in the direction opposite to the perceived distortion.

Why does spatial filtering not appear to work with this illusion? This illusion and its variations have one major difference from any other illusion which involves lines that intersect with angles. The short lines that intersect the long parallel lines do so at the same angle with the same lines. This is not true of other geometric illusions, such as the Lukiesh (1922) or Orbison (1939), having many intersecting lines. Therefore, the uniform effects of spatial filtering occur on all the same components of the Zöllner illusion but act differentially on the other geometric illusions. However, spatial filtering affects the strength of the illusion upon rotation.

The variation of the Zöllner illusion may be too coarsely quantized for this analysis, or the filtered image causes and/or allows another mechanism to create the perceived distortion. Further research is needed. Clearly, in comparison to all the other results on the filtering of illusions, the Zöllner illusion and its variations seem to be in a class by themselves.

## 12.6 Illusions of Contrast

### 12.6.1 The Hermann Grid Illusion

The Hermann Grid illusion (Hermann, 1870) is shown in Figure 60,a. Note the grey patches (reversed contrast) that appear in the white intersections. These grey patches, almost completely absent in the fovea, are strongest with peripheral viewing. This observation suggests that low-pass filtering in the peripheral retina contributes to the illusion.

A digitized version of the Hermann Grid illusion is shown in Figure 60,b. The results of spatially filtering this illusion are shown in Figure 60,c where real intensities at the intersections are clearly seen. Figure 23,d,1 shows another variation of this illusion. Note the grey patches at each intersection of the white squares in the MTF filtered picture (Figure 23,d,3). They grey patches correspond to the perceived illusory patches. (The reader should note that this illusion is also present at the intersections of the figures of Figure 23.) A space-variant filter would be needed to produce the gradations of brightness that are seen by the spatially inhomogeneous retina.

Rotating Figure 60,a by 45 degrees causes prominent lines of reversed contrast rather than patches. This observation suggests that postretinal anisotropic spatial filtering may also be a component of this illusion.

### 12.6.2 The Ehrenstein Illusion

The Ehrenstein illusion (Ehrenstein, 1925), shown in Figure 61,a, produces increased contrast at intersections of the lines. Recent studies by Spillmann, Fuld, and Gerrits (1976) suggested that this illusion is also present without eye movements. It persists with dichoptic presentation, scotopic vision, and with low contrast. It differs from the Hermann Grid illusion because it is seen in both the fovea and periphery. These findings led Spillmann, et al., to conclude that the enhanced contrast may result from postretinal factors.

Spatially filtering this illusion (Figure 61,b) results in increased contrast at the intersections of the lines shown in Figure 61,c. The magnitude of the illusion decreases if it is rotated by 45 degrees, which suggests that anisotropic spatial filtering is one filtering component that is also present.

### 12.6.3 The Benussi Ring Illusion

The Benussi Ring illusion (Benussi, 1902) shown in Figure 62,a,1, is an example of simultaneous contrast. The part of the grey ring on the white surround is seen as somewhat darker than the part of the ring on the black surround. The contrast of this illusion is enhanced if the edge that bisects the black and white area is fixated. This forces the illusion to

be observed in the periphery which emphasizes low spatial frequencies. Also, placing a black or white line over the same edge increases the contrast of the illusion.

The ability of the MTF and low-pass filter to produce images corresponding to the perceived contrast differences is shown in Figure 62,a,2,a,3. As with the geometric illusions, the slight contrast reversal that is seen from filtering by the MTF is much greater with the low-pass filter. Numerical printouts of the low-pass filtered image (Figure 62,e,f) confirm the perceived contrast differences of the grey ring.

A second study on the effect of adding a line across the edge that bisects the black and white area was made (Figure 62,b,1,c,1,d,1). The contrast between the ring and white surround was changed so that there should be a difference between the contrast of the white line and the white surround.

A comparison between filtered images of the Benussi ring (Figure 62,b,1) and an added white (Figure 62,c,1) and black line (Figure 62,d,1) reveals only slight increased contrast of the two sides of the ring (Figure 62,b,c,d,2). There must be at least one other mechanism responsible for the perceived increased contrast with the added lines. For example, the added lines could physically separate the illusion into two parts, each of which is filtered separately. In Section 13.3.1 segregation of parts of an object due to a line are discussed and a possible reason is suggested for how the addition of a simple line increases this illusion.

## 12.7 Subjective Contours: the Kanizsa Triangle

The Kanizsa triangle (the Kanizsa, 1955, version of the Schumann, 1904, illusion) represents a class of illusions which provide contours that are perceived but are not physically present in the original object. (See Coren, 1972, for review.) In Figure 63,1,a, a black triangle formed by the white features may be seen. Ginsburg (1975) showed that there is a physical intensity distribution that generally corresponds to the shape of the perceived black triangle after ideal low-pass filtering (Figure 63,1,f). The intensity distribution of the black triangle is enhanced if the low-pass filter is prefiltered by the MTF (Figure 63,1,e). If the visual system has similar filtering characteristics, then a physical triangular form will exist in the filtered image of some range of spatial frequencies.

This illusion persists, although greatly diminished, if the sectorized disks are replaced with dots (Gregory, 1972, Figure 63,2,a). Similar reductions in the shape of the intensity distribution that form the illusory triangle are seen in the low-pass filtered object (Figure 63,2,e,f).

### 12.7.1 Comparison Between Solid and Outline Kanizsa Triangle

The results of this filtering predict that it is the low spatial frequencies rather than the high spatial frequencies that provide the illusory triangle. This prediction was tested using a solid and outline version of the Kanizsa triangle. The original triangles (Figure 64,a,1,b,1) are Fourier transformed to create the magnitude spectra shown in the contour plots of Figure 64,a,2,b,2. Although the magnitude of the low spatial frequencies is greatly reduced in the outline triangle, the highest magnitude is at the third vertical harmonic. It is about 28 percent of the same value in the solid triangle (see arrows in Figure 64,a,2,b,2). The 16-level contour plots after low-pass filtering are shown in Figure 64,a,3,b,3. Note that the contour plot of the solid triangle creates a more homogeneous and better defined triangular region than that of the outline triangle. Figure 64,a,4,b,4 shows filled-in contour values outside the original features that range from 18 to 256. Figure 64,a,5,b,5 shows a 32 by 32 pel, 16-level numerical printout of the window section of Figure 64,a,4,b,4.

Both the reduced magnitude spectra and the less well defined illusory triangle predict a decreased illusion from the outline triangle. This prediction is confirmed by noting that the solid triangle produces a stronger illusory triangle than does the outline triangle at any viewing distance.

The dependence of the strength of the illusion on the low spatial frequencies has also been shown by Dumais and Bradley (1976). Using only the sectorized disks of the Kanizsa triangle, they found that the strength of the subjective triangle increased as the size of the object decreased from 18.9 to 1.2 degrees of visual angle. The strongest subjective triangles were reported for a pattern of small size (1.2 to 4.8 degrees) under very dim illumination (0.10 log lux) conditions that make the filtering characteristics of the visual system low-pass rather than band-pass (see Section 5.2.1).

It is not clear whether only one band of low spatial frequencies provides the illusion in this and other subjective contours. There may be other mechanisms, i.e., other bands of spatial frequencies that also contribute to the sharpness of the perceived illusion, as discussed in Section 12.8.3. Further research using spatial filters made from experimental data about the channel filters is required.

## 12.8 Discussion

The demonstrations with the MTF and band-pass spatial filters have suggested that, with the exception of the Zöllner-type illusion, the geometric distortions that are perceived may be due to two-dimensional spatial filtering by mechanisms in the visual system.

In general, all the MTF filtered images of geometric illusions so far show some spatial distortions that are consistent with perceived distortions. The distortions of the filtered images increase with further spatial filtering. As with the previous filtering of form and texture, the particular shape and bandwidth of the filter were not critical. However, there are small changes in the intensity distributions of the filtered images whose importance have to be determined from further research. These small differences were found between the MTF(L) and MTF(H) spatial filters, e.g., Figure 53. Therefore, since the only difference between these filters is the low frequency attenuation characteristic, the amount of lateral inhibition and the amount of contrast that contributes to the degree of distortion in these objects are clearly important.

In addition to the general filter shape, the size of the illusion also has some effect on the magnitude of the distortion. For example, the MTF spatial filters used were scaled to show distortions at and just above threshold with objects about 0.5 degrees in size. Increasing the size of the objects to 2 degrees, and using the same shape MTF(H) filter, shows predominant effects of lateral inhibition. An example is shown in Figure 65, a with a large size Ponzo illusion. Here the MTF causes only slight smoothing (Figure 65,b), with low intensity light and dark regions surrounding the lines that can be seen after log transformation (Figure 65,c). Examination of the MTF(H)L picture reveals that the upper horizontal line is slightly shorter by 1 pel when compared with the lower. This is opposite to the perceived distortion. But, this object was filtered using a spatially homogeneous filter. The retina is not perfectly spatially homogeneous over 2 degrees, and this filtered object does not represent the spatial information available to other bandpass mechanisms of the visual system. It merely demonstrates the difference that one can expect to find in different size objects filtered with similar spatial filters. However, when this object is low-pass filtered (Figure 65,d,e), the perceived distortion is evident as before.

The distorting effects of patterns similar to the illusions have also been demonstrated. Furthermore, it should be clear from the filtered dot patterns shown in Figures 23,b-g and 26 why dots or other fragmented objects arranged in the shape of these geometric illusions provide the perceived distortions (if the illusion distortions are judged from the low spatial frequencies of the objects).

In general, these demonstrations have shown the relative importance of filter shape, bandwidth, size and configuration of the illusion, and contrast. These are all interacting variables, some more important than others. It is clear that researchers will have to be very careful to control these variables before general statements can be made about visual distortions. The techniques presented here may offer firm quantitative predictions if these variables are controlled. All of these techniques can be refined and research is needed to determine which information in the filtered image the observer uses for length of line, for example, that can be related to the numerical computer printouts and contour plots. An initial attempt to determine that information is discussed in Section 12.8.1.

Does the concept of spatial filtering represent a unitary theory for perceived distortions? The answer is both yes and no. Since the visual system has to process spatial information with band-limited spatial mechanisms, some distortions like those demonstrated here must be present. In that sense, filtering is a unitary theory which differs from the other spatial theories that have been presented.

Certain distortions have been shown that cannot be accounted for by blurring or smoothing theories. The optics of the visual system, as discussed in Section 5.2.1, are good enough to pass the detail of objects that are processed at higher levels. Theories of lateral inhibition are inadequate to account for all of the perceived distortions. Since the known

mechanisms in the visual system are of finite size, there also has to be some spatial summation. As Ginsburg (1976) pointed out, the spatial filters that have been used incorporate both lateral inhibition and high-frequency attenuation (spatial summation). In sum, the proponents of various spatial theories of geometric distortions have been only partially correct.

The death-knell of a cognitive theory, i.e., inappropriate scaling (Gregory, 1963) as a unitary theory, has been sounded for many years and the numerous counter-examples will not be presented here. The interested reader is referred to Robinson (1972).

It is interesting to note that Gregory and Harris (1975) presented the results of an experiment that was supposed to show that the spatial filter theory failed when the inappropriate scaling theory predicted a negligible illusion from a Müller-Lyer figure under certain scaling conditions. However, Ginsburg (1976) pointed out that Gregory and Harris created the conditions under appropriate scaling whereby the fins of the Müller-Lyer figures appear at "right angles" in depth planes away from the shafts. Under reversed stereo projection, depth was "labile." Julesz (1971) demonstrated the destruction of the Müller-Lyer illusion by separation of the shafts into separate depth planes by means of random dot stereograms. Therefore, Gregory and Harris's results could have been predicted from the two-dimensional filter theory. If the illusion features could not interact spatially in the *same* depth plane, then the filtering would act on the pattern elements in *each* depth plane. However, they would not be able to distort each other's spatial distribution and would not produce illusion distortions.

Since spatial filtering of the kind presented here cannot offer an explanation of the Zöllner-type illusions, it cannot be considered a unitary theory. Nor would the author expect it to be. Clearly, factors such as pattern of eye scan, individual strategies to determine the spatial position and extent of lines, and even inappropriate scaling effects (if based upon the filtered image, e.g., different intensities and sizes corresponding to different depth planes, as was discussed in Section 11.6) would seem to have some input to the final response of the observer (Ginsburg, 1971,a,b). However, the filtering results presented here suggest that these may be, at best, second and third order variables.

The techniques presented in this dissertation can be used to determine the extent of distortions due to spatial filtering and other variables. For example, the distortions due not only to lateral inhibition can be determined by using a Gaussian low-pass filter—a filter that only produces spatial summation.

What is the site of the spatial filtering that can produce such distortions? Clearly any spatial filtering will cause the vast majority of geometric illusions to have distortions. Forcing judgements of line length, contrast, etc., in the peripheral retina increases errors due to the reduced spatial frequency resolution found in the periphery. In general, all the distortions change to some degree upon orientation. When the distortions were measured against general experimental findings, the degrees of distortion corresponded best to those illusions filtered with spatial filters with bandwidth similar to those required to create generalized forms in previous chapters—two octaves. The only orientation-selective mechanisms in the visual system that have bandwidths of two octaves have been found in the cortex (see Section 7.3). Thus, the cortex may be the major site of the filtered image from which distortions are perceived.

#### 12.8.1 Predicting the Perceived Length of the Müller-Lyer Illusion from Filtered Images

Pressey and Bross (1973) reported the perceived change in the length of the shaft of a configuration of the Müller-Lyer illusion having long and short fins. There were nine gaps ranging from 0 to 20 percent of the length of the shaft between the fins and the shaft. The subjects selected a line that appeared to be equal to the length of the shaft for each gap size. The perceived change in shaft length plotted as a function of gap size is shown in Figure 66 by the inverted U-shaped functions. Cornell (1978), using that paradigm, reported an initial attempt to predict the perceived length of a configuration of the Müller-Lyer illusion from filtered images. He used the same set of illusions; however, the subjects used the method of adjustment to match the length of a line to the perceived length of the shaft.

The results of Cornell's experiment are shown in Figure 66. Those experimental curves were compared to theoretical curves determined from filtered images. The nine illusions were digitally filtered using one-, two-, and three-octave ideal and channel band-pass filters having centre frequencies of 1, 2, 4, 8, 16, 32, and 64 cycles per size of the illusion. The theoretical length of the shafts was determined from the distance between the 0.25, 0.50, 0.75, and 1.00 percent

values of the peak amplitudes of the shafts of the filtered images. The best fit to the experimental data, shown in Figure 66, is from the filtered images from the two-octave channel filters having centre frequencies of 2 and 4 cycles per size of the illusion—the range of low spatial frequencies that are predicted from the previous filtering (see Section 12.3.1).

Six of nine illusion configurations were predicted well. However, the three configurations having the greatest gap size were not predicted well; the length of the lines of the filtered images were, in general, too short compared to the perceived length. There are several hypotheses as to why those data could not be predicted. First, the theoretical length of the shaft was determined from the filtered images using filters whose bandwidth was based on the overall size of the illusion, i.e., from fin tip to fin tip. Although this assumption appears reasonable for six of the illusions, the magnitude of the perceived illusion may not be based on the overall size for the remaining three illusions because of the large gaps between the fins and the shaft. It is possible that the overall size of the illusion with large gaps is taken as the shaft and one fin. This hypothesis could be tested by comparing the magnitude of the perceived illusion with and without one fin. If the perceived magnitude of the illusion remains the same under those conditions, then the theoretical shaft length should be determined from a filtered image containing only one fin and the shaft. This would reduce the shrinkage of the shaft so it may better correspond to the perceived shaft length. Second, the amplitude values used to determine the theoretical shaft length may not correspond to those used by subjects for those illusion configurations. Third, the theoretical values were determined from filtered images based on a single channel of a certain shape and bandwidth. Two or more channels may be interacting in unknown ways, producing the effect of requiring different filter shapes and bandwidth for those more complex configurations of the illusion. Of course, these three factors may be interacting simultaneously. Future research will be required to test these hypotheses.

These results that show certain agreement between some of the theoretical and experimental data are good, even without agreement with all the data. The general shapes of the curves are similar. The underestimation, peaking to overestimation, and then the decreasing of the perceived shaft length is predicted by the filtered images. The overestimation and underestimation, shown to be between  $\pm 15$  percent of the length of the shaft, is predicted. Finally, the location of zero and peak values of the perceived shaft length are closely predicted. In sum, these initial results, attempting to quantitatively relate the perceived length of a complex object from filtered images based upon biological data, are promising.

### 12.8.2 Filtered Images, Eye Scans, and Illusions

Another important clue about the possible site where the distortion is already present comes from eye scans that have been measured on illusions. It seems clear that the low spatial resolution of the peripheral retina forces the observer to make eye scans to place the fovea over various parts of an object to provide greater detail.

It may be that the mechanism that guides the foveal fixation is already dealing with low spatial frequency images. Yarbus (1967) showed eye scan paths for the Müller-Lyer illusion (Figure 67). (He also found that the illusion persisted without eye movements. Thus, theories attributing geometric distortions to inappropriate eye movement appear untenable.)

The author calculated the average distance between the different fixation spots in the traces of the eye scans shown in Figure 67. The ratio of the average distance between the large fixation spots of the inward to outward going fins is about 0.80. Pressey (1972) graphed data from Heymans (1896) that showed a 0.84 ratio between the distance of a line with fins at 45 degrees outward and fins at 90 degrees. The ratios from the computer printouts are 0.85 [MTF(H)], 0.78 [MTF(L)], and 0.75 [MTF(H) (5 by 5)]. These values were determined by counting the number of pels of approximately the same intensity at the ends of the shafts of the filtered images. The illusion was coarsely quantized and the end points that an observer uses in making line length judgements have yet to be fully determined. However, the values presented here are close enough to other experimental results, e.g., Cornell (1978), to suggest that it is the low-pass filtered image that may guide certain eye scans.

Further evidence for certain eye scans being directed by spatial information in filtered images is given. Eye scan paths of a portrait of a young girl (Figure 68,a,b) and a bust of Nefertiti (Figure 69,a,b) are from Yarbus (1967). These pictures were digitized (Figures 68,c,69,c) and filtered as before to create the filtered images shown in Figures 68,d,e. Note that the density of eye scans corresponds well to the regions of large contrast differences of the major features, e.g., nose, eyes, and mouth, seen in filtered images.

The suggestion that certain eye scans may be directed by spatial information contained in a filtered image is also supported by the fact that the fovea is directed to objects in the periphery that have relatively low resolution.

### 12.8.3 Why Are the Details of Illusions Seen as Distorted?

The perceived distortion of many illusions shown in this dissertation corresponded well to the distortions found in their low-pass filtered images. Using this approach, Cornell (1978) found that the theoretical data from the low-pass channel filtered illusions predicted well the perceived length of the shaft for six of nine configurations of the Müller-Lyer illusion. However, it is reasonable to ask why, if these data suggest that the perceptual space for distortions of illusions is the low-pass filtered image, the details of the illusions are seen as distorted, i.e., the high spatial frequencies of the objects. This question is answered by assuming that there are channels in the visual system, with a bandwidth of about two octaves, that provide a hierarchy of filtered images similar to those shown for the portraits in Figure 83, as discussed in Chapter 14. The filtered images may combine to create the global picture that is seen. Based upon that assumption, there are, in general, two possible combinational rules that would distort the high spatial frequencies. Details of the filtered images from the higher spatial frequency channels might follow the contours of the filtered images from the lower spatial frequency channels, or they may be spatially shifted by inhibition from the contours of the filtered images from the lower spatial frequency channels. The author has tried to determine experimentally the combinational rules of filtered images from channel filtering by attempting to relate the intensity distribution of combinations of filtered images to the perception of the tile illusion (Schachar, 1976). Good agreement between the intensity distribution of the resulting filtered image and the brightness distribution of the perceived illusion was obtained when the resulting filtered image was created from an envelope of several filtered images of which the intensity at each point in space was the maximum value of each filtered image. This approach may be used to determine if the low-pass filtered image can distort the high-pass filtered image when they are combined. Much further research will be needed in this area before the actual combinational rules for filtered images from channels in the visual system are known to fully explain why the details of illusions are seen as distorted.

### 12.9 Summary

This chapter has provided numerous demonstrations showing filtered images of illusions that contained distortions that, in general, corresponded well to perceived distortions. The only exception was the Zöllner illusion. These results suggested that the primary reason for seeing most illusions is that spatially band-limited mechanisms in the visual system cause filtering that distorts the geometric and brightness distributions of the original objects. This explanation was tested experimentally with very good initial results. Finally, a relationship between filtered images and eye scans was postulated.

The next chapter further pursues the filtering concept for perception on more complex visual phenomena: multistable objects.

## CHAPTER 13

### MULTISTABLE OBJECTS

#### 13.1 Introduction

An example of a simple multistable object is monocular rivalry, discussed in Section 6.2.4, which occurs when two crossed gratings perceptually alternate. There are more complex objects that change shape or can be interpreted in two or more ways that are also classed as multistable objects. Attneave (1971) provides a good review article for the interested reader. Can the concept of spatial filtering offer any insight into the perception of multistable objects? This is examined next.

#### 13.2 Multistability Due to the Different Sizes of Objects in One Scene

Certain scenes are multistable because they contain objects of different sizes in one picture. An example of such multistability is shown in Figure 70.a. This picture is a portion of "Slave Market with Apparition of the Invisible Bust of Voltaire" by Salvador Dali. As Attneave (1971) pointed out, either the bust or the people predominate at different viewing distances. With reference to the overall size of the picture, the bust is larger, thus having predominantly lower spatial frequencies than that of the people. A prediction of this picture in terms of filtering suggests that the bust and people will segregate into two predominantly different spatial frequency channels. This notion is demonstrated next.

The original picture was sampled into 128 by 128 discrete picture elements (pels) that resulted in Figure 70.b. The details of the people are considerably reduced by this form of low-pass filtering. Additional low-pass (24 by 24, Figure 70.c) spatial filtering eliminates the people, but the bust remains well resolved. Further spatial filtering removes even the bust and leaves only general low frequency forms from the original picture (Figure 70.d). (This intensity distribution is interesting in itself in that it seems to show the areas of the original picture to which one first attends upon initially viewing the picture. This observation has been made by the author on many other patterns that have been filtered similarly, and further suggests that filtered images may provide information for eye scan mechanisms (see Section 12.8.21.) Thus, the people lie in a spatial frequency region greater than 24 c/pw, whereas the bust can be found from about 8 to 24 c/pw. These results are further demonstrated.

The bust was enlarged to twice the size of the original picture in order to capture more of the detail of the faces found in the eye sockets of the bust (Figure 70.e). As found in the previous study, the faces are lost with moderate filtering and the bust remains with further low-pass filtering.

Which form will predominate at different viewing distances can perhaps be best explained in terms of the filtering characteristics of the visual system: contrast sensitivity function and retinal inhomogeneity. Contrast sensitivity is generally greatest at about 1 to 5 c/d of visual angle. Therefore, as the viewing distance changes, the predominant spatial frequency band for each of the forms will be seen at different levels of visual sensitivity. View Figure 70.e so that the faces are within the fovea, about 1 degree. The ratio between the sizes of the faces and the bust is about 1:8. Therefore, the third harmonic of each face (determined as approximately the minimum spatial frequency necessary for the recognition of faces from previous studies, see Section 10.2) is at about 3 c/d, whereas the third harmonic of the bust is at about 0.38 c/d. Since the major portion of the bust falls outside the fovea where retinal inhomogeneity reduces contrast sensitivity to high spatial frequencies even further, it seems reasonable that the faces dominate our perception at such close viewing distances (when viewed without eye scans).

If the picture is viewed at a distance so that the bust subtends about 2 degrees, the third harmonic of the bust is 3 c/d, whereas the third harmonic of the faces is 24 c/d. Since contrast sensitivity is reduced greatly at 24 c/d compared to 3 c/d, the bust seems to predominate, although the faces are still recognizable. At a third viewing distance so that the bust subtends 1 degree of visual angle, the third harmonic of the bust is 6 c/d. However, the third harmonic for the faces is 48 c/d, near the limit of our normal visual acuity. At this distance, the bust is clearly dominant over the faces.

There are, of course, other factors such as set, selective attention, and other picture clues that can contribute to whether



the people or the bust is more noticeable. Note that the figure of the man on the left side of the picture resting his head on his hand is about the same size as that of the bust and would cause a similar spatial frequency band to be attended to if noticed first (and vice versa). A similar situation exists for the people figures in the background. It seems that Dali knew quite well how to induce the visual system to perceive different size objects to create a multistable picture (Fisher, 1967).

The adequacy of the low spatial frequencies for the classification of forms can also be demonstrated using these patterns. If the large busts are viewed at a distance, they all look alike (at about 45 yards). Moving slowly towards the pictures causes the busts on the right to be seen as different from the ones on the left as their higher spatial frequencies rise above their threshold. The busts are recognized at about 13 yards, when the third harmonic is about 16 c/d and the fourth harmonics are at about 42 c/d and 56 c/d, respectively. These results are consistent with other findings that have shown that about four harmonics are sufficient for form recognition (Ginsburg, 1971,a,b; Woodhouse and Campbell, 1977).

Note that the recognition of the busts requires a higher spatial frequency than that of the faces. The studies of filtered portraits (Chapter 10) suggest that the critical features of the face for recognition are the position of the eyes, nose, and mouth. Since the bust is a three-quarter profile and there is only a small separation between the nose and the mouth, these features would be at a higher spatial frequency than those of a frontal view of the other faces in the picture.

### 13.3 The Bisected Circle

One of the most fundamental patterns which exhibits figure-ground properties is a circle bisected by a serpentine line as shown in Figure 71.a. Either side can become figure with equal ease. Note that the side that becomes the figure appears to be brighter than the other side and that the serpentine line appears to belong to the figure, not to the ground. Informal observation of this pattern suggests that eye scans may not play a very large role in determining which side is seen as figure and which is seen as ground. It may be that some unbalanced information from the object is needed in order for some mechanism to segregate one side from the other.

Figure 71.b,c,d shows simpler versions of this object made to further investigate this kind of figure-ground separation when the serpentine line is replaced by a straight line. The asymmetric object shown in Figure 71.b,c results in figure-ground more readily than the symmetric object shown in Figure 72.d. This demonstration suggests that the basic information being used for the separation of figure and ground in these objects is size or area differences between sections of the objects created by the position of the line. The filter concept suggests that there is some band of spatial frequencies that form an image which reflects the differences between size or area in these patterns. To examine this notion, these digitized versions (Figure 72.a,1-d,1) were sequentially low-pass filtered and the images examined for global information that could be used to segregate sections of the patterns. Such information was found in the lowest spatial frequencies of the patterns, in particular, the fundamental frequency as seen in the plots of the filtered images of Figure 72.a,2-d,2. Note how this very low spatial frequency information reflects the asymmetry of these patterns. These results suggest that the distribution of spectral energy in a filtered image formed by the very low spatial frequencies can provide spatial regions for the segregation of figure from ground.

These results are interesting because they provide a function for a region of spatial frequencies that were not needed for the demonstrations in Chapters 9 and 10. In those studies, the removal of the very low spatial frequencies from the object still resulted in recognizable forms, although the contrast was reduced. These images found from the very low spatial frequencies (less than 1 cycle per object) could also provide the position (phase) information with which the lines, i.e., high spatial frequencies, of each section of the patterns could become associated (see Section 12.8.3). Furthermore, suppressing the intensity distribution in one area by inhibition or selective attention would "highlight" the other area causing it to become the figure. Thus, it may be that the very low spatial frequencies "spotlight" the different areas of objects with which the images from the higher spatial frequencies can be associated; one pattern becomes the figure and the other the ground. This post hoc explanation suggests why the figure seems brighter than the ground and also on which side a common line or contour should appear.

#### 13.3.1 An Experiment: Segregation of Two Areas by a Line

The segregation property of lines in objects, e.g., the creation of local areas or regions for analysis, discussed in

Section 13.3, has a testable prediction: Certain information contained in an area of an object should be harder to extract if the object is physically partitioned by a sharp dividing line into two different areas. For example, the light and dark bars of a square-wave grating are easily seen having only one db difference in contrast. Does such a small difference produce similar results if a line is put between the bars putatively segregating them? This was determined in the following experiment.

A 2-degree bipartite field with and without a 6-minute line placed over the common edge of the bipartite field was presented on an oscilloscope to two subjects. The task of the subject was to adjust the contrast of one side of the field, starting at zero contrast, until the difference in contrast between the two sides was just detectable. The procedure was then reversed, starting with a high contrast bipartite field. The contrast was decreased until no contrast difference was seen between the two sides. The measurements were alternated for 30 trials. Voltage readings that corresponded to the contrast were recorded for each measurement. The average voltage measurement without the line was 84.9 mv (SD = 11.06) for the first subject, and 80.7 mv (SD = 14.4) for the second subject. The average voltage with the line was 309 mv (SD = 99.4) for the first subject and 783.1 mv (SD = 144.4) for the second subject. Thus, the first subject required about 4 times (11.2dB) more contrast to discriminate the contrast of the bipartite field with than without a line. The second subject needed about 10 times (19.7 dB) more contrast to perform the same task with the line. These results show that the contrast information that was available from the bipartite field without the line was greatly reduced when the line was present. These results also suggest that the line segregated the bipartite field into two separate regions, at least in terms of contrast information. Further experiments are planned to determine the spatial frequency and contrast properties of lines that provide that segregation.

#### 13.4 The Rubin Face-Vase Object

The Rubin Vase-Face object (or Candlestick illusion) (Rubin, 1921) is another example of multistability because of figure-ground reversal. As shown in Figure 73,a, either a vase or the profiles of faces in silhouette can be seen. As one is seen to predominate as the figure, the other is seen as the background, or vice versa. The multistability of this object has been explained previously in terms of filtered images (Ginsburg, 1971,a,b; Ginsburg, et al., 1976). It was suggested that if the observer attended to the lower spatial frequencies, then the smoothed image would provide sufficient information for the perception of the vase (or candlestick) but not sufficient information for the perception of the faces (Figure 73,d). However, if the observer was attending to the higher spatial frequencies, for example, by focusing his attention on the details of the pattern, the faces were reported.

The ambiguity of the Rubin face-vase object can be reduced if the overall size of the vase is made larger than the distance between the forehead and chin of the faces, as shown in Figure 73,e. This configuration of the figure appears to provide a stronger segregation of figure-ground because the information about the vase and faces is further separated in size, i.e., spatial frequency. The greater the difference in size between two patterns, the more easily they can be separated by filtering.

The segregation of figure-ground in these subjects is aided by a difference in contrast between the vase and faces. The vase is formed by a white on black contour, whereas the faces are formed by black on white contours. However, figure-ground reversal can still occur with this object if only the outline is present, as shown in Figure 73,f. Note that the outline still provides low spatial frequencies that allow the segregation of the vase and faces by filtering (although the low frequencies will be of lower energy in the outline form than in the solid form, as was shown in Section 12.7.11).

Note also that the filter explanation for this multistable object is consistent with the previous filtering results which showed that the low spatial frequencies provide the basic information about object form. Many different configurations of this object can also result in the perception of vases or goblets or candlesticks and silhouetted faces. The lower spatial frequencies of those different objects can provide generalized form information that would allow different interpretations of the filtered image.

The reversibility of these figures can easily be overcome if they are viewed at a distance such that the band of spatial frequencies that provide the face information is attenuated to the degree that only the lower spatial frequencies of the vase remain.

### 13.5 Multistable Dot Patterns

Atkinson, et al. (1973), reported the perceptual effect of another type of multistable object which exhibited monocular rivalry. The uniform field of dots shown in Figure 74,a can be seen to shift perceptually from horizontal to vertical columns, and sometimes even into rectangular shapes. What are the possible bases for such perceptual shifts? One possibility is that different populations of mechanisms tuned to similar ranges of spatial frequency and orientation shift their relative activity.

The analogue in transform space is the attenuation of certain parts of the transform. By shifting the spatial filter either vertically or horizontally (Figure 74,c,1-f,1), some vertical and horizontal substructures can be seen in the filtered images (Figure 74,c,2-f,2). Note that the structure of the pattern changes as a whole. Just as viewing of two or three of the dots cannot form a separate group from the rest of the dots, neither can the filtering. The "common fate" of the perception of the dots also applies to the filtered image that is created by spatial filtering.

One simple prediction based on these results of filtering is that adapting one set of orientation channels should bias perception and cause the dots to group in the other orientation. The reader can demonstrate this effect by gazing over any one of the three gratings shown in Figure 75 for about 2 to 3 minutes and then inspecting the original dot pattern, Figure 74,a. The dots should appear to be grouped in a different orientation than that of the adapting grating.

This is just one simple example of orientation-selective multistability. The next example is more complex.

### 13.6 Multistable Triangles

An example of three-dimensional multistability is shown in Figure 76,a,2. Initially reported by Attneave (1968, 1971), such fields of equilateral triangles are perceived as a unit, all appearing to point randomly in one of three directions. Furthermore, these perceptual fluctuations of orientation are accompanied by uniform changes in the shape of the triangles (typically, the equilateral triangles are perceived as isosceles triangles) and the triangles can appear in depth (like a set of pyramids lit on one side by the sun).

It is quite surprising that the triangles, separated by considerable distances, should all appear to look alike. Such visual processing must clearly go beyond just describing pattern features and must involve some holistic processing over the entire visual space in order for the triangles to share a "common fate." Attneave's analysis of such phenomena (Attneave, 1971, p 70) "... supposes the perceptual system employs something quite like a Cartesian coordinate system to locate and describe things in space."

Atkinson, et al. (1973), have suggested that the alternation of the triangles may be linked to the same mechanism of such visual phenomena as monocular rivalry. Perhaps an investigation that incorporates the filtering concepts mentioned above can offer additional insight, especially as to a possible reason why distributed objects behave in such a unitary manner.

The magnitude spectrum of the triangles is shown in Figure 76,a,1. Note that the spatial information of the triangles is now available in three spatial frequency/orientation regions (channels), containing approximately equal energy. The vertical sides of the triangles are transformed into the horizontal channel. The 60-degree and 120-degree sides transform into the 120-degree and 60-degree channels, respectively. Previous filtering results suggest that the low spatial frequencies provide sufficient information to classify forms. The results of such filtering, in which over half of the higher spatial frequencies are removed (Figure 76,b,1) and an inverse transform reconstructs the pattern, are shown in Figure 76,b,2. Note smoothed triangles with no intensity biases towards any orientation. However, filtering has removed equal spatial frequency information from each orientation. The orientation channels are next treated independently of one another.

Further spatial filtering passed two of the three orientation channels shown in Figure 76,c,2. Note that the triangles now point in one direction, appear isosceles in shape, and have intensity gradients such that they appear in depth. If a second combination of two orientation channels is filtered, the triangles now appear pointed in another direction (Figure 76,d,2). The final combination of two orientation channels reveals the third orientation in which the triangles can appear, the effects once again being accompanied by changes in shape and depth (Figure 76,e,2). Thus, two-dimensional filtering by quasi-independent spatial frequency/orientation channels in the visual system could provide a basis for the mechanisms behind such complex three-dimensional multistability.

Some of the finer points of the filtering are now considered. Can the triangles be made to appear to point in any other directions by such filtering? The answer is no. For example, passing only one orientation channel would result in only one side of each triangle being reconstructed. The effect would be to reverse the contrast of the edges of the triangles in these pictures. Do the channels have to be completely independent of one another to observe such phenomena? In other words, can these kinds of effects require that the two channels that are filtered not contain energy from the third? The answer is no. Figure 76.f,2 shows the information that is contained in the three orientation channels, where one is less filtered out than the other two. Note the isosceles shape of the triangles. Can such filtering extract similar orientation-specific information for one or several triangles without affecting the other? The answer again is no. Although such filtering could create slight variations in the intensity distribution from one triangle to another, as seen from these results, their spatial information can be acted upon only as a whole (this point will be expanded later). These several results appear to be a very important correlate to perception. The visual system appears unable to manipulate these objects any more or less than the filtering.

As Attneave (1968) noted, similar triangles and diamonds require special pattern configurations in order for them not to appear as a group that shifts orientation in unison. If the triangles are arranged in collinear units, such as shown in Figure 77.a,1, then subgroups of the triangles appear to group independently of one another. Furthermore, the triangles within a particular subgroup tend to orient themselves along a common axis.

What could be the basis for the common axis in each group? One possibility is the axis formed by the low spatial frequencies of the objects. This is shown in Figure 77.a,2. These results suggest that the filtered image formed by the low spatial frequencies could provide a common axis at different orientations on which the subgroups arrange themselves. A similar analysis was used for Figure 77.b,1,b,2.

Another correlate between the filtered triangles and perception is that of depth. The intensity distributions of the filtered triangles convey a sense of depth by appearing to point out of the page. Since the filtering is a linear process, it may be possible, with further experiments, to directly relate the depth conveyed from the intensity distribution to the spatial frequencies and orientation passed by the filter. The relationship between intensity distribution and depth found with filtered images of multistable objects is the same relationship that was found for the monocular texture gradient discussed in Section 11.6.

This analysis is not without predictions. Similar filtering of scalene triangles required more critical orientation selectivity of the filter. The results of filtering, shown in Figure 78, are consistent with the psychophysical data discussed in Section 6.2 that the orientation selectivity in the human visual system has an effective half-width of about  $\pm 15$  degrees. The psychophysical data suggest that scalene triangles having an acute angle of about 15 degrees or less fluctuate much less readily than equilateral triangles. Those results further suggest that triangles will fluctuate much less readily as the shape of the triangles is changed from equilateral to scalene in a series of decreasing ranges of the acute angles.

Finally, these filtering results predict that adaptation to gratings that are collinear with any side of the triangles should adapt the orientation channels in the visual system tuned to that orientation, thus increasing the tendency of the triangles to point in the direction orthogonal to the adapted side. This prediction was tested and confirmed on several subjects using both binocular and interocular adapting and testing conditions. Binocular adaptation produced stronger effects than did monocular adaptation. Furthermore, since the effect was found with the technique of interocular transfer (that is, adapting one eye and testing the other), the fluctuation is not simply a result of after-images. This result suggests that orientation-selective cortical mechanisms underlie the multistability of such patterns. The reader is invited to confirm these results by adapting to the patterns in Figure 75. Georgeson (1976) also found that adapting to gratings can affect the perception of multistable triangles.

Future experiments are planned to perform more detailed investigation of the effect of the spatial frequency and orientation of the gratings on such multistable patterns.

### 13.7 Summary

The results reported in this chapter extend the application of the spatial filter concept from static to certain dynamic

changes in perception. Seemingly unrelated perceptual phenomena were related in common terms — spatial frequency and orientation. These results, in particular those concerning the multistable triangles, will be used to argue for an analogy between the transform and filtering that have been used and the way the visual system appears to process spatial objects (see Section 19.9.3.1).

Before a general discussion of these results, one more investigation is discussed. All of the spatial filtering presented thus far has considered the spatial information in either the overall MTF or one bandwidth for each object. If the visual system has a range of different channels, then what is the full range of information that is contained in the channels? The investigation of that information is presented in the next chapter.

## CHAPTER 14

### SPATIAL INFORMATION FROM A BANK OF CHANNELS

#### 14.1 Introduction

Most of the filtering discussed in the previous sections concentrated on the effects of the overall MTF and the information contained in limited bands of spatial frequencies of objects. Certain differences in the shape and bandwidth of various spatial filters were found to produce little spatial differences in the filtered images. However, the visual system contains mechanisms tuned to different ranges of spatial frequency. This section examines more closely the effects of different shapes and bandwidths and the information contained in different bands of spatial frequencies. In particular, a complex object is filtered using a bank of spatial filters having ideal band-pass and "channel" weighting functions tuned to different ranges of spatial frequency.

#### 14.2 Methods

Both ideal band-pass filters and filtering based on the tuning characteristics of channels—the double exponential function that was found from experimental data (see Section 8.2.1)—were used for weighting functions. The bandwidth of these spatial filters was obtained from experimental data—one and two octaves at half amplitude (see Section 6.1). The filters are isotropic; creating spatial filtering for all the orientation channels would result in too large a set of data to be practical at this time.

The complex object that was filtered is the portrait of Figure 28.a. The main reason for using the same portrait was to determine if the different image processing systems, IAF and SEMPER, using different input and output devices would produce similar results.

The one- and two-octave bandwidth filters were centred at octave intervals of 1, 2, 4, 8, 16, 32, 64 and 128 c/f. Thus, the one- and two-octave filters represent a discrete band of overlapping channels whose centre frequency,  $f_c$ , is separated by one octave. A one-octave band-pass filter, centred a half-octave higher than those centre frequencies, was used to determine how critical the centre frequency was in providing certain spatial information contained in a complex object.

The original portrait (Figures 79-83,a) was made up of 256 by 256 pels and contained 190 grey levels. The picture values at the border of the portrait were tapered using five-line average taper to reduce spectral energy due to edge effects. A thin, vertically tapered line along the left side of the portrait was inserted as a control for the effects of filtering in the high frequency regions. It will be shown that the high spatial frequencies contain so little energy that the line was needed to convince the reader that the original portrait was filtered.

The spatial filtering was done as described in Section 3.2. The amplitude values of the reconstructed portraits were not normalized and thus reflected the actual amount of energy in the spectral bandwidth that was passed by each filter. Every attempt was made to process the film and prints in the same manner. However, with such a large set of pictures, some variation was unavoidable. The slight variations do not affect the interpretations of the results.

#### 14.3 Comparing Band-Pass and Channel Filtering of a Portrait

The one-octave ideal band-pass filter (Figure 79) greatly reduced the amount of general form or detailed information about the face. This lack of information is especially apparent when a comparison is made between these results and information contained in the two-octave band-pass filtered portraits shown in Figure 80. The hint of a face in the one-octave filtered portrait shown in Figure 79,d is clearly captured by the two-octave filter shown in Figure 80,d. Note that the two-octave filter centred at 16 c/f provides almost all the information about the portrait except for the fine details. The details are found in the portraits filtered from higher spatial frequencies.

The two-octave band-pass filtered portraits contain considerably more information than do the one-octave band-pass

filtered objects. Could the centre frequency be too low for the one-octave band-pass filter to be able to pass that increased information? This is unlikely because the one-octave band-pass filtered portrait centred a half-octave above the centre frequency used previously has little gain in information, as shown in Figure 81. The basic form of the face is reduced in Figure 81.d. There is a slight increase in the amount of information contained in Figure 81.f, but even this increase does not provide as much information as Figure 80.f. There are, of course, many other possible centre frequencies that might provide a little more information about the original portrait than the two used here. However, it is highly unlikely that a shift in centre frequency for the one-octave filter could, in general, provide the amount of information for the portrait that was passed by the two-octave filter.

There is little information about the portrait in the high spatial frequencies, as shown in Figures 79-80.h. The highest spatial frequencies in the last quarter of the spectrum, 96 to 128 c/f, contain virtually no information. Only the thin control line is visible (Figure 81.i). Similar results using the one- and two-octave channel filters are shown in Figures 82 and 83.

#### 14.3.1 General Discussion

Note that the *periodic* ripples that were present in the ideal band-pass filtered portraits are gone in the channel filtered portraits. However, note that the ripples on both sides of any edges in the ideal band-pass filtered portraits can still be seen in the channel filtered portraits. The absence of the periodic ripples in the channel filtered portrait is due to the positive and negative exponential taper of the channel filter. Any taper of the abrupt cutoff of an ideal band-pass filter will reduce the periodic ripples (e.g., see Brigham, 1974). The particular distribution of the light and dark ripples is due to the finite bandwidth and shape of the filters. The line-spread function of this type of filter was shown in Figure 4.b to have positive and negative weighting, i.e., "lateral inhibition." The square-wave response was shown in Figure 4.c. Thus, the light and dark ripples at the edges of these filtered portraits are the kind of contrast changes that can be expected in spatial objects from the effects of spatial filters producing lateral inhibition.

Note that the filtering that produced the effects of lateral inhibition has not produced edge sharpening. There are no edges in any filtered portrait that are seen as sharper than the same edges in the original portrait. The effect of filtering due to lateral inhibition is to increase the contrast of edges, i.e., to enhance the edges by reducing the contrast away from the edges.

The increased contrast of the edges is similar to the contrast distribution seen from Mach bands (see Ratliff, 1965; Patel, 1966; Cornsweet, 1970). Since the spatial frequencies of any figure that produces Mach bands will be filtered differently by the MTF as viewing distance changes, and Mach bands remain over relatively large ranges of viewing distance, it is unlikely that Mach bands can result from any one filter. However, assume that each channel filter has the same filter shape. As the object that produces a Mach band is viewed from different distances, it would be filtered by different channels with similar filter shapes and its appearance would not change until the viewing distance became very close or very far.

The reader is encouraged to compare the general information about the face of the two-octave band-pass filtered portraits of Figures 80, 83.d with the MTF low-pass filtered portraits of Figure 28.a,b,c.3,4. The previous filtered portraits were done with the square-shaped spatial filter over the same bandwidth as the present filtering. The general information about the face in all these filtered portraits is very similar. These results further suggest that spatial filters having different weighting functions can provide similar spatial information about objects. This particular result is important because it means that many facets of perception can be investigated with a generalized set of spatial filters without great concern about the precise shape or bandwidth of the actual channels in the visual system.

The major difference between the filtered portraits resulting from the different spatial filters is the contrast. Thus, the particular shape and bandwidth of the channels will most likely be important, primarily for those perceptual correlates that require more precise contrast information, e.g., the contrast of Mach bands. The shape and bandwidth of the channel filters is also probably important for refining measurements of lines and angles of geometric illusions and defining the resolution of objects under threshold conditions to relate the filtered images to experimental data.

The fidelity of the filtered portraits in providing the spatial information actually present in the original portrait is easily

tested. The reader should view the two-octave channel filtered portraits from a distance sufficient to make the original portrait just a grey patch. At that distance, the original portrait will look similar to the first filtered portrait containing only the very low spatial frequencies ( $f_c = 1$ ) because the visual system is acting like a low-pass filter. Slowly moving closer results in the original portrait looking like the filtered portrait from the second channel ( $f_c = 2$ ). Moving closer still will provide a good agreement between the original portrait and the filtered portrait from the third channel ( $f_c = 4$ ). As one moves even closer, a difference in contrast will be noticed because the original portrait will be seen with the combined channels whose individual contributions are shown separately in the channel filtered portraits. However, each higher channel provides different amounts of resolution. The good agreement of the degree of resolution seen between the original and the filtered portraits will be seen as one moves closer still.

#### 14.3.1.1 Information Contained in a Hierarchy of Filtered Images

Note the different information about the portrait that can be found in each of the seven two-octave bandwidth channels of Figure 83. The existence of an object is evident from the large regions of different contrast in the first channel ( $f_c = 1$ ). The gross elliptical shape of an object that appears right side up is seen in the second channel ( $f_c = 2$ ). The third channel ( $f_c = 4$ ) definitely provides enough information to classify the object as a face. The identification of the face needs a little more information. The fourth channel ( $f_c = 8$ ) suggests that the face is that of a woman from the hair style, etc. Identification would seem possible given a limited set of similarly filtered portraits to choose from. Clearly, the face in the fifth channel ( $f_c = 16$ ) is the same as that of the original channels; and identification could present no problem, given any large set of other portraits. If information about the details of the portrait is needed—e.g., the hair across her forehead, the texture of her hair, size of the pupils, outline of her lips—then that information is found in the two remaining channels ( $f_c = 32, 64$ ). (These last two channels are also needed to see the control line.) Thus, these seven channels provide the full spectrum of information that is needed for any perceptual task.

It is interesting to note that central vision contains an array of about 200 by 200 cones. Requiring two cones to sample the high spatial frequency results in 100 spatial harmonics. This portrait contains 128 two-dimensional harmonics. This resolution would allow only up to about 7 channels whose centre frequencies were separated by one octave.

These results also suggest a possible reason for having inhibition between spatial frequency channels (Tolhurst, 1972). In addition to sharpening up the bandwidth of channel filters, inhibition between channels further reduces the spatial information that is extracted from an object. Inhibition between channels could reduce the number of channels needed to provide relevant information about an object. If there were complete inhibition between channels over a two-octave bandwidth, then, for a two-octave bandwidth channel, only information contained in the channels with centre frequencies 1, 4, 16 and 64 would be processed. The filtered portraits from these four channels can be seen to contain sufficient information for the existence ( $f_c = 1$ ), general form of a face ( $f_c = 4$ ), identification of a face ( $f_c = 16$ ) and details of the face ( $f_c = 64$ ). If the inhibition is less strong between channels, then seven overlapping two-octave-wide channels would be possible. Thus, by having inhibition between channels, the spatial information required for relevant perceptual tasks can be separated into 4 to 7 semi-discrete channels.

In summary, this portrait, filtered using the same shape and bandwidth filter as that found in a wide variety of neurophysiological and psychophysical studies, demonstrates the amount and kind of spatial information that can be contained in banks of quasi-discrete channels in the visual system (assuming linearity, of course). These demonstrations further suggest that the particular shape and bandwidth are not critical in conveying similar spatial information about objects in similar region of spatial frequency. Seven octaves of overlapping channels centred one octave apart provide a lexicon of spatial information in a hierarchy of filtered images about the existence, the basic form and identification, and resolution of the finest detail of a complex object.



## CHAPTER 15

### GENERAL DISCUSSION AND SUMMARY OF THE RESULTS OF SPATIAL FILTERING

#### 15.1 The Classification of Simple and Complex Objects

A wide variety of objects have been spatially filtered. A narrow band of one to two octaves (about three harmonics) of low spatial frequencies provided similar generalized form information from discriminably different objects of the same class. These results demonstrated the Gestalt concept that the whole is different from the sum of the parts. Similar results were obtained with a complex object—a portrait. Again the low spatial frequencies provided general forms from a wide variety of discriminably different portrait configurations.

Experimental evidence supported the notion that low spatial frequencies provide sufficient information for the classification of an object. Ginsburg (1971,a,b) showed that subjects could learn random letter arrays which contained only low spatial frequencies at the same rate and with the same success as the original high spatial frequency letters. Woodhouse and Campbell (1977) have shown that four harmonics are sufficient to provide face recognition with a small number of faces. Part IV of this dissertation will provide evidence that an experiment done hundreds of times each day throughout the world—visual testing with the Snellen letter acuity chart—supports the suggestion that a small number of spatial frequencies are sufficient for the classification of objects.

#### 15.2 Visual Textures

The initial studies showed that filtering by the anisotropic MTF only reduced the detail of objects. The next study with visual textures showed that the anisotropy of the MTF segregated objects that differed only in orientation. Certain first and second order problems with texture arrays and random dot patterns appeared explicable in terms of the filter concept. The perception of a monocular texture gradient also had a correlate to the filtered image. The knowledge gained from the initial studies of texture was used to extract complex forms from a real scene.

#### 15.3 Visual Illusions

Visual illusions were investigated next. The MTF and low-pass filters provided distortions of filtered images that corresponded well to the distortions that were perceived. It seems no coincidence that the most robust distortions and the best results of an experiment that tested the filter theory were found with spatial filters whose bandwidth was the same as that which provided general form information in the demonstrations of the previous chapters. Only one visual illusion, the Zöllner illusion, did not yield to a simple explanation by spatial filtering.

A relationship was suggested between eye scans and certain regions of contrast of the filtered image of visual illusions. The anisotropy of the MTF offered an explanation of why certain geometric distortions change on rotation.

#### 15.4 Multistable Objects

Certain multistable objects were examined next in which many different alternating perceptions were unified by the concept of filtering by spatial frequency/orientation channels. An explanation of some multistable objects was given from the difference in size of the objects in one scene. Other multistable objects considered the segregation problem and how filtered images could favour different areas for analysis. Explanations of still other multistable objects suggested selective filtering of specific orientation channels.

#### 15.5 A Hierarchy of Filtered Images

Finally, a detailed study on a portrait compared ideal band-pass filters with biologically derived channel filters. The results of the study showed little difference between the forms from the two different kinds of filters. However, a bank of two-octave-wide filters provided more information in almost all the images than did the one-octave-wide filters.

Seven filtered images created from two-octave-wide channels provided information about the portrait that ranged from the basic form and recognition to the finest detail.

This hierarchy of filtered images is suggested as the kind of spatial information that is available to an observer. It helps answer the following question.

### 15.6 Why Don't We See the Basic Forms of Objects?

An important point to be considered is: Why are discrete pattern elements observed in detail, such as the dots of a dot *G*, and not just the low spatial frequencies that have been shown to contain the relevant form information? One explanation is that there is a hierarchy of filtered images, each of limited bandwidth. Although there is an ever increasing amount of evidence that mechanisms in the visual system filter the intensity distribution of the retinal image using quasi-independent spatial frequency/orientation channels, limited and unstable manipulation of such information can be seen only under somewhat special and isolated conditions (monocular rivalry, for example). If the visual system could isolate the information from any different spatial frequency channel independently of all the others at the early stages of processing, then the *G* form could be seen. But "seeing" the information in all the different spatial frequency bands would result in chaos for perception. Objects would be seen at will varying in resolution from diffuse forms to mere outlines. What appears to be seen, in general, is the detail in objects from the activity of all the channels limited only by the resolution lost by the filtering of the early stages of the visual system, as was demonstrated by the MTF spatial filters.

If a parallel set of filtered images is assumed to exist, then it follows that another stage of visual processing may attend specifically to the image(s) that contain the low spatial frequencies of the form. One channel would provide an image that contained generalized form information which was somewhat independent of the channels that contained the higher spatial frequency images. Since that low spatial frequency channel has been demonstrated to provide sufficient information for identification, it might provide the input to memory. This processing scheme could provide the basis for classification of objects, despite small discriminable differences. It may also offer a coherent explanation of why objects are correctly classified at distances at which only the low spatial frequencies are passed by the visual system as well as at closer distances where the details of the pattern are seen.

### 15.7 Predicting the Identification of Complex Objects by the Filtering Characteristics of the Human Visual System

This part of the dissertation presented a filter concept that offers possible explanations of a wide variety of visual phenomena. The preceding filtering demonstrated that a single channel with a bandwidth of one to two octaves passed sufficient spatial information for the classification and identification of many objects. Can this information be used to predict the identification of complex objects by the filtering characteristics of the human visual system? One obvious experiment to help answer this question is the removal of a one- to two-octave spatial frequency bandwidth which was shown to be important for the classification and identification of the object and to determine if performance was degraded in some specified way. The main problem with this approach is that it assumes that mechanisms in the visual system behave as perfect filters—that high spatial frequencies which are removed are not replaced by some mechanism in the visual system. This assumption cannot be justified for several reasons. First, as mentioned in Section 5.2.1, the fact that the sizes of retinal receptive fields change with retinal location means that the initial sampling of the retinal image is nonuniform. Unless the filtered image is first prefiltered with space variant filtering characteristics of the retina, the retinal image will be filtered in an unspecified manner. Second, the retinal image is not static. The eye is in constant motion due to voluntary and involuntary saccades. The motion will smear the retinal image in a complex fashion. For example, the sharp edges of a high-pass filtered image will suffer some degree of smoothing at the retina. The effect of eye movements may be reduced by short presentation times in a tachistoscope. However, that would introduce additional filtering by the temporal properties of the visual system. Stabilizing the image would cause it to disappear altogether. Third, Campbell, Howell, and Robson (1971) showed that, at low spatial frequencies, the higher harmonics can generate the appearance of a square-wave grating even when the fundamental component has been removed. The missing fundamental has been "filled in." This filling-in phenomenon also tends to occur between sharp edges of other patterns (O'Brien, 1958; Craik, 1966; Cornsweet, 1970). Until this filling-in mechanism is understood and quantified, it will be assumed that edges of objects provide sufficient information for the creation of certain low

spatial frequencies. For example, Figure 31,c showed that the edges of a portrait also contained low spatial frequencies. The outline subjective contour of Figure 64,a,1 also had low frequency components. In sum, although it is operationally easy to remove low spatial frequencies from objects, this provides no guarantee that those spatial frequencies will not be replaced to some degree by mechanisms in the visual system and that they will not generate other spatial frequencies. Although these caveats suggest caution in interpreting experiments in which bands of spatial frequencies are removed, the author has attempted such an analysis with some success with an analysis of the Kanizsa triangle (see Section 12.7.1).

On the other hand, rather than filtering objects to test the hypothesis, the filtering characteristics of the visual system could be modified to reduce sensitivity over selected ranges of spatial frequency using adaptation techniques (Section 6.1.1). Further, masking techniques (Section 6.1.2) could be used to reduce visibility of certain ranges of spatial frequencies of objects.

Another possibility is to use abnormal filter characteristics. For example, if a subject had an abnormal visual condition in which only one channel functioned, then one hypothesis is that the subject would be able to identify only those objects at the limited range of distances over which the relevant low spatial frequencies of the object fell within the bandwidth of that channel. Such a subject who had what appeared to be only a 3 c/d channel due to keratoconus (a disease affecting the shape of the cornea) was reported by Ohzu and Kawara (1975). Unfortunately, they reported no further investigation of this patient due to the rapid decline of his vision.

There are, however, other abnormal visual conditions which result in selective losses in contrast sensitivity. For example, Bodis-Wollner (1972) investigated the contrast sensitivity of 16 patients with cortical lesions. He found that the greatest loss in contrast sensitivity occurred at the high spatial frequencies. One subject suffering from a meningioma pressing on the left occipital lobe had a mid-frequency loss from about 4 to 12 c/d. Selective losses in contrast sensitivity at some spatial frequencies of amblyopes have also been found in studies reported by Itoi, Kato, Sugimachi, Kawamura, Ohzu, and Kawara (1975).

These selective losses in sensitivity to some spatial frequencies could be used to test the hypothesis that a one- to two-octave band of spatial frequencies of objects is required for their identification. Assume that mechanisms in the visual system cannot perfectly replace any high spatial frequency information that is removed by filtering. This dissertation has presented many examples of low-pass filtered images whose brightness distribution appeared very similar to that of the original object when viewed at the appropriate distance such that the visual system low-pass filtered the original object to the same degree as the filtered image. Thus, unlike the high-pass filtered images, there is no evidence that the visual system creates high spatial frequencies from low-pass filtered images to any high degree. If high-pass spatial filtering removes bands of spatial frequencies that remain relevant for identification, and those spatial frequencies that remain fall within a range of decreased visual sensitivity, then reduced identification would be predicted.

Another experiment could also be used to test the same hypothesis; namely, the reduced identification of objects could be related to a variety of contrast sensitivity functions having reduced sensitivity over different ranges of spatial frequencies. Adaptation and masking techniques could be used to reduce sensitivity. However, since the abnormal filtering characteristics of subjects previously reported appear to be robust, they do not require the additional procedures and assumptions of adaptation and masking; and, since investigating those characteristics may provide additional clues about vision, abnormal vision was selected as the means to test the hypothesis.

Based on preceding considerations, it was decided to study abnormal vision to find similar patients with reduced contrast sensitivity over different ranges of spatial frequencies. Since research into abnormal vision was somewhat outside the main thrusts of this dissertation, this research is appended in Chapters A-1 through A-4. Contrast sensitivity functions showing losses in sensitivity at low, middle, and high spatial frequencies were obtained from subjects having amblyopia and multiple sclerosis. Only one subject had contrast sensitivity over a narrow range of spatial frequencies. Unfortunately, illness prevented her from being used in further experiments. One subject had a narrow-band loss—a "notch," in her contrast sensitivity function that was to be used to test reduced visual performance over predicted ranges of sizes of objects. Sensitivity increased over that narrow range of spatial frequencies before the experiment was conducted. However, the gain in sensitivity resulted in an increase in Snellen letter acuity that was

related to the lower spatial frequencies of Snellen letters, as predicted (Section 18.3). (This interesting result suggested that visual performance can be increased for certain cases of amblyopia using grating stimuli (Section A-3.5). Although no single narrow-band channels or notches were obtained from the other subjects, the number of subjects tested did provide a wide range of abnormal contrast sensitivity functions used to test the hypothesis that a one- to two-octave bandwidth of the low spatial frequencies of Snellen letters can be used to predict Snellen letter acuity from the contrast sensitivity function. That research, requiring knowledge about the relationship between the contrast sensitivity function and the identification of objects, is presented in the next three chapters.

#### PART IV

#### RELATING CONTRAST SENSITIVITY TO THE IDENTIFICATION OF COMPLEX OBJECTS

"Consider your verdict," the King said to the Jury.  
"Not yet, not yet!" the Rabbit hastily interrupted,  
"There's a good deal to come before that."

*from Alice in Wonderland*

## CHAPTER 16

### SNELLEN LETTER ACUITY AND SPATIAL FREQUENCY

#### 16.1 Introduction

The next three chapters attempt to determine if the threshold measurements with sine-wave gratings can predict the suprathreshold measurements of Snellen letter acuity. This requires knowledge about the relevant spatial frequencies that make up each Snellen letter and the minimum (threshold) contrast required for their identification. Since it has been shown that the visual system is linear at threshold for one-dimensional waveforms (Campbell and Robson, 1968) and two-dimensional sinusoids (Carlson, et al., 1977), it could be expected that Snellen letter acuity can be predicted from contrast sensitivity to sine-wave gratings.

There have been previous attempts to predict Snellen letter acuity from the cutoff spatial frequency obtained from contrast sensitivity measurements with little success (Gstalter and Green, 1971; Bodis-Wollner, 1972; and Bodis-Wollner and Diamond, 1976). However, the band-pass filtering presented in this dissertation has shown that many objects can be identified correctly from a range of one to two octaves (2 to 4 c/o) of low spatial frequencies. Thus, the relationship between Snellen letter acuity and contrast sensitivity is determined by considering the minimum spatial frequencies of the letters required for their identification.

#### 16.2 The Theoretical Minimum Number of Spatial Frequencies Necessary for Identification of Snellen Letters

The spatial frequency components that make up each Snellen letter were determined as follows. Each Snellen letter was formed on a 5 by 5 element square grid. The lines that formed each part of the letter were one element wide. The size of each letter on line 6 of a standard Snellen chart, viewed at a distance of 6 meters (6/6), subtends 5 minutes of arc, and the width of the lines that form each letter subtends 1 minute of arc. In order to be consistent with definitions in the previous sections, the fundamental spatial frequency of the letters was taken as the reciprocal of the letter size. Thus, the fundamental spatial frequency of each letter on Snellen line 6/6 is 12 c/d.

The Nyquist frequency (see Section 2.4) can be used to determine the minimum theoretical sampling limit for the spatial information of the Snellen letters. Since the Snellen letters are based on a 5 by 5 sampling element grid, the theoretical minimum number of spatial frequencies is half the number of the sampling elements, or 2.5 cycles per letter width (c/l). This means that each line pair, i.e., adjacent black and white lines, of a Snellen letter will be sampled by one cycle of sine wave. Hence, the theoretical minimum number of spatial frequencies required to form each Snellen letter is 2.5 c/l in the x and y dimensions and 3.5 c/l along the diagonals (i.e.,  $2.5 \times \sqrt{2}$ ). The spatial frequencies in c/d necessary to pass the first 2.5 cycles of Snellen letters on each line are shown in Figure 84. (In keeping with the previous analysis, one cycle across the letter corresponds to one harmonic. However, since this analysis deals with half-cycles, half-harmonics is a meaningless term and cycles rather than harmonics will be used in the subsequent analysis.) Note that letters on line 6/6 have their 2.5 c/l at 30 c/d. The spatial frequency for 2.5 c/l for Snellen line 6/3—the limit of visual acuity—is 60 c/d.

It must be emphasized that this analysis is not based explicitly on the line width of the letters. Rather, this analysis assumes that it is the minimum filtering or sampling of the features of the letters that is important for visual processing—an assumption based on the filtering results from previous sections that showed that, generally, only a two-octave bandwidth was necessary for the identification of many objects.

#### 16.3 Spatial Filtering of Snellen Letters

Typical Snellen letters were filtered to see how many cycles were actually required for identification. The minimum number of cycles required for the identification of any object can be determined from the minimum viewing distance. However, the pictures of the filtered images provide the advantages of magnification, which allows an easier and more stable determination of the features of the filtered image than those seen at distances that produce the same degree of filtering. The two Snellen letters that were chosen to be filtered are the most easily identified letter L and the relatively

more difficult letter E. Those letters, shown in Figure 85, were synthesized by low-pass filtering from 0.5 to 3 c/l in half-cycle steps using the techniques previously discussed in Sections 4.2.1 and 4.2.2. The contrast of all the letters is 76 percent. Note that the L required only up to and including 1.5 c/l for identification whereas the E requires 2.5 c/l. These results suggest why the L has been found to be more visible than the E in Snellen acuity (Sheard, 1922; Lebensohn, 1965).

Sufficient information for the identification of the L and E can also be shown to exist in band-pass regions of 2.5 cycles from 1.5 to 3 c/l (Figure 85,a,b,7) and 2 cycles from 2 to 3 c/l (Figure 85,a,b,8). However, the contrast of each letter is reduced relative to the surround, and each is clearly less visible in comparison to the low-pass filter letters when viewed at a distance. Thus, for the present, it will be assumed that the relevant spatial frequencies for the identification of Snellen letters are from 1.5 to 2.5 c/l.

Another point to be emphasized is the lack of need of precise phase information by filtering mechanisms to capture the basic form of an object. There is little difference between the filtered Ls from 1.5 to 3 c/l and the Es with 2.5 and 3 c/l, even though the individual lines that form the letters are being filtered by spatial frequencies that differ in position (phase) relative to the lines of each letter. These points are important to an understanding of how objects can be identified without critically matched templates, features, or receptive fields.

It is clear from these filtering results that 1.5 to 2.5 c/l can provide sufficient information for the identification of Snellen letters. The next piece of information that is needed in order to relate Snellen letter acuity to contrast sensitivity is the contrast of the Snellen letters required for their identification. This is obtained in the next chapter.

## CHAPTER 17

### THE MINIMUM CONTRAST REQUIRED FOR THE DETECTION AND IDENTIFICATION OF SNELLEN LETTERS

#### 17.1 Introduction

Knowledge of both the minimum contrast and minimum number of spatial frequencies can provide a pair of numbers that can be used to determine the minimum information required for the identification of Snellen letters. The previous chapter presented evidence that about 1.5 to 2.5 cycles per letter is sufficient for the identification of Snellen letters. This experiment determines the minimum contrast necessary for the identification of Snellen letters.

#### 17.2 Methods

A 35 mm slide of the standard Snellen letter chart shown in Figure 86 was projected full size onto a white matte surface and viewed from the standard six meters by five subjects with normal or corrected vision of 6/6 or better. The contrast of the chart was controlled by the crossed polaroid system discussed in Section A-2.4. The mean luminance was 20 foot-lamberts. In order to insure that each Snellen line was viewed under identical conditions, the slide that projected the Snellen chart was positioned to place each line of letters between two fixed blue markers before each trial. The subjects were told that they would see a standard Snellen letter chart—lines of capital block letters.

The threshold contrast for the detection of letters of each Snellen line was used as a reference level for the contrast required for letter identification. The subject was told to report any inhomogeneity between the blue markers as the contrast of the letters was slowly increased from zero contrast by the experimenter. That response determined the contrast noted for detection. The contrast was slowly increased further until the subject, making a forced guess, could correctly identify at least 50 percent of the letters on each line. This response indicated the minimum contrast necessary for the identification of the letters of the Snellen line. This method was repeated for each subject for each line from 6/60 to 6/5.

These methods provide only general values of the minimum contrast for the detection and identification of Snellen letters. Each different letter has its own detection threshold which may be slightly different from other letters of the same size due to physical differences between each letter. Further, the contrast required for at least 50 percent correct identification of letters of each Snellen line does not represent the same level of subject performance because of the different number of letters in each line. A higher level of performance is required to correctly report 4 of 8 letters for small letters than to correctly report 1 of 2 letters for the large letters. However, since these factors are present in the normal measure of Snellen acuity, they are merely noted and not corrected for in these measurements. These factors could be corrected by using binominal probabilities.

A criterion of at least 50 percent correct identification of the letters on each Snellen line was used in an attempt to get an average contrast value of the different letters on each line. Pilot studies showed that most subjects required significantly more contrast to identify the remaining 1 or 2 letters on the smaller Snellen lines. It was felt that increasing the contrast to allow the correct identification of all the letters would not reflect the average contrast necessary for the identification of most letters. Since identification of over 50 percent of the letters was used as a criterion to determine the minimum contrast of the identification of each line, 2.5 c/l of each letter cannot be assumed to be used for identification. The average number of 2 c/l found from filtering of the L (1.5 c/l) and E (2.5 c/l) is used in the subsequent analysis for the minimum number of spatial frequencies required for the identification of Snellen letters.

#### 17.3 Results and Discussion

The mean contrast required for the detection and identification of at least 50 percent of the letters for each Snellen line for the five subjects is shown in Figures 87 and 88. The reciprocal of those contrast values, contrast sensitivity, is shown in Figure 89,a. The values of size and spatial frequency noted along the abscissa correspond to the width and fundamental cycle of the Snellen letters for each corresponding Snellen line.



The results, shown in Figures 88 and 89, are as expected; higher contrast (lower contrast sensitivity) is required for both detection and identification as the letters get smaller. Note that the detection threshold is constant for Snellen lines 6/60 to 6/18. This result appears reasonable if detection is based upon the half and first cycles per letter reaching threshold, which, on a line 6/60 to 6/18, range from 0.6 to 4 c/d. Since those spatial frequencies occur around the peak of the contrast sensitivity function, 1 to 2 c/d, they reach threshold with similar amounts of contrast.

A similar argument can be made for the nearly simultaneous detection and identification seen on lines 6/60 and 6/36. Since the relevant range of spatial frequencies for the detection and identification of those letters can be seen, from Figure 84, to occur from 0.6 to 4 c/d and those spatial frequencies occur around the peak of the contrast sensitivity, letters of those sizes will reach detection and identification threshold at similar levels of contrast.

It should be noted that letters larger than those on line 6/60 would be expected to have thresholds similar to letters on lines 6/60 to 6/18. Since the letters are made of bars and the contrast sensitivity to square waves is approximately constant below about 1 c/d, the detection of spatial frequencies below 1 c/d would remain relatively constant. However, further research will be needed to determine how well this approach will predict the identification of objects having fundamental frequencies less than 1 c/d.

The curves in Figure 89, a show that as the letters get smaller, increased contrast is required to identify the letters after they are detected. This result is understandable if detection and identification of the Snellen letters on the average require the first and second cycle per letter to reach detection and identification threshold, respectively. Figure 84 shows that 1 to 2 c/l occurs at 1.2 and 2.8 c/d for letters on line 6/60, and 12 and 24 c/d for letters on line 6/6. Since, after peak sensitivity, the contrast sensitivity function decreases exponentially with increasing spatial frequency (Campbell and Green, 1965), more contrast should be required to identify letters on line 6/6, where the relevant spatial frequencies are 12 and 24 c/d, than when the letters are on line 6/60.

The minimum number of cycles of the Snellen letters that were used by the subjects for detection and identification can be obtained from Figure 89, b in which contrast sensitivity of the detection and identification of Snellen letter is plotted against linear spatial frequency. Regression lines were determined using the least squares method. The correlation coefficient ( $r$ ) for the regression line of the identification data is 0.994. Two different regression lines have been plotted for the detection data. Note that the first four data points are horizontal because detection occurred at the peak of the contrast sensitivity for those Snellen letters. Since the contrast sensitivity peak can shift to somewhat different spatial frequencies due to experimental conditions (see Section 5.2.1), an argument can be made that the first four data points for detection threshold could change under different viewing conditions. Thus, regression lines were computed with (solid lines,  $r = 0.976$ ) and without (dashed line,  $r = 0.962$ ) the first three data points. The bandwidth of the identification-to-detection threshold ratio determined from the intercept of the regression lines to the spatial frequency axis is 56/23, or 2.55 cycles, using all the detection data points and 52.6/23, or 2.37 cycles, excluding the first three detection data points. These values are in quite good agreement with both the theoretical analysis (Section 16.2) and the filtering analysis (Section 16.3) that suggested that the detection and identification of Snellen letters require about 1.5 to 2.5 c/l.

Note that this result does not mean that a 0 to 2.5 c/l bandwidth is being used for detection and identification. Rather, it means that some range of spatial frequencies determined by multiplying the lowest spatial frequency by 2.5 is being used. For example, if detection is due to a half-cycle of a letter reaching threshold, then identification would occur when the  $2.5 \times 0.5$  cycle, or 1.25 c/l, reaches threshold.

The ratio of the contrast required for identification versus detection of Snellen letters is also shown in Figure 90. A regression line determined using the least squares method is shown to fit well with a correlation coefficient of 0.994. Note that the regression line crosses the spatial frequency axis at about 30 c/d. The second harmonic required for identification would be at 60 c/d, which is the theoretical cutoff spatial frequency, i.e., the limit of visual acuity. This result supports the data very well.

Why should the ratio of detection to identification of Snellen letters be a straight line? As previously noted, the contrast sensitivity function decreases exponentially from peak to minimum sensitivity with increasing spatial frequency when plotted on a log contrast sensitivity versus log spatial frequency scale. If the ratio of spatial frequencies used for the detection and identification of Snellen letters remains the same for all different size letters and the detection and

identification thresholds are a function of the shape of the contrast sensitivity function, then the ratio should be a straight line when plotted on a linear ratio versus log spatial frequency scale.

To determine the generality of the finding that detection and identification of Snellen letters requires about 2 c/1, ratios are plotted of contrast sensitivity of 1.5, 2, and 3 spatial frequencies from values obtained from contrast sensitivity measurements of the author (see Figures 90 and 91). Also plotted is the ratio of the threshold contrast of two spatial frequencies from Figure 3 of Campbell and Robson (1968). Slopes of the ratios of contrast sensitivity curves are slightly steeper than the slope of the data. However, considering the different experimental conditions used to collect these data, the general agreement between the theoretical slopes in the data are quite good, especially for the ratio of two spatial frequencies.

It is concluded that there is good agreement between the theoretical and experimentally determined number of cycles sufficient for the identification of Snellen letters. Now that the contrast sensitivity and the general range of spatial frequency required for identification of Snellen letters have been determined, the Snellen acuity of abnormal visual systems will be determined from values of the contrast sensitivity functions obtained from certain abnormal visual systems to test the predictive power of this analysis.

## CHAPTER 18

### THE RELATIONSHIP BETWEEN CONTRAST SENSITIVITY AND SNELLEN LETTER ACUITY IN NORMAL AND ABNORMAL VISION

#### 18.1 Introduction

The contrast sensitivity of ten subjects with abnormal vision was measured—one subject with abnormal retinal correspondence, three amblyopes, and six patients having multiple sclerosis (see Chapters A-1—A-5). The previous spatial filtering showed that 1.5 to 2.5 c/1 are required for the identification of Snellen letters. The experiments in Chapter 17 determined the minimum contrast required for the identification of at least 50 percent of the letters on each line of a standard Snellen chart. These data, combined in Figure 92, were used in an attempt to predict Snellen acuity of these subjects based upon their contrast sensitivity measurements.

#### 18.2 Predicting Snellen Acuity of Subjects Having Amblyopia, Abnormal Retinal Correspondence, and Multiple Sclerosis

The measured and predicted Snellen letter acuity of ten subjects is shown in Figures 93 and 94. With the exception of the initial measurements of Snellen acuity in subject A. H., the Snellen acuity was also measured by other clinicians. The values under the measured contrast sensitivity column in Figure 93 were obtained from contrast sensitivity functions of the subjects whose data are shown in Chapters A-3 — A-4. These values represent the contrast sensitivity at the spatial frequency of 2 c/1 for the Snellen line that determined the Snellen acuity. Extrapolation by eye was used where necessary to obtain the value of contrast sensitivity below those measures. Since the Snellen letters are made from bars, each value of contrast sensitivity was multiplied by 1.27 to correct for the difference in detection between the fundamental frequency of square- and sine-wave gratings. The predicted Snellen acuity was determined from the contrast sensitivity values listed in Figure 92.

The contrast required to identify at least 50 percent of the Snellen letters on each Snellen line and the average second spatial frequency of the letters required for identification provided a pair of numbers that represent one point on the contrast sensitivity function. Values of contrast sensitivity close to or exceeding the predicted contrast sensitivity determined the predicted Snellen letter acuity. For example, the predicted contrast sensitivity for a measured Snellen letter acuity of 6/6 is 7.1 at 24 c/d. If the measured contrast sensitivity at 24 c/d was 7.1 or more, then the predicted Snellen acuity was also 6/6. If the measured contrast sensitivity was less than 7.1, the pair of spatial frequencies and contrast sensitivities for the next largest Snellen lines were compared until the measured values were in agreement with the predicted values. The values in the two columns of the predicted Snellen letter acuity were determined from both the average and the  $\pm 2$  standard error range of contrast sensitivity required for the detection of the Snellen letters.

A comparison between the predicted and measured Snellen letter acuity shows perfect agreement for 8 of 22 eyes, and 16 of 22 eyes can be predicted within one Snellen line using the average contrast sensitivity criteria. (The two different sets of Snellen acuity of subject A.H. are considered separately.) Using the  $\pm 2$  standard error criteria, the Snellen letter acuity predicted using contrast sensitivity shows 11 of 22 eyes in agreement, and 17 of 22 eyes can be predicted within one Snellen line. The Snellen letter acuity of the other 5 of 22 eyes can be predicted within two Snellen lines.

There is better agreement between the measured and the predicted Snellen letter acuity using the  $\pm 2$  standard error than the average standard error of the contrast sensitivity required for the identification of the Snellen letters. These results suggest that contrast sensitivity used to predict Snellen acuity is somewhat higher than that used by the subjects for their measured Snellen acuity. One obvious reason for this result is that the predicted Snellen acuity was based on less than 100 percent letter identification. The measured Snellen acuity typically required the identification of all the Snellen letters on the line that determined acuity. Thus, requiring all the letters on a line to be identified would require more contrast than was used in these experiments. More contrast would reduce contrast sensitivity and increase the agreement between the measured and the predicted Snellen letter acuity based upon the average contrast sensitivity required for the identification of the Snellen letters. Of course, other factors, such as the use of different criteria and task for the detection of gratings and the identification of Snellen letters and different experimental conditions, would

have an effect and should be investigated.

It is concluded that there is good agreement between predicted and measured Snellen letter acuity based upon contrast sensitivity measurements. These results are especially encouraging because of the different patterns being compared, i.e., one-dimensional sine-wave gratings and two-dimensional letters. Furthermore, there was a difference in equipment, methods, and criteria used to obtain the data. Such good agreement between predicted and measured Snellen letter acuity suggests the power of contrast sensitivity measurements for accurate descriptions of the overall filtering characteristics of the visual system used for the detections and identification of objects.

### 18.3 Relating Snellen Letter Acuity to the Contrast Sensitivity of an Amblyope with a Notch in Her Contrast Sensitivity Function

From Figure 92, the initial Snellen acuity of 6/36 obtained from amblyope A. H. requires up to 4 c/d of resolution for the first 2 c/1. According to her initial contrast sensitivity, as shown in Figure 99, this range of spatial frequencies corresponds to the region of decreasing sensitivity after the peak sensitivity at 1 c/d. Although the 4 c/d component of the letter falls within the least sensitive region of the notch, the contrast sensitivity at 4 c/d is similar to that at 10 c/d and greater than that of 5 c/d. The data in Figure 99 show that the Snellen acuity of 6/36 of the amblyopic eye of A. H. is a factor of 7 less than the acuity of her normal eye, 6/5. The spatial frequency for 2 c/1 of Snellen line 6/5 is 28.8 c/d (Figure 84). If the acuity in her amblyopic eye is a factor of 7 less than that of the normal eye, then the highest spatial frequency that was used by her amblyopic eye for Snellen acuity is about 4 c/d. Since that spatial frequency corresponds to 2 c/1 for letters on line 6/36, those values of spatial frequency greater than about 4 c/d — after the least sensitive point in her notch — were not used for the identification of Snellen letters. Indeed, from Figures 92 and 99 it can be seen that the sensitivity at those spatial frequencies is too low to provide spatial information for Snellen acuity greater than about 6/36. Thus, the factor of 7 decrease in Snellen acuity from her normal to her abnormal eye corresponds well to the factor of 7 decrease of the usable range of spatial frequencies as determined from the contrast sensitivity in Figure 92.

A similar analysis can be made for the increased contrast sensitivity from 2 to 8 c/d and the concomitant increase of Snellen acuity from 6/36 to 6/18 in her amblyopic eye. From Figure 84, the first 2 c/1 on line 6/18 occurs at 8 c/d. The region of greatest increase in contrast sensitivity in her amblyopic eye is from 2 to 9 c/d (Figure 110). The sensitivity at 4 c/d increased by about a factor of 10 from her initial measurements. The increased contrast sensitivity from 2 to 9 c/d is in good agreement with the predicted sensitivity required to identify the Snellen letters on line 6/18.

These results provide additional evidence that suggests the existence of narrowly tuned mechanisms in the visual system — channels — which are used in the identification of complex objects.

The initial Snellen acuity of amblyope A. H. was 6/5 (R) and 6/36 (L). Her initial contrast sensitivity predicted 6/9 (R) and 6/60 (L). Although this analysis is close to predicting her initial Snellen acuity, further analyses of these results are interesting. The two letters A and V from the Snellen chart of Figure 86, required for identification for 6/36 acuity, were not filtered to determine the minimum number of spatial frequencies necessary for identification. The general criterion of 2 c/1 for letter identification may be too high. A criterion of 1.5 c/1 does predict 6/5 (R) and 6/36 (L). One final note is that her initial contrast sensitivities are among the lowest obtained. Slightly higher values would have resulted in agreement between measured and predicted Snellen acuity.

### 18.4 Predicting Snellen Acuity from Data of Other Amblyopes

The number of cycles required for the identification of Snellen letters versus contrast sensitivity, shown in Figure 92, appears to enable prediction of Snellen letter acuity from contrast sensitivity measurements obtained by other researchers. Levi and Harwerth (1977) showed the contrast sensitivity measurements of three subjects. Subjects M. M., L. N., and M. R. had Snellen acuities of 20/20 (R-6/6), 20/200 (L-6/60); 20/200 (R-6/60), 20/20 (L-6/60); and 20/30 (R-6/9), 20/20 (L-6/6). The Snellen letter acuities of 20/20 were just outside the -2 standard error of the predicted contrast sensitivity but were closer to 20/20 than 20/30, the next Snellen line. The 20/200 and 20/50 acuities could be predicted from Figure 92. Considering the different Snellen test charts, equipment, methods, and criterion differences in the measurements, the agreement between their data and the results reported here supports the predictive power of the previous analysis.

### 18.5 Summary

The abnormal filtering characteristics of individuals with amblyopia and multiple sclerosis were determined. One amblyope had a unique, highly spatial frequency selective region (4 to 8 c/d) of decreased contrast sensitivity (notch) to both stationary and moving sine-wave gratings. Increased sensitivity of the spatial frequencies of that highly selective notch occurred with a concomitant increase in two lines of Snellen acuity.

An attempt was made to link the results of filtering objects reported in Part III of this dissertation with the Snellen letter acuity of these subjects. Full predictive power required knowledge of the minimum contrast required for the identification of Snellen letters. An experiment provided these data. The minimum contrast and range of spatial frequencies required for Snellen letter acuity were related to the two cycles per letter generally found necessary to provide the minimum amount of information required to identify Snellen letters. That data enabled Snellen letter acuity to be predicted within one Snellen line for 17 of 22 eyes.

In sum, the following approach has been shown to successfully predict, at least to a first approximation, the identifications of complex objects — Snellen letters — from the spatial filtering characteristics of the visual system using contrast sensitivity measurements. First, the *minimum* number of spatial frequencies sufficient for identification was determined by spatial filtering. Second, those spatial frequencies sufficient for identification were required to exceed contrast threshold determined from contrast sensitivity measurements of the observer. This approach, similar to that used by Campbell and Robson (1968) to determine the detection and identification of square waves, assumes first-order approximation of linearity of the visual system. The extent to which this approach will predict the identification of the other objects will require further research (discussed further in Section 19.10). However, these results clearly support the findings in the first part of the dissertation which suggest that a one- to two-octave channel can provide sufficient information for the identification of objects.

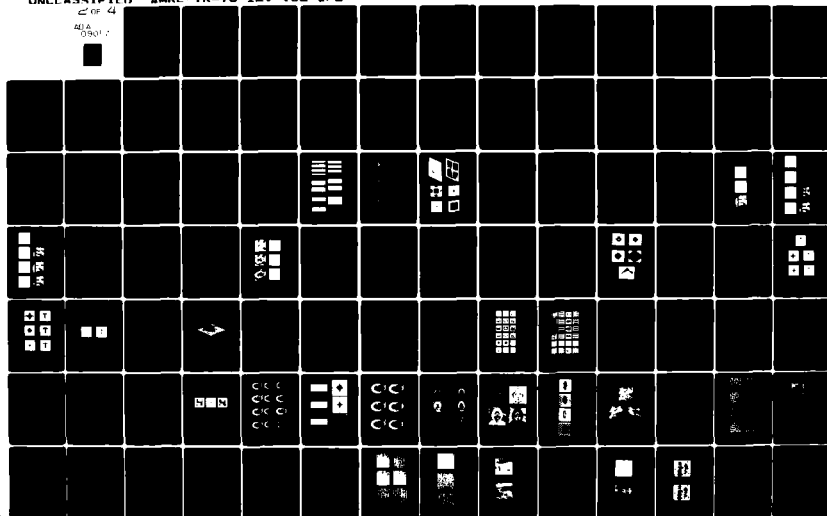
AD-A090 117

AIR FORCE AEROSPACE MEDICAL RESEARCH LAB WRIGHT-PATT--ETC F/6 6/16  
VISUAL INFORMATION PROCESSING BASED ON SPATIAL FILTERS CONSTRAI--ETC(U)  
DEC 78 A P GINSBURG  
AMRL-TR-78-129-VOL-1/2

UNCLASSIFIED

NL

41A  
09017



## CHAPTER 19

### GENERAL DISCUSSION AND CONCLUSIONS ABOUT HOW THE FILTER CONCEPT RELATES TO THE OVERALL PROBLEMS OF PERCEPTION

#### 19.1 Introduction

The previous chapters have shown how the concept of spatial filtering, based upon known filtering properties of mechanisms found in mammalian visual systems, can offer a parsimonious explanation of many aspects of visual perception. There are many alternatives to one or more of the explanations of the filtered images. It is an impossible task to counter all the potential criticisms of the somewhat cavalier manner in which certain long-standing problems in perception have been treated, e.g., the Gestalt principles. However, the aim of this dissertation is the presentation of a sufficient number of examples to demonstrate the parsimony of the filter concept with many different aspects of perception.

Several questions immediately arise about how the results may fit into the overall scheme of visual processing. What is the relationship, for example, between spatial filtering and memory or selective attention? What are the implications for machine pattern recognition? What problems in visual perception does the filter concept appear to solve? And, what problems remain? These and other questions will be considered in this final chapter.

#### 19.2 The Relationship between Spatial Filtering and Higher Visual Processing

Although the concept of spatial filtering by channels in the visual system appears to offer reasonable and testable explanations of many perceptual problems, there is still an overall cognitive structure that has to deal with the filtered information. For example, as one moves from the simple multistable objects to more complex objects such as the man-girl figure of Fisher (1968), decision boundaries that are a natural concomitant to any pattern classification system must also be taken into account (Ginsburg, et al., 1976).

Although the concept of a hierarchy of filtered images appears to predict the possible patterns that are available to an observer, it cannot predict which pattern will be seen and reported by an observer at a particular moment under free viewing conditions (excluding biasing by adaptation, masking, etc.). This aspect of visual processing is suggested to be one of the major cognitive elements of perception in which "nonsensory" concepts of Hebb (1949), such as attention, context, motivation, and set, are relevant. Indeed, based on data from several perceptual tasks, it has been argued that the filtering concept must be used in conjunction with such concepts as "set" and "selective attention," even for machine pattern recognition (Ginsburg, 1971,a,b; Ginsburg, 1973; Ginsburg, et al., 1976).

Perception involves both physiological and cognitive mechanisms. A major problem is the isolation of the different aspects of perception that are predominantly due to physiological and/or cognitive mechanisms. The filtering approach appears to offer a powerful tool in the solution of such problems. Clearly, cognitive mechanisms must be constrained by the nature, i.e., the bandwidth, of the physiological mechanisms.

#### 19.3 Implications for Machine Pattern Recognition

It was the initial success of machine pattern recognition using filtered transforms that prompted the author to apply the concept of spatial filtering to problems of visual perception (Ginsburg, 1971,a,b).

Kabrisky, Tallman, Day, and Radoy (1970) reported the results of successful machine pattern recognition using hand-printed alphanumeric patterns based on a model of the human visual system. The central concept of the machine algorithm is spatial filtering in a two-dimensional transform domain. The input pattern is transformed and spatially filtered. The low frequency components of the input pattern are then compared to the low frequency components of certain patterns stored in memory using a Euclidean distance metric (cross-correlation). Minimum Euclidean distance between the input pattern and a pattern stored in memory classifies them as the same.

It is a general tenet of pattern recognition that if the correct features of patterns are chosen, then the measure needed to classify patterns as the same will be simple. Incorrect feature selection usually leads to complex classification schemes. Cross-correlation of patterns (minimum Euclidean distance) is a simple classification measure.

A review of the early results of application of the filtered transforms to the general classification problem can be found in Carl and Hall (1972). It is interesting to note that, in general, the three or four harmonics that were required for a high percentage of correct classifications of a large number of different objects are the same as those found to be so important for most of the filter demonstrations presented in this dissertation.

Machine pattern recognition based upon filtered transforms is not perfect. It fails in some cases, but generally it fails with the same patterns that a human observer also fails to classify. The machine, so far, is generally limited to isolated objects. It is hoped that some of the rules for the segregation of objects presented in this dissertation will help solve the segregation problem.

The point made in this section is that the filter concept that has been presented in this dissertation does work for machine pattern recognition for the class of objects tested on the machine, e.g., hand-printed alphanumerics. Extension of some of the results of the filtering presented in this dissertation may help in the construction of a "seeing" machine. Minimally, the filter concept based on visual information processing should help reduce the choice between numerous algorithms which exist for feature detector concepts.

The author has attempted to combine the previous machine pattern recognition techniques with the same results of the spatial filtering reported here into schemes for machine pattern recognition (Ginsburg, 1973).

#### 19.4 Some Problems in Object Recognition That the Spatial Filter Concept Can Help to Solve

Sutherland (1968) listed twelve sets of facts which he claimed should be explained by any theory of object recognition. Since that list covers the major problems in object recognition, it is used here as a general guide in discussing what the filtering concept can and cannot offer in the solution of such problems.

##### 19.4.1 Size Invariance

Biological visual systems are able to identify similar objects even when their size varies over a considerable range. If an object is decomposed into components of size or spatial frequency (as by Fourier analysis), then changing the size of an object will change the range of size or spatial frequency that the object is decomposed into by a scaling factor (as shown in Figure 3). The ratio of the sizes or spatial frequencies will remain the same. Thus, if a system is able to extract the ratio of sizes or spatial frequencies of an object, then classification of different sizes of objects could be easily achieved. Blakemore and Campbell (1969) recognized the importance of such a scheme to account for size invariance.

The simplicity and power of such a scheme is even more attractive when the size or spatial frequency components are based upon the overall size of the object. It was shown previously that three to four spatial frequencies easily provide the basic information about the form of an object. Thus, the ratio of those few spatial frequencies could be used to provide the information required to classify an object over large ranges of different sizes, assuming that the relative amplitudes remain constant.

##### 19.4.2 Invariance to Retinal Position

Objects can be correctly classified as the same over different regions of the retina. This ability is limited by the loss of visual acuity in the peripheral retina. The power of the low spatial frequencies to provide uniform form information across the inhomogeneous retina was discussed in Section 5.2.1. Another attractive property of the Fourier transform is that the magnitude of the spatial frequencies is translationally invariant, e.g., see Bracewell (1965). If phase is eliminated, there are very many different patterns that could be reconstructed from spatial frequencies that have the same magnitude. However, consider two different kinds of phase — explicit and implicit. Explicit phase will be used to define the relative position of the object with respect to retinal space. Implicit phase will be used to define the relative position of the spatial frequencies of the object with respect to the object. In other words, certain mechanisms in the



visual system that respond to stimulation at specific regions of visual space provide explicit phase information about that object. Certain mechanisms that respond to certain spatial information and are independent of where the object is in visual space provide implicit phase along with spatial information of the object. Pollen, Lee, and Taylor (1971) recognized that complex cells have the property of translational invariance. The role of the complex cells may be to extract position invariant spatial information about objects. If the magnitude ratio of spatial frequencies of an object is extracted along with an implicit phase, then size and position invariant object recognition may be accomplished.

#### 19.4.3 Recognition of Objects When Their Contrast Is Reversed

The decrease in the recognition of objects when their contrast is reversed was discussed in Section 10.7. The harmonic analysis of an object, typified by Fourier analysis, will be somewhat different for objects whose contrast is reversed, suggesting one reason why photographic negatives are difficult to recognize.

#### 19.4.4 Equivalence of Objects That Are Solid or Outline

Data in Section 10.6 showed that information from the low spatial frequencies of an edge type portrait compared well to similar information of other portraits. In Section 12.7 the subjective contours were shown to be physically present from the low spatial frequencies of a solid and outline Kanizsa triangle.

It is not clear whether only one global band of low spatial frequencies could be used for the recognition of all line objects. It may be that segmentation of parts of such objects must come first to isolate regions over which the low spatial frequencies are then used for recognition, as was discussed in Section 13.3. Much more work is needed in this area before a clear picture will form.

#### 19.4.5 Nonequivalence of Recognizing Rotated Shapes

As Sutherland (1968) pointed out, a major mistake that many researchers in the field of pattern recognition make is to assume that a rotated object will be treated as the original nonrotated object.

Several examples in the preceding sections, e.g., Figures 19 and 53, showed how the shape of objects will change as a function of the anisotropic spatial filtering properties of the visual system.

Machine pattern recognition studies based upon filtered two-dimensional transforms (see Section 19.3) failed to classify objects correctly when they were rotated more than about  $\pm 15$  degrees. Of course, this angle depended on the shape of the object as well as the bandwidth of the filter that was used.

The inability of the machine to classify rotated objects correctly corresponds to human inability, in general, to classify rotated objects. Good agreement between the machine and human observers was obtained by correlating the errors made by the machine with the errors made by subjects in the identification of rotated capital letters (Ginsburg, 1971,a,b). However, this work is only a beginning. Clearly, there are certain objects, such as letters and faces, that are quite difficult to recognize when they are rotated. There are many other objects that present no problem, e.g., furniture and cutlery. Whether several different orientations of such objects are stored in memory because they are seen often having different orientations is not clear. It is noted that typesetters, because they are exposed to various orientations of printed material, can recognize such material with ease at any orientation. This observation suggests that the facility to recognize rotated objects is at least partly a learned ability.

Thus, if the visual system encodes spatial information about objects by using orientation channels, then the price that is paid is the loss of rapid object recognition of rotated objects (Blakemore and Campbell, 1969). The two-dimensional transform analysis presented in this dissertation offers a quantitative means with which to investigate the recognition of rotated objects.

#### 19.4.6 Similarity and Confusion Between Shapes

The successes as well as the failures of the machine in recognizing objects prompted many experiments of similarity

judgement with a wide variety of objects (see Ginsburg, et al., 1976 for a review). In those studies, subjects as well as the machine were required to rank order the similarity of objects. The machine rank ordered the objects by cross-correlating (minimum Euclidean distance) only their low spatial frequencies. The correlation coefficient between the machine and the subjects from such experiments was generally above 0.9. The low spatial frequencies of objects used to create the filtered images such as shown in this dissertation seem to capture at least some of the important form information that can be used in classifying the basic form of objects as the same or different.

#### 19.4.7 Recognition with Local Variations of Shape

Pattern recognition with local distortion of shape is accomplished quite easily as other people's handwriting is read (assuming basic legibility, of course). Machine pattern recognition has also been quite successful with such tasks (see Section 19.3). Examples have been shown of discriminably different objects having similar forms when low-pass filtered, e.g., Figure 26. Low-pass filtering may offer a quite reasonable solution to the local distortion problem.

#### 19.4.8 Segmentation

The segmentation problem (physically isolating objects or parts of objects in complex scenes for further analysis) is perhaps one of the major remaining problems to be understood and solved. The isolation of edges is clearly an important prerequisite for segmentation, as many previous researchers have realized. The plethora of edge extracting techniques exists mainly because of the almost infinite number of features and algorithms that can be specified.

Constraining segmentation techniques to those that the visual system may use greatly delimits that number. The author has used a simple first order metric, based on contrast differences that appear to exist to some extent at different levels of the visual system, as an aid to segmentation; but this work has far to go. The visual system may be using information from a hierarchy of filtered images to aid segmentation. It also may be the case that spatial frequency (size), orientation, and contrast can be used only as *general* information to aid segmentation. Clearly, there is no evidence that the visual system has the capability to extract values of those properties to the degree of accuracy that has been suggested by other researchers, e.g., Marr (1976).

The inhomogeneous filtering properties of the retina may play an important part in segmentation in many ways. For example, it reduces the amount of detail available across the retina for any segmentation process. By providing the visual system with an inhomogeneous filtered image, it almost has to force global processes onto the lower spatial frequencies of objects that cross through the central retina. The use of the low spatial frequencies of scenes should reduce the amount of information required to isolate large objects, as shown by the filtered images in Section 11.4.

#### 19.4.9 Recognition of Complex Scenes

Sutherland (1968) noted that the human can recognize a complex scene in presentation times as brief as 100 milliseconds. Although small inconsistencies may not be detected, large systematic ones are easily noticed. If, for example, a patch of some object is presented in some quadrant of a picture or a blank is left in some scene, it is easily reported. However, provided that there are no gross differences, small inconsistencies may go undetected. The paradox is: If *all* the information about the scene is being processed, why can't the details of each part of the picture be reported (Sutherland, 1968)?

One way that the preceding observations are a paradox is if the assumption is made that the visual system always processes all the information in a complex scene all the time. Many researchers assume that because all the detailed information can be described in a complex scene, the visual system must be processing all that detail as the scene is viewed. However, as the introduction to this dissertation and subsequent reviews of the filtering characteristics of mammalian visual systems stressed, much information has to be thrown away at various levels in the visual system. Since the low spatial frequencies of objects and textures have been shown to convey much information about shape, symmetry, etc., then the details—i.e., the high spatial frequencies—need not be processed at all for form recognition. In other words, there is no paradox if the visual system uses spatial filters to segregate relevant from irrelevant information about objects at very early stages of processing.

The price that the visual system pays for such a scheme is susceptibility to certain visual illusions and other "failures"

such as the previous paradox suggested by Sutherland. However, this is a small price to pay for rapid, global processing. It seems that the evolutionary pressures that shaped the design of visual systems were survival needs. The early visual systems had to do processing with minimum information in a rapid manner to determine whether the organism was to eat or be eaten. The organism could not care if there was any detailed information above that which was required to do that task. Thus, spatial detail exceeding that which is necessary to perform specific tasks becomes redundant.

As pointed out in the previous sections on segmentation, more research will have to be done before the analysis of complex scenes can be explained. The complex scenes that were processed in this dissertation, e.g., Figure 44, are just a beginning. However, it seems clear that such an analysis should be approached by considering the minimum amount of information, from low-pass filtered images, required to perform certain tasks rather than high spatial frequency details.

#### 19.4.10 Perceptual Learning

Sutherland (1968) suggested that it is important for an adequate theory of pattern recognition to be able to account for perceptual learning, i.e., the ability to recognize that a new object belongs to a certain class of objects that have been learned.

Tallman (1970) used the basic concept of a filtered transform to build an adaptive pattern recognition scheme. Once the machine was trained on an initial set of objects (the low spatial frequencies of similar objects were averaged), any subsequent errors in classification of new objects resulted in a shift in the average spatial frequencies to include the new object. In other words, the decision boundary based upon the feature space of the low spatial frequencies was shifted to accept this new pattern. The machine, albeit in a crude manner, learned. It has a long way to go to compete with human performance, but it is a powerful beginning that is consistent with the concepts reported in this dissertation.

The results of filtering suggest that classification of objects can be based on information from their low spatial frequencies. If the visual system is indeed storing just a few low spatial frequencies about objects in memory, the classification of objects into certain classes can be made quite easily. There are clearly other higher perceptual processes involved with learning than just the extraction of certain ranges of spatial frequencies. However, the filtering reported here offers at least a quantitative beginning with which to look at those other processes.

#### 19.4.11 Redundancy

Sutherland (1968) used Julesz-type random dot pictures as an example of the failure of the visual system to see differences between certain pictures even though acuity limitations were not involved. He also asked how "We . . . take advantage of the redundancy of our visual environment in forming the classes of picture that we do form." As discussed in Section 11.4, the filtering of random dot patterns can offer a simple explanation for the first observation.

The discussion of machine classification in Section 19.3 and the low-pass filtered images shown in this dissertation suggest an answer to the second question. Redundancy of information plays an important role in communication systems. The results of the filtering of many objects have shown that the high spatial frequencies are redundant for the classification of those objects.

If one point is to be made from the filter concept, it is that spatial information required for the classification of objects and the spatial information about an object that is redundant are interrelated. It is perhaps no accident that the low-pass filtering provides the basic form of objects with the minimum of spatial information. Consider the tremendous amount of redundancy in pattern information that has been shown. A 7 by 7 matrix of spectral coefficients provided sufficient information for the classification of many objects. Furthermore, such information was necessary for the generalization of forms that were made up of discrete pattern elements. A 7 by 7 matrix provides 96 spectral coefficients if the zero spatial frequency term is excluded. However, half of these coefficients are redundant due to the symmetry properties of the sine and cosine parts of the Fourier transform. Thus, 24 real (cosine) and 24 imaginary (sine) components have been used. (Both sine and cosine terms are necessary in order to preserve the phase information.)

It should be emphasized that this 7 by 7 matrix is a general value. Some objects will require less information and some

objects more. Furthermore, not all the spatial frequency/orientation pairs of spectral information in a 7 by 7 matrix will be needed for all objects. This fact should be evident from looking at the various magnitude spectra. The 7 by 7 matrix should be viewed as a general box size into whose slots the relevant spectral components from objects are put.

Rate-distortion theory (Shannon, 1960) is a field that attempts to deal with information that has to be transmitted over a noisy channel with finite error. It is suggested that the spatial filtering typified in this dissertation may lead to the value of  $D$ , the measure needed to specify the average distortion of an object. Such a measure is required to specify the cost of errors in a communication system.

#### 19.4.12 Physiological Evidence

The physiological and psychophysical evidence which was used to support and to specify the spatial filters of this dissertation has been discussed in Chapters 5-7.

#### 19.4.13 Summary

The previous discussions have shown briefly how the filter concept can begin to offer certain explanations to the major problems of pattern recognition. The filter concept has attempted to go beyond explanations of certain individual problems to provide a quantitative structure and concept that appears to unify the different classes of certain perceptual problems—Gestalt laws, texture analysis, visual illusions, and multistability. Furthermore, monocular depth perception and memory have been discussed, as well as memory within the concept of filtering. Although machine pattern recognition of three-dimensional solid objects and overlapping objects has not been attempted so far using these kinds of techniques, it does appear that they may be equally solvable within the context of the filtering presented in this dissertation.

### 19.5 Why Are the Low Spatial Frequencies More Important than the High Spatial Frequencies?

Objects can still be correctly identified from just the high spatial frequencies. If so, then why emphasize the importance of the low spatial frequencies? Four reasons for the importance of low spatial frequencies over the high spatial frequencies in the processing of spatial information are given in the following paragraphs.

First, it has been shown that only a small number of spatial frequencies are needed to provide a quantitative description of the basic form of an object. The minimum number of spatial frequencies required to correctly classify an object provides a firm criterion for their selection, whereas higher spatial frequencies do not (e.g., see Section 9.4). There is a large set of possible high spatial frequencies that could be selected that can satisfy the criteria of representing the object. Also, any set of high spatial frequencies would have to contain a larger number of spatial frequencies than the minimum set of low spatial frequencies. For example, a bandwidth of two octaves with a centre frequency of 2 would have spatial frequencies for 2 to 8, or 7 integer spatial frequencies. This would increase the memory store in either a machine or a biological system.

Second, most of the spectral energy is found in the low spatial frequencies of objects. This was shown even for outline objects. It is not too surprising that the spectral region containing most of the energy of an object also contains most of the important form information about the object.

Third, it has been shown repeatedly that the low spatial frequencies provide the basic form of an object independent of the particular features that make up the form. The high spatial frequencies, although able to convey the basic form implicitly, do not solve the problem of generalization; another stage of processing would have to be used to extract the basic form from such high spatial frequencies.

Fourth, any serious attempt to understand how the human visual system processes the objects it sees must contend with the spatial information that is lost under everyday viewing conditions. The low spatial frequencies contain the only spatial information that can survive reduced illumination, low contrast, minimum retinal sampling from distance viewing, inhomogeneous retinal sampling from close viewing, movement, etc.

Of course, the high spatial frequencies play an important role in providing information about the details of objects without which some discriminations would be impossible. However, from these practical and realistic considerations, it is the low rather than the high spatial frequencies that appear to contain the important general information of spatial objects for machines and biological visual systems.

#### 19.6 What Is the Bandwidth and Shape of the Channels?

The reader may expect one specific bandwidth and filter shape to come out of this study. But that is not the result. Several detailed examples of filtered images have shown that similar forms can exist from a *general* band of several harmonics filtered with *different* functions. This is not a weakness of the filter concept in an attempt to understand visual perception but, rather, a strength. What the filtering results suggest is that a large amount of spatial information can be extracted from objects without the need to invoke complex mechanisms to extract and manipulate *precise* features from objects.

The previous discussions (Chapters 6 and 7) of the bandwidths of channels from neurophysiological and psychophysical data suggest a certain continuum of both bandwidth and shape. This kind of a continuum is what one would expect from a biological system. It is suggested that any serious theory about visual information processing must contend with spatial information in such a *continuum* of bandwidths and shapes of channels.

#### 19.7 What Could Be the Basis for the One- to Two-Octave-Wide Channels?

There is a common factor to the biological data (see Chapters 6 and 7), machine pattern recognition techniques (see Section 19.3), and the filtering that has been presented in this dissertation. All three systems extract spatial frequency (size) and orientation information in a two-dimensional space. Furthermore, using neurophysiological and psychophysical techniques, one- to two-octave bandwidths have been found repeatedly for channels in biological systems. Similar bandwidths have been found to provide successful machine pattern recognition when the algorithms were based upon filtered transforms. Finally, it has been shown often by the author, using both optical and digital filtering techniques, that a channel bandwidth of one to two octaves can provide information about the basic forms of many objects.

Is the similar channel bandwidth that has been found to be important for processing objects in three different systems a happy coincidence, or does it reflect some basic unit of spatial information? Further research is needed to answer that question fully. It is suggested, however, that the one- to two-octave bandwidth does represent a fundamental unit of spatial information processing in the visual system.

It seems that the, roughly, two to four harmonics that make up the one- to two-octave channel bandwidth found in mammalian visual systems reflect some basic physiological substructure. It also seems reasonable that this unit is found at the earliest processing of spatial information in the visual system. Once the optical image is filtered by the retinal ganglia, no more information about the *local* (explicit, see Section 19.4.2) spatial information of an object is available to higher visual processes. Thus, implicit (see Section 19.4.2) phase information about an object would remain and be limited by the extent of overlap of receptive fields in the retina. Robson (1975) determined that the number of overlapping receptive fields in any one area of the retina of cat is about three.

Further supportive evidence for the one- to two-octave channel bandwidth comes from the data of Wilson and Bergen (1977). They compared two sets of data collected to determine the spatial inhomogeneity, local variation, and probability summation over the retina. Analysis of the line-spread function and thresholds taken at different parts of the retina suggested that there might be just four different receptive field sizes at each retinal eccentricity.

It should be stressed that these data do not mean that there are narrow one- to two-octave-wide channel bandwidths at the retina. They mean that the local spatial information is collected by relatively wideband channels in clumps of three or four receptive fields. What is suggested, then, is that as the spatial information is filtered into narrower channels at the higher stages of visual processing, the integrity of the initial implicit phase is maintained to provide a fundamental unit of up to about four harmonics of spatial information.

Are there any other clues, in addition to the results of spatial filtering, that also suggest that spatial processes are limited

to about four harmonics? Atkinson, Campbell, and Francis (1976) found that the limit for counting linear arrays of dots or lines with only one glance (150 msec presentation time) with total accuracy is from 2 to 4 dots, depending upon the dot spacing. In a further study, Atkinson, Francis and Campbell (1976) reported that if the stimuli have large differences in orientation (90 degrees) and a large intergroup space, three times the interdot interval, then accurate counting within each subgroup can take place.

These results suggest that spatial information used in counting is limited to the initial bandwidth of mechanisms in the visual system. Large numbers of dots would require a larger bandwidth to provide sufficient sampling for a counting mechanism.

After learning of these results, the author went back to some early filtering on 4 by 4 dot arrays (Figure 95,a). The fundamental frequency,  $f_1$ , of the dots is  $32/14$ , or 2.29 cycles per array (c/a);  $f_2 = 4.57$  c/a;  $f_3 = 6.86$  c/a; and  $f_4 = 9.15$  c/a. Therefore, there should be discriminably different dots from a spatial filter whose bandwidth is from one to two octaves — in this case, from 4.5 c/a to 9.15 c/a. The results of the spatial filtering are shown in Figure 95,b,c,d; the dots are clearly discriminable when the third harmonic of the array is captured by a 7 by 7 spatial filter, 6.86 c/a (Figure 95,c). The mathematics required to relate the bandwidth required to discriminate the number of elements in an array is given by the array theorem, e.g., see Hecht and Zajac (1974). (Briefly, the Fourier transform of an array of similar objects is given by the product of the Fourier transform of an array of point sources by the Fourier transform of the elements.)

## 19.8 What Is the Minimum Number of Spatial Frequencies Necessary for the Identification of Objects?

There is no *one* number. Each task and each object requires slightly different numbers of spatial frequencies or harmonics. For example, to detect the presence of an object requires only very low spatial frequency, less than the fundamental spatial frequency of the object. The classification of Snellen letters requires from about 1.5 to 2.5 cycles per letter. The identification of a face from a small class of faces requires about 4 cycles per face width. The number of spatial frequencies (referenced to the overall size of the object) which are required will be based on the part of the object required to do the particular task. For example, if one needs to discriminate a square wave from a sine wave, then the detection of the third harmonic is sufficient (Campbell and Robson, 1968).

In optics, the number of spatial frequencies required to allow objects to be classified and discriminated was suggested to be the half-power point of the central maximum of the particular feature relevant for the particular task (Ginsburg, 1971,a,b). The half-power point in terms of discrete harmonics of an object is about the first harmonic. That is, the detection of the fundamental harmonic of the particular feature necessary to perform the specific task appears to be sufficient. Additional spatial information will be redundant for *that* task for a certain percentage of the time. This assertion is supported by an experiment performed by Quine (1971) showing that a notch contained in a filtered image of a large square was correctly identified at the 75 percent correct level when the half-power point of the notch was passed by the filter.

## 19.9 The Roles That Fourier Analysis Can Play in Spatial Vision

### 19.9.1 Fourier Analysis as a Metric

Both the theoretical and practical reasons for using Fourier analysis as a means to describe spatial information in simple and complex objects have been discussed.

Furthermore, Fourier transformation has provided the features of objects that have been used to yield a measure of similarity of objects for human and machine experiments (Section 19.3). Although there are other transforms that could be used, the vast literature on the Fourier transform, the simplicity of obtaining the Fourier transform by means of optical diffraction, and the general availability of digital computer programmes for the Fourier transform have motivated its use in this dissertation.

### 19.9.2 Fourier Analysis as a Tool for Spatial Filtering

The two-dimensional Fourier transform has been used to analyze objects with respect to spatial frequency and

orientation to allow selective filtering along those stimulus dimensions. Very simple spatial filters were used to extract certain regions of spatial frequency and orientation information.

It is emphasized that all the filtering that has been done using band-pass spatial filters in the Fourier domain could be done by convolving the object with the Fourier transform of the band-pass spatial filters. Once the problem is solved in a linear transform domain, then it is very simple to apply that solution to the space domain. However, besides being more complicated, convolution techniques do not offer insight into thinking about the filtering process by mechanisms that range in size and orientation that a two-dimensional transform would, i.e., the magnitude and phase spectra of the Fourier transform.

### 19.9.3 The Fourier Transform as a Model of Visual Information Processing

The author has gained much insight into two-dimensional spatial filtering from the two-dimensional Fourier analysis, making an analogy between Fourier analysis and the mechanisms in the visual system. Thus, the author has used Fourier analysis as a model of encoding visual spatial information by mechanisms tuned to different spatial frequencies (sizes) and orientation. The model aspect of the Fourier analysis will now be discussed.

There appears to be a good relationship between the filtering properties of the sinusoids of the two-dimensional Fourier transform and visual mechanisms. Note the weighting functions of the sinusoidal filters of the transform (Figure 2). As can be seen in the upper right corner of each sinusoid, the schematic weighting functions have similar properties to certain receptive fields described in terms of feature detectors, e.g., Barlow, et al. (1972). The cosine harmonics have filtering properties of line detectors. The sine harmonics have the filtering properties of edge detectors. Such sinusoids could even be called fuzzy bar or edge detectors.

In general, these finite sinusoids have similar periodicity to the line weighting functions of complex cells in the visual cortex of cat found by Glezer, et al. (1973), and Pollen and Ronner (1975). Although the shape is similar (a closer fit would be obtained by tapering the sinusoids with a cosine function), there is no evidence for such narrowly tuned neurons. However, the two-dimensional sinusoids have provided an intuitive jump between a Fourier-like transform and cortical mechanisms tuned to different ranges of spatial frequency and orientation.

Thus, two-dimensional analysis, typified by the Fourier transform, can provide not only a tool but also an analogue from which to view the decomposition of any object into the same stimulus domain or feature space that has been found relevant from biological data—spatial frequency (size) and orientation.

#### 19.9.3.1 From a Local to a Global Harmonic Analysis

There is a more subtle aspect of the magnitude spectrum that appears to be particularly relevant to the analysis of such objects as the multistable triangles. That is, the magnitude spectrum represents the spectral decomposition of all the patterns within the pattern space of analysis or aperture. In the case of the triangles, all the triangles in the picture constitute the pattern space. Therefore, any one spectral region that is filtered in the magnitude spectrum will affect each pattern similarly, as was shown with the triangles (Figures 76 and 77). Although the end result of such a process appears to be an analogue to our own perception, it does represent additional mechanisms, or at least interconnections between known mechanisms, that go beyond our present knowledge of visual processes.

Consider, as an example, the analysis of each triangle by known visual mechanisms. Each triangle excites mechanisms of similar spatial frequency (size) and orientation, in different regions of visual space. Thus, each triangle can be considered undergoing a local Fourier-like transformation. This represents the first stage of an actual Fourier transform. However, in order to obtain the pattern information analogous to the magnitude spectrum, there have to be other channels that pool or act upon each local spectrum over similar ranges of spatial frequency and orientation and cover large regions of visual space. Without such processes, it seems highly unlikely that all the mechanisms could act in unison to produce the global multistable perceptions of the triangles that were observed. Thus, spatial information may be pooled from a local harmonic analysis into a more global harmonic analysis along the stimulus dimensions of spatial frequency (size) and orientation.

Although such mechanisms offer a reasonable explanation of the perception of a field of similar but randomly positioned equilateral triangles, the mechanisms appear to be limited to regions of visual space that contain similar pattern orientation and patterns that are close to one another. As previously discussed in Section 13.6, triangles (in particular spatial configurations) do not generally appear as a group that changes orientation in unison. However, all the triangles within a subgroup do appear to point in similar orientations, as shown in Figure 77. The local grouping seems to depend upon the similarity and proximity of each pattern within a region and, further, certain regions can be analyzed somewhat independently of other regions. Thus, the concept of a local harmonic analysis for each pattern could lead to a more global harmonic analysis at the next processing level, determined by the spatial arrangements and the similarity of the patterns at an earlier processing level. A completely random arrangement of similar patterns will allow a global transform to extend over all of visual space. Structured arrangements of similar patterns restrict the transform grouping over regions of visual space within which the substructure is uniform, e.g., the collinearity and proximity of the triangles of Figure 77.

One of the rules that determine the extent to which similar spatial frequency and orientation information will pool to form a more global region might be the classical grouping concepts such as similarity and proximity. These concepts were shown to be physically realizable from the low spatial frequencies of classical Gestalt grouping patterns (Section 9.5). Perhaps it is the low spatial frequency images of visual space that aid in the formation of localized harmonic analyses.

It is from this point of view that the Fourier transform is an analytical tool as well as a model with which to analyze and view the way that visual mechanisms seem to be processing the objects that are observed.

This analysis, in agreement with other studies, suggests that a two-dimensional Fourier-like transform domain can provide a good first approximation to the stimulus domain in which visual mechanisms are processing the pattern information (Kabisky, 1967; Campbell and Robson, 1968; Ginsburg, 1971; Pollen, et al., 1971; Glezer, et al., 1973; Maffei and Fiorentini, 1973; DeValois, 1976).

Of course, this does *not* mean that one should expect to see a Fourier spectrum at some level of the visual system. Rather, a sufficient condition for such a view is that mechanisms tuned to different ranges of spatial frequency (size) and orientation within local regions of visual space are used as units of information somewhat independently of mechanisms tuned to different spatial frequencies (sizes) and orientations.

The term Fourier-like is used because there are many other two-dimensional transforms that would satisfy the requirement of decomposing patterns into different sizes and orientations. The decomposition of patterns with perfect, infinitely long sinusoids is not a prerequisite for the preceding analysis. Although a linear mathematical process has been used to create the pictures in this dissertation, the visual system does not seem to be strictly linear. Indeed, previous results with machine pattern recognition and filtering have been quite successful using other linear as well as nonlinear two-dimensional functions to transform and classify patterns (Kabisky and Carl, 1971). It appears that almost any quasi-periodic set of size and orientation functions would suffice at this level of analysis.

The important concept of this dissertation is filtering — not what the particular filtering elements are. However, since a particular transform must be chosen in order for any analysis to be done, one is chosen for the best compromise between being a good tool and a good model. For example, both the Fourier and Walsh transforms have been used for pattern analysis, e.g., see Ginsburg et al. (1976). However, the Fourier transform has been shown to provide more consistent correlates to everyday perception, e.g., Gestalt grouping and visual illusions, than does a Walsh transform (Ragsdale, 1972). This is not too surprising when one considers that sinusoids are more like the spatial properties of receptive fields than the rectangular-shaped Walsh functions (which are, incidentally, literal bar and edge detectors).

Again, the important concept is not so much the particular two-dimensional transform components in a two-dimensional space. It is unlikely that the use of an analytical set of functions that approximate the spatial properties of the receptive fields will, at *this* level of analysis, substantially change the filtering results to date. However, there are sure to be some phenomena that will be better observed with a closer approximation to the properties of the receptive fields.



### 19.10 Future Investigations

The next stage to this research is to try to determine the rules by which the channels combine. A hierarchy of filtered images appears needed to provide both the general and detailed spatial information about objects. The results of some of the contrast illusions, e.g., the subjective contours, suggest that certain parts of low band-pass filtered images "peek" through in places where there is no pattern. Further, it is possible that the classic problem of Mach bands results from the overall filtered image when the channels combine. This research will continue based on the combinational rules outlined in Section 12.8.3.

The author hopes to learn some of the combinational rules from continued studies of abnormal vision. Clearly, the *contrast matching studies of the amblyope*, discussed in Chapter A-4, present a more complex interrelationship between spatial frequency and contrast than had been previously considered.

Another major area that will be investigated further is the relationship between single and/or multiple spatial frequencies of complex patterns and the contrast sensitivity function to predict the identification of any arbitrary pattern, especially for those objects having a fundamental frequency greater than 1 c/d. This will require more detailed examination of the relevant spatial frequencies of patterns in terms of their two-dimensional spectra and the mechanisms in the visual system that detect spatial stimuli.

The hierarchy of filtered images provides a reasonable construct that allows different spatial information about an object to be attended to at will. Just as either the entire orchestra or only the woodwind section of the orchestra can be attended to, similarly either the entire portrait or only the form of the portrait can be attended to. The certain parallels between the visual and auditory systems suggest that the concept of a hierarchy of filtered images may be relevant to the auditory and other sensory systems.

## SUMMARY

This dissertation investigated visual information processing using spatial filters that are constrained by biological data. The four parts of this dissertation were (1) a theoretical background to Fourier analysis, (2) a review of the literature relating to the spatial filtering characteristics of mammalian visual systems, (3) visual information processing in terms of spatial filtering, and (4) the relating of contrast sensitivity to the identification of complex objects. The common denominator in all the investigations that have been reported is spatial filtering. The major goal of the dissertation was to attempt to explain certain aspects of visual information processing in the visual system with a filter concept. The results of this attempt are summarized below:

(1) Biological data from cat, monkey, and man, gathered using neurophysiological and psychophysical methods, provide much evidence for the existence of mechanisms tuned to different regions of spatial frequency and orientation. In general, the spatial frequency bandwidth is one to two octaves and the orientation bandwidth is  $\pm 15$  degrees. The overall filtering characteristic of the visual system is the envelope of the activity of those mechanisms and can be determined by contrast sensitivity and contrast matching functions.

(2) Two-dimensional spatial filters were made based upon the general and specific filtering properties of the overall (MTF) and individual mechanisms (channels). These spatial filters were used to filter a wide variety of objects.

(3) The perceptual problems of the classification of simple and complex objects — Gestalt principles, visual textures, visual illusions, and multistability — with few exceptions, have yielded gracefully to the concept of spatial filtering. Parsimony reigned as explanations for these seemingly disparate visual phenomena were given in terms of the known two-dimensional filtering properties of the visual system.

(4) A detailed study using generalized and biologically derived band-pass spatial filters further demonstrated the power of a general filter concept for visual information processing. The full spectrum of perceptual information about a complex object from basic form to the finest detail was available with only seven two-octave-wide band-pass filters (channels). These results led to the concept of a hierarchy of filtered images.

(5) In general, the MTF filter provided the details of objects that correspond to what is seen. One- to two-octave band-pass filters appeared to provide the generalized information that is perceived about objects. The specific bandwidth and shape of the spatial filters were not important for the class of objects and perceptual problems discussed in this dissertation.

(6) Combining the filtering concepts of the minimum information required for the identification of objects with data from an experiment that determined the minimum amount of contrast required for the identification of Snellen letters demonstrated the predictive power of the filter concept. The Snellen acuity of 17 of 22 eyes of amblyopes and patients suffering from multiple sclerosis could be predicted within one Snellen line. The increase of spatial sensitivity over a narrow range of spatial frequency of one amblyope resulted in a concomitant increase in Snellen letter acuity. Especially interesting was that the increased Snellen acuity could be explained from the minimum number of spatial frequencies required for letter identification. These results appear to provide the first direct evidence for the existence of narrow-band mechanisms in the visual system which are used in the identification of complex objects. Thus, the ability to establish a relationship between Snellen letter acuity and contrast sensitivity suggests that the filter concept is neither blind nor empty.

In general, these results support the view that the MTF is the window which reduces the range of size of objects that can be seen. The much narrower and orientation-selective filters that make up the MTF appear to filter relevant form information. The outputs of all the individual filters appear to be presented simultaneously to create the global picture that is seen.

The picture that emerges from these studies is that visual perception may be structured from a hierarchy of filtered images, each image representing one level of visual information. This hierarchy of filtered images may be the keyboard from which the harmony of visual perception is obtained.

## REFERENCES

- Andrews, H. C., 1970, *Computer Techniques in Image Processing*, New York: Academic Press.
- Atkinson, J., Campbell, F. W., Fiorentini, A., and Maffei, L., 1973, The dependence of monocular rivalry on spatial frequency, *Perception*, 2, 127-133.
- Atkinson, J., Campbell, F. W., and Francis, M. R., 1976, The magic number  $4 + 0$ : a new look at visual numerosity judgements, *Perception*, 5, 327-334.
- Atkinson, J., Francis, M. R., and Campbell, F. W., 1976, The dependence of the visual numerosity limit on orientation, color, and grouping in the stimulus, *Perception*, 5, 335-342.
- Attneave, F., 1954, Some informational aspects of visual perception, *Psychol. Rev.*, 61, 183-193.
- Attneave, F., 1968, Triangles as ambiguous figures, *Am. J. Psychol.*, 181, 447-453.
- Attneave, F., 1971, Multistability in perception, *Scient. Am.*, 225, 62-71.
- Attneave, F., 1972, Personal communication.
- Barlow, H. B., 1961, Some possible principles underlying the transformations of sensory messages, in *Sensory Communication*, W. A. Rosenblith, ed., New York: John Wiley, pp. 217-234.
- Barlow, H. B., Narashimhan, R., and Rosenfeld, A., 1972, Visual pattern analysis in machines and animals, *Science*, 177, 567-575.
- Beck, J., 1966.a, Perceptual grouping produced by changes in orientation and shape, *Science*, 154, 538-540.
- Beck, J., 1966.b, Effect of orientation and of shape similarity on perceptual grouping, *Percept. Psychophys.*, 1, 300-302.
- Beck, J., 1967, Perceptual grouping produced by line figures, *Percept. Psychophys.*, 2, 491-495.
- Beck, J., 1972, Similarity grouping and peripheral discriminability under uncertainty, *Am. J. Psychol.*, 85, 1-19.
- Békésy, G. von, 1968, Brightness distribution across Mach bands measured with flicker photometry and the linearity of sensory nervous interaction, *J. Opt. Soc. Am.*, 58, 1-8.
- Benussi, F., 1902, Über den einfluss der farbe auf grösse der Zöllnerischen täuschung, *Z. für Psychol.*, 29, 264-351 and 385-433.
- Bishop, P. O., Henry, G. H., and Smith, Q. J., 1971, Binocular interaction fields of single units in the cat striate cortex, *J. Physiol.*, 216, 39-68.
- Blakemore, C. and Campbell, F. W., 1969, On the existence of neurons in the human visual system selectively sensitive to the orientation and size of retinal images, *J. Physiol.*, 203, 237-260.
- Blakemore, C. B., Carpenter, R. H. S., and Georgeson, M. A., 1970, Lateral inhibition between orientation detectors in the human visual system, *Nature*, 228, 37-39.
- Blakemore, C. B., Muncey, J. P. J., and Ridley, R. M., 1973, Stimulus specificity in the human visual system, *Vision Res.*, 13, 1915-1933.

- Blakemore, C. B. and Nachmias, J., 1971, The orientation specificity of two visual after-effects, *J. Physiol.*, 213, 157-174.
- Bodis-Wollner, I., 1972, Visual acuity and contrast sensitivity in patients with cerebral lesions, *Science*, 178, 769-771.
- Bodis-Wollner, I. and Diamond, S. P., 1976, The measurement of spatial contrast sensitivity in cases of blurred vision associated with cerebral lesions, *Brain*, 99, 695-710.
- Borish, I. M., 1970, *Clinical Refraction*, New York: The Professional Press, Inc.
- Bracewell, R., 1965, *The Fourier Transform and Its Applications*, New York: McGraw-Hill.
- Braddick, O., Campbell, F. W., and Atkinson, J., 1977, Channels in vision: basic aspects, to appear in *Handbook of Sensory Physiology*, Vol. VIII: Perception, Held, R., Leibowitz, H., and Teuber, H. L., eds., Heidelberg: Springer-Verlag.
- Breitmeyer, B. G. and Ganz, L., 1976, Implications of sustained and transient channels for theories of visual pattern masking, saccadic suppression, and information processing, *Psychol. Rev.*, 83, 1-36.
- Brentano, F., 1892, Uber ein optisches paradoxen, *Z. Psychol.*, 3, 349-358.
- Brigham, E. O., 1974, *The Fast Fourier Transform*, New Jersey: Prentice-Hall, Inc.
- Burian, H. M., 1967, The behavior of the amblyopic eye under reduced illumination and the theory of functional amblyopia, *Doc. Ophthalmol.*, 23, 188-202.
- Campbell, F. W., 1974, The transmission of spatial information through the visual system, in *The Neurosciences Third Study Program*, Schmitt, F. O. and Worden, F. G., eds., Cambridge, Mass.: The M.I.T. Press, 95-103.
- Campbell, F. W., Carpenter, R. H. S., and Levinson, J. Z., 1969, *J. Physiol.*, 204, 283-298.
- Campbell, F. W., Cooper, G. F., and Enroth-Cugell, C., 1969, The spatial selectivity of the visual cells of the cat, *J. Physiol.*, 203, 223-235.
- Campbell, F. W., Cleland, B. G., Cooper, G. F., and Enroth-Cugell, C., 1968, The angular selectivity of visual cortical cells to moving gratings, *J. Physiol.*, 198, 237-250.
- Campbell, F. W., Gilinsky, A. S., Howell, E. R., Riggs, L. A., and Atkinson, J., 1973, The dependence of monocular rivalry on orientation, *Perception*, 2, 123-125.
- Campbell, F. W. and Green, D. G., 1965, Optical and retinal factors affecting visual resolution, *J. Physiol.*, 181, 576-593.
- Campbell, F. W. and Gubisch, R. W., 1966, Optical quality of the human eye, *J. Physiol.*, 186, 558-578.
- Campbell, F. W. and Howell, E. R., 1972, Monocular alteration: a method for the investigation of pattern vision, *J. Physiol.*, 225, 15-21.
- Campbell, F. W., Howell, E. R., and Robson, J. G., 1971, The appearance of gratings with and without the fundamental Fourier component, *J. Physiol.*, 217, 17-18.
- Campbell, F. W. and Kulikowski, J. J., 1966, Orientation selectivity of the human visual system, *J. Physiol.*, 187, 437-445.

- Campbell, F. W., Kulikowski, J. J., and Levinson, J. Z., 1966, The effect of orientation on the visual resolution of gratings, *J. Physiol.*, 187, 427-436.
- Campbell, F. W. and Maffei, L., 1970, Electrophysiological evidence for the existence of orientation and size detectors in the human visual system, *J. Physiol.*, 207, 635-652.
- Campbell, F. W. and Robson, J. G., 1964, Application of Fourier analysis to the modulation response of the eye, *J. Opt. Soc. Am.*, 54, 581.
- Campbell, F. W. and Robson, J. G., 1968, Application of Fourier analysis to the visibility of gratings, *J. Physiol.*, 197, 551-566.
- Carl, J. W. and Hall, C. P., 1972, The application of filtered transforms to the general classification problem, *IEEE Trans. Comput.*, C-21, 785-790.
- Carlson, S. K., Cohen, R. W., and Gorog, I., 1977, Visual processing of simple two-dimensional sine-wave luminance gratings, *Vision Res.*, 17, 351-358.
- Carter, B. E. and Henning, G. B., 1971, The detection of gratings in narrow-band visual noise, *J. Physiol.*, 219, 355-365.
- Chiang, C., 1968, A new theory to explain geometrical illusions produced by crossing lines, *Percept. Psychophys.*, 3, 174-176.
- Cleland, B. G., Dubin, M. W., and Levick, W. R., 1971, Sustained and transient neurons in the cat's retina and lateral geniculate nucleus, *J. Physiol.*, 217, 473-496.
- Cooper, G. R. and McGillem, C. D., 1967, *Methods of Signal and System Analysis*, New York: Holt, Rinehart, and Winston Inc.
- Coren, S., 1972, Subjective contours and apparent depth, *Psychol. Rev.*, 79, 359-367.
- Cornell, C. O., 1978, Quantitative Predictions of Length in the Müller-Lyer Illusion as Perceived by the Human Visual System, MS Thesis GE/EE/78M-9, Wright-Patterson Air Force Base, Ohio: Air Force Inst. Technol.
- Cornsweet, T., 1970, *Visual Perception*, New York: Academic Press.
- Craik, K. J. W., 1966, *The Nature of Psychology*, Sherwood, S. L., ed., Cambridge: Cambridge University Press. Posthumous publication of his Ph.D. thesis: *Visual Adaptation*, 1940, University of Cambridge.
- Cutrona, L. J., 1965, Recent developments in coherent optical technology, in *Optical and Electro-Optical Information Processing*, Tippett, J. T., ed., Cambridge: M.I.T. Press, 123-141.
- Daitch, J. M. and Green, D. G., 1969, Contrast sensitivity of the human peripheral retina, *Vision. Res.*, 9, 947-952.
- Davidson, M., 1968, Perturbation approach to spatial brightness interaction in human vision, *J. Opt. Soc. Am.*, 58, 1300-1308.
- Day, R. H., 1972, Visual spatial illusions: a general explanation, *Science*, 175, 1335-1340.
- Dealy, R. S. and Tolhurst, D. J., 1974, Is spatial frequency adaptation an after-effect of prolonged inhibition?, *J. Physiol.*, 241, 261-270.
- DeValois, K. K., 1977, Spatial frequency adaptation can enhance contrast sensitivity, *Vision Res.*, 17, 1057-1065.

- DeValois, R. L., 1976, Color coding and lateral interactions, abs. Workshop on Spatial Contrast, Amsterdam, The Netherlands (4-9 January).
- Duke-Elder, W. S., 1949, Text-Book of Ophthalmology, Vol. IV, London: Henry Kimpton.
- Dumais, S. T. and Bradley, D. R., 1976, The effect of illumination level and retinal size on the apparent strength of subjective contours, *Percept. Psychophys.*, 19, 229-245.
- Ebbinghaus, H., 1902, *Grundzüge der Psychologie*, Leipzig: Veit, Vols. I & II.
- Ehrenstein, W., 1925, Versuche über die beziehungen zwischen bewegungs und gestaltwahrnehmung, *A. Psychol.*, 95, 305-352.
- Eichelman, W. H., 1970, Changes in the relative discriminability of slant and configuration differences, Ph.D. Thesis, Univ. of Oregon.
- Eichelman, W. H. and Ginsburg, 1977, A. P., Functional effects of anisotropic spatial filtering in visual discrimination (submitted for publication).
- Enroth-Cugell, C. and Robson, J. G., 1966, The contrast sensitivity of retinal ganglion cells of the cat, *J. Physiol.*, 187, 517-552.
- Estevéz, O. and Cavanus, C. R., 1976, Low-frequency attenuation in the detection of gratings: sorting out the artifacts, *Vision. Res.*, 16, 497-500.
- Flom, M. D., Weymouth, F. W., and Kahneman, D., 1963, Visual resolution and contour interaction, *J. Opt. Soc. Am.*, 53, 1026-1045.
- Fick, A., 1851, *De Errone Quodam Optic Asymmetria Bulbi Effecto*, Marburg: Koch.
- Fisher, G. H., 1967, Ambiguous figure treatments in the art of Salvador Dali, *Percept. Psychophys.* 2, 328-330.
- Fisher, G. H., 1968, Ambiguity of form: old and new, *Percept. Psychophys.* 4, 189-192.
- Ganz, L. and Day, R. H., 1965, An analysis of the satiation-fatigue mechanisms of figural after-effects, *Am J. Psychol.*, 78, 345-361.
- Georgeson, M. A., 1976, Personal communication.
- Georgeson, M. A. and Sullivan, G. D., 1975, Contrast constancy: deblurring in human vision by spatial frequency channels, *J. Physiol.*, 252, 627-656.
- Gibson, J. J., 1950, *The Perception of the Visual World*, Boston: Houghton Mifflin.
- Ginsburg, A. P., 1971,a, Psychological Correlates of a Model of the Human Visual System, MS Thesis GE/EE/71S-2, Wright-Patterson Air Force Base, Ohio: Air Force Inst. Technol.
- Ginsburg, A. P., 1971,b, Psychological correlates of a model of the human visual system, *Proc. 1971 National Aerospace Electronics Conference (NAECON)*, Dayton, Ohio: IEEE Trans. on Aerospace and Electronic Systems, 283-290.
- Ginsburg, A. P., 1973, Pattern recognition techniques suggested from psychological correlates of a model of the human visual system, *Proc. 1972 National Aerospace Electronics Conference (NAECON)*, Dayton, Ohio: IEEE Trans. on Aerospace and Electronic Systems, 309-316.

- Ginsburg, A. P., 1975, Is the illusory triangle physical or imaginary?, *Nature*, 257, 219-220.
- Ginsburg, A. P., 1976, Are negligible illusions under appropriate scaling surprising?, *Perception*, 5, 119.
- Ginsburg, A. P., Carl, J. W., Kabrisky, M., Hall, C. F., and Gill, R. A., 1976, Psychological aspects of a model for the classification of visual images, in *Advances in Cybernetics & Systems*, J. Rose, ed., London: Gordon and Breach, Science Publishers Ltd., 1289-1305.
- Ginsburg, A. P., Cook, F. H., and Mott-Smith, J. C., 1972, Image Analysis Facility: An Interactive Digital Computer System, Research Report AFCRL-72-0115, Air Force Cambridge Research Laboratories, Bedford, Mass.
- Glezer, V. D., Ivanoff, V. A., and Tscherbach, T. A., 1973, Investigation of complex and hypercomplex receptive fields of visual cortex of the cat as spatial frequency filter, *Vision. Res.*, 13, 1875-1904.
- Goldstein, A. and Rosenfeld, A., 1964, Optical correlation for terrain type discrimination, *Photo. Eng.*, 30, 639-646.
- Graham, N., 1975, Spatial frequency channels in human vision: detecting edges without edge detectors to appear in *Visual Coding and Adaptability*, Harris, C. S., ed., Hillsdale, New Jersey: Lawrence Erlbaum Assoc.
- Graham, N., 1977, Visual detection of a periodic spatial stimuli by probability summation among narrow band channels, *Vision Res.*, 17, 637-652.
- Graham, N. and Nachmias, J., 1971, Detection of grating patterns containing two spatial frequencies: a comparison of single channel and multi-channel models, *Vision Res.*, 11, 251-259.
- Gregory, R. L., 1963, Distortion of visual space as inappropriate constancy scaling, *Nature*, 199, 678-680.
- Gregory, R. L., 1972, Cognitive contours, *Nature*, 238, 51-52.
- Gregory, R. L. and Harris, J. P., 1975, Illusion-destruction by appropriate scaling, *Perception*, 4, 203-220.
- Grosvenor, T., 1954, The effect of duration and background luminance upon the brightness discrimination of the amblyope, *Am. J. Optom. and Arch. Am. Acad. Optom.*, 31, 639-652.
- Gstalter, R. J. and Green, D. G., 1971, Laser interferometric acuity in amblyopia, *J. Ped. Ophthal.*, 8, 251-256.
- Harmon, L., 1973, The recognition of faces, *Scient. Am.*, 229, 71-82.
- Harmon, L. D. and Julesz, B., 1973, Masking in visual recognition: effects of two-dimensional filtered noise, *Science*, 180, 1194-1197.
- Hawkins, J. K., 1970, Textural properties for pattern recognition, in *Picture Processing and Psychopictorics*, Lipkin, G. S. and Rosenfeld, A., eds., New York: Academic Press, 347-370.
- Hay, G. A. and Chesters, M. S., 1972, Signal-transfer functions in threshold and suprathreshold, *J. Opt. Soc. Am.*, 62, 990-998.
- Hebb, D. O., 1949, *The Organization of Behavior*, New York: John Wiley.
- Hecht, E. and Zajac, A., 1974, *Optics*, London: Addison-Wesley.
- Helmholtz, H. von, *Handbuch der Physiologischen Optik*, Leipzig: Voss. Part I (1856), Part II (1860), Part III (1866). The first two parts were published in the same volume as the third part in 1866. This was called the first edition. Translation by J. P. C. Southall of the third (1909) edition was published as *Treatise on Physiological Optics*, 1962, New York: Dover.

Henning, G. B., Hertz, B. G., and Broadbent, D. E., 1975, Some experiments bearing on the hypothesis that the visual system analyzes spatial patterns in independent bands of spatial frequency, *Vision Res.*, 15, 887-897.

Hermann, L., 1870, Eine erscheinung simultanen kontrastes, *Pflüg. Arch. ges. Physiol.*, 3, 13-15.

Hess, R. F., 1974, Eye movements and the contrast sensitivity function in squint amblyopia, abs. XXVI Inter. Cong. of Physiol. Sci., Sydney, Aust., Oct. 13-17.

Heymans, G., 1896, Quantitative intersuchungen über das "optische paradoxen", *Z. Psychol.*, 9, 221-255.

Hilz, R. and Cavanaugh, C. R., 1974, Functional organization of the peripheral retina: sensitivity to periodic stimuli, *Vision Res.*, 14, 1333-1337.

Hotopf, W. H. N., 1975, Personal communication.

Hubel, D. H. and Wiesel, T. N., 1959, Receptive fields of single neurons in the cat's striate cortex, *J. Physiol.* 148, 574-591.

Hubel, D. H. and Wiesel, T. N., 1962, Receptive fields, binocular interaction, and functional architecture in the cat's visual cortex, *J. Physiol.*, 160, 106-154.

Hubel, D. H. and Wiesel, T. N., 1968, Receptive fields and functional architecture of monkey striate cortex, *J. Physiol.*, 195, 215-243.

Hubel, D. H. and Wiesel, T. N., 1974, Sequence regularity and geometry of orientation columns in the monkey striate cortex, *J. Comp. Neurol.*, 158, 267-293.

Itoi, M., Kato, K., Sugimachi, Y., Kawamura, M., Ohzu, N., and Kawara, Y., 1975, Clinical application of modulation transfer function, *Jap. J. Clin. Ophthal.*, 30, 313-321.

Johnston, H. R., El-Sum, H., Rudin, M., Sikorsky, E., and Feigenbaum, S., 1964, Rapid cartographic processing system study, AD 545068, National Tech. Info. Service, Springfield, Va.

Julesz, B., 1962, Visual pattern discrimination, *IRE Trans. of Info. Th.*, IT-8, 84-92.

Julesz, B., 1971, *Foundations of Cyclopean Perception*, Chicago: Univ. of Chicago Press.

Julesz, B., 1975, Experiments in the visual perception of texture, *Scient. Am.*, 232, 34-43.

Kabricky, M., 1967, A proposed model for visual information processing in the human brain, in *Models for the Perception of Speech and Visual Form.*, Wathen-Dunn, W., ed., Cambridge, Mass.: MIT Press, 354-361.

Kabricky, M. and Carl, J. W., 1971, Sequence filtered densely connected transforms for pattern recognition, in *Proc. 4th Hawaii Inter. Conf. on System. Sci.*, Honolulu, Hawaii, 223-228.

Kabricky, M., Tallman, O., Day, C. M., and Radoy, C. M., 1970, A theory of pattern perception based on human physiology, *Ergonomics*, 13, 129-142.

Koboyashi, T., 1956, Analytical study of displacement in visual perception, *Jap. Psychol. Res.*, 3, 37-44.

Kanizsa, G., 1955, Marzini quasi-perceptivi in campi con stimolazione omogenea, *Rivista di Psicologia*, 49, 17-30.

Koffka, K., 1935, *Principles of Gestalt psychology*, New York: Harcourt, Brace.



- Kuffler, S. W., 1953, Discharge patterns and functional organization of mammalian retina, *J. Neurophysiol.*, 16, 37-68.
- Kulikowski, J. J., 1971, Stimulus parameters affecting spatial and temporal resolutions of human vision, *Vision Res.*, 11, 83-93.
- Kulikowski, J. J., 1976, Effective contrast constancy and linearity of contrast sensation, *Vision Res.*, 16, 1419-1431.
- Kulikowski, J. J., Abadi, R., and King-Smith, P. E., 1973, Orientational selectivity of grating and line detectors in human vision, *Vision Res.*, 13, 1479-1486.
- Kulikowski, J. J. and King-Smith, P. E., 1973, Spatial arrangement of line, edge, and grating detectors revealed by sub-threshold summation, *Vision Res.*, 13, 1455-1478.
- Kulikowski, J. J. and Tolhurst, D. J., 1973, Psychophysical evidence for sustained and transient detectors in human vision, *J. Physiol.*, 232, 149-162.
- Künnapas, T. M., 1955,a, An analysis of the "vertical-horizontal illusion", *J. Exp. Psychol.*, 49, 134-140.
- Künnapas, T. M., 1955,b, Influence of frame size on apparent length of a line, *J. Exp. Psychol.*, 50, 168-170.
- Lange, R. V., Sigel, C., and Stecher, S., 1973, Adapted and unadapted spatial frequency channels in human vision, *Vision Res.*, 13, 2139-2145.
- Lebensohn, J. E., 1965, Visual charts and refraction, *Int. Ophthal. Clin.*, 5, 2-17.
- Legge, G., 1977, Space domain properties of a spatial frequency channel in human vision (submitted for publication).
- Lendaris, G. G. and Stanley, G. L., 1970, Diffraction pattern sampling for automatic pattern recognition, *Proc. IEEE*, 58, 198-216.
- Levelt, W. J. M., 1965, On Binocular Rivalry, Soesterberg, The Netherlands: Inst. for Percep.
- Levi, M. and Harwerth, R. S., 1977, Spatio-temporal interactions in anisometric and strabismic amblyopia, *Invest. Ophthal. Vis. Sci.*, 16, 90-95.
- Lipson, S. G. and Lipson, H., 1969, *Optical Physics*, Cambridge: Cambridge University Press.
- Loeb, J., 1895, Über den nachweis von kontrasterscheinungen im gebiete der raumempfindungen des auges, *Pflüg. Arch. ges. Physiol.*, 60, 509-518.
- Luckiesh, M., 1922, *Visual Illusions*, New York: Dover.
- Luedde, 1922, *Am. J. Ophthal.*, 3, 441-456.
- Lumsden, C. E., 1970, The neuropathology of multiple sclerosis, in *Handbook of Clinical Neurology*, Vinken, P. J. and Brugh, G. W., eds., New York: American Elsevier Co. Inc., Vol. 9.
- Lyle, T. K. and Wybar, K. C., 1970, *Practical Orthoptics in the Treatment of Squint*, London: H. K. Lewis & Co. Ltd.
- Mach, E., 1865, Über die wirkung der räumlichen vertheilung des lichtreizes auf die netzhaut, *Sitzungsberichte der Mathematisch-Naturwissenschaftlichen, Vienna: Klasse der Kaiserlichen Akademie der Wissenschaften*, 52/2, 303-322.

- Maffei, L. and Fiorentini, A., 1973, The visual cortex as a spatial frequency analyser, *Vision Res.*, 13, 1255-1267.
- Maffei, L. and Fiorentini, A., 1977, Spatial frequency rows in the striate visual cortex, *Vision Res.*, 17, 257-264.
- Marr, D., 1976, Early visual processing, Mass. Inst. Tech. Art. Intel. Memo 340.
- Martin, 1890, *An. d'Oc.*, ciii, 5, 299; civ, 101 (as reported by Duke-Elder, 1949).
- McCullough, C., 1955, The variation in width and position of Mach bands as a function of luminance, *J. Exp. Psychol.*, 49, 141-152.
- Meur, G., 1964, Etude des sommations spatiales rétinienne dans les amblyopies fonctionnelles, *Bull. Soc. Belge Ophthal.*, 137, 377-393.
- Michelson, A. A., 1927, *Studies In Optics*, Chicago: University of Chicago Press.
- Miller, E. A., 1954, Nature and cause of impaired vision in the amblyopic eye of a squinter, *Am. J. Optom.*, 31, 615-623.
- Miller, E. A., 1955, Investigation of the nature and cause of impaired acuity in amblyopia, *Am. J. Optom.*, 32, 10-29.
- Mitchell, D. E., Freeman, R. D., Millidot, M., and Haegerstrom, G., 1973, Meridional amblyopia: evidence for modification of the human visual system by early visual experience, *Vision Res.*, 13, 535-558.
- Mitchell, D. E., Freeman, R. D., and Westheimer, G., 1967, Effect of orientation on the modulation sensitivity for interference fringes on the retina, *J. Opt. Soc. Am.*, 57, 246-249.
- Mostafavi, H., and Sakrison, D., 1976, Structure and properties of a single channel in the human visual system, *Vision Res.*, 16, 957-968.
- Movshon, J. A. and Blakemore, C. B., 1973, Orientational specificity and spatial selectivity in human vision, *Perception*, 2, 53-60.
- Müller-Lyer, F. C., 1896, Zur lehre von den optischen täuschungen. Über kontrast und konfluxion, *Z. Psychol.*, 9, 1-16.
- Müller-Lyer, F. C., 1889, Optische urteilstäuschungen, *Arch. Physiol.*, suppl. band, 263-270.
- Obonai, T., 1954, Induction effects in estimates of extent, *J. exp. Psychol.*, 47, 57-60.
- O'Brien, V., 1958, Contour perception, illusion and reality, *J. Opt. Soc. Am.*, 48, 112-119.
- Ohzu, H. and Kawara, T., 1975, The modulation transfer function of the human visual system and its clinical applications, *Tokyo J. Med. Sci.*, 83, 63-78.
- Olson, R. K. and Attneave, F., 1970, What variables produce similarity grouping?, *Am. J. Psychol.*, 83, 1-21.
- O'Neill, E. L., 1963, *Introduction to Statistical Optics*, Reading, Mass.: Addison-Wesley.
- Orbison, W. D., 1939, Shape as a function of the vector field, *Am. J. Psychol.*, 31-45.
- Oyama, T., 1960, Japanese studies on the so-called geometrical-optical illusions, *Psychologia*, 3, 7-20.
- Pantle, A., 1974, Visual information processing of complex imagery, Research Report AMRL-TR-74-43, Aerosp. Med. Res. Lab., Wright-Patterson AFB, Ohio.

- Pantle, A. and Sekuler, R., 1968, Size detecting mechanisms in human vision, *Science*, 162, 1146-1148.
- Patel, A. S., 1966, Spatial resolution by the human visual system: The effect of mean retinal luminance, *J. Opt. Soc. Am.*, 56, 689-694.
- Pickett, R. M., 1970, Visual analysis of texture in the detection and recognition of objects, in *Picture Processing and Psychopictories*, Lipkin, B. S. and Rosenfeld, A., eds., New York: Academic Press, 289-308.
- Pollen, D. A., Lee, J. R., and Taylor, J. H., 1971, How does the striate cortex begin the reconstruction of the visual world?, *Science*, 173, 74-77.
- Pollen, D. A. and Ronner, S., 1975, Periodic excitability changes across receptive fields of complex cells in striate and parastriate cortex of the cat, *J. Physiol.*, 245, 667-697.
- Polyak, S. L., 1957, *The Vertebrate Visual System*, Chicago: University of Chicago Press.
- Ponzo, M., 1912, Rapports de contraste angulaire et l'appréciation de grandeur des astres à l'horizon, *Arch. Ital. de Biol.*, 58, 327-329.
- Pressey, A. W., 1972, The assimilation theory of geometric illusions: an additional postulate, *Percept. Psychophys.*, 11, 28-30.
- Pressey, A. W. and Bross, M., 1973, Assimilation theory and the reversed Müller-Lyer illusion, *Perception*, 2, 211-217.
- Pressey, A. W. and den Heyer, K., 1968, Observations on Chiang's "new" theory of geometrical illusions, *Percept. Psychophys.*, 4, 313-314.
- Quick, R. F. and Reichert, T., 1975, Spatial frequency selectivity in contrast detection, *Vision Res.* 15, 637-643.
- Quina, K. and Pollack, R. H., 1972, Effects of test line position and age on the magnitude of the Ponzo illusion, *Percept. Psychophys.*, 4, 12, 253-255.
- Quine, D. H., 1971, Applications of Fourier optics to visual pattern recognition, unpublished special study, Wright-Patterson Air Force Base, Ohio: Air Force Inst. Technol.
- Ragsdale, W. O., 1972, A Digital Simulation of Psychological Correlates of a Model of the Human Visual System, MS Thesis GE/EE/72-19, Wright-Patterson Air Force Base, Ohio: Air Force Inst. Technol.
- Ratliff, F., 1965, *Mach Bands. Quantitative Studies on Neural Networks in the Retina*, San Francisco: Holden-Day.
- Regan, D., Silver, R., and Murray, T. J., 1977, Visual acuity and contrast sensitivity in multiple sclerosis: hidden visual loss, *Brain*, 100, 563-579.
- Reade, F., 1969, Illusions of bent line, *Percept. Psychophys.*, 5, 273-274.
- Robinson, J. O., 1972, *The Psychology of Visual Illusion*, London: Hutchinson and Co.
- Robson, J. G., 1966, Spatial and temporal contrast sensitivity functions of the human eye, *J. Opt. Soc. Am.*, 56, 1141.
- Robson, J. G., 1975, Receptive fields: neural representation of the spatial and intensive attributes of the visual image, in *Handbook of Perception*, Vol. V: Seeing, Carterette, E. C. and Friedman, M. P., eds., New York: Academic Press, 81-116.

- Rubin, E., 1921, Visuell Wahrgenommene Figuren, Copenhagen: Glydendalske.
- Sachs, M., Nachmias, J., and Robson, J. G., 1971, Spatial frequency channels in human vision, *J. Opt. Soc. Am.*, 61, 1176-1186.
- Schachar, R. A., 1976, Optical transforms and the pincushion grid illusion, *Science*, 192, 389-391.
- Schade, O. H., 1956, Optical and photoelectric analog of the eye, *J. Opt. Soc. Am.*, 46, 721-739.
- Schumann, F., 1900, Beiträge zur analyse der gesichtswahrnehmungen, *A. Psychol.*, 23, 1-32; 24, 1-33.
- Schumann, F., 1904, Einige beobachtungen über die zusammenfassung von gesichtseindrucken zu Einheiten, *Psychologische Studien*, 1, 1-32.
- Sekuler, R., 1974, Spatial vision, *A. Rev. Psych.*, 25, 195-232.
- Shannon, C. E., 1960, Coding theorems for a discrete source with a fidelity criterion, in *Information and Decision Processes*, Machol, R. E., ed., New York: McGraw-Hill, 93-124.
- Sharpe, C. R. and Tolhurst, D. J., 1973, Orientation and spatial frequency channels in peripheral vision, *Vision Res.*, 13, 2103-2112.
- Sheard, C., 1922, Some factors affecting visual acuity tests, *Am. J. Phys. Opt.*, 3, 177-208.
- Shultz, T., 1976, Personal communication.
- Spillmann, L., Fuld, K., and Gerrits, H. J. M., 1976, Brightness contrast in the Ehrenstein illusion, *Vision Res.*, 16, 713-719.
- Stone, J. and Dreher, B., 1973, Projection of X- and Y-cells of the cat's lateral geniculate nucleus to areas 17 and 18 of visual cortex, *J. Neurophysiol.*, 36, 551-574.
- Stromeyer, C. F. and Klein, S., 1975, Evidence against narrow-band spatial frequency channels in vision: the detectability of frequency modulated gratings, *Vision Res.*, 15, 899-910.
- Stromeyer, C. F. and Julesz, B., 1972, Spatial-frequency masking in vision: critical bands and spread of masking, *J. Opt. Soc. Am.*, 62, 1221-1232.
- Sutherland, N. S., 1968, Outlines of a theory of pattern recognition in animals and man, *Proc. of the Royal Society, Series B*, 171, 297-317.
- Tallman, G. H., 1970, Processing of visual imagery by an adaptive model of the visual system: its performance and its significance, Research Report AMRL-TR-70-45, Aerosp. Med. Res. Lab., Wright-Patterson AFB, Ohio.
- Thomas, J. P., 1970, Model of the function of receptive fields in human vision, *Psychol. Rev.*, 77, 121-134.
- Tolhurst, D. J., 1972, Adaptation to square-wave gratings: inhibition between spatial frequency channels in human visual system, *J. Physiol.*, 226, 231-248.
- Tolhurst, D. J., 1973, Separate channels for the analysis of the shape and the movement of a moving visual stimulus, *J. Physiol.*, 231, 385-402.
- Tolhurst, D. and Movshon, A., 1976, Personal communication.

Van Nes, F. L., Koenderink, J. J., Nas, H., and Bouman, M. A., 1967, Spatiotemporal modulation transfer function in the human eye, *J. Opt. Soc. Am.*, 57, 1082-1088.

Vogt, K. M., 1939, Aug., ciii, 291 (as reported by Duke-Elder, 1949).

Von Noorden, G. K., 1967, Classification of amblyopia, *Am. J. Ophthal.*, 63, 238-244.

Wald, G. and Burian, H. M., 1944, The dissociation of form vision and light perception in strabismic amblyopia, *Am. J. Ophthal.*, 27, 950-967.

Watanabe, A., Mori, T., Nagata, S., and Hiwatashi, K., 1968, Spatial sine-wave response of the human visual system, *Vision Res.*, 8, 1245-1263.

Wenderoth, P. and Beh, H., 1977, Component analysis of orientation illusions, *Perception*, 6, 57-75.

Wilson, H. R. and Bergen, J., 1977, A four-mechanism model for spatial vision, paper presented at Assoc. Res. Vis. and Ophthal. (ARVO), Sarasota, Fla.

Woodhouse, J. M. and Campbell, F. W., 1977, Face recognition: minimum information requirements (submitted for publication).

Wundt, W., 1893, *Grundzuge der physiologischen psychologie*, Leipzig: Englemann.

Wundt, W., 1898, Die geometrisch-optischen täuschungen, *Abhandl. Math-phys. der sachs. Ges. Wiss.*, 24, 53-178.

Yarbus, A. L., 1967, *Eye Movements and Vision*, New York: Plenum Press.

Zöllner, F., 1860, Über eine neue art von pseudoskopie und ihre beziehungen zu den von plateau und Oppel beschriebenen bewegungsphänomenen, *Ann. Phys. Chem.*, 185, 500-523.

Zöllner, F., 1862, Über eine neue art anorthoskopischer zerrbilder, *Amm. Phys.*, 117, 477-484.

## **VOLUME II**

"If sight were to deceive us as to the position and distance of external objects, we should at once become aware of the delusion on attempting to grasp or to approach them. This daily verification by our other senses of the impressions we receive by sight produces so firm a conviction of its absolute and complete truth that the exceptions taken by philosophy or physiology, however well grounded they may seem, have no power to shake it."

Hermann von Helmholtz, 1869

## LIST OF ILLUSTRATIONS

### Figure

- 1 Two-Dimensional Sinusoids
- 2 Three-Dimensional View of Two-Dimensional Sinusoids
- 3 Two- and Three-Dimensional Magnitude Spectra of Two Different Size Squares
- 4 Examples of One-Dimensional Ideal Band-Pass Filters
- 5 Examples of Two-Dimensional Band-Pass Filters
- 6 Three-Dimensional View of Two-Dimensional Ideal Low-Pass Filters with Their Point-Spread Functions
- 7 Examples of Two-Dimensional Spatial Filtering on the Bridge of Sighs
- 8 A Sine-Wave Grating Whose Spatial Frequency Is Changing Logarithmically
- 9 A Square- and Sine-Wave Grating Whose Contrast Is Changing Logarithmically
- 10 A Sine-Wave Grating Whose Spatial Frequency and Contrast Are Changing Logarithmically
- 11 Changing the Contrast of a Portrait
- 12 A Typical Contrast Sensitivity Function
- 13 Contrast Matching Functions
- 14 Normalized Contrast Sensitivity Functions for 0, 45, 90 Degrees from the Averaged Data of Campbell, Kulikowski, and Levinson (1966)
- 15 Table of Digital Data for One Quadrant of a Two-Dimensional Contrast Sensitivity Function
- 16 Pictures of the MTF(L) and MTF(H) Spatial Filters
- 17 Comparison of the Filter Characteristics of the Sinc Function (Solid Line), a Simple Cell in the Visual Cortex of Cat (Filled Circles), and the Shape of a Psychophysical Channel Determined by Adaptation (Dashed Line)
- 18 A Diagram of an Ideal Low-Pass Digital Transform Filter that Passes the First Four Harmonics
- 19 Spatial Filtering a Letter T
- 20 Two- and Three-Dimensional Contour Plots of a Filtered Letter T
- 21 Sequential Low-Pass Filtering of a Letter T after MTF(L) Filtering
- 22 Sequential Low-Pass Filtering of a Letter T after MTF Filtering
- 23 Filtered Objects



24	Contour Plots of a Synthesized Dot Letter G
25	Contour Plots of a High-Pass Filtered Dot Letter G
26	Similar Forms from Low Spatial Frequencies of Four Discriminably Different Letter G's
27	An Example of Closure from the Low Spatial Frequencies of a Discrete Line Letter H
28	The Effects of MTF and Low-Pass Filtering on Three Variations of a Portrait
29	Log Magnitude Spectra of Portraits in Figure 28
30	Variable Low-Pass Filtering of Original and Coarsely Quantized Portraits
31	Low-Pass Filtering of Other Portrait Variations
32	Portraits Having Reversed Contrast
33	Isolating a Rectangular Form From Oblique Lines by Spatial Filtering
34	Isolating Oblique Structure in a Real Scene
35	Similarity Grouping of Pairs and Arrays of Letters
36	Similarity Grouping of Arrays of Letters that Differ in Orientation
37	Similarity Grouping of an Array of Letters that Differ in Configuration
38	Numerical Printouts of the Magnitude Spectra of an L and T
39	Numerical Printouts of the Filtered Arrays of Figure 37
40	Examples of Letter Arrays Used in Beck's (1966b) Similarity Grouping Experiment
41	Numerical Printouts of MTF(H) Filtered Pairs of Letters
42	Isolating Form and Symmetry from a Random Dot Pattern
43	Isolating an Area of Different Size Objects in a Random Dot Pattern
44	Analyzing a Complex Scene
45	Filtering a Monocular Texture Gradient (from Gibson, 1950)
46	The Poggendorff Illusion
47	Numerical Printouts of the Filtered Poggendorff Illusion
48	Correcting the Poggendorff Illusion
49	Numerical Printouts of an Illusion Due to Error in Aligning Edges
50	Müller-Lyer Illusions
51	Contour Plot of MTF Filtered Müller-Lyer Illusion of Figure 50,c,3

52	The Ponzo Illusion
53	The 90 Degree Configuration of the Horizontal-Vertical Line Illusion
54	Numerical Printouts of Two Configurations of the Horizontal-Vertical Line Illusion
55	Numerical Printouts of the L Configuration of the Horizontal-Vertical Line Illusion with Variations of a Frame
56	Simple Line Illusions
57	Numerical Printouts and Contour Plots of the MTF Filtered Titchner Illusion
58	Numerical Printouts of an Illusion of Misjudged Distance
59	The Zöllner Illusion
60	The Hermann Grid Illusion
61	The Ehrenstein Illusion
62	The Benussi Ring Illusion
63	Variations of the Kanizsa Triangle
64	Contour Plots and Numerical Printouts of Low-Pass Filtered Solid and Outline Versions of the Kanizsa Triangle
65	The Ponzo Illusion (Large Sized)
66	Theoretical and Experimental Data for the Magnitude of the Müller-Lyer Illusion
67	Eye Scan Paths from the Müller-Lyer Illusion (from Yarbus, 1967)
68	Eye Scan Paths from a Portrait of a Young Girl (from Yarbus, 1967)
69	Eye Scan Paths from a Bust of Nefertite (from Yarbus, 1967)
70	Portion of "Slave Market with Apparition of the Invisible Bust of Voltaire" by Salvador Dali
71	Variations of the Bisected Circle
72	Numerical Printouts of Variations of the Bisected Circle
73	The Rubin Face-Vase Object
74	Multistable Dot Pattern
75	Square-Wave Gratings at Three Orientations
76	Multistable Triangles — Equilateral and Random
77	Numerical Printouts of Equilateral Multistable Triangles and Collinear Multistable Diamonds

78	Multistable Triangles — Scalene and Random
79	One-Octave Band-Pass Filtered Portrait
80	Two-Octave Band-Pass Filtered Portrait
81	One-Octave Band-Pass Filtered Portrait Having a Higher Centre Frequency
82	One-Octave Channel Filtered Portrait
83	Two-Octave Channel Filtered Portrait
84	Table of First 2.5 Cycles of Letters Associated with Each Snellen Line Number
85	Synthesis of Snellen Letters
86	Snellen Letter Acuity Chart Used in Experiments
87	Table of Contrast and Contrast Sensitivity Required for Detection and Identification of Snellen Letters
88	The Percent Contrast Required for the Detection and Identification of Snellen Letters for Each Snellen Line
89	Contrast Sensitivity Required for the Detection and Identification of Snellen Letters for Each Snellen Line
90	Ratio of Contrast Required for Identification Versus Detection of Snellen Letters as a Function of Snellen Line Number
91	Contrast Sensitivity Function of Subject A.G.
92	Table of Cycles and Associated Contrast Sensitivity Required for the Identification of Snellen Letters
93	Table of Predicted Snellen Letter Acuity from the Contrast Sensitivity of 10 Subjects
94	Measured Versus Predicted Snellen Letter Acuity
95	Spatial Filtering a 4 by 4 Dot Array
96	Curve for Determining the Percent Contrast from the Polarizer Angle
97	Contrast Sensitivity Functions and Difference Between Eyes Curve: Amblyope J.P.
98	Contrast Sensitivity Functions and Difference Between Eyes Curve: Amblyope M.B.
99	Contrast Sensitivity Functions and Difference Between Eyes Curve: Amblyope A.H.
100	Contrast Sensitivity Functions and Difference Between Eyes Curve: Amblyope A.H.
101	Average Contrast Sensitivity Functions and Difference Between Eyes Curve of Figures 99 and 100
102	Decrease in Difference Between Eyes Curve for the First Two Test Sessions: Amblyope A.H.
103	Contrast Sensitivity Functions and Difference Between Eyes Curve: Effect of Abnormal Retinal Correspondence (ARC)

- 104 Contrast Sensitivity Functions and Difference Between Eyes Curve: Amblyope A.H.
- 105 Contrast Sensitivity Functions and Difference Between Eyes Curve: Amblyope A.H.
- 106 Average Contrast Sensitivity Functions and Difference Between Eyes Curve of Figures 104, 105
- 107 Decrease in Difference Between Eyes Curve: Amblyope A.H.
- 108 Average from Three Sets of Contrast Sensitivity Functions and Difference Between Eyes Curves: Amblyope A.H.
- 109 Contrast Sensitivity Functions and Difference Between Eyes Curve: Amblyope A.H.
- 110 Decrease in Difference Between Eyes Curve from the Initial to the Final Test Session: Amblyope A.H.
- 111 Contrast Sensitivity Functions and Difference Between Eyes Curve: Amblyope A.H.
- 112 Contrast Sensitivity Functions and Difference Between Eyes Curve: Amblyope A.H.
- 113 Contrast Sensitivity Functions and Difference Between Eyes Curve: Amblyope A.H.
- 114 Contrast Sensitivity Versus Time: Amblyope A.H.
- 115 Average Contrast Matching Functions for Both Eyes of Amblyope A.H.
- 116 Contrast Matching Functions from Three Separate Test Sessions: Amblyope A.H.
- 117 Difference Between Eyes Curves for Each Contrast Match for Three Separate Test Sessions: Amblyope A.H.
- 118 Average Difference between Eyes Curves for Three Contrast Matches of Figure 115
- 119 Contrast Matching Functions over a Finer Spatial Frequency Range
- 120 Difference Between Eyes Curves for Each Contrast Match for Two Separate Test Sessions, (Figures 119a, b) and Their Average (Figure 119c)
- 121 Contrast Sensitivity Functions and Difference Between Eyes Curve: Multiple Sclerosis C.H.
- 122 Contrast Sensitivity Functions and Difference Between Eyes Curve: Multiple Sclerosis S.S.
- 123 Contrast Sensitivity Functions and Difference Between Eyes Curve: Multiple Sclerosis H.R.
- 124 Contrast Sensitivity Functions and Difference Between Eyes Curve: Multiple Sclerosis A.J.
- 125 Contrast Sensitivity Functions and Difference Between Eyes Curve: Multiple Sclerosis M.D.
- 126 Contrast Sensitivity Functions and Difference Between Eyes Curve: Multiple Sclerosis B.M.

## FIGURES

A brief explanation of symbols used in the figure captions follows.

### MTF Filters

MTF indicates that the spectrum or image has been spatially filtered using a filter based on the two-dimensional contrast sensitivity function shown in Figure 16. MTF(L) and MTF(H) indicate that the spatial filter has different amounts of low spatial frequency attenuation: threshold and suprathreshold. The MTF filters are discussed in Section 8.1.

### Band-Pass Filters

(U by V) indicates the spatial frequency bandwidth of a two-dimensional spatial filter in the U, V transform domain. U and V are the number of spatial frequencies passed by the filter along the U and V axis. (U by V - 1) is a band-pass filter which passes U and V spatial frequencies minus the fundamental frequency,  $f_1$ . Thus, (5 by 5) means that 5 times  $f_1$  spatial frequencies of the object in the U, V dimensions have been passed by the filter. Band-pass filters are discussed in Sections 4.2 and 9.1.

### Log Transformation

An L after the MTF or (U by V) means that the intensity values of the filtered images were log transformed to increase the visibility of the low contrast features in the pictures. The technique of log transformation is discussed in Section 9.2.

### References to Chapters and Sections

The numbers in parentheses after the figure number refer to the chapter and section in the text of Volumes I and II in which the figure is discussed in detail. Thus (2.5.1) means that the figure is discussed in Chapter 2, Section 5.1.

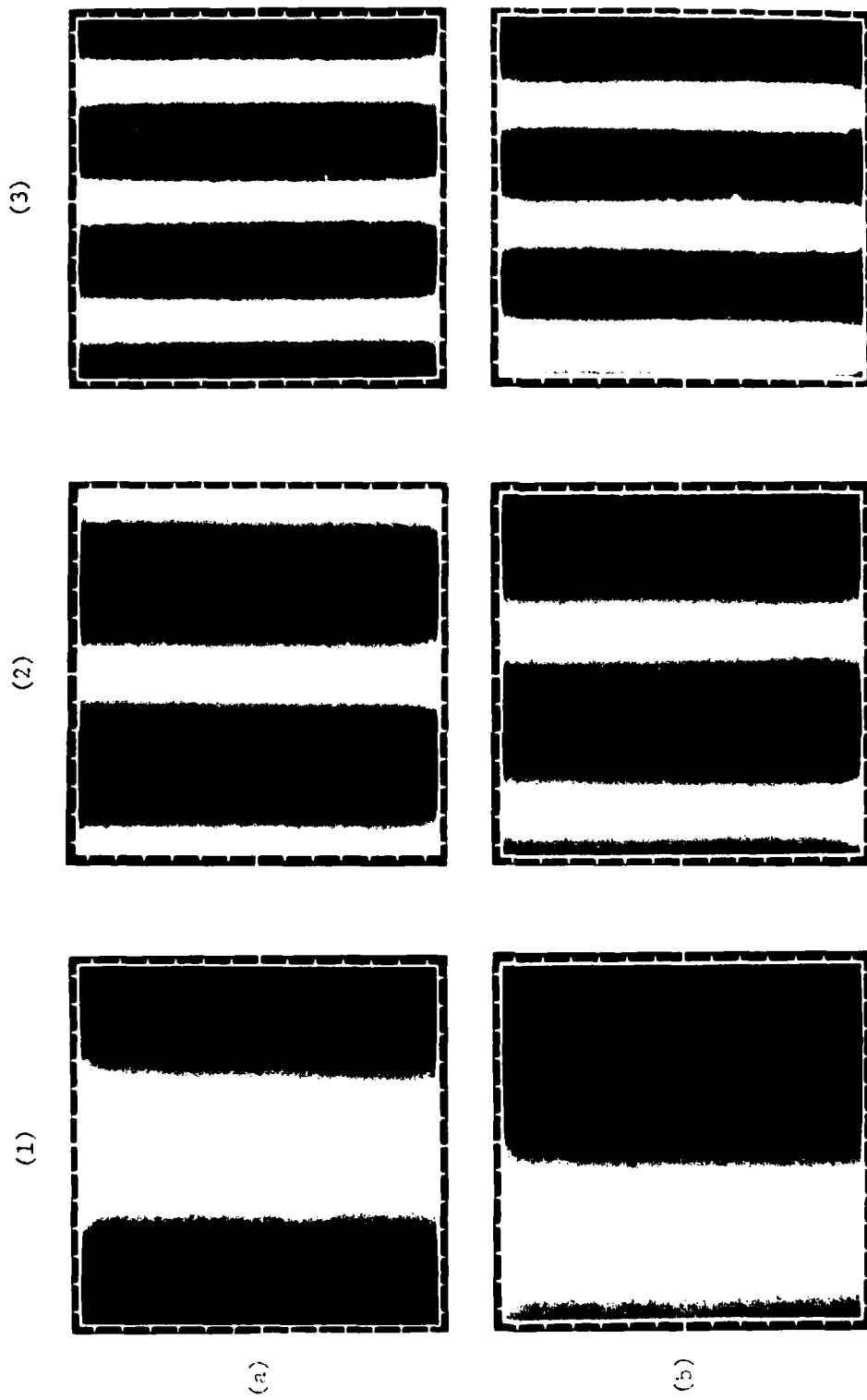


Figure 1. Two-Dimensional Sinusoids: (a) Sine Gratings; (b) Cosine Gratings Having 1 cycle; (2) Sinusoidal Gratings Having 2 Cycles; (3) Sinusoidal Gratings Having 3 Cycles. (Sections 2.5, 1, 5, 1)

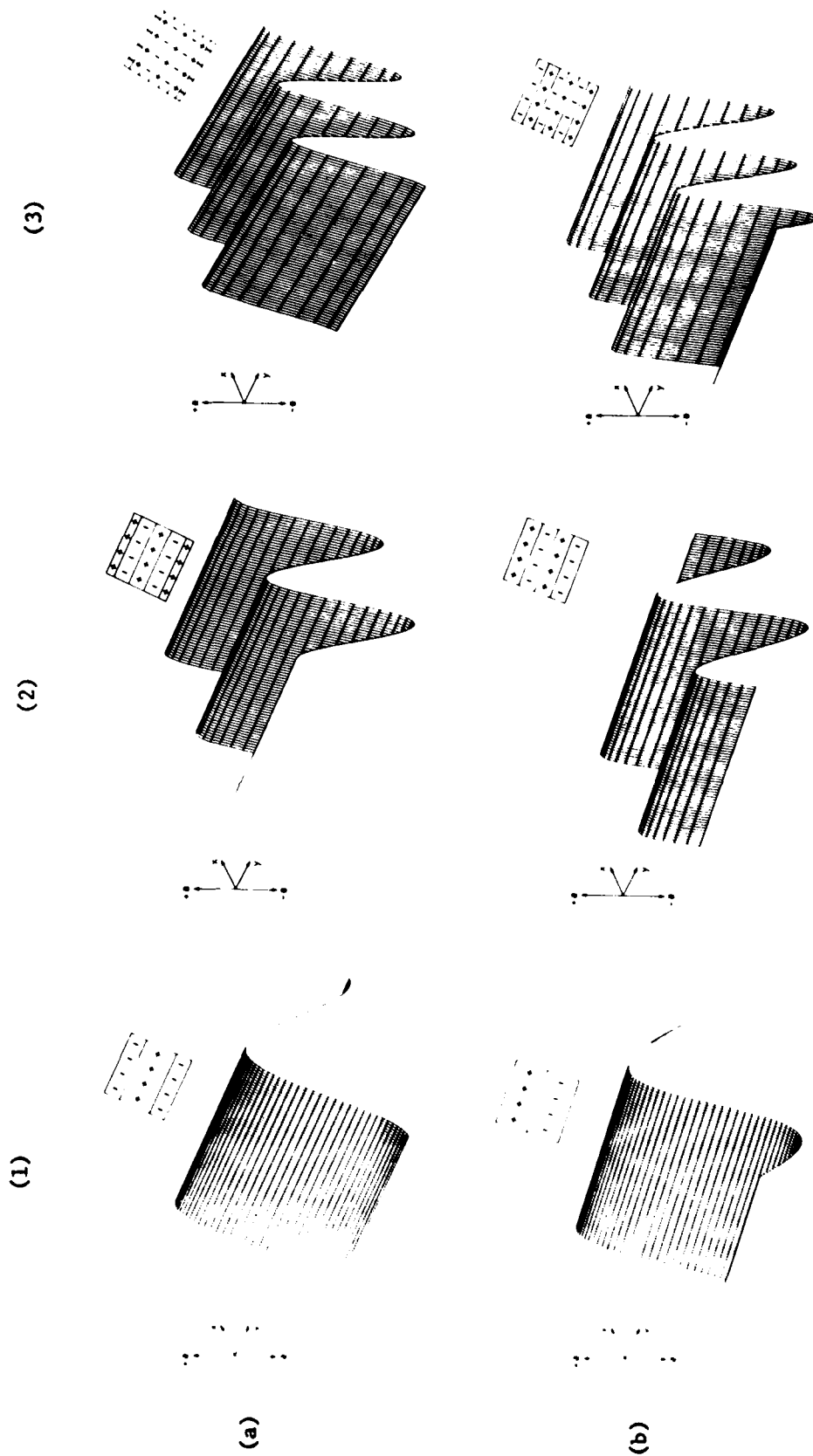


Figure 2. Three-Dimensional View of Two-Dimensional Sinusoids: (a) Sine Gratings; (b) Cosine Gratings; (1) Sinusoidal Gratings Having 1 Cycle; (2) Sinusoidal Gratings Having 2 Cycles; (3) Sinusoidal Gratings Having 3 Cycles.  
(Sections 2.5.1, 5.1)

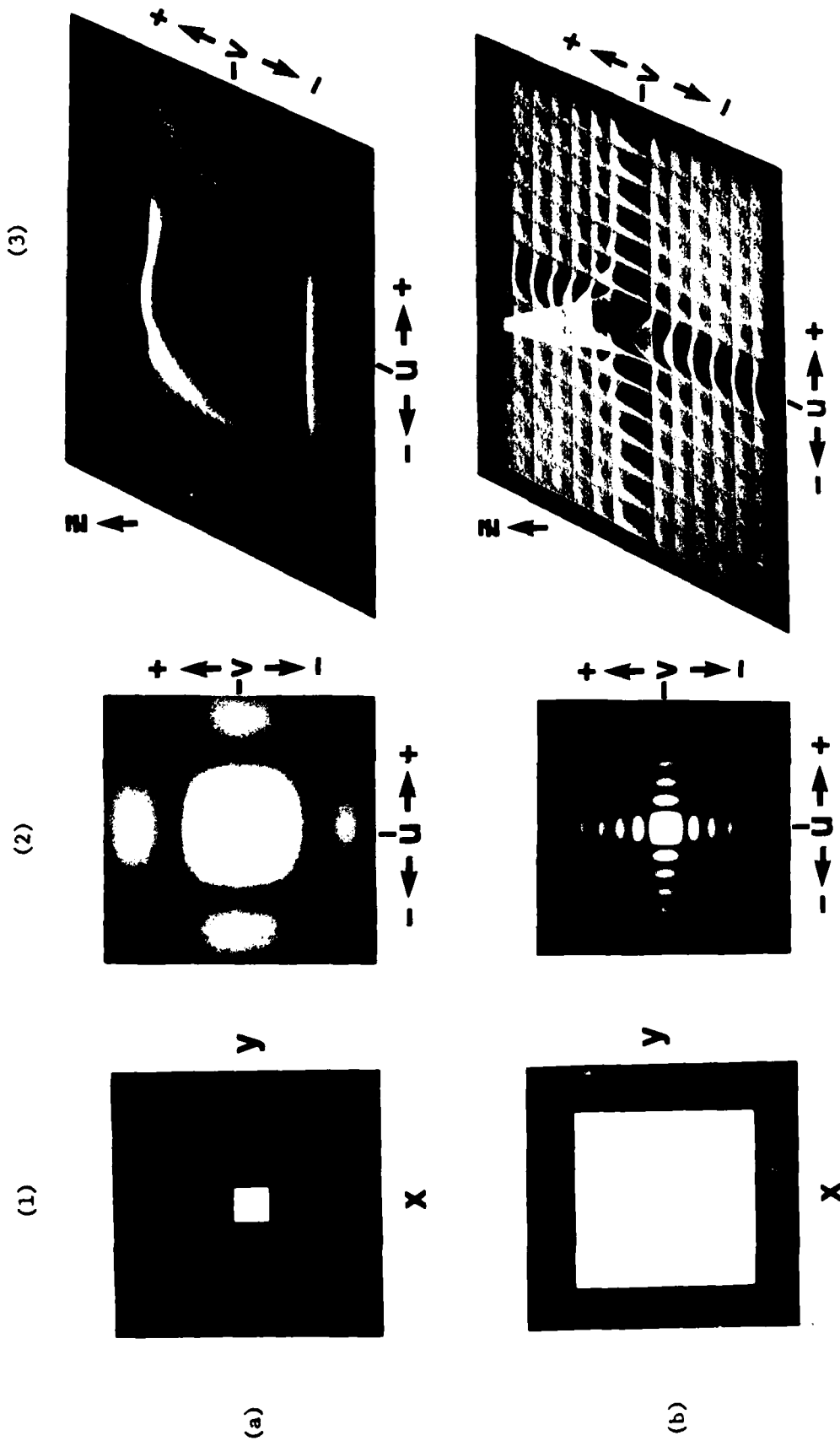


Figure 3. Two- and Three-Dimensional Magnitude Spectra of Two Different Size Squares: (a) Small Square; (b) Large Square; (1) Square; (2) Two-Dimensional Magnitude Spectra; (3) Three-Dimensional Magnitude Spectra. (Section 3.3.1)



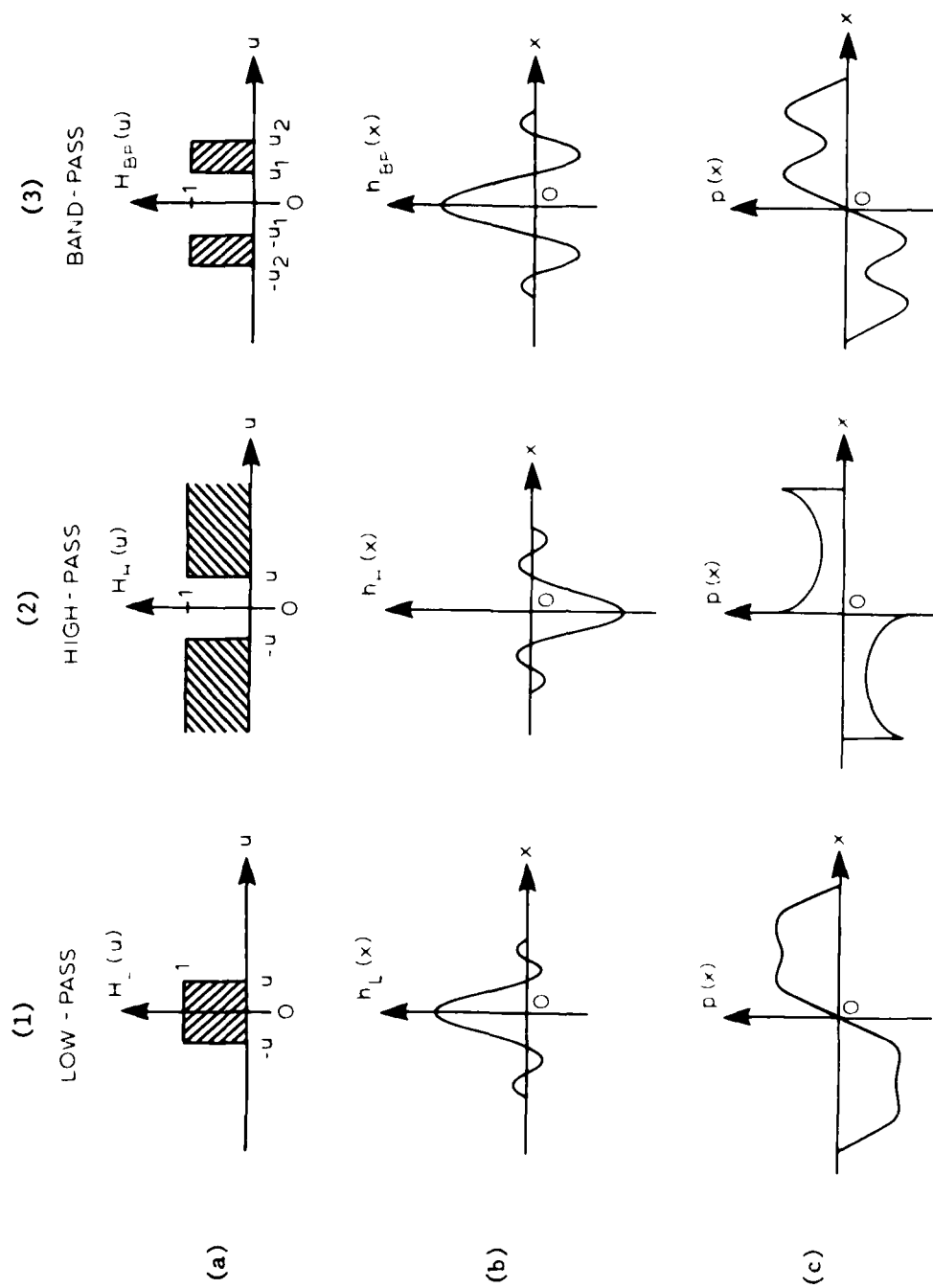


Figure 4. Examples of One-Dimensional Ideal Band-Pass Functions: (a) Transform Filters; (b) Space Filters (Line-Spread Functions); (c) General Square-Wave Response; (1) Low-Pass Filter; (2) High-Pass Filter; (3) Band-Pass Filter. (Sections 4.2.1, 8.2.1)

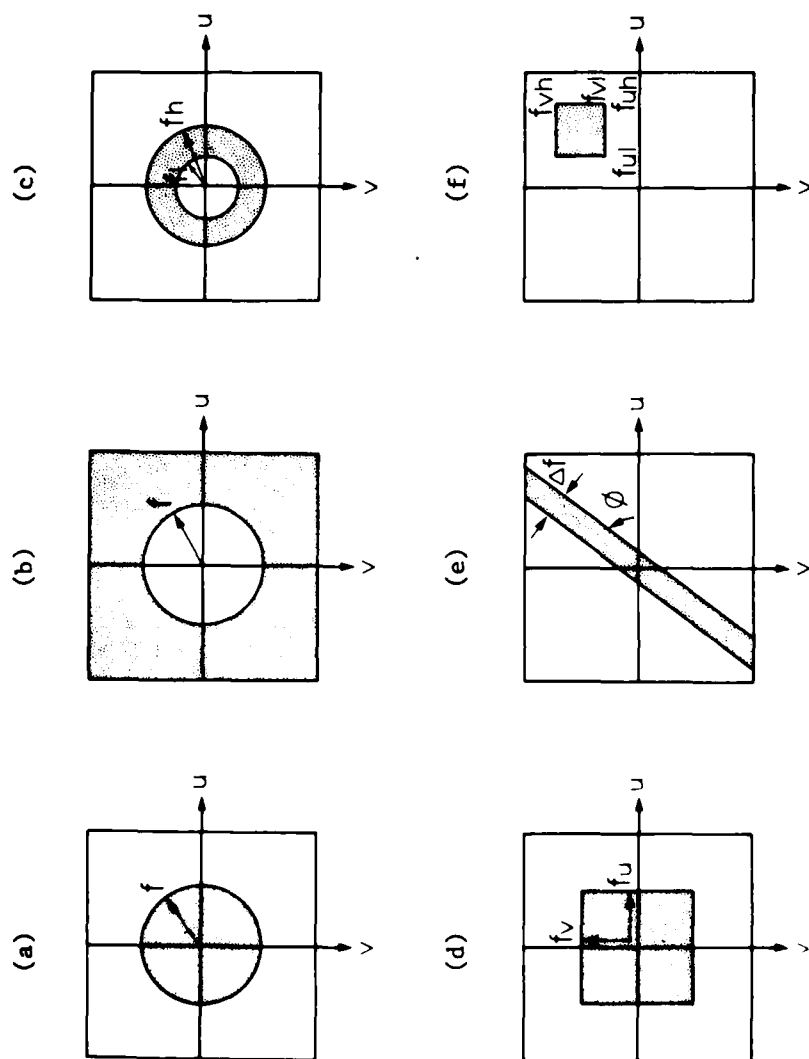
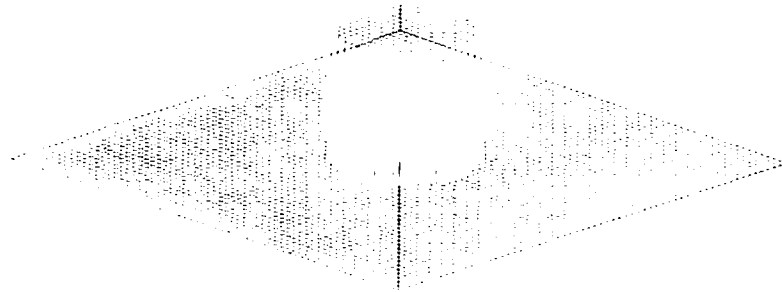


Figure 5. Examples of Two-Dimensional Band-Pass Filters: (a) Low-Pass Circle Filter; (b) High-Pass Circle Filter; (c) Band-Pass Circle Filter; (d) Low-Pass Square Filter; (e) Orientation Selective Band-Pass Filter; (f) Orientation and Spatial Frequency Selective Band-Pass Filter. (Section 4.2.1)

(a)

(1)



(2)

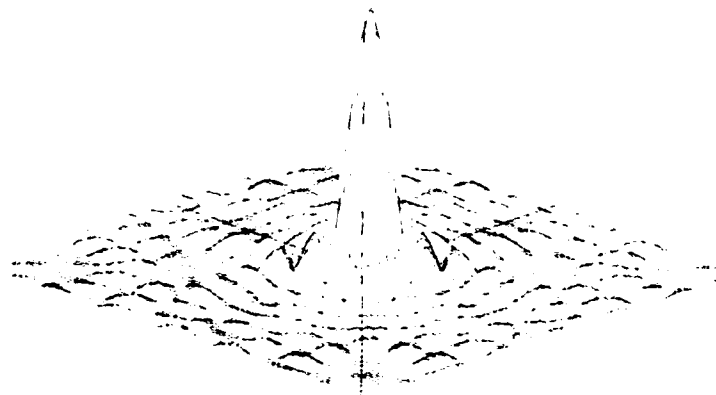
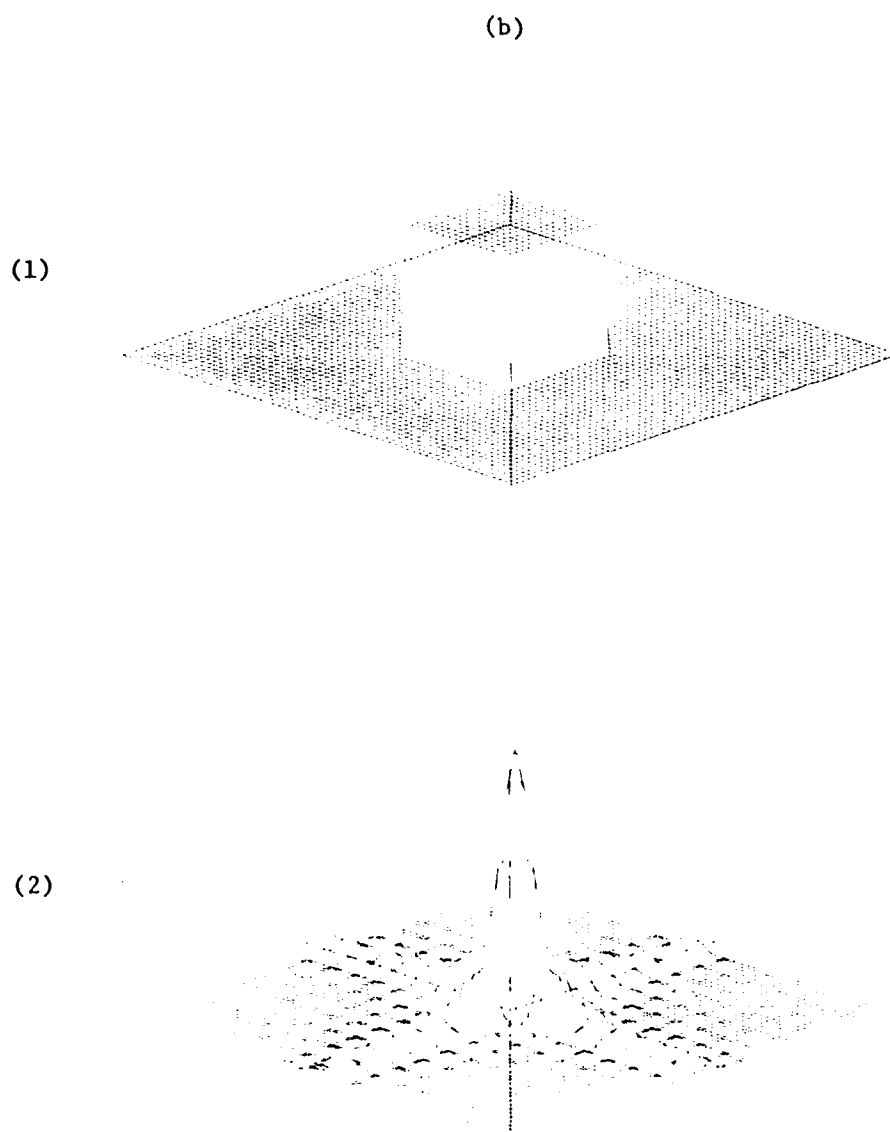


Figure 6. Three-Dimensional View of Two-Dimensional Ideal Low-Pass Filters with Their Point-Spread Functions: (a) Circle Functions; (b) Square Functions; (1) Low-Pass Filters; (2) Filter Point-Spread Functions. (Sections 4.2.2, 8.2.1)



**Figure 6. Three-Dimensional View of Two-Dimensional Ideal Low-Pass Filters with Their Point-Spread Functions: (a) Circle Functions; (b) Square Functions; (1) Low-Pass Filters; (2) Filter Point-Spread Functions. (Sections 4.2.2, 8.2.1) (cont.)**

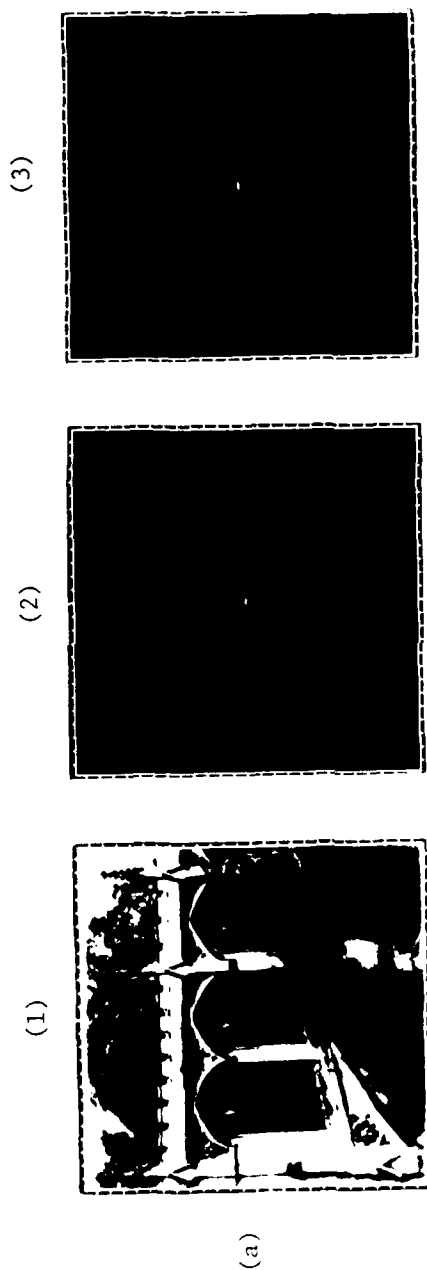


Figure 7. Examples of Two-Dimensional Spatial Filtering on the Bridge of Sighs: (a) Original Digitized Scene; (b) Low-Pass (12 Harmonics) Filtered Scene; (c) Low-Pass (18 Harmonics) Filtered Scene; (d) High-Pass (Greater than 12 Harmonics) Filtered Scene; (e) High-Pass (Greater than 18 Harmonics) Filtered Scene; (f) Scene Filtered Passing the Horizontal Spectral Components; (g) Scene Filtered Passing the Vertical Spectral Components; (h) Scene Filtered Passing the Oblique Spectral Components; (i) Scene Filtered Passing a Small Spectral Area that Contains the Periodicity of the Portals. The Filtered Spectra Are Above and the Respective Filtered Images Are Below for Figures 7b-i. (1) Digitized Scene; (2) The Magnitude Spectra; (3) The Magnitude Spectra Sectioned, Normalized, and Recombined to Show the High Frequencies. (Section 4.2.3)

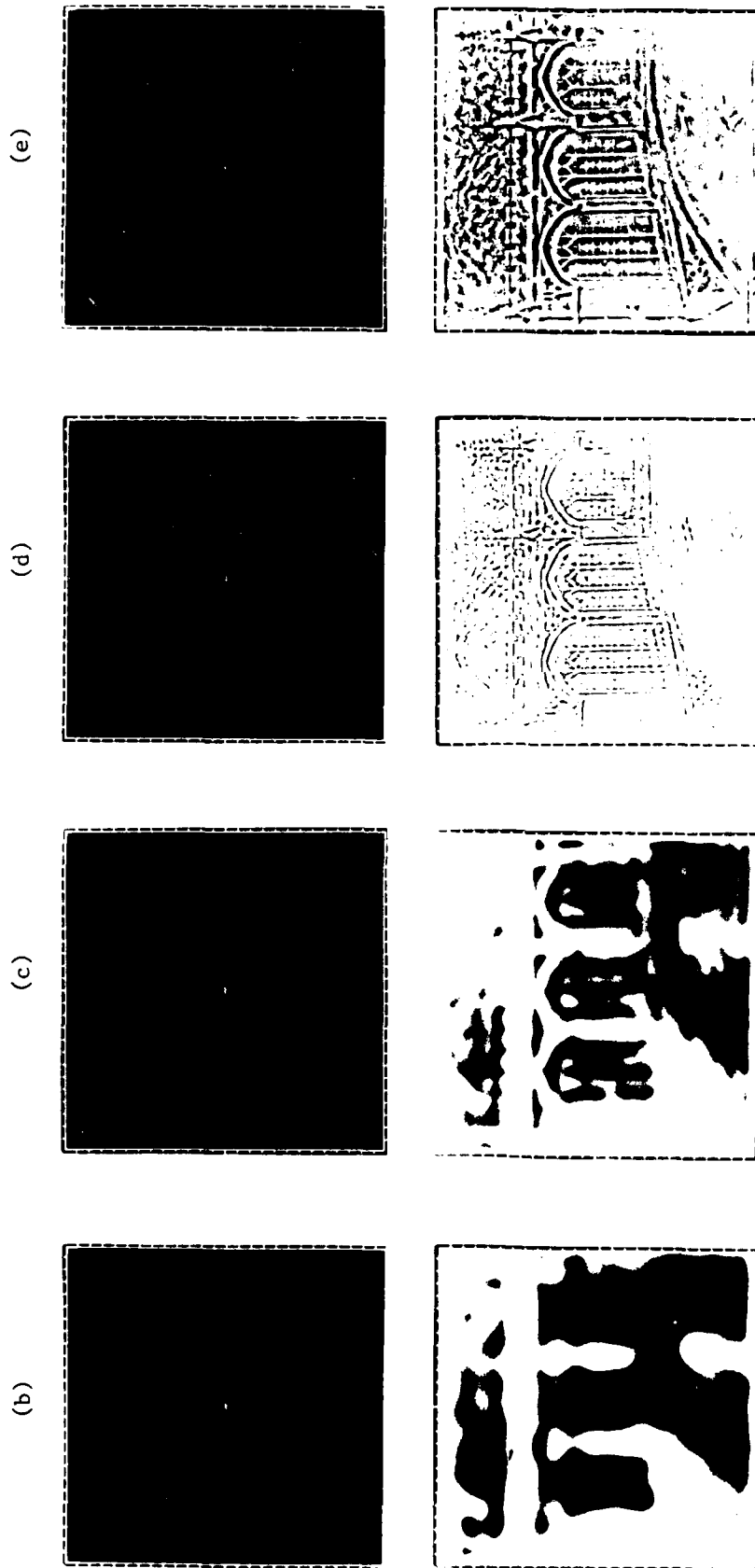


Figure 7. Examples of Two-Dimensional Spatial Filtering on the Bridge of Sighs: (a) Original Digitized Scene; (b) Low-Pass (12 Harmonics) Filtered Scene; (c) Low-Pass (18 Harmonics) Filtered Scene; (d) High-Pass (Greater than 12 Harmonics) Filtered Scene; (e) High-Pass (Greater than 18 Harmonics) Filtered Scene; (f) Scene Filtered Passing the Horizontal Spectral Components; (g) Scene Filtered Passing the Vertical Spectral Components; (h) Scene Filtered Passing the Oblique Spectra Components; (i) Scene Filtered Passing a Small Spectral Area that Contains the Periodicity of the Portals. The Filtered Spectra Are Above and the Respective Filtered Images Are Below for Figures 7b-i. (1) Digitized Scene; (2) The Magnitude Spectra; (3) The Magnitude Spectra Sectioned, Normalized, and Recombined to Show the High Frequencies. (Section 4.2.3) (cont.)

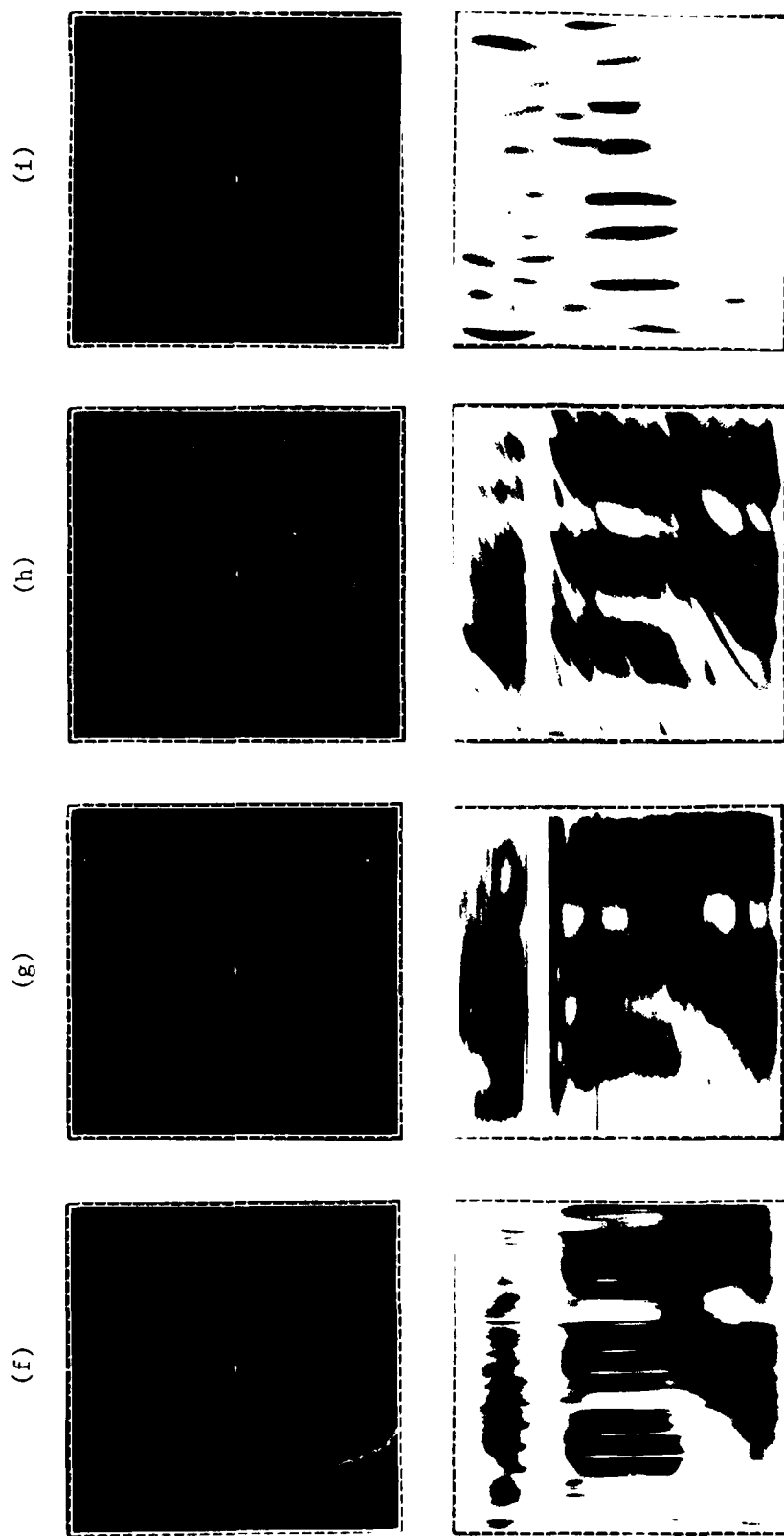


Figure 7. Examples of Two-Dimensional Spatial Filtering on the Bridge of Sighs: (a) Original Digitized Scene; (b) Low-Pass (12 Harmonics) Filtered Scene; (c) Low-Pass (18 Harmonics) Filtered Scene; (d) High-Pass (Greater than 12 Harmonics) Filtered Scene; (e) High-Pass (Greater than 18 Harmonics) Filtered Scene; (f) Scene Filtered Passing the Horizontal Spectral Components; (g) Scene Filtered Passing the Vertical Spectral Components; (h) Scene Filtered Passing the Oblique Spectral Components; (i) Scene Filtered Passing a Small Spectral Area that Contains the Periodicity of the Portals. The Filtered Spectra Are Above and the Respective Filtered Images Are Below for Figures 7b-i. (1) Digitized Scene; (2) The Magnitude Spectra Sectioned, Normalized, and Recombined to Show the High Frequencies. (Section 4.2.3) (cont.)

Figure 8. A Sine-Wave Grating Whose Spatial Frequency Is Changing Logarithmically. (Section 5.1)



**Figure 9. A Square- and Sine-Wave Grating Whose Contrast Is Changing Logarithmically. (Section 5.1)**



Figure 10. A Sine-Wave Grating Whose Spatial Frequency and Contrast Are Changing Logarithmically. (Section 5.1)

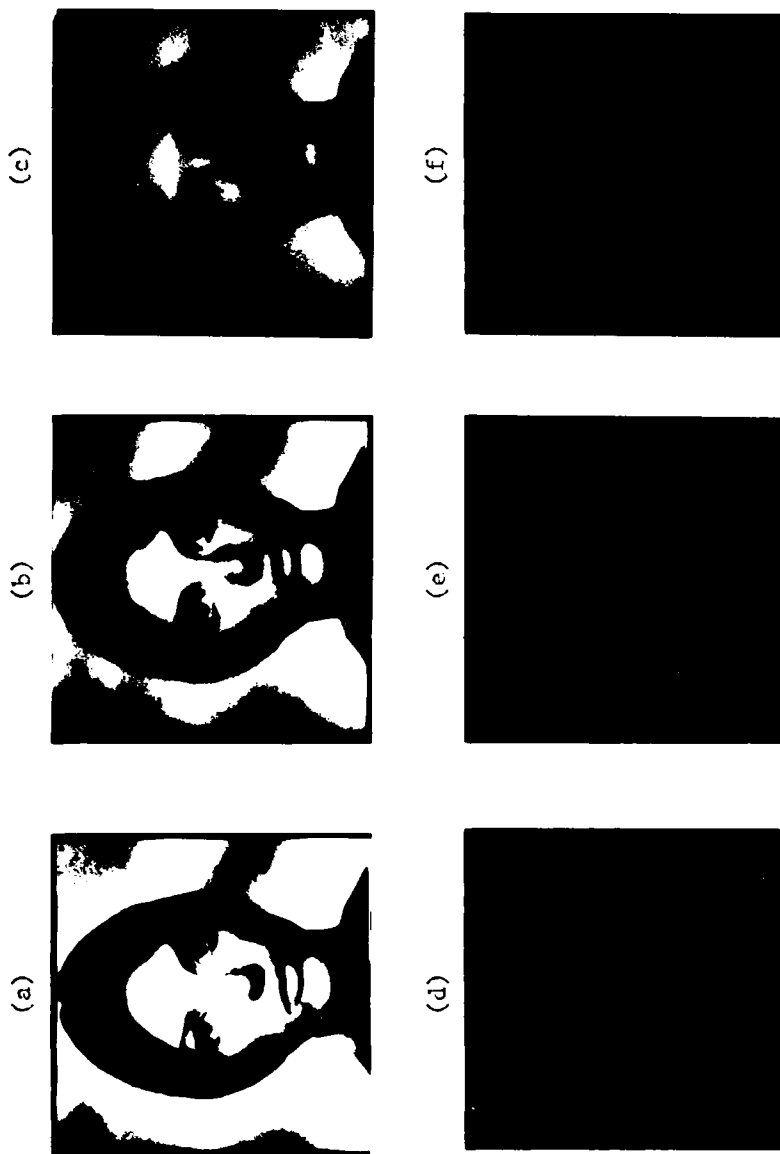


Figure 11. Changing the Contrast of a Portrait: (a) 100%; (b) 75%; (c) 50%; (d) 25%; (e) 12%; (f) 6%. (Section 5.1)

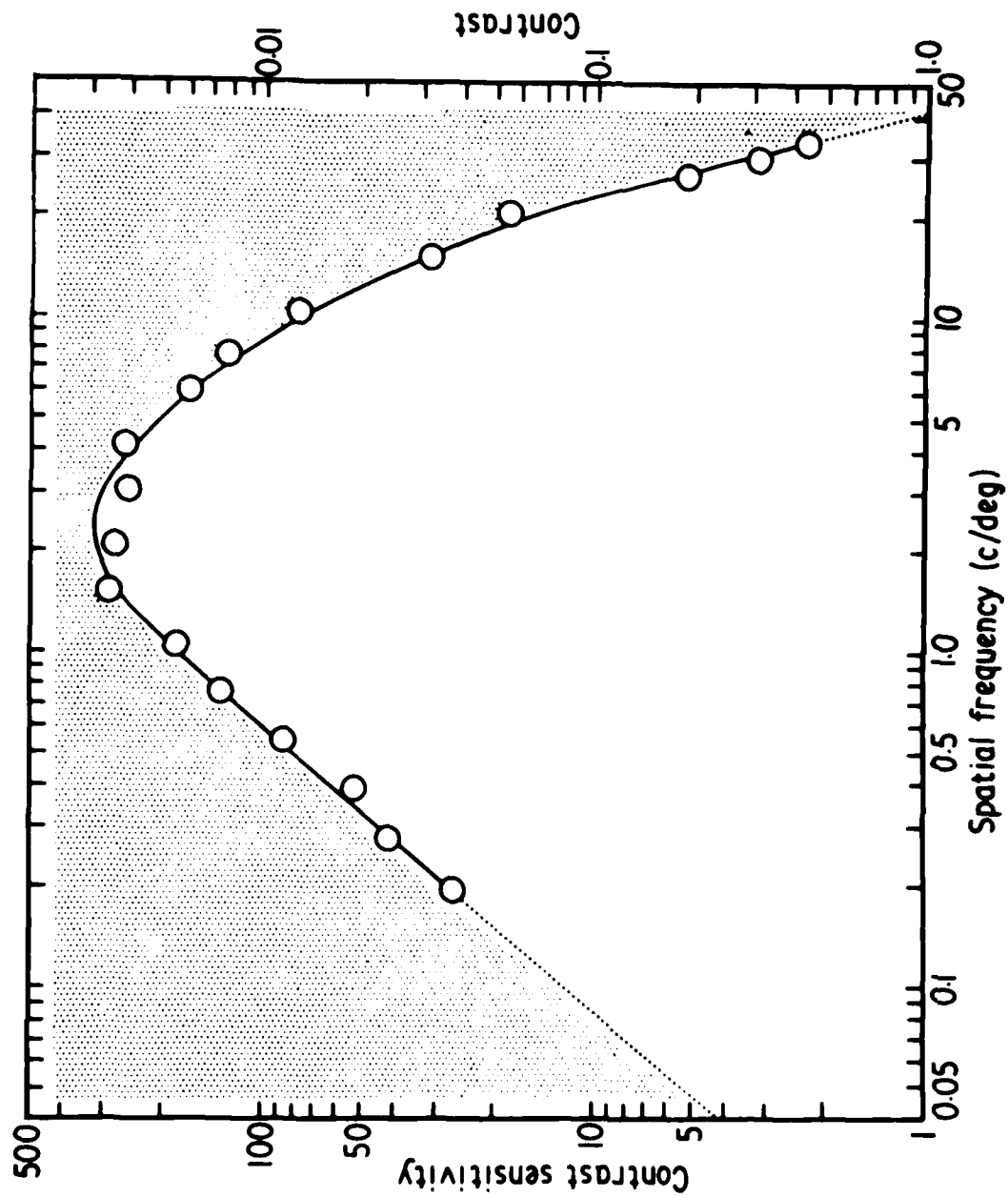


Figure 12. A Typical Contrast Sensitivity Function. (Section 5.2)

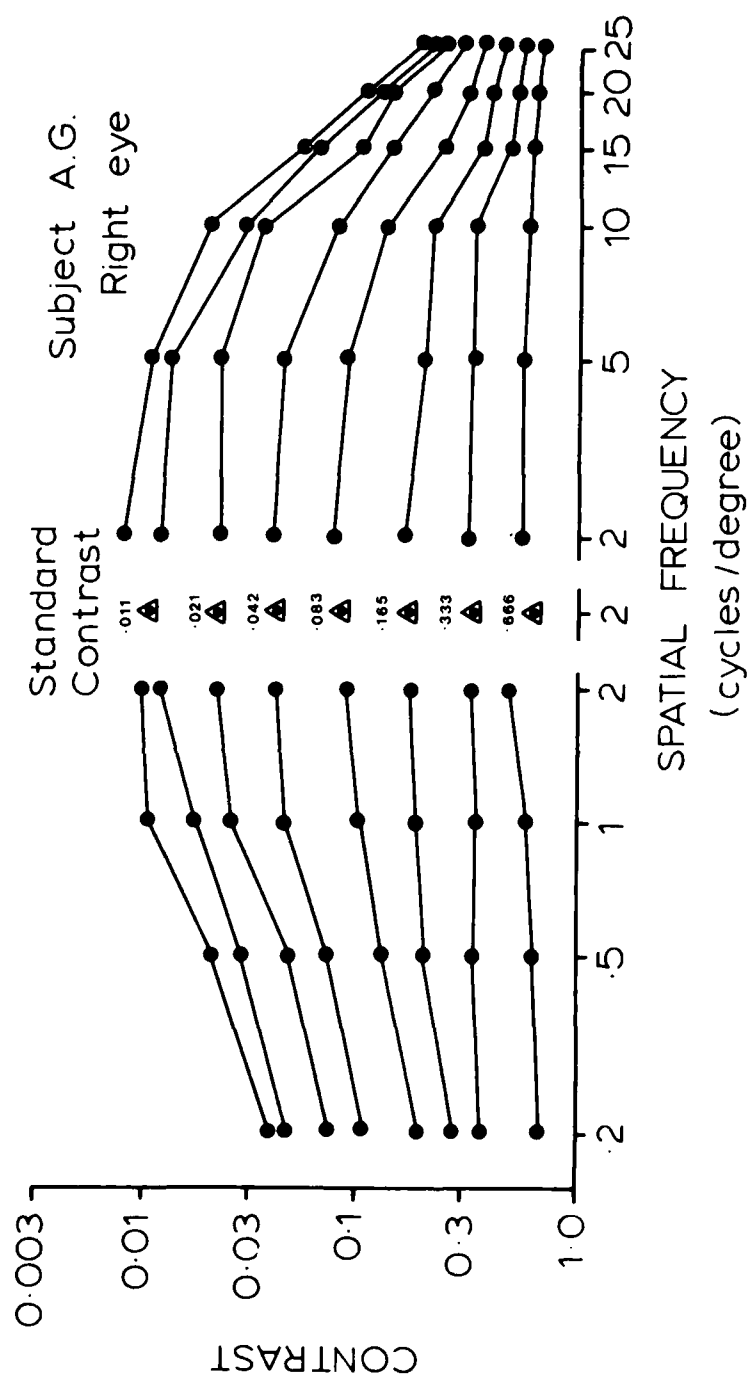


Figure 13. Contrast Matching Functions. (Sections 5.4, A-2.3)

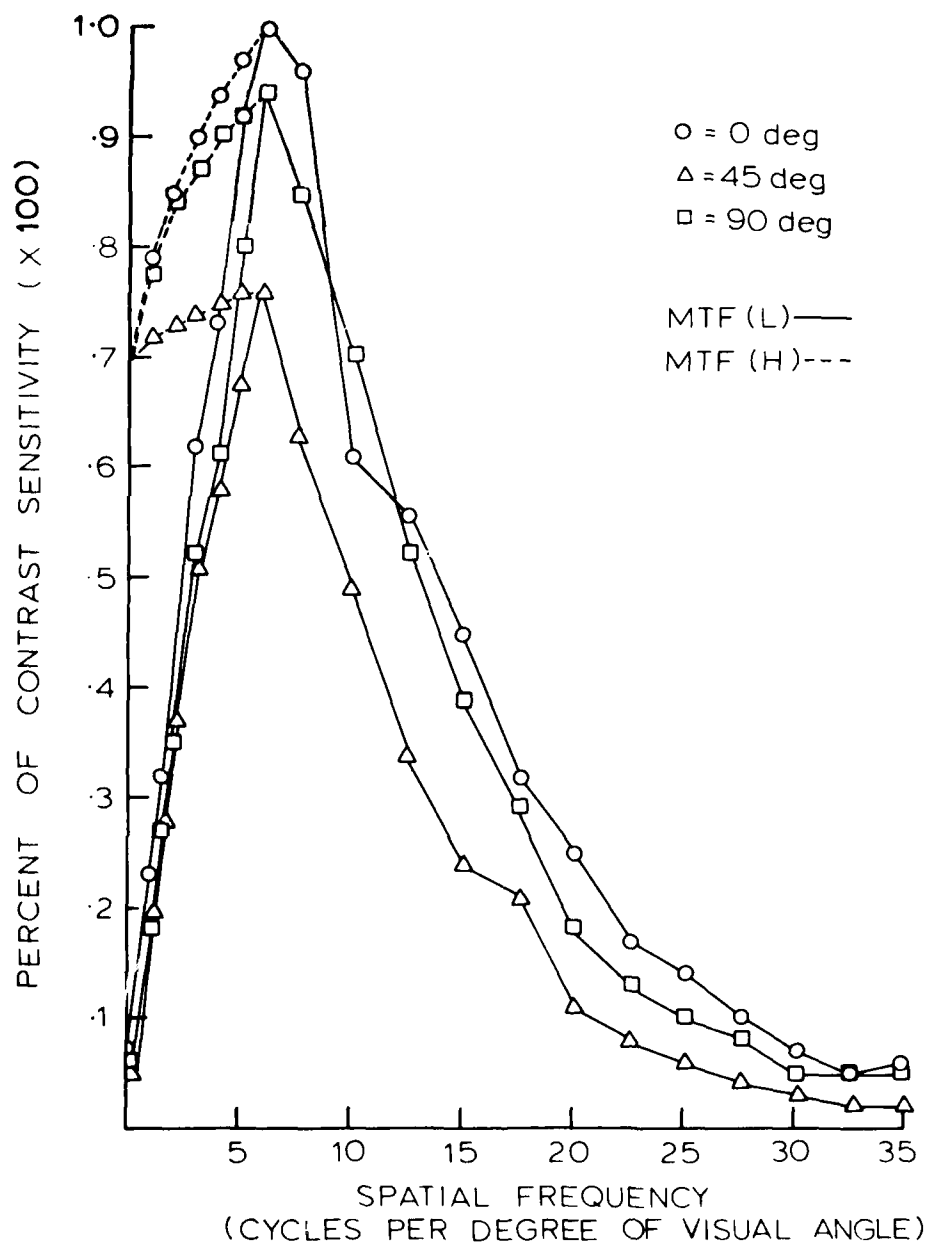


Figure 14. Normalized Contrast Sensitivity Functions for 0, 45, 90 Degrees from the Averaged Data of Campbell, Kulikowski, and Levinson (1966). (Section 8.11)

HORIZONTAL  
SPATIAL FREQUENCY  
(cycles per degree)

0	99	23	47	60	73	92	99	98	92	75	61	59	56	54	49	45	40	35	30	28	25	22	19	16	15	14	13	11	10	8	7	6
1	19	20	42	56	68	87	95	94	88	75	61	59	56	54	49	45	40	35	30	28	25	22	19	16	15	14	13	11	10	8	7	6
2	35	34	51	64	72	80	88	87	82	71	58	57	55	53	46	45	40	35	30	28	25	22	19	16	15	14	13	11	10	8	7	6
3	54	52	59	58	69	82	81	76	67	57	54	54	52	44	44	42	38	32	28	26	23	22	19	16	15	14	13	11	10	8	7	6
4	61	60	68	67	76	79	76	70	64	55	53	50	50	42	40	38	32	27	26	22	23	20	18	15	14	13	11	9	8	7	6	5
5	80	77	72	81	78	68	66	61	53	51	50	48	46	38	36	36	31	26	24	22	20	18	15	14	13	12	10	9	7	6	5	4
6	94	88	82	75	72	64	61	58	50	47	45	44	36	34	34	30	25	23	21	20	17	14	12	11	10	9	7	6	5	4	3	3
7	98	84	73	72	68	61	57	49	45	43	41	41	34	32	32	29	24	22	21	19	16	14	12	11	10	9	8	7	6	5	4	4
8	82	79	73	68	64	53	50	44	43	39	36	32	32	36	30	28	23	20	18	15	13	12	12	10	9	8	7	6	5	4	5	4
9	78	74	71	60	55	52	47	40	38	32	29	30	28	28	27	22	18	19	20	18	14	13	11	10	9	8	7	6	5	4	3	3
10	70	68	63	57	53	51	42	40	34	29	38	35	26	25	24	21	18	19	17	17	12	11	11	10	9	8	7	6	5	4	3	3
11	63	61	58	52	48	44	39	37	30	29	25	24	25	23	20	17	17	19	16	12	10	10	9	8	7	6	5	4	3	3	3	3
12	56	55	54	45	43	41	32	30	28	27	25	24	22	19	16	17	15	14	11	11	10	10	9	8	7	6	5	5	4	3	3	3
13	50	49	47	43	36	34	30	29	28	26	24	23	18	15	15	13	12	14	10	11	9	9	8	7	6	5	5	4	3	3	3	3
14	44	43	42	40	34	32	30	29	26	25	24	19	15	15	11	11	11	10	9	9	9	8	7	6	5	4	5	4	3	3	3	3
15	39	38	37	36	31	30	29	26	25	20	19	16	16	11	10	9	9	9	9	8	7	7	6	5	4	4	3	3	3	3	3	3
16	35	34	33	32	28	27	27	21	20	17	16	12	12	10	10	9	8	8	8	7	7	6	5	4	4	3	3	3	3	2	2	2
17	31	30	29	29	24	23	22	18	17	17	13	12	11	9	9	8	7	7	7	7	6	5	4	3	3	3	3	3	2	2	2	2
18	27	26	25	25	19	19	18	13	11	10	10	10	9	9	8	8	7	6	5	5	5	4	4	3	3	3	2	2	2	2	2	2
19	23	22	21	20	15	14	14	11	11	10	10	10	9	9	8	8	7	7	5	5	5	4	4	3	3	3	2	2	2	2	2	2
20	18	17	16	15	14	12	12	11	11	9	9	9	9	9	8	8	7	7	5	5	4	4	3	3	3	3	2	2	2	2	2	2
21	16	15	14	13	13	12	12	12	10	10	9	9	9	9	8	7	6	5	5	4	4	3	3	3	3	3	2	2	2	2	2	2
22	15	14	13	12	12	10	10	10	9	9	9	8	6	6	6	6	5	4	4	3	3	3	3	3	2	2	2	2	2	2	2	2
23	13	12	11	10	10	10	10	10	10	9	9	8	8	6	6	5	5	4	4	3	3	3	3	2	2	2	2	2	2	2	2	2
24	12	12	11	10	10	10	10	10	8	8	8	7	7	6	6	5	5	3	3	3	3	2	2	2	2	2	2	2	2	2	1	1
25	11	11	11	10	10	8	8	8	8	7	7	6	6	5	5	5	5	3	3	3	2	2	2	2	2	2	2	2	2	2	1	1
26	9	9	9	9	8	7	7	7	7	6	6	5	5	4	4	4	3	3	3	2	2	2	2	2	2	2	2	2	2	1	1	1
27	8	8	8	8	7	6	6	6	5	5	5	5	4	4	4	4	3	3	3	2	2	2	2	2	2	2	2	2	2	1	1	1
28	7	7	7	7	6	5	5	5	5	5	5	4	4	4	4	4	3	3	3	2	2	2	2	2	2	2	2	2	2	1	1	1
29	6	6	6	6	5	5	5	5	5	5	4	4	4	4	4	4	3	3	3	2	2	2	2	2	2	2	2	2	2	1	1	1
30	5	5	5	5	5	5	5	5	5	5	4	4	4	4	3	3	3	2	2	2	2	2	2	2	2	2	2	2	2	1	1	1
31	5	5	5	5	5	5	5	5	5	5	4	4	4	4	3	3	2	2	2	2	2	2	2	2	2	2	2	2	2	1	1	1

VERTICAL  
SPATIAL FREQUENCY  
(cycles per degree)

Figure 15. Table of Digital Data for One Quadrant of a Two-Dimensional Contrast Sensitivity Function:  
(a) MTF(L) Filter; (b) MTF(H) Filter. (Section 8.1)

	0	1	2	3	4	5
0	99	79	85	80	94	97
1	77	72	78	83	87	93
2	83	77	75	77	82	86
3	87	80	75	74	78	81
4	90	84	78	77	78	79
5	92	86	80	81	78	68

Figure 15. Table of Digital Data for One Quadrant of a Two-Dimensional Contrast Sensitivity Function:  
(a) MTF(L) Filter; (b) MTF(H) Filter. (Section 8.1) (cont.)



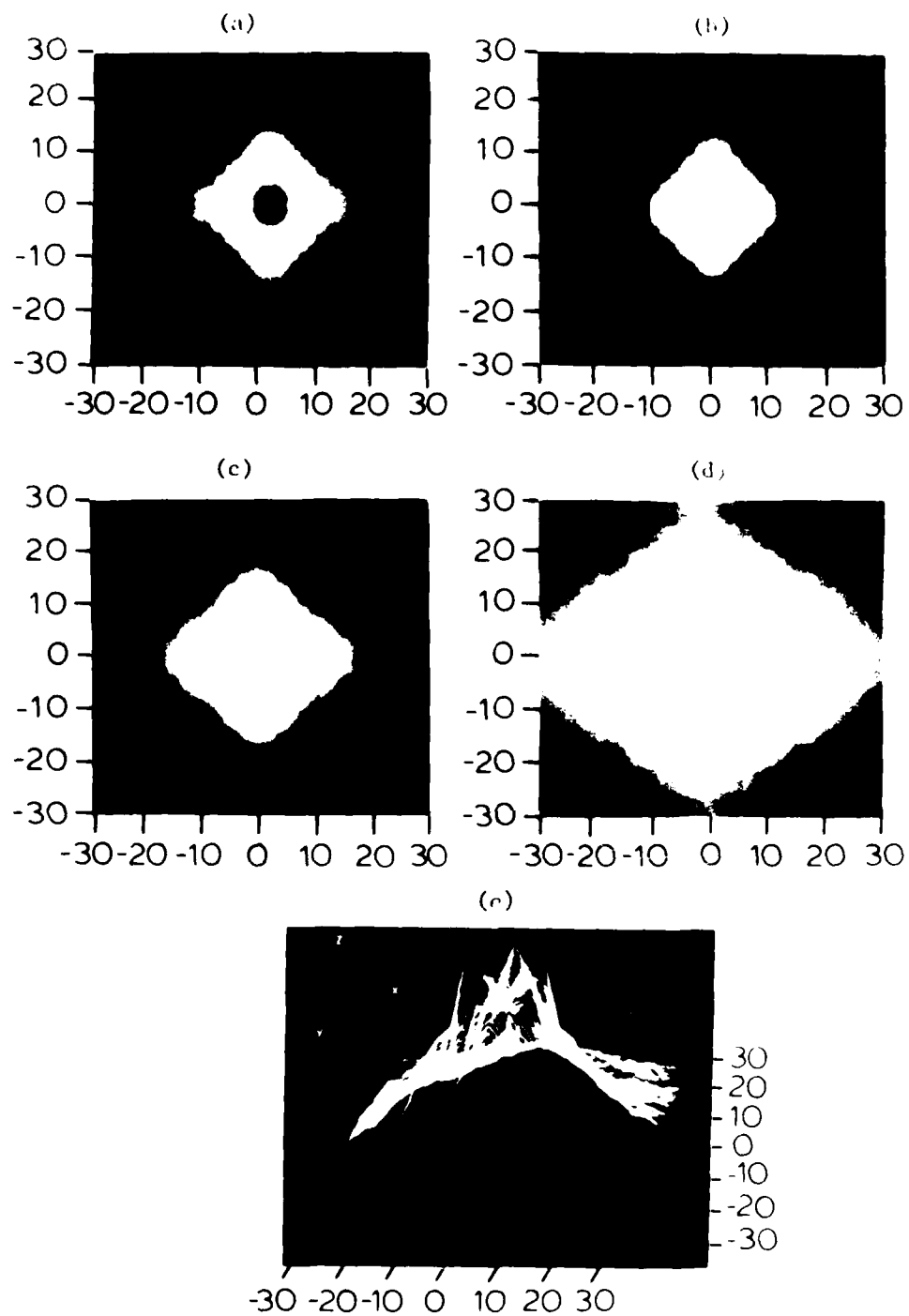


Figure 16. Pictures of the MTF(L) and MTF(H) Spatial Filters. High Visual Sensitivity Corresponds to High Intensity: (a) MTF(L); (b) MTF(H); (c) and (d) Underexposed Versions of b; (e) Three-Dimensional View of b. (Section 8.1)

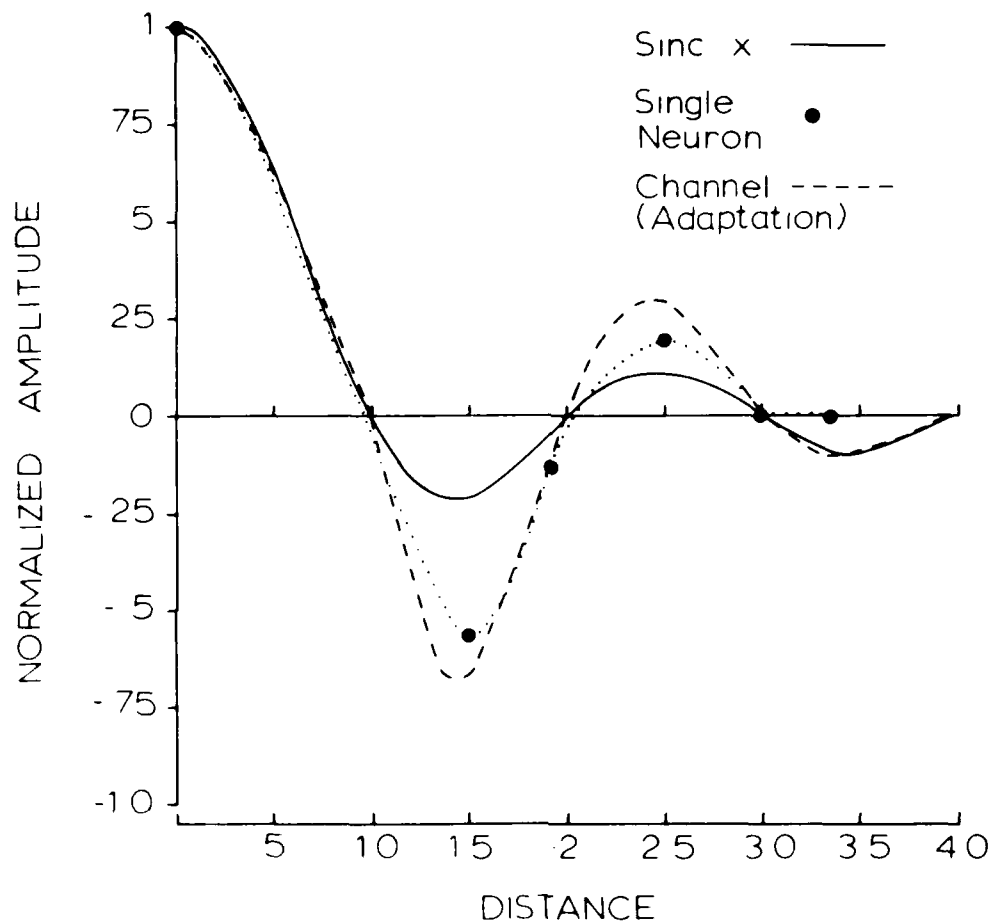


Figure 17. Comparison of the Filter Characteristics of the Sinc Function (Solid Line), a Simple Cell in the Visual Cortex of Cat (Filled Circles), and the Shape of a Psychophysical Channel Determined by Adaptation (Dashed Line). (Section 8.2.1)



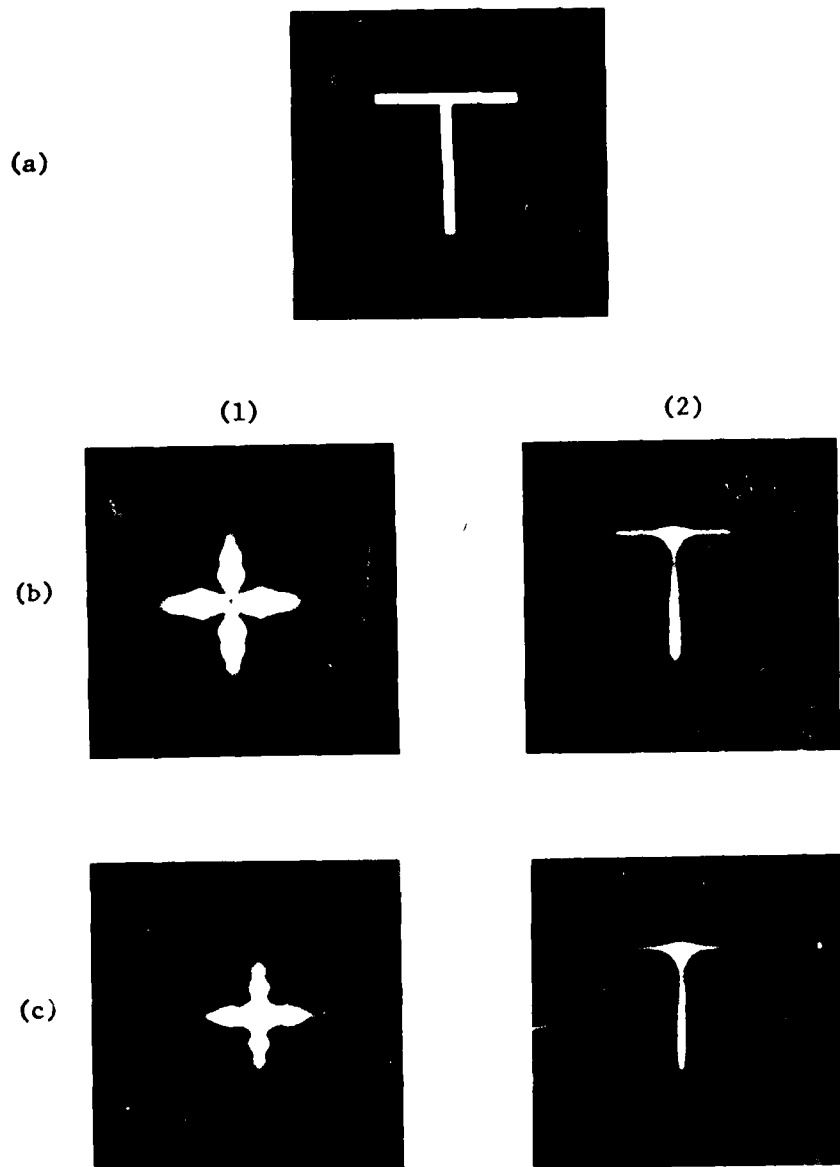


Figure 19. Spatial Filtering a Letter T: (a) Original Illusion; (b) MTF(L) Filtered Images; (c) MTF(H) Filtered Images; (d) MTF(H)L Filtered Images; (e) MTF(H) (6 by 6) L Filtered Images; (f) Low-Pass (6 by 6-1) Filtered Images; (g) Magnitude Spectra; (h) Filtered Letters. (Sections 9.1, 9.2)

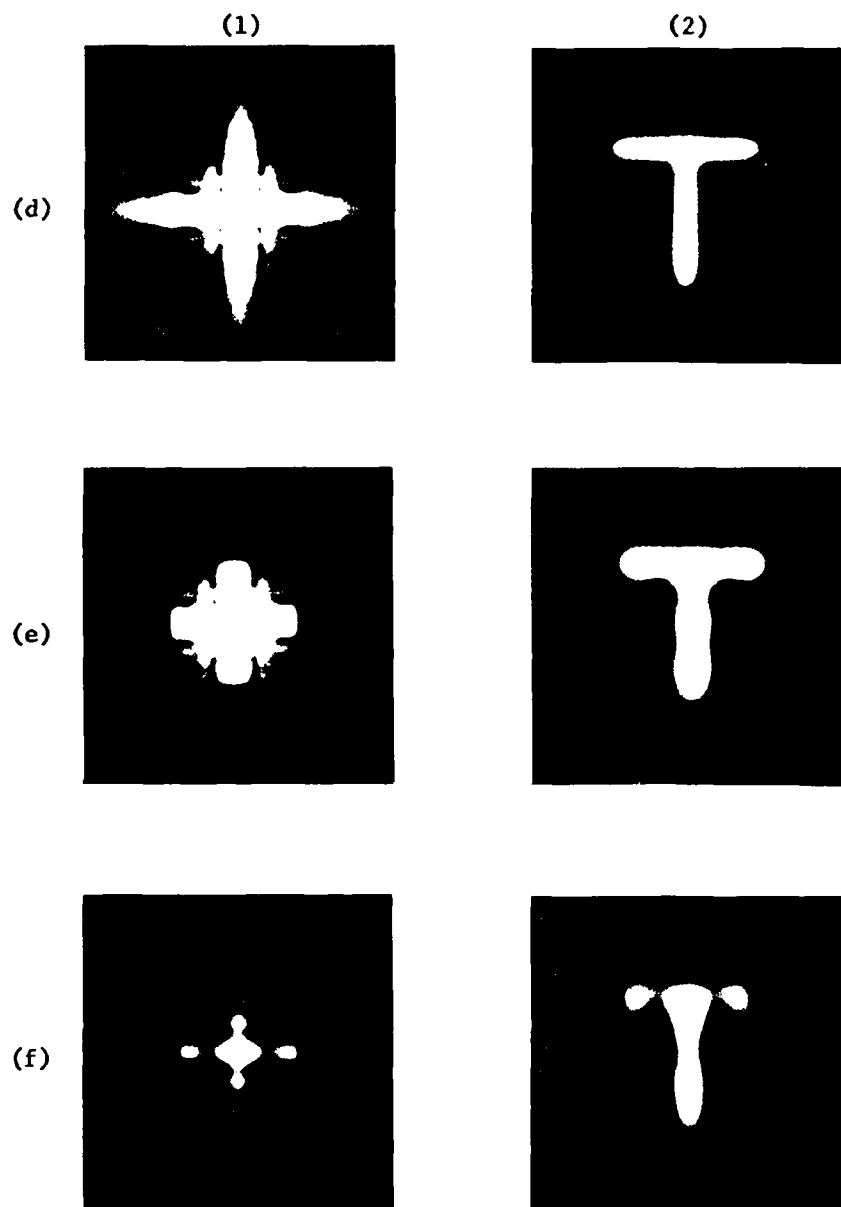


Figure 19. Spatial Filtering a Letter T: (a) Original Illusion; (b) MTF(L) Filtered Images; (c) MTF(H) Filtered Images; (d) MTF(H)L Filtered Images; (e) MTF(H) (6 by 6)L Filtered Images; (f) Low-Pass (6 by 6) Filtered Images; (g) Low-Pass (6 by 6 ~ 1) Filtered Images; (1) Magnitude Spectra; (2) Filtered Letters. (Sections 9.1, 9.2) (cont.)

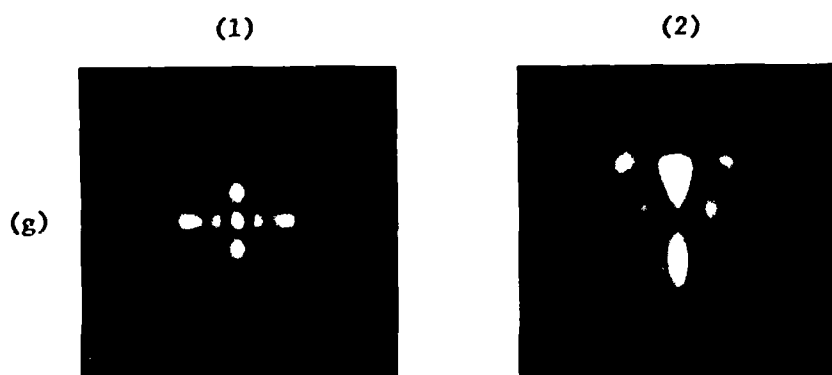


Figure 19. Spatial Filtering a Letter T: (a) Original Illusion; (b) MTF(L) Filtered Images; (c) MTF(H) Filtered Images; (d) MTF(H)L Filtered Images; (e) MTF(H) (6 by 6)L Filtered Images; (f) Low-Pass (6 by 6) Filtered Images; (g) Low-Pass (6 by 6 - 1) Filtered Images; (1) Magnitude Spectra; (2) Filtered Letters. (Sections 9.1, 9.2) (cont.)

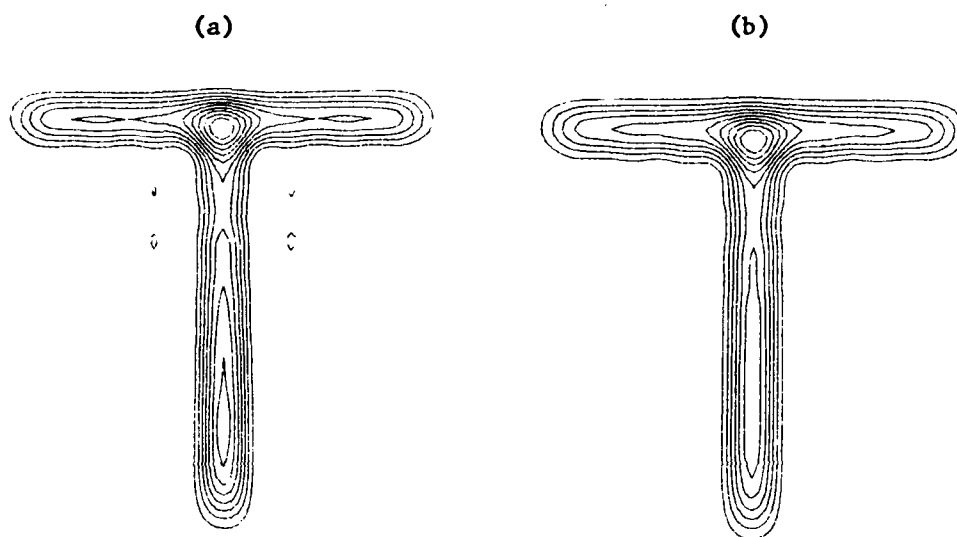


Figure 20. Two- and Three-Dimensional Contour Plots of a Filtered Letter T:  
 (a) Two-Dimensional Plot after Filtering with  $MTF(L)$ ;  
 (b) Two-Dimensional Plot after Filtering with  $MTF(H)$ ;  
 (c) Three-Dimensional Plot after Filtering with  $MTF(L)$ ;  
 (d) Three-Dimensional Plot after Filtering with  $MTF(L)^2$ ;  
 (e) Three-Dimensional Plot after Filtering with  $MTF(H)^2$ .  
 (Sections 9.2, 12.3.3)

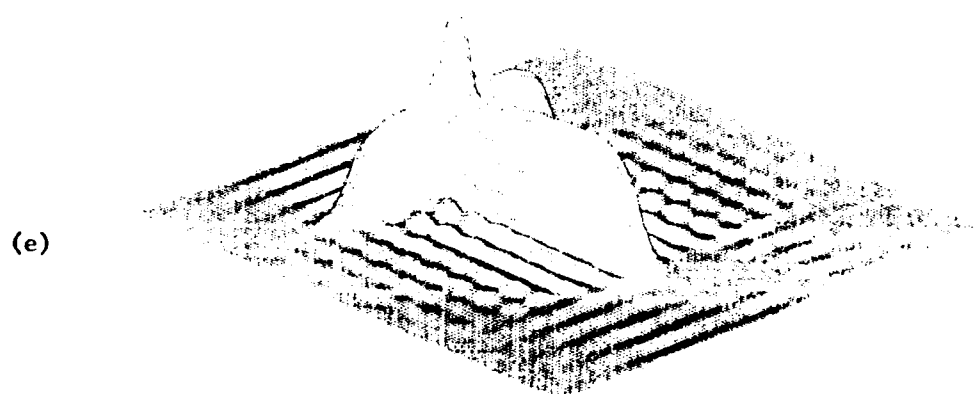
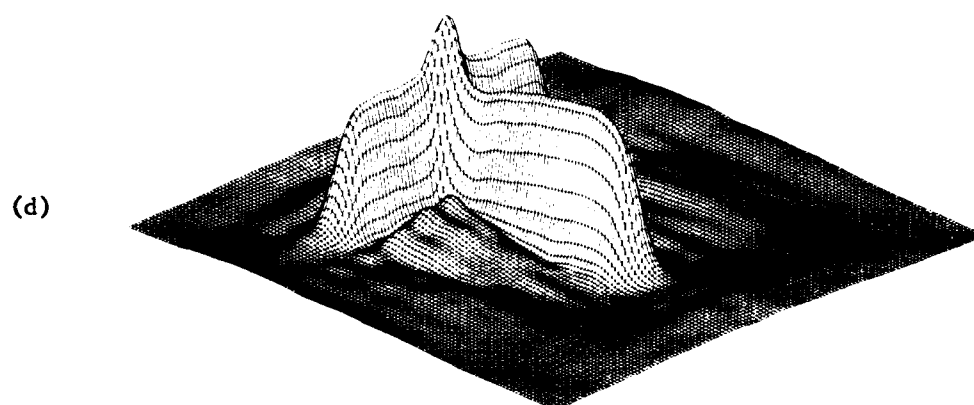
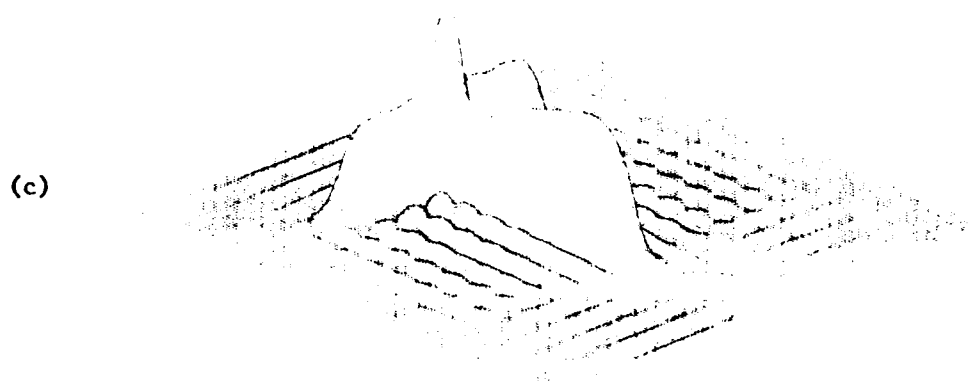


Figure 20. Two- and Three-Dimensional Contour Plots of a Filtered Letter T:  
 (a) Two-Dimensional Plot after Filtering with  $MTF(L)$ ;  
 (b) Two-Dimensional Plot after Filtering with  $MTF(H)$ ;  
 (c) Three-Dimensional Plot after Filtering with  $MTF(L)$ ;  
 (d) Three-Dimensional Plot after Filtering with  $MTF(L)^2$ ;  
 (e) Three-Dimensional Plot after Filtering with  $MTF(H)^2$ .  
 (Sections 9.2, 12.3.3) (cont.)



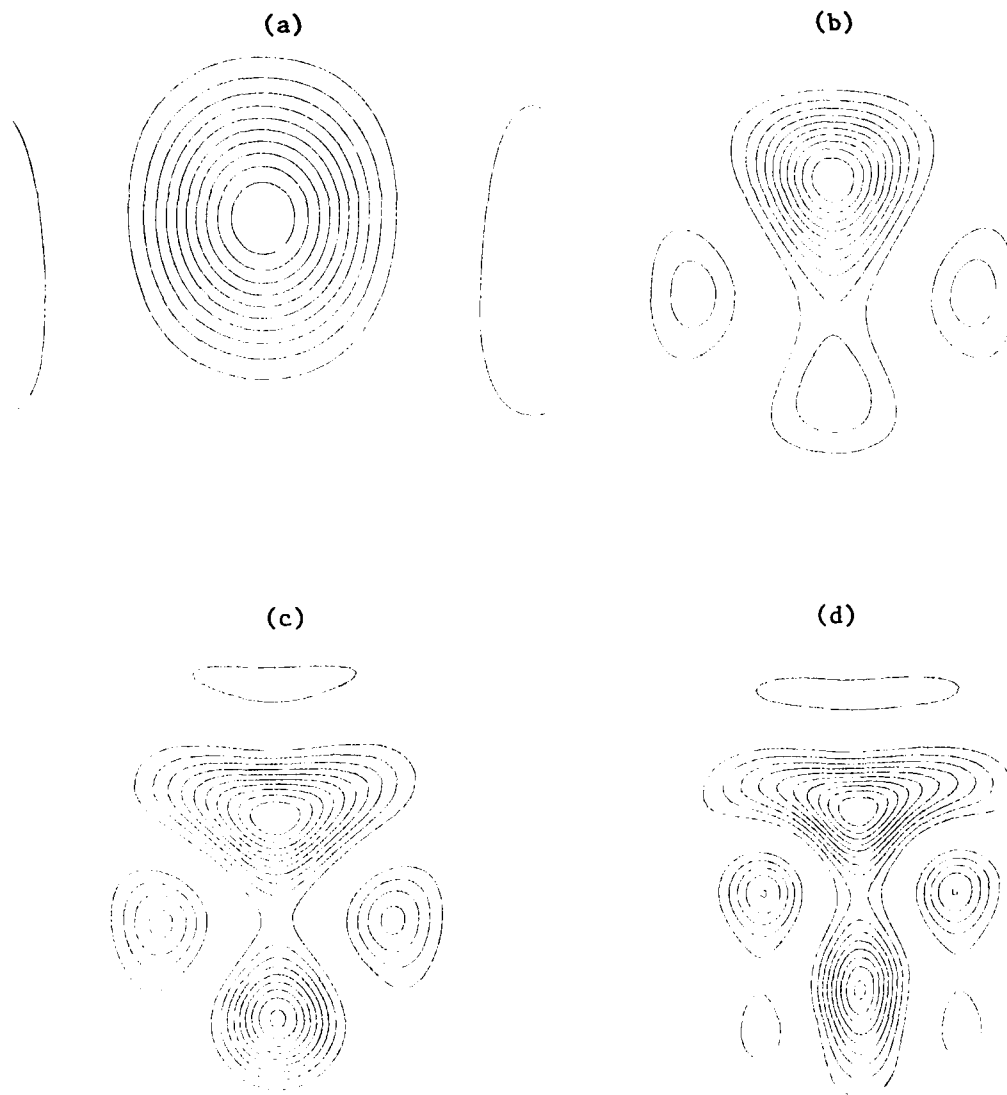


Figure 21. Sequential Low-Pass Filtering of a Letter T after MTF(L) Filtering: (a) Low-Pass (1 by 1) Filtered Letter T; (b) Low-Pass (2 by 2) Filtered Letter T; (c) Low-Pass (3 by 3) Filtered Letter T; (d) Low-Pass (4 by 4) Filtered Letter T; (e) Low-Pass (5 by 5) Filtered Letter T; (f) Low-Pass (6 by 6) Filtered Letter T. (Section 9.2)

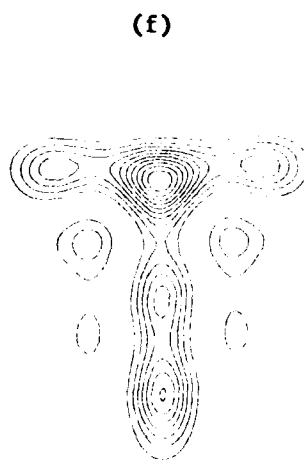
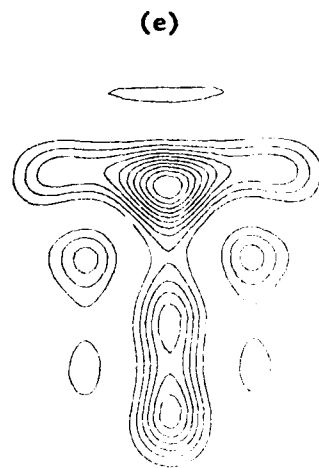


Figure 21. Sequential Low-Pass Filtering of a Letter T after MTF(L) Filtering: (a) Low-Pass (1 by 1) Filtered Letter T; (b) Low-Pass (2 by 2) Filtered Letter T; (c) Low-Pass (3 by 3) Filtered Letter T; (d) Low-Pass (4 by 4) Filtered Letter T; (e) Low-Pass (5 by 5) Filtered Letter T; (f) Low-Pass (6 by 6) Filtered Letter T. (Section 9.2) (cont.)

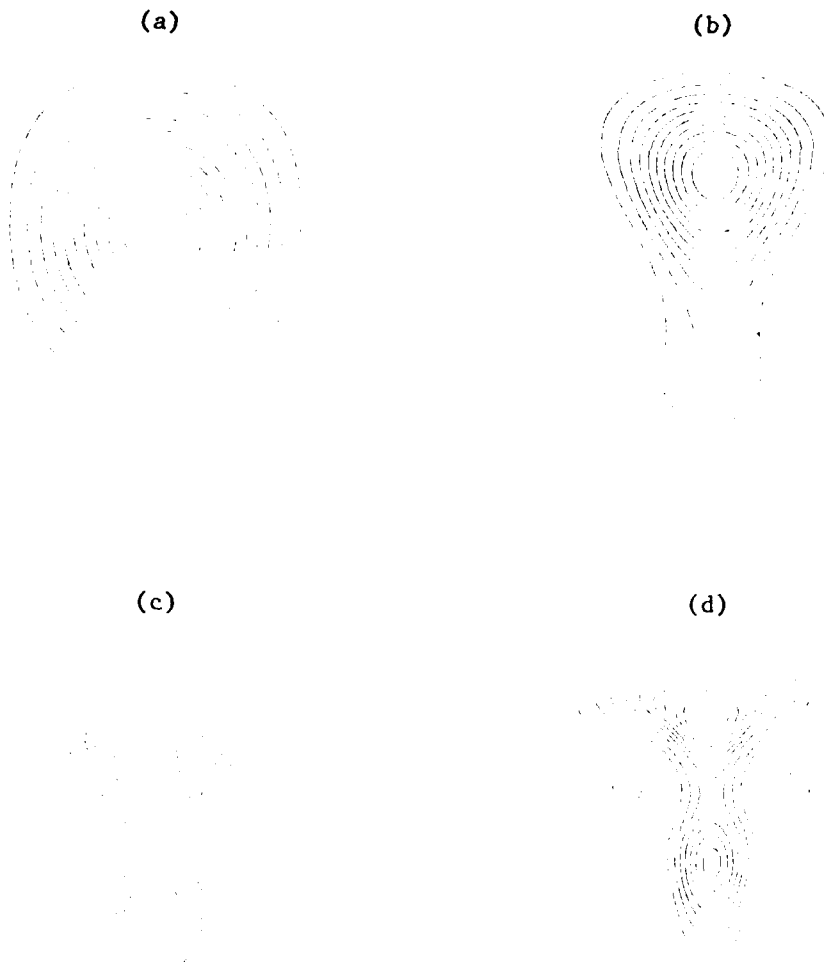


Figure 22. Sequential Low-Pass Filtering of a Letter T after MTF(H) Filtering: (a) Low-Pass (1 by 1) Filtered Letter T; (b) Low-Pass (2 by 2) Filtered Letter T; (c) Low-Pass (3 by 3) Filtered Letter T; (d) Low-Pass (4 by 4) Filtered Letter T; (e) Low-Pass (5 by 5) Filtered Letter T; (f) Low-Pass (6 by 6) Filtered Letter T. (Section 9.2)

(e)



(f)



Figure 22. Sequential Low-Pass Filtering of a Letter T after MTF (H) Filtering: (a) Low-Pass (1 by 1) Filtered Letter T; (b) Low-Pass (2 by 2) Filtered Letter T; (c) Low-Pass (3 by 3) Filtered Letter T; (d) Low-Pass (4 by 4) Filtered Letter T; (e) Low-Pass (5 by 5) Filtered Letter T; (f) Low-Pass (6 by 6) Filtered Letter T. (Section 9.2) (cont.)

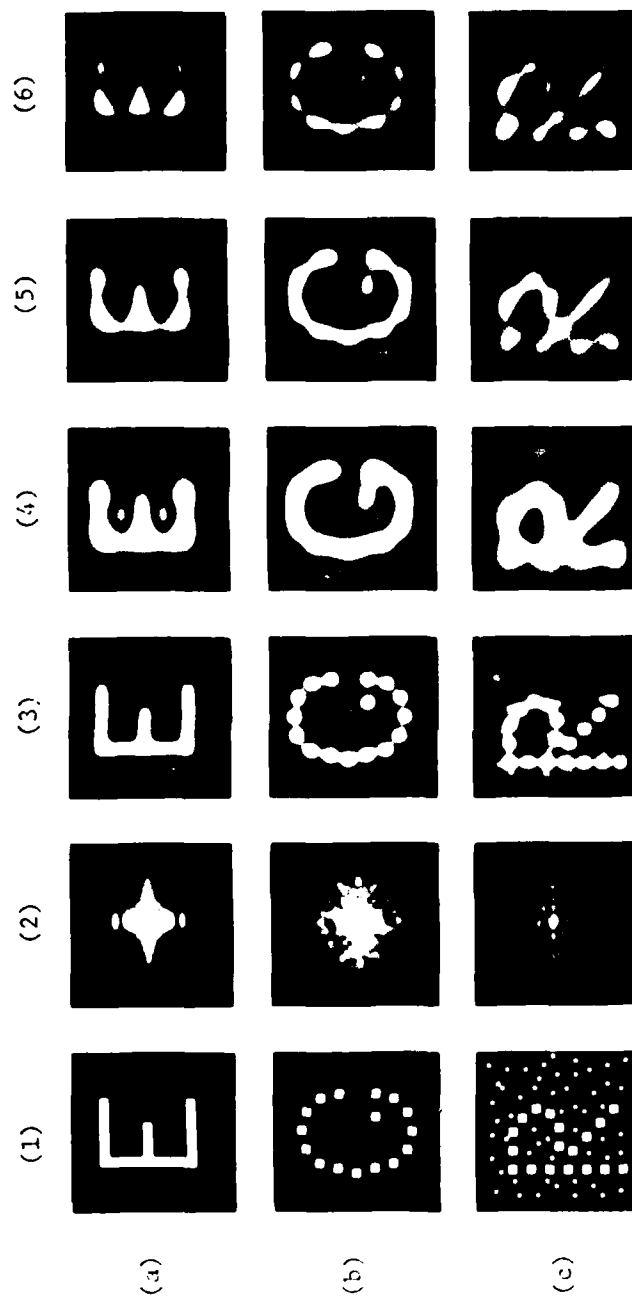


Figure 23. Filtered Objects: (a) Letter E; (b) Dot Letter G; (c) Dot Letter R in Noise; (d) Dot-Whole; (e) Dot-Proximity; (f) Dot-Line-Similarity; (g) Dot-Line Proximity; Similarity; (1) Original Objects; (2) MTF Filtered Magnitude Spectra; (3) MTF Filtered Images; (4) MTF 4 by 4 Low-Pass Filtered Images; (5) Low-Pass 4 by 4 Filtered Images; (6) Low-Pass 4 by 4 - 1) Filtered Images, (Sections 9,2, 9,3, 9,4, 9,5, 9,6, 12,6, 1)

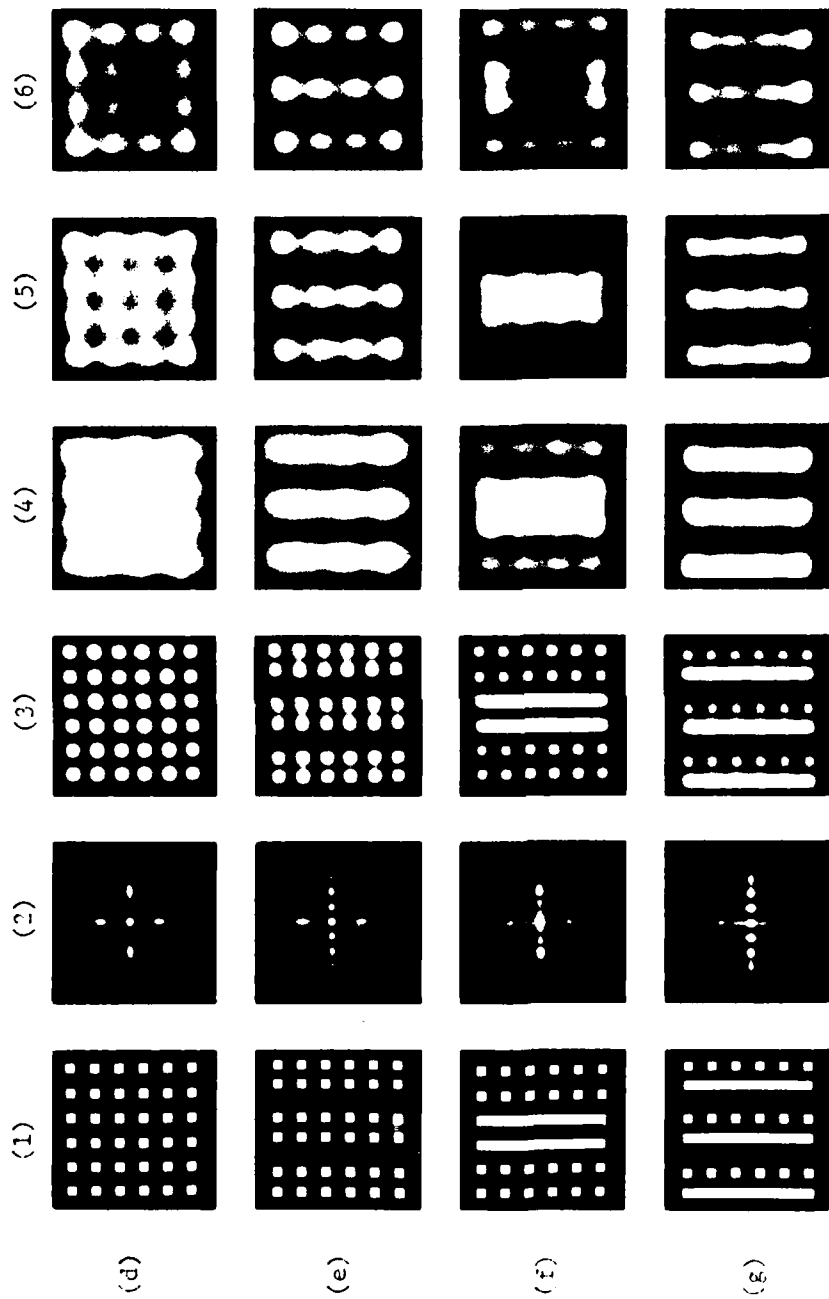


Figure 23. Filtered Objects: (a) Letter E; (b) Dot Letter G; (c) Dot Letter R in Noise; (d) Dot-Whole; (e) Dot-Proximity; (f) Dot-Line-Similarity; (g) Dot-Line Proximity Similarity; (1) Original Objects; (2) MTF Filtered Magnitude Spectra; (3) MTF Filtered Images; (4) MTF (4 by 4) Filtered Images; (5) Low-Pass (4 by 4) Filtered Images; (6) Low-Pass (4 by 4 - 1) Filtered Images. (Section 9.2, 9.3, 9.4, 9.5, 9.6, 12.6, 1)

(a)

(b)

(c)

(d)

Figure 24. Contour Plots of a Synthesized Dot Letter G: (a) Low-Pass (1 by 1) Filtered Letter; (b) Low-Pass (2 by 2) Filtered Letter; (c) Low-Pass (3 by 3) Filtered Letter; (d) Low-Pass (4 by 4) Filtered Letter; (e) Low-Pass (5 by 5) Filtered Letter; (f) Low-Pass (6 by 6) Filtered Letter; (g) Low-Pass (7 by 7) Filtered Letter. (Section 9.4)

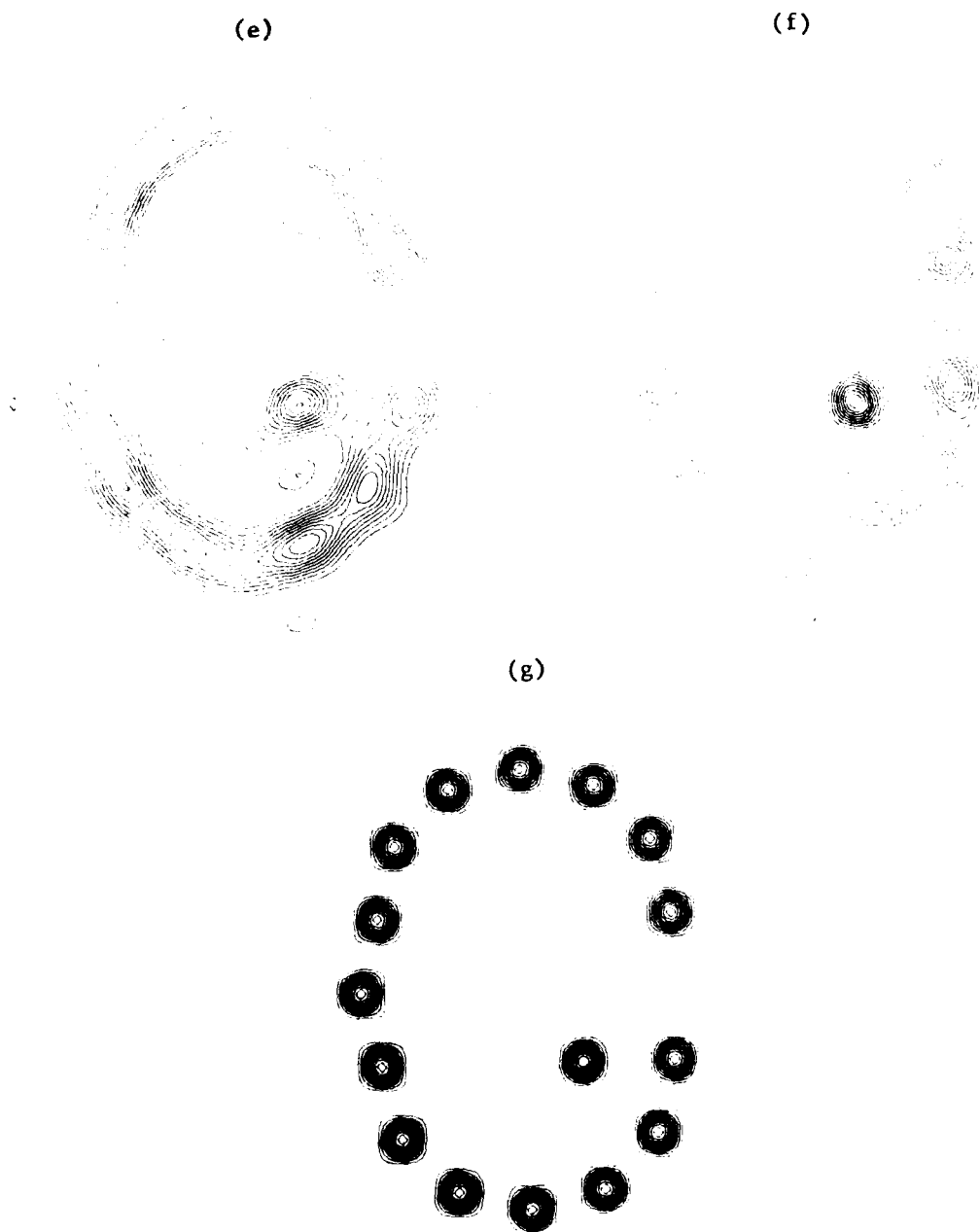


Figure 24. Contour Plots of a Synthesized Dot Letter G: (a) Low-Pass (1 by 1) Filtered Letter; (b) Low-Pass (2 by 2) Filtered Letter; (c) Low-Pass (3 by 3) Filtered Letter; (d) Low-Pass (4 by 4) Filtered Letter; (e) Low-Pass (5 by 5) Filtered Letter; (f) Low-Pass (6 by 6) Filtered Letter; (g) Low-Pass (7 by 7) Filtered Letter. (Section 9.4) (cont.)



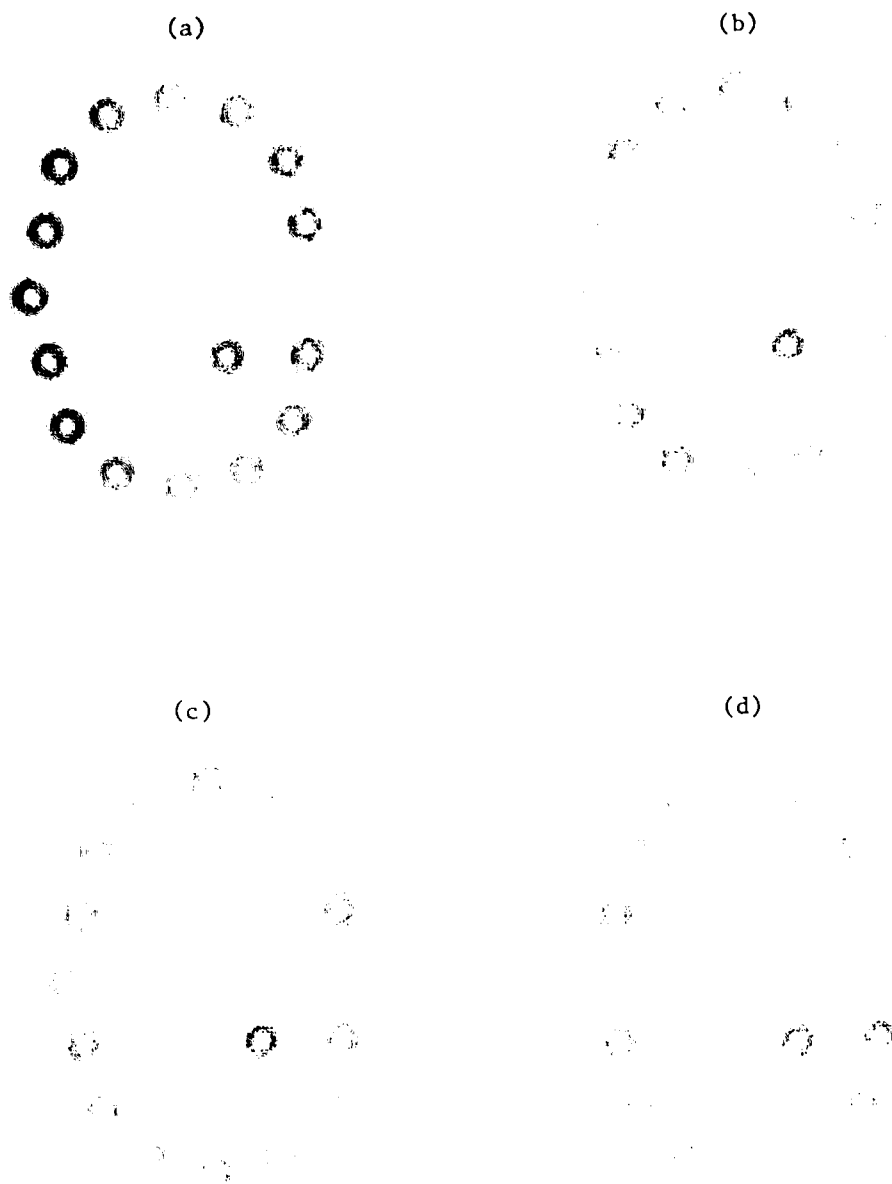


Figure 25. Contour Plots of a High-Pass Filtered Dot Letter G. There Are 16 Spatial Harmonics and the Low Spatial Frequencies Are Sequentially Removed One at a Time: (a) High-Pass (-1 by 1) Filtered Letter; (b) High-Pass (-2 by 2) Filtered Letter; (c) High-Pass (-3 by 3) Filtered Letter; (d) High-Pass (-4 by 4) Filtered Letter; (e) High-Pass (-5 by 5) Filtered Letter; (f) High-Pass (-6 by 6) Filtered Letter; (g) High-Pass (-7 by 7) Filtered Letter; (h) High-Pass (-8 by 8) Filtered Letter; (i) High-Pass (-9 by 9) Filtered Letter; (j) High-Pass (-10 by 10) Filtered Letter. (Section 9.4)

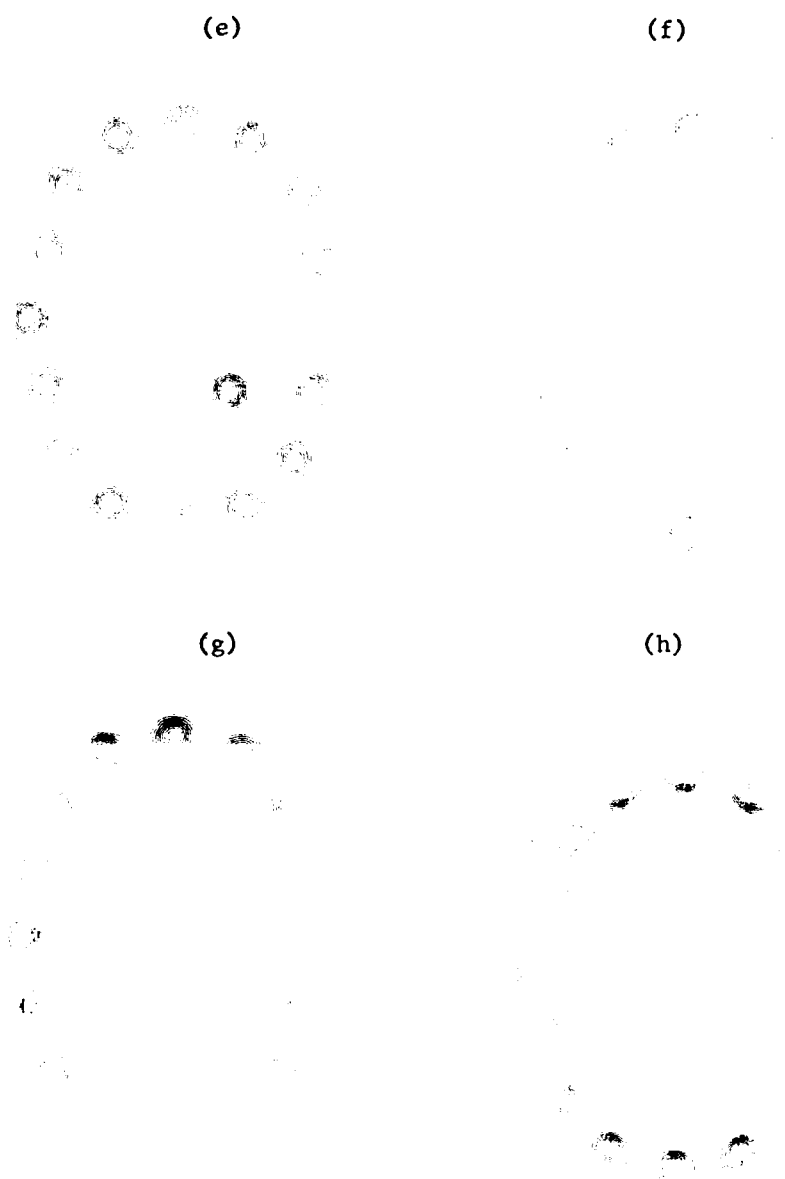
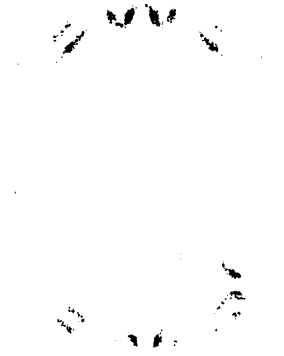


Figure 25. Contour Plots of a High-Pass Filtered Dot Letter G. There Are 16 Spatial Harmonics and the Low Spatial Frequencies Are Sequentially Removed One at a Time: (a) High-Pass (-1 by 1) Filtered Letter; (b) High-Pass (-2 by 2) Filtered Letter; (c) High-Pass (-3 by 3) Filtered Letter; (d) High-Pass (-4 by 4) Filtered Letter; (e) High-Pass (-5 by 5) Filtered Letter; (f) High-Pass (-6 by 6) Filtered Letter; (g) High-Pass (-7 by 7) Filtered Letter; (h) High-Pass (-8 by 8) Filtered Letter; (i) High-Pass (-9 by 9) Filtered Letter; (j) High-Pass (-10 by 10) Filtered Letter. (Section 9.4) (cont.)

(1)



(j)

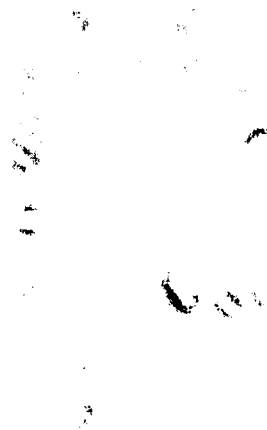


Figure 25. Contour Plots of a High-Pass Filtered Dot Letter G. There Are 16 Spatial Harmonics and the Low Spatial Frequencies Are Sequentially Removed One at a Time: (a) High-Pass (-1 by 1) Filtered Letter; (b) High-Pass (-2 by 2) Filtered Letter; (c) High-Pass (-3 by 3) Filtered Letter; (d) High-Pass (-4 by 4) Filtered Letter; (e) High-Pass (-5 by 5) Filtered Letter; (f) High-Pass (-6 by 6) Filtered Letter; (g) High-Pass (-7 by 7) Filtered Letter; (h) High-Pass (-8 by 8) Filtered Letter; (i) High-Pass (-9 by 9) Filtered Letter; (j) High-Pass (-10 by 10) Filtered Letter. (Section 9.4) (cont.)

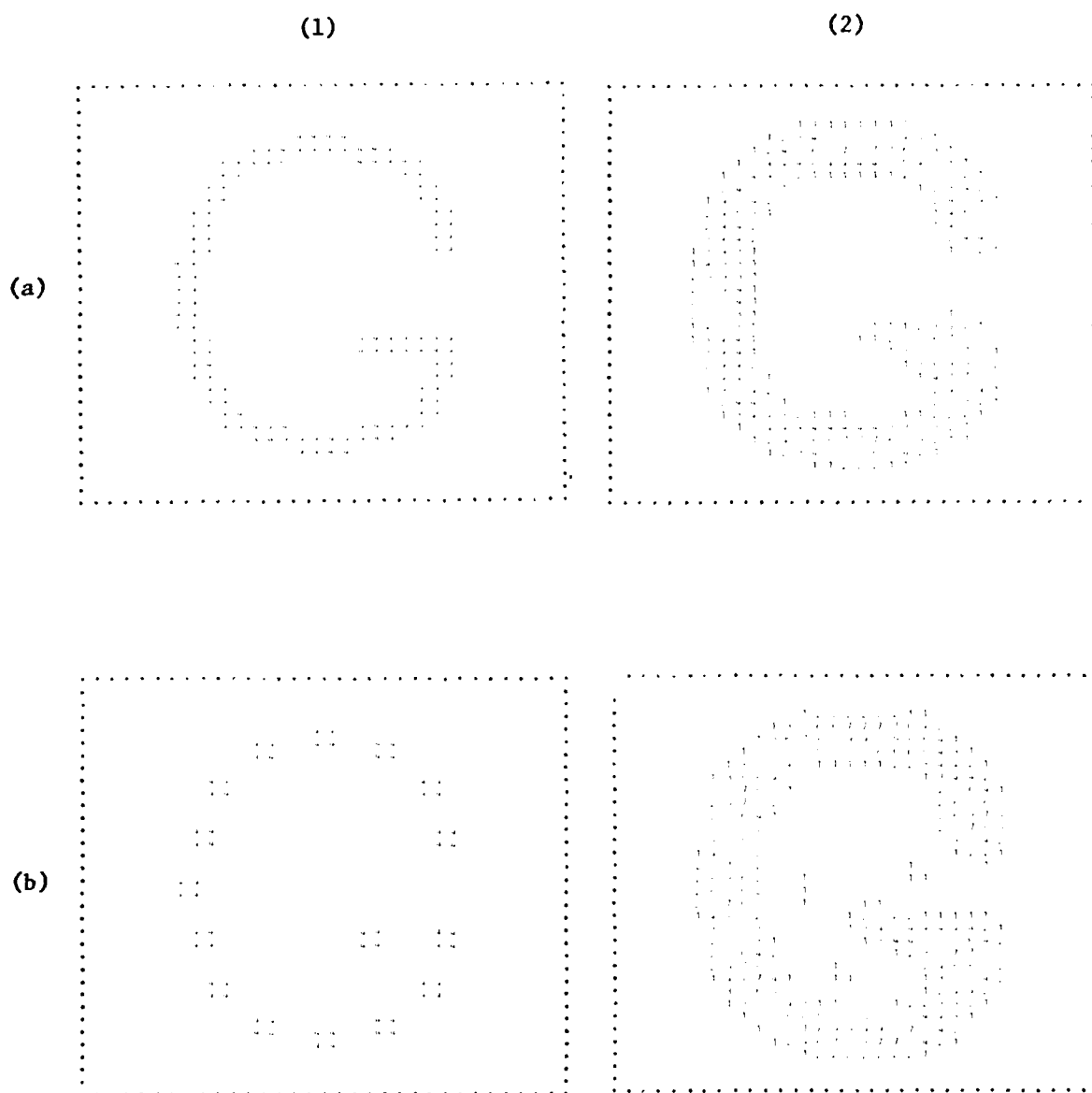


Figure 26. Similar Forms from Low Spatial Frequencies of Four Discriminably Different Letter G's: (a) Full G; (b) Dot G; (c) Serif G; (d) Slash G; (1) Original Letters; (2) Low-Pass (4 by 4) Filtered Letters. (Section 9.4.1)

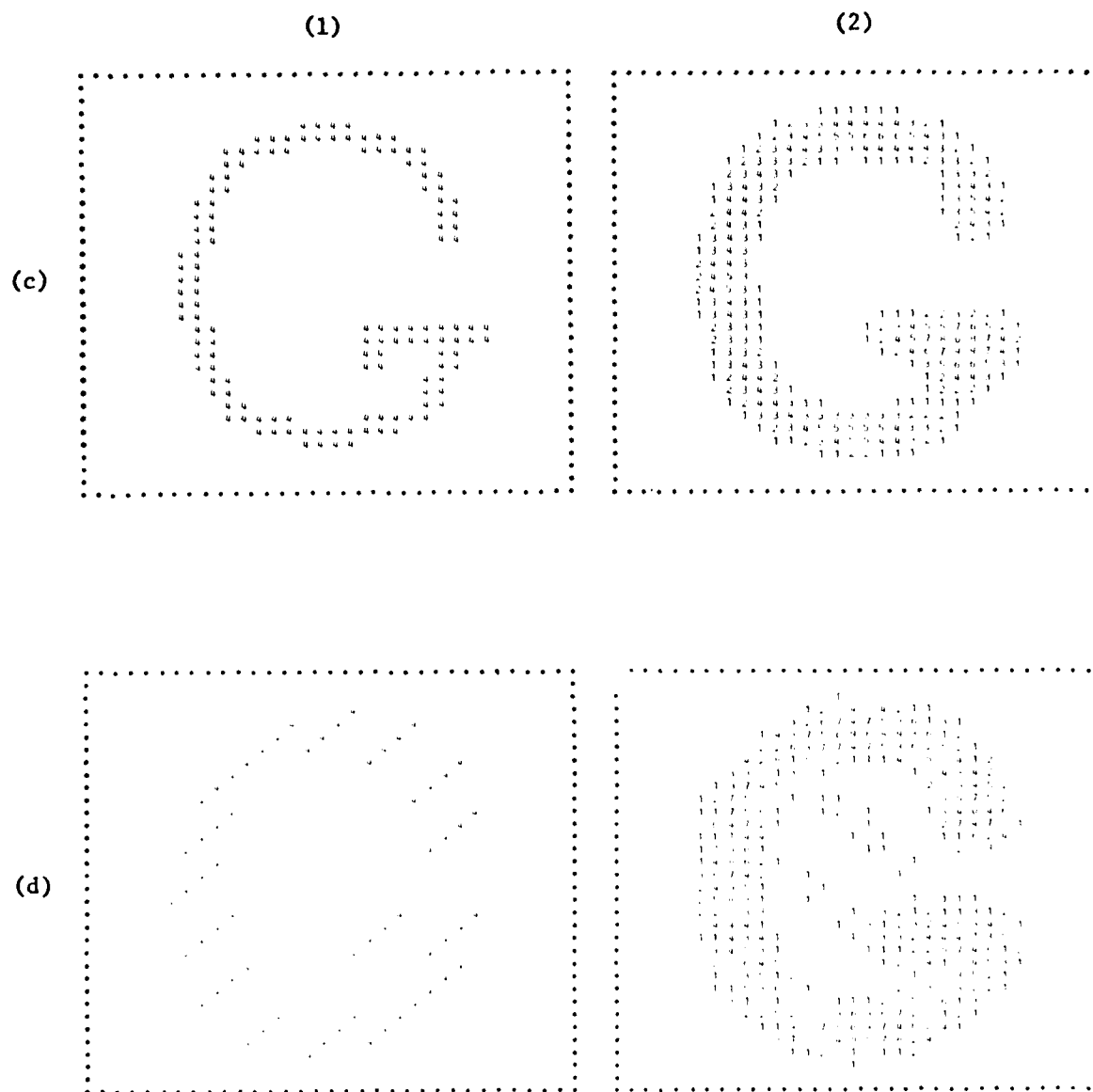
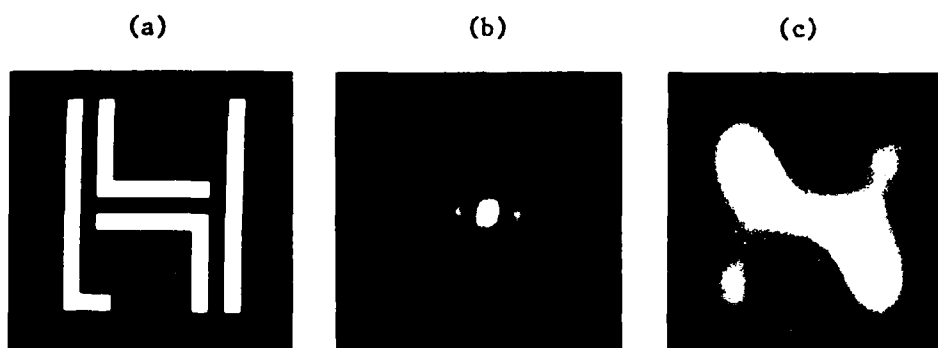


Figure 20. Similar Forms from Low Spatial Frequencies of Four Discriminably Different Letter G's: (a) Full G; (b) Dot G; (c) Serif G; (d) Slash G; (1) Original Letters; (2) Low-Pass (4 by 4) Filtered Letters. (Section 9.4.1) (cont.)



**Figure 27. An Example of Closure from the Low Spatial Frequencies of a Discrete Line Letter H:**  
 (a) Original Object; (b) Low-Pass (4 by 4) Filtered Magnitude Spectrum; (c) Low-Pass (4 by 4) Filtered Image. (Section 9.6)



Figure 28. The Effects of MTF and Low-Pass Filtering on Three Variations of a Portrait: (a) Original Portraits; (b) Coarsely Quantized Portraits; (c) Portraits with Random Noise Added; (1) Portraits; (2) MTF Filtered Portraits; (3) MTF 10.2 by 10.3 Filtered Portraits; (4) Low-Pass 10.2 by 10.3 Filtered Portraits. (Sections 10.2, 10.3, 10.4)

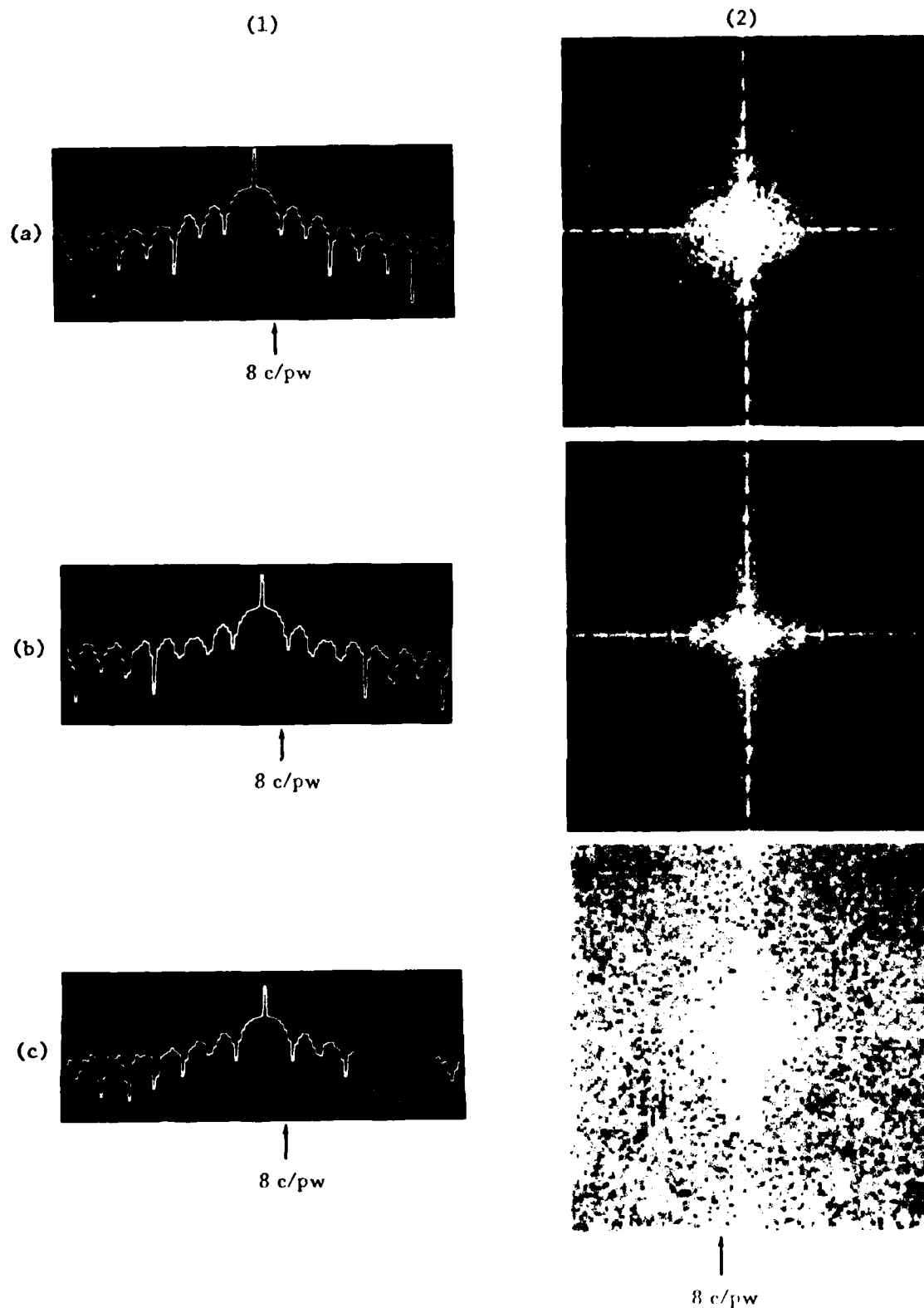


Figure 29. Log Magnitude Spectra of Portraits in Figure 28: (a) Original Portrait Spectra; (b) Coarsely Quantized Portrait Spectra; (c) Portrait with Random Noise Added Spectra; (1) One-Dimensional; (2) Two-Dimensional. (Sections 10.2, 10.3, 10.4)



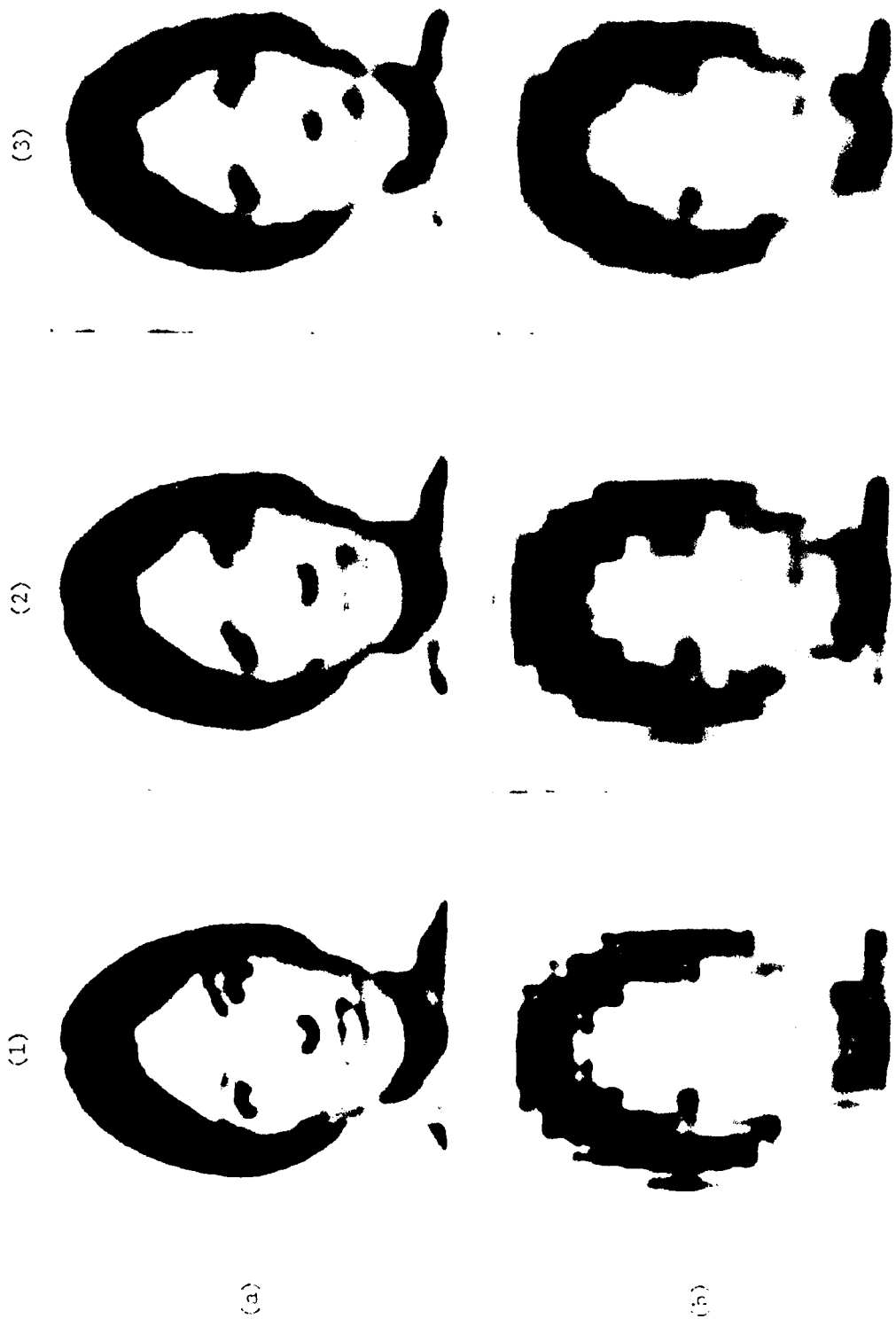


Figure 30. Variable Low-Pass Filtering of Original and Coarsely Quantized Portraits: (a) Original Portraits; (b) Coarsely Quantized Portraits; (1) Low-Pass (24 by 24) Filtered Portraits; (2) Low-Pass (16 by 16) Filtered Portraits; (3) Low-Pass (12 by 12) Filtered Portraits. (Section 10.3.1)

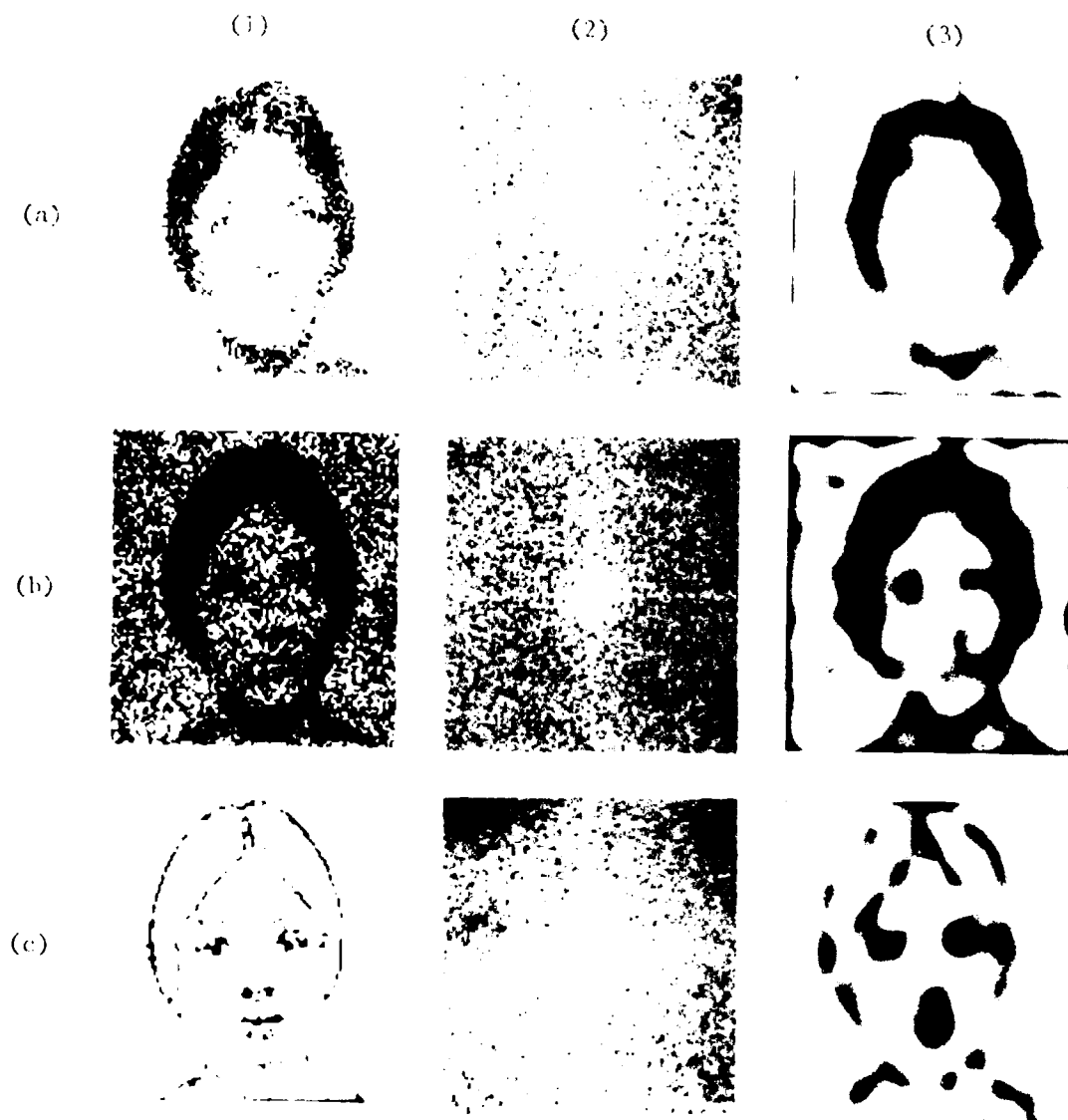


Figure 31. Low-Pass Filtering of Other Portrait Variations: (a) a Second Portrait with Random Noise Added; (b) Portrait with Inclusive-OR Random Noise Added; (c) a Binary Line Portrait; (1) Original Portraits; (2) Two-Dimensional Log Magnitude Spectra; (3) Low-Pass (3 by 3) Filtered Portraits. (Sections 10.4, 10.5, 10.6)



Figure 32. Portraits Having Reversed Contrast: (a) Edge Enhanced; (b) Binary Valued;  
(1) Original; (2) Reversed Contrast. (Section 10.7)

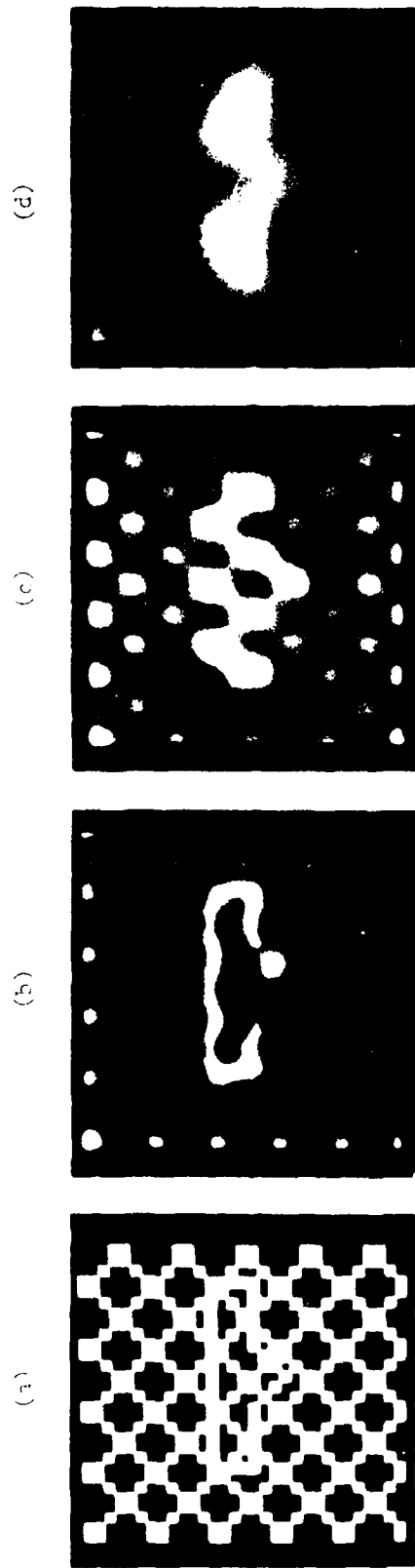


Figure 11. Isolating a Rectangular Form From Oblique Lines by Spatial Filtering: (a) Original Object; (b) MTF Filtered Image; (c) Low-Pass Filtered Image; (d) Filtered Image. (Section 11.2.1)

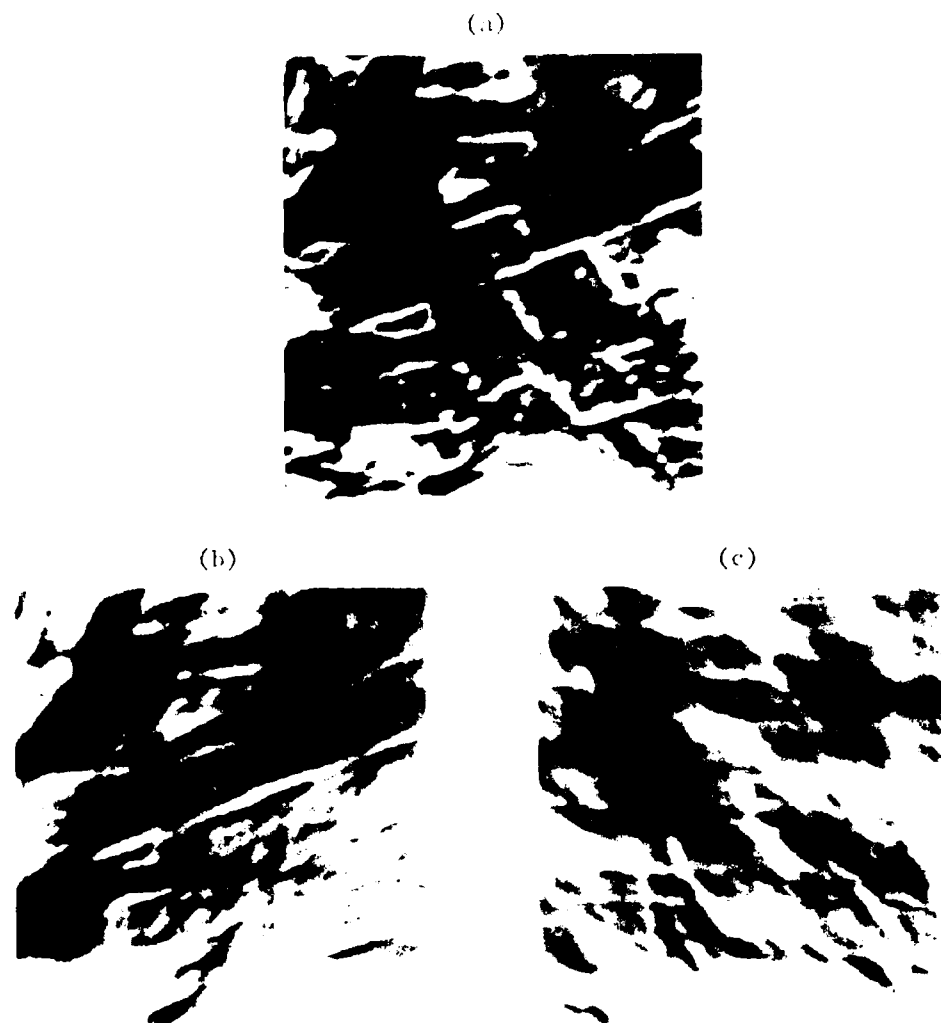
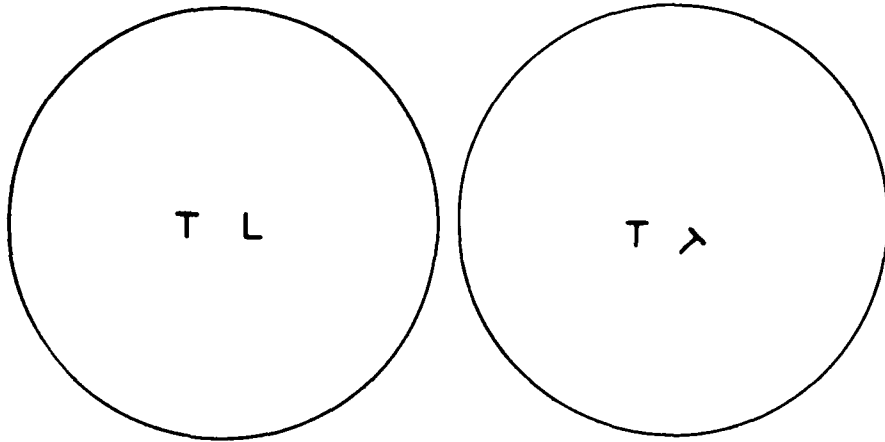


Figure 31. Isolating Oblique Structure in a Real Scene: (a) Original Scene; (b) Left Obliques Enhanced by Passing Right Oblique Spatial Frequencies; (c) Right Obliques Enhanced by Passing Left Oblique Spatial Frequencies. (Section 11.2.2)

(a)



(b)

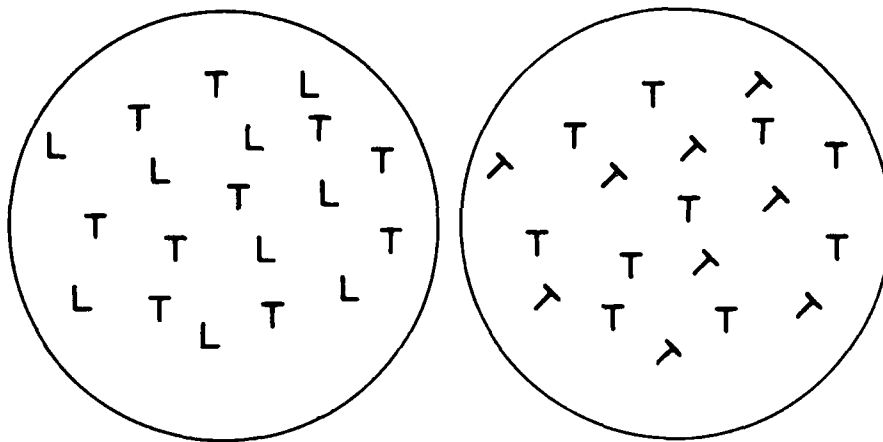


Figure 35. Similarity Grouping of Pairs and Arrays of Letters: (a) Letter Pairs; (b) Letter Arrays. (Section 11.3.1)

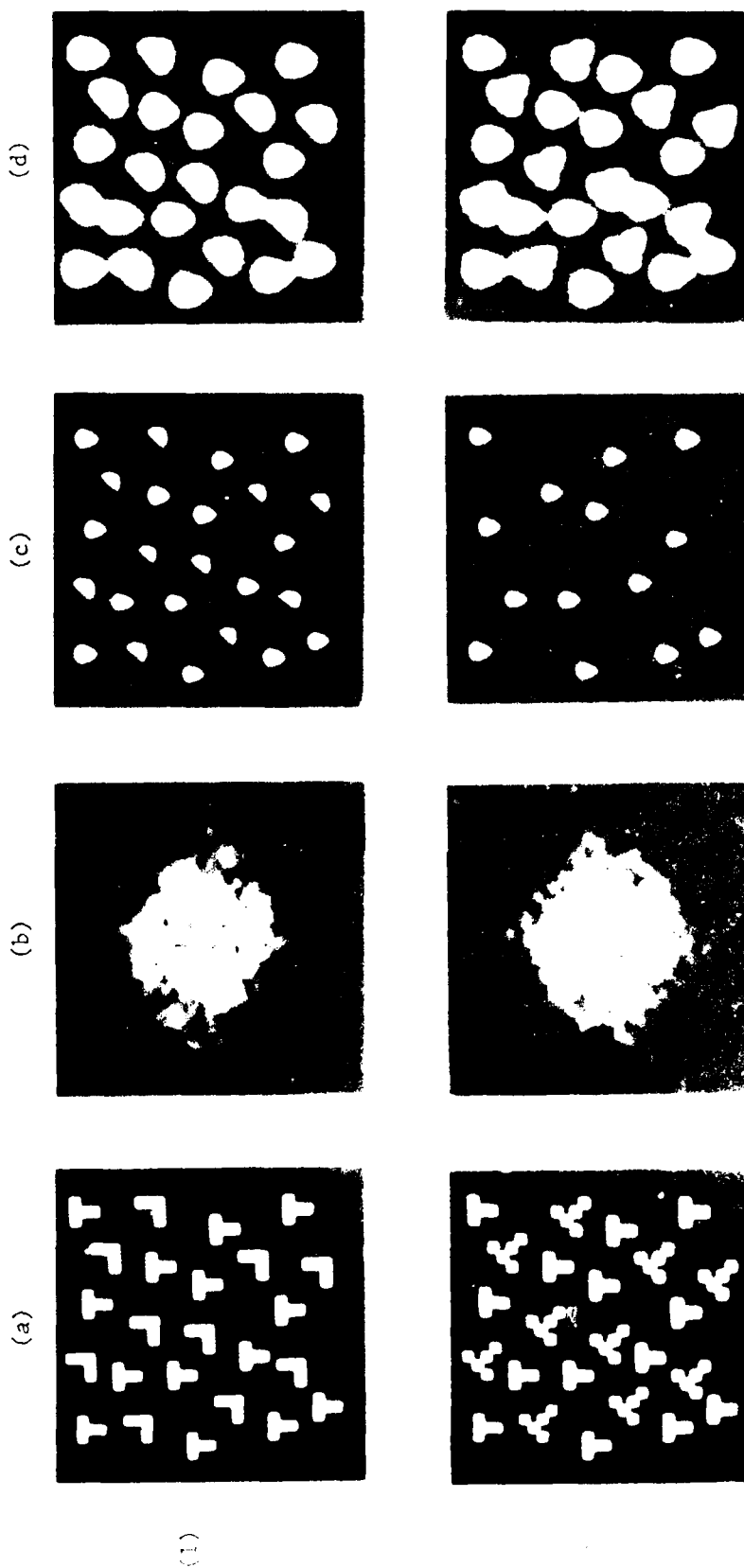


Figure 30. Similarity Grouping of Arrays of Letters that Differ in Orientation: (a) Original Arrays; (b) MTF Filtered  
Magnitude Spectra; (c) MTF(1) Filtered Arrays; (d) MTF(1) Filtered Arrays; (e) T-L Arrays; (f) T-slanted T  
Arrays; (g) T-L Arrays; (h) T-slanted T Arrays.

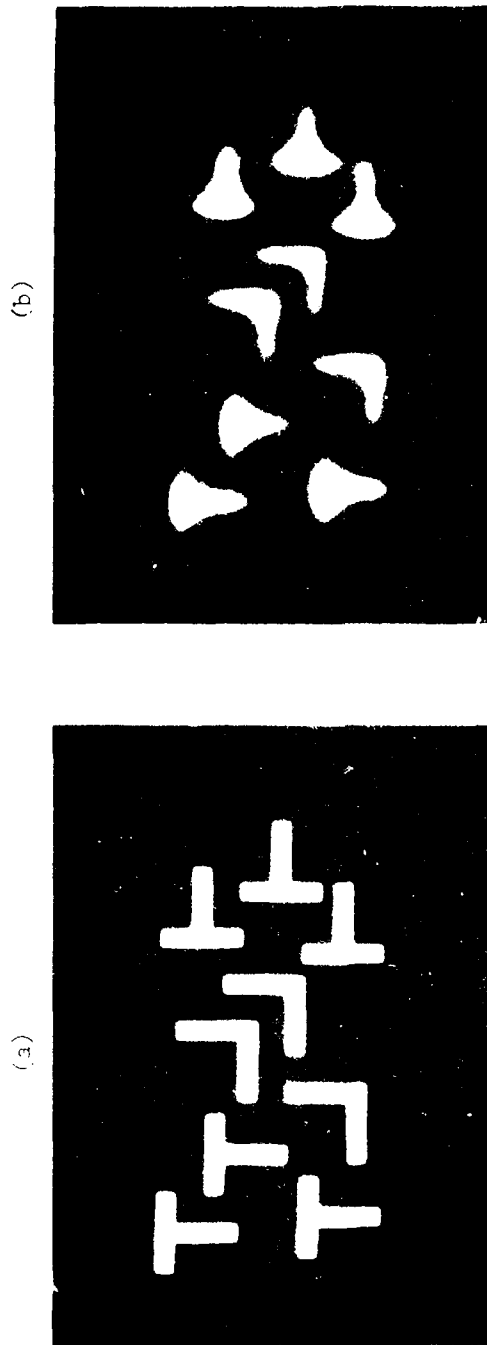


Figure 3.7. Similarity Grouping of an Array of Letters that Differ in Configuration: (a) Original Array; (b) MTF Filtered Array. (Section 11.3.2)



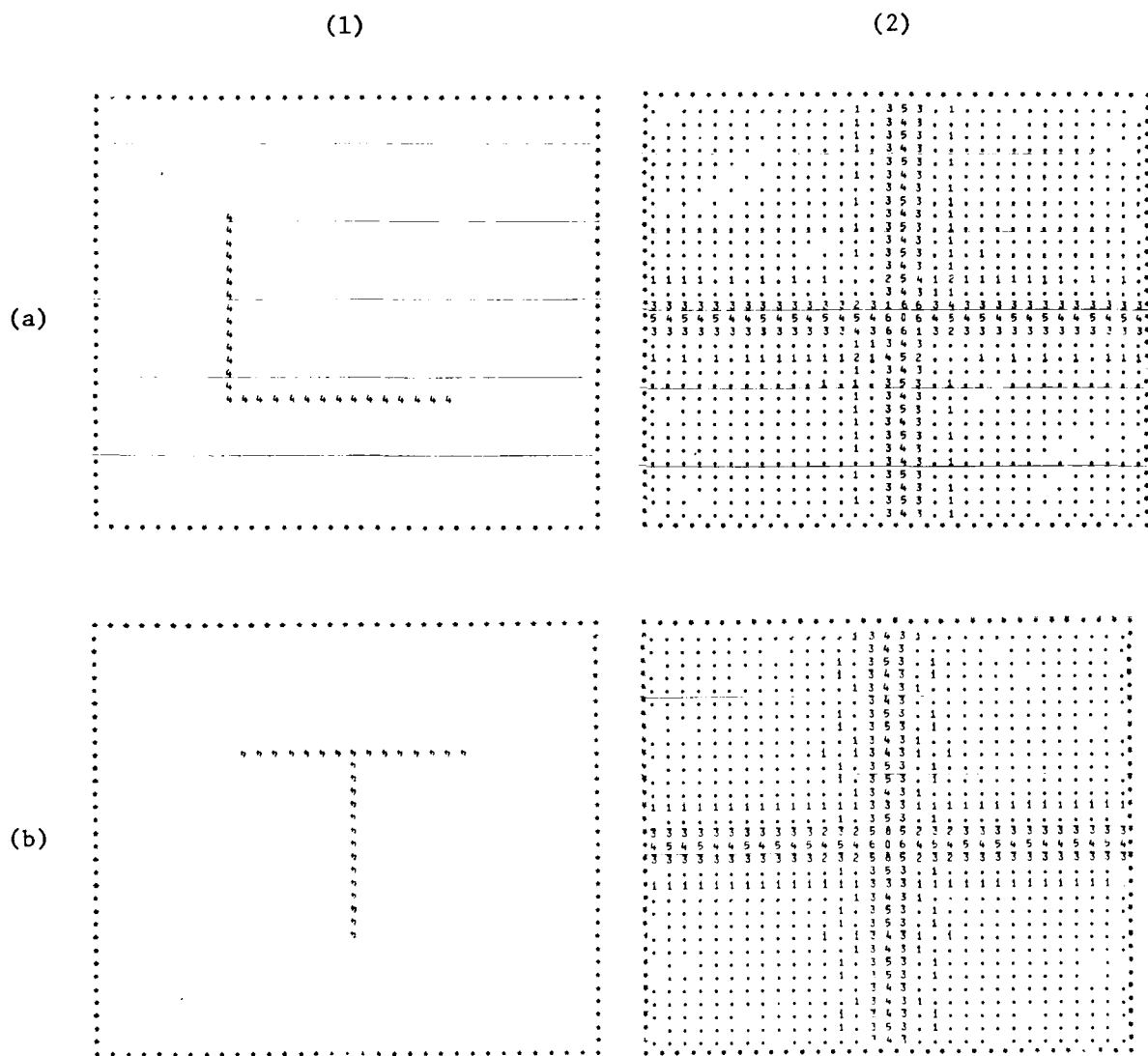


Figure 38. Numerical Printouts of the Magnitude Spectra of an L and T: (a) Letter L; (b) Letter T; (1) Numerical Printouts of Letters; (2) Magnitude Spectra of Letters. (Section 11.3.2)

(a)

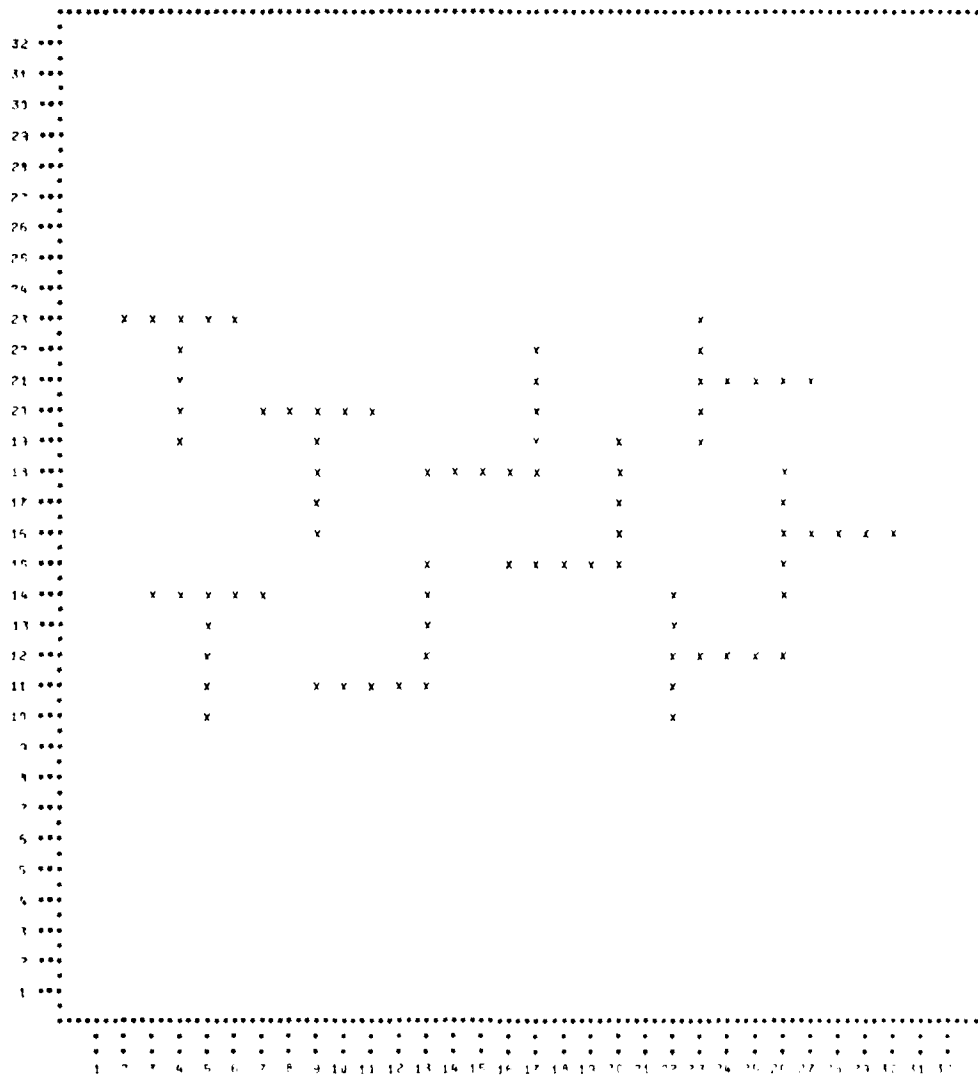


Figure 39. Numerical Printouts of the Filtered Arrays of Figure 37:  
(a) Original Array; (b) MTF Filtered Array. (Section 11.3.2)

(b)

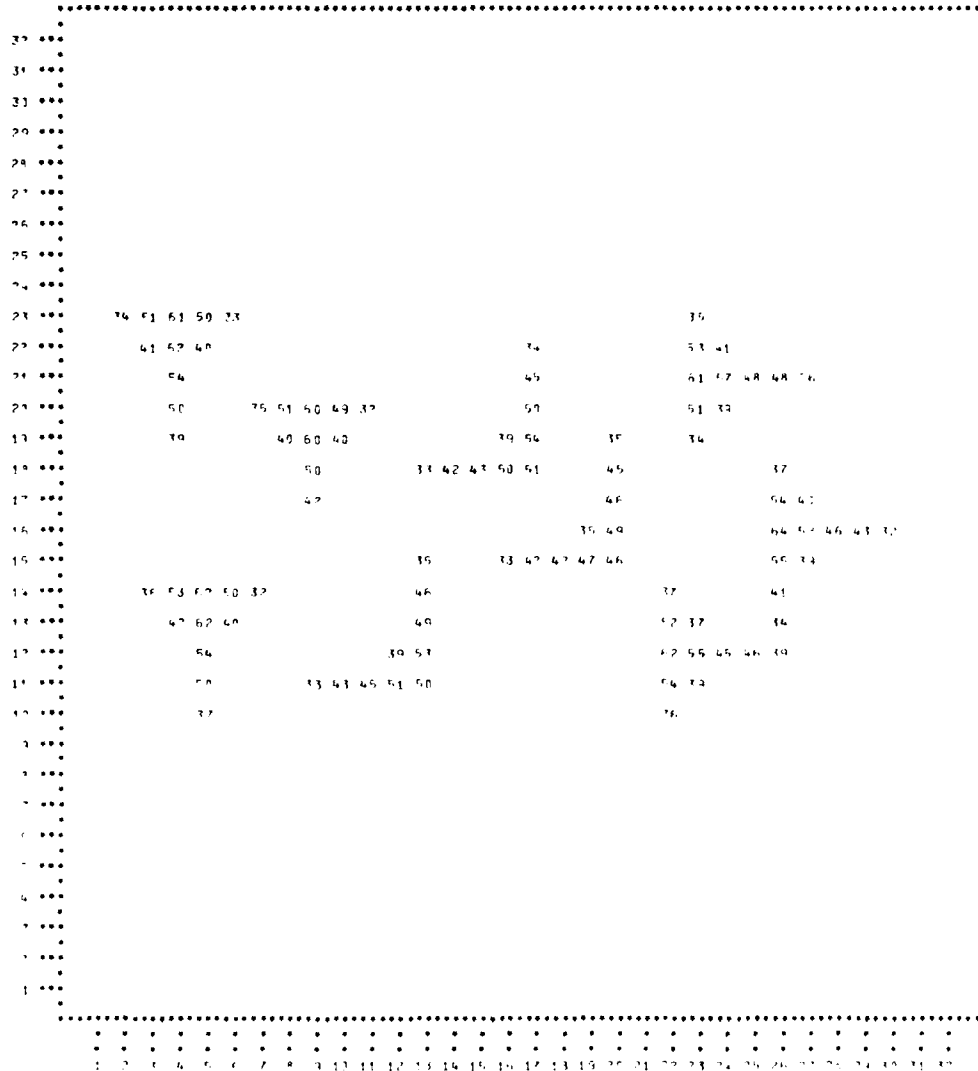


Figure 39. Numerical Printouts of the Filtered Arrays of Figure 37: (a) Original Array; (b) MTF Filtered Array. (Section 11.3.2) (cont.)

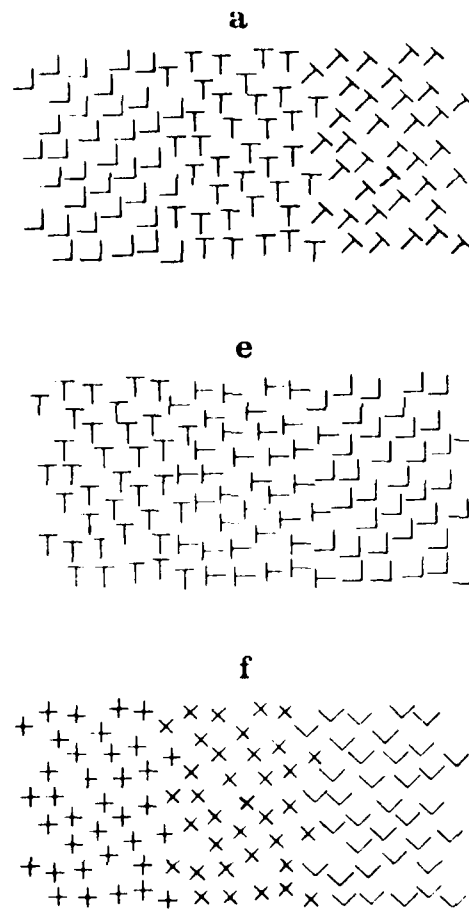


Figure 40. Examples of Letter Arrays Used in Beck's (1966b) Similarity Grouping Experiment. (Section 11.3.2)

(a)

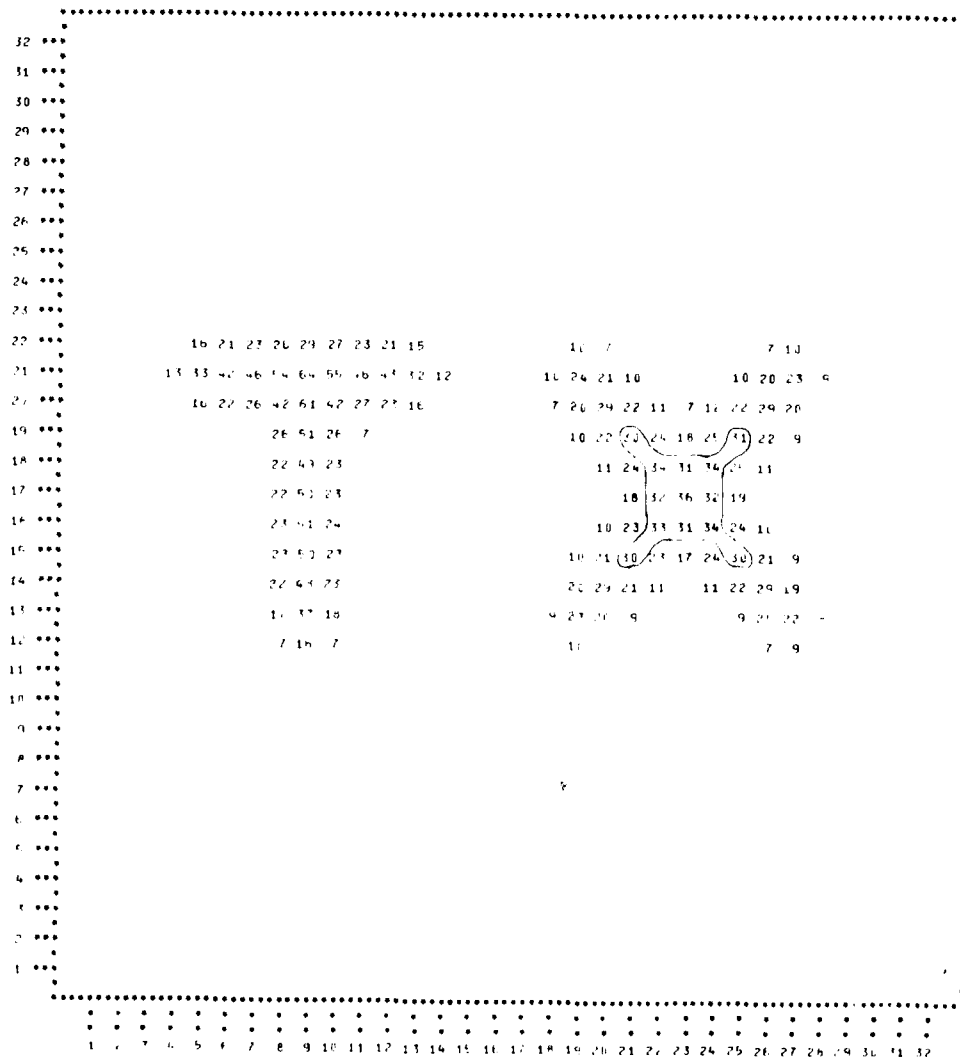


Figure 41. Numerical Printouts of MTF(H) Filtered Pairs of Letters: (a) T-X;  
 (b) T-Tilted T. (Section 11.3.3)



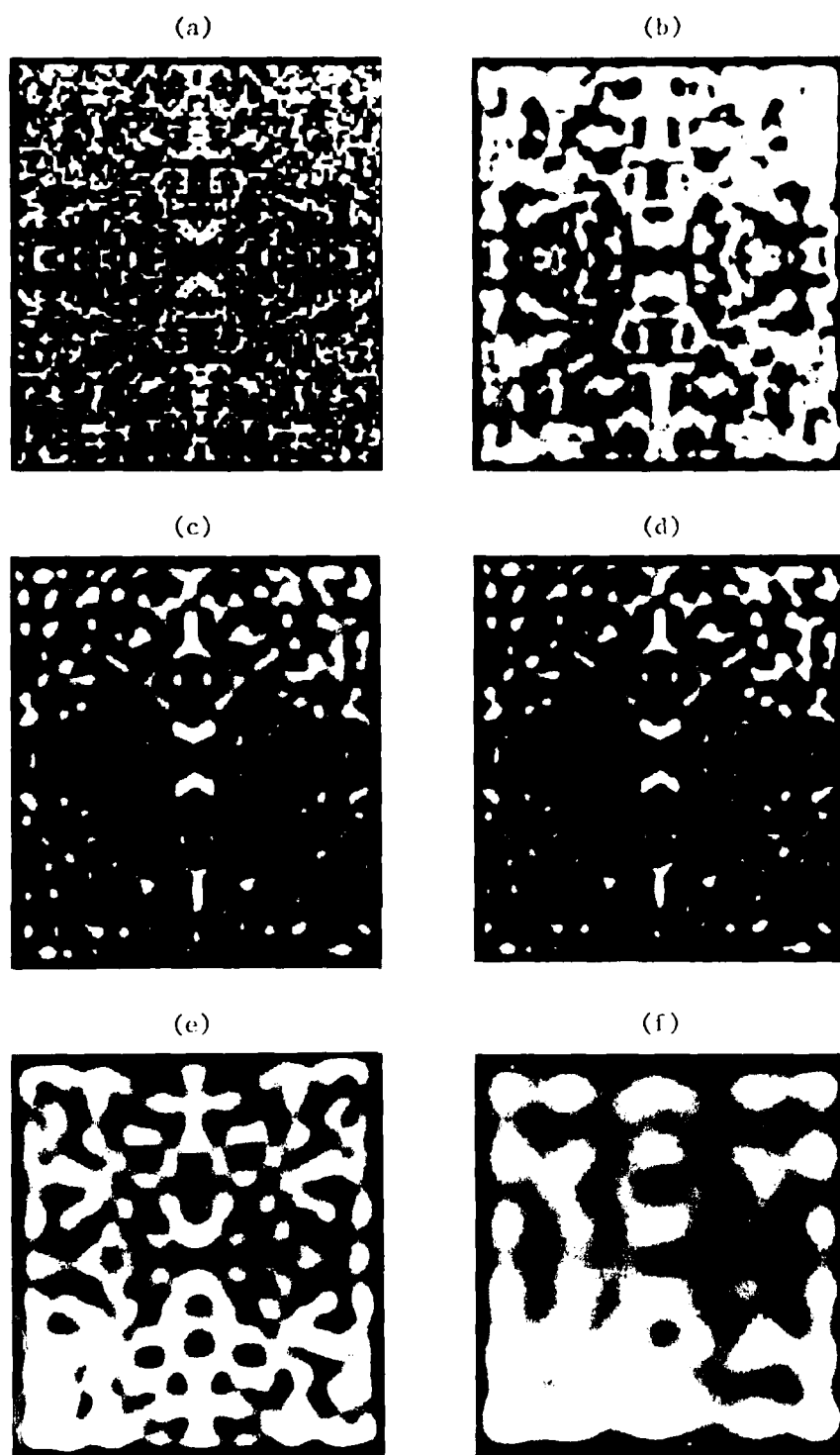


Figure 12. Isolating Form and Symmetry from a Random Dot Pattern:  
 (a) Original Pattern; (b) MTF Filtered Image; (c) Low-Pass (24  
 by 24) Filtered Image; (d) Image Created from the Upper 30  
 Percent of the Intensity Values of c; (e) Low-Pass (16 by 16)  
 Filtered Image; (f) Low-Pass (8 by 8) Filtered Image.  
 (Section 11.4.1)

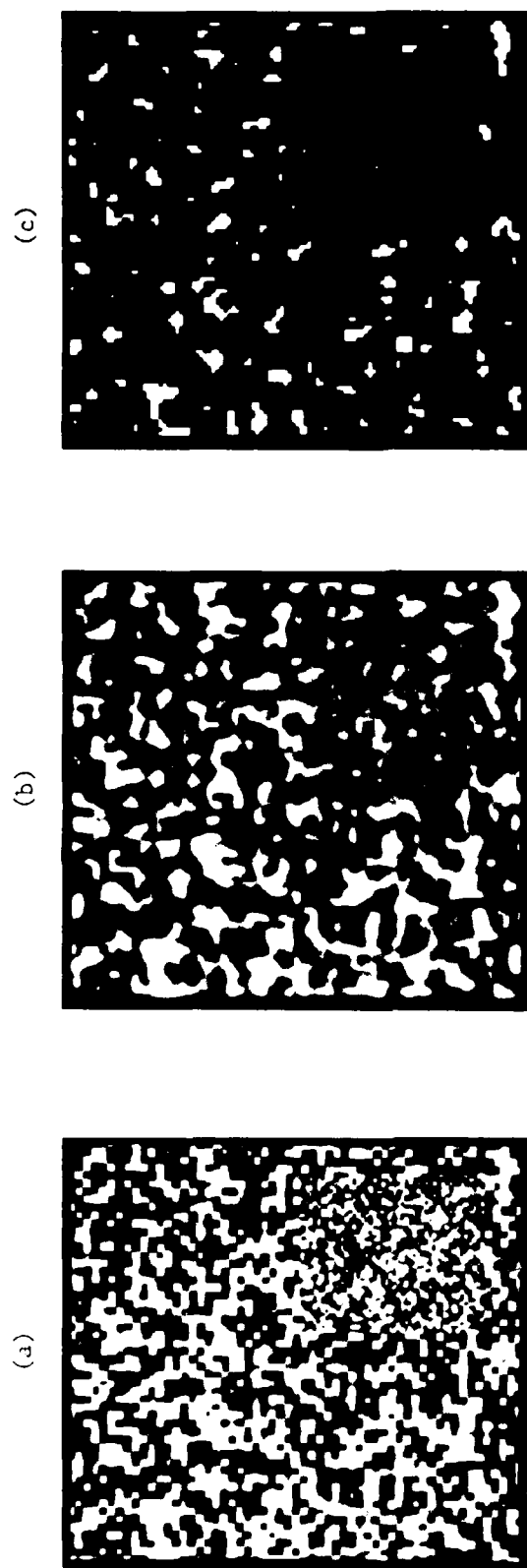


Figure 13. Isolating an Area of Different Size Objects in a Random Dot Pattern: (a) Original Pattern; (b) MTF Filtered Pattern; (c) Binary Pattern Created from the Upper 30 Percent of the Intensity Values of b. (Section 11.4.2)



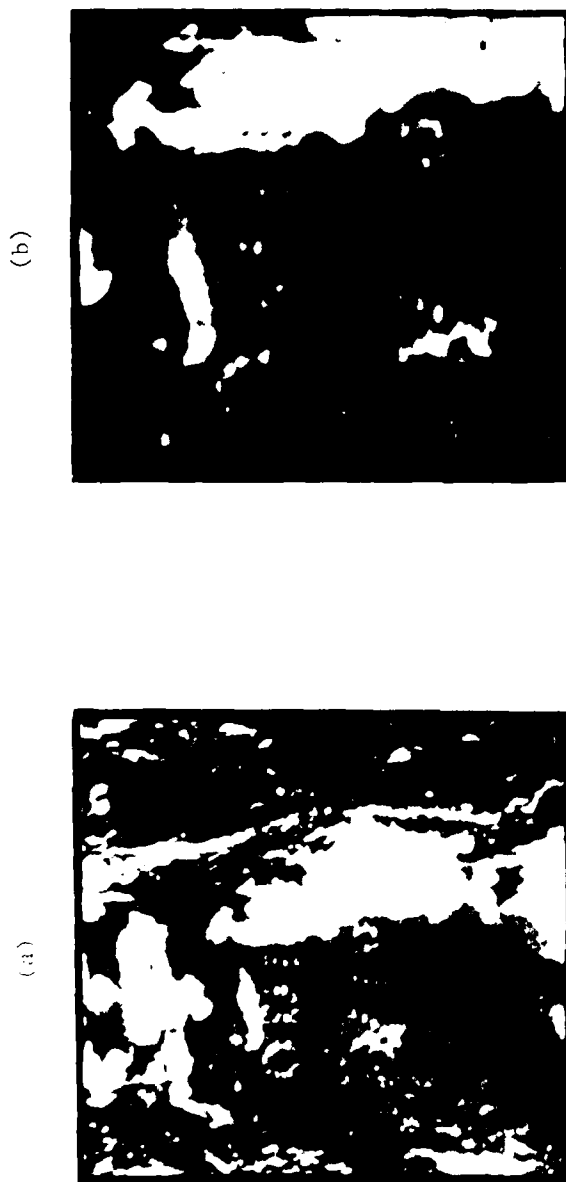


Figure 44. Analyzing a Complex Scene: (a) Original Scene; (b) Enlarged Area of Interest; (c) Log Transform of (b); (d) Low-Pass (24 by 24) Filtered Version of (c); (e) Figure (c) Digitized to 128 by 128 Pels with Approximately 30 Percent of the Lowest Picture Values Made White; (f) Removing the White Picture Values From (e); (g) MTF Filtered Dots; (h) Low-Pass (24 by 24) Filtered Dots. (Section 11.5)

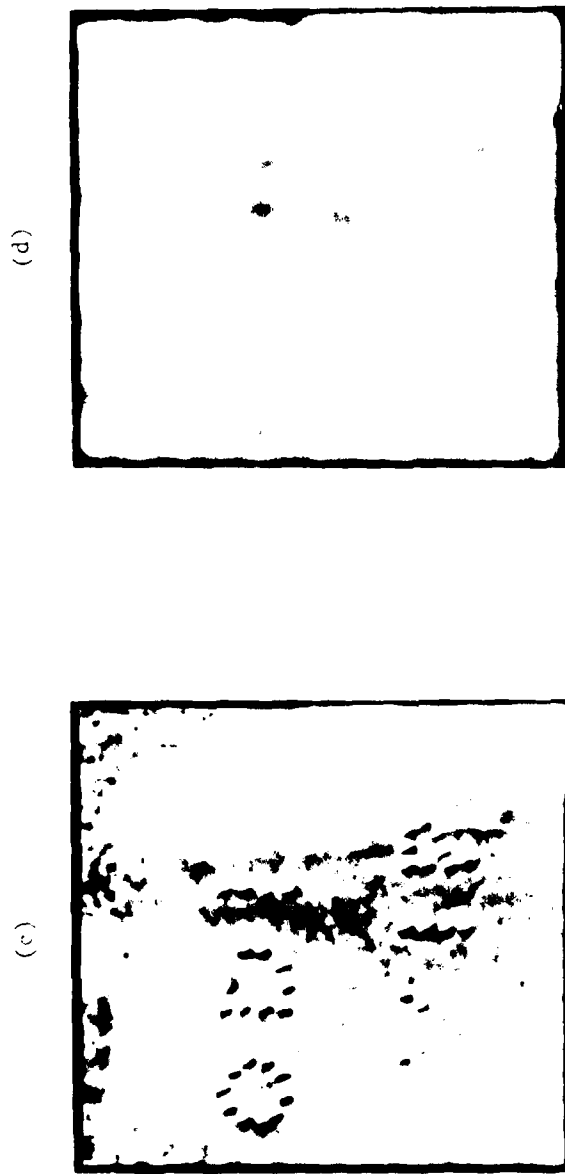


Figure 44. Analyzing a Complex Scene: (a) Original Scene; (b) Enlarged Area of Interest; (c) Log Transform of b; (d) Low-Pass (24 by 24) Filtered Version of c; (e) Figure c Digitized to 128 by 128 Pels with Approximately 30 Percent of the Lowest Picture Values Made White; (f) Removing the White Picture Values From c; (g) MTF Filtered Dots; (h) Low-Pass (24 by 24) Filtered Dots. (Section 11.5) (cont.)

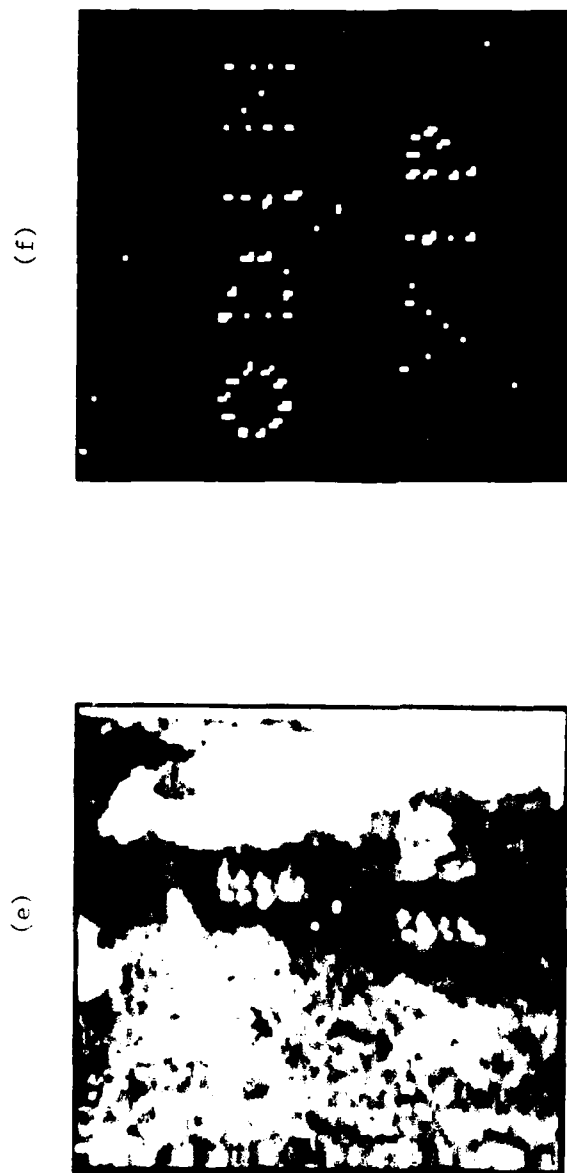


Figure 44. Analyzing a Complex Scene: (a) Original Scene; (b) Enlarged Area of Interest; (c) Log Transform of b; (d) Low-Pass (24 by 24) Filtered Version of c; (e) Figure c Digitized to 128 by 128 Pels with Approximately 30 Percent of the Lowest Picture Values Made White; (f) Removing the White Picture Values From c; (g) MTF Filtered Dots; (h) Low-Pass (24 by 24) Filtered Dots. (Section 11.5) (cont.)

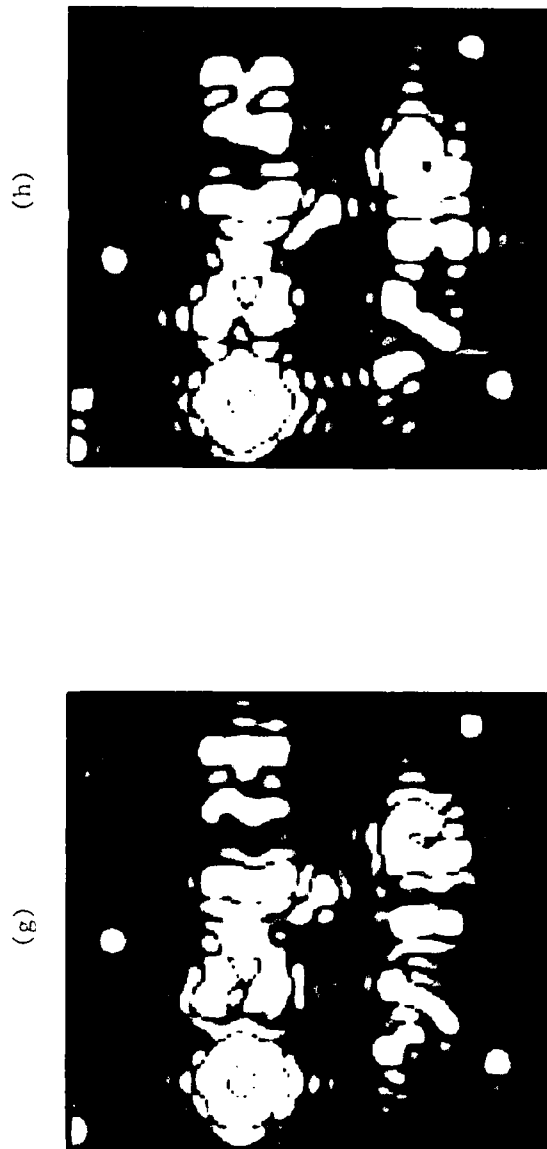


Figure 44. Analyzing a Complex Scene: (a) Original Scene; (b) Enlarged Area of Interest; (c) Log Transform of b; (d) Low-Pass (24 by 24) Filtered Version of c; (e) Figure c Digitized to 128 by 128 Pels with Approximately 30 Percent of the Lowest Picture Values Made White; (f) Removing the White Picture Values From e; (g) MTF Filtered Dots; (h) Low-Pass (24 by 24) Filtered Dots. (Section 11.5) (cont.)

(a)

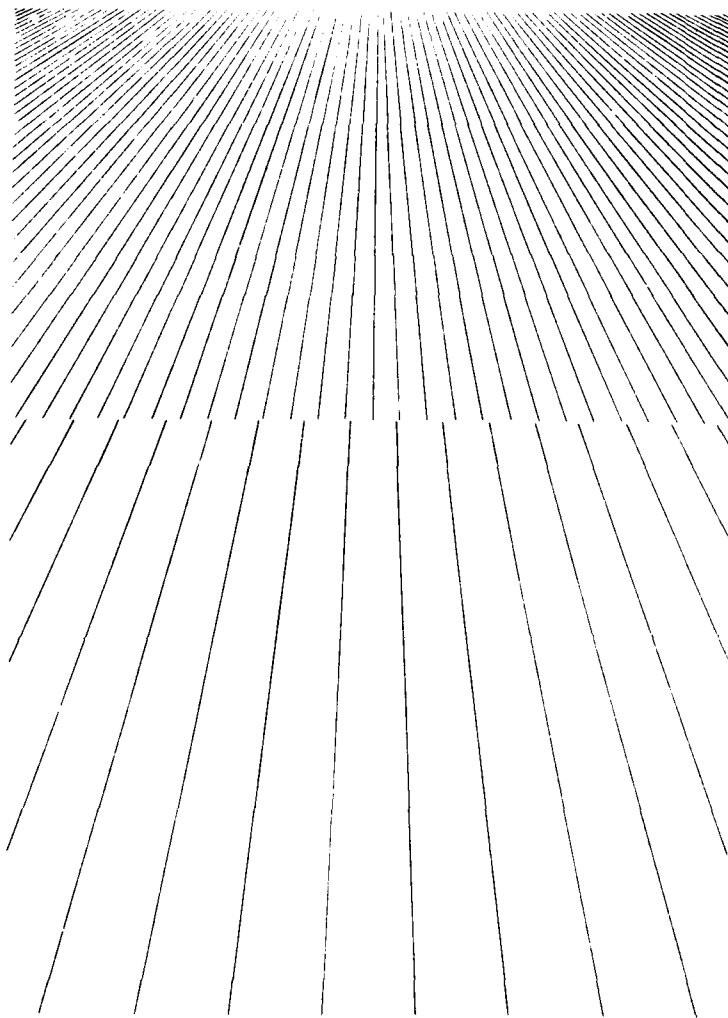


Figure 45. Filtering a Monocular Texture Gradient (from Gibson, 1950): (a) Original Texture Gradient; (b) Digitized Version of a; (c) MTF Filtered Texture Gradient. (Section 11.6)

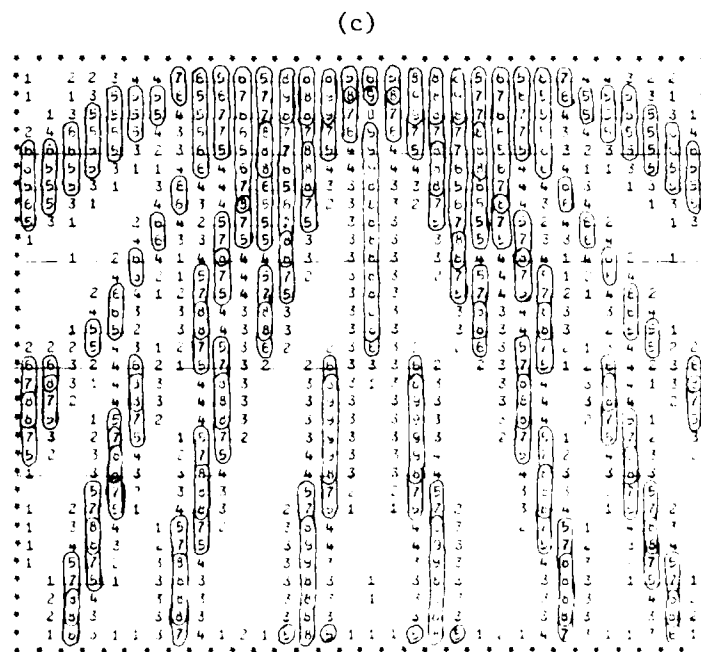
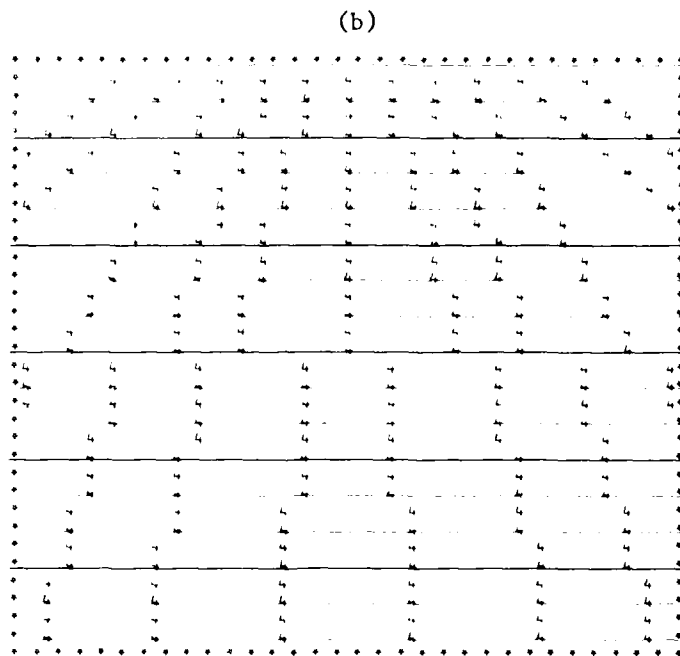


Figure 45. Filtering a Monocular Texture Gradient (from Gibson, 1950): (a) Original Texture Gradient; (b) Digitized Version of a; (c) MTF Filtered Texture Gradient. (Section 11.6) (cont.)

AD-A090 117

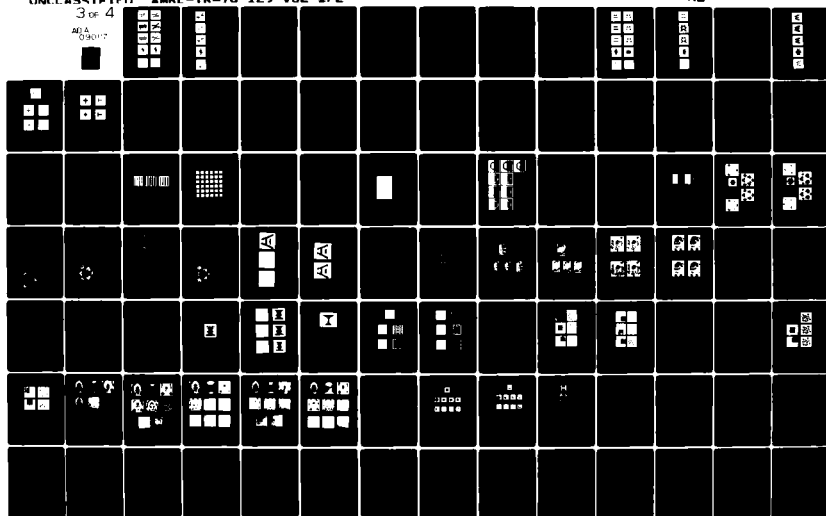
AIR FORCE AEROSPACE MEDICAL RESEARCH LAB WRIGHT-PATT--ETC F/6 6/16  
VISUAL INFORMATION PROCESSING BASED ON SPATIAL FILTERS CONSTRAI--ETC(U)  
DEC 78 A P GINSBURG  
AMRL-TR-78-129-VOL-1/2

UNCLASSIFIED

3 of 4

ALA  
03017

ML



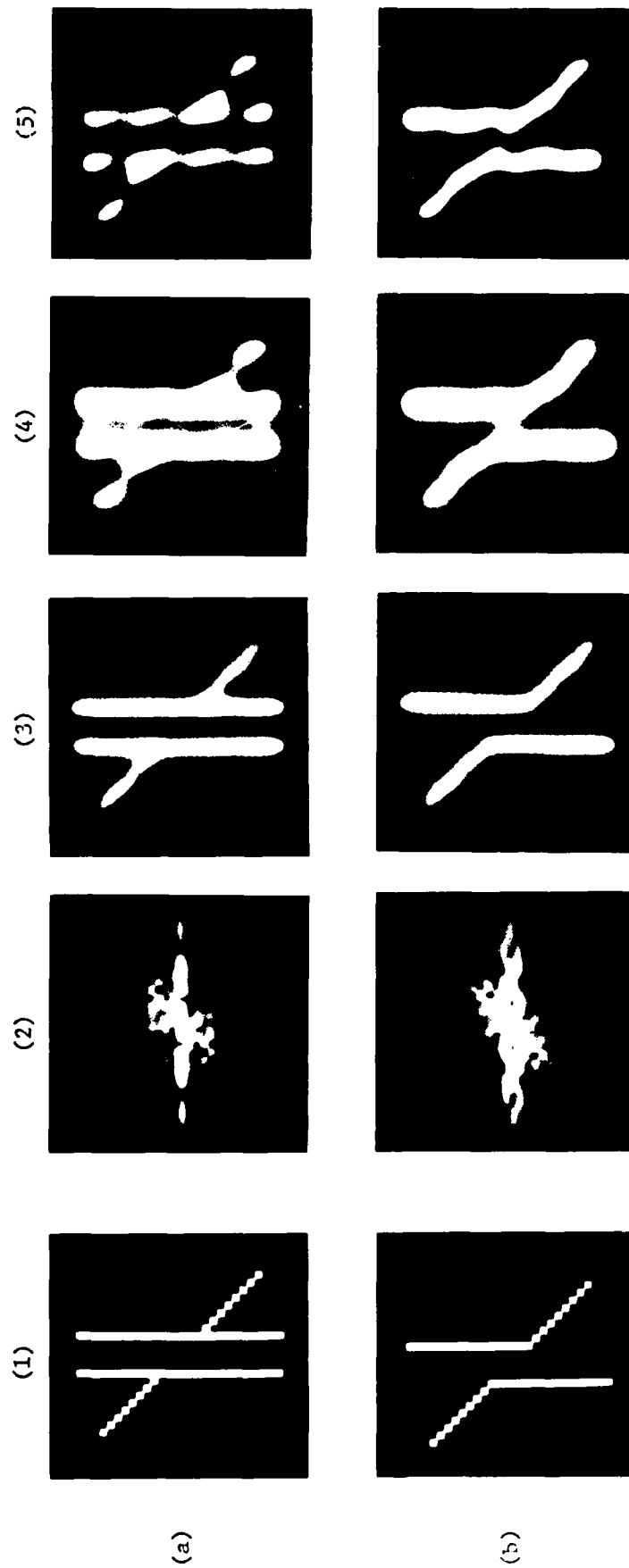


Figure 46. The Poggendorf Illusion: (a) Standard Illusion; (b) Obtuse Angles Only Illusion; (c) Acute Angles Only Illusion; (1) Original Illusions; (2) MTF Filtered Magnitude Spectra; (3) MTF Filtered Illusions; (4) MTF (5 by 5) L Filtered Illusions; (5) Low-Pass (5 by 5) Filtered Illusions. (Section 12.2)



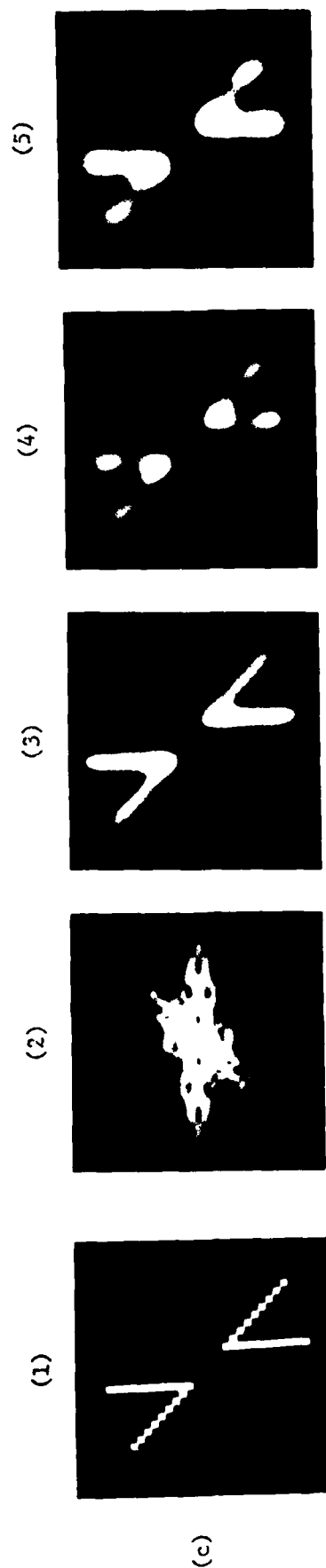


Figure 46. The Poggendorff Illusion: (a) Standard Illusion; (b) Obtuse Angles Only Illusion; (c) Acute Angles Only Illusion; (1) Original Illusions; (2) MTF Filtered Magnitude Spectra; (3) MTF Filtered Illusions; (4) MTF(5 by 5)L Filtered Illusions; (5) Low-Pass (5 by 5) Filtered Illusions. (Section 12.2) (cont.)

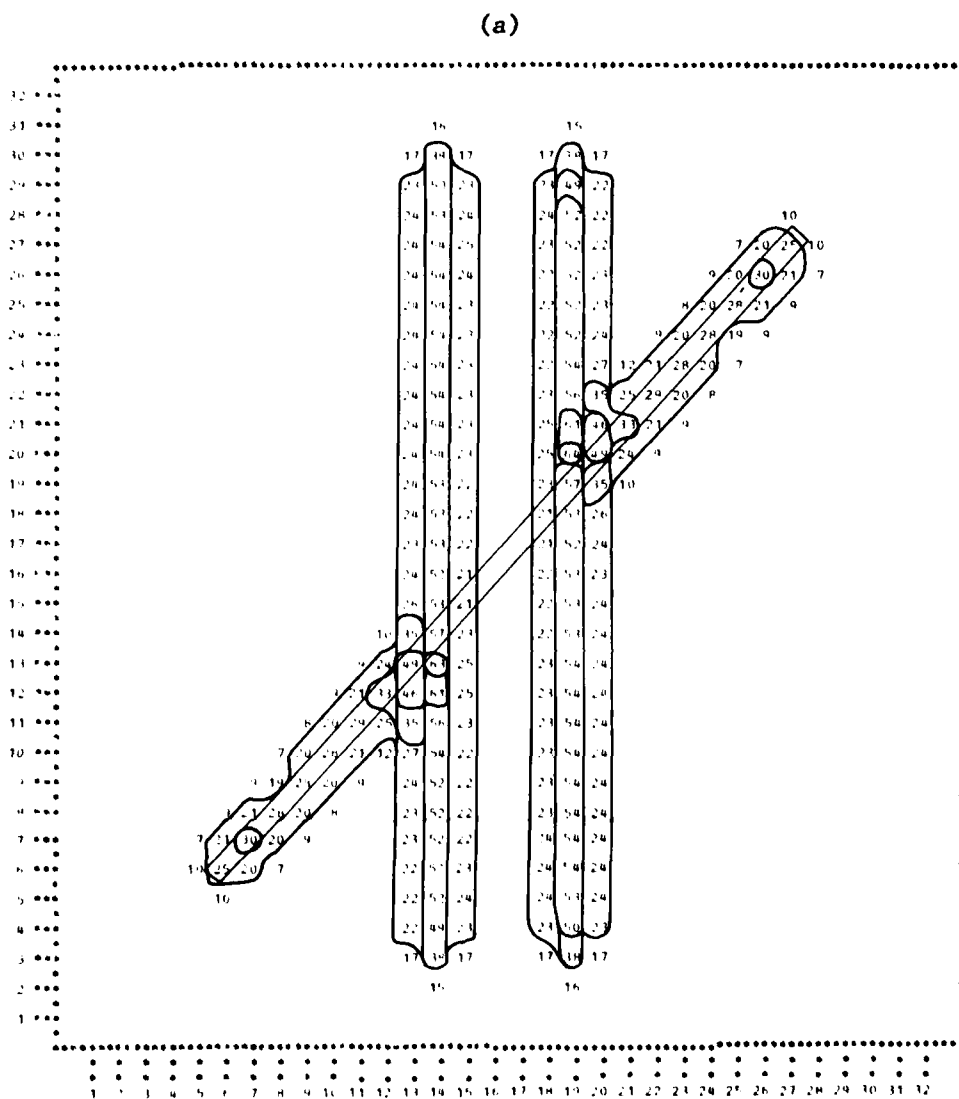


Figure 47. Numerical Printouts of the Filtered Poggendorff Illusion: (a) MTF Filtered Illusion; (b) MTF (5 by 5) Filtered Illusion; (c) Inverse MTF ( $MTF^{-1}$ ) Filtered Illusion. (Section 12.2.1)

(b)

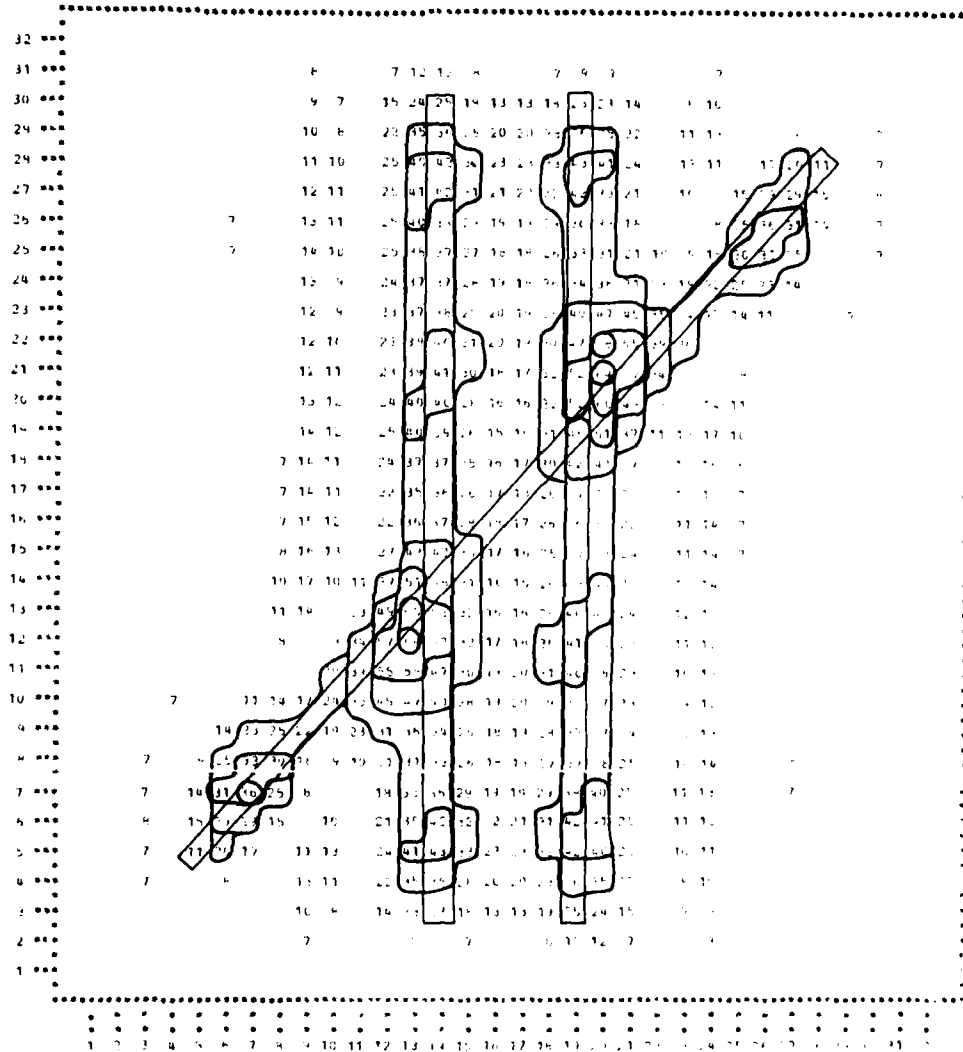


Figure 47. Numerical Printouts of the Filtered Poggendorff Illusion: (a) MTF Filtered Illusion; (b) MTF (5 by 5) Filtered Illusion; (c) Inverse MTF (MTF-1) Filtered Illusion. (Section 12.2.1) (cont.)

(c)

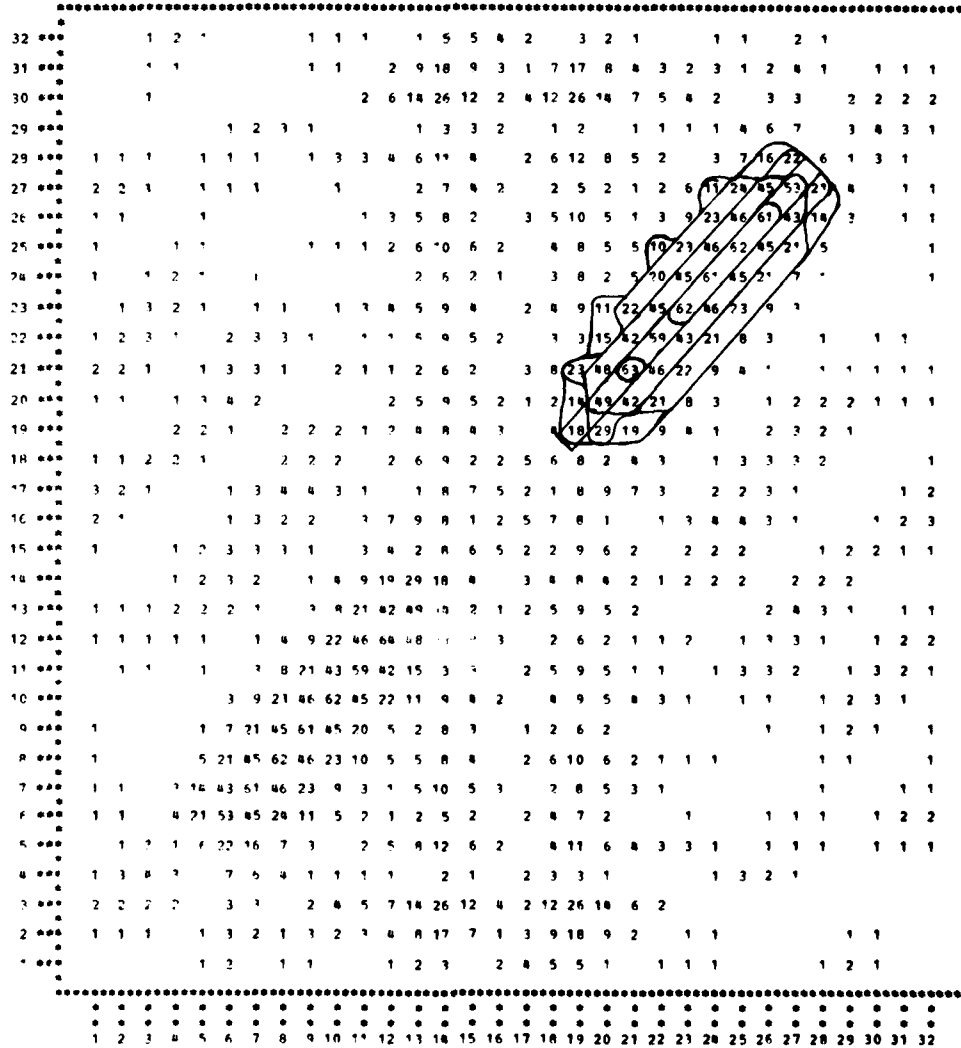


Figure 47. Numerical Printouts of the Filtered Poggendorff Illusion: (a) MTF Filtered Illusion; (b) MTF (5 by 5) Filtered Illusion; (c) Inverse MTF ( $MTF^{-1}$ ) Filtered Illusion. (Section 12.2.1) (cont.)

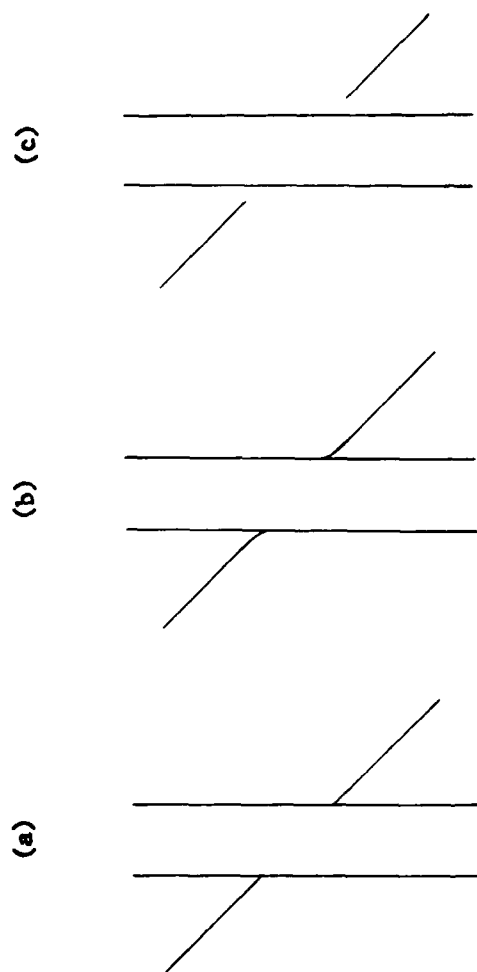


Figure 48. Correcting the Poggendorff Illusion: (a) Original Illusion; (b) "Corrected" Illusion; (c) Variation of the Poggendorff Illusion. (Section 12.2.1)

(a)

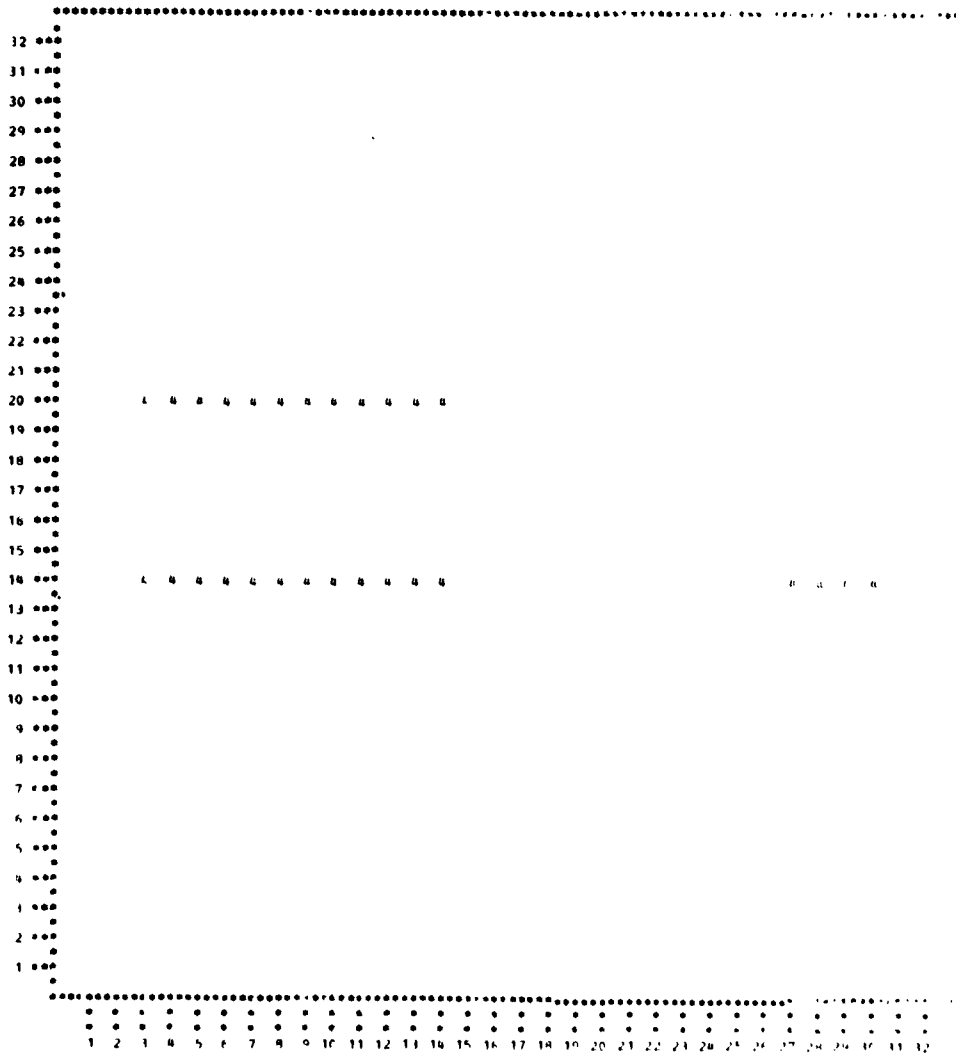


Figure 49. Numerical Printouts of an Illusion Due to Error in Aligning Edges: (a) Original Illusion; (b) MTF Filtered Illusion. (Section 12.2.2)

(b)

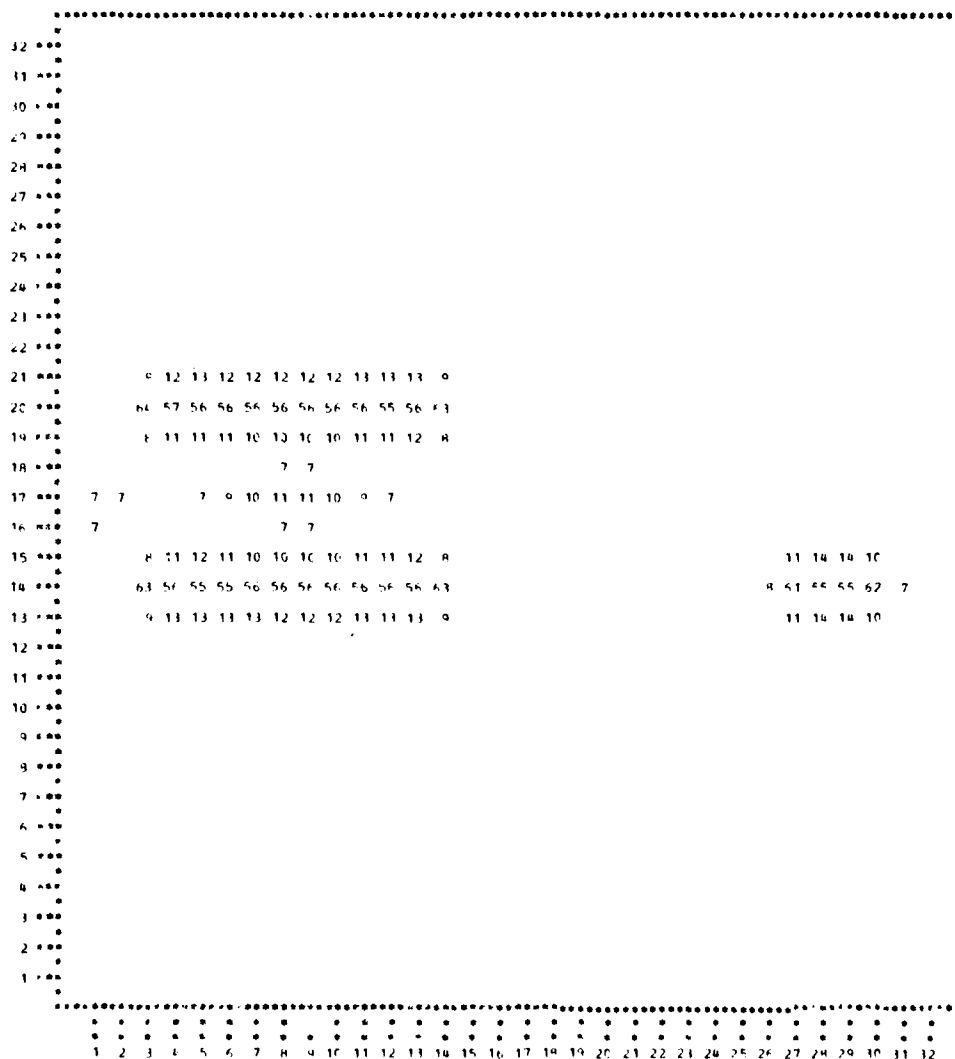


Figure 49. Numerical Printouts of an Illusion Due to Error in Aligning Edges: (a) Original Illusion; (b) MTF Filtered Illusion. (Section 12.2.2) (cont.)

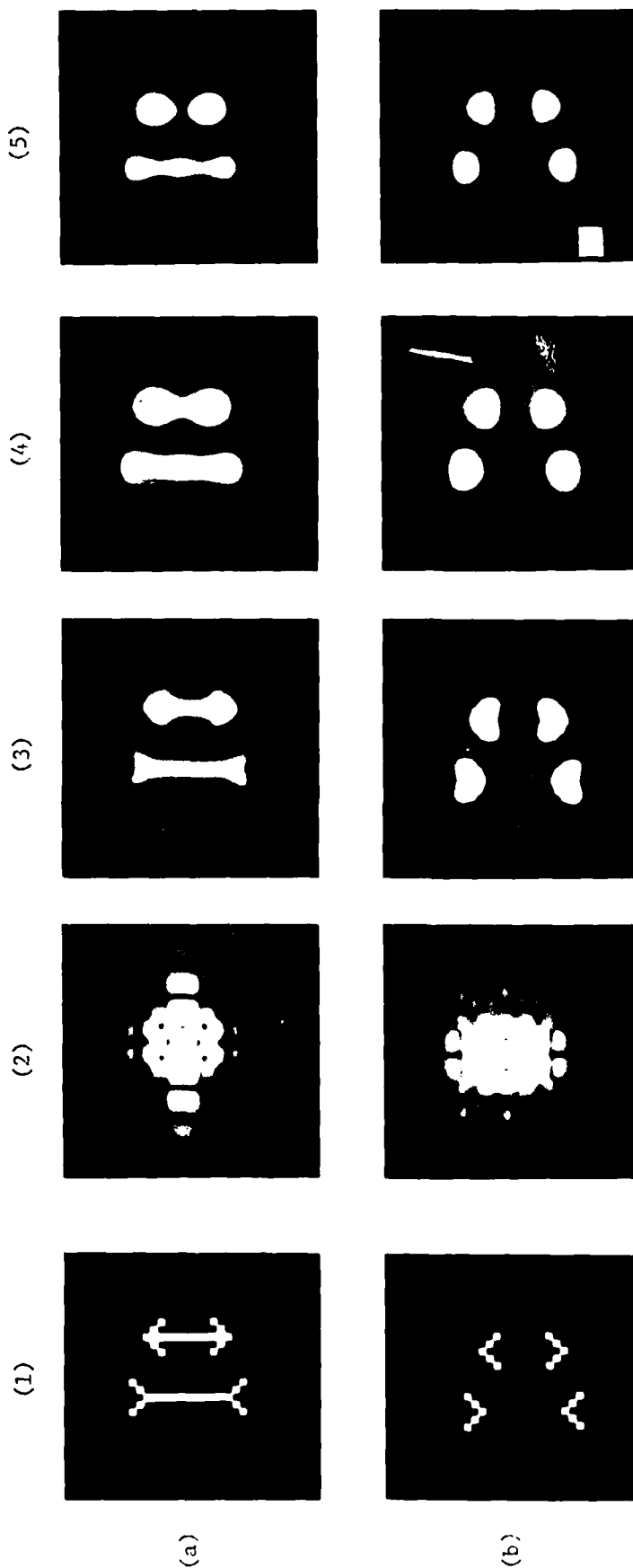


Figure 50. Müller-Lyer Illusions: (a) Standard Müller-Lyer Illusion; (b) Müller-Lyer Illusion with Fins Only; (c) Müller-Lyer Illusion with Unequal Size Fins Going in the Same Direction; (1) Original Illusions; (2) MTF Filtered Magnitude Spectra; (3) MTF Filtered Illusions; (4) MTF (5 by 5) L Filtered Illusions; (5) Low-Pass (5 by 5) Filtered Illusions. (Section 12.3.1)



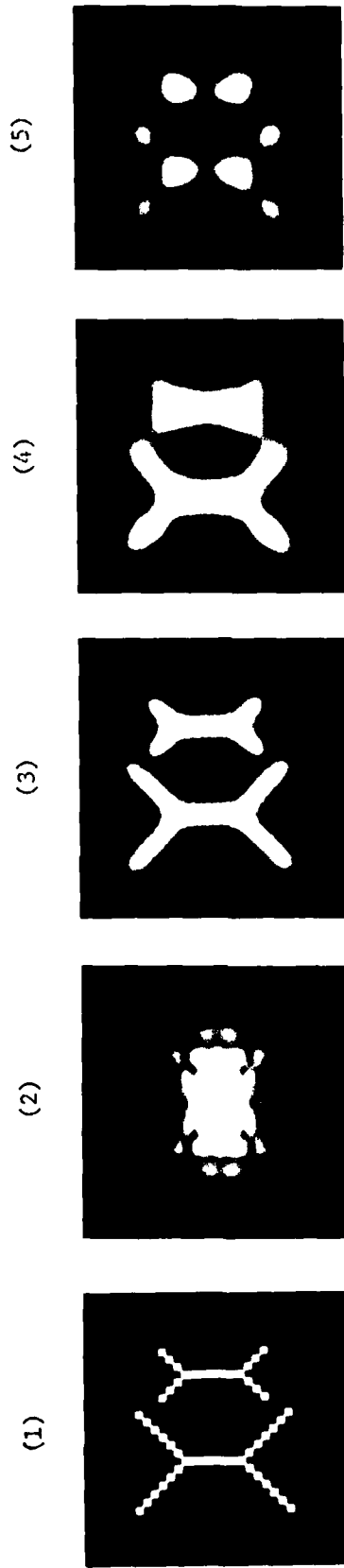


Figure 50. Müller-Lyer Illusions: (a) Standard Müller-Lyer Illusion; (b) Müller-Lyer Illusion with Fins Only; (c) Müller-Lyer Illusion with Unequal Size Fins Going in the Same Direction; (1) Original Illusions; (2) MTF Filtered Magnitude Spectra; (3) MTF Filtered Illusions; (4) MTF (5 by 5) Low-Pass (5 by 5) Filtered Illusions; (5) Filtered Illusions. (Section 12.3.1) (cont.)

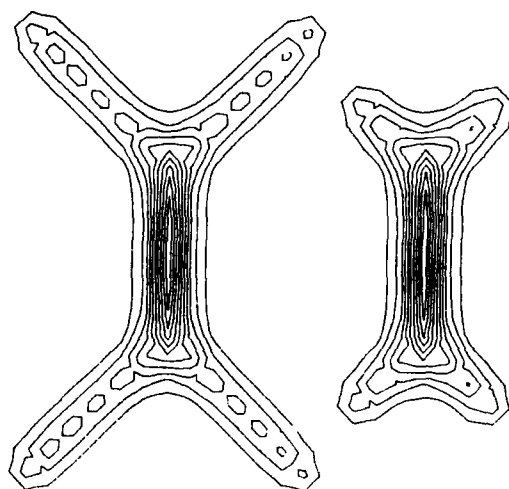


Figure 51. Contour Plot of MTF Filtered Müller-Lyer Illusion of Figure 50,c,3. (Section 12.3.1)

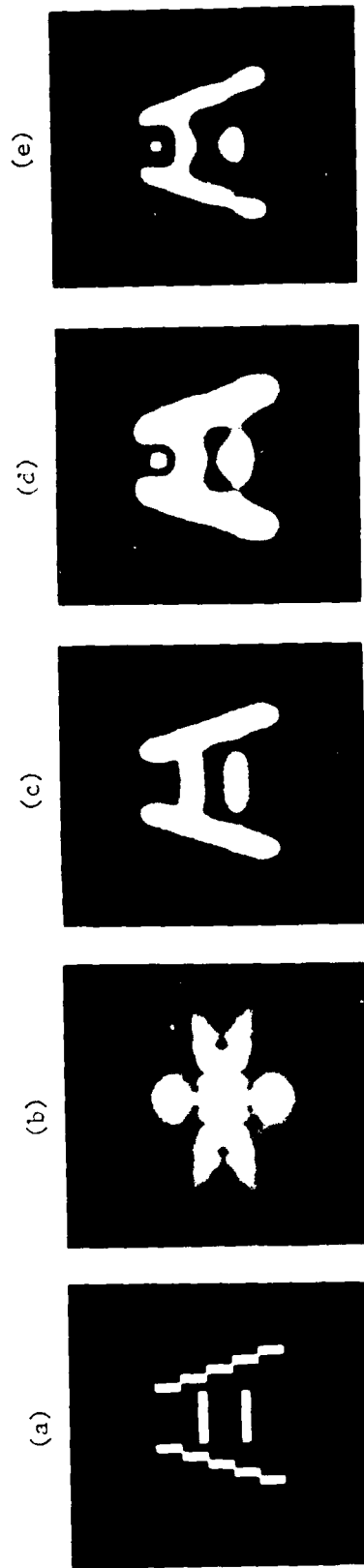


Figure 5.2. The Ponzo Illusion: (a) Original Illusion; (b) MTF Filtered Magnitude Spectrum; (c) MTF Filtered Illusion; (d) MTF (6 by 6) Filtered Illusion; (e) Low-Pass (6 by 6) Filtered Illusion. (Section 12.3.2)

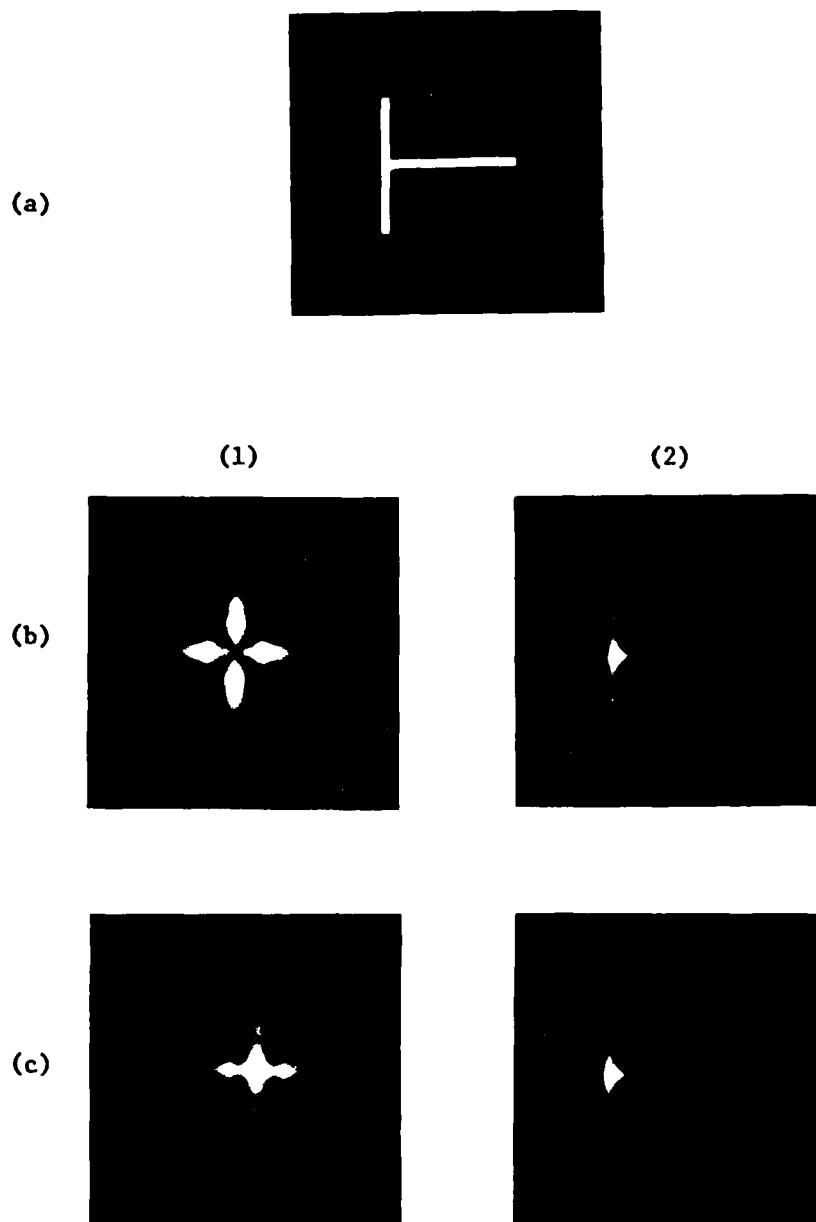


Figure 53. The 90 Degree Configuration of the Horizontal-Vertical Line Illusion:  
 (a) Original Illusion; (b) MTF(L) Filtered Images; (c) MTF(H) Filtered  
 Images; (d) MTF(H)L Filtered Images; (e) MTF(H) (6 by 6) Filtered  
 Images; (1) Filtered Magnitude Spectra; (2) Filtered Illusions.  
 (Section 12.3.3)

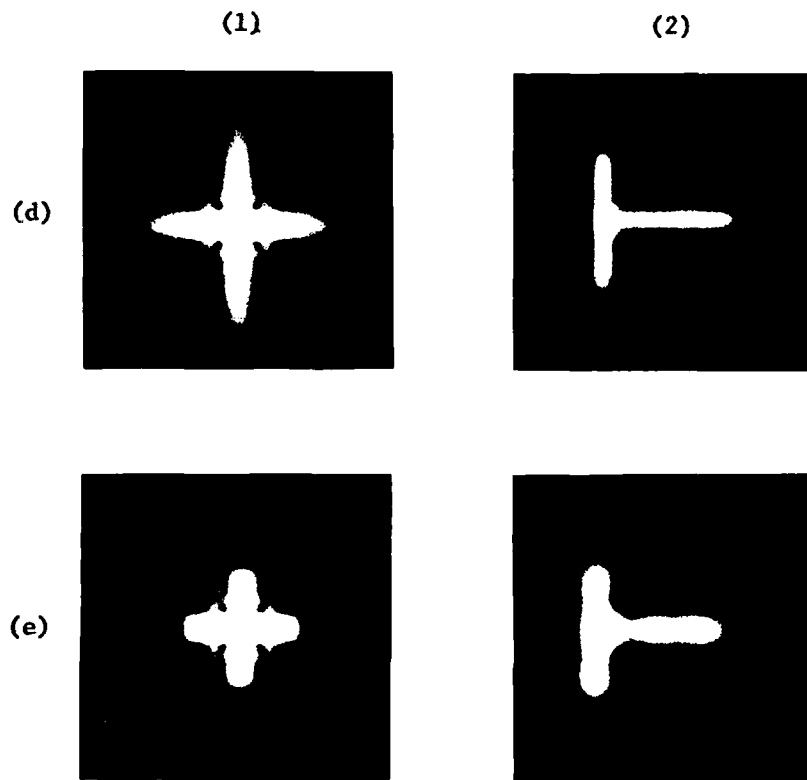
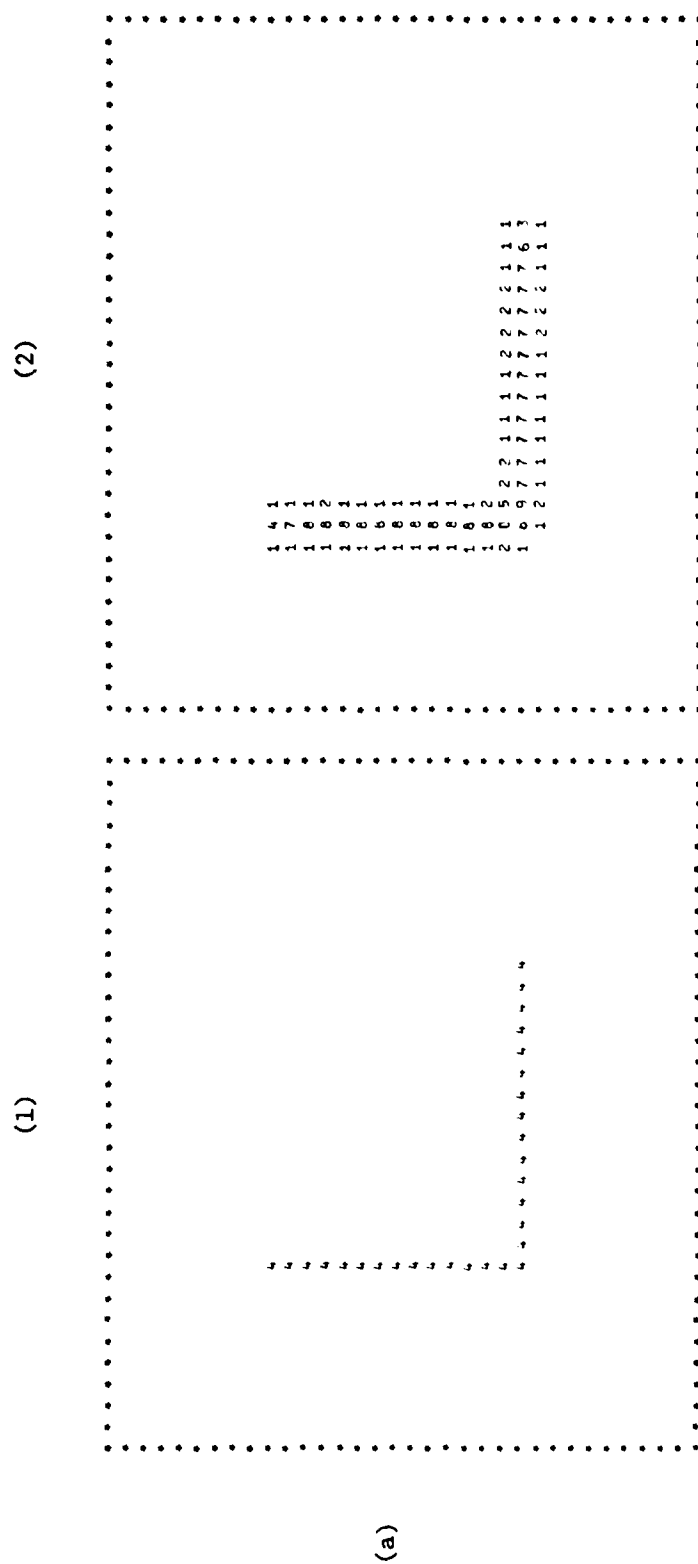


Figure 53. The 90 Degree Configuration of the Horizontal-Vertical Line Illusion: (a) Original Illusion; (b) MTF(L) Filtered Images; (c) MTF(H) Filtered Images; (d) MTF(H)L Filtered Images; (e) MTF(H) (6 by 6) Filtered Images; (1) Filtered Magnitude Spectra; (2) Filtered Illusions. (Section 12.3.3) (cont.)

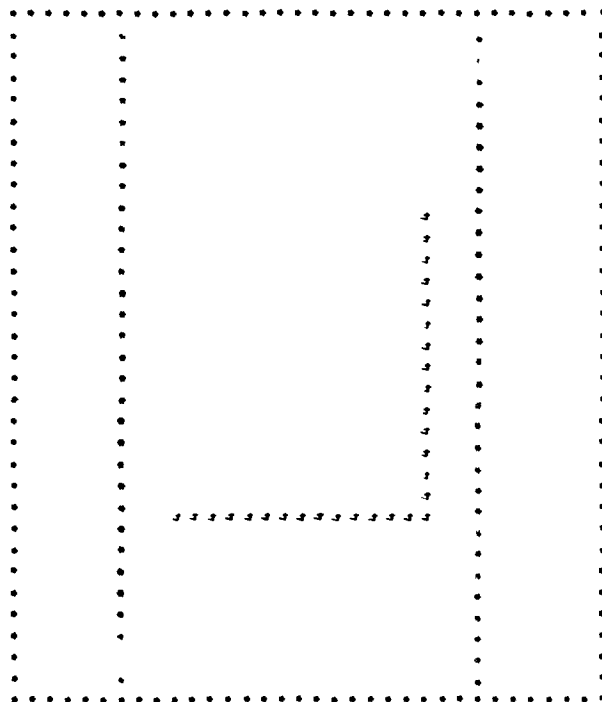
**Figure 54. Numerical Printouts of Two Configurations of the Horizontal-Vertical Line Illusion: (a) Original Illusion; (b) Illusion Rotated 90 Degrees; (1) Original Illusions; (2) MTF Filtered Illusions. (Section 12.3.3)**







(1)



(b)

(2)

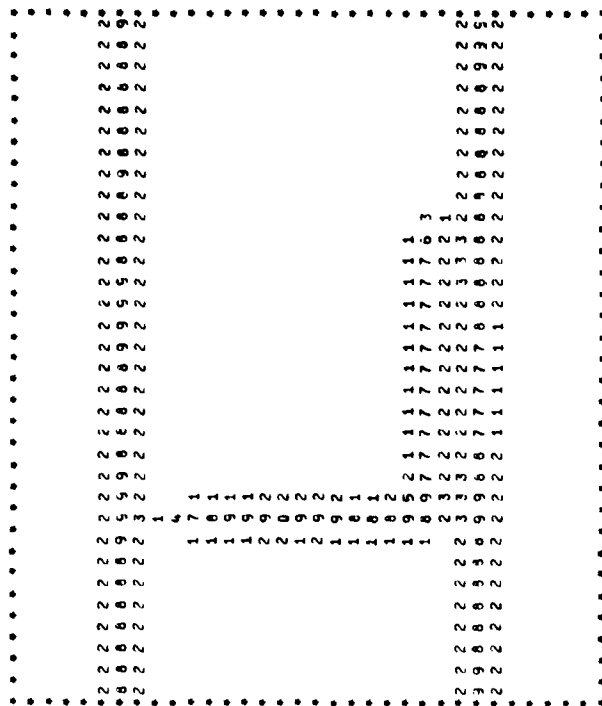
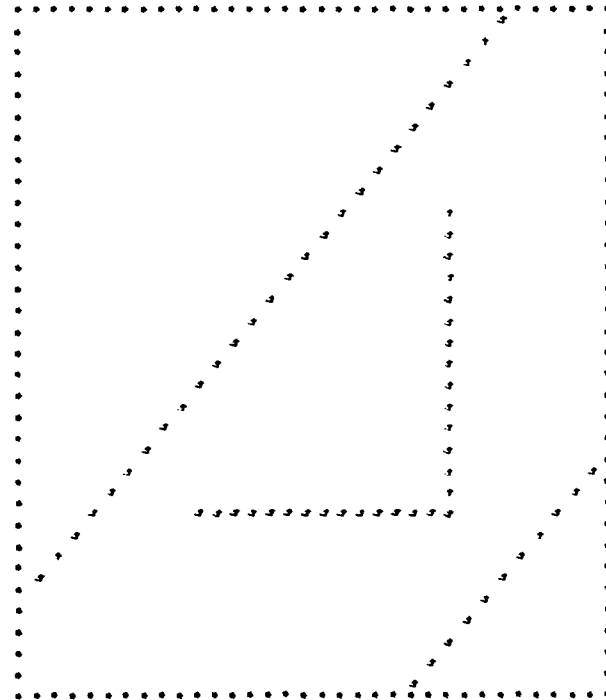
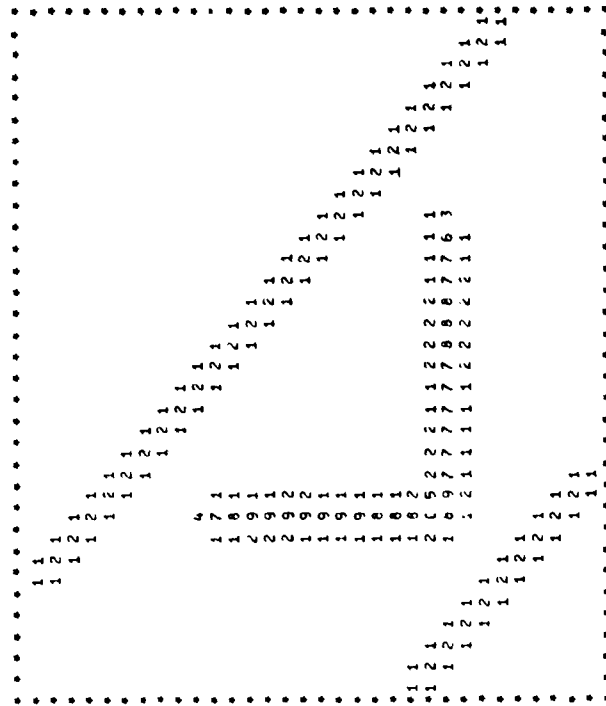


Figure 55. Numerical Printouts of the L Configuration of the Horizontal-Vertical Line Illusion with Variations of a Frame:  
(a) Configuration without a Frame; (b) Configuration with a Frame; (c) Configuration Rotated within a Frame;  
(1) Original Configurations; (2) MTF Filtered Configurations. (Section 12.3.3) (cont.)

(1)



(2)



(c)

Figure 55. Numerical Printouts of the L Configuration of the Horizontal-Vertical Line Illusion with Variations of a Frame:  
(a) Configuration without a Frame; (b) Configuration with a Frame; (c) Configuration Rotated within a Frame;  
(1) Original Configurations; (2) MTF Filtered Configurations. (Section 12.3.3) (cont.)

(a)

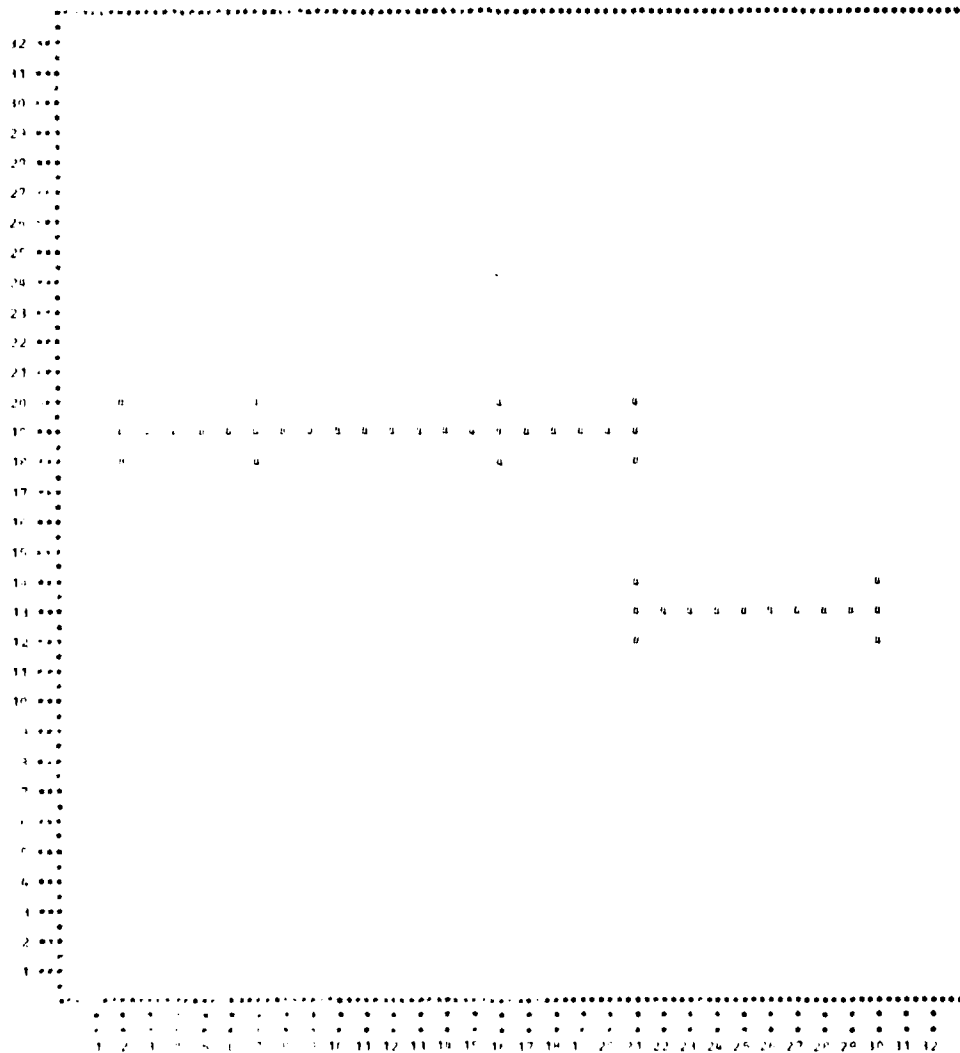


Figure 56. Simple Line Illusions: (a) Illusion One; (b) Illusion Two;  
(c) Numerical Printout of MTF Filtered Illusion One;  
(d) Numerical Printout of MTF Filtered Illusion Two;  
(e) Iso-Contour Plots of MTF Filtered Illusion One;  
(f) Iso-Contour Plots of MTF Filtered Illusion Two.  
(Section 12.3.4)

(b)

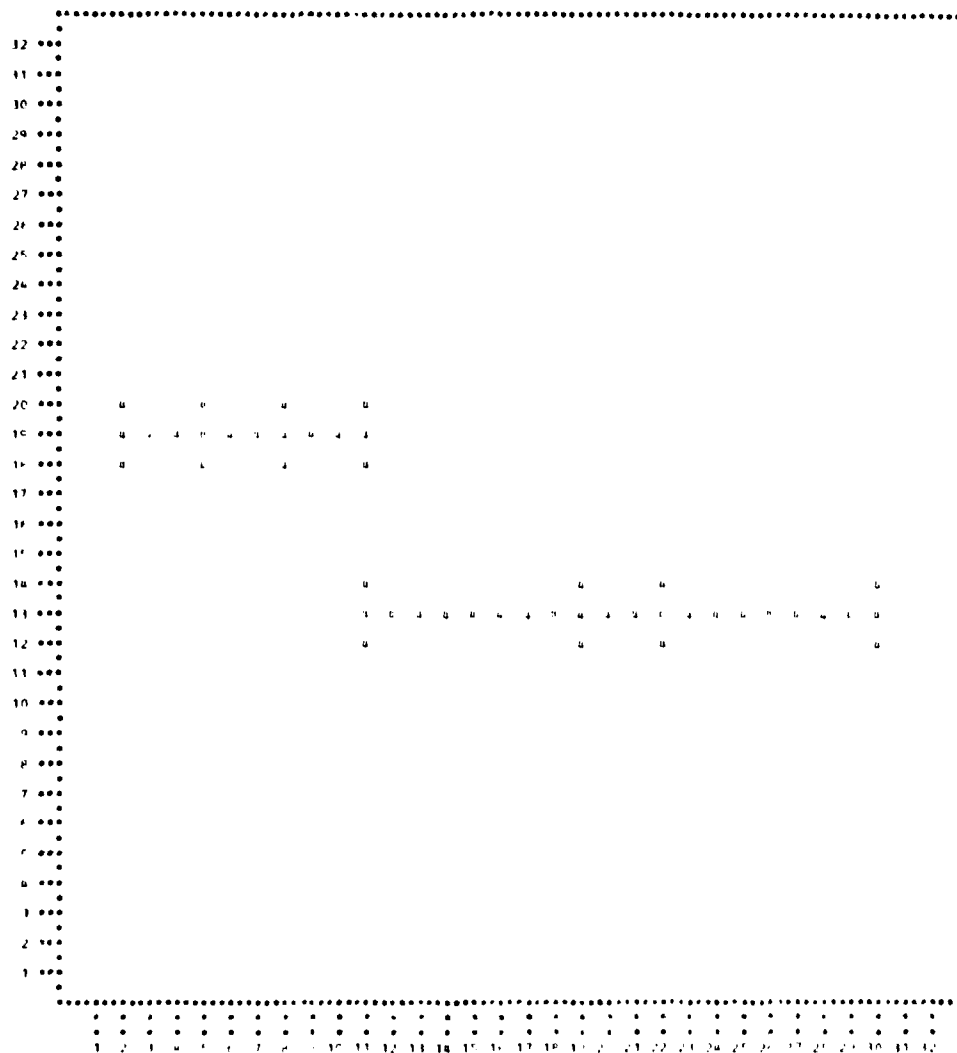


Figure 56. Simple Line Illusions: (a) Illusion One; (b) Illusion Two;  
 (c) Numerical Printout of MTF Filtered Illusion One;  
 (d) Numerical Printout of MTF Filtered Illusion Two;  
 (e) Iso-Contour Plots of MTF Filtered Illusion One;  
 (f) Iso-Contour Plots of MTF Filtered Illusion Two.  
 (Section 12.3.4) (cont.)

(c)

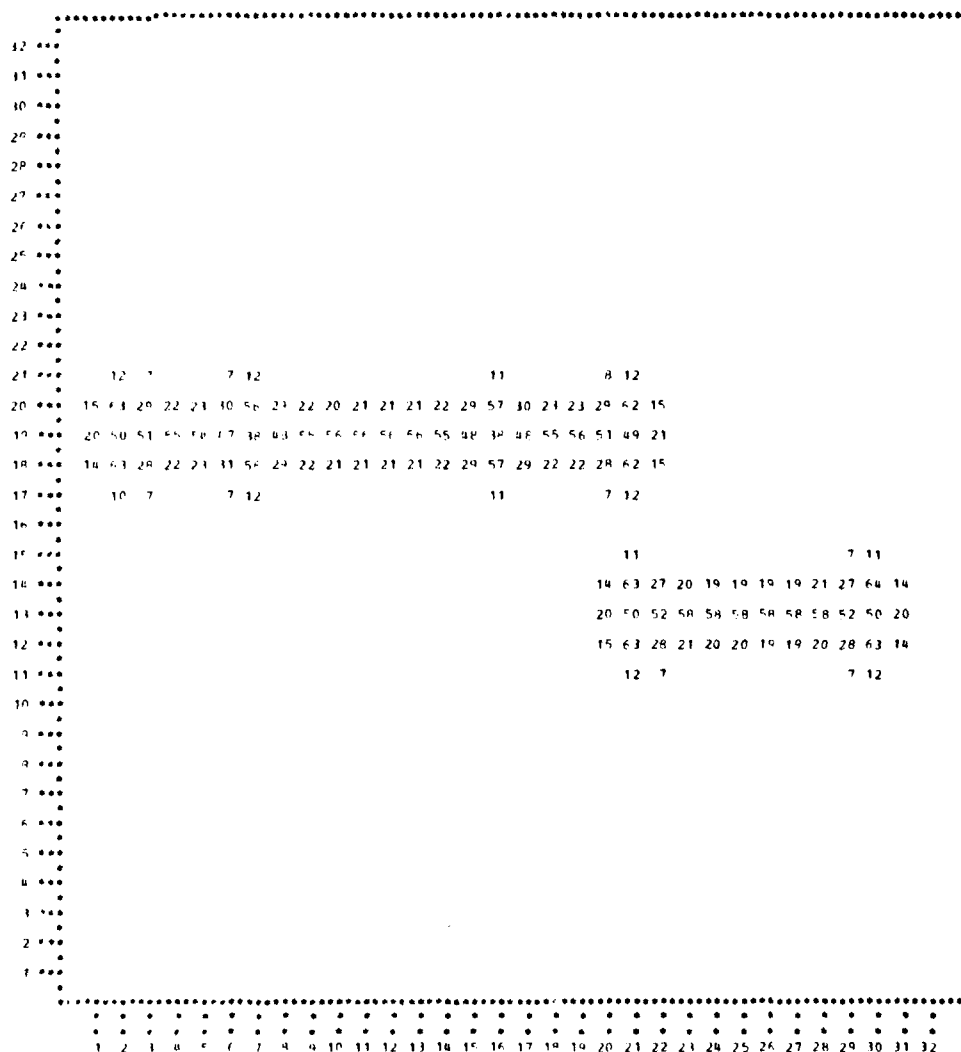
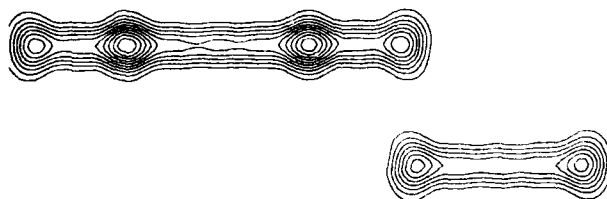


Figure 36. Simple Line Illusions: (a) Illusion One; (b) Illusion Two; (c) Numerical Printout of MTF Filtered Illusion One; (d) Numerical Printout of MTF Filtered Illusion Two; (e) Iso-Contour Plots of MTF Filtered Illusion One; (f) Iso-Contour Plots of MTF Filtered Illusion Two. (Section 12.3.4) (cont.)

[illegible]

209

(e)



(f)

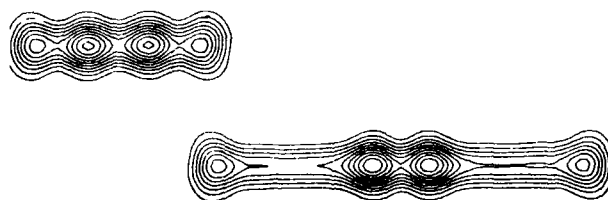


**Figure 56. Simple Line Illusions: (a) Illusion One; (b) Illusion Two;  
(c) Numerical Printout of MTF Filtered Illusion One;  
(d) Numerical Printout of MTF Filtered Illusion Two;  
(e) Iso-Contour Plots of MTF Filtered Illusion One;  
(f) Iso-Contour Plots of MTF Filtered Illusion Two.  
(Section 12.3.4) (cont.)**





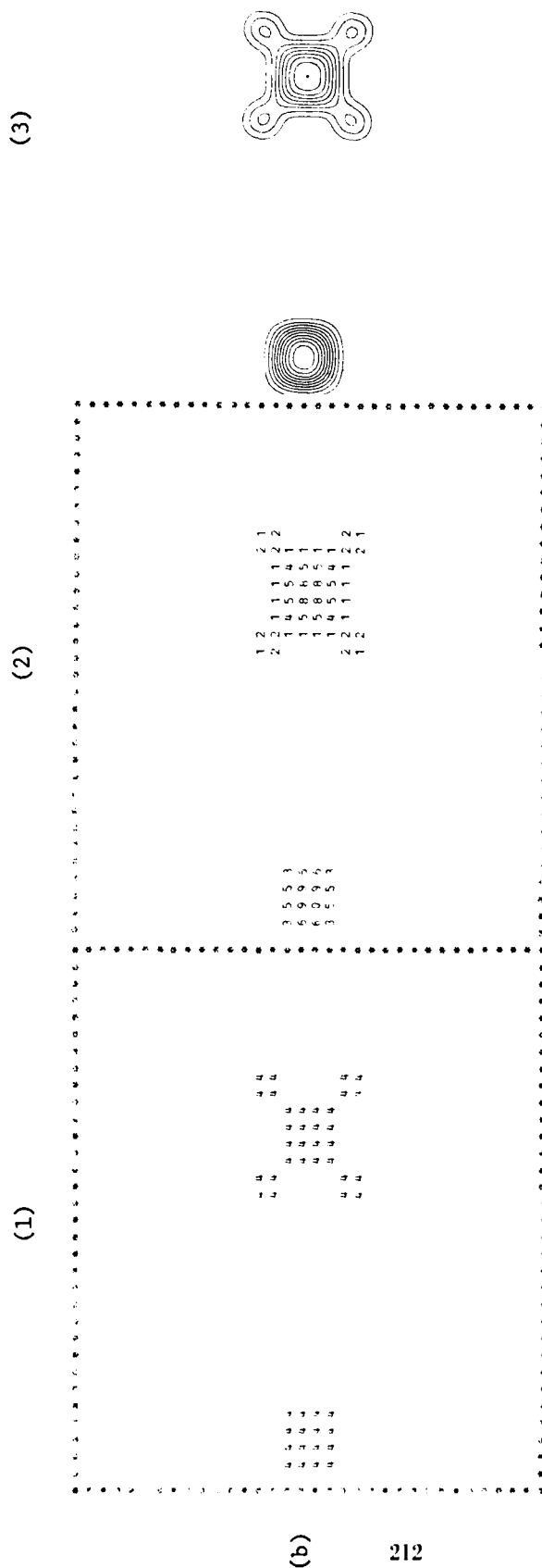


Figure 57. Numerical Printouts and Contour Plots of the MTF Filtered Titchner Illusion: (a) Large Square Surround; (b) Small Square Surround; (1) Original Illusions; (2) MTF Filtered Illusions; (3) Contour Plot of Illusions. (Section 12.4.1) (cont.)

(a)

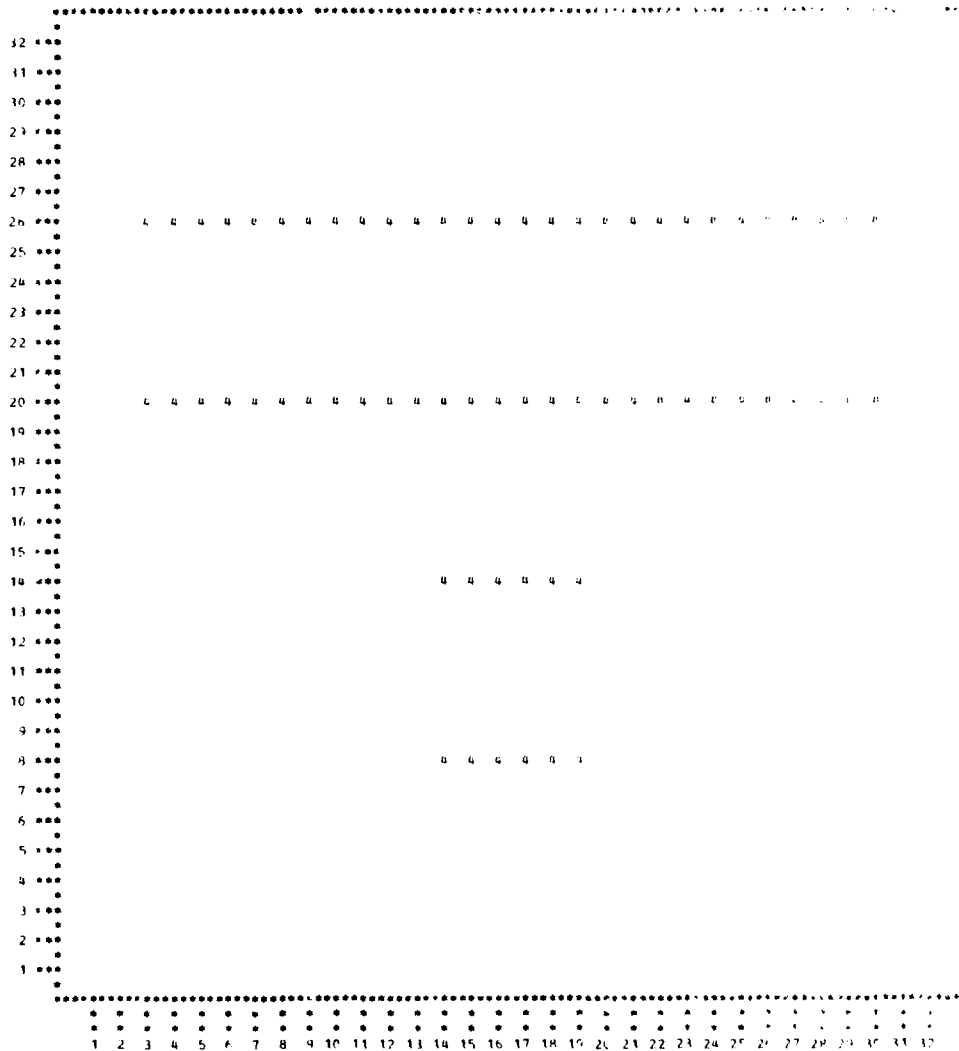
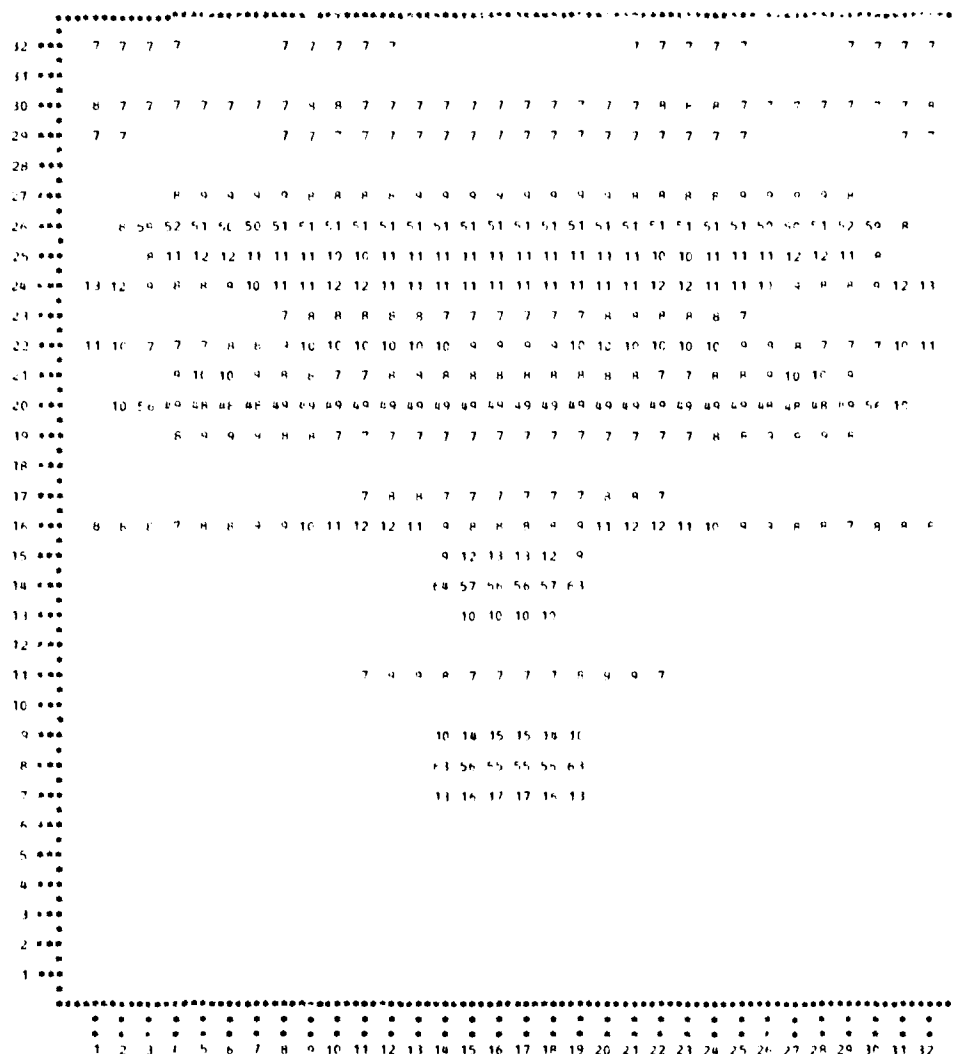


Figure 58. Numerical Printouts of an Illusion of Misjudged Distance: (a) Original Illusion; (b) MTF Filtered Illusion. (Section 12.4.2)

(b)



**Figure 58. Numerical Printouts of an Illusion of Misjudged Distance: (a) Original Illusion; (b) MTF Filtered Illusion. (Section 12.4.2) (cont.)**

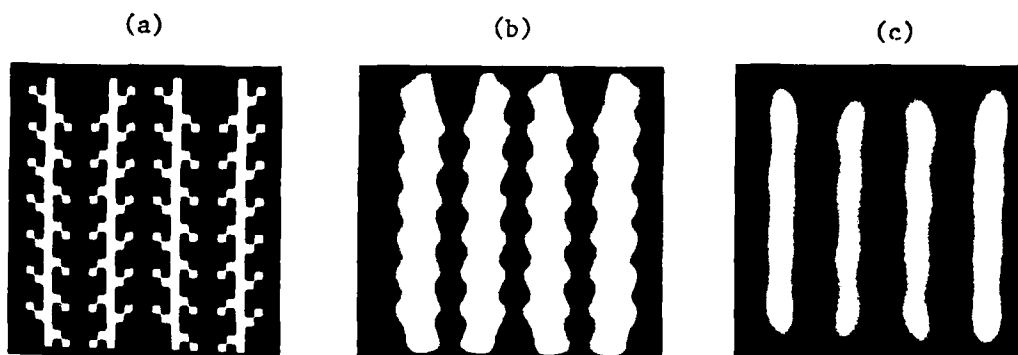


Figure 59. The Zöllner Illusion: (a) Original Illusion; (b) MTF Filtered Illusion; (c) Low-Pass (4 by 4) Filtered Illusion. (Section 12.5)

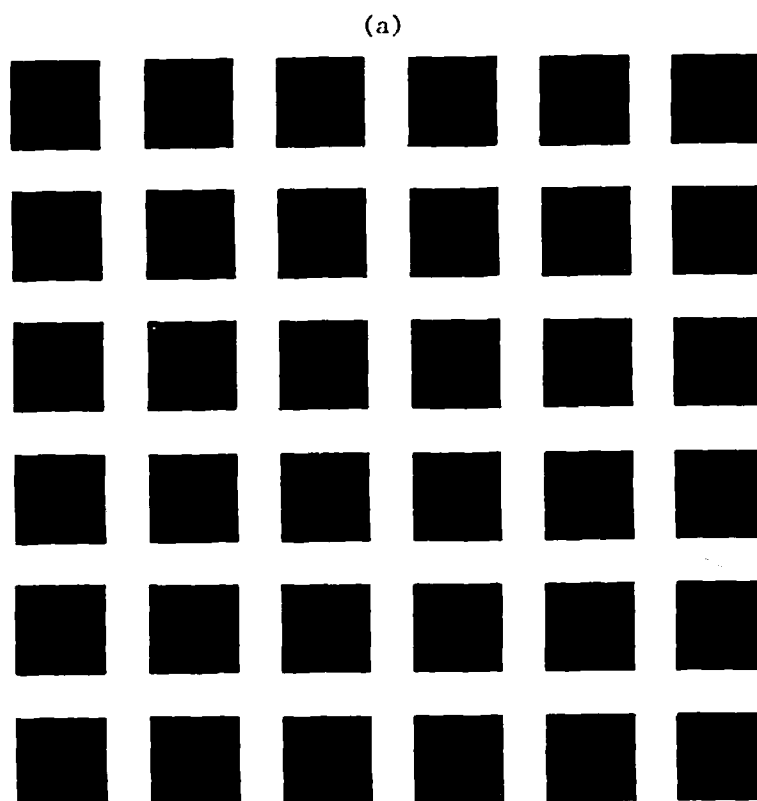


Figure 60. The Hermann Grid Illusion: (a) Original Illusion;  
(b) Digitized Version of Illusion; (c) MTF Filtered Illusion.  
(Section 12.6.1)

[illegible]

217

(c)

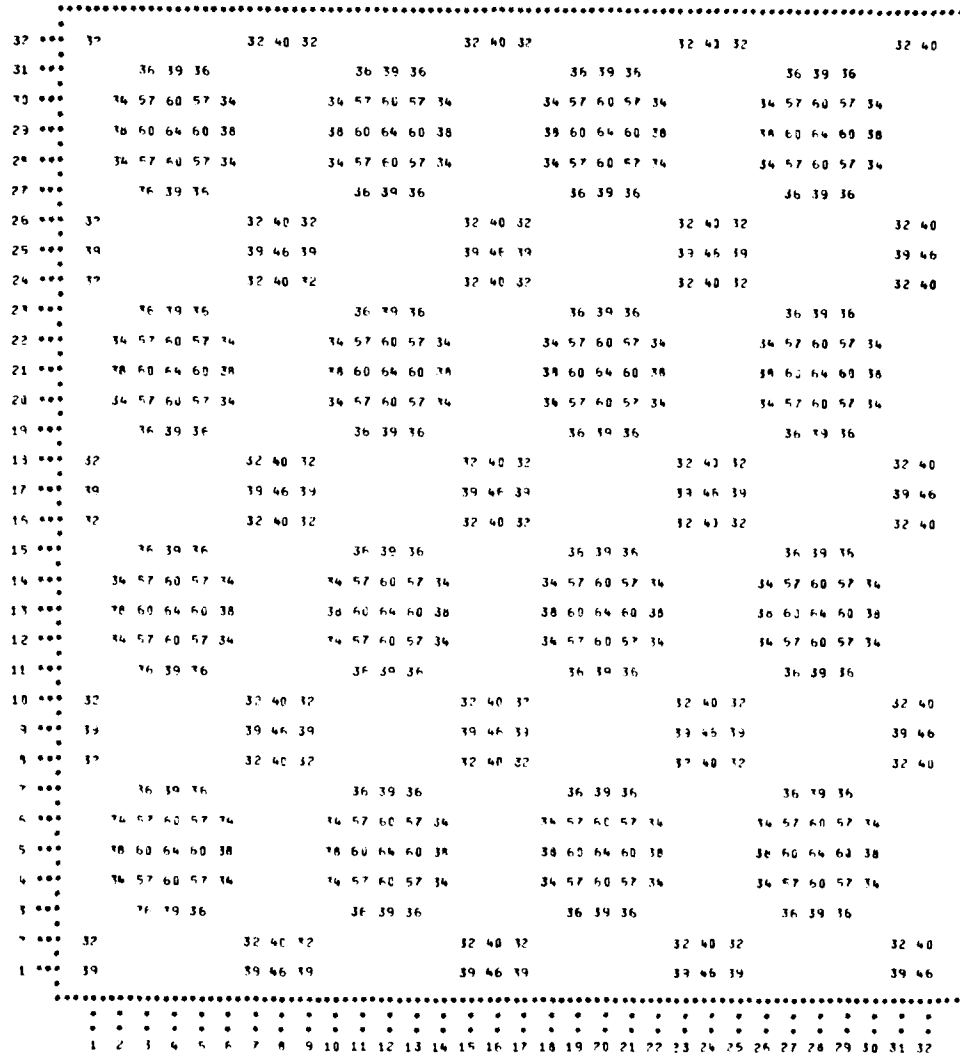


Figure 60. The Hermann Grid Illusion: (a) Original Illusion; (b) Digitized Version of Illusion; (c) MTF Filtered Illusion. (Section 12.6.1) (cont.)

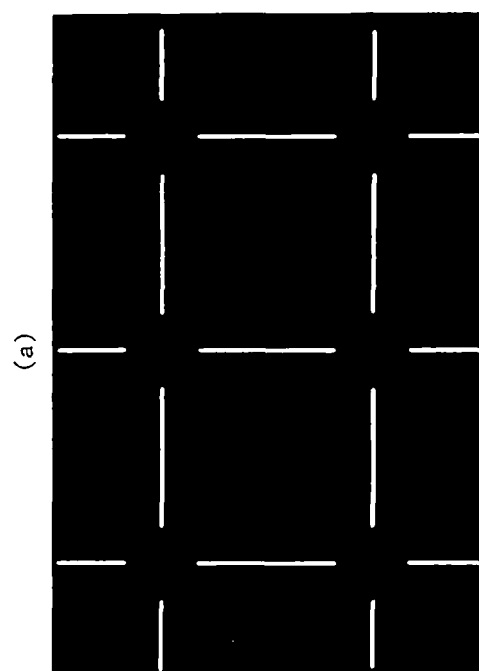


Figure 6.1. The Ehrenstein Illusion: (a) Original Illusion; (b) Digitized Version of the Illusion; (c) MTF Filtered Illusion.  
(Section 12.6.2)



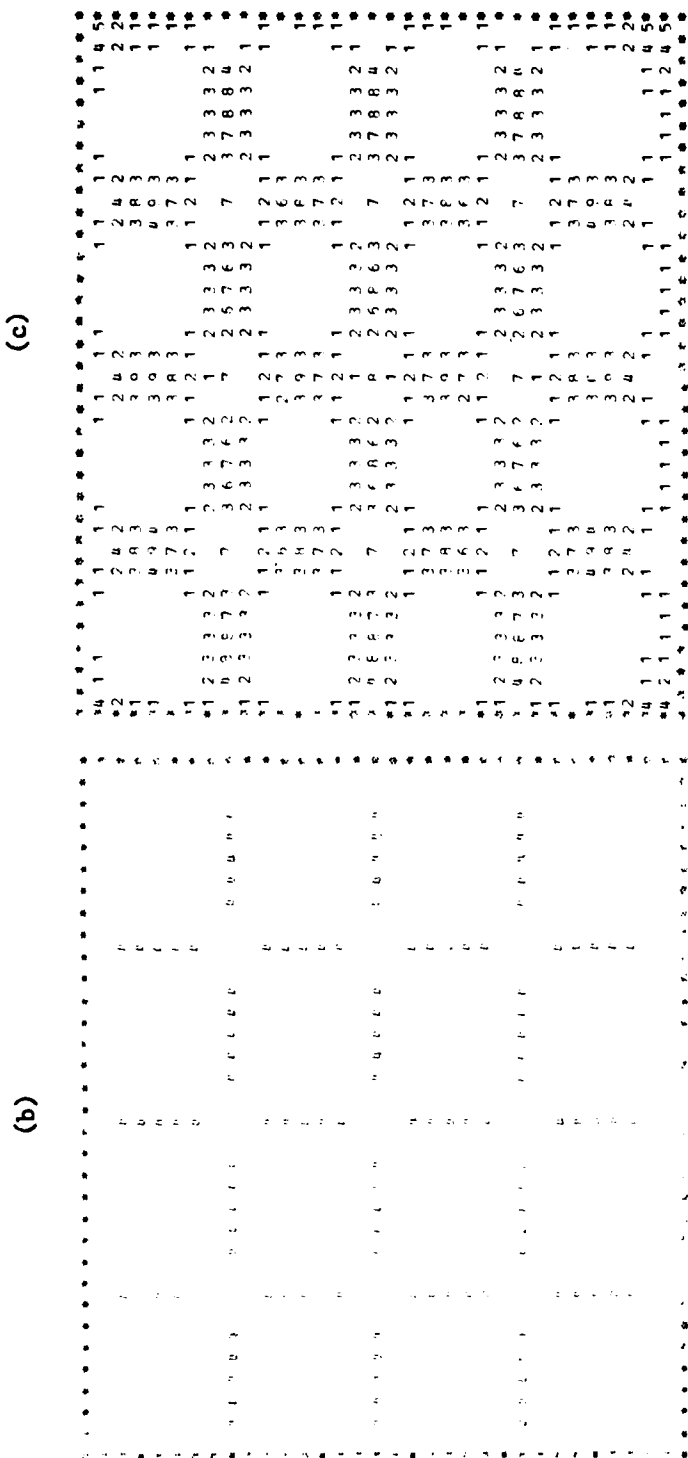


Figure 61. The Ehrenstein Illusion: (a) Original Illusion; (b) Digitized Version of the Illusion; (c) MTF Filtered Illusion.  
(Section 12.6.2) (cont.)

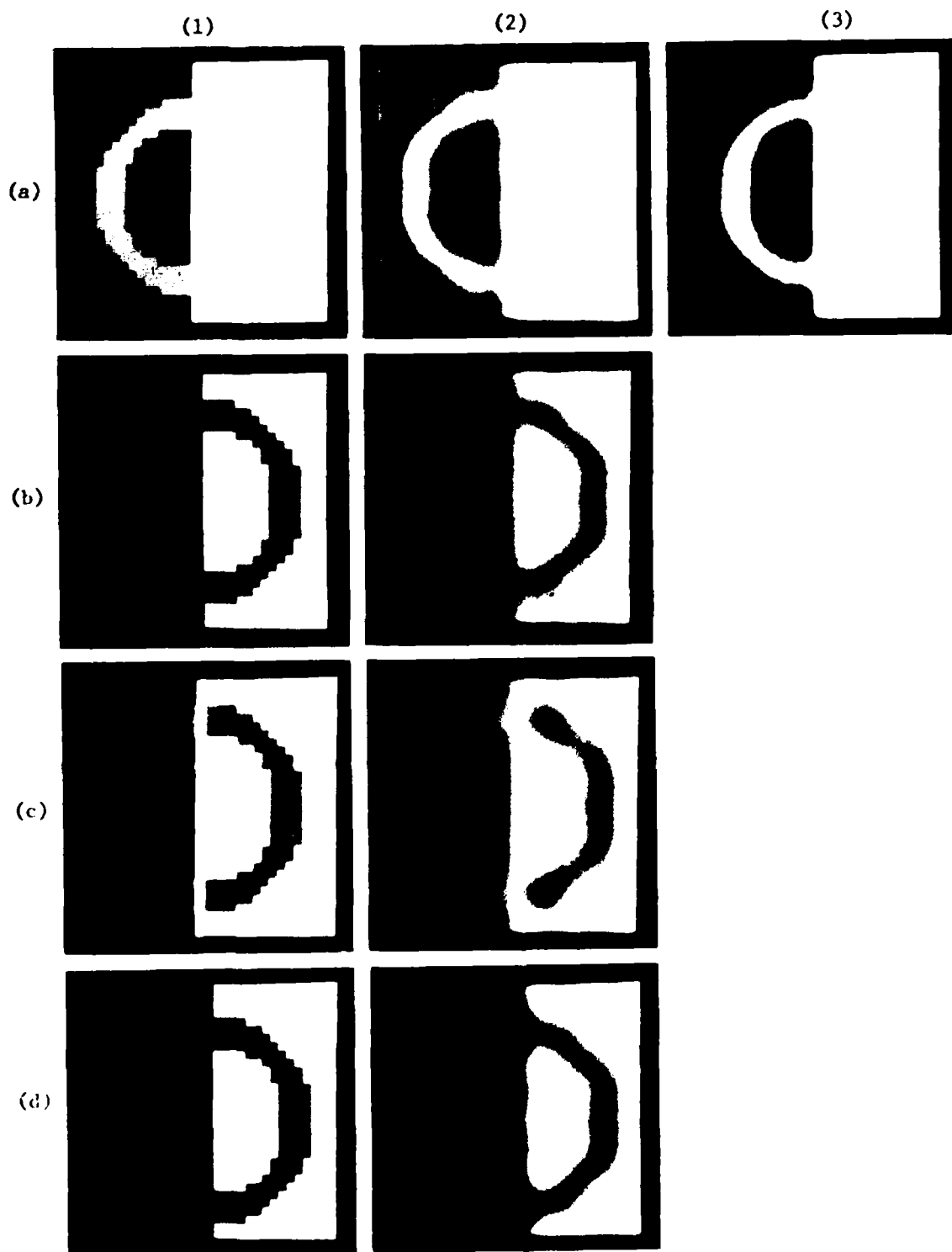


Figure 6.2 The Benussi Ring Illusion: (a) Original Illusion; (b) Illusion with Different Contrast; (c) (b) with a White Line; (d) (b) with a Black Line; (e) Numerical Printout of Original Illusion; (f) Numerical Printout of Low-Pass 5 by 5 Filtered Illusion; (g) Low-Pass 5 by 5 Filtered Illusion without Sinc Function Smoothing; (h) High-Pass 5 by 5 Filtered Illusion with Sinc Function Smoothing; (1) Unfiltered Illusions; (2) Low-Pass 5 by 5 Filtered Illusions; (3) MTF Filtered Illusion (Section 12.6.3)

(e)

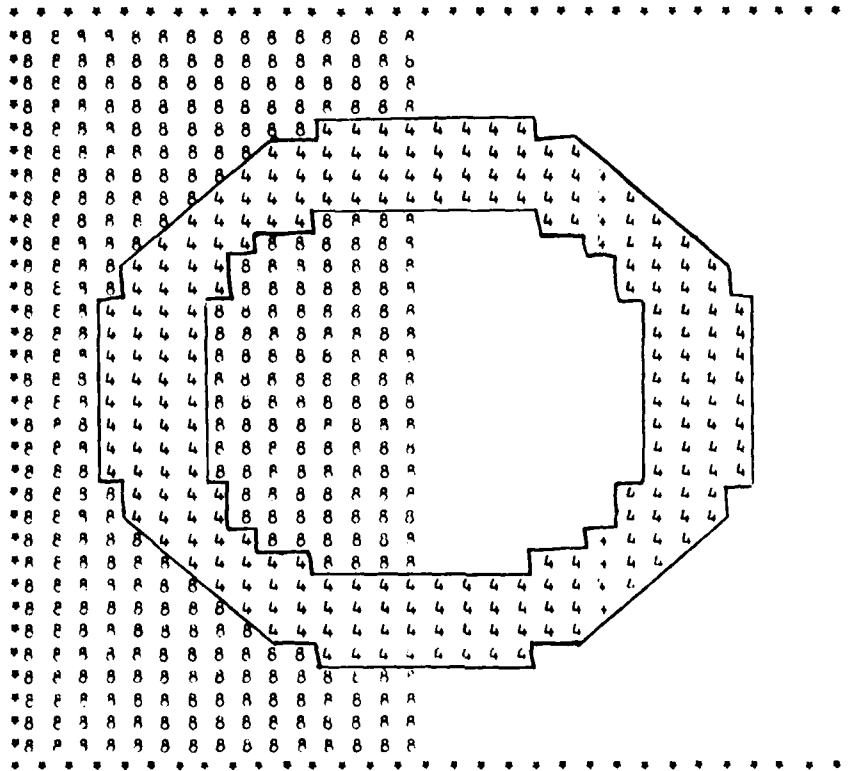


Figure 62. The Benussi Ring Illusion: (a) Original Illusion; (b) Illusion with Different Contrast; (c) b with a White Line; (d) b with a Black Line; (e) Numerical Printout of Original Illusion; (f) Numerical Printout of Low-Pass (5 by 5) Filtered Illusion; (g) Low-Pass (5 by 5) Filtered Illusion without Sine Function Smoothing; (h) High-Pass (5 by 5) Filtered Illusion with Sine Function Smoothing; (i) Unfiltered Illusions; (2) Low-Pass (5 by 5) Filtered Illusions; (3) MTF Filtered Illusion. (Section 12.6.3) (cont.)

(f)

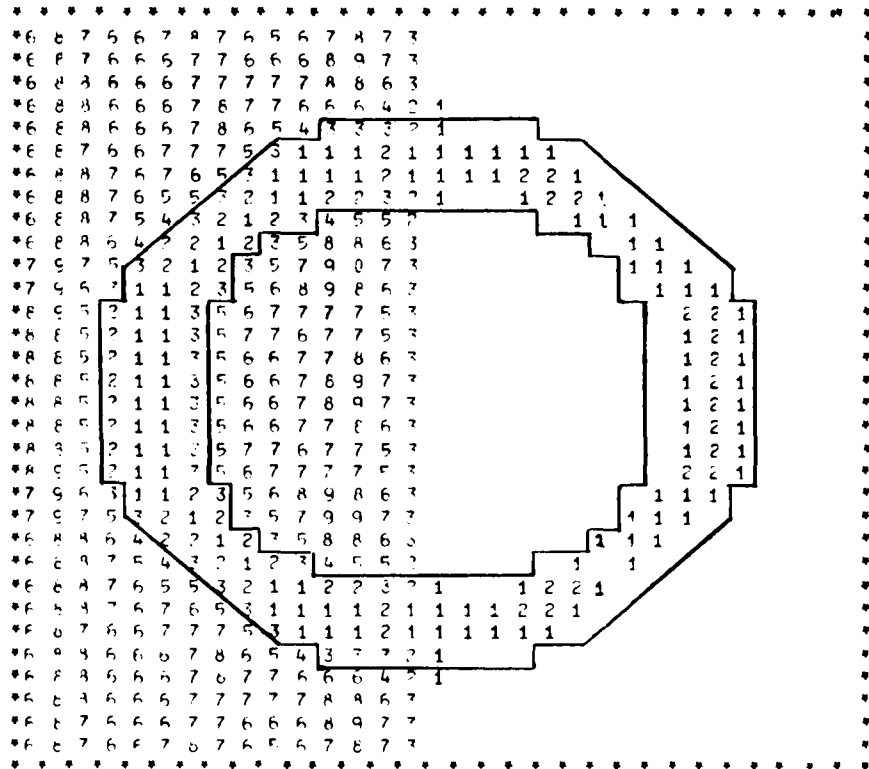
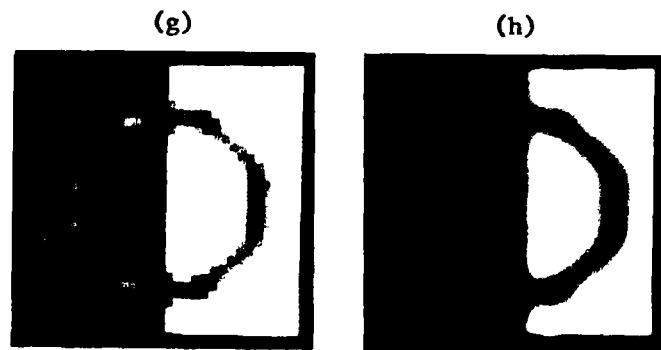


Figure 62. The Benussi Ring Illusion: (a) Original Illusion; (b) Illusion with Different Contrast; (c) b with a White Line; (d) b with a Black Line; (e) Numerical Printout of Original Illusion; (f) Numerical Printout of Low-Pass (5 by 5) Filtered Illusion; (g) Low-Pass (5 by 5) Filtered Illusion without Sine Function Smoothing; (h) High-Pass (5 by 5) Filtered Illusion with Sine Function Smoothing; (i) Unfiltered Illusions; (j) Low-Pass (5 by 5) Filtered Illusions; (k) MTF Filtered Illusion. (Section 12.6.3) (cont.)



**Figure 62. The Benussi Ring Illusion:** (a) Original Illusion; (b) Illusion with Different Contrast; (c) b with a White Line; (d) b with a Black Line; (e) Numerical Printout of Original Illusion; (f) Numerical Printout of Low-Pass (5 by 5) Filtered Illusion; (g) Low-Pass (5 by 5) Filtered Illusion without Sinc Function Smoothing; (h) High-Pass (5 by 5) Filtered Illusion with Sinc Function Smoothing; (1) Unfiltered Illusions; (2) Low-Pass (5 by 5) Filtered Illusions; (3) MTF Filtered Illusion. (Section 12.6.3) (cont.)

(1)

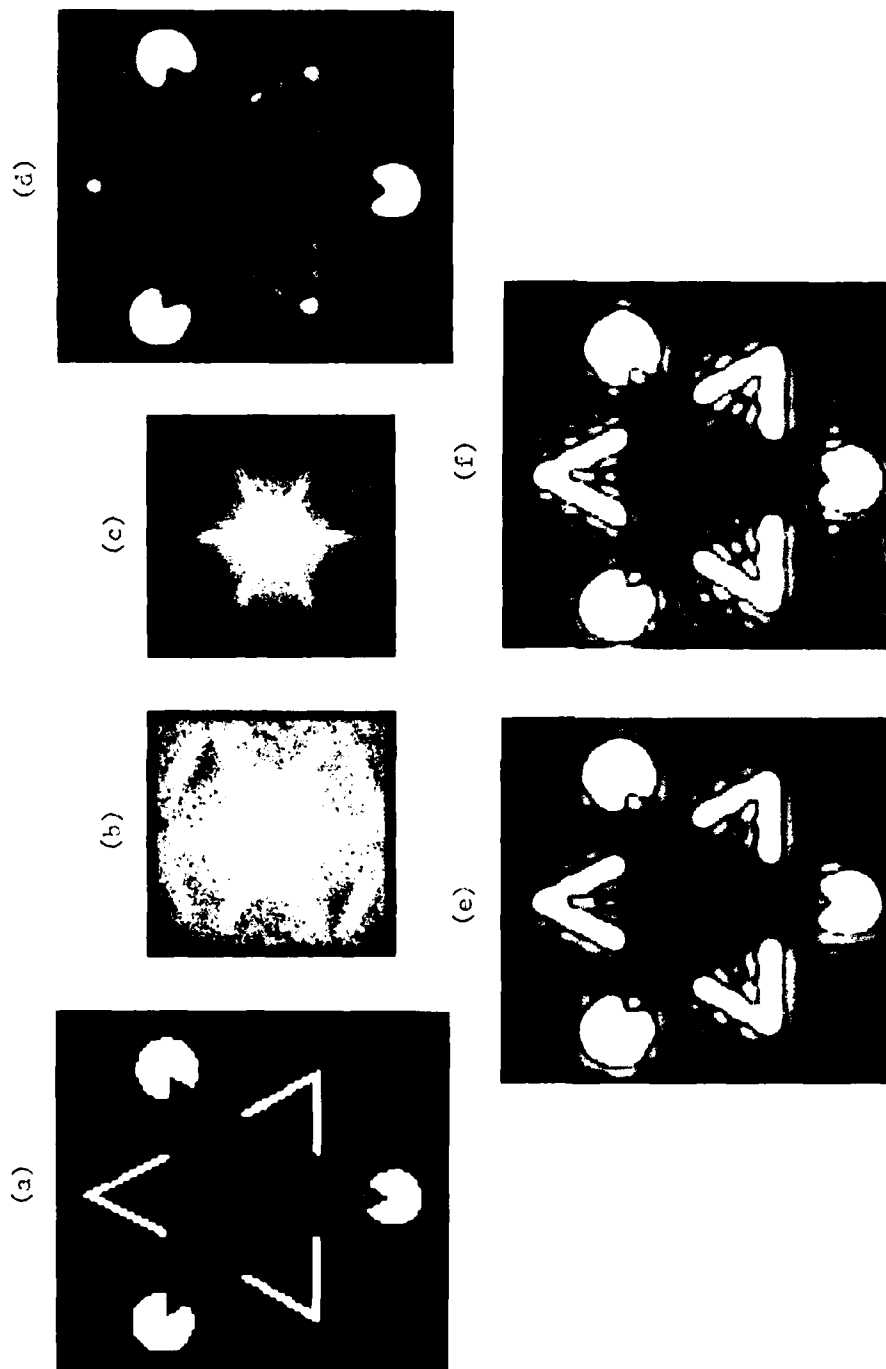


Figure 63. Variations of the Kanizsa Triangle: (a) Original Triangles; (b) Fourier Magnitude Spectra of (a); (c) MTF (L) Filtered Magnitude Spectra; (d) MTF (L) Filtered Triangles; (e) Low-Pass (16 by 16) Filtered Triangles; (f) MTF (L) Low-Pass (16 by 16) Filtered Triangles; (1) Original Illusion (from Ginsburg, 1975); (2) Illusion with Dots Replacing the Sectors in 1. (Section 12.7)

(2)

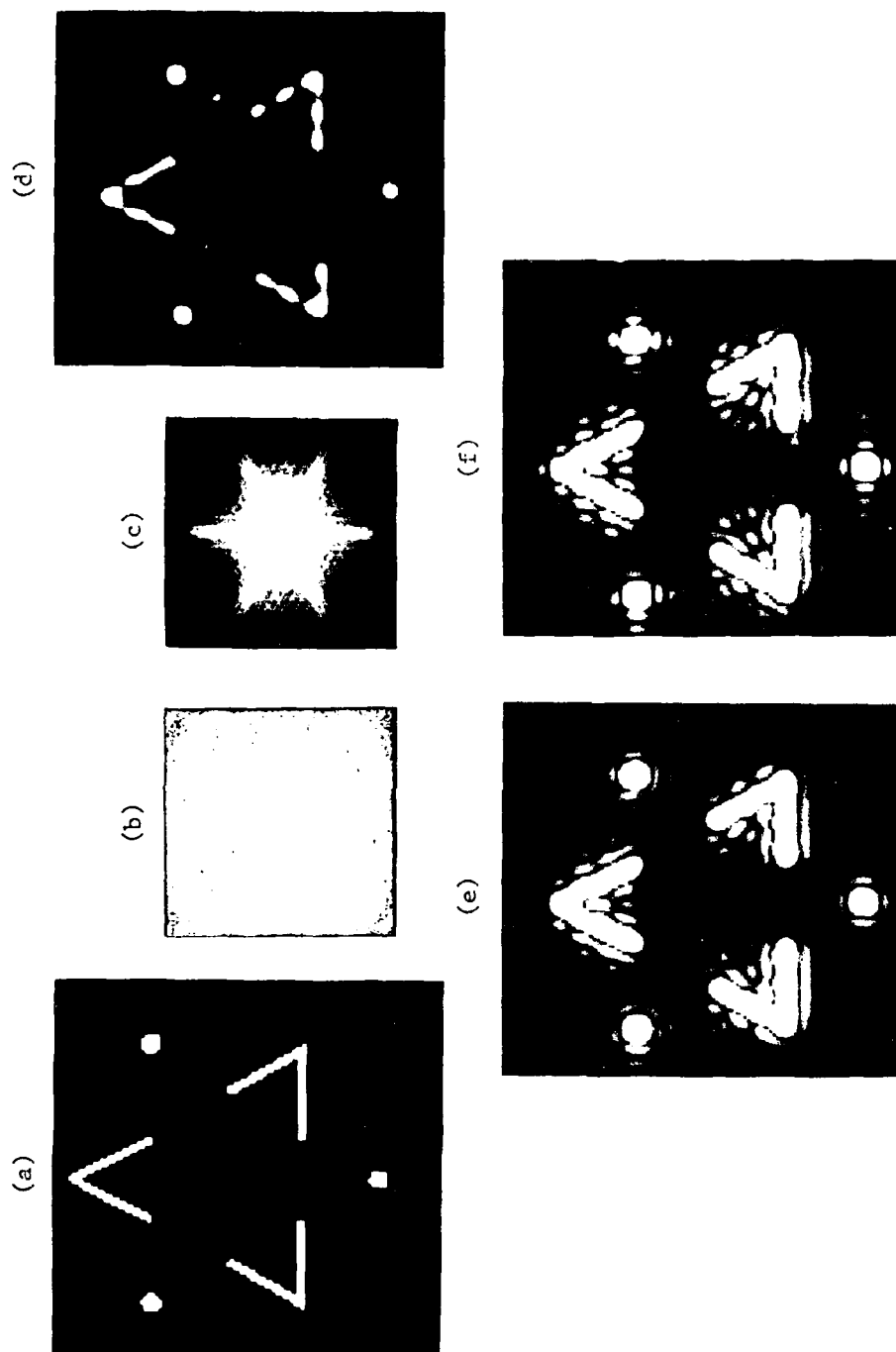


Figure 63. Variations of the Kanizsa Triangle: (a) Original Triangle; (b) Fourier Magnitude Spectra of a; (c) MTF (L) Filtered Magnitude Spectra; (d) MTF (L) Filtered Triangles; (e) Low-Pass (16 by 16) Filtered Triangles; (f) MTF (L) Low-Pass (16 by 16) Filtered Triangles; (1) Original Illusion (from Ginsburg, 1975); (2) Illusion with Dots Replacing the Sectorized Disks in 1. (Section 12.7 (cont.))

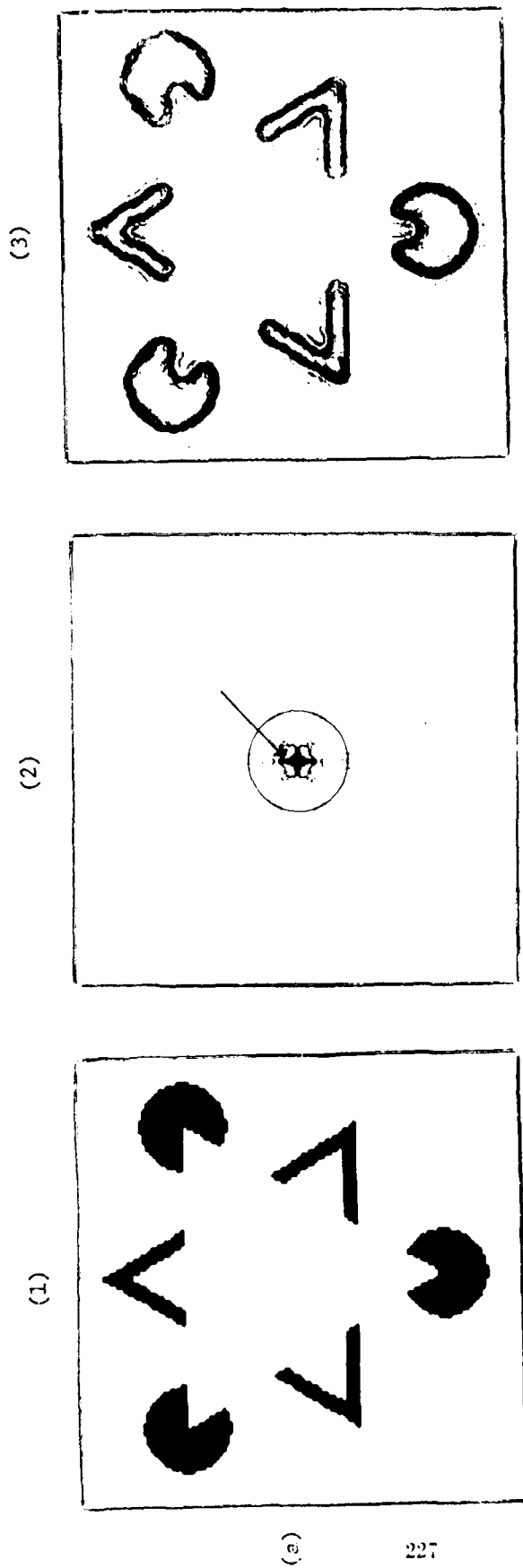


Figure 64. Contour Plots and Numerical Printouts of Low-Pass Filtered Solid and Outline Versions of the Kanizsa Triangle:  
 (a) Solid Triangle; (b) Outlined Triangle; (1) Original Triangles; (2) Magnitude Spectra of Triangles; (3) 16 Level  
 Contour Plots of Low-Pass (14 by 14) Filtered Triangles; (4) Contour Values Between 18 and 25 Percent of the  
 Maximum Values of 3 Are Filled in; (5) 32 by 32 Pel 16 Level Numerical Printout of the Window Section of 4.  
 (Section 12.7.1)



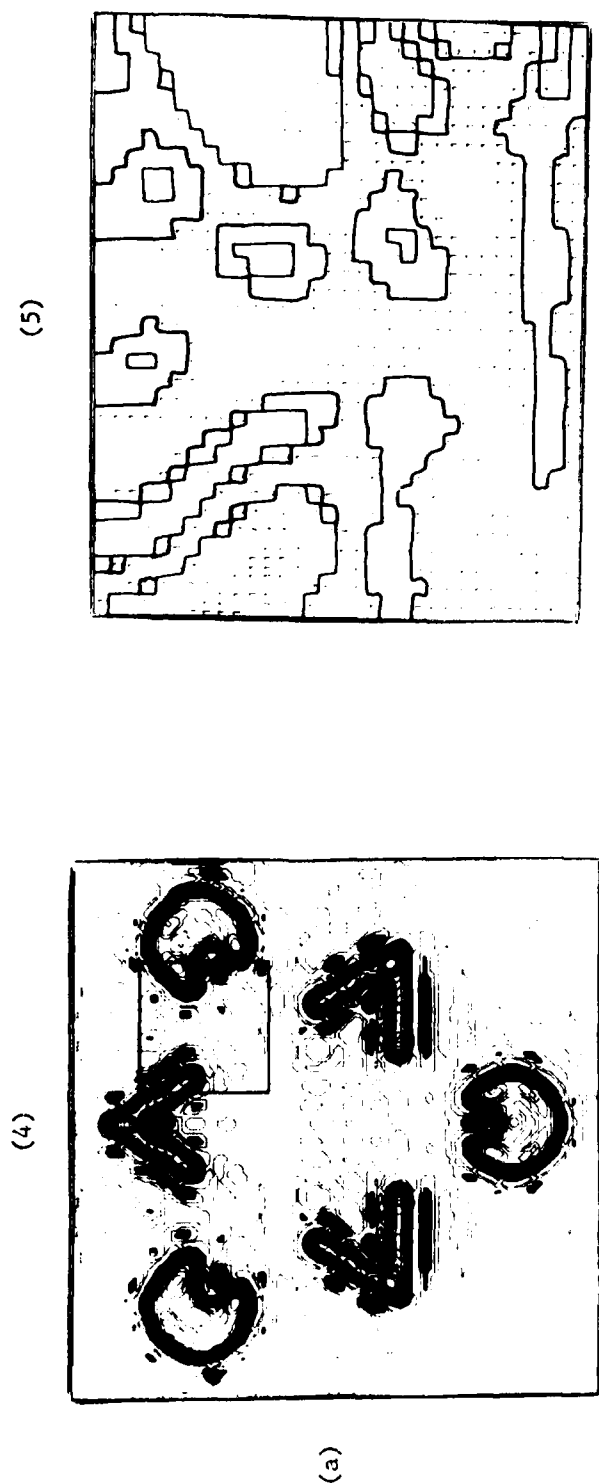


Figure 64. Contour Plots and Numerical Printouts of Low-Pass Filtered Solid and Outline Versions of The Kanizsa Triangle:  
 (a) Solid Triangle; (b) Outlined Triangle; (1) Original Triangles; (2) Magnitude Spectra of Triangles; (3) 16 Level  
 Contour Plots of Low-Pass (14 by 14) Filtered Triangles; (4) Contour Values Between 18 and 25 Percent of the  
 Maximum Values of 3 Are Filled in; (5) 32 by 32 Pel 16 Level Numerical Printout of the Window Section of 4.  
 (Section 12.7.1) (cont.)

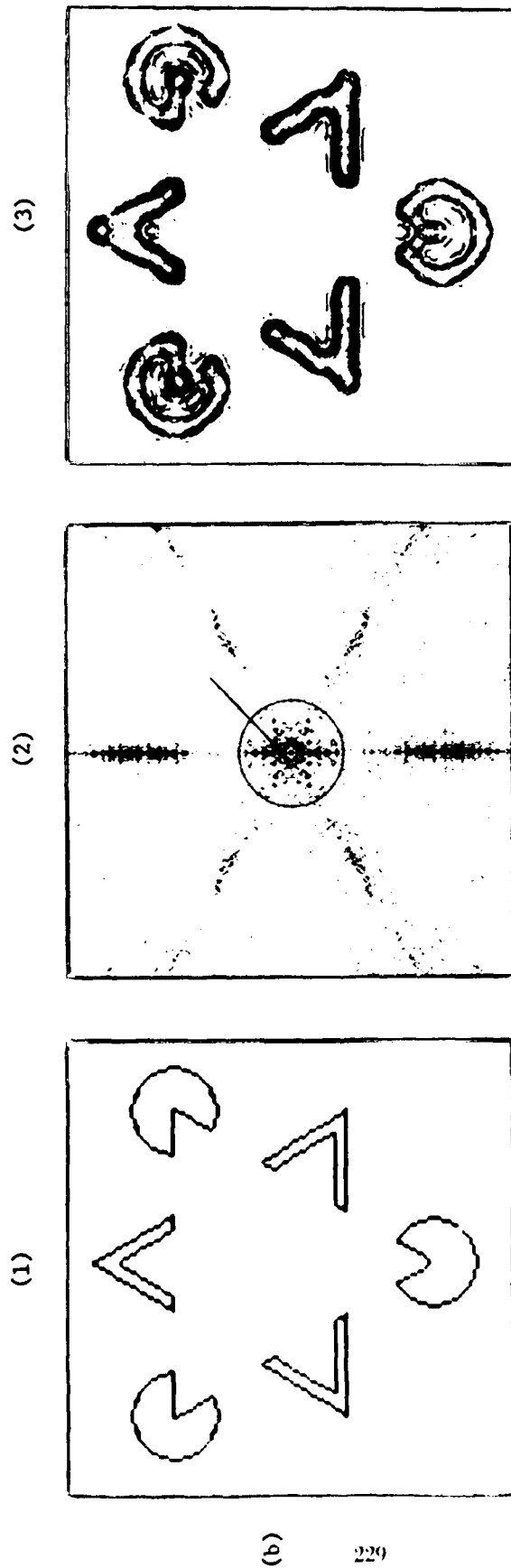


Figure 6-4. Contour Plots and Numerical Printouts of Low-Pass Filtered Solid and Outline Versions of the Kanizsa Triangle; (a) Solid Triangle; (b) Outlined Triangle; (1) Original Triangles; (2) Magnitude Spectra of Triangles; (3) 16 Level Contour Plots of Low-Pass (14 by 14) Filtered Triangles; (4) Contour Values Between 18 and 25 Percent of the Maximum Values of 3 Are Filled in; (5) 32 by 32 Pel 16 Level Numerical Printout of the Window Section of 4. (Section 12.7.1) (cont.)

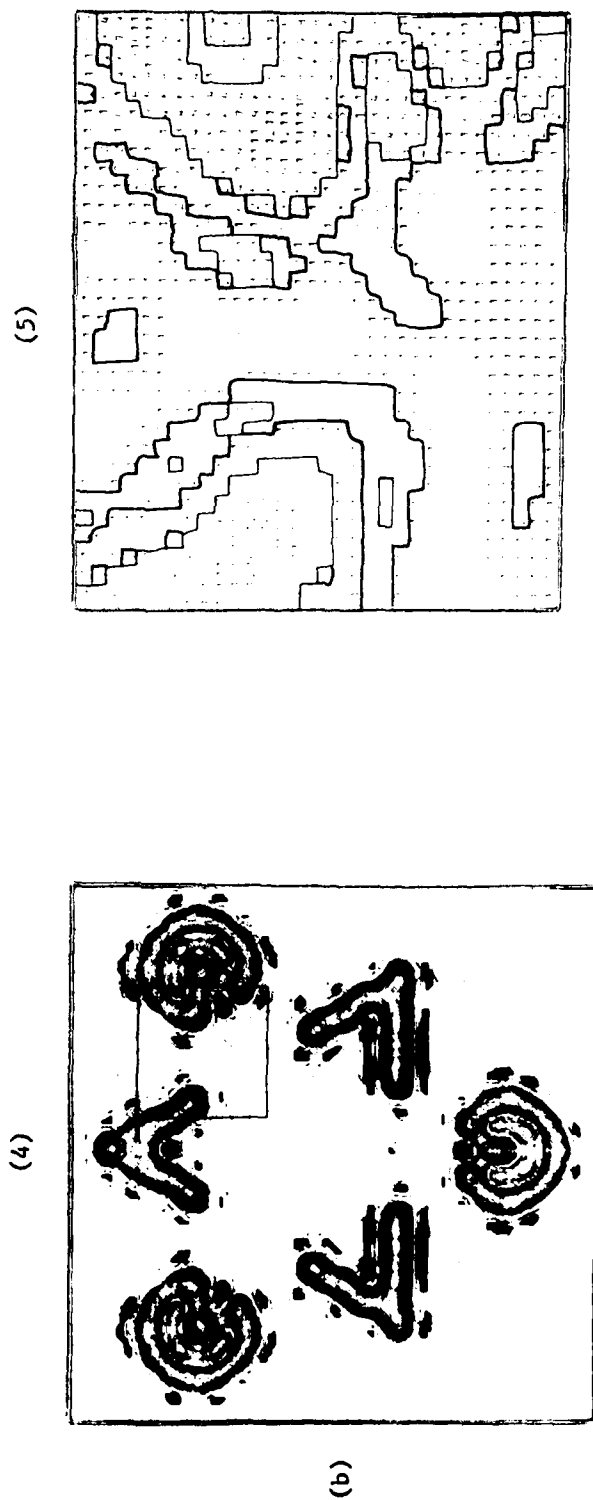


Figure 64. Contour Plots and Numerical Printouts of Low-Pass Filtered Solid and Outline Versions of the Kaniza Triangle:  
 (a) Solid Triangle; (b) Outlined Triangle; (2) Magnitude Spectra of Triangles; (3) 16 Level  
 Contour Plots of Low-Pass (14 by 14) Filtered Triangles; (4) Contour Values Between 18 and 25 Percent of the  
 Maximum Values of 3 Are Filled in; (5) 32 by 32 Pel 16 Level Numerical Printout of the Window Section of 4.  
 (Section 12.7.1) (cont.)

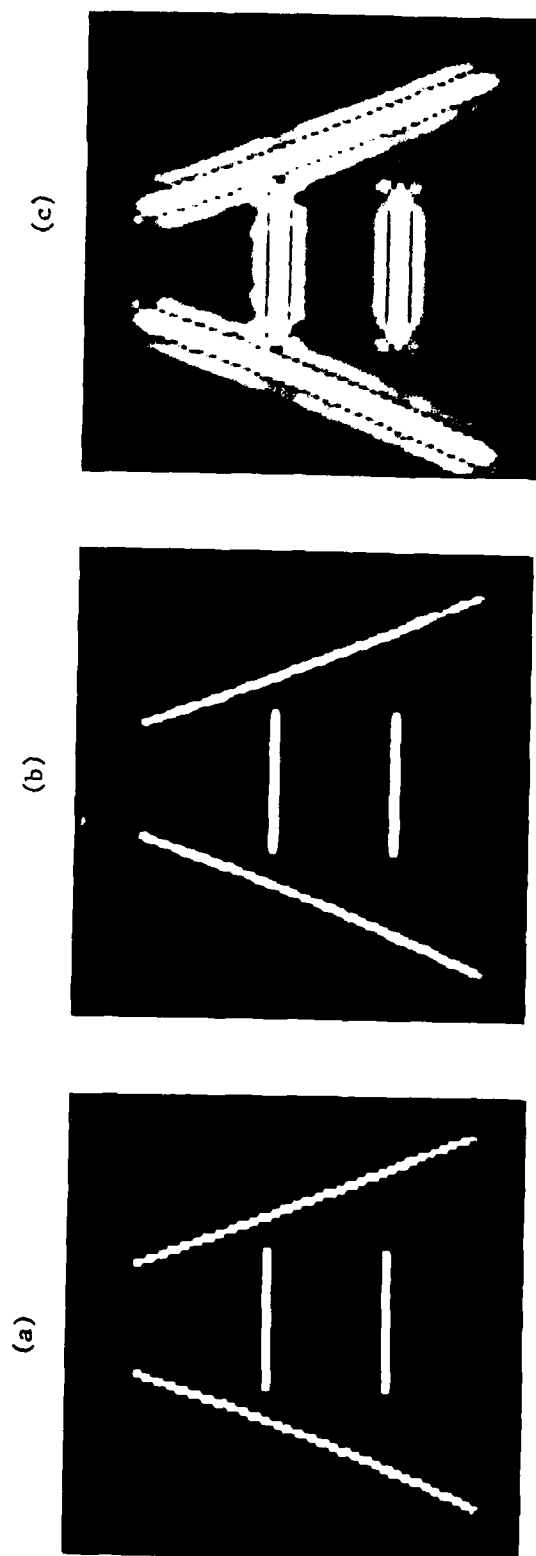


Figure 65. The Ponzo Illusion (Large Sized): (a) Original Illusion; (b) MTF Filtered Illusion; (c) MTF(L)L Filtered Illusion; (d) MTF(L) (5 by 5) Filtered Illusion; (e) Low-Pass (5 by 5) Filtered Illusion. (Section 12.8)

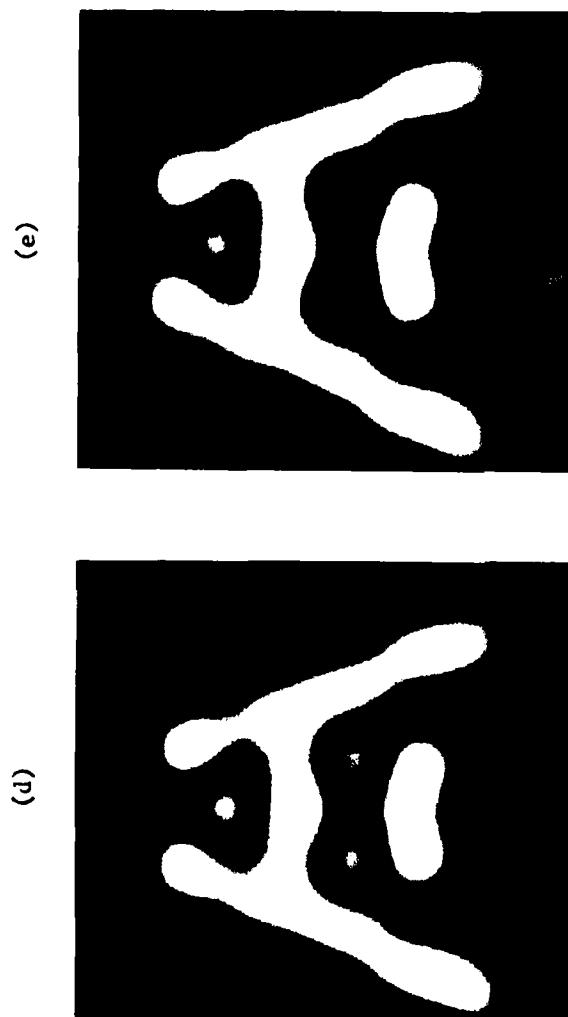


Figure 65. The Ponzo Illusion (Large Sized): (a) Original Illusion; (b) MTF Filtered Illusion; (c) MTF(L) Filtered Illusion; (d) MTF(L) (5 by 5) Filtered Illusion; (e) Low-Pass (5 by 5) Filtered Illusion. (Section 12.8) (cont.)

# THEORETICAL AND EXPERIMENTAL DATA FOR THE MAGNITUDE OF THE MÜLLER - LYER ILLUSION

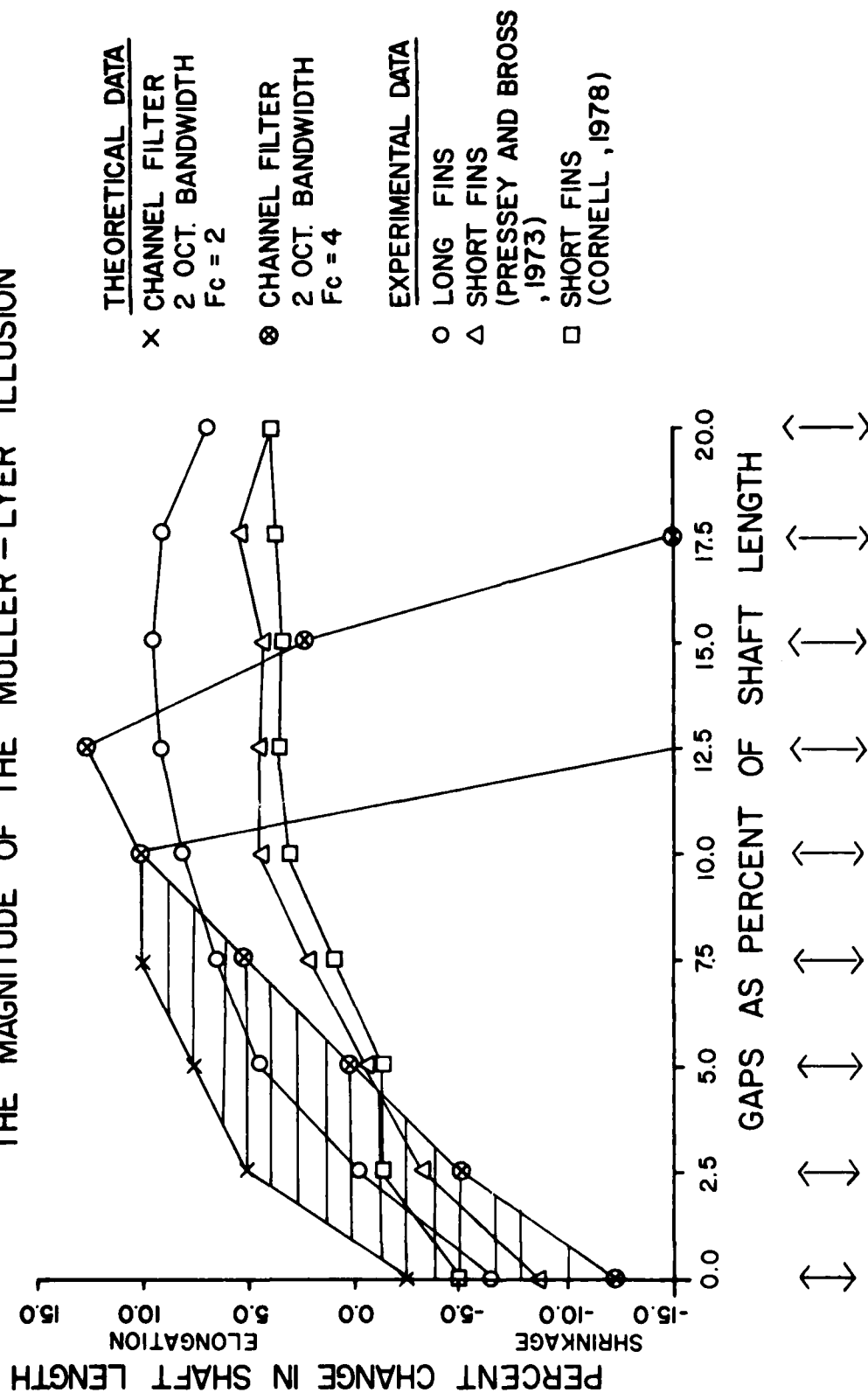


Figure 66. Theoretical and Experimental Data for the Magnitude of the Müller-Lyer Illusion. (Section 12.8.1)

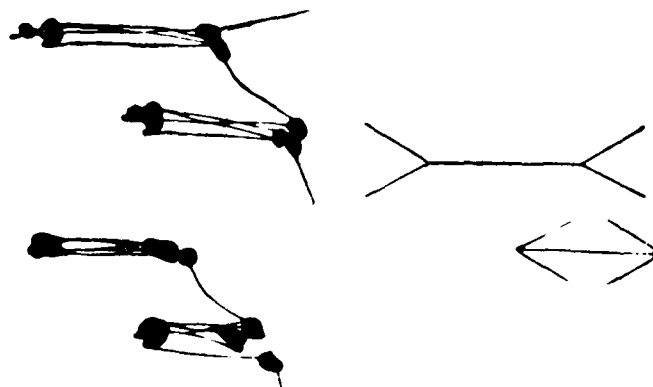


Figure 67. Eye Scan Paths from the Müller-Lyer Illusion (from Yarbush, 1967).  
(Section 12.15.1)

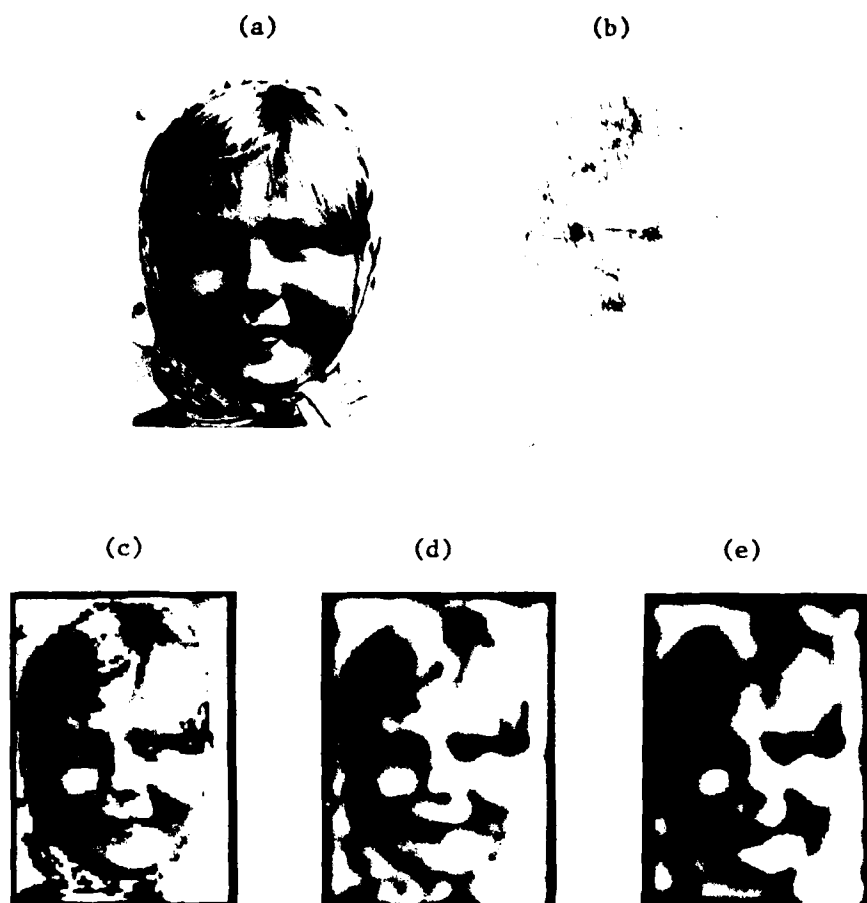


Figure 68. Eye Scan Paths from a Portrait of a Young Girl (from Yarbus, 1967): (a) Original Portrait; (b) Eye Scan Paths; (c) Digitized Portrait; (d) Low-Pass (24 by 24) Filtered Portrait; (e) Low-Pass (16 by 16) Filtered Portrait. (Section 12.8.2)



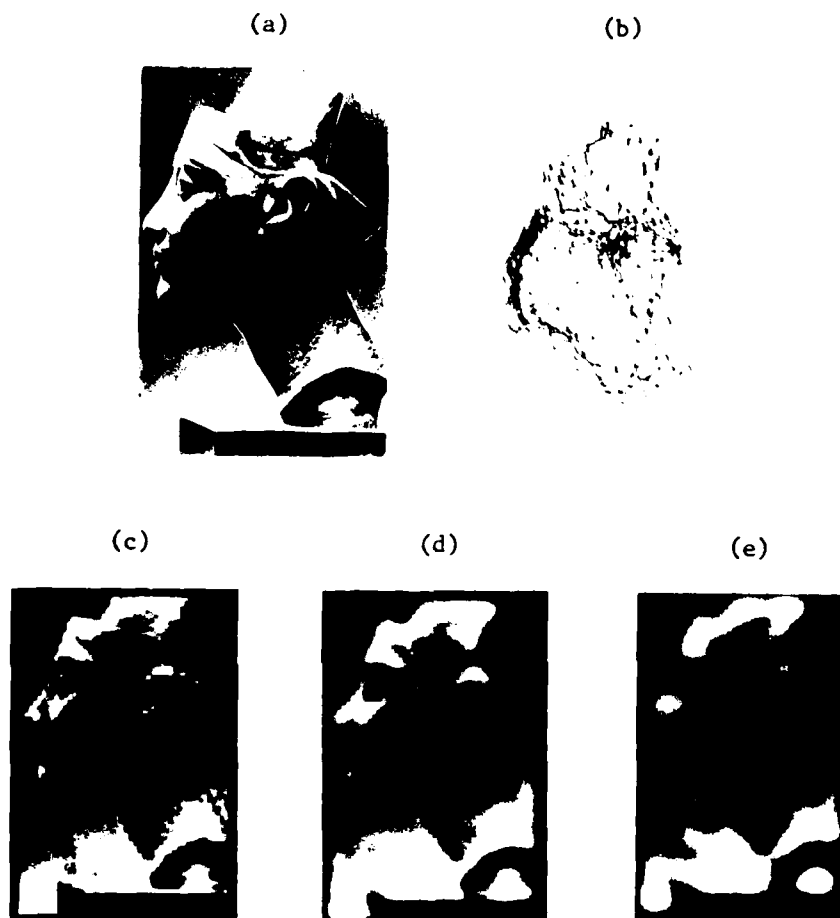


Figure 69. Eye Scan Paths from a Bust of Nefertite (from Yarbus, 1967):  
 (a) Original Portrait; (b) Eye Scan Paths; (c) Digitized Portrait;  
 (d) Low-Pass (24 by 24) Filtered Portrait; (e) Low-Pass (16 by  
 16) Filtered Portrait. (Section 12.8.2)



Figure 70. Portion of "Slave Market with Apparition of the Invisible Bust of Voltaire" by Salvador Dali: (a) Original Picture; (b) Original Picture Digitized to 128 by 128 Pels; (c) Low-Pass (24 by 24) Filtered Picture; (d) Low-Pass (8 by 8) Filtered Picture; (e) Bust Enlarged to Two Times the Original; (f) Low-Pass (24 by 24) Filtered Picture; (g) Low-Pass (16 by 16) Filtered Picture; (h) Low-Pass (8 by 8) Filtered Picture. (Section 13.2)

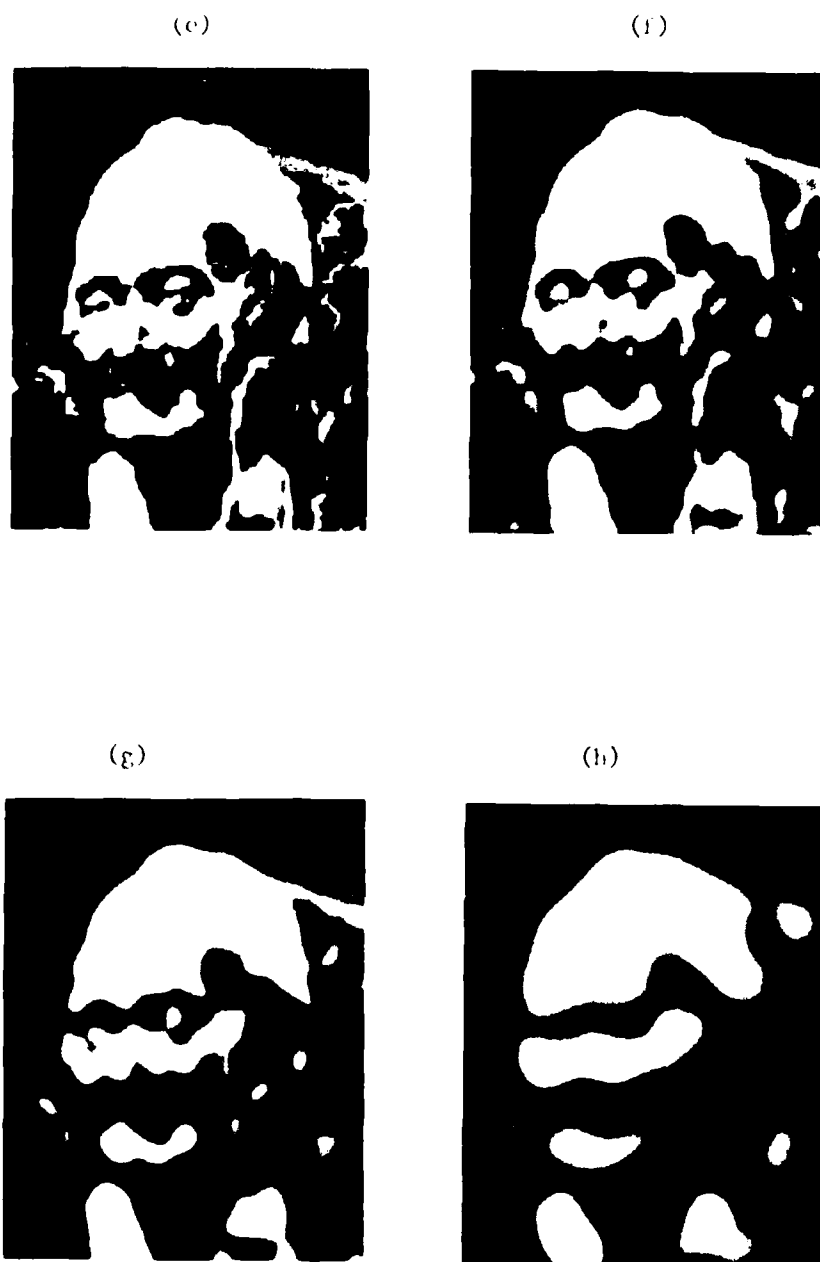


Figure 70. Portion of "Slave Market with Apparition of the Invisible Bust of Voltaire" by Salvador Dalí: (a) Original Picture; (b) Original Picture Digitized to 128 by 128 Pels; (c) Low-Pass (24 by 24) Filtered Picture; (d) Low-Pass (8 by 8) Filtered Picture; (e) Bust Enlarged to Two Times the Original; (f) Low-Pass (24 by 24) Filtered Picture; (g) Low-Pass (16 by 16) Filtered Picture; (h) Low-Pass (8 by 8) Filtered Picture. (Section 13.2) (cont.)

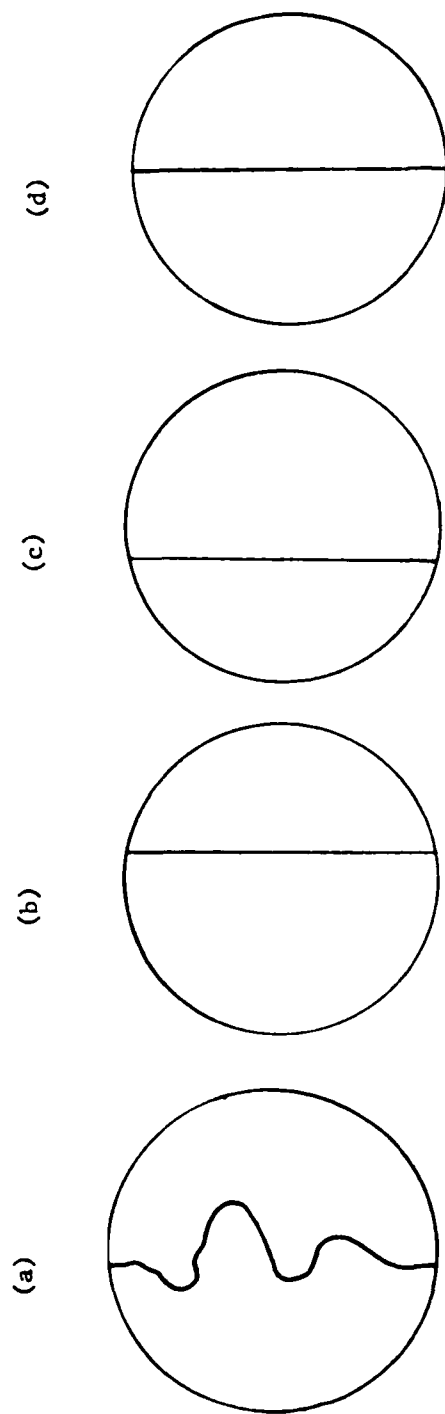


Figure 71. Variations of the Bisected Circle: (a) Original Version of Bisected Circle; (b) Variation 1 of Bisected Circle; (c) Variation 2 of Bisected Circle; (d) Variation 3 of Bisected Circle. (Section 13.3)

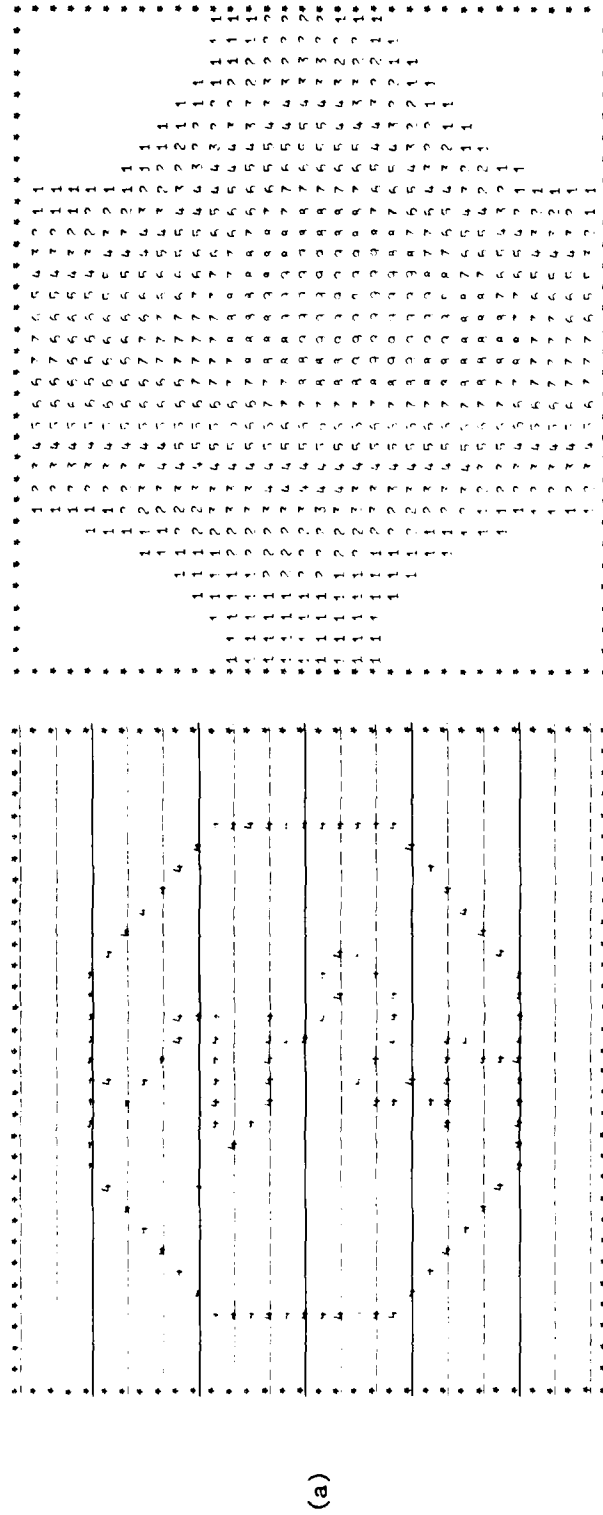
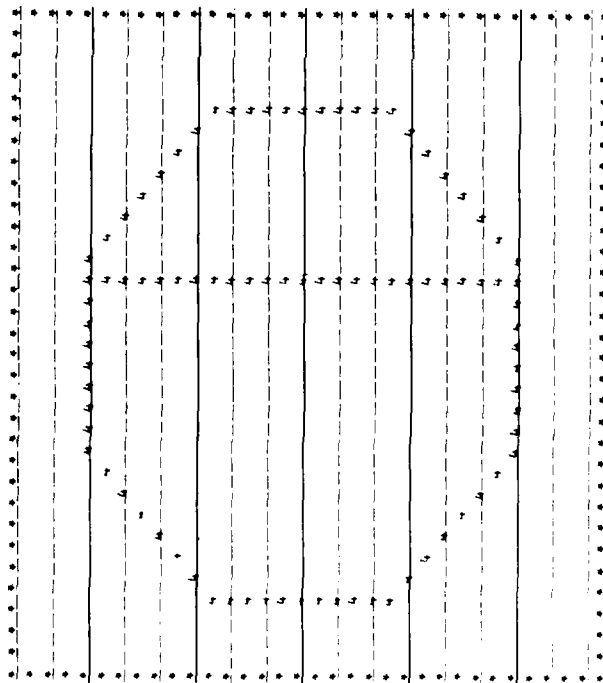
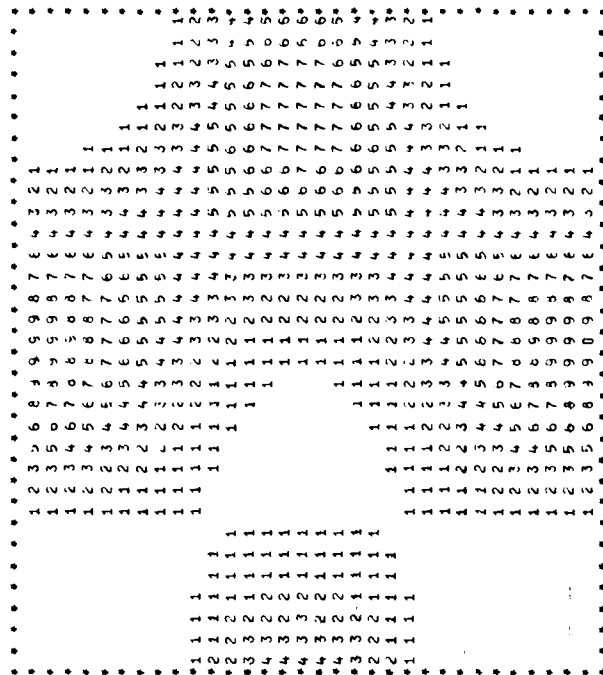


Figure 72. Numerical Printouts of Variations of the Bisected Circle: (a) Original Bisected Circle; (b) Simplified Version 1 of a; (c) Simplified Version 2 of a; (d) Simplified Version 3 of a; (1) Original Variations; (2) Low-Pass (1 by 1) Filtered Images. (Section 13.3)

(1)



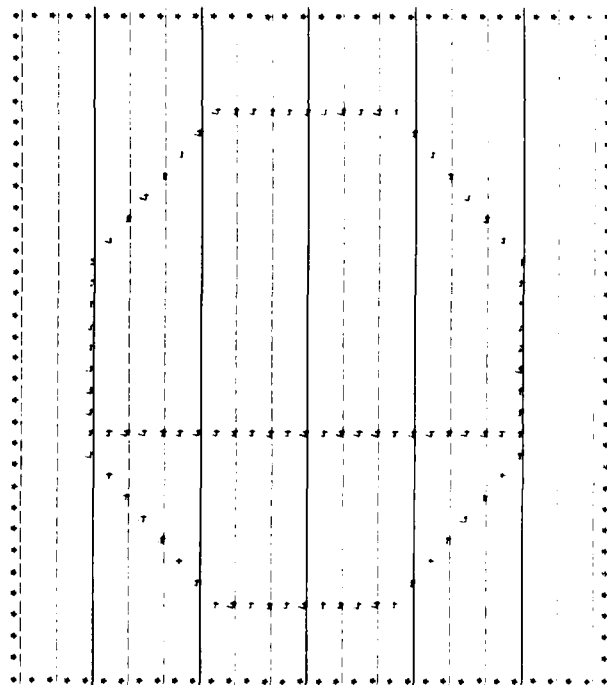
(2)



(b)

Figure 72. Numerical Printouts of Variations of the Bisected Circle: (a) Original Bisected Circle; (b) Simplified Version 1 of a; (c) Simplified Version 2 of a; (d) Simplified Version 3 of a; (1) Original Variations; (2) Low-Pass (1 by 1) Filtered Images. (Section 13.3) (cont.)

(1)



(c)

(2)

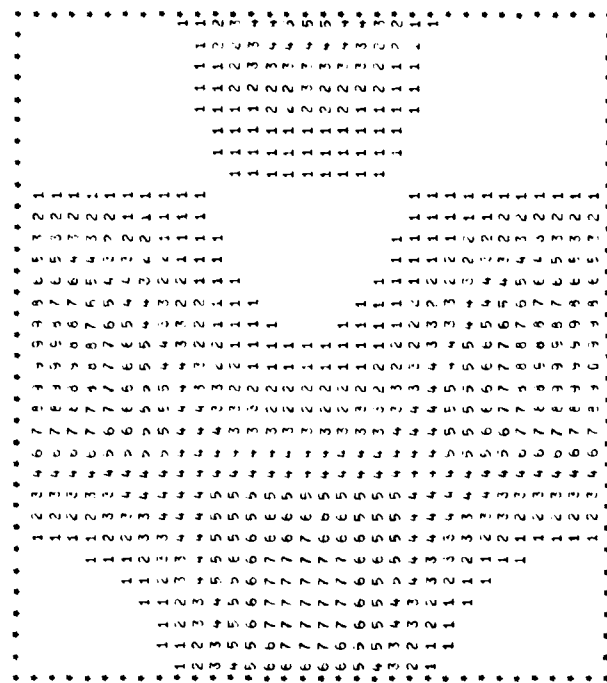


Figure 72. Numerical Printouts of Variations of the Bisected Circle: (a) Original Bisected Circle; (b) Simplified Version 1 of a; (c) Simplified Version 2 of a; (d) Simplified Version 3 of a; (1) Original Variations; (2) Low-Pass (1 by 1) Filtered Images. (Section 13.3) (cont.)

(2)

(d)

**Figure 7.2. Numerical Printouts of Variations of the Bisected Circle: (a) Original Bisected Circle; (b) Simplified Version 1 of a; (c) Simplified Version 2 of a; (d) Simplified Version 3 of a; (1) Original Variations; (2) Low-Pass (1 by 1) Filtered Images. (Section 13.3) (cont.)**



(a)

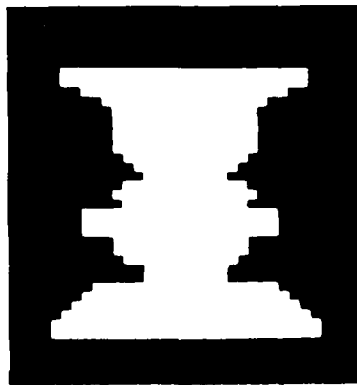


Figure 73. The Rubin Face-Vase Object: (a) Original Object; (b) Low-Pass (8 by 8) Filtered Images; (c) Low-Pass (6 by 6) Filtered Images; (d) Low-Pass (4 by 4) Filtered Images; (e) and (f) Two Variations of the Rubin Face-Vase Object; (1) Magnitude Spectra; (2) Filtered Images. (Section 13.4)

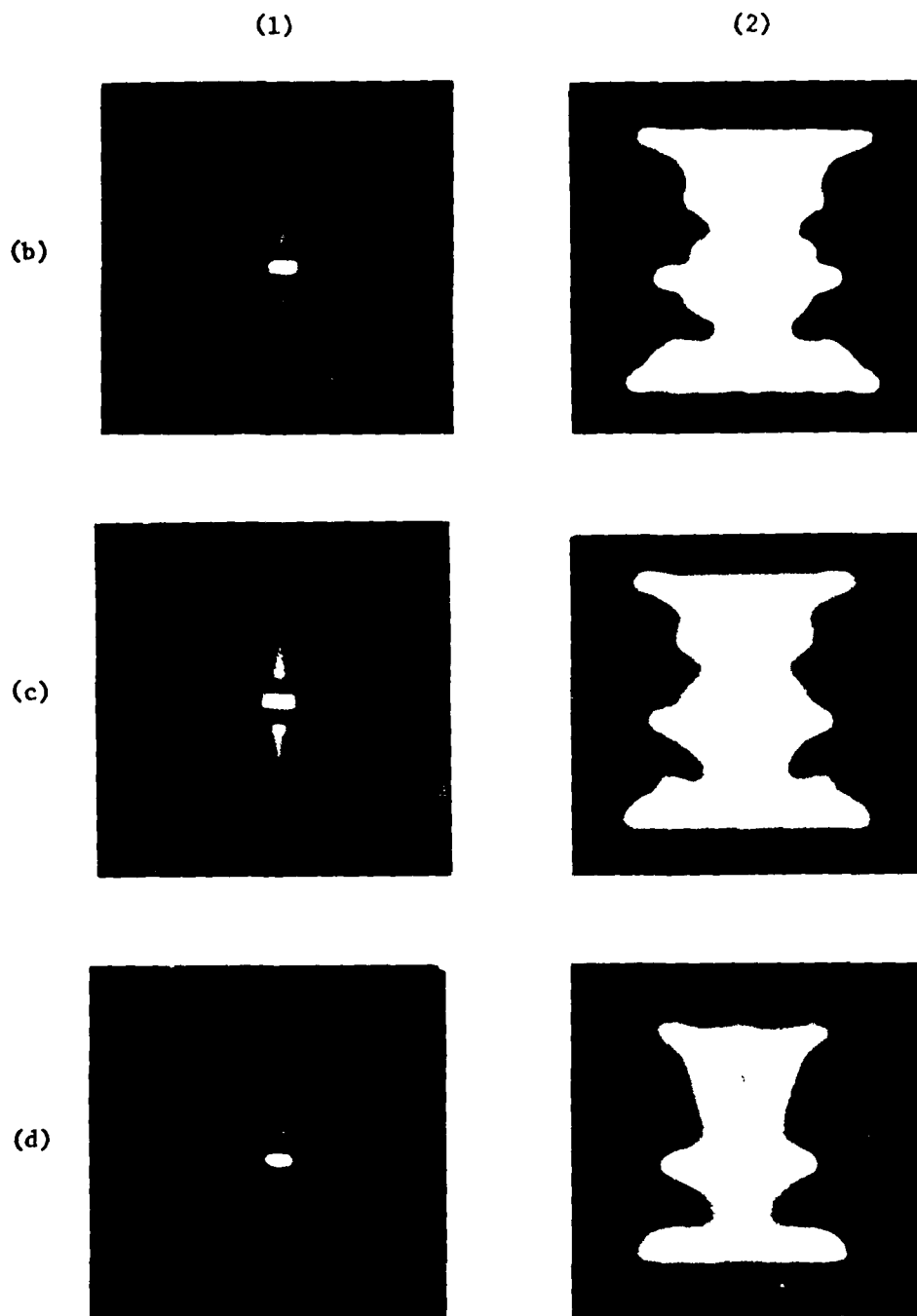
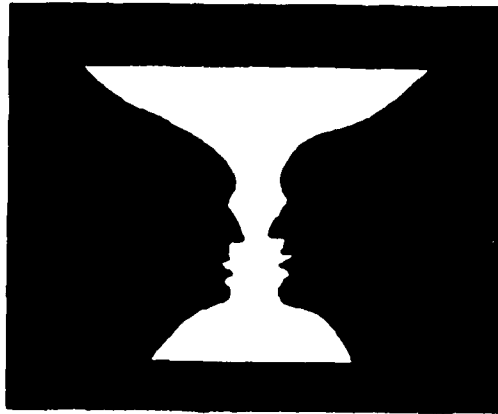


Figure 73. The Rubin Face-Vase Object: (a) Original Object; (b) Low-Pass (8 by 8) Filtered Images; (c) Low-Pass (6 by 6) Filtered Images; (d) Low-Pass (4 by 4) Filtered Images; (e) and (f) Two Variations of the Rubin Face-Vase Object; (1) Magnitude Spectra; (2) Filtered Images. (Section 13.4) (cont.)

(e)



(f)

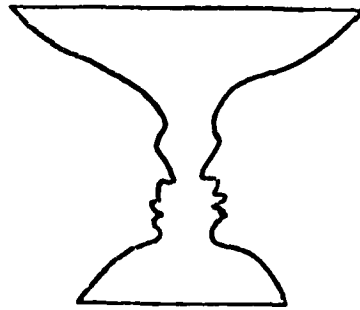


Figure 73. The Rubin Face-Vase Object: (a) Original Object; (b) Low-Pass (8 by 8) Filtered Images; (c) Low-Pass (6 by 6) Filtered Images; (d) Low-Pass (4 by 4) Filtered Images; (e) and (f) Two Variations of the Rubin Face-Vase Object; (1) Magnitude Spectra; (2) Filtered Images. (Section 13.4) (cont.)

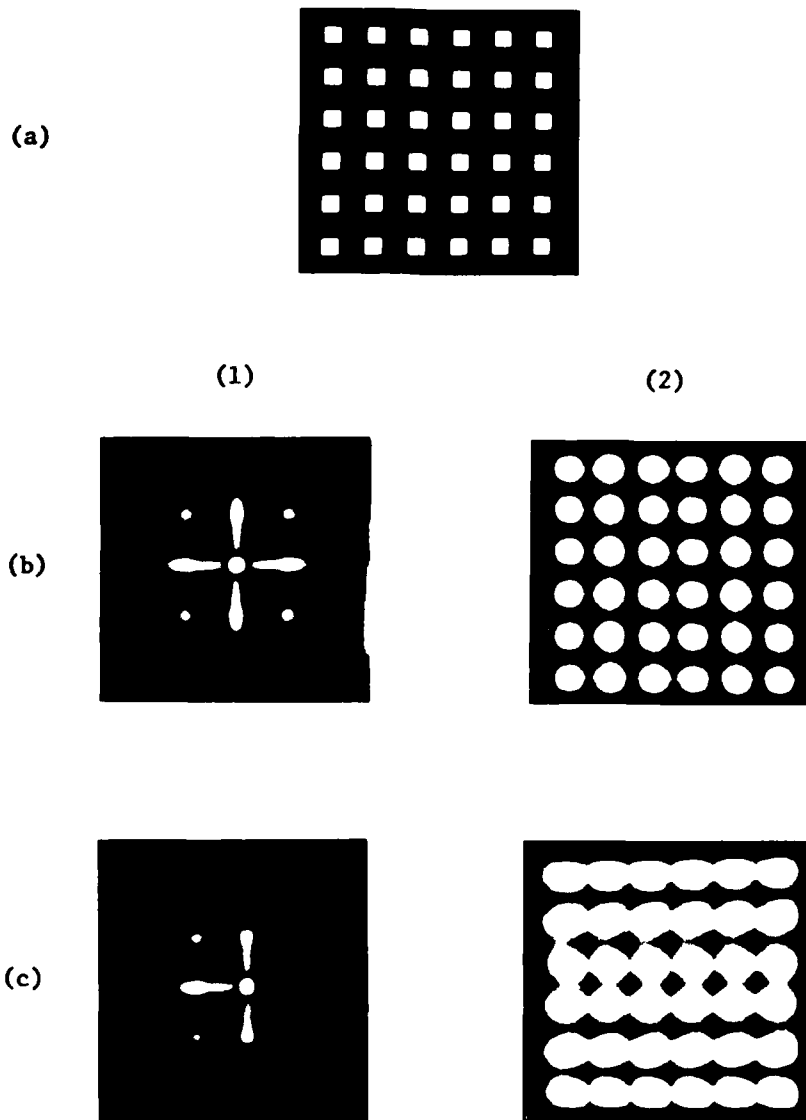


Figure 74. Multistable Dot Pattern: (a) Original Pattern; (b) MTF(L) Filtered; (c) Low-Pass (6 by 6) Filtered, Shifted (-6,0) Harmonics; (d) Low-Pass (6 by 6) Filtered, Shifted (-7,0) Harmonics; (e) Low-Pass (6 by 6) Filtered, Shifted (0,-6) Harmonics; (f) Low-Pass (6 by 6) Filtered, Shifted (0,-7) Harmonics; (1) Filtered Magnitude Spectra; (2) Filtered Dot Patterns. (Section 13.5)

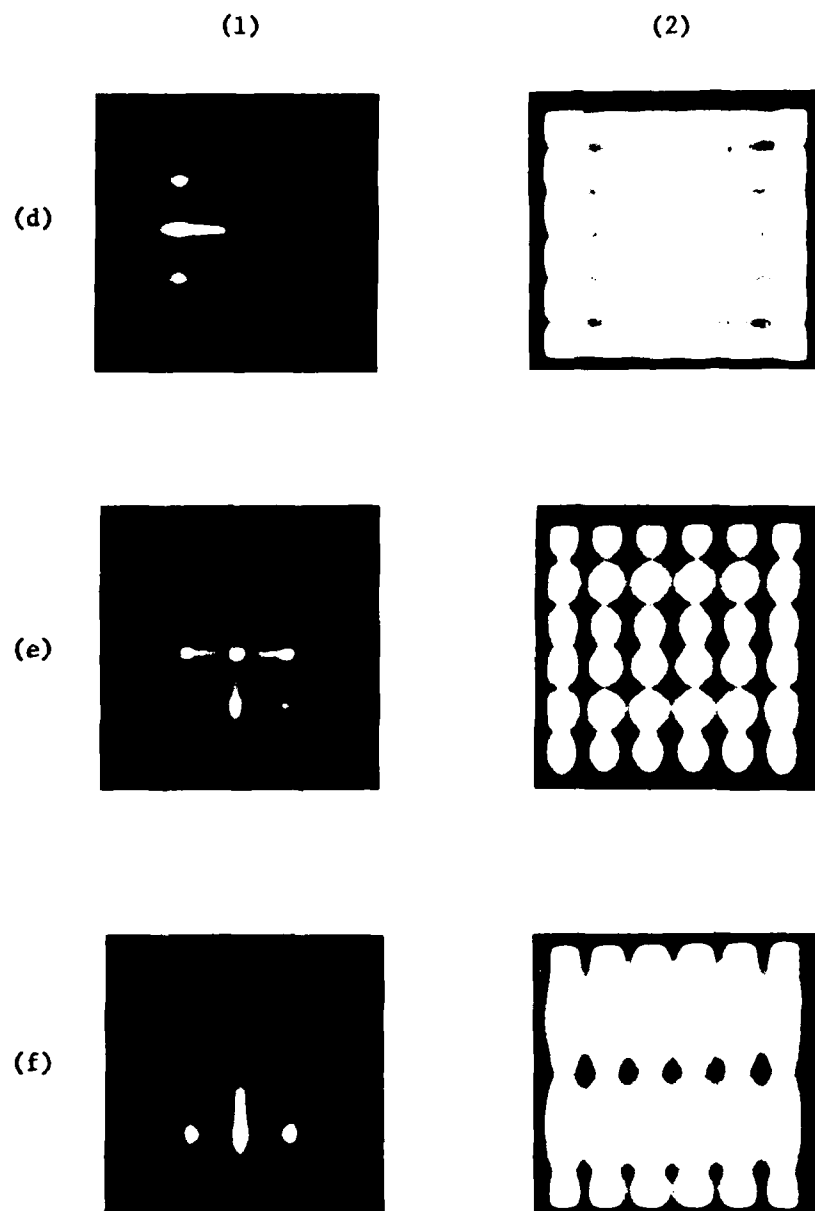


Figure 74. Multistable Dot Pattern: (a) Original Pattern; (b) MTF(L) Filtered; (c) Low-Pass (6 by 6) Filtered, Shifted (-6,0) Harmonics; (d) Low-Pass (6 by 6) Filtered, Shifted (-7,0) Harmonics; (e) Low-Pass (6 by 6) Filtered, Shifted (0,-6) Harmonics; (f) Low-Pass (6 by 6) Filtered, Shifted (0,-7) Harmonics; (1) Filtered Magnitude Spectra; (2) Filtered Dot Patterns. (Section 13.5) (cont.)

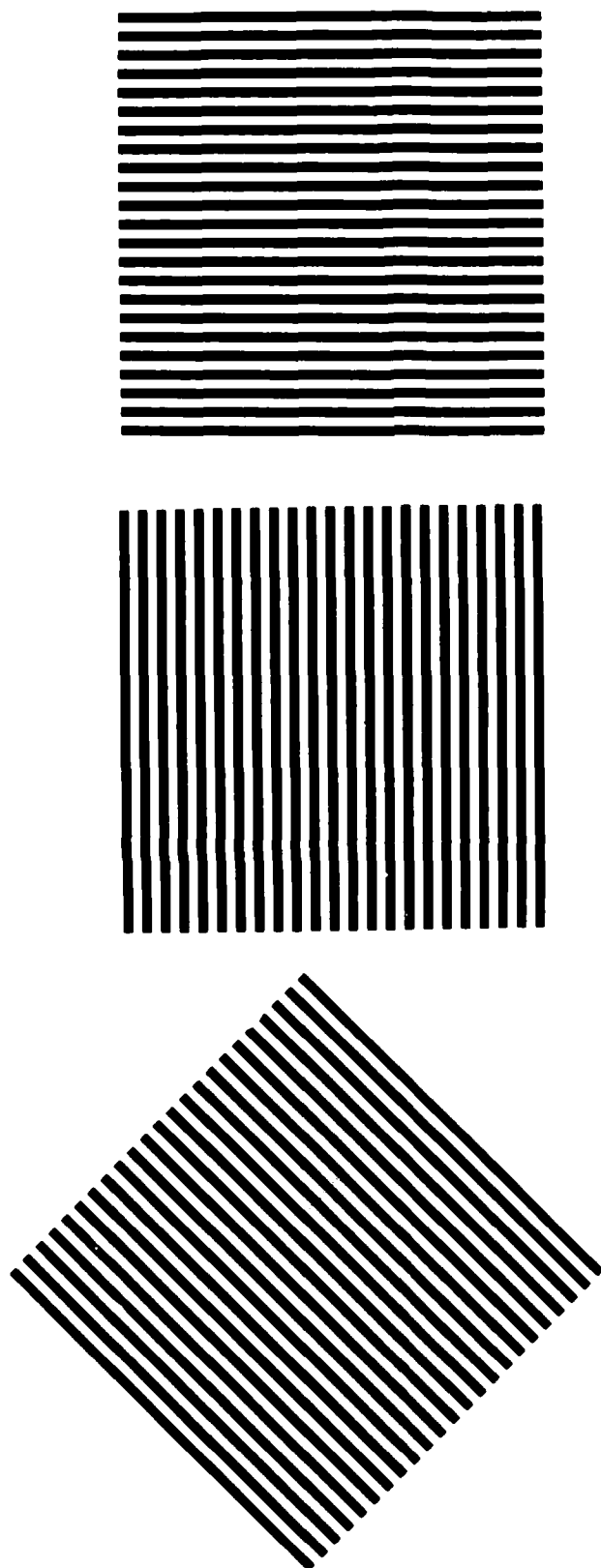


Figure 15. Square-Wave Gratings at Three Orientations. (Sections 13.5, 13.6)

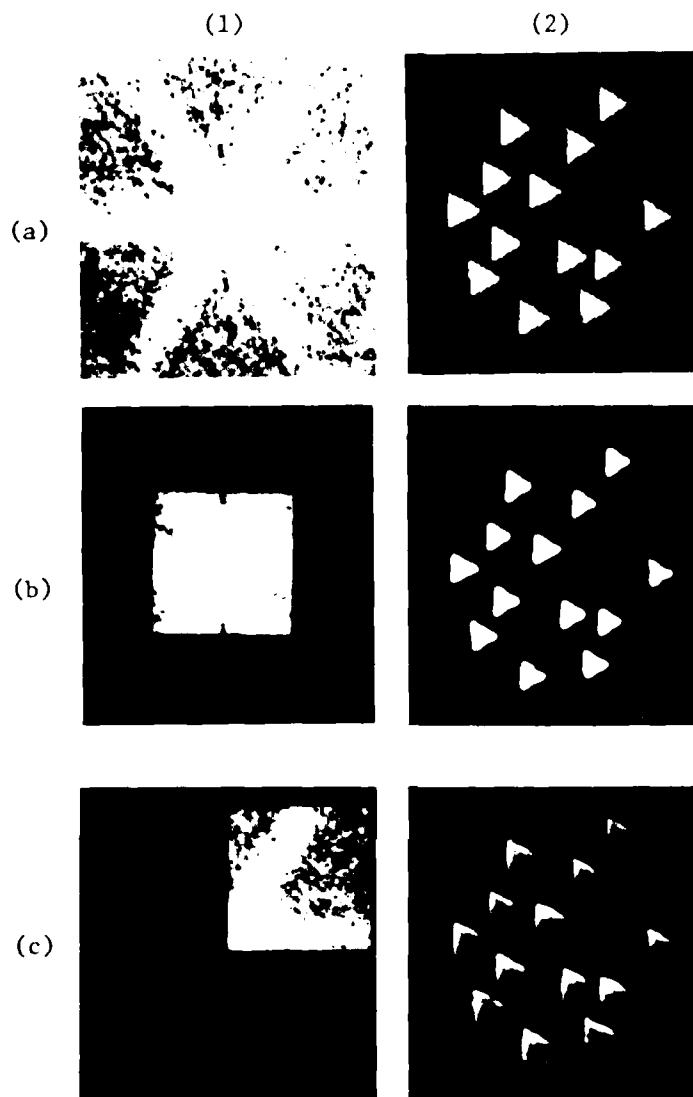


Figure 76. Multistable Triangles — Equilateral and Random:  
 (a) Original Images; (b) Low-Pass (24 by 24) Filtered  
 Images; (c), (d), and (e) Low-Pass (24 by 24) Filter  
 Shifted over the Magnitude Spectrum to Filter Three  
 Different Combinations of Two Channels; (f) Combination  
 of Three Channels; (1) Magnitude Spectra; (2) Triangles.  
 (Section 13.6)

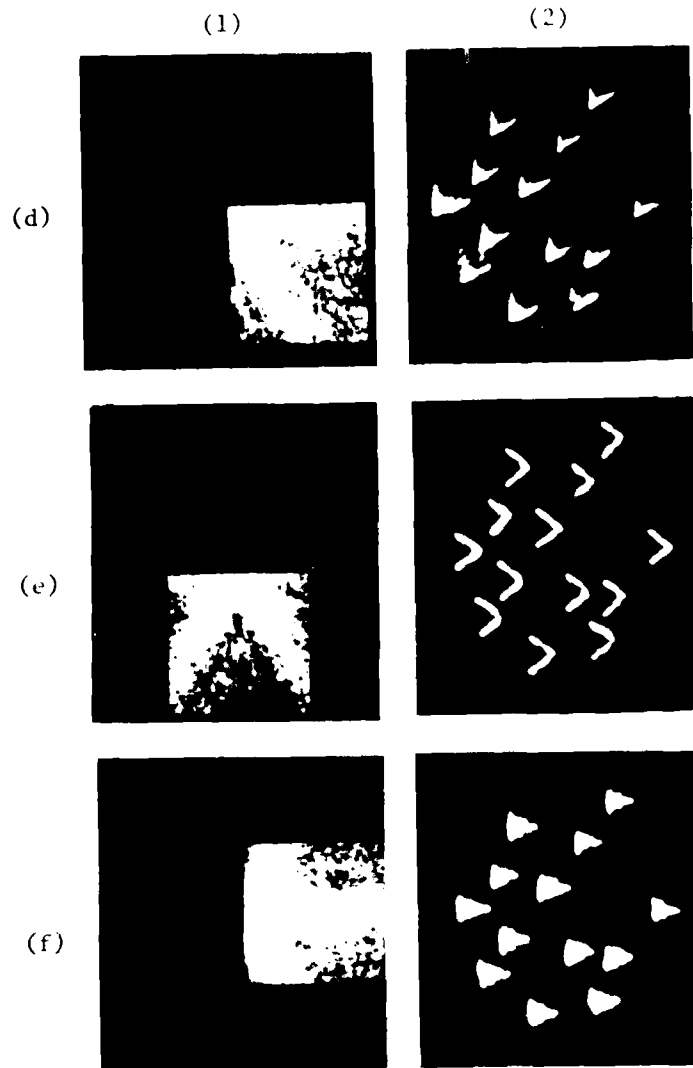


Figure 76. Multistable Triangles — Equilateral and Random:  
 (a) Original Images; (b) Low-Pass (24 by 24) Filtered  
 Images; (c), (d), and (e) Low-Pass (24 by 24) Filter  
 Shifted over the Magnitude Spectrum to Filter Three  
 Different Combinations of Two Channels; (f) Combination  
 of Three Channels; (1) Magnitude Spectra; (2) Triangles.  
 (Section 13.6) (cont.)



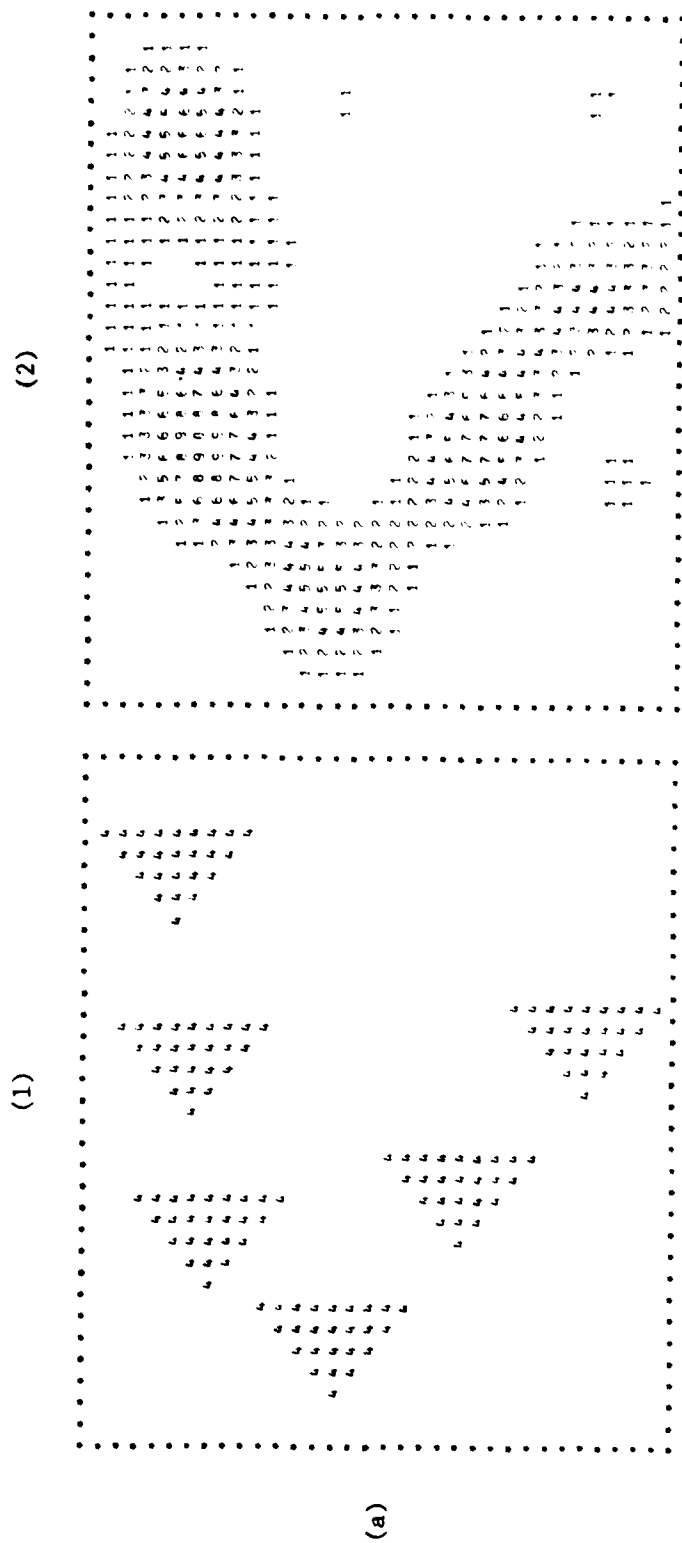


Figure 7.7. Numerical Printouts of Equilateral Multistable Triangles and Collinear Multistable Diamonds; (a) Equilateral Multistable Triangles; (b) Collinear Multistable Diamonds; (1) Original Objects; (2) Low-Pass (2 by 2) Filtered Images; (Section 1.3.6)

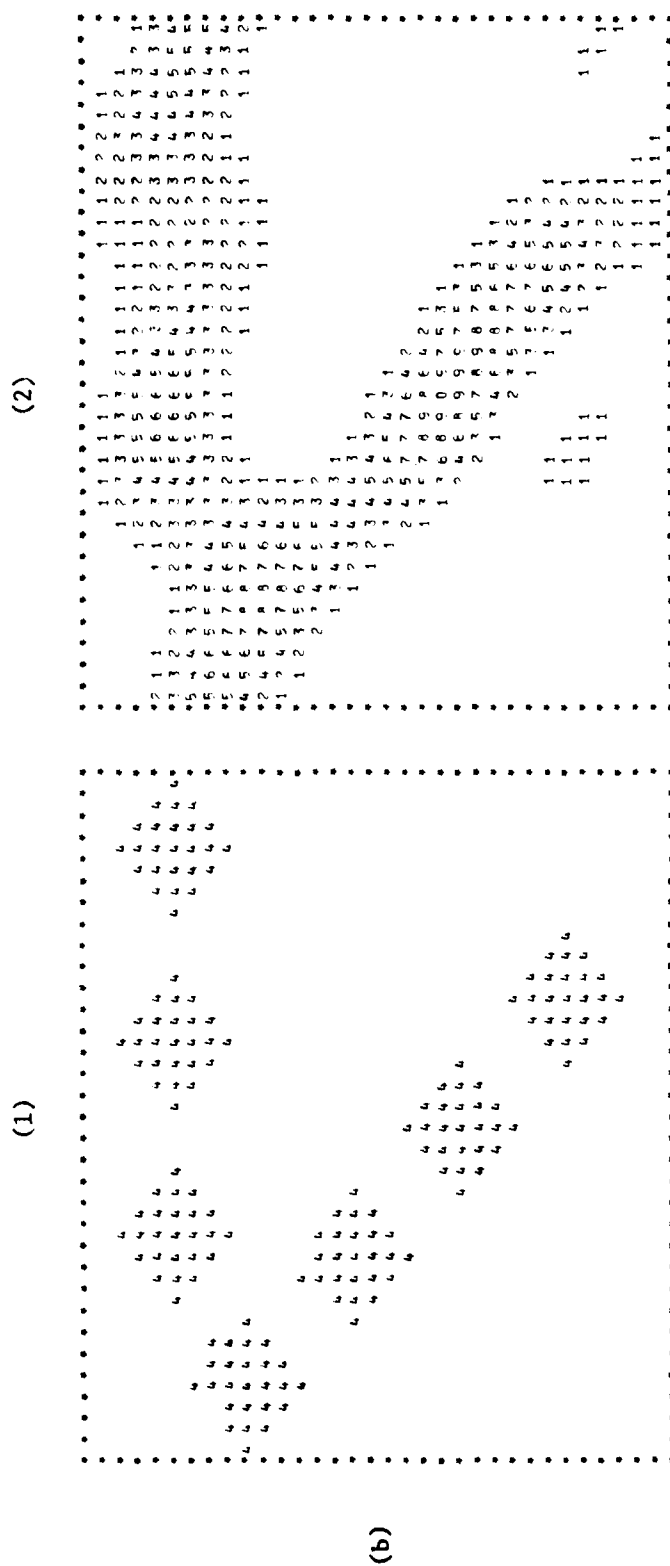


Figure 7.7. Numerical Printouts of Equilateral Multistable Triangles and Collinear Multistable Diamonds: (a) Equilateral Multistable Triangles; (b) Collinear Multistable Diamonds: (1) Original Objects; (2) Low-Pass (2 by 2) Filtered Images. (Section 13.6) (cont.)

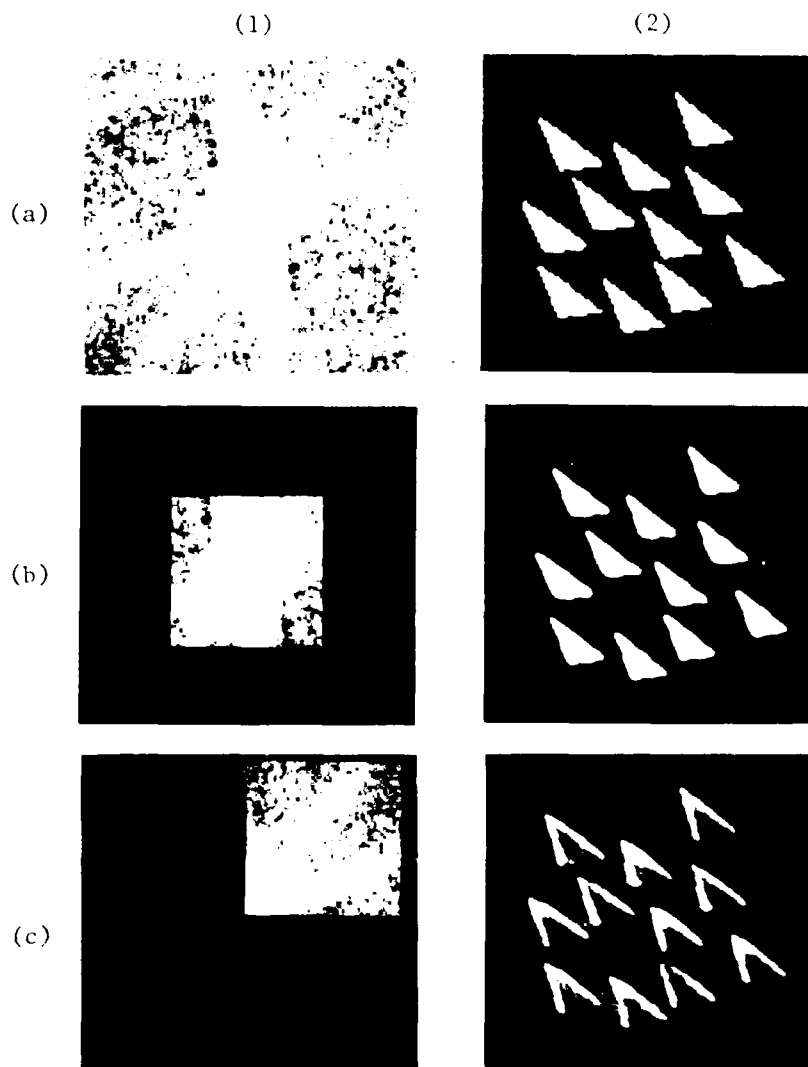


Figure 78. Multistable Triangles — Scalene and Random:  
 (a) Original Images; (b) Low-Pass (24 by 24) Filtered  
 Images; (c), (d), and (e) Low-Pass (24 by 24) Filter  
 Shifted over the Magnitude Spectrum to Filter Three  
 Different Combinations of Two Channels; (1) Magnitude  
 Spectra; (2) Triangles. (Section 13.6)

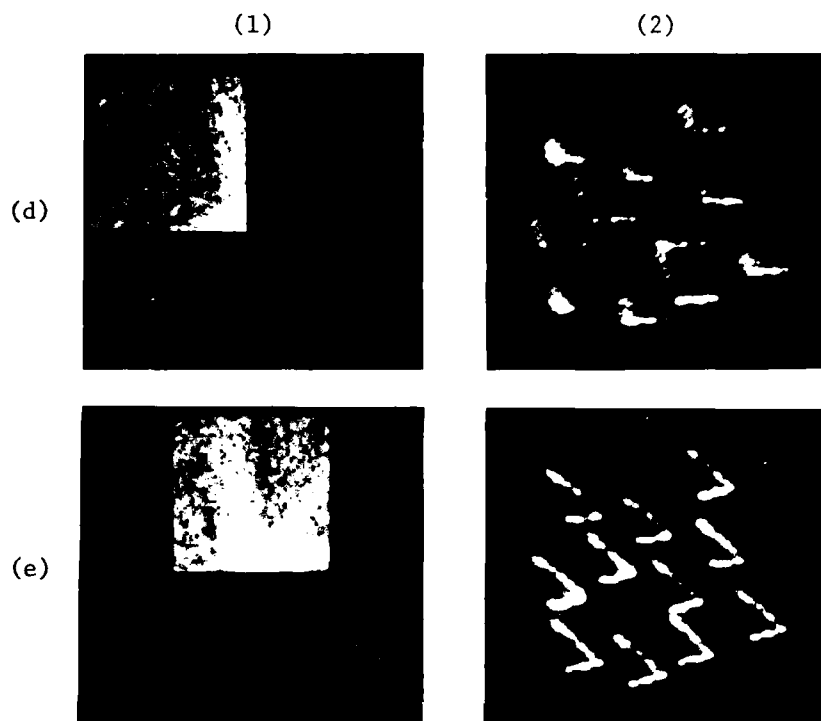


Figure 78. Multistable Triangles — Scalene and Random: (a) Original Images; (b) Low-Pass (24 by 24) Filtered Images; (c), (d), and (e) Low-Pass (24 by 24) Filter Shifted over the Magnitude Spectrum to Filter Three Different Combinations of Two Channels; (1) Magnitude Spectra; (2) Triangles. (Section 13.6) (cont.)

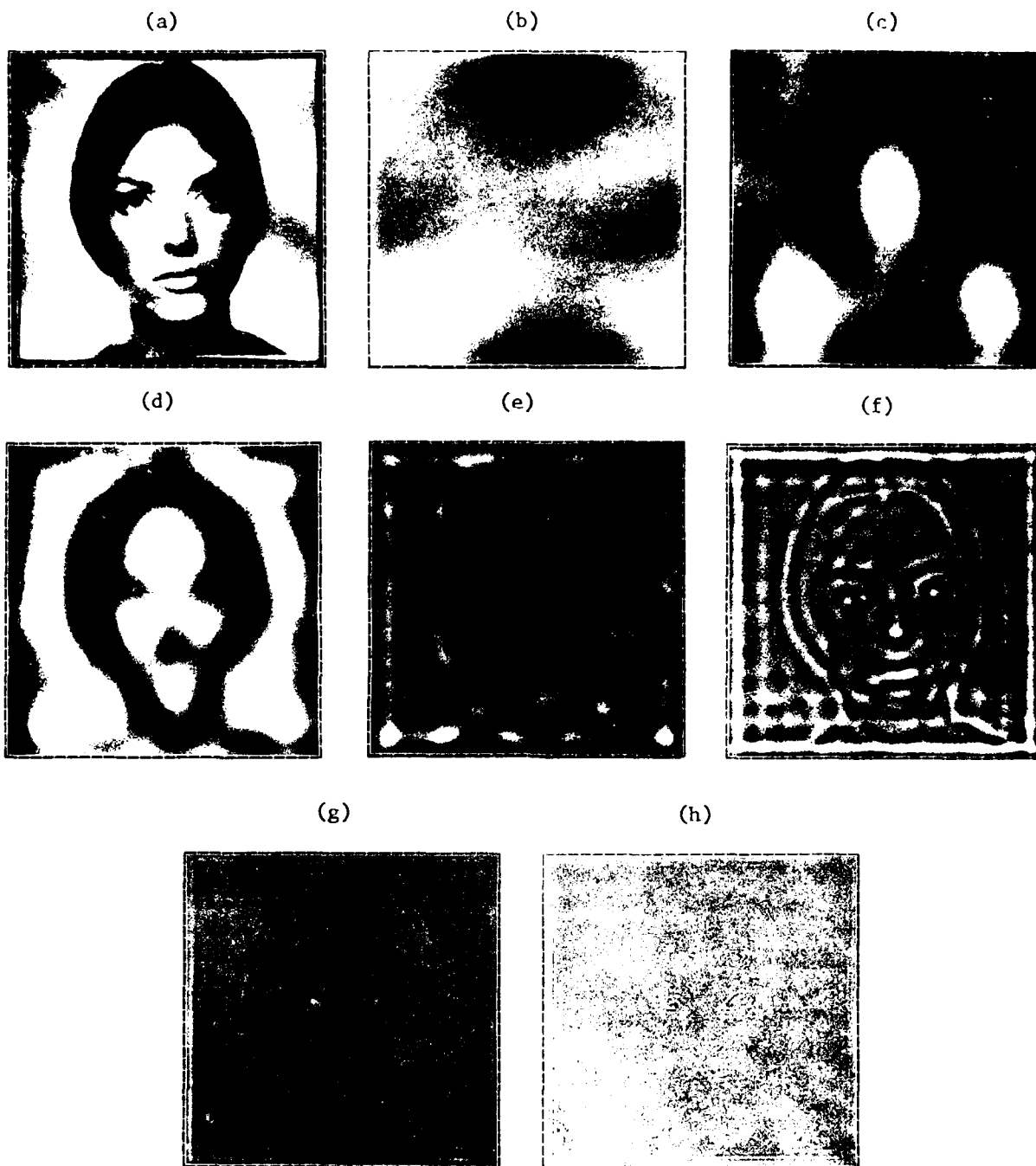


Figure 79. One-Octave Band-Pass Filtered Portrait.  $f_c$  = Centre Frequency of Filter: (a) Original Portrait; (b)  $f_c = 1$ ; (c)  $f_c = 2$ ; (d)  $f_c = 4$ ; (e)  $f_c = 8$ ; (f)  $f_c = 16$ ; (g)  $f_c = 32$ ; (h)  $f_c = 64$ . (Section 14.3)

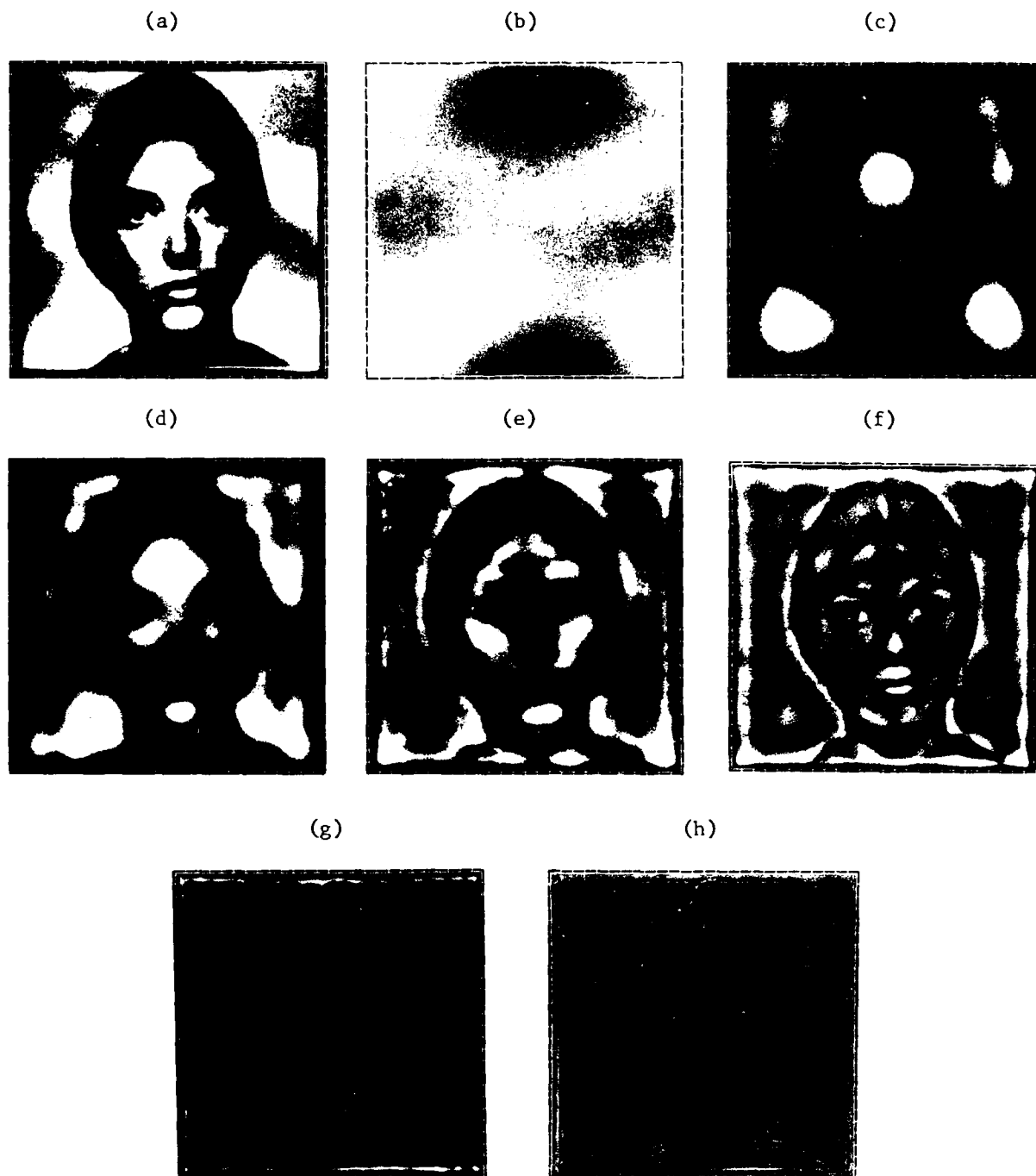


Figure 80. Two-Octave Band-Pass Filtered Portrait.  $f_c$  = Centre Frequency:  
 (a) Original Portrait; (b)  $f_c = 1$ ; (c)  $f_c = 2$ ; (d)  $f_c = 4$ ; (e)  $f_c = 8$ ;  
 (f)  $f_c = 16$ ; (g)  $f_c = 32$ ; (h)  $f_c = 64$ . (Section 14.3)

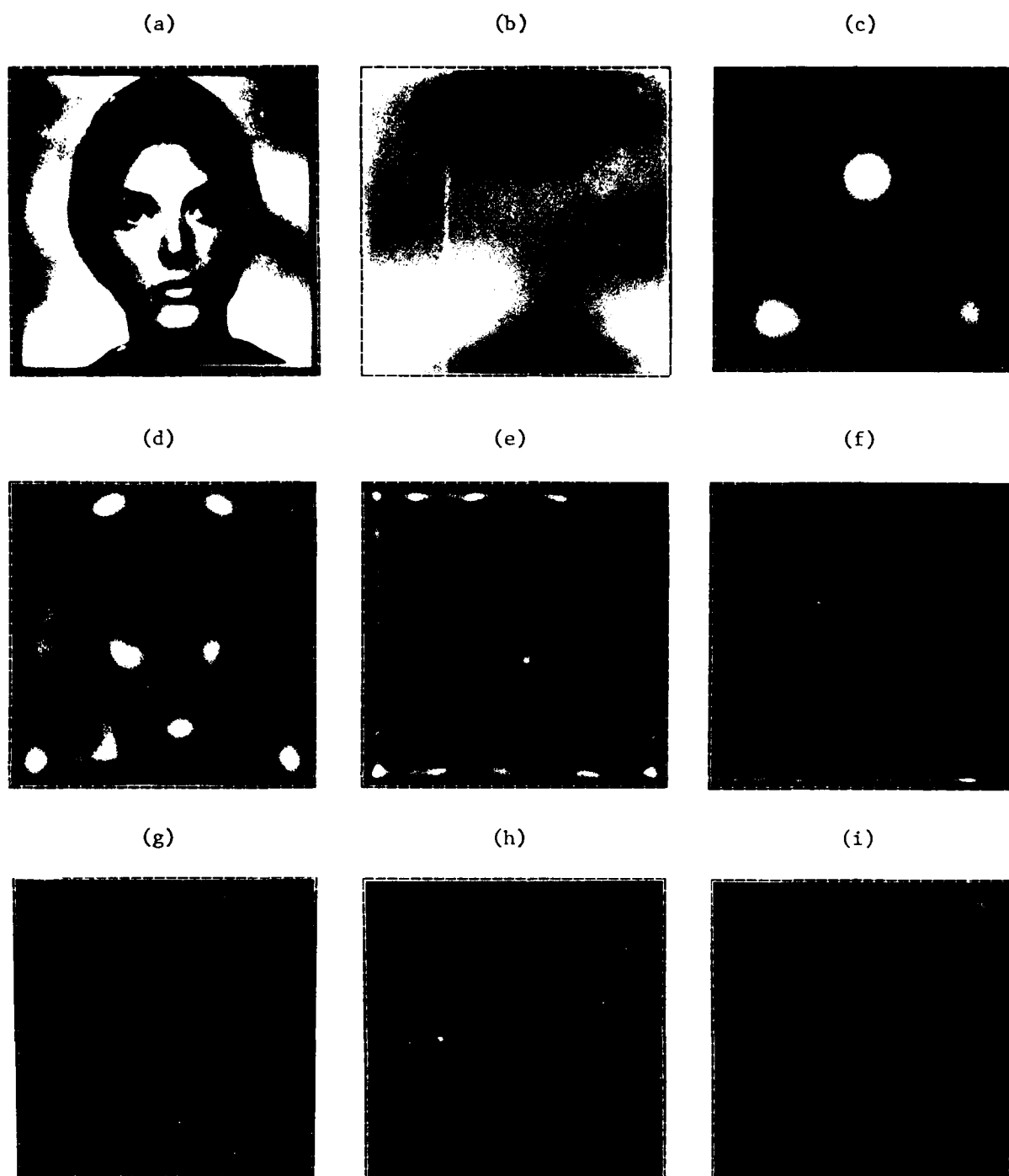


Figure 81. One-Octave Band-Pass Filtered Portrait Having a Higher Centre Frequency.  $f_c$  = Centre Frequency of Filter: (a) Original Portrait; (b)  $f_c = 2$ ; (c)  $f_c = 4.5$ ; (d)  $f_c = 9$ ; (e)  $f_c = 18$ ; (f)  $f_c = 36$ ; (g)  $f_c = 72$ ; (h)  $f_c = 112$ ; (i)  $f_c = 128$ . (Section 14.3)

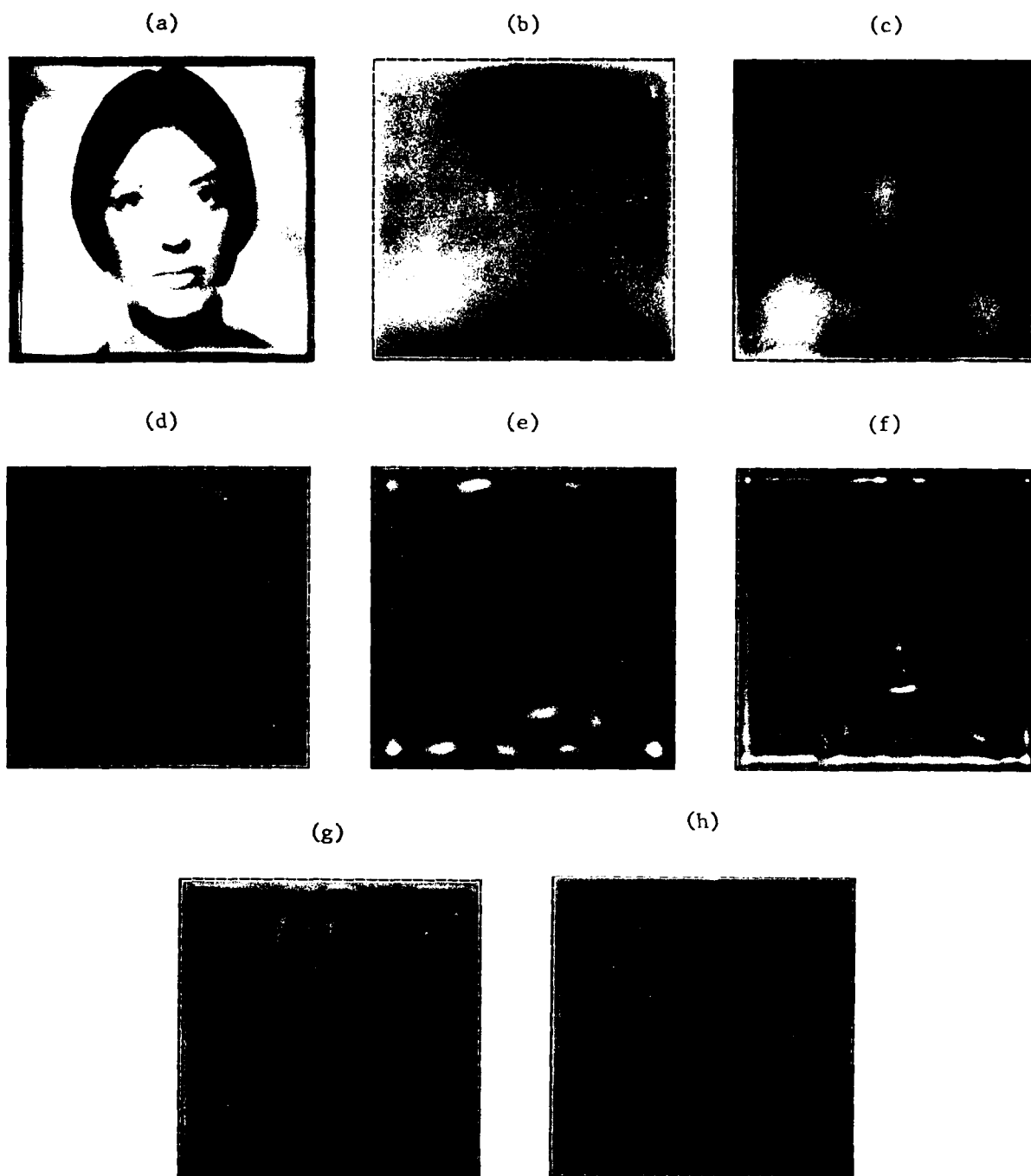


Figure 82. One-Octave Channel Filtered Portrait.  $f_c$  = Centre Frequency of Filter: (a) Original Portrait; (b)  $f_c = 1$ ; (c)  $f_c = 2$ ; (d)  $f_c = 4$ ; (e)  $f_c = 8$ ; (f)  $f_c = 16$ ; (g)  $f_c = 32$ ; (h)  $f_c = 64$ . (Section 14.3)



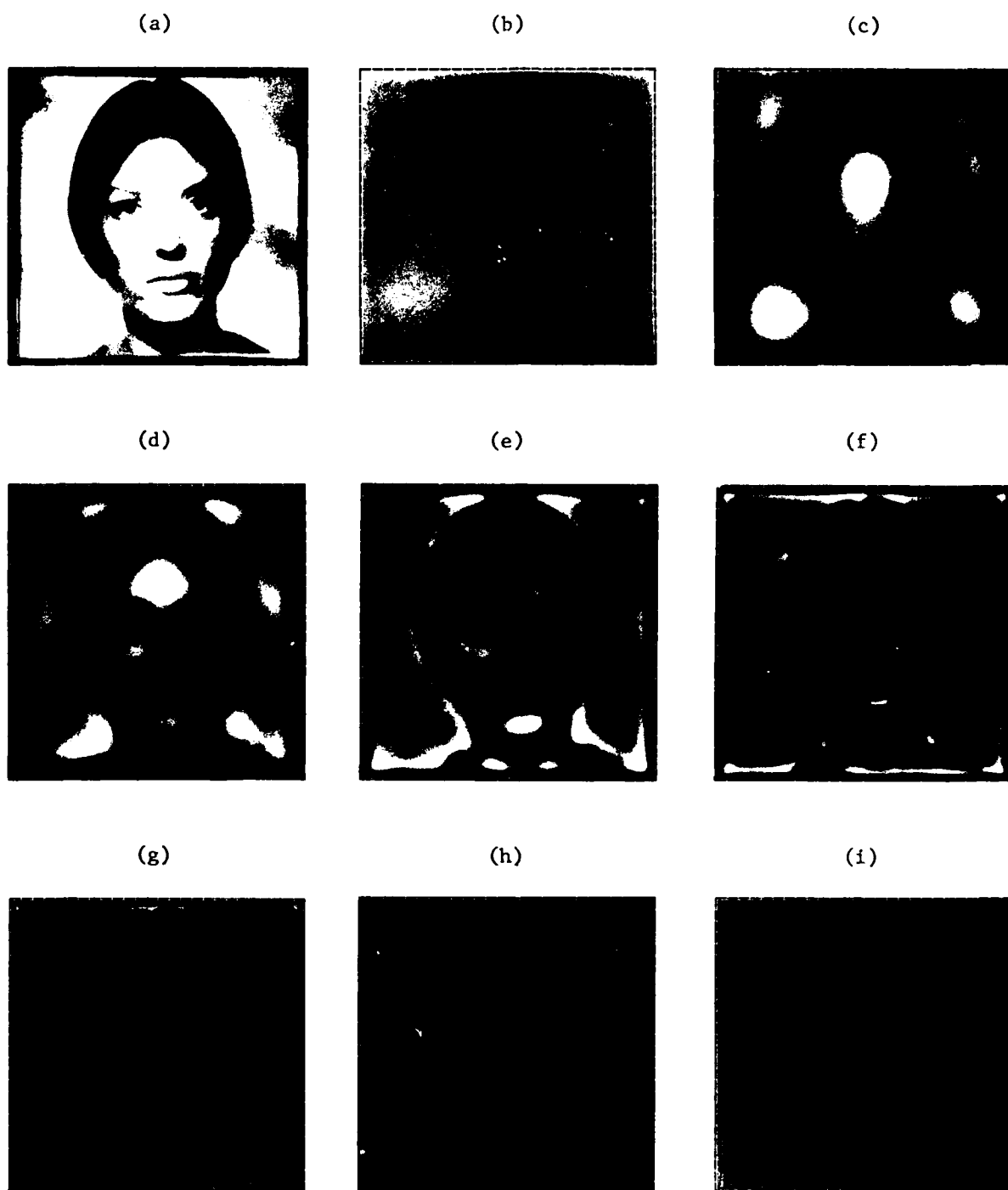


Figure 83. Two-Octave Channel Filtered Portrait.  $f_c$  = Centre Frequency of Filter: (a) Original Portrait; (b)  $f_c = 1$ ; (c)  $f_c = 2$ ; (d)  $f_c = 4$ ; (e)  $f_c = 8$ ; (f)  $f_c = 16$ ; (g)  $f_c = 32$ ; (h)  $f_c = 64$ ; (i)  $f_c = 128$ . (Section 14.3)

<u>SNELLEN LINE NUMBER</u>		<u>SIZE OF LETTER</u>			<u>SPATIAL FREQUENCIES OF LETTERS (c/d)</u>				
		<u>min</u>	<u>c/d</u>	<u>.5</u>	<u>1.0</u>	<u>1.5</u>	<u>2.0</u>	<u>2.5</u>	
6/60	20/200	50.0	1.2	0.6	1.2	1.8	2.8	3.0	
6/36	20/120	30.0	2.0	1.0	2.0	3.0	4.0	5.0	
6/24	20/80	20.0	3.0	4.5	3.0	4.5	6.0	7.5	
6/18	20/60	15.0	4.0	2.0	4.0	6.0	8.0	10.0	
6/12	20/40	10.0	6.0	3.0	6.0	9.0	12.0	15.0	
6/9	20/30	7.5	8.0	4.0	8.0	12.0	16.0	20.0	
6/6	20/20	5.0	12.0	6.0	12.0	18.0	24.0	30.0	
6/5	20/15	4.2	14.4	7.2	14.4	21.6	28.8	36.0	
6/3	20/10	2.5	24.0	12.0	24.0	36.0	48.0	60.0	

Figure 84. Table of First 2.5 Cycles of Letters Associated with Each Snellen Line Number. (Section 16.2)

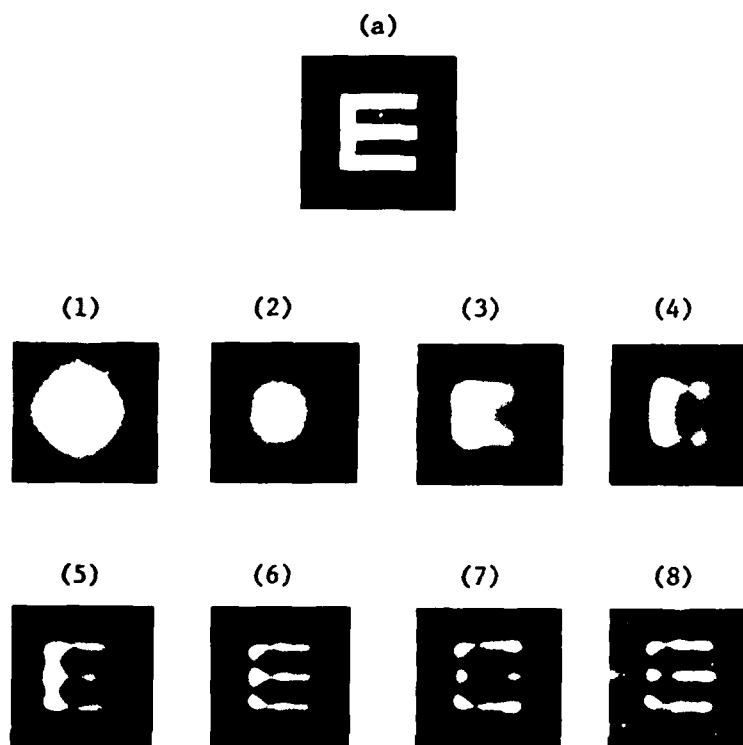


Figure 85. Synthesis of Snellen Letters: (a) Letter E; (b) Letter L;  
 (1) Low-Pass (1.5 c/Letter) Filtered Letters;  
 (2) Low-Pass (1.0 c/Letter) Filtered Letters;  
 (3) Low-Pass (1.5 c/Letter) Filtered Letters;  
 (4) Low-Pass (2.0 c/Letter) Filtered Letters;  
 (5) Low-Pass (2.5 c/Letter) Filtered Letters;  
 (6) Low-Pass (3.0 c/Letter) Filtered Letters;  
 (7) Band-Pass (1.5 - 3 c/Letter) Filtered Letters  
 (8) Band-Pass (2 - 3 c/Letter) Filtered Letters.  
 (Section 16.3)

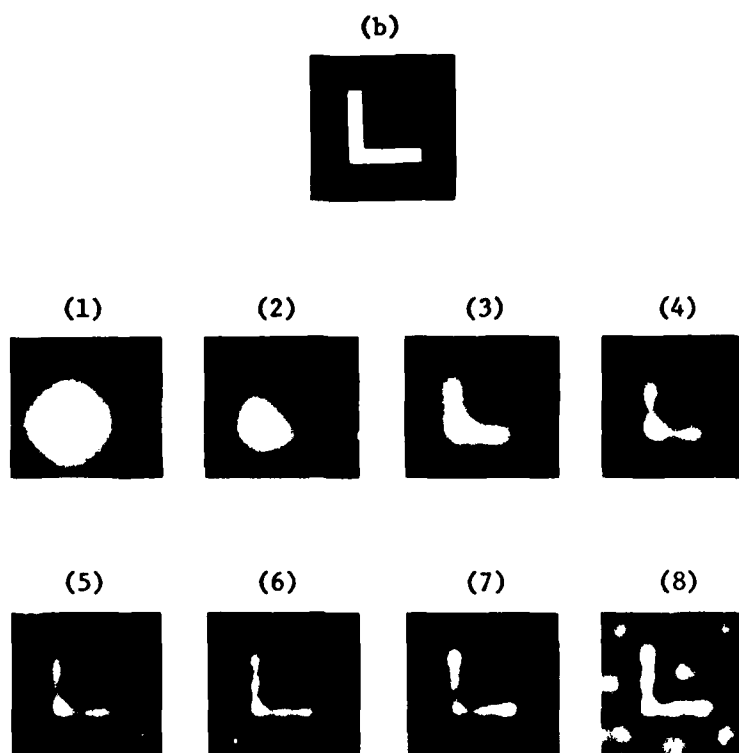


Figure 85. Synthesis of Snellen Letters: (a) Letter E; (b) Letter L;  
 (1) Low-Pass (.5 c/Letter) Filtered Letters;  
 (2) Low-Pass (1.0 c/Letter) Filtered Letters;  
 (3) Low-Pass (1.5 c/Letter) Filtered Letters;  
 (4) Low-Pass (2.0 c/Letter) Filtered Letters;  
 (5) Low-Pass (2.5 c/Letter) Filtered Letters;  
 (6) Low-Pass (3.0 c/Letter) Filtered Letters;  
 (7) Band-Pass (1.5 - 3 c/Letter) Filtered Letters;  
 (8) Band-Pass (2 - 3 c/Letter) Filtered Letters.  
 (Section 16.3) (cont.)

H  
A V  
L T J  
V O A  
T X A L  
O A N V Z  
H Z N V T U E  
N O H X E Z A U

Figure 86. Snellen Letter Acuity Chart Used in Experiments. (Section 17.2)

SNELLEN LINE NUMBER	POLAROID ANGLE FOR EACH SUBJECT (DEG)				AVERAGE POLAROID ANGLE (DEG)	CONTRAST			CONTRAST SENSITIVITY		
	JF	DP	HH	CH		-2 S.E.	AVE	+2 S.E.	-2 S.E.	AVE	+2 S.E.
6/60	D 11	11.8	13	11	11.9	.021	.024	.028	35.7	42.4	47.6
	I 14	11.8	13	11	12.5	.022	.025	.031	32.3	39.9	45.5
6/36	D 9	12	12	13.2	12.2	.017	.025	.033	30.3	40.9	58.8
	I 11.5	12	13	13.5	13.0	.023	.028	.033	30.3	36.6	43.5
6/24	D 9	12	13	13	13.4	.018	.025	.034	29.4	40.5	55.6
	I 14	14	15	15.5	14.9	.032	.036	.041	34.4	27.7	30.3
6/18	D 12	12.2	10	12	12.0	.019	.024	.030	33.3	41.2	52.6
	I 15.5	14	17	15.9	15.6	.037	.040	.460	21.7	25.1	27.0
6/12	D 11.2	14.5	14	15	14.2	.026	.034	.043	23.3	29.3	38.5
	I 15.8	17.2	21	20	19.1	.047	.060	.076	13.3	16.6	31.3
6/9	D 12	16.8	17	12	14.9	.026	.036	.050	20.0	27.5	38.5
	I 21	21	28	25	23.8	.072	.092	.113	8.8	10.8	13.9
6/6	D 13	17.5	17	18	16.1	.03	.042	.059	16.9	23.7	29.4
	I 28	30	27	29	29.8	.120	.140	.164	6.1	7.1	8.3
6/5	D 21	18	18	19	19.0	.054	.060	.068	14.7	16.6	18.5
	I 35	50	-	50	45.0	.217	.28	.369	2.7	3.6	4.6

D = DETECTION THRESHOLD

I = IDENTIFICATION THRESHOLD

Figure 87. Table of Contrast and Contrast Sensitivity Required for Detection and Identification of Snellen Letters.  
(Section 17.3)

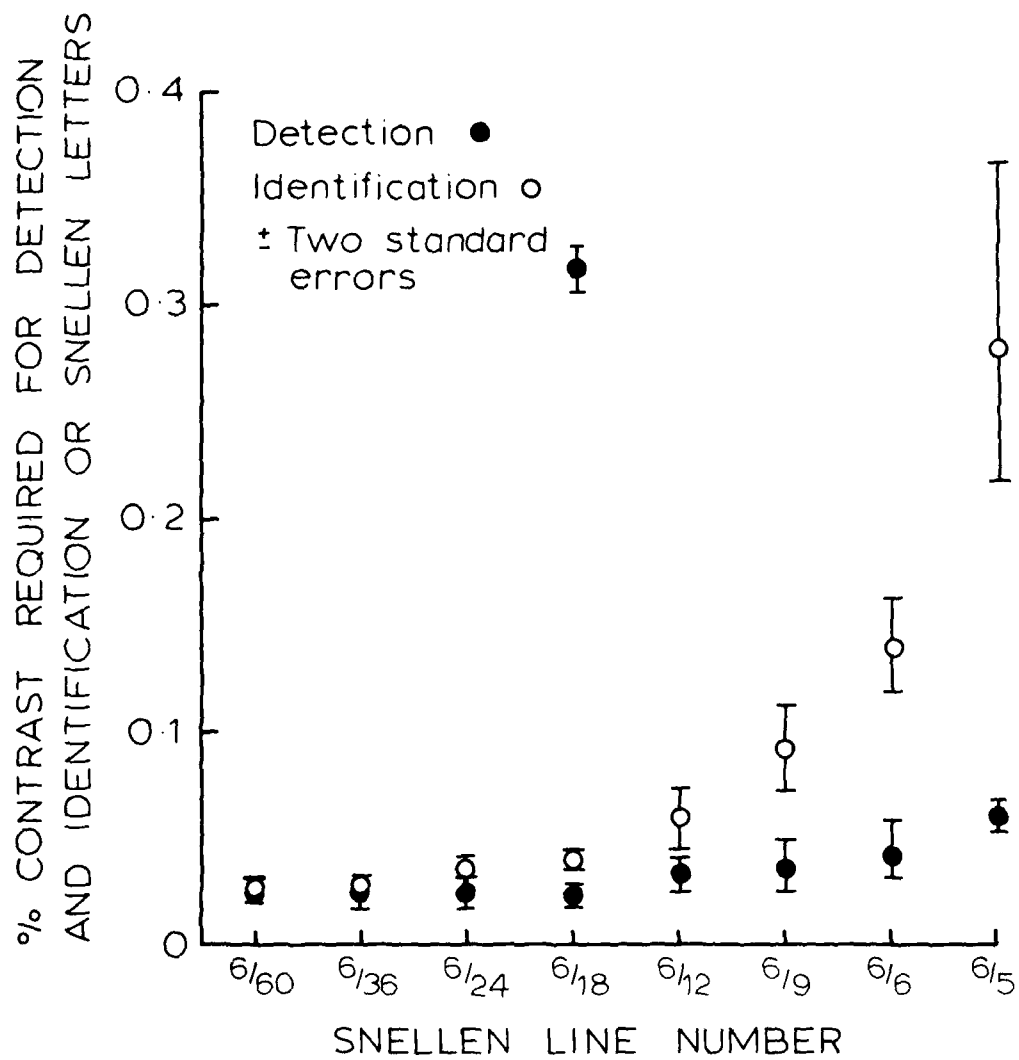


Figure 88. The Percent Contrast Required for the Detection and Identification of Snellen Letters for Each Snellen Line. (Section 17.3)

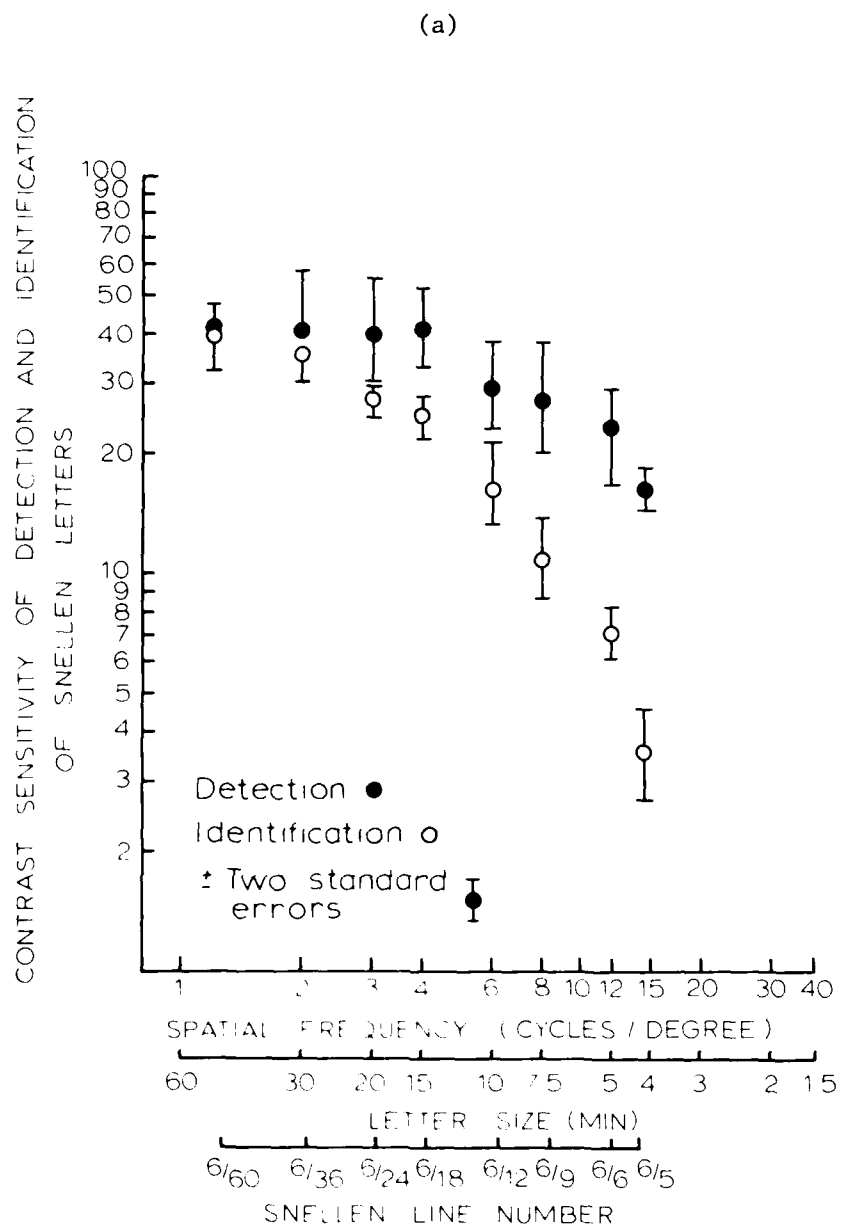


Figure 89. Contrast Sensitivity Required for the Detection and Identification of Snellen Letters for Each Snellen Line: (a) Log Contrast Sensitivity - Log Spatial Frequency; (b) Log Contrast Sensitivity - Linear Spatial Frequency. (Section 17.3)



CONTRAST SENSITIVITY OF DETECTION AND IDENTIFICATION  
OF SNELLEN LETTERS

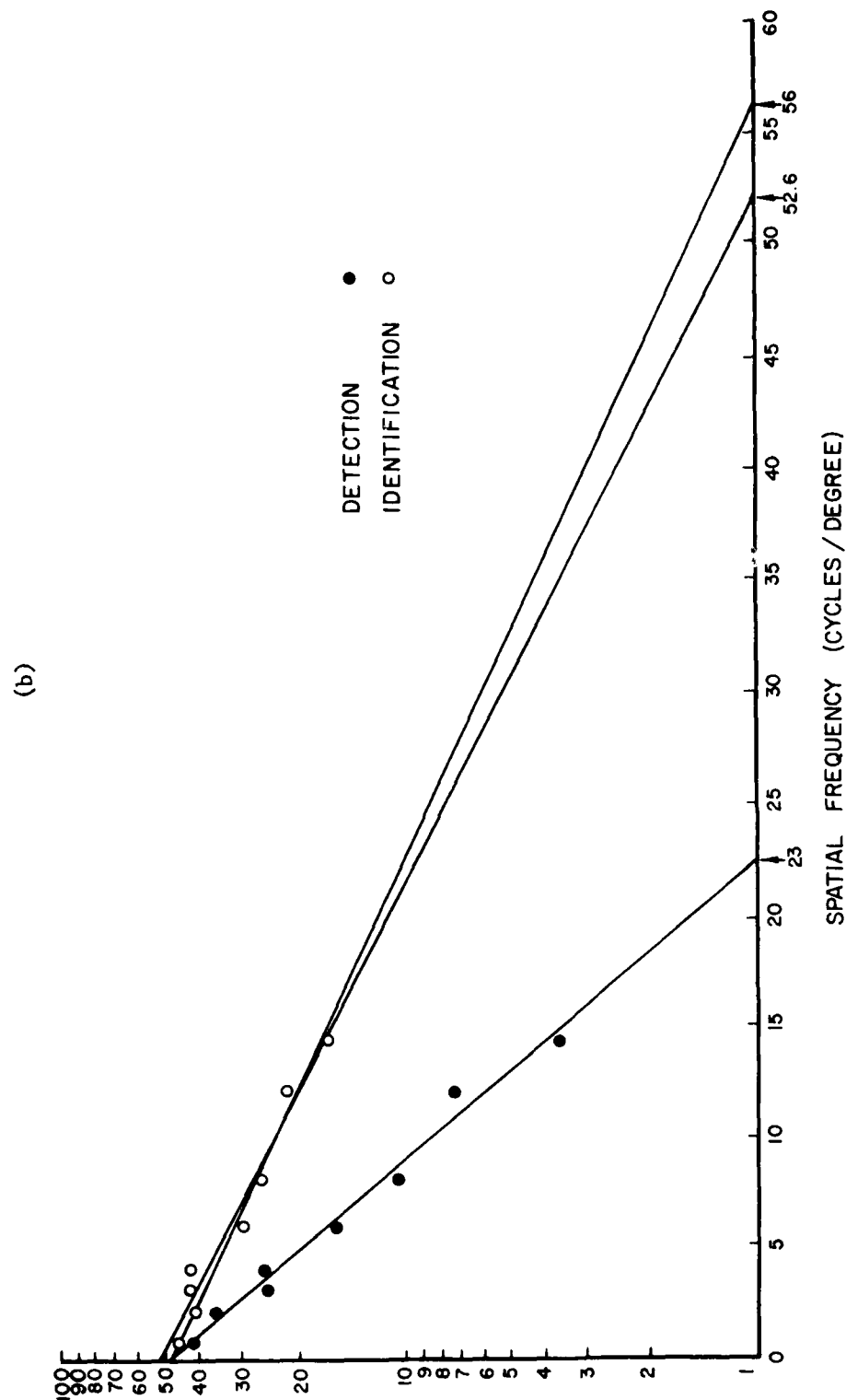


Figure 80. Contrast Sensitivity Required for the Detection and Identification of Snellen Letters for Each Snellen Line:  
(a) Log Contrast Sensitivity - Log Spatial Frequency; (b) Log Contrast Sensitivity - Linear Spatial Frequency.  
(Section 17.3) (cont.)

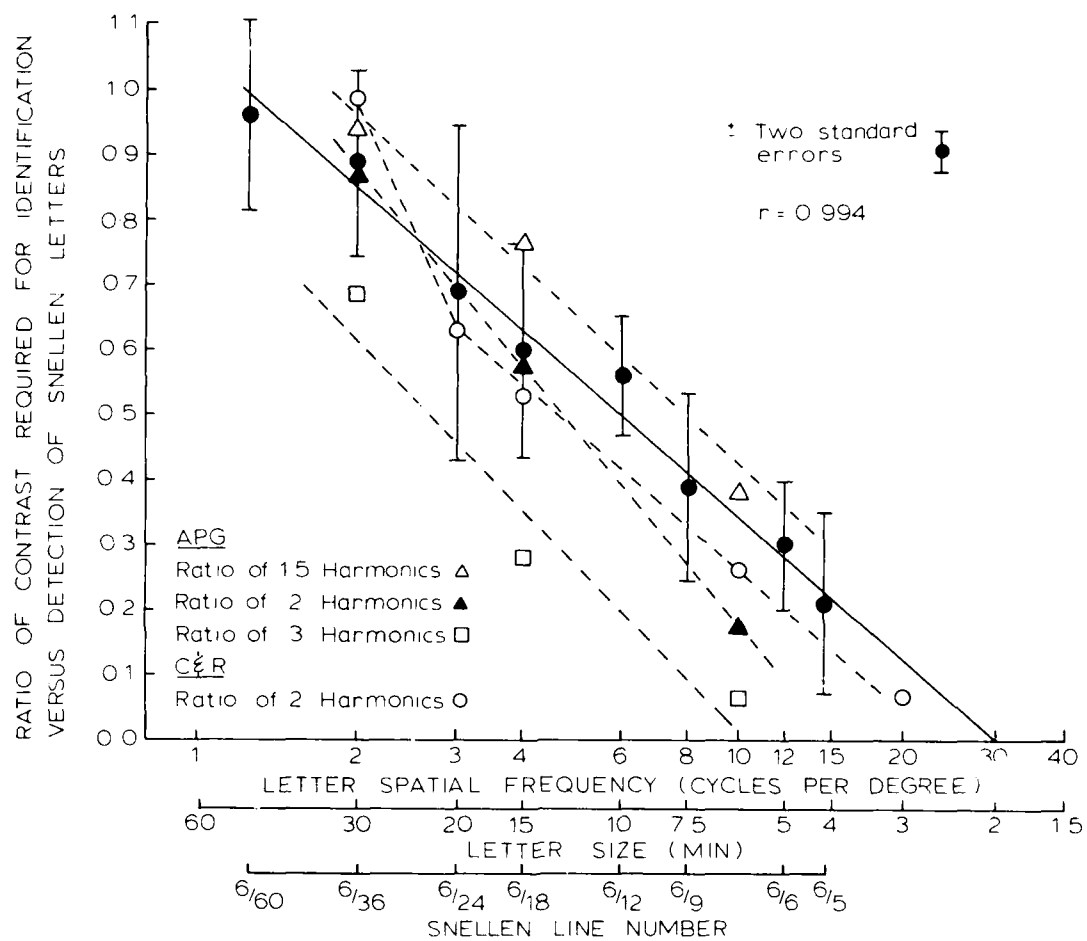


Figure 90. Ratio of Contrast Required for Identification Versus Detection of Snellen Letters as a Function of Snellen Line Number. (Section 17.3)

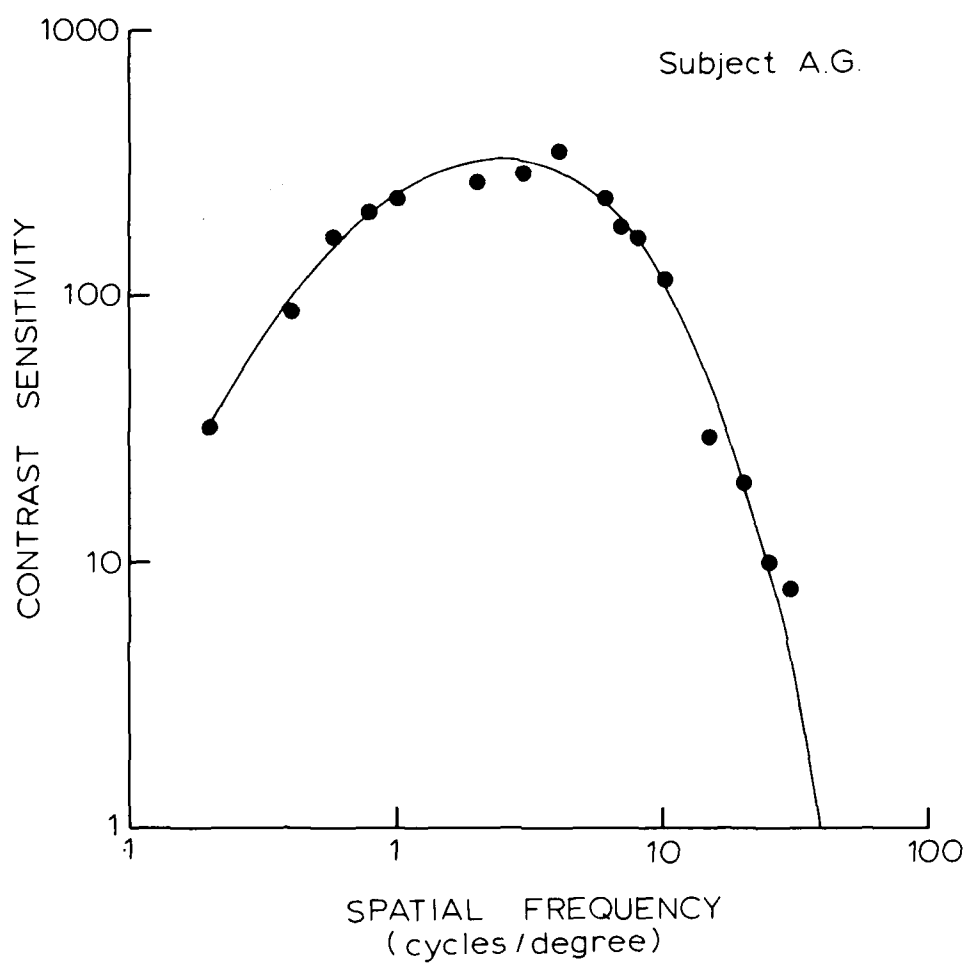


Figure 91. Contrast Sensitivity Function of Subject A.G. (Section 17.3)

<u>SNELLEN LINE NUMBER</u>		<u>SPATIAL FREQUENCIES OF LETTERS REQUIRED FOR IDENTIFICATION</u>			<u>CONTRAST SENSITIVITY REQUIRED FOR IDENTIFICATION</u>		
		<u>(c/d)</u>					
		<u>1.5</u>	<u>2.0</u>	<u>2.5</u>	<u>-2 S.E.</u>	<u>AVE</u>	<u>+2 S.E.</u>
6/60	20/200	1.8	2.4	3.0	32.3	39.9	45.5
6/36	20/120	3.0	4.0	5.0	30.3	35.6	43.5
6/24	20/80	4.5	6.0	7.5	24.4	27.7	30.3
6/18	20/60	6.0	8.0	10.0	21.7	25.1	27.0
6/12	20/40	9.0	12.0	15.0	13.3	16.6	21.3
6/9	20/30	12.0	16.0	20.0	8.8	10.8	13.9
6/6	20/20	18.0	24.0	30.0	6.1	7.1	8.3
6/5	20/15	21.6	28.8	36.0	2.7	3.6	4.6

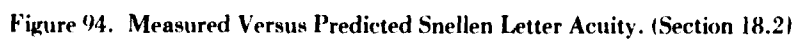
Figure 92. Table of Cycles and Associated Contrast Sensitivity Required for the Identification of Snellen Letters. (Section 18.1, 18.2)

SUBJECT	MEASURED SNELLEN LETTER ACUITY	MEASURED CONTRAST SENSITIVITY	PREDICTED SNELLEN LETTER ACUITY		
			AVE	$\pm 2$ S.E.	
JP	6/5(R)	3.2	6/6(R)	6/5(R)	*
	6/9(L)	8.9	6/12(L)	6/9(L)	*
MB	6/4(R)	3.6	6/4(R)	6/4(R)	*
	2/60(L)	51.2	6/60(L)	6/60(L)	
AH	6/5(R)	1.5	6/9(R)	6/9(R)	
	6/36(L)	10.2	6/60(L)	6/60(L)	†
AH	6/5(R)	6.2	6/5(R)	6/5(R)	*
	6/18(L)	24.1	6/18(L)	6/18(L)	*
RH	6/9(R)	15.2	6/9(R)	6/9(R)	*
	6/5(L)	6.4	6/5(L)	6/5(L)	*
MD	6/6(R)	2.5	6/12(R)	6/9(R)	†
	6/6(L)	1.3	6/18(L)	6/18(L)	
JJ	6/6(R)	2.3	6/9(R)	6/9(R)	†
	6/9(L)	4.8	6/24(L)	6/18(L)	
SS	6/6(R)	8.9	6/6(R)	6/6(R)	*
	6/6(L)	3.6	6/9(L)	6/9(L)	†
BM	6/6(R)	4.5	6/9(R)	6/9(R)	†
	6/6(L)	1.5	6/18(L)	6/18(L)	
HR	6/6(R)	3.8	6/9(R)	6/9(R)	†
	6/12(L)	5.1	6/18(L)	6/12(L)	*
CH	6/6(R)	15.2	6/6(R)	6/6(R)	*
	6/6(L)	8.9	6/6(L)	6/6(L)	*

\* = AGREEMENT BETWEEN MEASURED AND  
PREDICTED SNELLEN LETTER ACUITY

† = AGREEMENT OFF BY ONE SNELLEN LINE

Figure 93. Table of Predicted Snellen Letter Acuity from the Contrast Sensitivity of 10 Subjects.  
(Section 18.2)



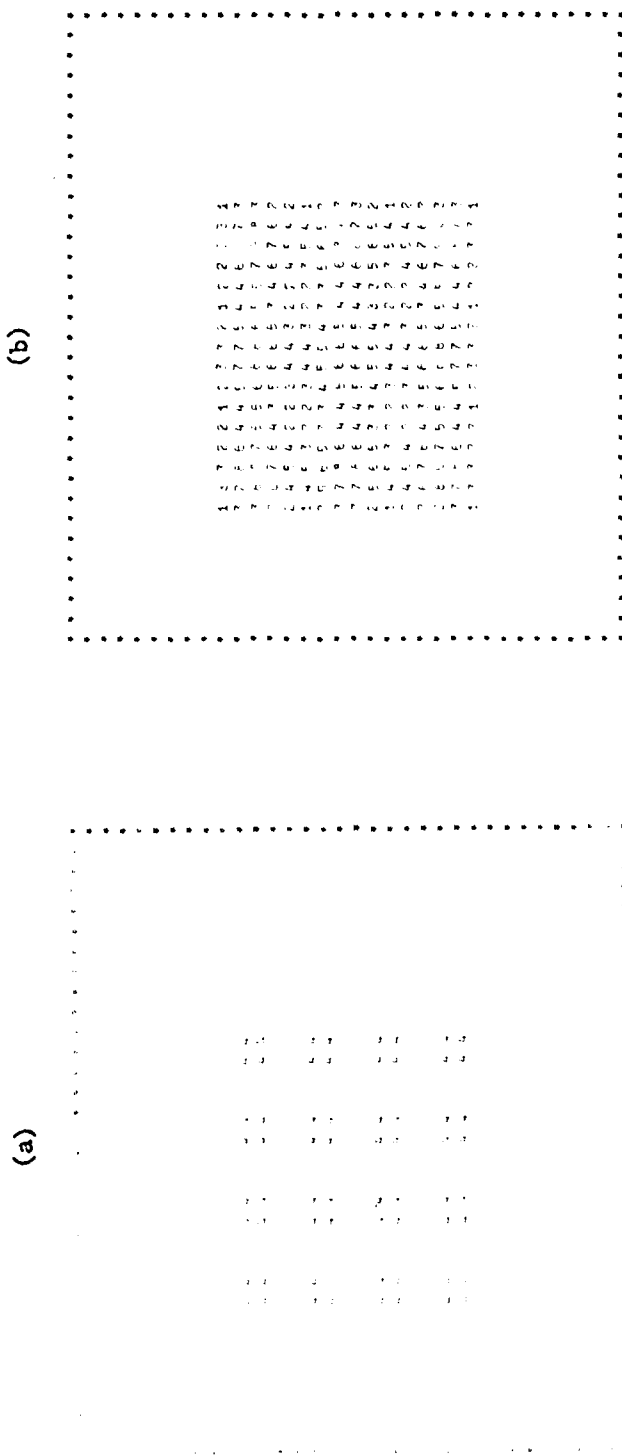


Figure 95. Spatial Filtering a 4 by 4 Dot Array: (a) Original Array; (b) Low-Pass (6 by 6) Filtered Array; (c) Low-Pass (7 by 7) Filtered Array; (d) Low-Pass (8 by 8) Filtered Array. (Section 19.7)



Figure 9.5. Spatial Filtering a 4 by 4 Dot Array: (a) Original Array; (b) Low-Pass (6 by 6) Filtered Array; (c) Low-Pass (7 by 7) Filtered Array; (d) Low-Pass (8 by 8) Filtered Array. (Section 19.7) (cont.)



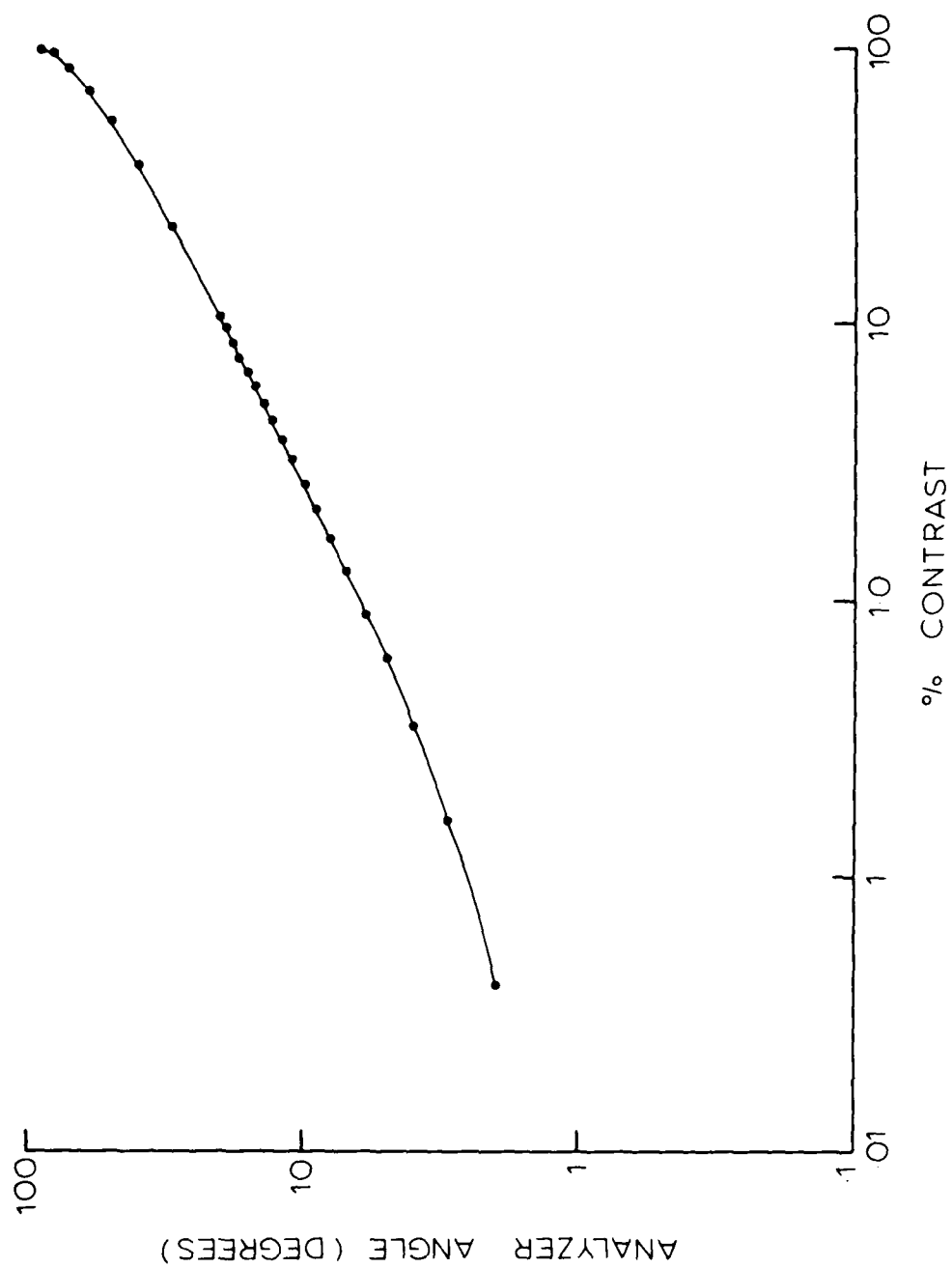


Figure '6). Curve for Determining the Percent Contrast from the Polarizer Angle. (Section A-2.4)

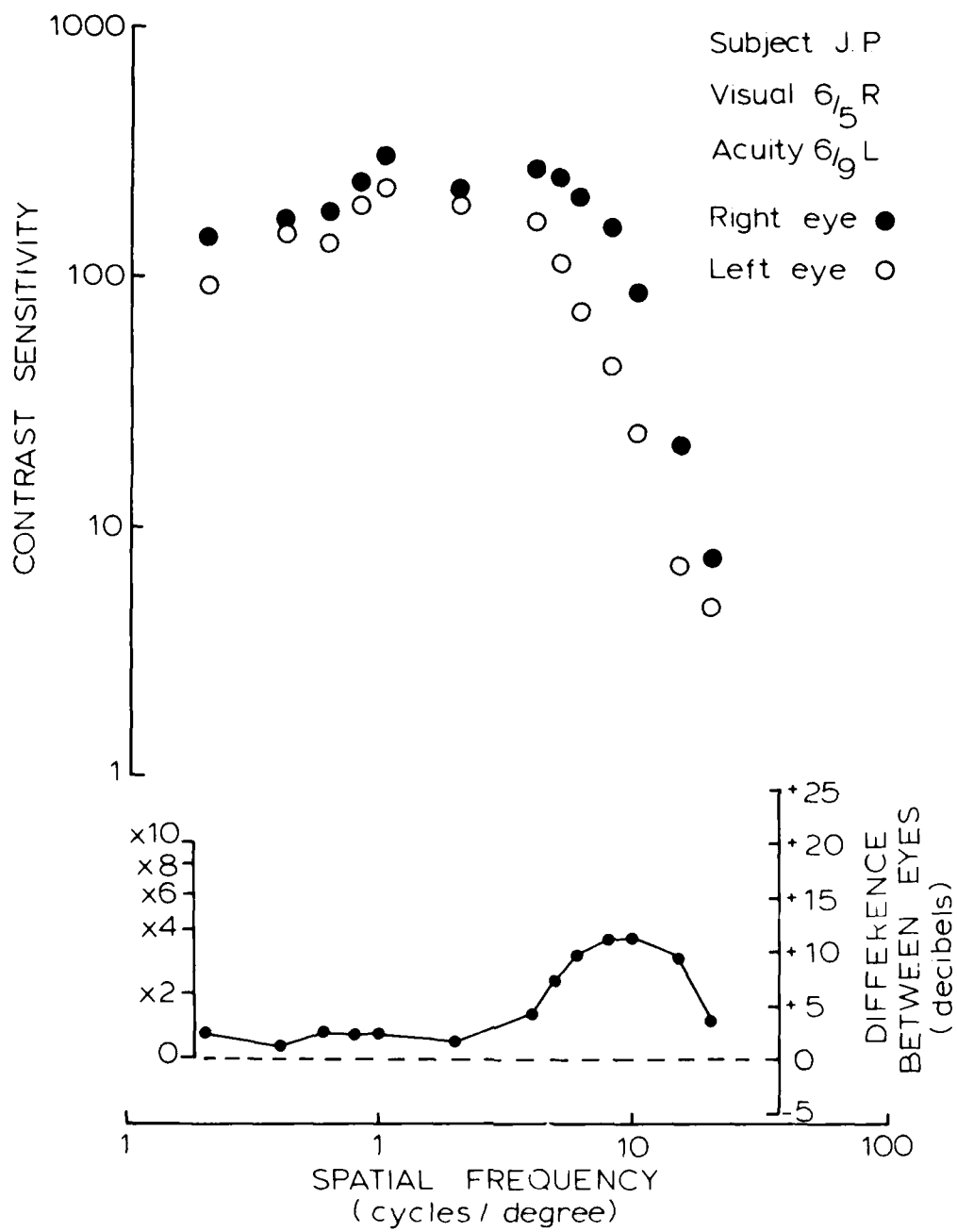


Figure 97. Contrast Sensitivity Functions and Difference Between Eyes Curve  
 Amblyope J.P. Loss at All Frequencies. Stationary Sine-Wave Gratings.  
 (Section A-3.2)

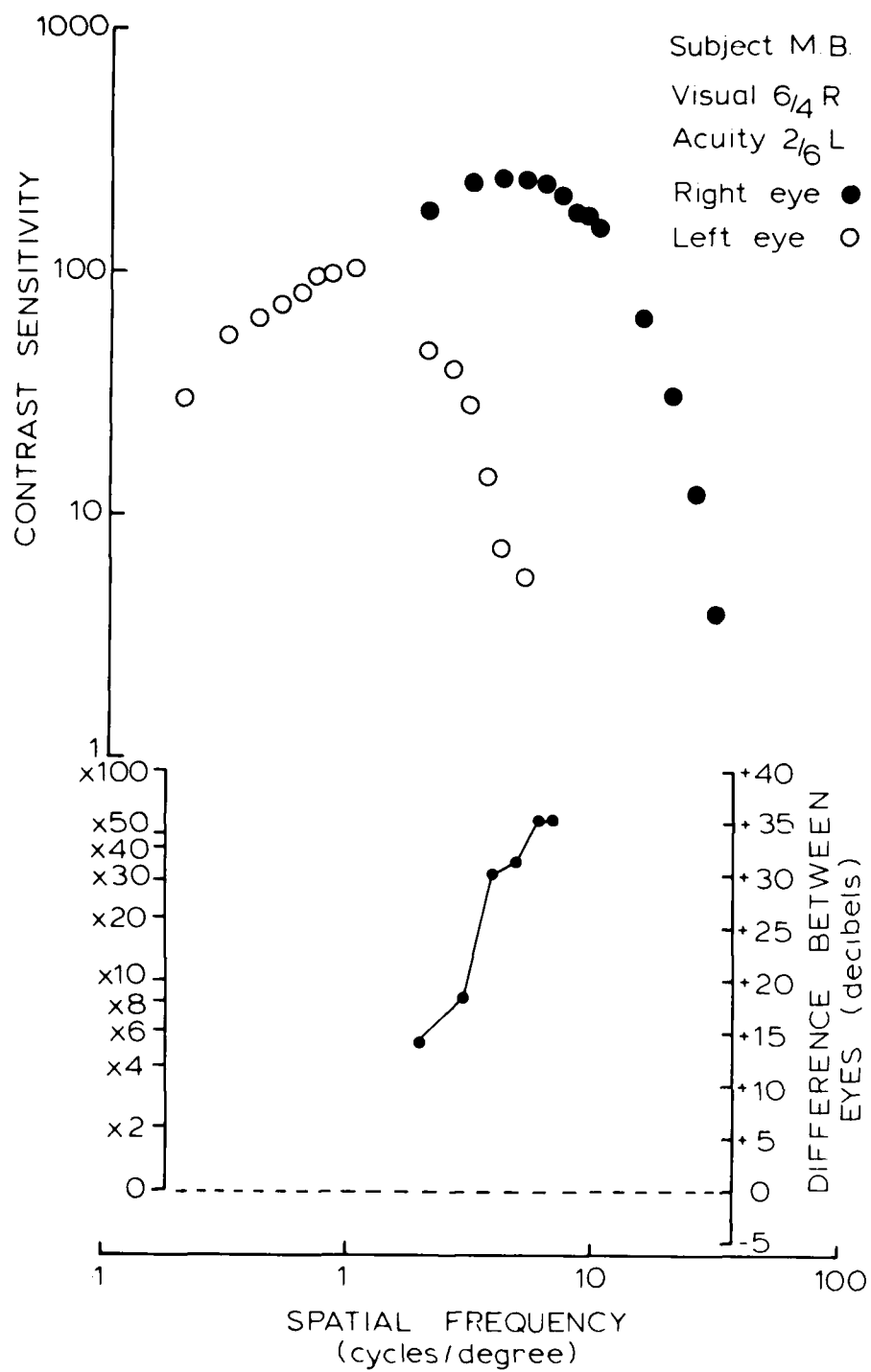


Figure 98. Contrast Sensitivity Functions and Difference Between Eyes  
 Curve: Amblyope M.B. Loss at High Frequencies. Stationary  
 Sine-Wave Gratings. (Section A-3.3)

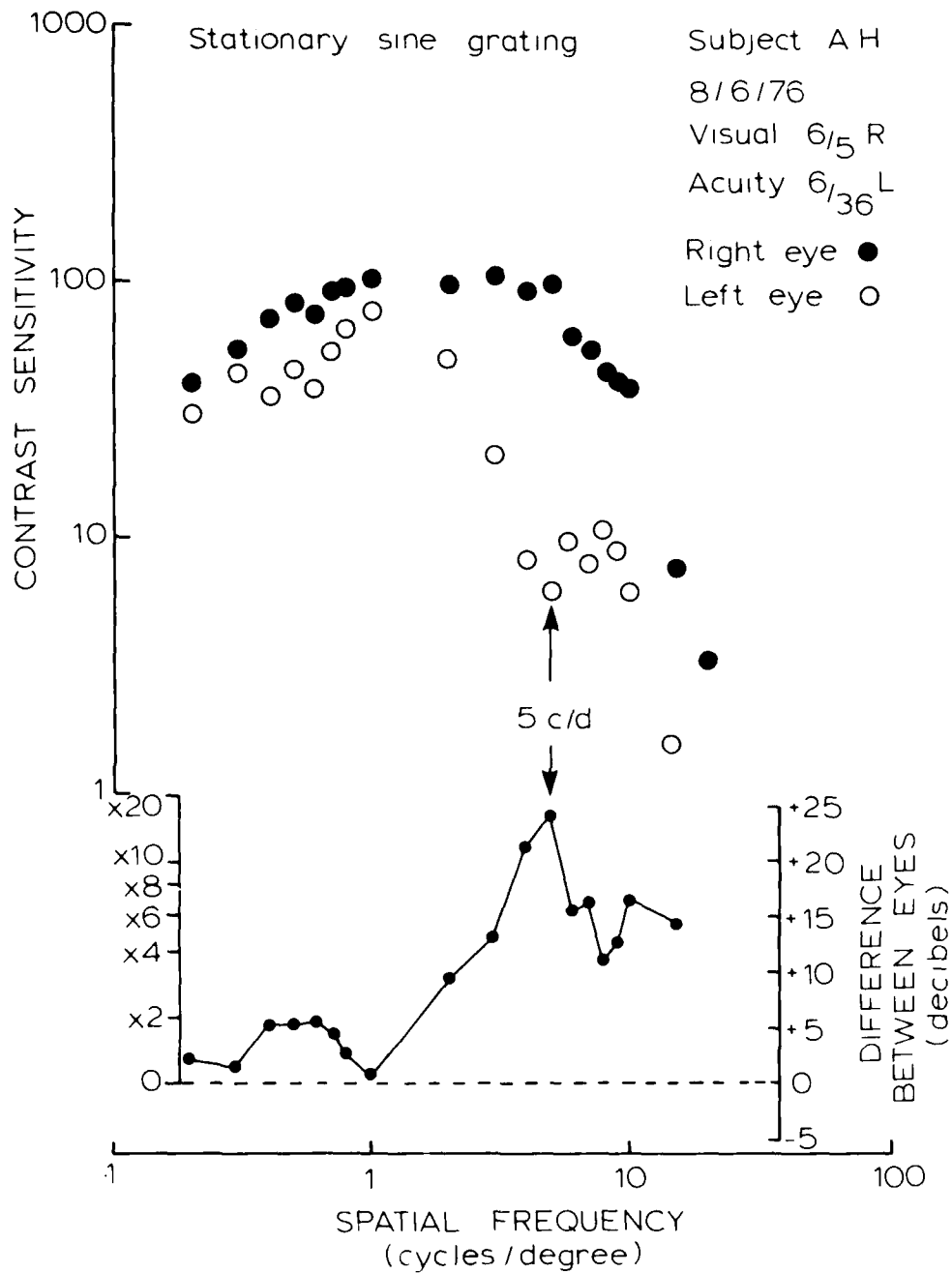


Figure 99. Contrast Sensitivity Functions and Difference Between Eyes Curve:  
Amblyope A.H. Loss at High Frequencies and Selective Mid-Frequency  
Loss. Stationary Sine-Wave Gratings. (Section A-3.4.1)

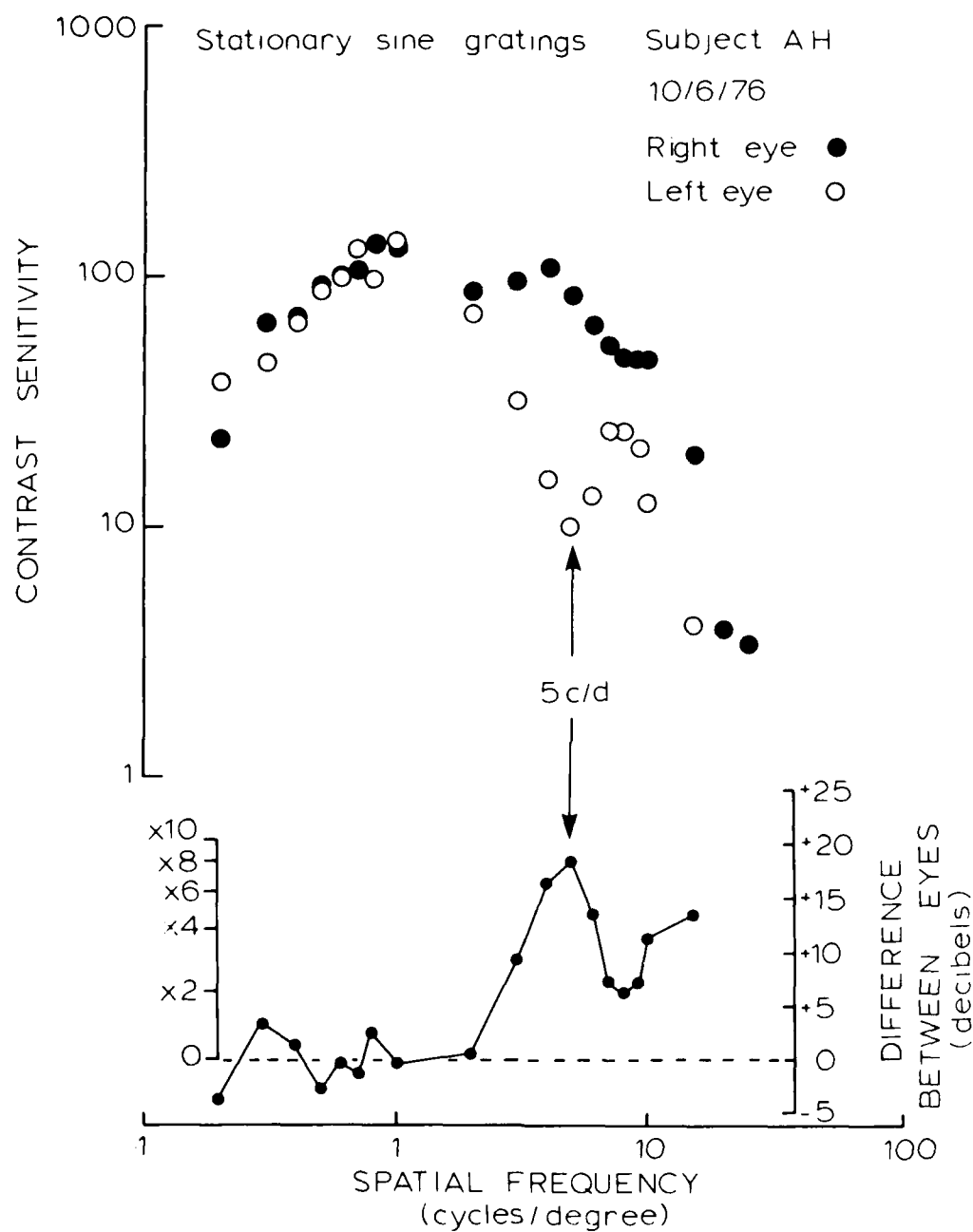


Figure 100. Contrast Sensitivity Functions and Difference Between Eyes Curve: Amblyope A.H. Loss at High Frequencies and Selective Mid-Frequency Loss. Stationary Sine-Wave Gratings. (Section A-3.4.1)

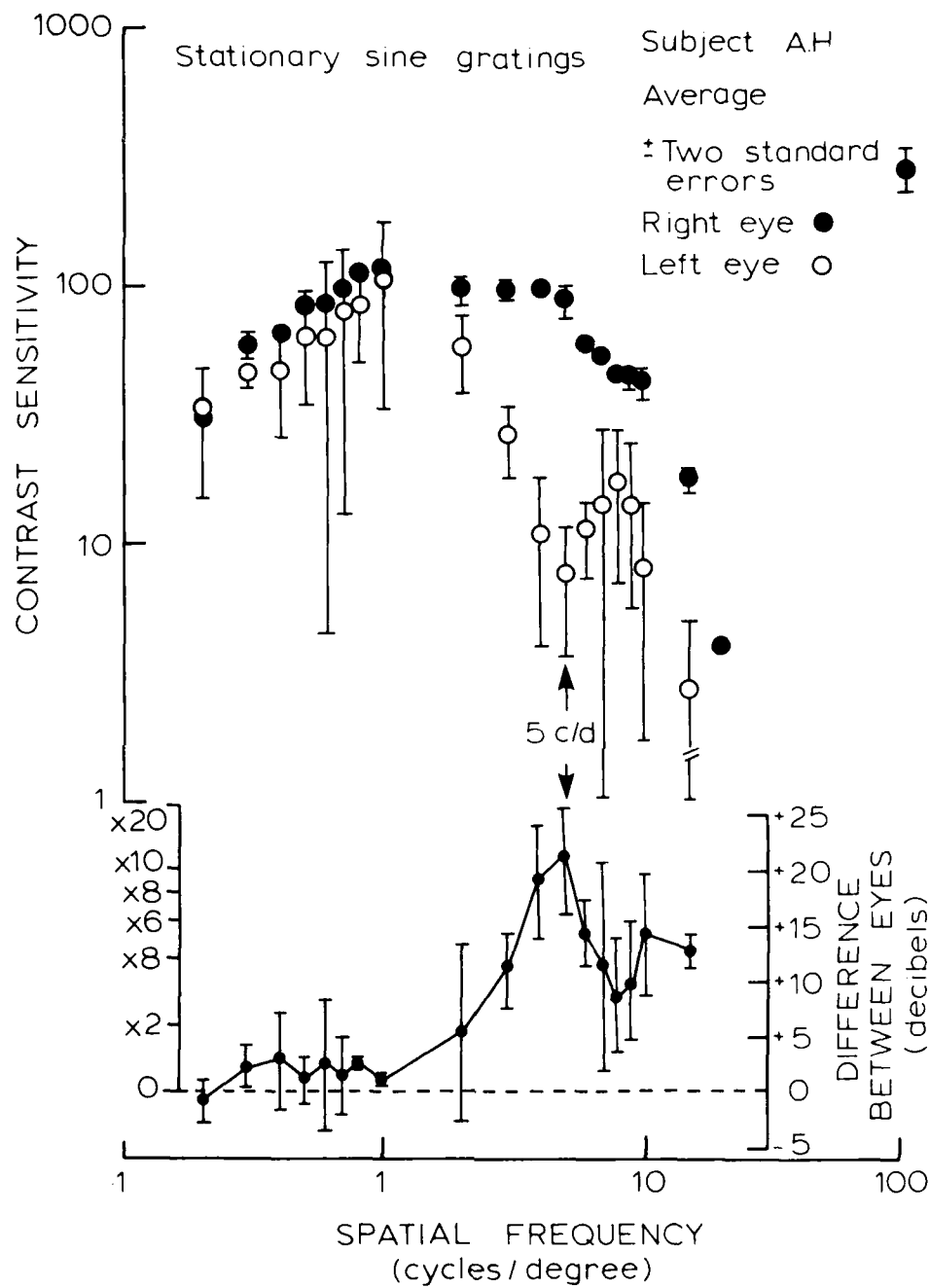


Figure 101. Average Contrast Sensitivity Functions and Difference Between Eyes  
Curve of Figures 99 and 100: Stationary Sine-Wave Gratings.  
(Section A-3.4.1)

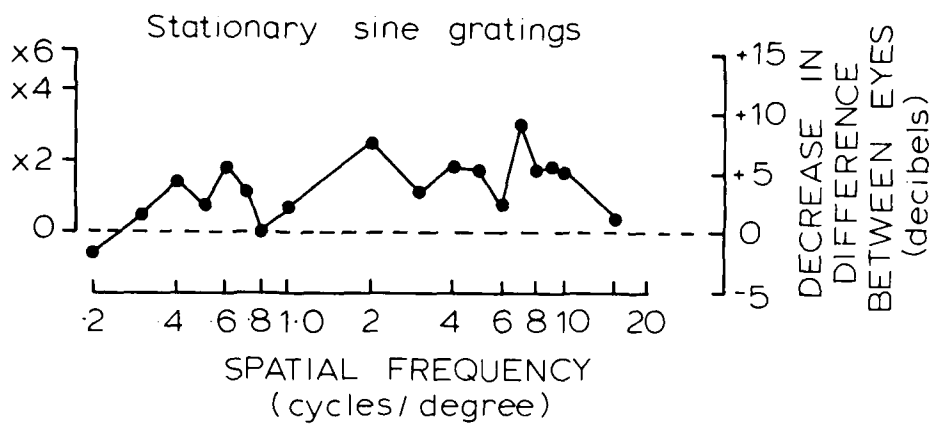


Figure 102. Decrease in Difference Between Eyes Curve for the First Two Test Sessions: Amblyope A.H. Stationary Sine-Wave Gratings. (Section A-3.4.1)

AD-A090 117

AIR FORCE AEROSPACE MEDICAL RESEARCH LAB WRIGHT-PATT--ETC F/6 6/16  
VISUAL INFORMATION PROCESSING BASED ON SPATIAL FILTERS CONSTRAI--ETC(U)  
DEC 78 A P GINSBURG

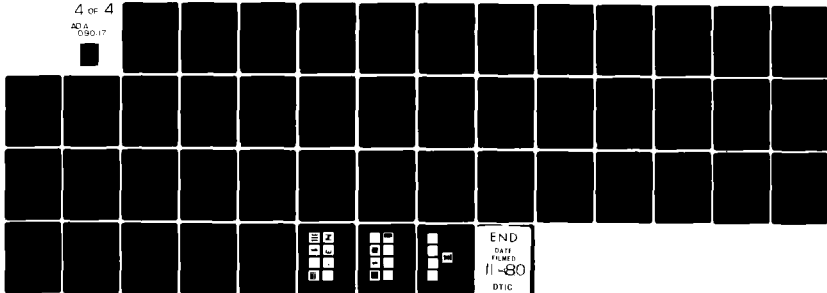
UNCLASSIFIED

AMRI-TR-78-129-VOL-1/2

NL

4 OF 4

AD A  
090 117



END  
DATE  
FILMED  
11-80  
DTIC



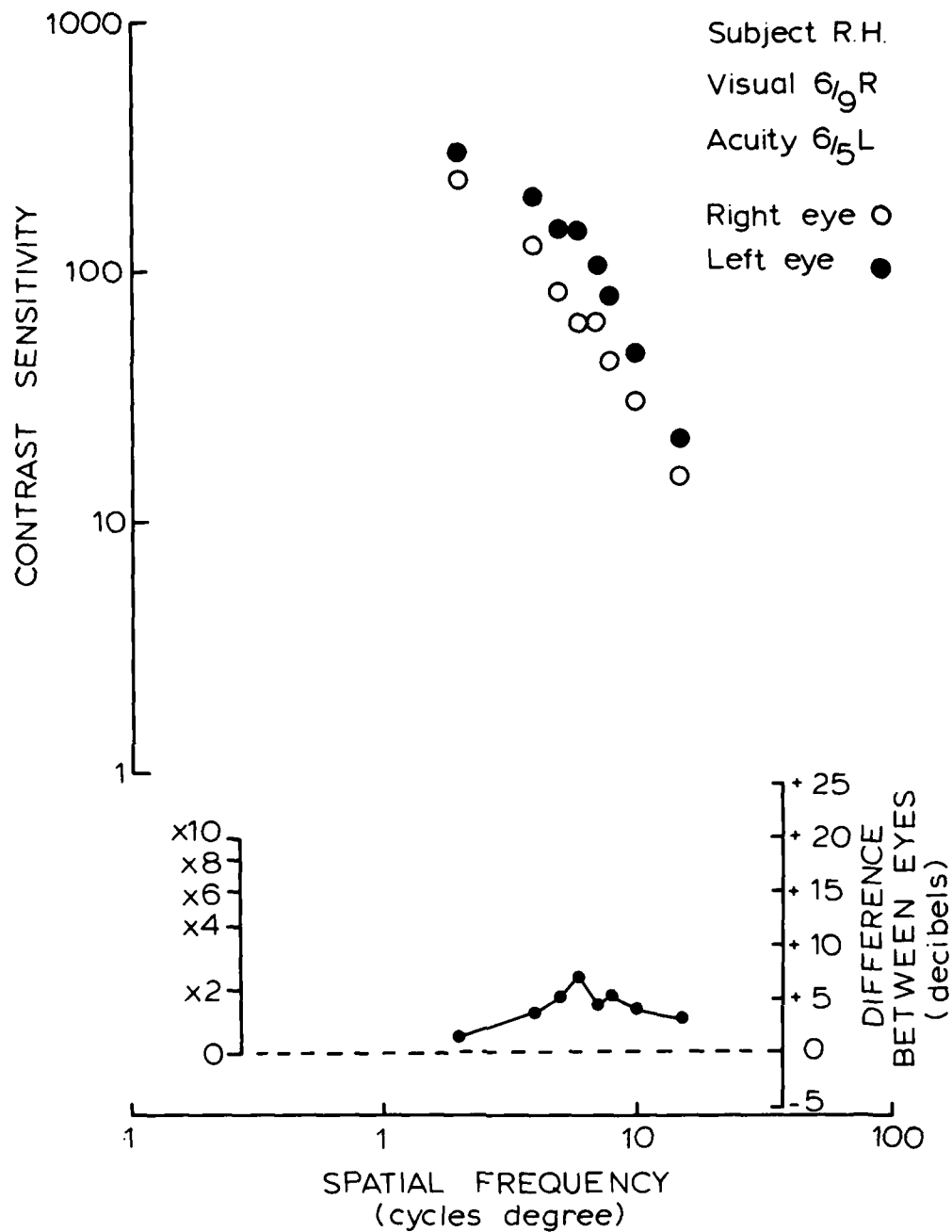


Figure 103. Contrast Sensitivity Functions and Difference Between Eyes Curve: Effect of Abnormal Retinal Correspondence (ARC). Stationary Sine-Wave Gratings. (Section A-2.4.1)

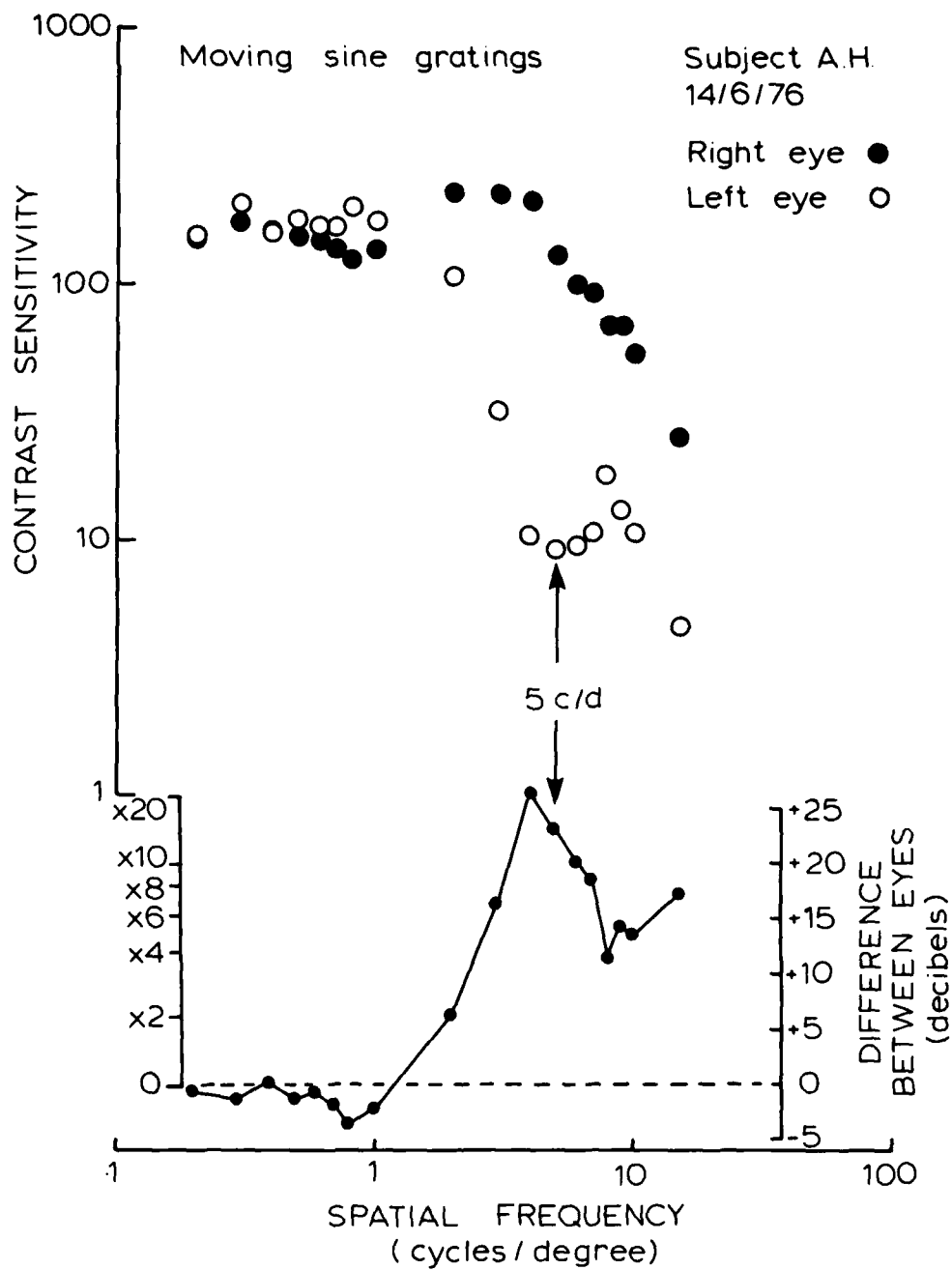


Figure 104. Contrast Sensitivity Functions and Difference Between Eyes Curve: Amblyope A.H. Loss at High Frequencies and Selective Mid-Frequency Loss. Moving Sine-Wave Gratings. (Section A-3.4.2)

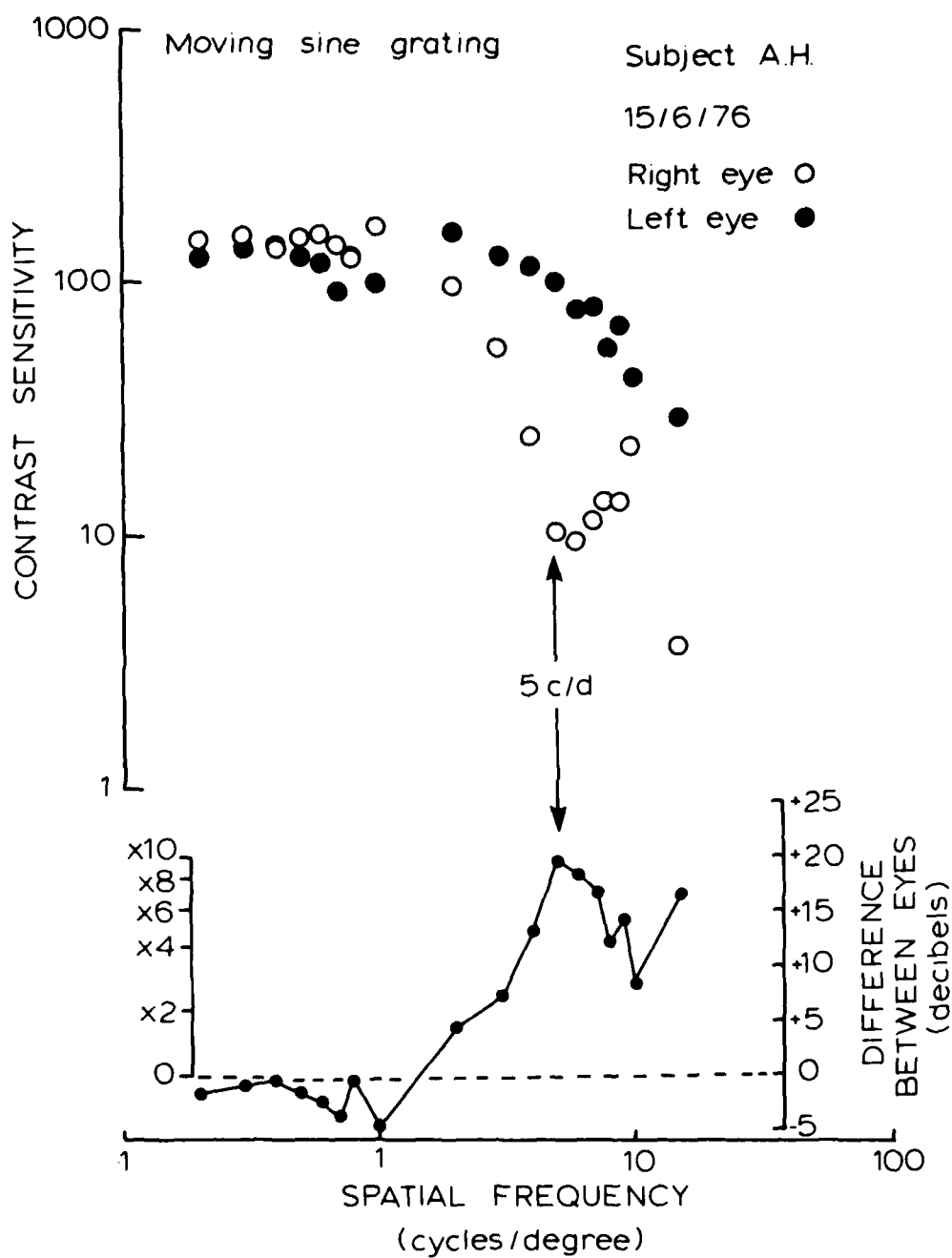


Figure 105. Contrast Sensitivity Functions and Difference Between Eyes Curve:  
Amblyope A.H. Loss at High Frequencies and Selective Mid-Frequency  
Loss. Moving Sine-Wave Gratings. (Section A-4.2)

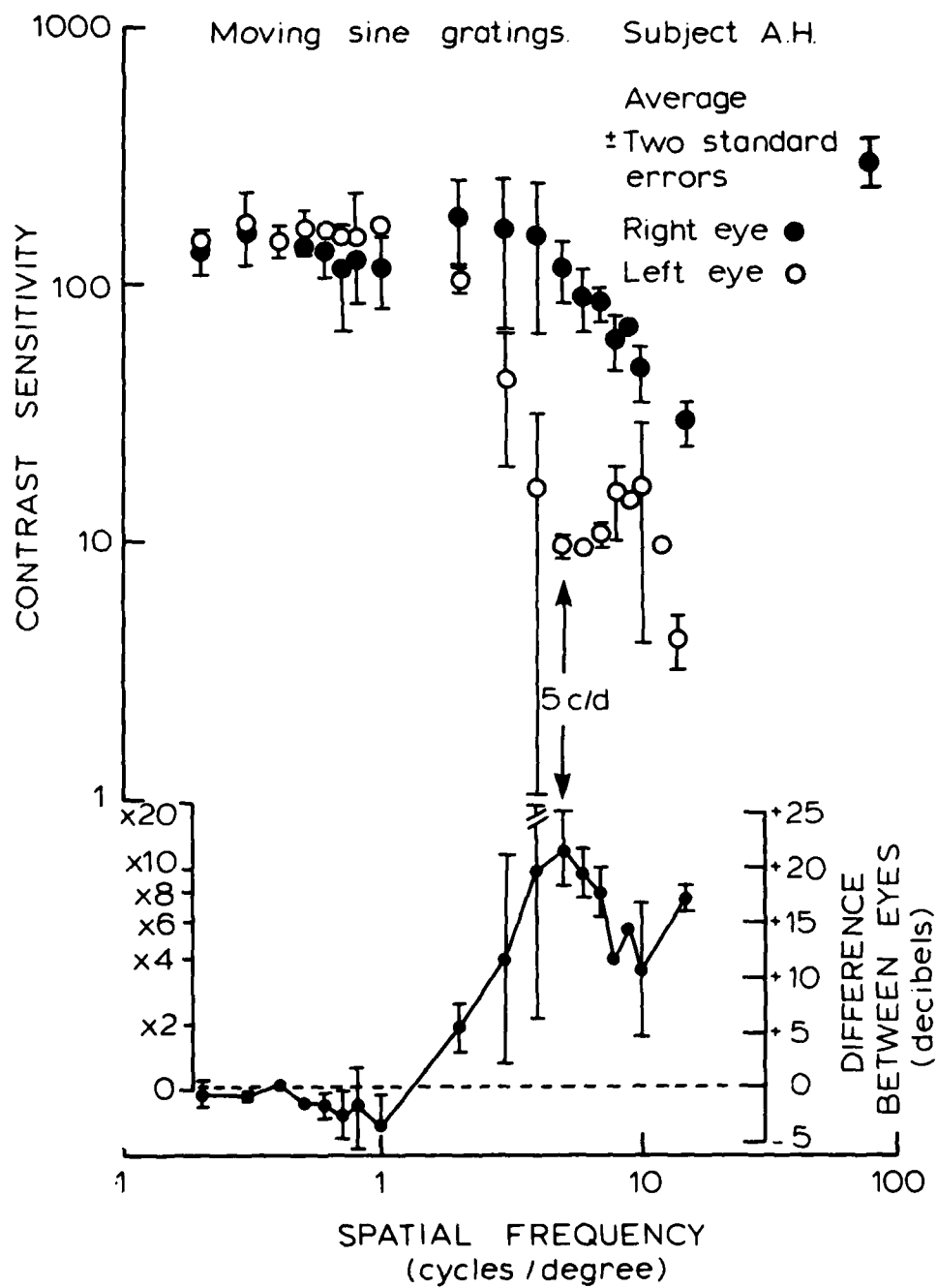


Figure 106. Average Contrast Sensitivity Functions and Difference Between Eyes  
 Curve of Figures 104, 105. Moving Sine-Wave Gratings. (Section A-3.4.2)

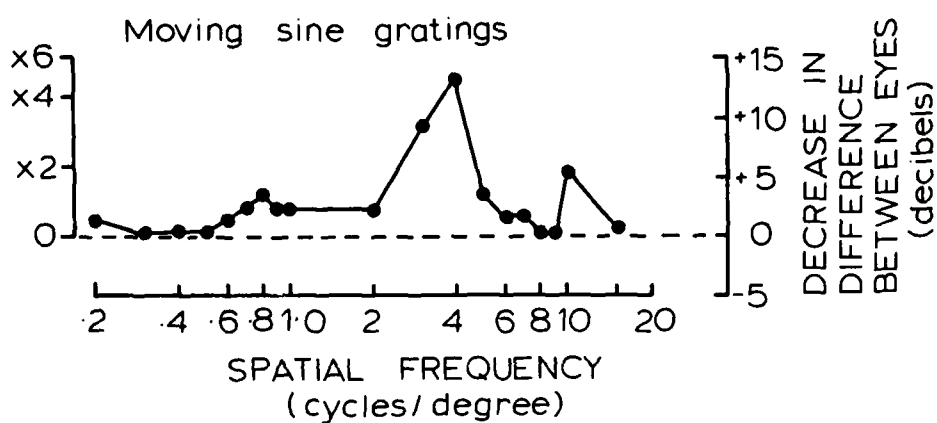


Figure 107. Decrease in Difference Between Eyes Curve: Amblyope A.H.  
Moving Sine-Wave Grating. (Section A-3.4.2)

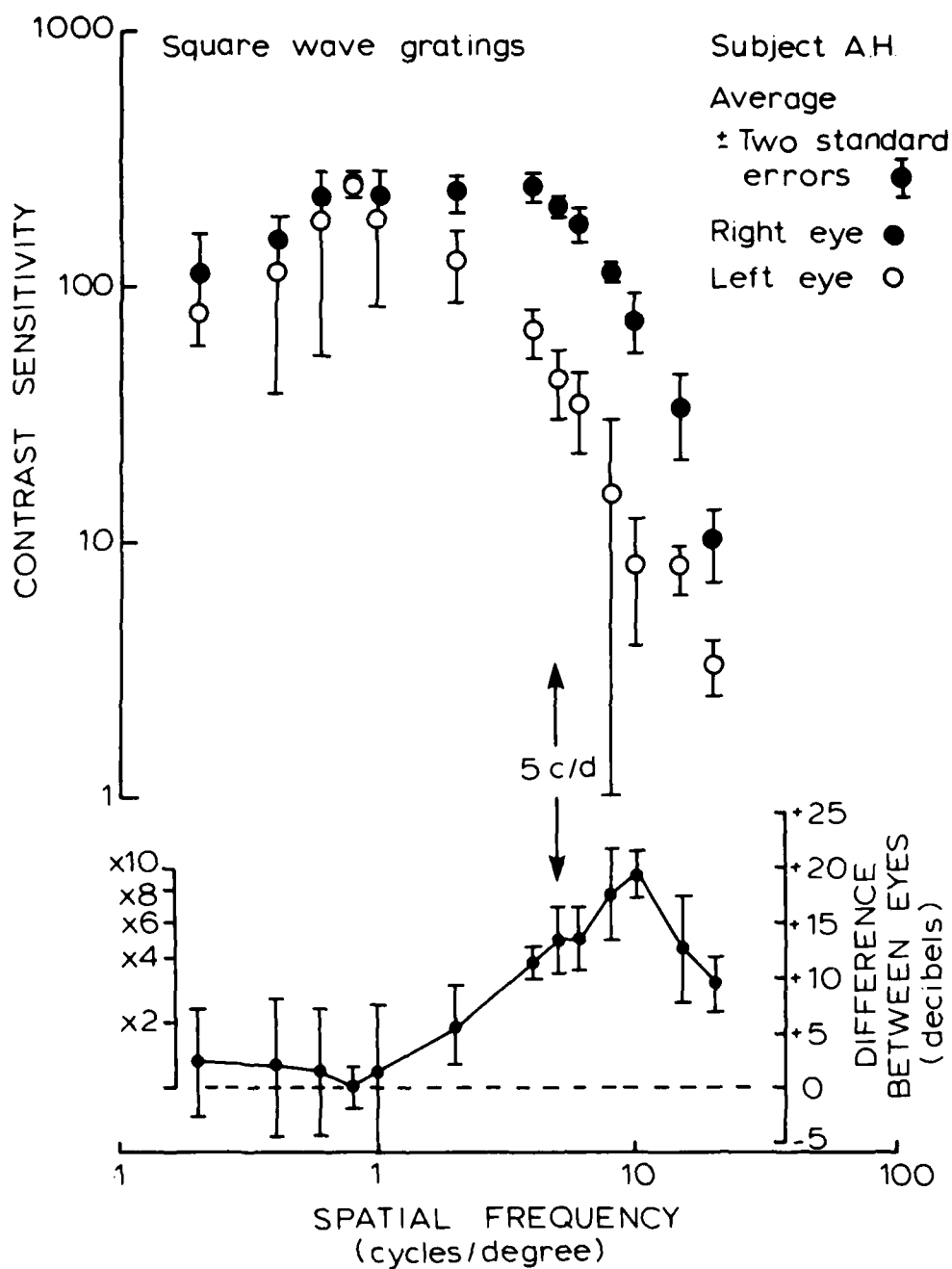


Figure 108. Average from Three Sets of Contrast Sensitivity Functions and Difference Between Eyes Curves: Amblyope A.H. Stationary Square-Wave Gratings. (Section A-3.4.3)

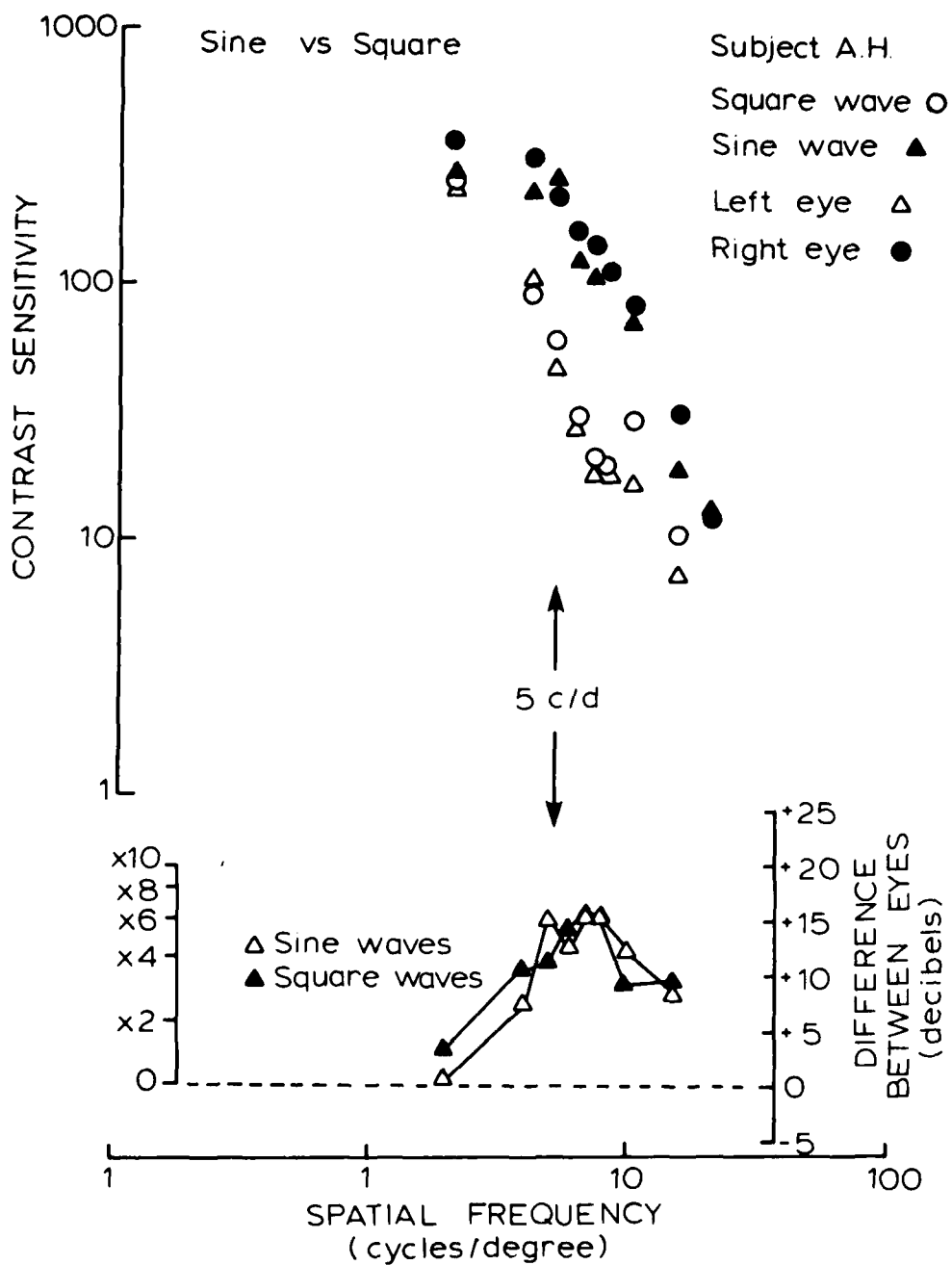


Figure 109. Contrast Sensitivity Functions and Difference Between Eyes Curve: Amblyope A.H. Stationary Sine- and Square-Wave Gratings from One Test Session. (Section A-3.4.3)

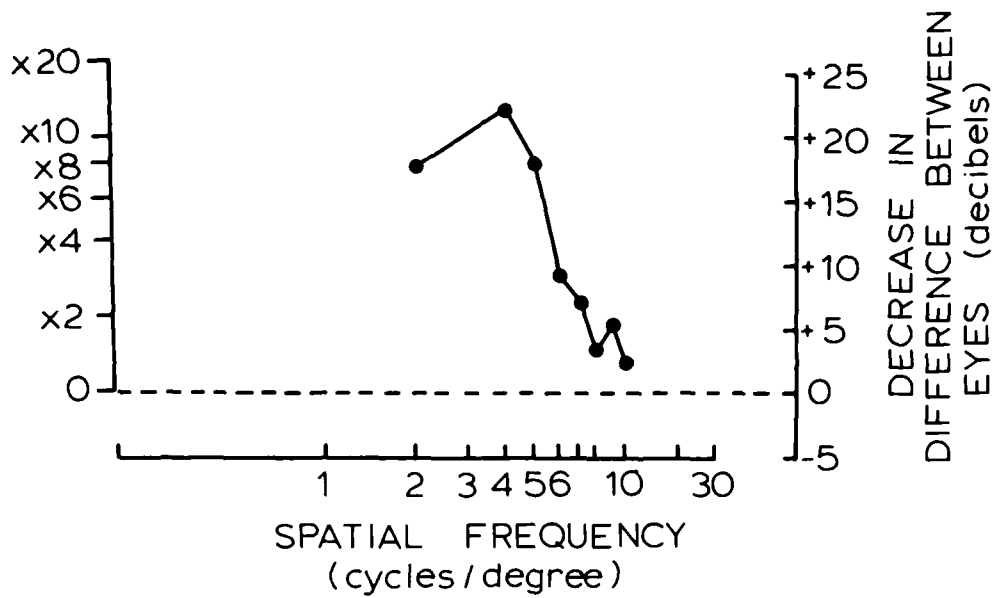


Figure 110. Decrease in Difference Between Eyes Curve from the Initial to the Final  
Test Session: Amblyope A.H. Stationary Sine-Wave Gratings. (Section A-3.5)



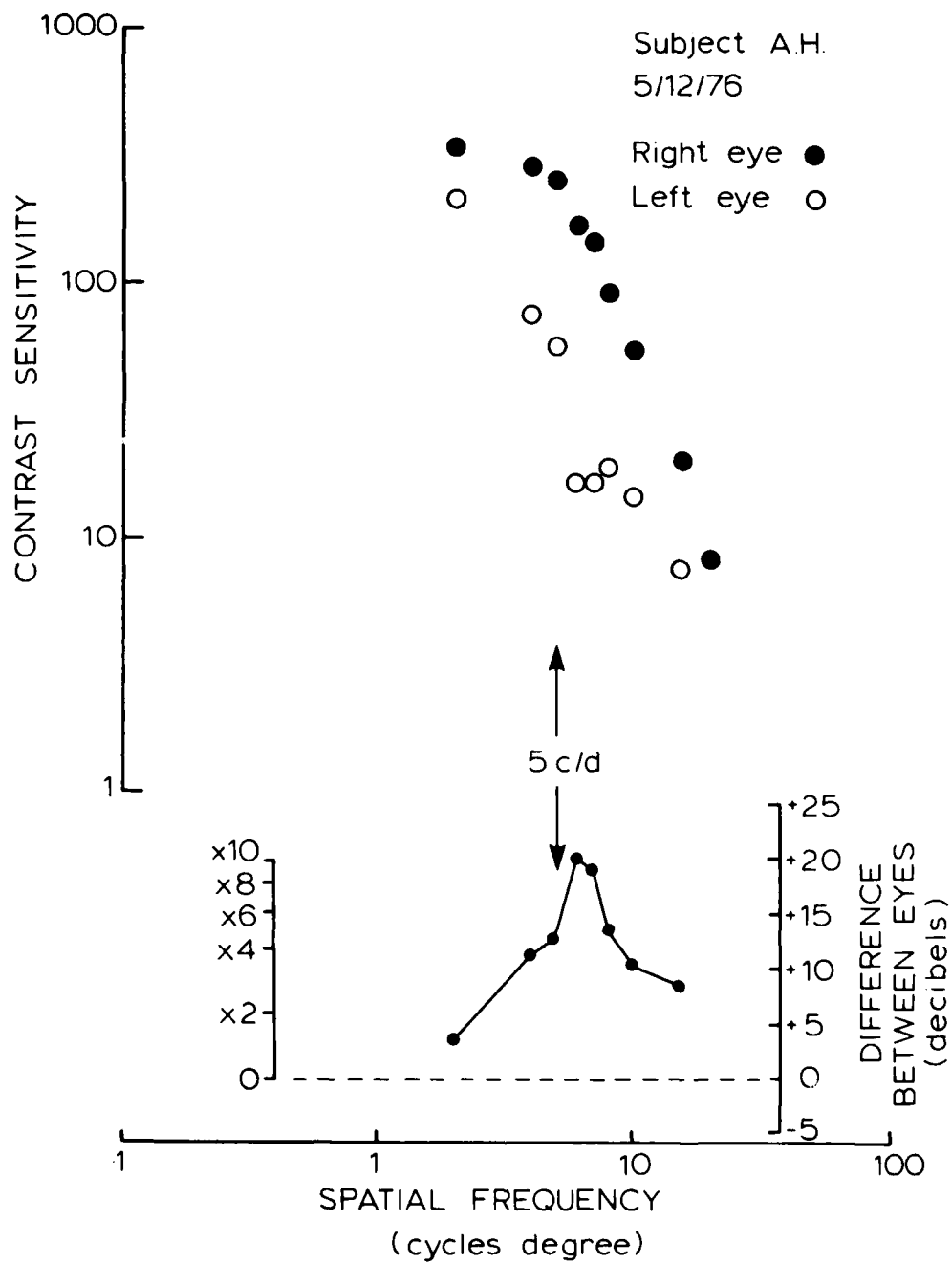


Figure 111. Contrast Sensitivity Functions and Difference Between Eyes Curve:  
Amblyope A.H. Stationary Sine-Wave Gratings. (Section A-3.5)

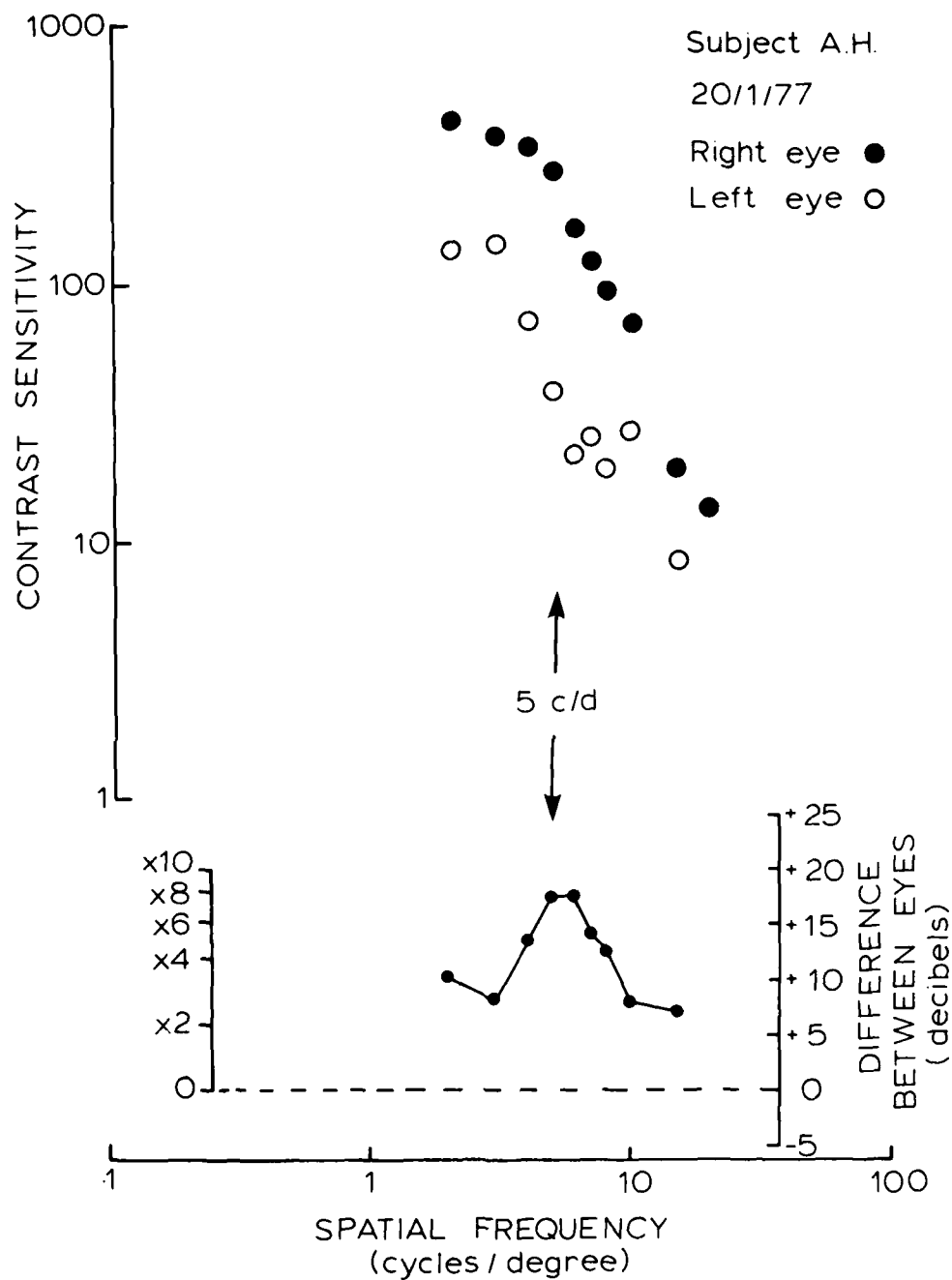


Figure 112. Contrast Sensitivity Functions and Difference Between Eyes Curve:  
Amblyope A.H. Stationary Sine-Wave Gratings. (Section A-3.5)

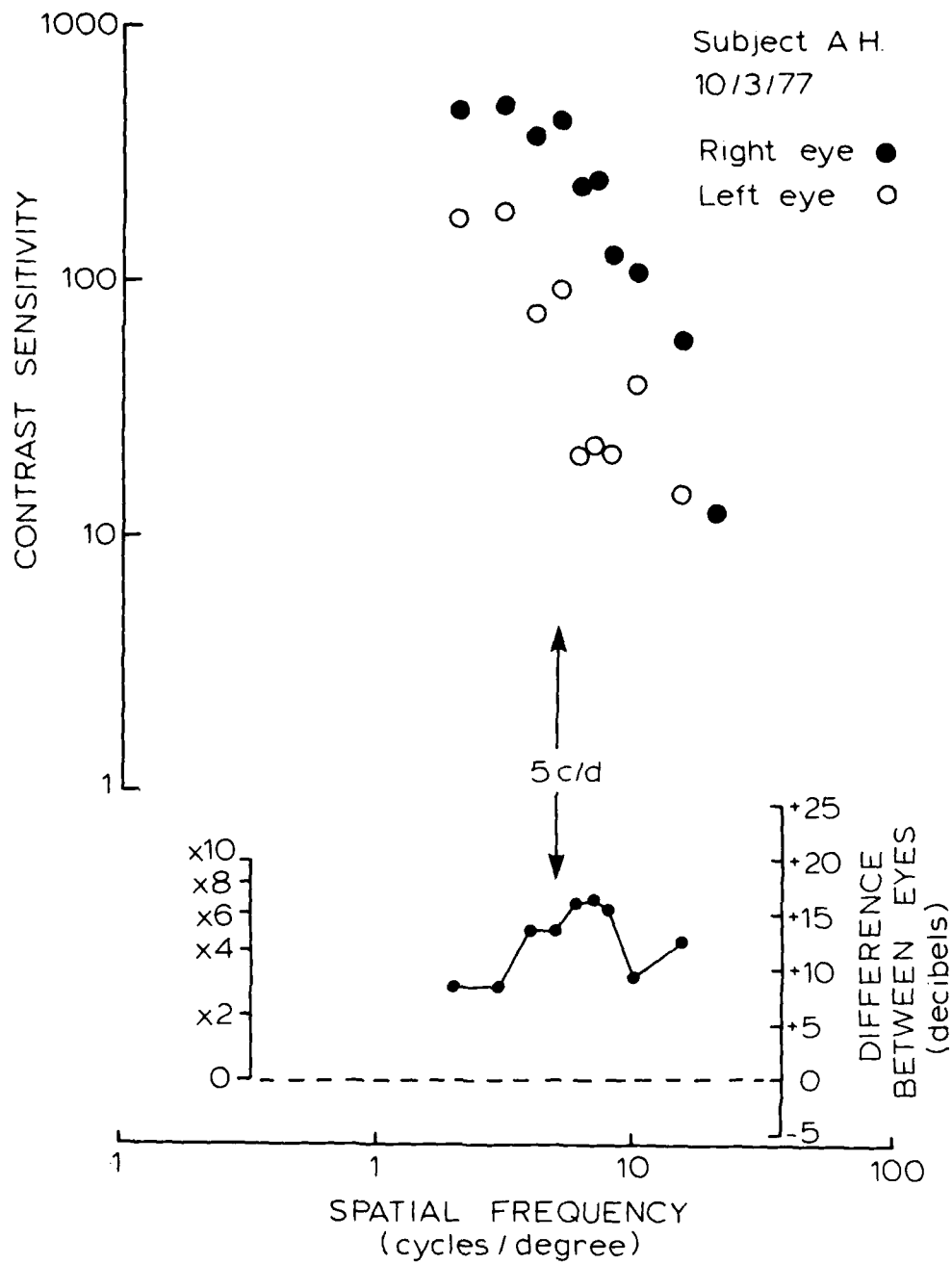


Figure 113. Contrast Sensitivity Functions and Difference Between Eyes Curve:  
Amblyope A.H. Stationary Sine-Wave Gratings. (Section A-3.5)

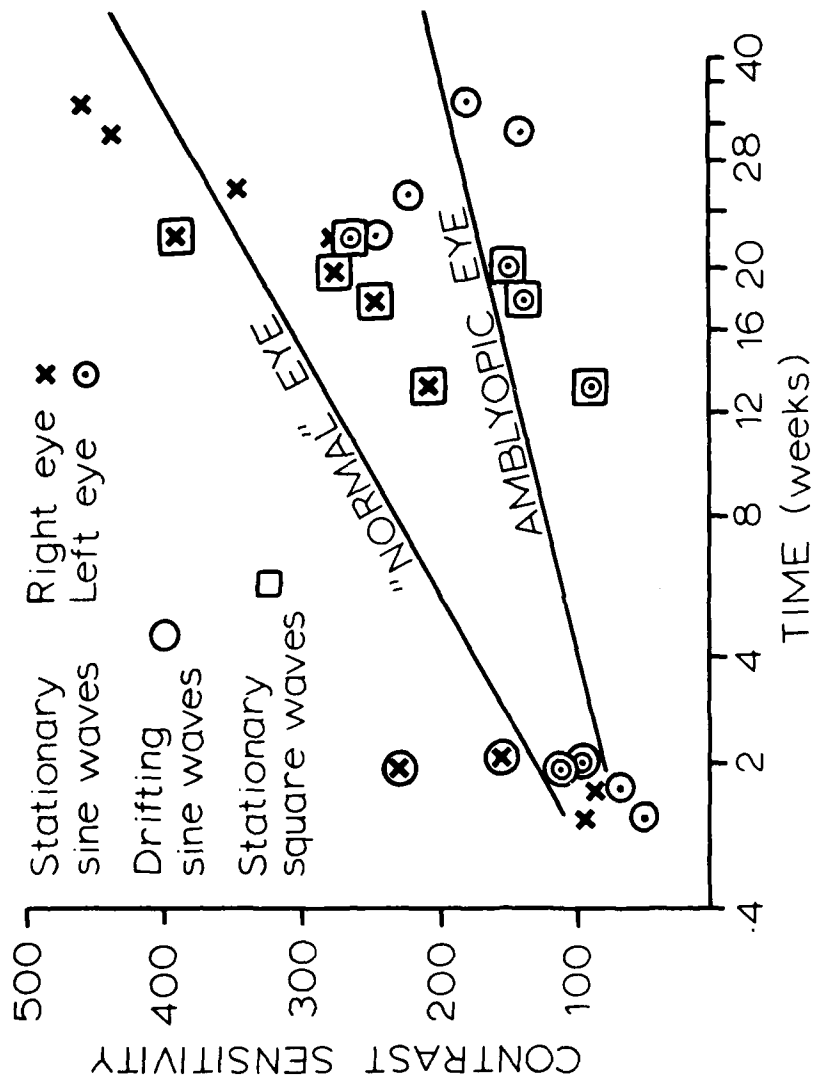


Figure 114. Contrast Sensitivity Versus Time: Amblyope A.H. (Section A-3.5)

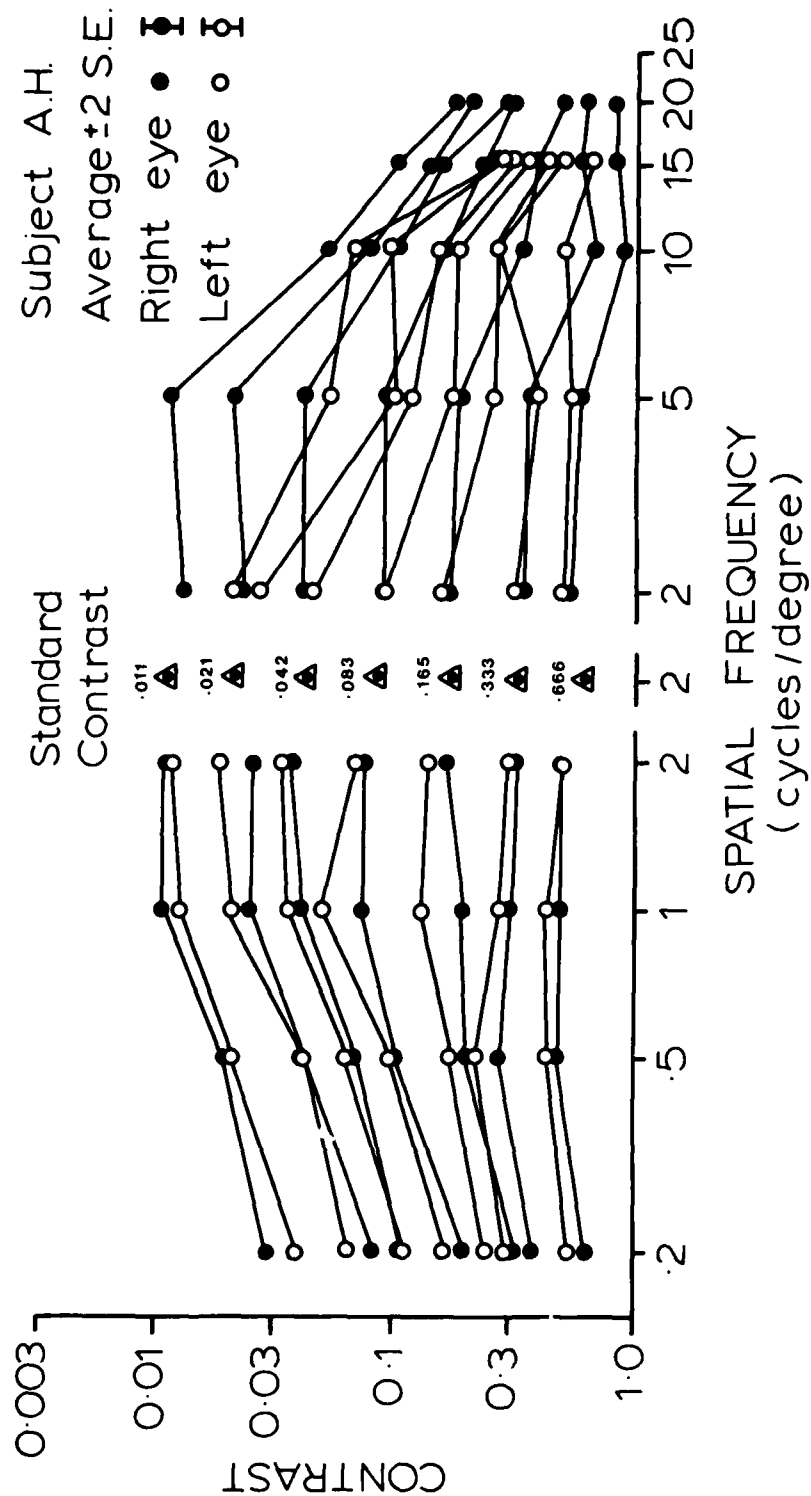


Figure 115. Average Contrast Matching Functions for Both Eyes of Amblyope A.H. (Section A-4.2)

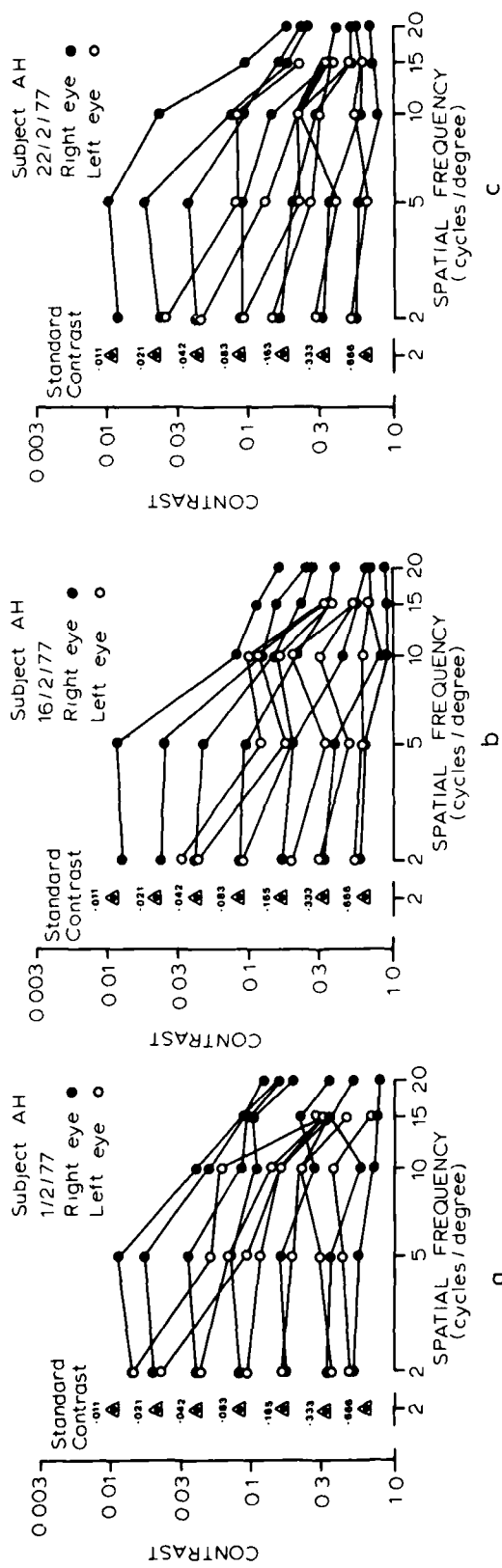


Figure 116. Contrast Matching Functions from Three Separate Test Sessions: Amblyope A.H. (Section A-4.2)

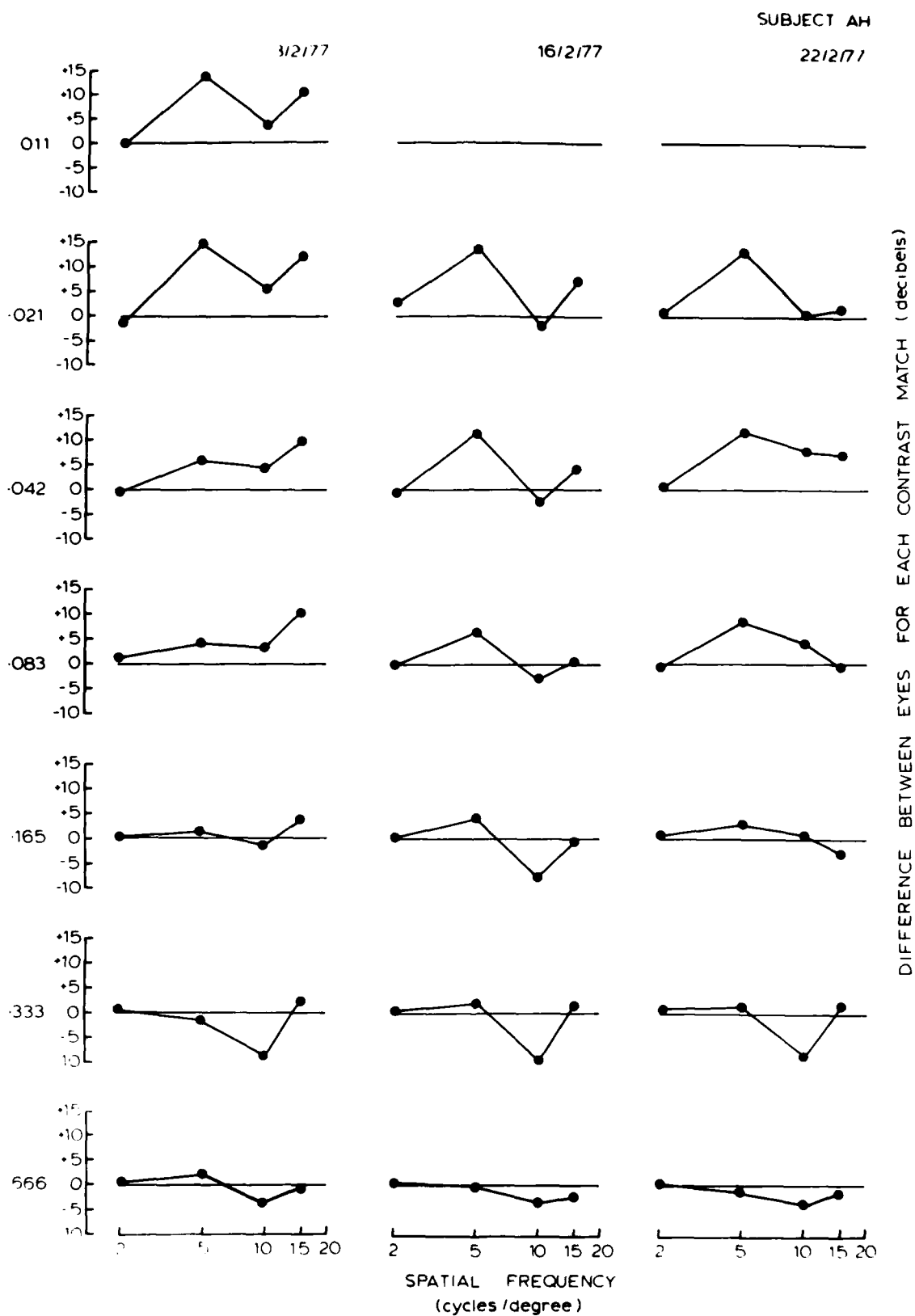


Figure 117. Difference Between Eyes Curves for Each Contrast Match for Three Separate Test Sessions: Amblyope A.H. (Section A-4.2)

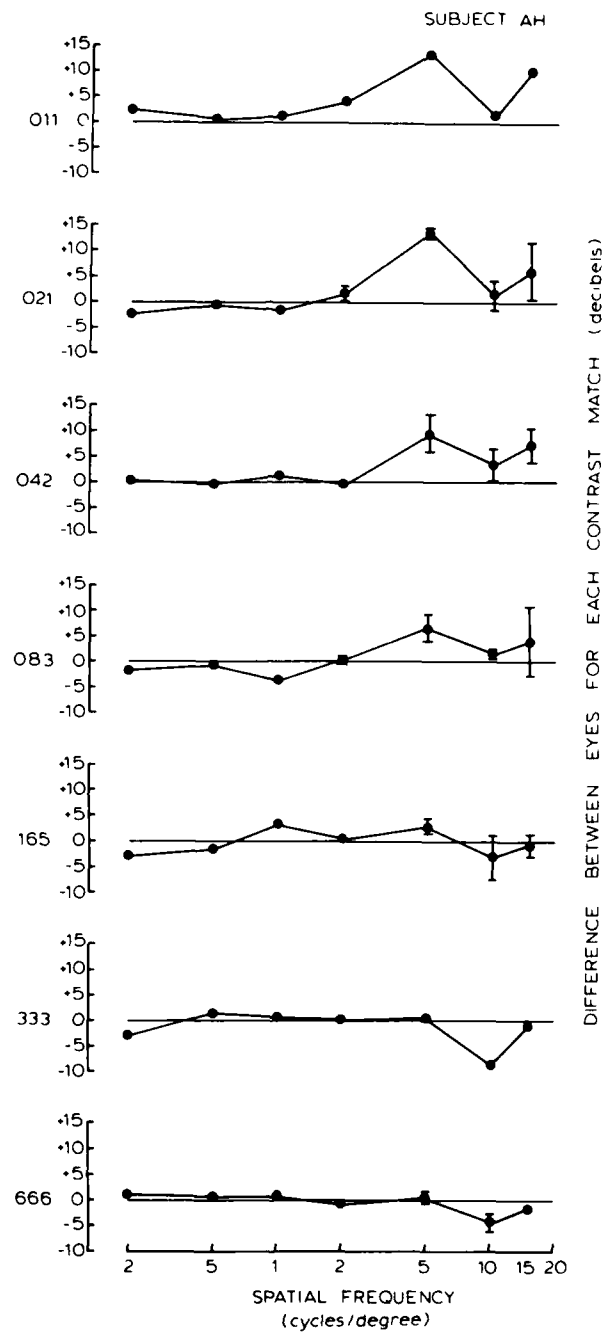


Figure 118. Average Difference Between Eyes Curves for Three Contrast Matches of Figure 115. Amblyope A.H. (Section A-4.2)



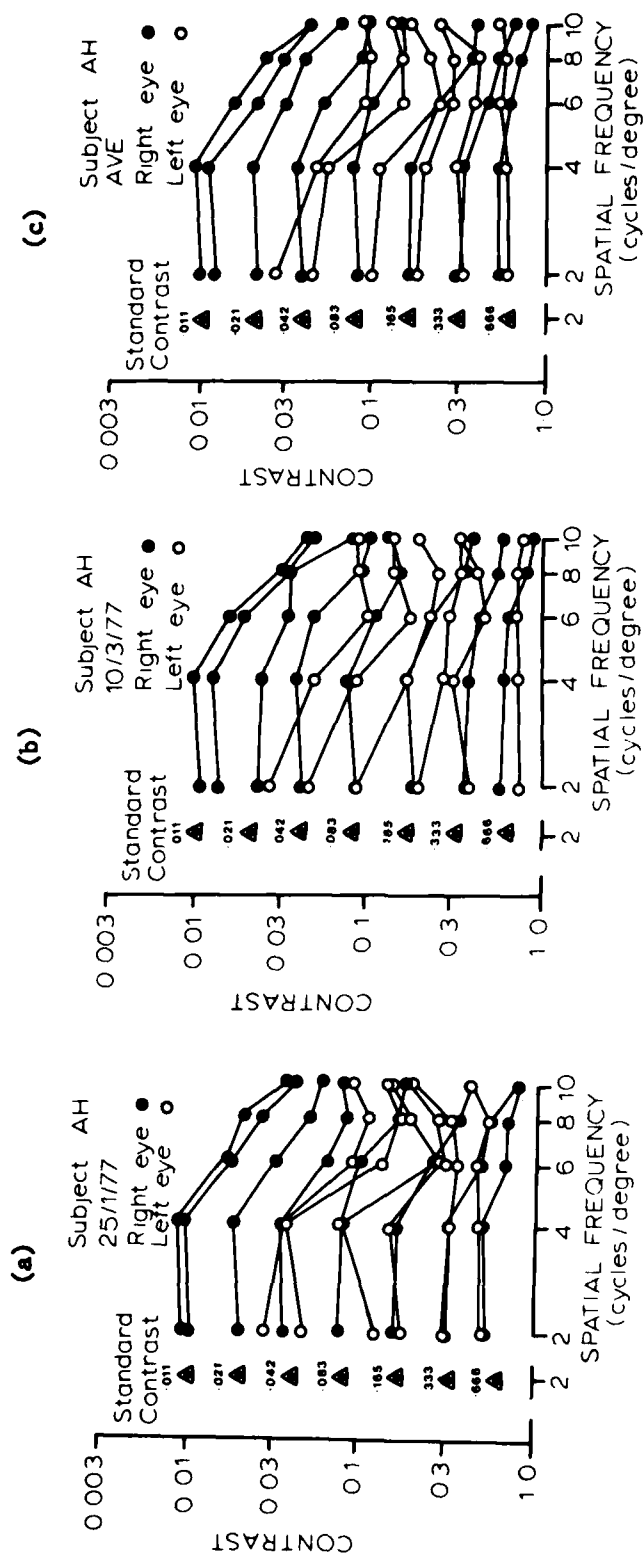


Figure 119. Contrast Matching Functions over a Finer Spatial Frequency Range. Two Separate Test Sessions (a, b) and Their Average (c): Amblyope A.H. (Section A-4.2)

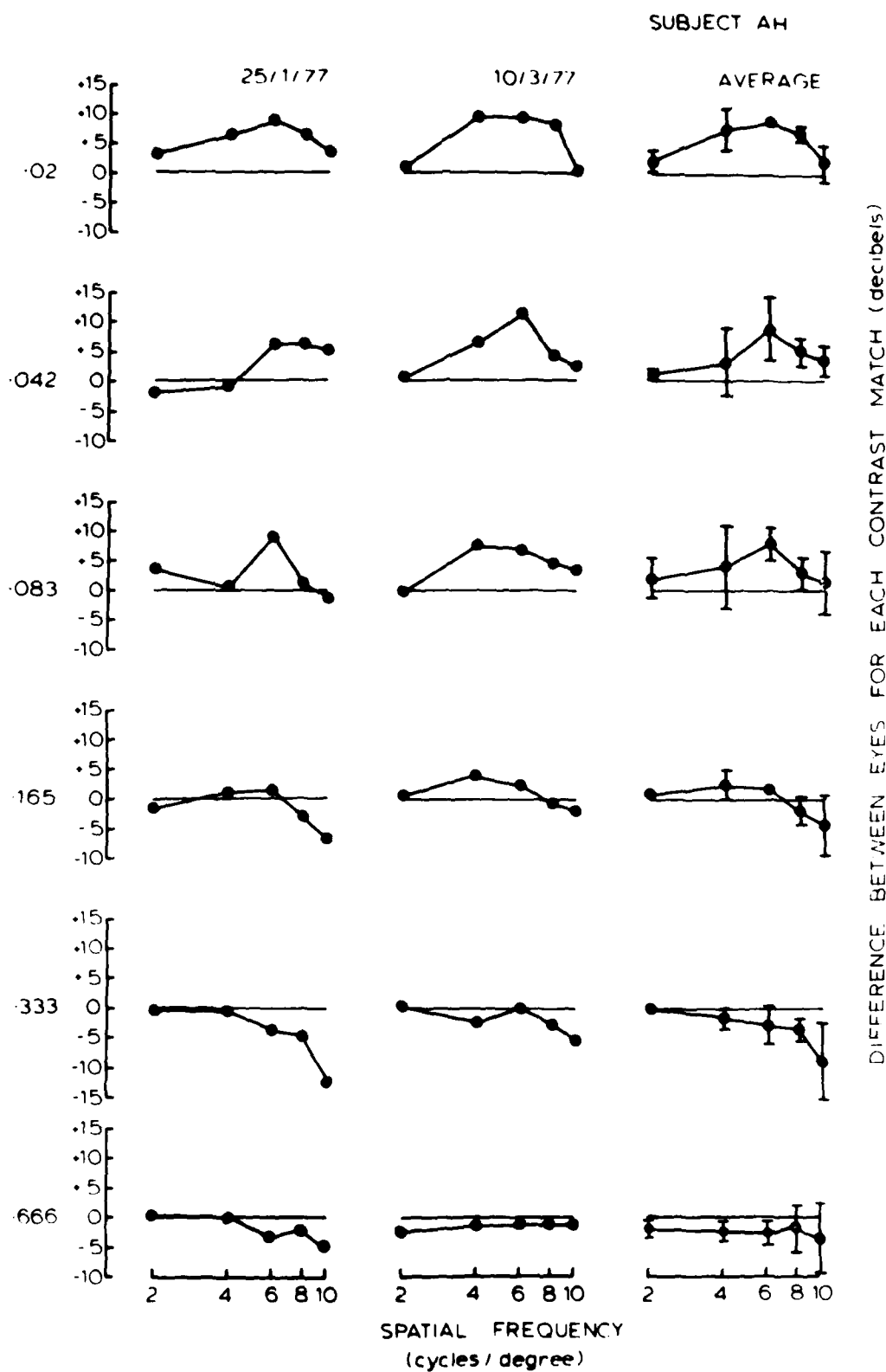


Figure 120. Difference Between Eyes Curves for each Contrast Match for Two Separate Test Sessions, (Figures 119a, b) and Their Average (Figure 119c): Amblyope A.H. (Section A-4.2)

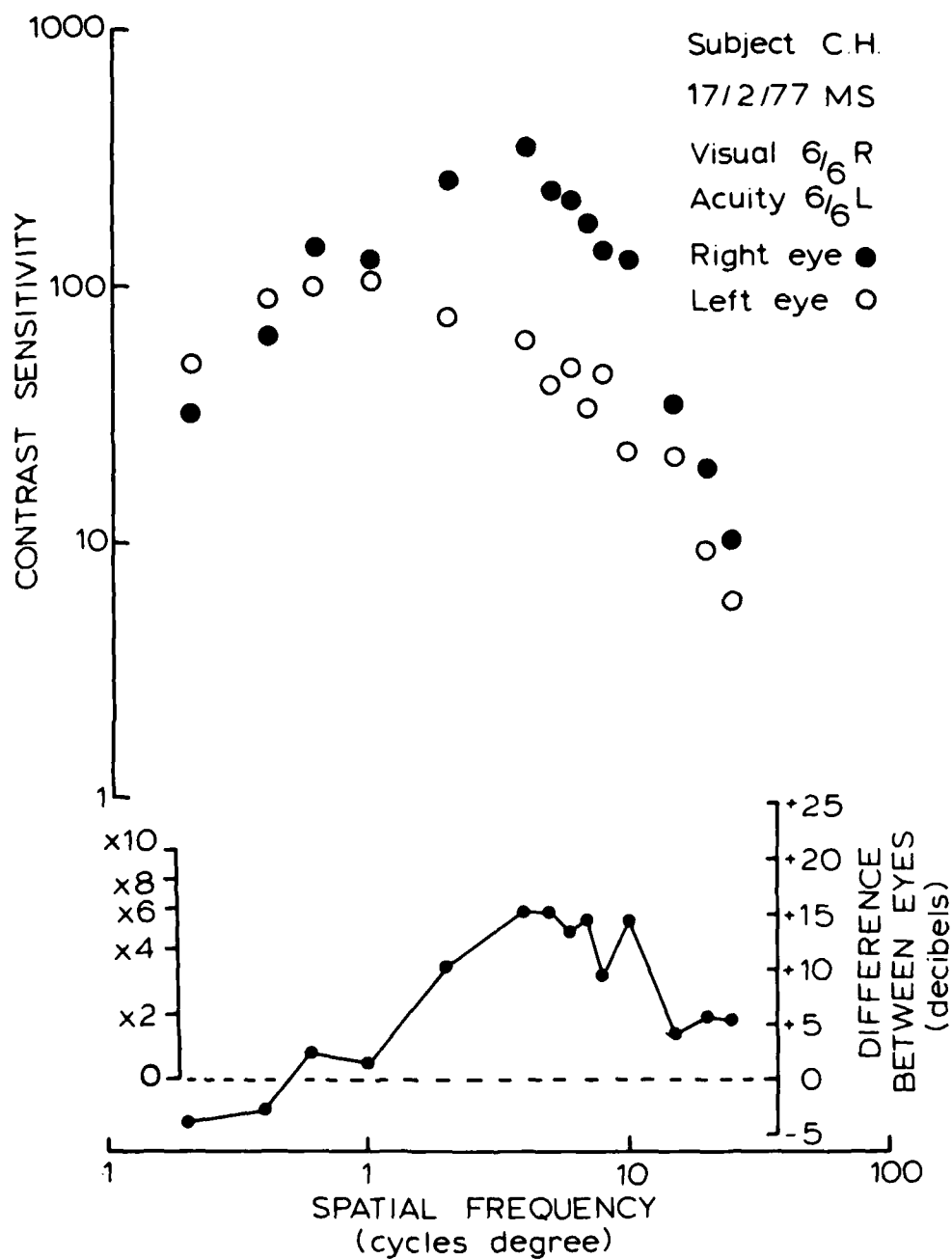


Figure 121. Contrast Sensitivity Functions and Difference Between Eyes Curve:  
Multiple Sclerosis C.H. Mid-Frequency Loss. (Section A-5.2)

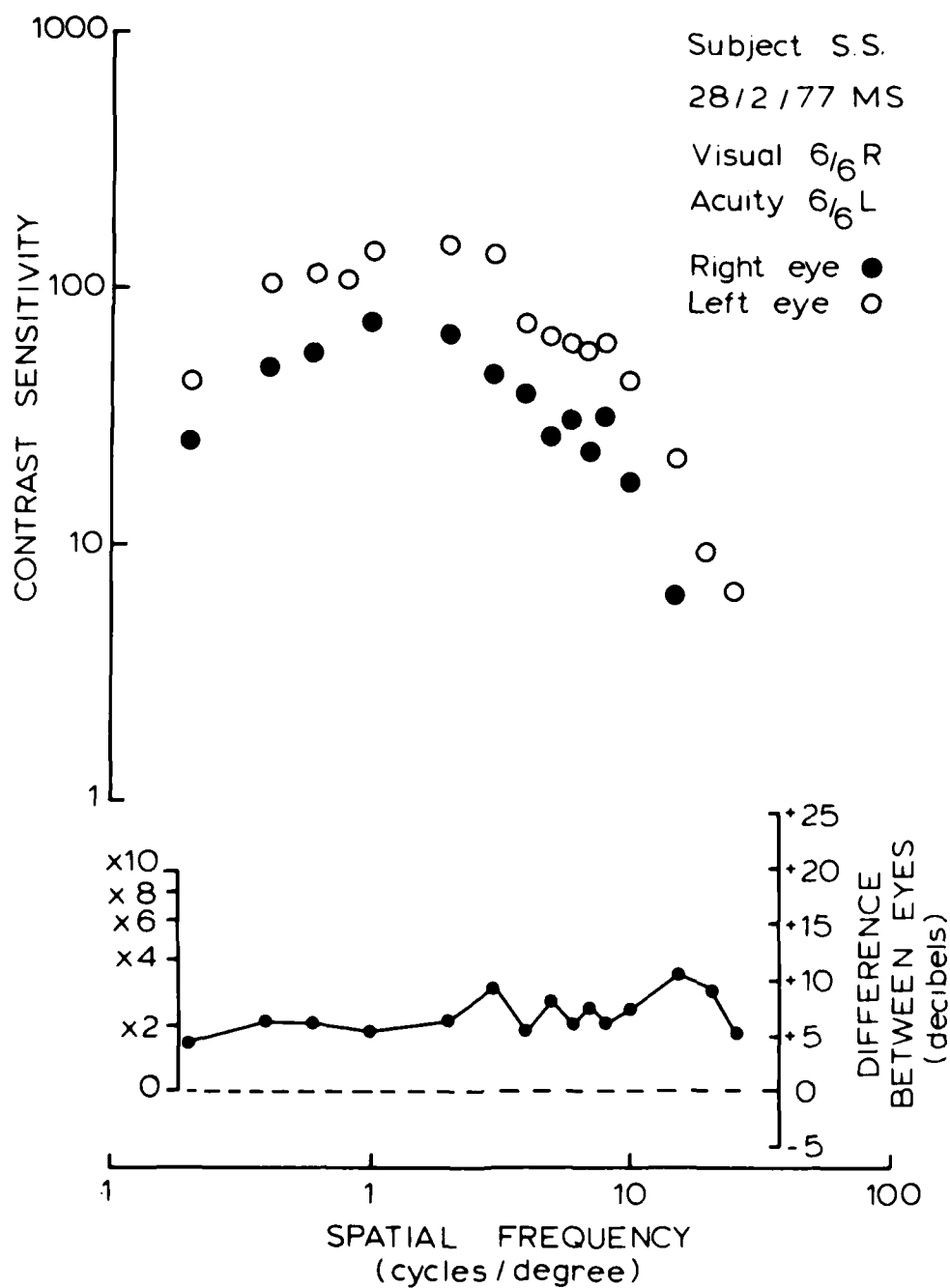


Figure 122. Contrast Sensitivity Functions and Difference Between Eyes Curve:  
Multiple Sclerosis S.S. All Frequency Loss. (Section A-5.2)

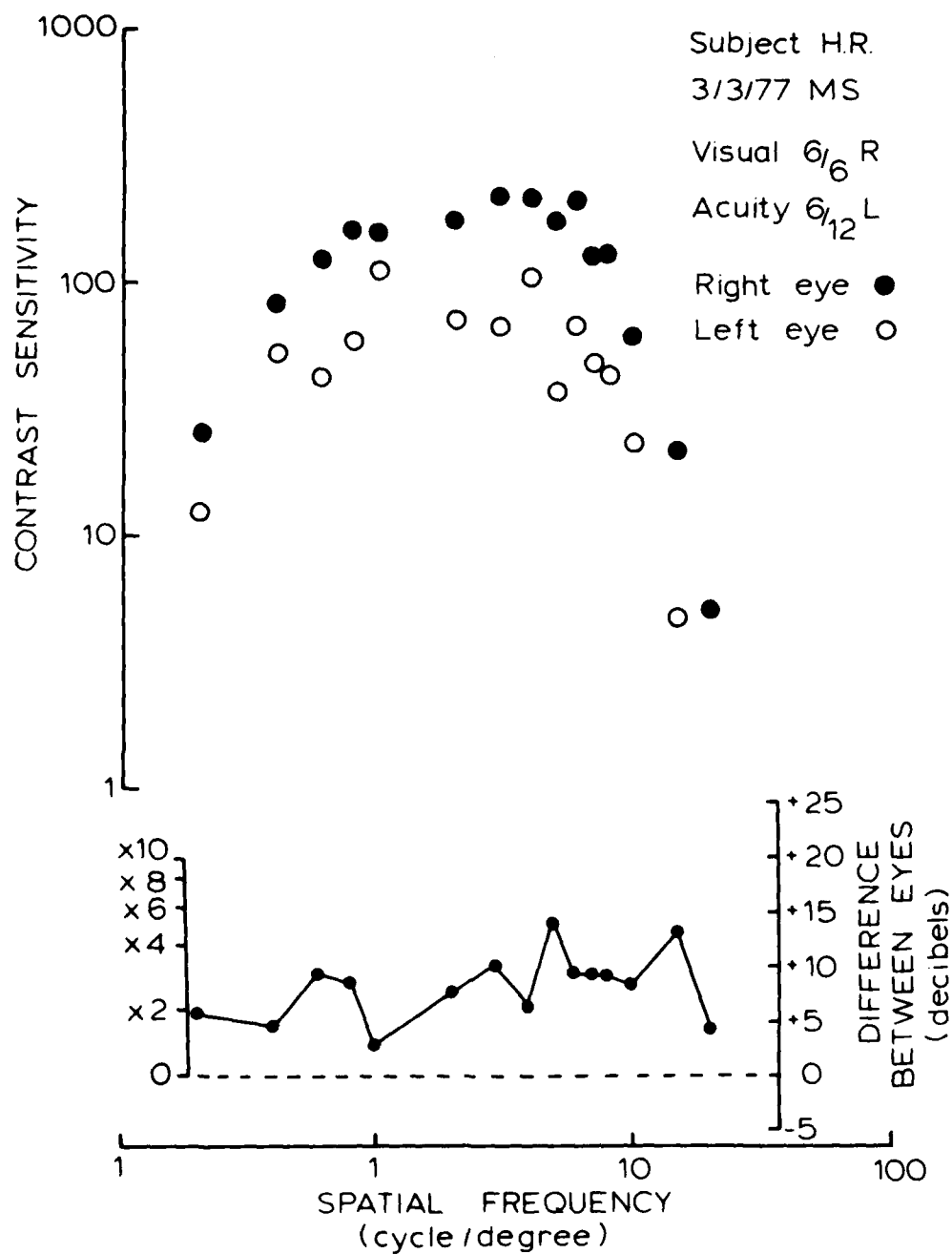


Figure 123. Contrast Sensitivity Functions and Difference Between Eyes Curve:  
Multiple Sclerosis H.R. All Frequency Loss. (Section A-5.2)

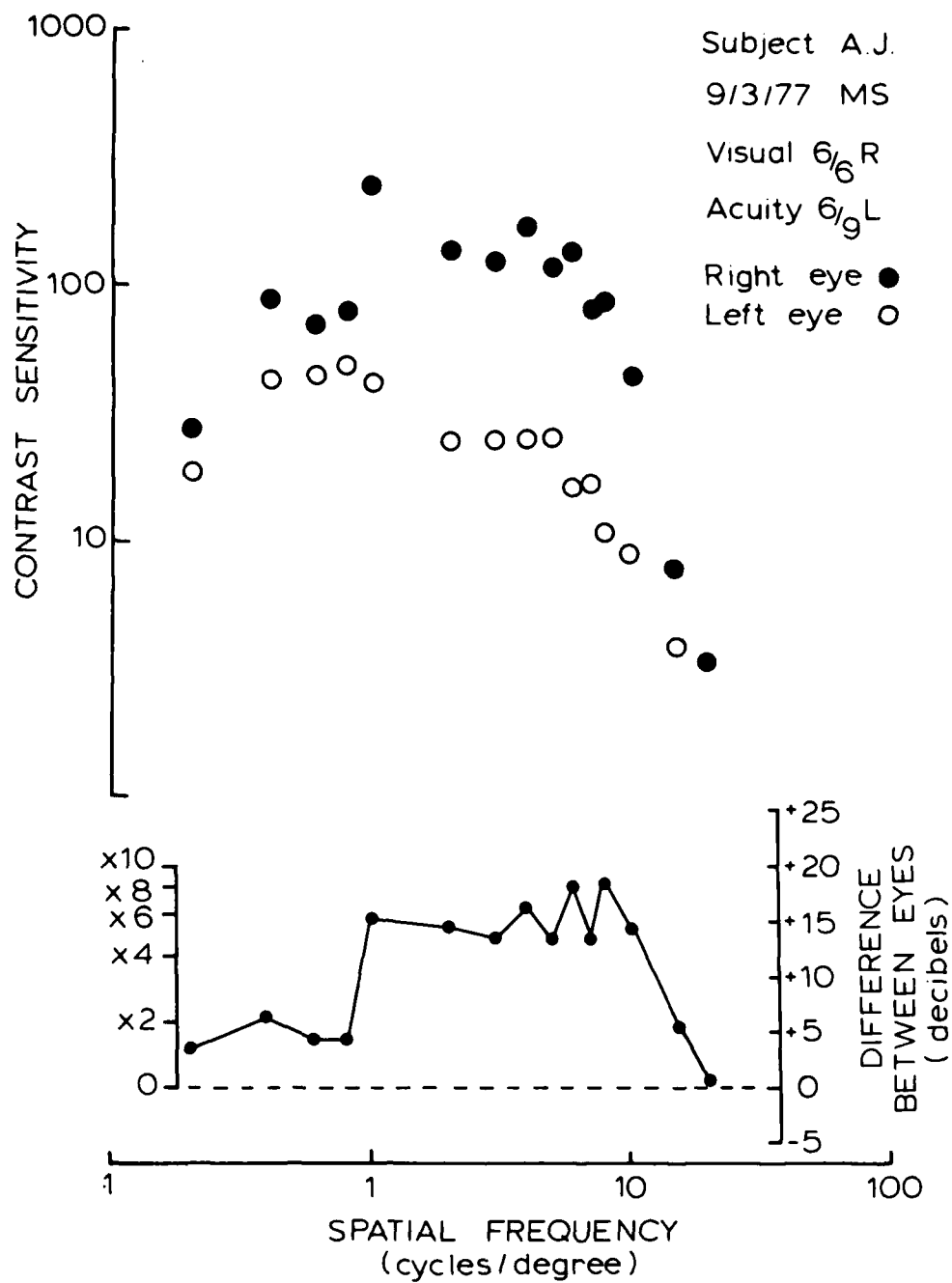


Figure 124. Contrast Sensitivity Functions and Difference Between Eyes Curve:  
Multiple Sclerosis A.J. Predominant Mid-Frequency Loss.  
(Section A-5.2)

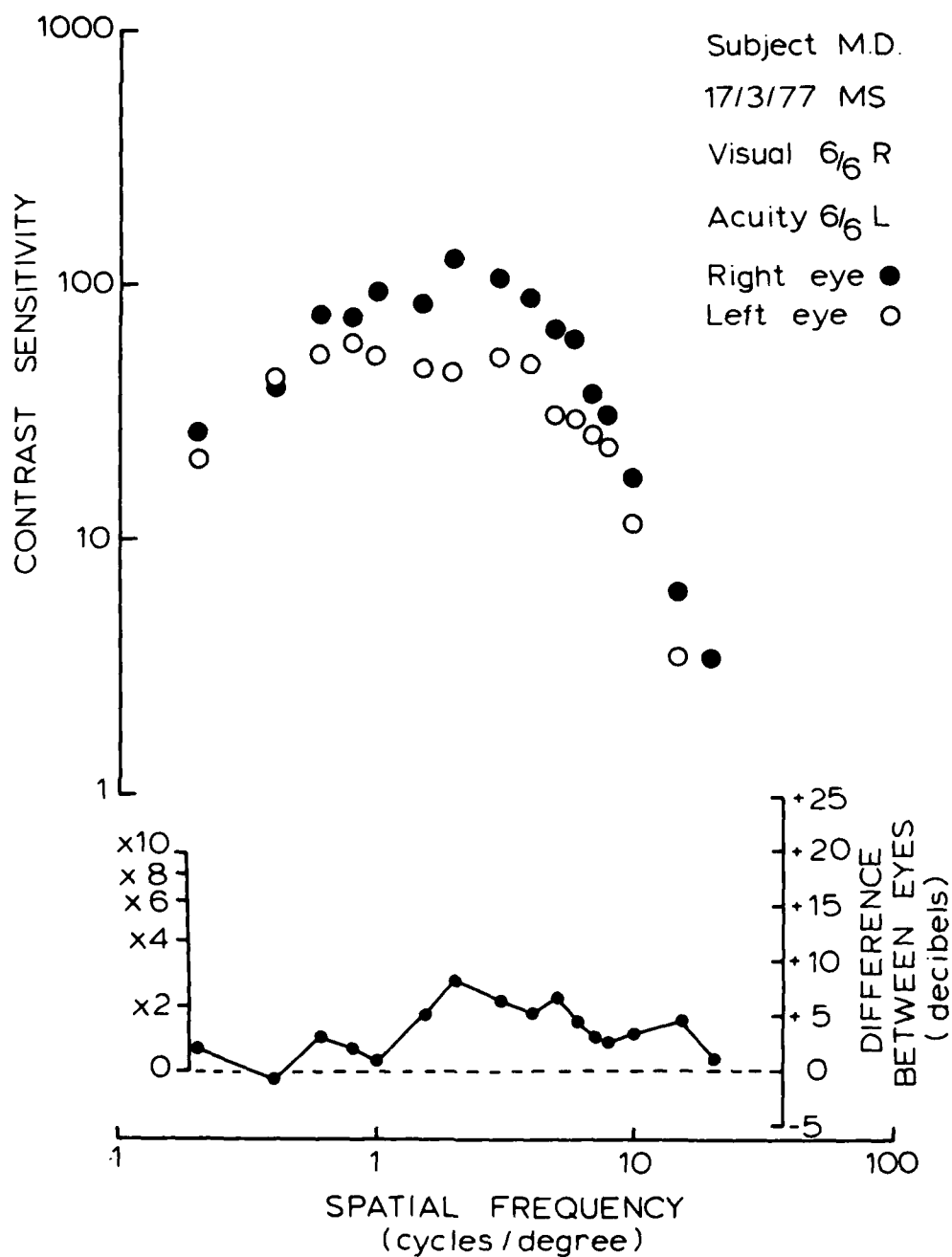


Figure 125. Contrast Sensitivity Functions and Difference Between Eyes Curve: Multiple Sclerosis M.D. Mid-Frequency Loss. (Section A-5.2)

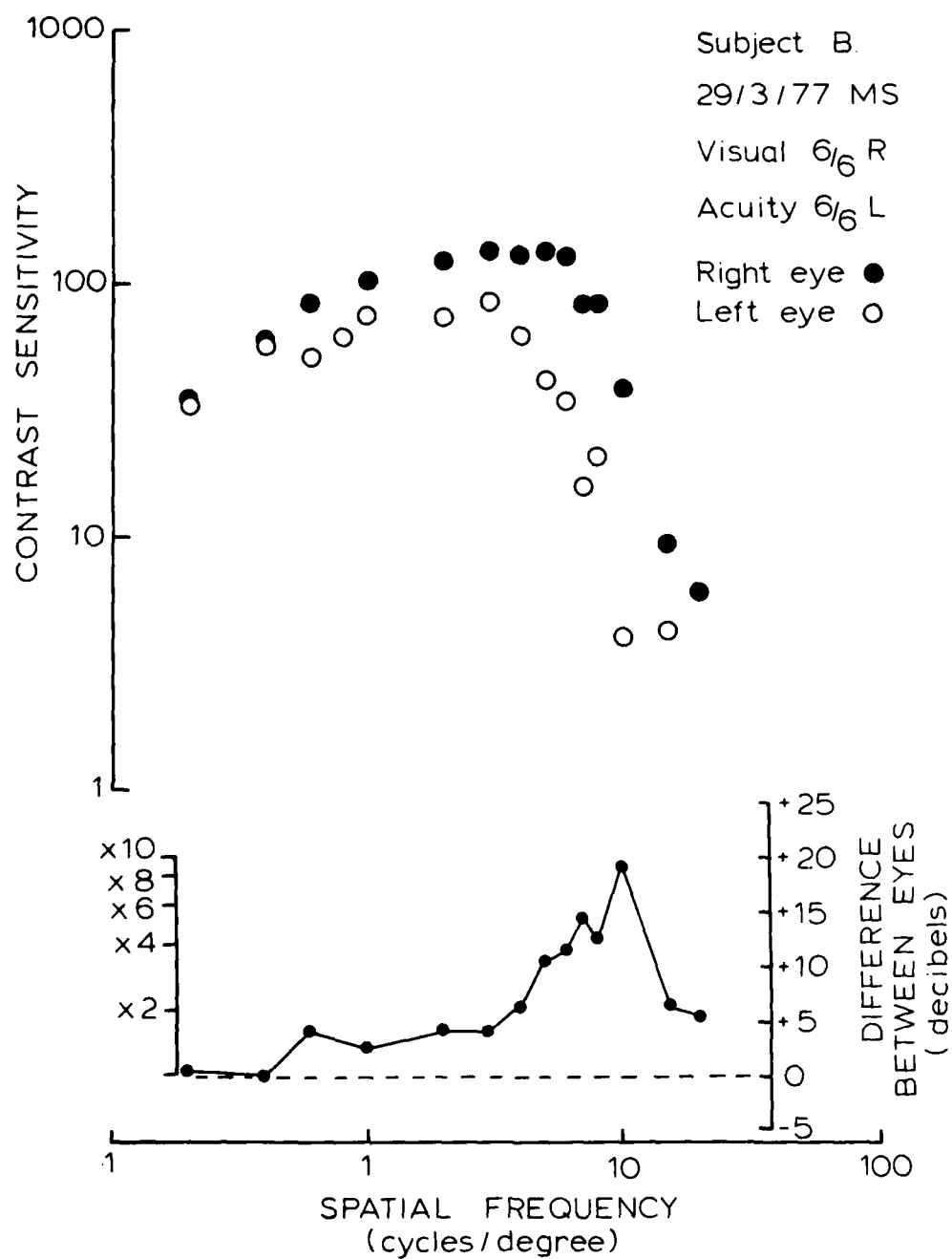


Figure 126. Contrast Sensitivity Functions and Difference Between Eyes Curve:  
Multiple Sclerosis B.M. Predominant High-Frequency Loss.  
(Section A-5.2)



**APPENDIX A**

**INVESTIGATIONS INTO THE FILTERING  
CHARACTERISTICS OF ABNORMAL VISION**

## CHAPTER A-1

### THE FILTERING CHARACTERISTICS OF ABNORMAL VISION

#### A-1.1 Why Investigate Abnormal Vision?

Chapters 9-14 were concerned with the effects of the filtering characteristics of normal vision on the perception of many objects. In these appended chapters, the filtering characteristics of abnormal vision are examined. The motivation for this particular research is two-fold. First, an understanding of visual perception in an abnormal system may lead to a better understanding of how mechanisms of the normal visual system function. Second, a subject with a particular kind of abnormal vision could be used to test certain hypotheses based upon research in normal vision, as was discussed in Section 15.7.

#### A-1.2 Amblyopia

If the neurophysiological filtering properties of abnormal vision are to be investigated, then a condition should be chosen that is not optical in origin. Therefore, the abnormal visual conditions investigated were amblyopia and multiple sclerosis.

Initial investigations began with a visual disorder that affects about four percent of the population: amblyopia. The brief information about amblyopia presented in the following section has been gleaned from Duke-Elder (1949), Borish (1970), and Lyle and Wybar (1970). In general, amblyopia is described as a dimness of form vision that cannot be corrected by optical means. The most common cause of amblyopia is the lack of use of one eye early in life due to strabismus (squint). One eye becomes dominant and is used almost exclusively, to the detriment of the other eye.

Von Noorden (1967) provided a recent classification of different types of amblyopia. In addition to strabismic amblyopia, there is also amblyopia ex anopsia (amblyopia of disuse), anisometropic amblyopia (amblyopia due to a difference in the refractive power between the two eyes), aniseikonia (unequal size of images of each eye), congenital amblyopia (organic malfunction which includes receptor amblyopia secondary to nystagmus and achromatopia), and, finally, ametropic amblyopia (amblyopia due to poor refractive power of the eye). Although seemingly similar, Von Noorden distinguishes ametropic amblyopia from anisometropic amblyopia by noting that the interference in the visual system between unequal images that occurs in anisometropic or strabismic amblyopia never occurs in ametropic amblyopia.

An interesting comment on amblyopia was made by Duke-Elder (1949): "Every child may be said to be born bilaterally amblyopic, and it is only through the constant facilitation of reflexes cumulatively sustained by the reward of clear vision that epicritic vision is attained." Thus, normal development of the visual system may be needed to overcome an initial amblyopic state.

If an abnormal condition persists and is not corrected, amblyopia may result. This can cause two problems: confusion and diplopia (double vision). Confusion results from the spatial overlap of two different images, which occurs because corresponding retinal points are stimulated by two different images. Diplopia results from having the same images appearing side by side. This occurs because noncorresponding retinal points are stimulated by the same image.

The visual system uses three general adaptive mechanisms to inhibit or suppress vision in order to abolish or at least diminish confusion and diplopia: facultative inhibition, obligatory inhibition, and eccentric retinal fixation. Facultative inhibition only occurs in the squinting eye and disappears when it resumes fixation. Obligatory inhibition is a sequel to facultative inhibition and persists even when the squinting eye fixates. Eccentric retinal fixation may follow obligatory inhibition and refers to the nonfoveal receptors that assume a foveal form of projection as a point of reference for other retinal receptors. The change in fixation point is not too rewarding because the foveal type of projection cannot equal the foveal type of acuity. Eccentric retinal fixation is usually preceded by abnormal retinal correspondence.

Abnormal retinal correspondence (ARC) occurs when the projection of the retinal receptors of the squinting eye are centered on a retinal area other than the fovea and assume a foveal type of projection. It differs from eccentric retinal fixation by not being maintained as the fixation point when the squinting eye is used alone. In uncomplicated ARC the inhibition disappears on covering the nonsquinting eye and may be regarded as facultative, and a reasonable level of vision is maintained. However, in some cases of ARC the abnormal state is obligatory and remains after the nonsquinting eye is covered. In such cases, ARC is associated with eccentric retinal fixation and visual acuity is usually poor.

#### A-1.2.1 Early Psychophysical Studies of Amblyopia

The psychophysics of amblyopia has been extensively investigated over the last 35 years (see review by Burian, 1967). Amblyopes have normal light and dark adaptation and can localize points of light (Vogt, 1939; Wald and Burian, 1944). Miller (1954) investigated brightness discrimination and summation in amblyopia. He found that the differential luminance threshold under photopic conditions increased as the width of a stimulus line increased. However, decreasing the width of the line to less than 4 to 6 minutes in the normal eye and 10 minutes in the amblyopic eye did not affect threshold. Miller concluded, in agreement with the earlier results of Wald and Burian (1944), that the fovea of the amblyope behaved like the periphery of a dark adapted normal retina. Similar results were found by Grosvenor (1954) and Meur (1964).

In general, the spatial summation properties of the amblyopic fovea seem similar to those of the normal peripheral retina. The most accepted theory for reduced photopic functioning in the amblyopic fovea was put forward by Miller (1955): reduced lateral inhibition between foveal cones. Miller's theory is attractive because it seems to explain certain clinical phenomena, for example, the "crowding effect" in which acuity is higher for single letters than for lines of letters. Presumably, the reduced lateral inhibition between the foveal cones causes the letters to be smeared together and interferes with their legibility when formed in a line.

Although the crowding effect is usually associated with amblyopia, it was associated with visual acuity by Flom, Weymouth, and Kahneman (1963). They found that the effect of contour interaction with visual resolution is similar in both normal and amblyopic subjects.

All the evidence to date suggests that amblyopia results from cortical inhibition. For example, persons born with a high degree of astigmatism still retain poor vision in the astigmatic meridian even with correcting lenses (Martin, 1890; Luedde, 1922; Mitchell, Freeman, Millodot, and Haegerstrom, 1973). These findings strongly suggest that cortical mechanisms are involved in amblyopia since the cortex is the first site of orientation receptive fields. Furthermore, since the cortex contains binocularly excited neurons, it seems reasonable from an economy of effort viewpoint that the cortex should be involved in the suppression of diplopia.

#### A-1.2.2 Recent Studies of Amblyopia

Much general information about amblyopia has been found using the conventional psychophysical paradigms. However, the use of contrast sensitivity measurements is a more systematic approach which yields more quantitative information than could have been otherwise obtained.

Gstalder and Green (1971) measured the acuity of amblyopes using laser interferometric gratings, sine- and square-wave gratings, and Snellen letters. They found that acuity of amblyopes was greatest with gratings and greater with laser interferometric gratings than with Snellen letters. Although they suggested that the laser generated gratings resulted in the greatest acuity, luminance and criterion differences that existed in their experiments make that conclusion questionable. They also claimed that the measured contrast sensitivity was normal for low and medium spatial frequencies between 1 and 6 c/d for the amblyopic eye compared to the normal eye in the two subjects. However, the contrast sensitivity function shown in Figure 1 of their paper shows similar values only at 1 and 2 c/d. Furthermore, one measurement at 1 c/d does not constitute enough data with which to generalize about contrast sensitivity at the low spatial frequencies.

Hess (1974) in an extensive study using contrast sensitivity measurements found two general classes of strabismic

amblyopia. One class showed losses in contrast sensitivity predominantly over the high spatial frequencies. The second class showed losses in contrast sensitivity over the whole range of spatial frequencies. In their study of several clinical visual disorders, Itoi, Kato, Sugimachi, Kamamura, Ohzu, and Kawara (1975) showed selective spatial frequency losses at middle spatial frequencies in three strabismic amblyopes and two ametropic amblyopes. Unfortunately, they did not measure sensitivity below 2 c/d. Most recently, Levi and Harwerth (1977) investigated both spatial and temporal interactions using gratings in cases of anisometropic and strabismic amblyopia. They found a decrease in sensitivity at all spatial frequencies for both long (500 msec) and short (50 msec) grating presentations for the amblyopic eye. However, the contrast sensitivity for the low spatial frequencies was about the same in both the normal and the amblyopic eye if the grating was flickered at 10 Hz. Such results suggested that there are differences between the perception of static and dynamic patterns in the amblyopic eye.

Such selective spatial frequency losses in amblyopia are difficult to explain without a concept of channels tuned to limited ranges of spatial frequency in the visual system. With this limited background, the spatial stimuli and experimental procedures used to determine the filtering characteristics of some amblyopes are examined next.

## CHAPTER A-2

### THE GENERATION OF STIMULI AND EXPERIMENTAL PROCEDURES

#### A-2.1 The Generation of Spatial Stimuli

The visual stimuli were displayed on the face of a standard television cathode ray tube (CRT) using techniques developed by Schade (1956) and modified by Robson (1966). The display consisted of a raster of about 1000 lines achieved by applying a 250 Hz sawtooth waveform and a 150 Hz triangular waveform to the x- and y-axis of the CRT, respectively. One frame, the required time for the beam to form the raster along the x-axis, took about 4 msec. Both the frame frequency — about five times higher than the highest flicker frequency detectable by the visual system — and the high density of the lines were unresolvable for normal viewing distance.

The mean luminance of the raster was provided by a steady voltage into the z-axis of the CRT and was kept at about 40 foot-lamberts which is in the photopic range of vision. A P31 phosphor provided a short persistence light having a broad wavelength-spectrum with a maximum in the blue-green spectral region. The unmodulated raster appeared to be desaturated green that was spatially and temporally uniform.

##### A-2.1.1 Contrast

The raster was modulated by applying a modulation signal to the z-axis from a standard 500-10 kHz oscillator. Sinusoidal modulation produced a sinusoidal grating that did not change the mean luminance of the screen. As previously discussed, the depth of modulation about the mean luminance determined the contrast.

Over the range of contrasts studied, the luminance of the screen (measured by a linear photocell) varied linearly with the modulation voltage.

##### A-2.1.2 The Stimuli

The gratings used in all the experiments were vertically oriented with luminance varying along the horizontal axis about a constant mean luminance.

##### A-2.1.2.1 Stationary Gratings

A stationary grating was achieved by synchronizing the frame frequency of the CRT with the frequency of the z-axis modulation signal. The grating can be described by

$$L(x) = L(1 + m \cdot \sin 2\pi f_x x)$$

where  $L$  is the mean luminance,  $m$  is the contrast, and  $f$  is the spatial frequency. As a reminder, spatial frequency is defined as the number of cycles of the grating per degree of visual angle (c/d).

##### A-2.1.2.2 Moving Gratings

Gratings can be made to appear to move along the horizontal axis of the CRT. A moving grating can be described by

$$L(x, t) = L[1 + m \cdot \sin 2\pi(f_x x + V_t t)]$$

where  $V$  is the velocity of the movement in degrees of visual angle per sec (d/sec). Since  $V = f_t/f_x$ , where  $f_t$  is the temporal frequency in hertz, the moving grating can be described by

$$L(x, t) = L[1 + m \cdot \sin 2\pi(f_x x + f_t t)]$$

Using a trigonometric identity yields

$$\sin 2\pi(f_x x + f_t t) = \sin 2\pi f_x x \cdot \cos 2\pi f_t t + \cos 2\pi f_x x \cdot \sin 2\pi f_t t$$

That is, a moving grating is the sum of two sinusoidally modulated gratings that are 90 degrees out of phase with respect to both space and time.

### A-2.1.2.3 Split-Screen Gratings

The contrast matching experiments require the independent control of spatial frequency and contrast of two sinusoidal grating displays. In order to avoid any problems associated with matching two different display systems, a split-screen technique was used to provide the two independent displays using the same CRT. The split screen was made by using the trigger signal from the CRT that provided the frame rate to synchronize two oscillators and trigger a pulse generator. The pulse generator provided a signal at twice the frequency of the frame rate that was used to drive an electronic switch. The electronic switch alternately connected the output of each oscillator to the z-axis of the CRT which, in turn, created two half-frames on the CRT. Although two gratings were adjacent to one another on the same screen, the spatial frequency and contrast of each half-frame could be controlled independently.

The luminance distribution of the split screen can be described by

$$\begin{aligned} L(x) &= L(1 + m_1 \cdot \sin f_{x_1} x) \quad \text{for } x \leq 0, x/2 \\ &= L(1 + m_2 \cdot \sin f_{x_2} x) \quad \text{for } x > x/2, x \end{aligned}$$

A white 2 cm wide strip of cardboard was placed over the CRT to separate the two fields and prevent the subject from using any information from the portions of the gratings that were immediately adjacent to one another in the experiments.

### A-2.1.3 Determining Contrast

Contrast of the gratings was determined by passing the output of the oscillator through a potentiometer that attenuated the grating 39 dB in 0.025 log unit steps. The base contrast was determined with the attenuator set at zero. A neutral density filter of known value was placed over a square-wave grating that was displayed on the CRT. The oscillator output was then adjusted to make the light and dark bars appear to be of equal brightness. A neutral density of 0.3 was used to create a base contrast of 33 percent. Higher values of contrast were determined by a decade attenuator in series with the potentiometer and use of a nonzero setting for the base contrast. In this way, higher contrasts could be obtained by decreasing the decade attenuator.

The logarithmic potentiometer was mechanically linked to a second potentiometer which provided a linear output voltage in direct proportion to the logarithmic potentiometer. The output voltage went to the analogue/digital converter of a PDP 8/I digital computer for the calculation of contrast sensitivity.

The display screen was surrounded by a white card that was illuminated by a projector to about the same mean luminance as the CRT. This was done to reduce the fatigue of the observer that can occur when he makes many threshold measurements over a visual area that has large differences in contrast. Furthermore, it insures a constant level of adaptation of the eye as it wanders over the whole display.

## A-2-2. Measuring Contrast Sensitivity

The experimental condition for the observers during the measurement of contrast sensitivity was as follows. The subject randomly scanned a CRT across which a sine-wave grating of zero contrast was presented. A blank screen of uniform luminance was seen. The contrast of the grating was increased until it could only just be seen. The lowest contrast at which the grating was seen is called the contrast threshold. The reciprocal of the contrast threshold is called the contrast sensitivity.

The contrast of the grating was controlled by means of a potentiometer, as previously discussed. When the subject set the contrast threshold, he pressed a microswitch which enabled the computer to read the voltage across the potentiometer and to compute the contrast of the grating. At least ten consecutive measurements were made at each spatial frequency and the mean was computed and used to compute the value of contrast sensitivity. The viewing distance was 57 cm for the measurements of the spatial frequencies at and below 2 c/d. The viewing distance was 229 cm for the measurements of high spatial frequencies above 2 c/d. Appropriate lenses were placed before the eye being tested to provide in-focus gratings with minimum accommodative effort by the subject. The square grating field subtended 24.5 degrees by 19.3 degrees at 57 cm, and 6.1 degrees by 4.8 degrees at 229 cm.

This technique for obtaining threshold measurements is called the method of adjustment. It is a simple and popular

method for measuring contrast thresholds. But it is open to criticism, mainly because it is subjective and subjects can adopt different criteria for the amount of a grating that is seen at threshold. Other alternative techniques, such as the method of constant stimuli, requires a considerable amount of time for data collection. The time required for such measurements and the tedium involved would be unrealistic for the number of subjects and physical conditions (e.g., multiple sclerosis) that were used in these studies.

Another reason the method of adjustment was chosen is that the vast majority of data was to be used to compare the performance of one eye against the other eye in the same subject. Thus, small individual differences in the criterion for threshold would not be important so long as the criterion of the subject remained the same for each eye during each set of measurements.

The ascending method of adjustment was chosen. That is, the contrast threshold was obtained by increasing the contrast of the grating until it was seen rather than decreasing the contrast of a high contrast grating until it was not seen. Inexperienced subjects had no difficulty with this method which avoids any effects of adaptation of gratings of higher contrast that could result in a higher threshold (Blakemore and Campbell, 1969).

### A-2.3 Measuring a Contrast Match

A split-screen CRT with one side containing a vertical grating of one spatial frequency and contrast and the other side a vertical grating of another contrast and sometimes a different spatial frequency was used for measuring a contrast match. The subject adjusted the contrast of one of the gratings (the variable) until it appeared to be the same as that of the other grating (the standard). This procedure is called contrast matching.

The measurements reported here were made in a manner partially similar to that of Georgeson and Sullivan (1975) in an attempt to replicate their results. The major difference using this method was the selection of a standard grating of 2 c/d rather than 5 c/d because previous contrast sensitivity measurements using this apparatus were maximum at about 2 c/d. Thus, the contrast matches were made between a standard sinusoidal grating of 2 c/d and variable gratings whose spatial frequencies ranged from 0.2 to 25 c/d. The contrast of the standard grating ranged from 0.03 percent to 66 percent in 6 db steps. As with the measurement of contrast sensitivity, two viewing distances were used: 57 cm for spatial frequencies 2 c/d and below; 229 cm for spatial frequencies 2 c/d and above. Appropriate lenses were placed before the eye to create in-focus gratings with near zero accommodative effort by the subject. At 57 cm each field subtended 12 degrees by 19.3 degrees separated by a 1 degree wide strip of cardboard. A 2.5 degree strip separated the 3 by 4.8 degree fields when viewed from 229 cm. Monocular viewing was used and the observer was allowed as much time as desired to look back and forth at the two gratings.

The contrast of the standard grating was set by the experimenter. The contrast of the variable grating was adjusted by the observer with a logarithmic potentiometer for a contrast match. In general, five contrast matches for each condition were obtained at each session. The contrast of the standard grating was changed in either ascending or descending order for each frequency of the variable grating. The frequencies of the variable grating were quasi-random. Contrast threshold measurements were also determined in each session. The data were collected using the same computer techniques as used for the contrast sensitivity measurements except for minor changes in the computer programme to reduce the number of trials per block of runs and to accept a change in attenuation for each trial.

One major criticism of this method is that large effects from adaptation could occur from free inspection of high contrast gratings. However, a recent study of contrast matching by Kulikowski (1976) has shown that there is little if any difference in results of such measurements when comparing the method of adjustment (using long viewing time) to the method of constant stimuli (using short viewing time). Furthermore, each setting of contrast rarely took more than 10 seconds to make — a period of time much shorter than the usual 2 to 3 minutes used for adaptation studies (e.g., Blakemore and Campbell, 1969).

### A-2.4 Changing Contrast by Polarizers

A polarizer is an optical device whose input is natural light and whose output is some form of polarized light. Polarized light is light whose orientation (transmission axis) of the electric field is constant although the magnitude and sign vary with time. Let the amplitude of the electric field transmitted by the polarizer be  $E_0$ . If a second polarizer (called

an analyzer) is placed in the optical path of plane polarized light, only the component that is parallel to the transmission axis of the analyzer will reach the detector (assuming zero absorption). This component will be equal to  $E_0 \cos \phi$ , where  $\phi$  is the angle of rotation from the transmission axis. The irradiance,  $I$ , proportional to the square of the amplitude, reaching the detector is given by Malus's Law, e.g., see Hecht and Zajac (1974).

$$I(\phi) = I_0 \cos^2 \phi$$

Note that at  $\phi = 90$ , theoretically, no light is transmitted because the electric field that has passed through the polarizer is perpendicular to the transmission axis of the analyzer. At this rotation the two polarizers are said to be crossed. The resulting electric field is therefore parallel to what is called the extinction axis of the analyzer and has no component along the transmission axis. A more detailed account of polarization can be found in Hecht and Zajac (1974).

It is desirable to have a simple system that changes the contrast of complex objects. A crossed polarizer system allows a controlled amount of light to be reflected from an object. However, in order to change the contrast and keep the mean luminance constant, two crossed polaroid systems are needed. Constant mean luminance is achieved if the light from the two polarizers of orthogonal polarization is collected through one analyzer. As the analyzer is rotated, an increase in the light transmitted by one polarizer will be accompanied by a decrease in transmission of the same amount by the other polarizer. The overall effect of rotating the analyzer is to change the contrast of the object while maintaining constant mean luminance.

A crossed polarizing device was built with two projectors. The light transmitted from the projectors was directed through separate polarizers. The light from the polarizers was directed through one analyzer — a large circular piece of polaroid mounted on a rotating device. The analyzer angle was read directly in degrees from a scale fixed to its mount. The light from the two projectors was imaged onto the same surface area. Appropriate alignment of the polarizers produced maximum and minimum contrast of the object as the analyzer was rotated from 0 to 90 degrees.

The mean luminance of the combined projectors varied  $\pm 2$  percent as the analyzer angle rotated from 0 to 90 degrees. The mean luminance of the projected stimuli was determined using a linear photocell and the luminance of the other projector was set to that value.

Although the contrast of an object could be calculated directly from Malus's Law, in practice, any difference between the projectors, polarizers, and the alignment of the system will produce errors. Therefore, luminance values were obtained from a linear photocell as the analyzer rotated and were used to determine the contrast versus analyzer angle curve shown in Figure 96. The contrast of an object was calculated by multiplying the original contrast of the object by the contrast at the angle of the analyzer. Some of the predicted values of contrast generally differed by 10 percent from the measured values. Thus, it is quite important to measure calibration curves and not use Malus's Law when employing such polaroid systems.



## CHAPTER A-3

### CONTRAST SENSITIVITY FUNCTIONS OF AMBLYOPES

#### A-3.1 Methods

Contrast sensitivity functions were obtained using the methods discussed in Section A-2.2. Both the normal and the amblyopic eye were measured during the same session. Contrast sensitivity measurements for the same spatial frequency taken at two different viewing distances were not averaged to reduce any possible artifacts in the analysis of the data. Appropriate lenses were placed before each eye to provide in-focus gratings with minimum accommodative effort from the subject. This reduced any possible artifacts of the measurements due to different accommodative states of the eyes and also decreased fatigue due to eye strain. The reference to the normal eye is used only in a relative sense to distinguish the differences between the two eyes. It does not mean that the nonamblyopic eye is normal.

#### A-3.2 Sensitivity Loss at All Spatial Frequencies

Subject J. P. is a 32-year old woman with a minimal left convergent squint, left hyperopia (far-sighted) and left amblyopia with normal retinal correspondence. Her Snellen letter acuity was 6/5 for the right eye (R) and 6/9 for the left eye (L).

Regarding contrast sensitivity shown in Figure 97, a general loss is exhibited in her amblyopic eye at all spatial frequencies but most markedly at the higher spatial frequencies from 5 to 15 c/d. The difference in sensitivity between the eyes is more clearly seen in the lower curve of Figure 97 which shows a maximum difference in sensitivity of about 11 dB at 8 to 10 c/d. This loss of sensitivity at all spatial frequencies is typical of one class of amblyopes (Hess, 1974).

#### A-3.3 Sensitivity Loss at High Spatial Frequencies

A more severe case of high frequency loss was found in the amblyopic eye of subject M.B., a 62-year old woman diagnosed as a left anisometropic amblyope with Snellen letter acuity of 6/4 (R) and 2/60 (L). Even with corrective lenses, her contrast sensitivity measurements, shown in Figure 98, reveal large differences in sensitivity between her amblyopic and her normal right eye beginning at 2 c/d. No measurements could be obtained in her amblyopic eye for spatial frequencies greater than 5 c/d. Unfortunately, due to illness of the subject, threshold measurements at the lower ranges of spatial frequency could only be made for her amblyopic eye. However, the results obtained from her more normal eye suggest that there would be little, if any, difference between the eyes at the lower spatial frequencies. This general loss of sensitivity over the high spatial frequencies is typical of a second class of amblyopes (Hess, 1974).

Note that there is almost a 4 log unit (35 dB) difference between the sensitivity of the eyes at 5 c/d shown in the lower curve of Figure 99. There appears to be general agreement of Snellen acuity and contrast threshold measurements, indicating a large degradation in vision in the amblyopic eye.

Her amblyopic eye is quite spatial frequency selective. The bandwidth measured at half-sensitivity is about one octave with a centre frequency of 1 c/d. In general, the contrast sensitivity measurements of the amblyopic eye of this subject appear similar to measurements of a normal observer with + 3.5 diopters of blur (Campbell and Green, 1965). However, when questioned, the subject reported the appearance of objects not consistent with blur. Although this subject was quite verbal and fully trained in ophthalmic practice, she could not convey a meaningful description of what the amblyopic eye saw. She described colour and contrast as more vibrant in her amblyopic eye as compared to vision in her normal eye. Objects seemed to stand out from their background, take on a different texture, and "become more interesting."

An attempt was made to determine if vision in her normal eye could be degraded to the degree where objects would appear to be similar in both eyes. She viewed objects with her normal eye through several layers of semi-opaque plastic

and used lenses to diffuse and blur the objects. However, even with appropriate lenses in front of her amblyopic eye to correct for viewing distance, objects still appeared to be different when viewed by the two eyes. She could not equate the sharpness of objects between her two eyes with induced blur, and the semi-opaque cover over her normal eye caused objects to look foggy or misty. These curious observations were puzzling until contrast matching studies were made with another amblyope. A discussion of the possible reasons for not having been able to create visual conditions in her normal eye that were similar to those in her amblyopic eye is deferred until Section A-4.2 where the results of the contrast matching experiments are discussed.

An attempt to gain a more quantitative assessment of her subjective visual impressions was made by asking her to describe the filtered portraits shown in Figure 28. She reported the MTF filtered image (Figure 28,a,c,2) to be "better" portrait than the original (Figure 28,a,c,1) for both the original and coarsely quantized portraits. However, the low-pass filtered images of both the original and the coarsely quantized portraits appeared similar to their MTF filtered counterparts. These surprising results suggest that when there were no high spatial frequencies present to provide sharp detail such as edges, then her amblyopic eye saw the portraits as if they were blurred. The high spatial frequency detail in the original portraits appeared to interfere with perception in the amblyopic eye. Again these curious results were inexplicable until contrast matching measurements were made on another amblyope.

### A-3.4 Selective Loss at Mid-Spatial Frequencies

#### A-3.4.1 Stationary Sine-Wave Gratings

The most interesting and unique filtering characteristics came from subject A. H., a 20-year old female student who was diagnosed as having a left converging squint, left hyperopia, and amblyopia with a slight left eccentric fixation and abnormal retinal correspondence (ARC). Her Snellen acuity was 6/5 (R) and 6/36 (L) when she started the experiments. Her initial contrast sensitivity measurements shown in Figure 99 reveal large reductions in sensitivity for frequencies greater than 2 c/d. Especially note that there is a considerable decrease in sensitivity of just over one log unit in her amblyopic eye from 4 to 5 c/d, suggesting the possibility of a highly spatial frequency selective loss—a "notch" at 5 c/d.

A second set of measurements two days later produced results shown in Figure 100. Note especially the notch—the highly spatial frequency selective loss at 5 c/d suggested from the initial measurements. The contrast sensitivity in the amblyopic eye was increased over that in the initial measurements which resulted in about a 5 dB reduction in the difference between her normal and amblyopic eye at 4 to 5 c/d. This increase in sensitivity in the amblyopic eye does not appear to be due to a general practice effect. Note that the standard error of the average contrast sensitivity for both eyes, shown in Figure 101, reveals quite stable measurements from the normal eye, whereas the amblyopic eye has changed considerably.

The decrease in the contrast sensitivity difference between eyes is shown in Figure 102. The positive data points indicate increased sensitivity in the left eye over almost the whole range of spatial frequencies. This increase in sensitivity in the amblyopic eye from the first to the second set of measurements suggests caution in interpreting the visual characteristics of amblyopes from initial contrast sensitivity measurements. Furthermore, such results suggest the possibility of a plasticity in the mechanisms of amblyopia that are quite sensitive to stimulation. This increase in sensitivity occurred after the amblyopic eye was tested for only one hour two days previously.

Although all the data points are not statistically significant from one another, there is a trend towards increased contrast sensitivity in the amblyopic eye at the low spatial frequencies, below 2 c/d. This trend is evident in both Figures 99 and 100.

The surprising spatial frequency selective notch in contrast sensitivity is highly suggestive of depressed activity in about a  $\pm$  one-octave channel with a centre frequency of about 5 c/d. A review of the literature has not revealed similar findings except for data reported by Itoi, et al. (1976). Three patients having strabismic amblyopia and one patient having ametropic amblyopia appear to have highly selective losses in contrast sensitivity from 6 to 12 c/d. Unfortunately, there are too few spatial frequencies measured about the least sensitive spatial frequency to be certain.

The notch and general decrease in contrast sensitivity of the high spatial frequencies of subject A. H. are more similar to the contrast sensitivity obtained by + 3.5 diopters of blur by Campbell and Green (1965) than that of subject M. B. However, just as with subject M. B., no amount of optical defocus of her normal right eye could create vision of objects similar to that seen by her amblyopic eye. Once again the reason for this will be given in the discussion of contrast matching studies in Section A-4.2.

One possible cause of the notch may be abnormal retinal correspondence. (I am indebted to Jean Lowry of Addenbrooks Hospital, Cambridge, for pointing out this possibility.) Recall that ARC occurs when the peripheral retina assumes a central retinal projection instead of at the fovea and is not maintained as the fixation point when the normal eye is covered. It is possible for a subject to control the ARC. Dr. Wilkins at Addenbrooks Hospital, Cambridge, had a subject with three different fixation points that could be controlled at will (personal communication, 1977). Such findings suggest that subject A. H. could have been using different parts of her retina, and, hence, different regions of spatial sensitivity, during her measurements. For example, she could have been shutting off the foveal region during the measurements of lower to mid-spatial frequencies and then using the foveal region for the higher spatial frequencies. A notch in her contrast sensitivity function would represent the region of crossover from one retinal field to the other.

This hypothesis was tested by measuring the contrast sensitivity function of a subject that was not amblyopic but did have ARC. The results shown in Figure 103 do not reveal a notch in any region of the mid- to high spatial frequencies. This result suggests that ARC may not be the cause of the notch in subject A. H.

#### A-3.4.2 Moving Sine-Wave Gratings

The next experiments were designed to further probe the tuning characteristics of the notch. It was noticed that the subject seemed to move her head horizontally during the measurements with her amblyopic eye, as if to cause the grating to move across the retina. When queried, she claimed that, in general, she saw the grating better with her amblyopic eye if she kept it moving across her retina by constantly shifting her gaze.

It appears that two types of mechanisms in the visual system, transient (Y) and sustained (X), provide separate channels for viewing moving and stationary objects (Cleland, Dubin, and Levick, 1971; Kulikowski and Tolhurst, 1973). The behaviour of A. H., supported by her comments, suggested that she was attempting to avoid using or could not satisfactorily use her sustained system for viewing the stationary gratings and thus, by constantly shifting her gaze, she was attempting to use her transient system for the task. It is possible that her tuning characteristics resulted from partially inoperative sustained mechanisms over the middle range of spatial frequencies. This hypothesis was tested by measuring her contrast sensitivity to gratings that were moved horizontally at 5 Hz — a temporal frequency that provides maximum sensitivity for normal subjects.

The results in Figure 104 show that the mid-frequency notch has remained with the moving gratings. Note that the contrast sensitivity at the lower spatial frequencies remains at a constant value for both eyes. Such results are typical of the tuning characteristics obtained from moving gratings in normal subjects (Robson, 1966; Kulikowski and Tolhurst, 1973).

Note that there is a general trend for an increase in sensitivity in the amblyopic eye compared to the normal eye at the lower spatial frequencies in opposition to the data obtained with the stationary gratings. A second set of data collected the following day was similar (Figure 105). The average of the two measurements shown in Figure 106 reveals a smaller decrease in sensitivity between the eyes than did the results from the stationary gratings, except at 3 to 4 c/d. This smaller decrease in the difference between the eyes is shown in Figure 107. Finally, note that the relative contrast sensitivity around the notch at 5 c/d is generally the same for both the stationary and drifting gratings, although there is about a 5 dB increase in the difference curves at 7 to 9 c/d with moving gratings.

These results suggest that the mechanism (or mechanisms) responsible for the decreased sensitivity in this subject are common to both the transient and sustained visual systems. These results are in general agreement with those of Levi and Harwerth (1977) who investigated the spatio-temporal interaction of sine-wave gratings in four subjects that had

either ametropic or strabismic amblyopia. Similar to the results reported here, they found that the contrast sensitivity of the amblyopic and normal eyes remained the same at the higher spatial frequencies but increased at the lower spatial frequencies with flickering gratings. They found, at the lowest spatial frequency tested — 0.4 c/d, that the contrast sensitivity with gratings flickering at 10 Hz and with stationary gratings "is essentially equal," for both the normal and the amblyopic eyes of all their subjects. However, the individual measurements of subject A. H. were shown to contain trends of decreased contrast sensitivity to stationary gratings and increased contrast sensitivity to moving gratings in the amblyopic eye compared to the normal eye at the low spatial frequencies, 1 to 0.2 c/d. This increased sensitivity for the lower spatial frequencies for flickering gratings of the amblyopic eye over the normal eye is also evident in subject L. N. in Figure 1 of Levi and Harwerth, who may not be a strabismic amblyope (see their Table I). The results reported here, as well as the previous analysis of the data of Levi and Harwerth, do not support their conclusion that the transient channels for low spatial frequencies are normal in a strabismic or anisometropic amblyopic eye.

Although the notch of subject A. H. remained substantially the same for both stationary and moving gratings at 4 to 5 c/d, those spatial frequencies are equally well detected by both transient and sustained mechanisms (Tolhurst, 1973). Significant differences in that region of spatial frequency between stationary and moving gratings would be expected if the notch were caused by either the transient or sustained mechanisms. Thus, the results reported here, coupled with the previous analysis, suggest that both mechanisms may be involved in strabismic amblyopia. However, further research is needed to determine the relative importance of each mechanism in the overall loss of spatial vision that an amblyope suffers.

#### A-3.4.3 Sine-Wave Versus Square-Wave Gratings

The next step in this investigation was to determine whether a difference in contrast sensitivity existed for subject A.H. between sine-wave and square-wave gratings. Campbell and Robson (1968) showed that above 1 c/d the threshold of a square-wave grating is  $1.27 (4/\pi)$  greater than that of a sine-wave grating. This result was predicted from an assumption of linearity at threshold and that detection at threshold was based upon the energy of the Fourier components of the square wave.

The results of the contrast sensitivity measurements of square-wave gratings averaged over three sessions are shown in Figure 108. Note that the mid-frequency notch that was found using stationary and moving gratings has almost vanished. The peak difference in sensitivity of about 20 dB between the amblyopic and the normal eye has shifted from 4-7 c/d to 7-10 c/d. This increased sensitivity in the mid-frequency notch was quite surprising.

This result suggested that there was a difference in sensitivity to sine- and square-wave gratings which was tested by measuring the contrast sensitivity using square and sine waves during the same session. As can be seen from the results in Figure 109, little difference between contrast sensitivity to sine- and square-wave gratings was found. In general, the square waves were detected at a lower contrast than the sine waves, which is in general agreement with the results obtained by Campbell and Robson (1968). A closer agreement with the  $4/\pi$  difference between the contrast sensitivity of square- and sine-wave gratings is lacking, presumably due to the observer's lack of experience in performing such tasks and also the fact that the presentations of the sine and square waves were not alternated at each frequency for each measurement.

Only the high spatial frequencies were measured in Figure 109 and for the subsequent contrast sensitivity measurements due to the short time that the subject was available. She was usually able to be a subject for only two hours per week. Since the major changes in her contrast sensitivity function were at the high spatial frequencies, the exclusion of low spatial frequencies allowed more time to be used for the following contrast matching experiments.

#### A-3.5 Changes in Contrast Sensitivity in the Amblyopic Eye

The increased sensitivity from 4 to 7 c/d and the concomitant shift to a higher spatial frequency of the peak difference between the eyes has, in general, confirmed the previous results with square waves. The difference in contrast sensitivity between her eyes from her initial measurements to this last set is shown in Figure 110. There is over a ten-fold increase in the difference in sensitivity at 4 c/d; this decreases to less than half that value at 6 c/d! Large changes in

sensitivity over such a narrow range of spatial frequencies suggest a certain plasticity in highly tuned one-to-two-octave bandwidth mechanisms in the visual system.

Could such a change be due to artifacts such as misalignment or changes in the apparatus? Such factors can be ruled out because if, for example, the viewing distance was wrong or the oscillator malfunctioned, then general differences in sensitivity would be expected at all frequencies — not at those just around 4 c/d. However, the contrast sensitivity measurements below 2 c/d and above 10 c/d remained substantially the same. Furthermore, such artifacts should produce concomitant changes in the sensitivity measurements in the normal eye. Since there is no evidence for such changes in the normal eye, it was assumed that the change in sensitivity in her amblyopic eye reflected a real change in the state of her visual system.

The increase in sensitivity to the mid-range of spatial frequencies in the amblyopic eye should be reflected in another measure of acuity. Thus, the subject was tested for Snellen letter acuity in which, surprisingly, the amblyopic eye which was originally tested at 6/36 now tested at 6/18 — a gain in acuity of two lines. Upon testing, the subject, who had been tested with Snellen charts many times in the past, exclaimed, "I have never seen those lines before with my bad eye." A more detailed analysis that relates this subject's change in Snellen acuity to changes in contrast sensitivity can be found in Section 18.3.

In one sense, this subject's increase in Snellen letter acuity should not be too surprising. Quite striking increases in the performance of the visual systems of amblyopes have been reported by many researchers, e.g., Von Noorden (1967). Furthermore, Itoi, et al. (1975), also found increased contrast sensitivity with two amblyopes after 40 days and two months occlusion of the normal eye. Their data showed an increase predominantly in the middle spatial frequencies. The earlier notches were not present after occlusion. However, for some unexplained reason, the second measurements were made at spatial frequencies other than at the notch, and it is uncertain whether their results are the same as those reported here.

The improved performance in their cases was due to specific forms of therapy, e.g., occlusion. In other words, increased acuity occurred in certain types of amblyopes by working the heretofore suppressed amblyopic eye. What is interesting about the results reported here is that there was no conscious attempt to improve the sight in the amblyopic eye. Rather, the increased acuity was an inadvertent result of having the subject use the abnormal eye for comparatively difficult threshold measurements.

It would seem that the time span over which these results occurred, as well as the amount of time the subject spent in the experiment, is important. Her amblyopic eye was used only four times for about one hour each time over a period of one week for the collection of the data in the initial sensitivity measurements using stationary and moving gratings. A four-month break followed due to a summer holiday. Upon her return, the contrast sensitivity of the subject was determined using square-wave gratings, after which the combined sine- and square-wave measurements were made and Snellen letter acuity was remeasured. This increase in visual performance, if it can be replicated with other amblyopes, suggests that gratings may offer a powerful tool, not only in the assessment of amblyopia but as a possible means of therapy. In particular, it may be that only short exposure to gratings that are continuously shifted in spatial frequency might prove quite useful. Such patterns would stimulate all visual channels equally well.

The evidence of a substantial shift in a relatively narrow region of spatial frequency with time suggested that it would be of interest to measure A. H. periodically. Since she was about to go on an extended holiday of about one and one half months, another session was planned just before her departure. The results of the contrast sensitivity measurements made prior to her departure showed a slight decrease of contrast sensitivity in the amblyopic eye. The peak difference between eyes was about 20 dB from 6 to 7 c/d (see Figure 111). This change was not considered to be significant until the data that were obtained from measurements made after her return were found to be quite similar, as shown in Figure 112. Here, a peak difference in sensitivity of 17.5 dB was noted. The final measurements two months later are shown in Figure 113. The peak difference in sensitivity is 16 dB at 6 to 7 c/d. Although there is evidence for a slight decrease in the peak difference between eyes in spatial frequency, there was a consistent reduction of about 4 dB in these last three sets of measurements as compared to previous ones. Her Snellen acuity remained at 6/18. This subject was retested for contrast sensitivity and Snellen acuity after 10 months. No significant decrease in contrast sensitivity or Snellen acuity had occurred.

It can be concluded that, in general, A. H.'s loss of the highly selective spatial frequency notch has remained relatively stable for a period of about one and one-half years.

The peak contrast sensitivity of subject A. H. at 2 c/d increased considerably in both her normal and amblyopic eye over the 34-week period when measurements were made. This trend of increased sensitivity, shown in Figure 114, is seen from the straight lines that have been drawn by eye. Although both eyes have increased in sensitivity during the course of the experiments, the normal eye has increased at a higher rate than the amblyopic eye. Further research is needed to determine if the increased sensitivity resulted from practice effects and/or if the physiological sensitivity increased. Similar results of increased contrast sensitivity from normal subjects tested for over one year have been noted by DeValois (1977).

#### A-3.6 Summary

The results of determining contrast sensitivity functions of several amblyopes have been shown. One amblyope showed a unique highly spatial frequency selective region of decreased contrast sensitivity at mid-spatial frequencies. This region of decreased sensitivity showed an increase of over 20 dB from initial to final measurements. These novel results are concerned with threshold vision. The next study involved investigation of the suprathreshold vision of the same amblyope.

## CHAPTER A-4

### SUPRATHRESHOLD VISION OF AN AMBLYOPE

An attempt was made to make sine and square waves look similar to the amblyopic eye of subject A.H. by changing contrast. No systematic range of contrast produced consistent waveforms that she would call sine or square wave over the range of spatial frequencies tested — 1 to 7 c/d. Furthermore, an attempt was made to determine whether square waves could be seen as the same waveform in both eyes by changing only contrast. Again no systematic results were obtained. These negative results suggested a very complex interrelationship between contrast and spatial frequency.

One interesting result of the investigations of amblyopes was the inability of the subjects to describe, except in the most general terms, what they saw with their amblyopic eye. This result is curious because each had a relatively normal eye with which to compare vision in the amblyopic eye. Yet no optical means used to reduce acuity and/or contrast in the normal eye seemed to provide objects that appeared similar to those seen by the amblyopic eye. These results were surprising since the contrast sensitivity functions in two of the amblyopes were quite similar to those obtained with optical blur, as previously discussed.

There is, however, another factor to consider in attempts to equate the perception of suprathreshold objects that are composed of complex spatial frequency distributions to the perception of spatially pure objects such as gratings at threshold. Objects have many different spatial frequencies in two dimensions at many different levels of contrast. The results of contrast matching experiments which have been discussed suggest that the gain of mechanisms tuned to different ranges of spatial frequencies is at different levels of activity, depending upon contrast. Although the contrast matching functions are a well behaved family of functions (similar monotonic increasing and decreasing functions) for the normal observer (see Figure 13), there may be differences in contrast matching between a normal and amblyopic eye. And, such differences may account for the strange and poor descriptions of objects seen with an amblyopic eye.

Such considerations, as well as the desire to gather more quantitative data on amblyopia using a technique that has not been used before on amblyopes, prompted the next set of experiments — contrast matching.

#### A-4.1 Contrast Matching of a Normal Observer

Contrast matching data from a corrected astigmat, A. G., the author, were obtained in order to provide a reference for similar data that were collected from the amblyope A. H. The methods used were discussed in A-2.3. Figure 13 shows that the contrast matching data of subject A. G. provide a family of equal-contrast contours plotted similarly to the data of Georgeson and Sullivan (1975). The standard spatial frequency used was 2 c/d, the spatial frequency for which contrast sensitivity was maximal in previous measurements. The standard contrasts at the standard spatial frequency are represented by the triangular symbols. The connected open symbols represent the contrast of the test grating that appeared to match the contrast of the standard grating. A physical match between the standard and the test grating will result in equal contrast curves which are horizontal lines through the standard contrast symbols. Such results are evident, in general, from 0.2 to 10 c/d for the higher contrasts. However, at lower standard contrasts the equal-contrast curves approach the contrast sensitivity function. The uppermost curve is the contrast sensitivity function.

These results are in general agreement with similar measurements of other researchers, e.g., Watanabe, et al. (1968); Georgeson and Sullivan (1975).

#### A-4.2 Contrast Matching by an Amblyope

The contrast matching data for the amblyope A. H. are shown in Figure 115. The low spatial frequency contrast matching data from 0.2 to 2 c/d were based on the average of five trials. The high spatial frequency contrast matching data from 2 to 20 c/d were based on the average of three sessions of five trials each. As with the contrast sensitivity measurements, the normal and amblyopic eye were tested during the same session.

The contrast matches for the low spatial frequencies appear normal when compared to the results of subject A. G.

(Figure 13). The contrast measurement and contrast match at the low levels of contrast were as expected, showing a mid-frequency loss and cutoff. The highest curve is A. H.'s contrast sensitivity function. However, the results at high contrast were quite unexpected for both the normal and the amblyopic eye. The loss of sensitivity of the amblyopic eye shown by matches at 5 c/d at contrasts below 16.5 percent is not evident at the high contrasts of 33 percent and 66 percent. There is also a trend of increased sensitivity at 10 c/d, especially at the 33 percent contrast level. Note that this increased sensitivity at 10 c/d reverses at 15 c/d.

The contrast matches in the normal eye were as expected except at 10 c/d where an abnormal decrease in the ability to make a contrast match was evident in general for higher contrasts of 33 percent and 66 percent. Such losses at 10 c/d at the higher contrasts are not found in the contrast matches of subject A. G. Thus, A. H.'s "normal" eye may not be normal. These quite unexpected contrast and spatial frequency selective differences from the contrast match in her normal and amblyopic eye are reflected in each of the three testing sessions as shown in Figure 116.

The individual and average differences in contrast matches between the normal and amblyopic eye are seen more clearly in the difference curves of Figures 117 and 118. The differences in sensitivity between the normal and the amblyopic eye are expressed in decibels. The numbers on the left side of each set of curves are the standard contrasts. The three sets of measurements in Figure 117 are from three different test sessions. No data are shown for the standard contrast of 0.011 on the 16/3/77 or 22/2/77 test session because the subject could not do a contrast match at the 0.011 standard contrast. Thus, the results shown for the 0.021 standard contrasts for those measurements are the contrast sensitivity measurements.

Note the increased sensitivity of the amblyopic eye at 10 c/d at high contrast and the decreased sensitivity at 5 c/d at low contrast with respect to the other eye. Positive differences in Figures 117 and 118 mean that the normal eye matched more closely to the baseline contrast match at 2 c/d than the amblyopic eye. Negative differences reflect the reverse situation. The average differences between eyes in Figure 118 are the averages of the differences of all the measurements. The vertical lines indicate plus and minus two standard errors. This method of determining the average differences is only valid if the individual differences are of the same sign. If some individual differences are of opposite sign, then the numerical average will not reflect the degree to which the two eyes differ. This situation occurred primarily with the high standard contrast of 66 percent. Therefore, the average values for the differences between eyes for the standard contrast of 66 percent were determined from the absolute values of the individual differences. The sign was then chosen to reflect the eye which had the closest contrast matches to the baseline contrast match at 2 c/d. For example, an examination of the individual differences between eyes in Figure 116 showed that the amblyopic eye performed a contrast match better than the normal eye at 10 c/d. This result would not be evident in the average differences had not the latter analysis been used.

These surprising results can be seen in greater detail in the additional contrast matching data that were obtained over a more concentrated range of mid-spatial frequencies. The contrast matches of two sessions from 2 to 10 c/d in 2 c/d increments are shown in Figures 119.a and 119.b. The average results are shown in Figure 119.c. The difference curves are shown in Figure 120. Results similar to the previous measurements are evident. The decrease in sensitivity most evident at 6 and 8 c/d at low contrast is not found at contrasts of 33 percent and 66 percent. Her amblyopic eye shows increased sensitivity at 33 and 66 percent contrast. As in the previous results, her normal eye has lost sensitivity at 10 c/d for the high contrasts. Clearly, the state of both her normal and amblyopic eye changes as a function of spatial frequency and contrast.

Note that there is a greater difference between the contrast match at the higher standard contrasts in the first set of data (Figure 120.a) as when compared to the second set (Figure 120.b). The second set of data is similar to the first set primarily at lower contrasts. Almost two months elapsed between these particular measurements. It can only be conjectured whether these results are due to practice or whether they reflect a change of state of her visual system such as occurred with the previous contrast sensitivity and Snellen letter acuity measurements or normal variability. Further investigation is needed before any determination of such changes can be made.

#### A-4.3 Discussion

These results show that the mechanisms tuned to different spatial frequencies in the visual system of this amblyope do



not behave normally. Mechanisms for both the amblyopic and normal eye changed their sensitivity in a complex manner as a function of spatial frequency and contrast. The results of the contrast matches at low contrasts were consistent with the previous contrast sensitivity data. However, at high contrast the amblyopic eye appeared to overcompensate, requiring less contrast than should be required to do a contrast match. The normal eye at higher contrast appeared to undercompensate and required more contrast than was needed in comparison to the normal subject. Although the previous data from contrast matching, e.g., Georgeson and Sullivan (1975), can be interpreted as evidence for mechanisms in the visual system tuned to different ranges of spatial frequencies, the present data obtained from this amblyope most strongly demonstrated visual behaviour that is difficult to interpret in any other way. Furthermore, the overcompensation and undercompensation that were found suggest a much more complex gain system for the channels than was suggested by Georgeson and Sullivan (1975).

Although further research is needed to determine the rules of such channel behaviour, certain speculation can be made about possible reasons for overcompensation in the amblyopic eye and undercompensation in the normal eye. As noted in the introduction, the amblyope has two problems to overcome: confusion and diplopia. The amblyope can sometimes maintain binocular vision. A. H. does have limited stereopsis. Perhaps the overcompensation in her amblyopic eye and the undercompensation in her normal eye reflect a need of the visual system to maintain constant contrast for binocular mechanisms in a manner similar to a binocular brightness averaging mechanism proposed by Levelt (1965).

The gain of the least sensitive channel in the amblyopic eye may have been boosted (reduced inhibition) to compensate for the low sensitivity. If the gain mechanism had a similar or larger bandwidth than that of the channels, then a boost of gain of one channel would cause a boost of gain in adjacent channels. Since the channels are about one to two octaves wide, an increase in sensitivity for the 6 c/d channel would also cause a boost in higher and lower spatial frequencies, resulting in overcompensation, as was found at 10 c/d. Although this explanation seems reasonable, it does not help explain why the channels overcompensate at higher levels of contrast or why the channels at 3 c/d do not also show overcompensation. However, suppose that the gain of certain channels in the amblyopic eye was boosted and resulted in abnormally high sensitivity at certain levels of contrast. Then how is the contrast of these channels combined with the contrast of the channels in the other eye if, for example, an average contrast must be maintained? One solution would be a decrease in the gain of certain channels in the normal eye to compensate for the increased gain in the amblyopic eye.

This idea of a channel having abnormally low sensitivity could be reinterpreted in terms of a channel having abnormally high sensitivity. If the gain mechanism for the 10 c/d channel were abnormally high, it could reduce the output of other channels by inhibition. This explanation fits the data better because there did not seem to be any overcompensation at 3 c/d in the amblyopic eye and it is more likely (e.g., Harmon and Julesz, 1973) that high spatial frequencies inhibit low spatial frequencies than that low spatial frequencies inhibit high spatial frequencies. The rest of the argument follows as above. At present, these explanations are quite speculative. However, the contrast matching data clearly imply much more complex interactions between the normal and amblyopic eye than has been previously suggested.

If these quite unexpected results can be found with other amblyopes, then perhaps a beginning can be made to understand the difficulty that amblyopes (and possibly other individuals with different visual disorders) have in describing the characteristics of objects that they see. Furthermore, these results also suggest why no optical means could produce images in the normal eye that looked like the images seen with the amblyopic eye. Most objects contain many spatial frequencies at different contrast levels. The contrast matching experiments have shown that the sensitivity of the mechanisms in the visual system of this amblyope depends not only on the spatial frequency composition but also the contrast of spatial frequencies. It is not surprising that optical or other techniques which affect contrast at different spatial frequencies in a monotonic fashion cannot mimic the vision of an amblyope. The visual system of an amblyope appears to provide a much more complex picture of objects than has been suspected—a picture that, as one subject stated, is "more interesting."

Although it appears that the contrast matching studies help to explain the strange suprathreshold vision of the amblyope, there is another question to be answered from the original contrast sensitivity measurements—is there a relationship between the increased spatial frequency sensitivity in the amblyopic eye and the concomitant increase in Snellen letter acuity? This is examined in Section 18.3.

## CHAPTER A-5

### THE FILTERING CHARACTERISTICS OF PATIENTS HAVING MULTIPLE SCLEROSIS

#### A-5.1 Introduction

Multiple sclerosis (MS) is a disease which results from demyelination of conducting fibres in the nervous system. Demyelination in the visual system, typically of the optic nerve or chiasma, is almost always found *postmortem* in cases of MS (Duke-Elder, 1949, Vol. III; Lumsden, 1970). However, it is quite common for patients suffering from MS to complain of poor vision in one or both eyes and yet have normal Snellen acuity. Such reports suggest that MS patients may have selective losses in spatial frequency channels that are not sufficiently low to affect the range of spatial frequencies required for Snellen letter acuity but that do affect the general quality of vision. Motivated by the study of the abnormal filtering characteristics of amblyopia, a similar investigation was made with patients having MS.

#### A-5.2 Methods and Results

The contrast sensitivity functions of six MS patients were determined using the same methods discussed previously in Section A-2. The results are shown in Figures 121 to 126. The visual acuity of the subjects is shown in the upper right corner of each figure. The difference in sensitivity between eyes is plotted below the contrast sensitivity curves, in factors on the left, dB on the right. Compared with the contrast sensitivity curves of the amblyopes, there is generally little difference in sensitivity between the two eyes at the high spatial frequencies. However, each patient shows at least a 7 dB (greater than a factor of 2) difference in sensitivity between eyes over some range of spatial frequencies. Three general classes of sensitivity loss are evident; mid-spatial frequencies (subjects C. H., A. J., M. D.), all spatial frequencies (subject S. S., M. S.), high spatial frequencies (subject B. M.). One subject, C. H., showed an average of 3 dB increased sensitivity from 0.2 to 0.3 c/d in the left compared to the right eye. However, at 4 to 10 c/d, the right eye was about 14 dB more sensitive than the left eye.

#### A-5.3 Discussion

Clearly, the contrast sensitivity measurements provide a much more sensitive indication of the filtering characteristics of the visual system that is used for the everyday perception of objects than does Snellen letter acuity. The predominant mid-frequency losses in sensitivity, especially found with subjects C. H., A. J., and M. D., would be very difficult to explain by simple optical blurring which always degrades the high spatial frequencies more than the low. However, these results are consistent with selective losses in channels tuned to different ranges of spatial frequency.

These results are also in good agreement with a similar recent study by Regan, Silver, and Murray (1977). They found that 20 of 48 patients had losses in contrast sensitivity that could not be explained by refractive error. Sensitivity losses in the mid-spatial frequencies were evident in 10 of 20 patients. Three patients were reported to have selective losses at low- to mid-spatial frequencies. Since 8 of 14 patients with selective spatial frequency losses did not show any clinical evidence of visual impairment, they concluded that the contrast sensitivity measurements can aid the earlier diagnosis of MS.

The selective spatial frequency losses in contrast sensitivity found to accompany MS have not resulted in the large losses of Snellen letter acuity that were seen with the amblyopes. The only general difference between the contrast sensitivity functions of MS and amblyopia is the degree to which the contrast sensitivity is decreased over certain ranges of spatial frequency. This finding further suggests that Snellen letter acuity is based upon a certain level of contrast sensitivity over a relatively narrow range of high spatial frequencies.

The level of contrast sensitivity attained by these MS patients to their Snellen letter acuity is related in Section 18.2.

**APPENDIX B**

**TABLE OF CONTRAST SENSITIVITY  
FROM CAMPBELL, KULIKOWSKI, AND LEVINSON (1966)**

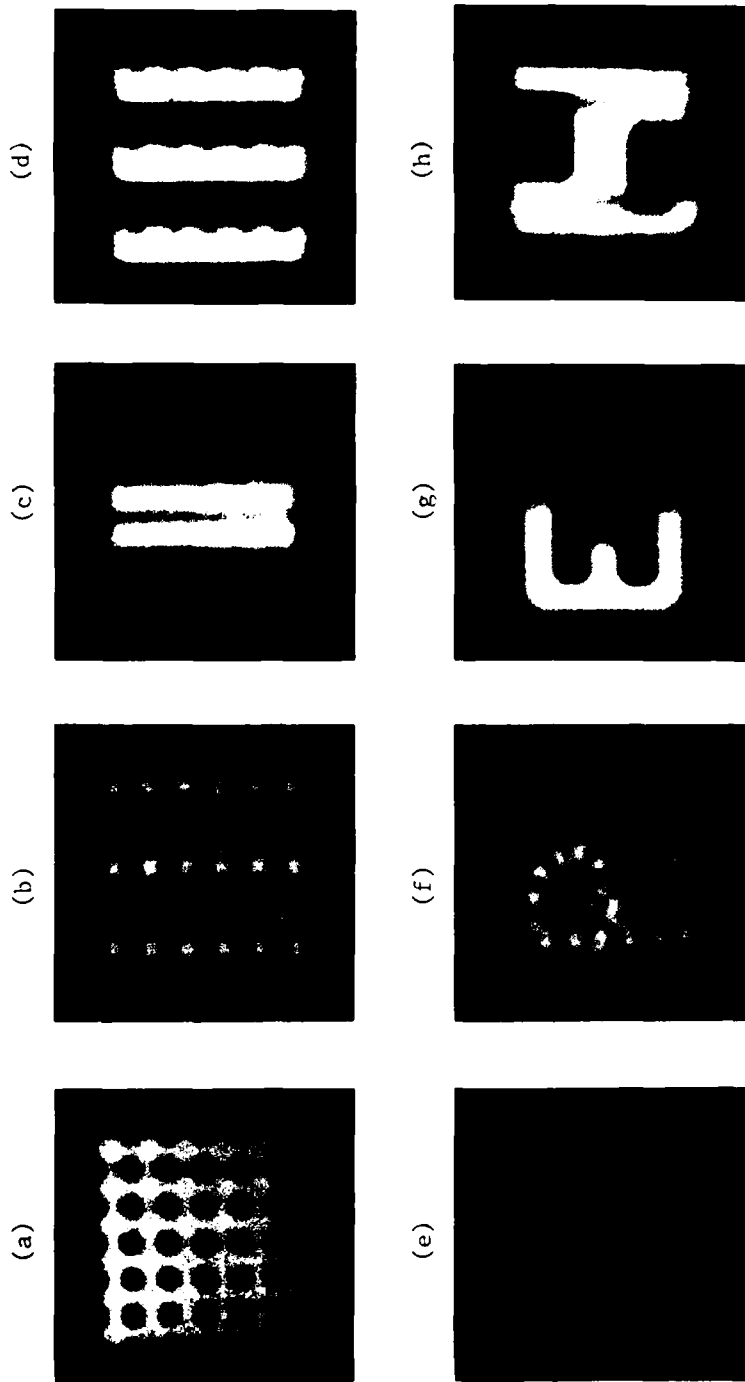
APPROXIMATED MTF SUBJECT DATA

SPATIAL FREQUENCY (c/d)	CONTRAST SENSITIVITY (0°)				CONTRAST SENSITIVITY (45°)				CONTRAST SENSITIVITY (90°)			
	INDIVIDUAL SUBJECT DATA			% RED	INDIVIDUAL SUBJECT DATA			% RED	INDIVIDUAL SUBJECT DATA			% RED
	a	b	c		a	b	c		a	b	c	
1.0	53.0	43.0	50.0	.23	47.0	40.0	43.0	.20		45.0	37.0	.19
1.5	77.0	75.0	55.0	.32	73.0	53.0	50.0	.28	60.0	55.5	60.0	.27
2.0	115.0	90.0	93.0	.47	95.0	70.0	73.0	.37	77.0	75.0	73.0	.35
3.0	165.0	110.0	120.0	.62	130.0	93.0	105.0	.51	85.0	125.0	120.0	.52
4.0	160.0	135.0	170.0	.73	145.0	97.0	130.0	.58	150.0	120.0	120.0	.61
5.0	230.0	170.0	185.0	.92	155.0	120.0	150.0	.68	140.0	180.0	190.0	.81
6.0	300.0	150.0	190.0	1.00	180.0		145.0	.76	250.0	170.0	180.0	.94
7.5	230.0	135.0	250.0	.96	135.0	120.0	150.0	.63	180.0	150.0	210.0	.85
10.0	135.0	105.0	150.0	.61	100.0	90.0	120.0	.49		130.0	170.0	.70
12.5	130.0	80.0	145.0	.56	70.0	60.0	90.0	.34				
15.0	110.0	57.7	120.0	.45	50.0	40.0	65.0	.24	110.0	85.0	130.0	.52
17.5	50.0	55.0	100.0	.32	37.0	30.0	70.0	.21	97.0	55.0	100.0	.39
20.0	47.0	35.0	75.0	.25	13.0	18.0	42.0	.11	45.0	48.0	92.0	.29
22.5	40.0	22.0	48.0	.17	16.0	8.0	25.0	.08	35.0	25.0	55.0	.18
25.0	30.0	18.0	40.0	.14	8.5	8.5	20.0	.07	27.0	18.0	42.0	.14
27.5	17.0	12.5	32.0	.10	6.0	7.3	13.0	.04	15.0	14.0	35.0	.10
30.0	13.0	12.0	22.0	.07	2.7	4.0	12.0	.03	14.0	15.0	25.0	.08
32.5	9.0	10.0	12.0	.05	2.3	3.5	8.0	.02	9.5	7.5	17.0	.05
									8.0	6.0	17.0	.05

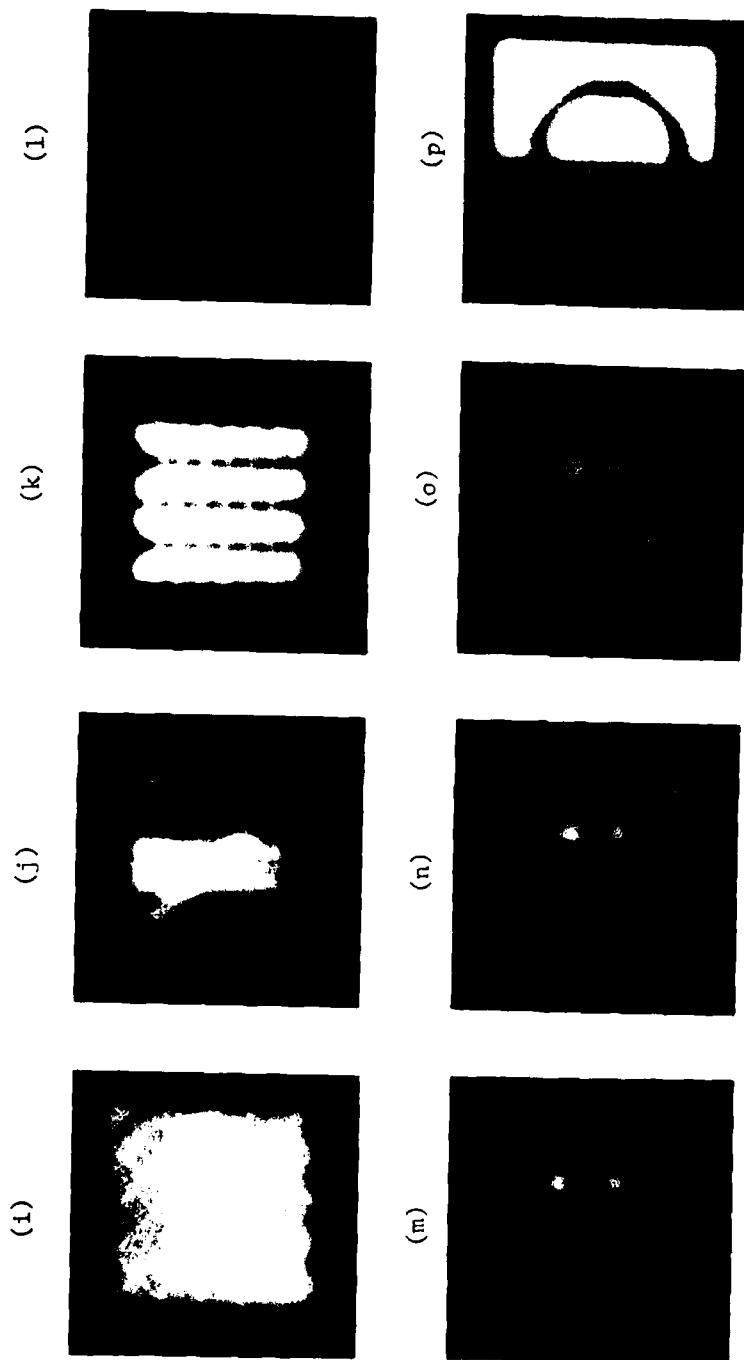
NOTE: The percent reduction (% Red) for all the angles (0, 45, 90) is normalized from the maximum value (213.3 @ 6.0 c/d @ 0°).

**APPENDIX C**

**OBJECTS THAT ARE BLURRED BY OPTICAL DEFOCUS  
TO ABOUT THE FOURTH HARMONIC**



Objects that are Blurred by Optical Defocus to About the Fourth Harmonic: (a) Dot-Whole; (b) Dot-Proximity; (c) Dot-Line-Similarity; (d) Dot-Line-Proximity/Similarity; (e) Dot Letter G; (f) Dot Letter R in Noise; (g) Letter E; (h) Discrete Line Letter H; (i) Isolating a Rectangular Form from Oblique Lines; (j) Poggendorff Illusion; (k) Zöllner Illusion; (l) Horizontal-Vertical Illusion; (m) Original Müller-Lyer Illusion; (n) Original Müller-Lyer Illusion with Further Blurring; (o) Müller-Lyer Illusion with Unequal Sized Fins Going in the Same Direction; (p) Benussi Ring Illusion; (q) Müller-Lyer Illusion with Fins Only; (r) Müller-Lyer Illusion with Fins Only with Further Blurring; (s) Ponzo Illusion; (t) Ponzo Illusion with Further Blurring; (u) Rubin Face-Vase Object.



Objects that are Blurred by Optical Defocus to About the Fourth Harmonic: (a) Dot-Whole; (b) Dot-Proximity; (c) Dot-Line-Similarity; (d) Dot-Line-Proximity/Similarity; (e) Dot Letter G; (f) Dot Letter R in Noise; (g) Letter E; (h) Discrete Line Letter H; (i) Isolating a Rectangular Form from Oblique Lines; (j) Poggendorff Illusion; (k) Zöllner Illusion; (l) Horizontal-Vertical Illusion; (m) Original Müller-Lyer Illusion; (n) Original Müller-Lyer Illusion with Further Blurring; (o) Müller-Lyer Illusion with Unequal Sized Fins Going in the Same Direction; (p) Benussi Ring Illusion; (q) Müller-Lyer Illusion with Fins Only; (r) Müller-Lyer Illusion with Fins Only with Further Blurring; (s) Ponzo Illusion; (t) Ponzo Illusion with Further Blurring; (u) Rubin Face-Vase Object. (cont.)



Objects that are Blurred by Optical Defocus to About the Fourth Harmonic: (a) Dot-Whole; (b) Dot-Proximity; (c) Dot-Line-Similarity; (d) Dot-Line-Proximity/Similarity; (e) Dot Letter G; (f) Dot Letter R in Noise; (g) Letter E; (h) Discrete Line Letter H; (i) Isolating a Rectangular Form from Oblique Lines; (j) Pogendorff Illusion; (k) Zöllner Illusion; (l) Horizontal-Vertical Illusion; (m) Original Müller-Lyer Illusion; (n) Original Müller-Lyer Illusion with Further Blurring; (o) Müller-Lyer Illusion with Unequal Sized Fins Going in the Same Direction; (p) Benussi Ring Illusion; (q) Müller-Lyer Illusion with Fins Only; (r) Müller-Lyer Illusion with Fins Only with Further Blurring; (s) Ponzio Illusion; (t) Ponzio Illusion with Further Blurring; (u) Rubin Face-Vase Object. (cont.)